ЖУРНАЛ
ЭКСПЕРИМЕНТАЛЬНОЙ И ТЕОРЕТИЧЕСКОЙ
ФИЗИКИ
Zhurnal Eksperimental'noi i Teoreticheskoi Fiziki

SOVIET PHYSICS JETP

VOL. 11, NO. 4 OCTOBER, 1960

A Translation
of the
Journal of Experimental and Theoretical Physics
of the
Academy of Sciences of the USSR

(Russian Original Vol. 38, No. 4, April, 1960)

Published by the
AMERICAN INSTITUTE OF PHYSICS
INCORPORATED

SOVIET PHYSICS
JETP

A translation of the Journal of Experimental and Theoretical Physics of the USSR.

A publication of the

AMERICAN INSTITUTE OF PHYSICS

Governing Board

Ralph A. Sawyer, *Chairman*
J. G. Baker
R. H. Bolt
Wallace R. Brode
Harvey Brooks
Dirk Brouwer
J. W. Buchta
Vernet E. Eaton
J. H. Elliott
Herbert A. Erf
S. A. Goudsmit
W. W. Havens, Jr.
Winston E. Kock
R. Bruce Lindsay
H. V. Neher
C. J. Overbeck
George E. Pake
Ray Pepinsky
Francis W. Sears
Frederick Seitz
John Strong
George E. Uhlenbeck
Mary E. Warga
Victor F. Weisskopf
William R. Willets

Administration

Elmer Hutchisson
Director
Wallace Waterfall
Secretary and Treasurer
Henry A. Barton
Administrative Consultant
W. C. Kelly
Director of Education
Eugene H. Kone
Director of Public Relations
Hugh C. Wolfe
Director of Publications
Kathryn Setze
Assistant Treasurer
Norma Frankel
Publications Editor
Alice Mastropietro
Circulation Manager
Edward Tober
Manager, Production and Distribution
Theodore Vorburger
Advertising Manager
Emily Wolf
Manager, Special Services

American Institute of Physics Advisory Board on Russian Translations

Robert T. Beyer, *Chairman*
J. George Adashko, Freeman Dyson, Dwight Gray,
Morton Hamermesh, Harold F. Weaver

Editor of Soviet Physics—JETP

J. George Adashko, 25 West 81st St., New York 24, New York

Soviet Physics—JETP is a monthly journal published by the American Institute of Physics and contains a complete translation of the Journal of Experimental and Theoretical Physics of the U.S.S.R. Academy of Sciences.

This translating and publishing project was undertaken by the institute in the conviction that dissemination of the results of researches everywhere in the world is invaluable to the advancement of science. The National Science Foundation of the United States has encouraged the project initially and is supporting it in large part by a grant.

The American Institute of Physics and its translators propose to translate faithfully all the material appearing in the original articles. The views expressed in the translations are therefore those of the original authors, and not those of the translators nor of the American Institute of Physics.

Volume 1 of Soviet Physics—JETP corresponds to Russian Volume 28 (1955). Two volumes are published annually, each of six issues. Each volume contains the translation of one volume of the Journal of Experimental and Theoretical Physics.

Beginning with Vol. 9(36), the transliteration of the names of Russian authors follows British Standard 2979, which is being adopted by a large number of scientific journals in the United States. The Library of Congress transliteration is followed in the earlier volumes.

Subscription Prices

Per Year (12 issues)	
General:	
United States and Canada	$75.00
Elsewhere	79.00
Libraries of non-profit degree-granting Institutions:	
United States and Canada	$35.00
Elsewhere	39.00
Back Numbers	$ 8.00

Subscriptions should be addressed to the American Institute of Physics, 335 East 45th Street, New York 17, New York.

SOVIET PHYSICS, JETP is published monthly by the American Institute of Physics, Inc. Second Class postage paid at Ann Arbor, Michigan.

Copyright by American Institute of Physics 1960

SOVIET PHYSICS
JETP

A translation of Zhurnal Éksperimental'noĭ i Teoreticheskoĭ Fiziki.

Vol. 11, No. 4, pp. 733-979 (Russ. orig. Vol. 38, No. 4, pp. 1017-1360, April, 1960) Oct.,1960

LONG-LIVED LUTETIUM ISOTOPES

V. A. ROMANOV, M. G. IODKO, and V. V. TUCHKEVICH

Leningrad Physico-Technical Institute, Academy of Sciences, U.S.S.R.

Submitted to JETP editor August 7, 1959

J. Exptl. Theoret. Phys. (U.S.S.R.) 38, 1019-1026 (April, 1960)

The conversion spectrum of the long-lived lutetium isotopes Lu^{173} and Lu^{174} was investigated. The relative conversion-line intensity in the soft region of the Lu^{173} spectrum (up to 250 kev) was measured. The per cent ratio of the M1 + E2 mixture for the 78.6- and 100.6-kev transitions is determined. The Lu^{174} spectrum contains conversion lines which can be ascribed to transitions connected with the isomer state of Lu^{174} ($E_\gamma = 44.7$ kev — M1 transition and $E_\gamma = 59.0$ kev — M3 transition). The half-life of the isomer state is ~90 days.

IN the study of the lutetium fraction separated from a tantalum target bombarded by fast (660 Mev) protons, a series of lines with a half-life considerably in excess of 32 days was observed in the conversion spectrum after the decay of the lutetium isotopes with relatively small half lives ($T_{1/2} < 8$ days), and after the decay of the Yb^{169} present in the source ($T_{1/2} = 32$ days). The measurements were carried out on a double-focusing spectrometer with an approximate transmission of 0.2% ($R_0 = 24$ cm., half-width ~ 0.3%). In many measurements the transmission was reduced to 0.1% in order to reduce the half width of the lines. In the soft region (< 30 kev) the width of the lines was greater than the instrument width, owing to the slowing down of the electrons in the source material.

The measurements were carried out with two sources. Source 1 was obtained by bombarding the tantalum target in the cyclotron for approximately 4 hours and separating the lutetium fraction 10 to 12 hours after the bombardment. To produce source 2, the target was irradiated for approximately three months, and the lutetium fraction was separated a week after the end of the irradiation. Source 2 was employed previously by Dzhelepov et al.[1,2]

The considerable number of the observed lines with long half-lives is due to the presence in the source of Lu^{173}, the spectrum of which has been relatively well studied.[1-3] Lu^{173} lines were observed in the spectra obtained with both sources. The relative line intensities obtained were in good agreement with those given by Bobrov et al.[1] with the exception of the Auger lines, whose intensities were obviously overestimated in their paper.

Figure 1 shows the strongest lines and the spectrum of the long-lived isotopes of lutetium, obtained with source 1. The figure shows the conversion lines without corrections for Hρ and for absorption in the source.

Table I lists the energies and relative intensities of the lines (without corrections for the absorption in the source) in the Lu^{173} spectrum. The intensities given were obtained with source 2. The relative intensities obtained with the thinner source 1 are the same, within the limits of errors, for all lines with the exception of Kγ 78.6 kev. This shows that the correction for absorption in the source and in the counter films is small, starting with an electron energy ~ 30 kev.

When measurements with source 1 were made at a reduced aperture ratio, the conversion lines from the L subshells were sufficiently well sepa-

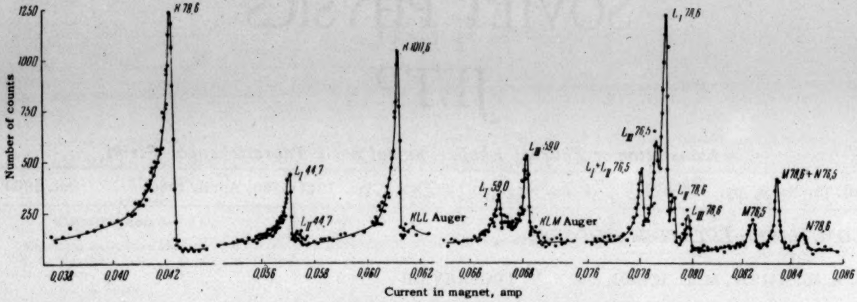

FIG. 1. Section of spectrum of long-lived lutetium isotopes.

TABLE I. Energy and relative intensity of the conversion lines in the Lu^{173} spectrum

No. of line	Identification of line	Line energy, kev	Relative intensity*	No. of line	Identification of line	Line energy, kev	Relative intensity*
1	$K\gamma$ 78.6	17.33	345±10	11	$L_I + L_{II}\gamma$ 100.6	90.14	19.3± 0.5
2	$K\gamma$ 100.6	39.32	100	12	$L_{III}\gamma$ 100.6	91.70	
3	*KLL*-Auger	—	33±1	13	$M\gamma$ 100.6	98.21	3.4
4	*KLM*-Auger	—	21.2±0.7	14	$N\gamma$ 100.6	100.43	1.4
	KLN-Auger	—		15	$K\gamma$ 171.3	110.0	1.4
5	*KMM*-Auger	—	4.0±0.7	16	$K\gamma$ 179.3	118.0	2.1
6	$L_I\gamma$ 78.6	68.15	98±3	17	$L\gamma$ 171.3	161.1	<0.3
7	$L_{II}\gamma$ 78.6	68.64		18	$L_I + L_{II}\gamma$ 179.3	169.5	1.1
8	$L_{III}\gamma$ 78.6	69.69		19	$L_{III}\gamma$ 179.3	170.6	
9	$M\gamma$ 78.6	76.22	18.9±0.6	20	$K\gamma$ 272.5	211.2	2.8±0.1
10	$N\gamma$ 78.6	78.15	6.0±0.2				

*The errors characterize the statistical dispersion and do not include the possible systematic errors.

rated for the different transitions. For the 78.6-kev γ transition the ratio obtained was $L_I : L_{II} : L_{III} = 1 : (0.24 \pm 0.005) : (0.164 \pm 0.003)$.

A comparison of the relations obtained with the theoretical values makes it possible to establish that this is a mixed transition, 95.5% M1 + 4.5% E2. For such radiation we have a theoretical ratio $(K/L)_{theor} = 5.1$. An experimental ratio $(K/L)_{exp} = 4.1$ was obtained with source 1 and $(K/L)_{exp} = 3.5$ was obtained with source 2. The deviation from the theoretical values is explained by absorption in the source material. A ratio $L_{III} : (L_I + L_{II}) = 0.075 \pm 0.002$ was obtained for the 100.6-kev γ transition. The transition is of the mixed type, 96% M1 + 4% E2. In this case $(K/L)_{theor} = 5.62$. The experimental ratio $(K/L)_{exp} = 5.4 \pm 0.2$ agrees, within the limits of errors, with the theoretical one. We see from a comparison of the theoretical and experimental values that the correction for absorption is small in this case.

For the 171.3-kev γ transition, an estimate of $K/L > 4.5$ was obtained. Such a K/L ratio is possessed by the transitions E1, M1, and M2. In the case of the 179.3-kev γ transition, the resultant ratios $L_{III} : (L_I + L_{II}) = 0.60$ and $K : L = 1.9$ indicate that this is an E2 transition. The theoretical ratios of the internal conversion coefficients for an E2 transition of the same energy are $L_{III} : (L_I + L_{II}) = 0.54$ and $K/L = 1.73$.

Gorodinskiĭ et al.[3] measured the relative intensities of the γ rays and the spectrum of Lu^{173}. Using the relative γ-ray and the relative conversion K-line intensities obtained in the present work, one can determine the K-shell internal-conversion coefficients. In this case it is best to normalize the internal-conversion coefficients against the 78.6-kev $L\gamma$ line (the multipolarity of the transition has been well established, and the line energy is sufficiently high).

Table II lists the relative γ-ray intensities

TABLE II. Relative intensities of the transitions in the spectrum of Lu^{173}

Transition energy, kev	I_γ [3]	I_k, rel. units	I'_γ, rel. units	α_k from I_k and ref. 3	$(\alpha_k)_{theor}$, from ref. 4			$I_{tot.}$
					E1	M1	E2	
78.6	1	—	90.3					713
100.6	0.52	100	38.3	2.13 (0)	2.80 (—1)	2.81 (0)	9.89 (—1)	166
171.3	0.31	1.4		5.0 (—2)	7.0 (—2)	6.58 (—1)	2.70 (—1)	22
179.3	0.11	2.1	9.4	2.1 (—1)	6.65 (—2)	5.88 (—1)	2.23 (—1)	13
272.5	1.85	2.8		1.7 (—2)	2.14 (—2)	1.77 (—1)	7.1 (—2)	134
351	0.11							10
570	0.15							14
630	0.26							24

I_γ, obtained in reference 3, the relative intensities I_k of the conversion K lines, the γ-ray intensities I'_γ, obtained from the conversion data and from the Sliv and Band tables,[4] and also the calculated K-shell internal-conversion coefficients α_k. The 100.6-kev K_γ line intensity is taken to be 100. A comparison of the calculated internal-conversion coefficients with the theoretical ones for the 100.6- and 179.3-kev γ transitions confirms the previously-established multipolarity and shows that 171.3- and 272.5-kev γ transitions are E1. Table II lists also the total relative intensities of the transitions, I_{tot}, calculated from our conversion data and the Sliv and Band tables.[4] The intensities of the 351-, 570-, and 630-kev γ transitions were taken from the paper by Gorodinskiĭ et al.[3] and it is assumed that in these cases $I_k \ll I_\gamma$.

The level scheme of Lu^{173} has been sufficiently well investigated.[1-3,5] The total intensities and the decay scheme yield the "population" of the excited levels of Yb^{173}. Figure 2 shows the level scheme of Yb^{173}. In our case the number of captures in the excited levels was 760 (I_k (γ100.6) = 100 units). The number of vacancies freed after the conversion was $\Sigma I_k = 605$. The total number of vacancies was 1365. If we take Gray's[6] Auger electron yield for Yb, $\alpha_k = 0.064 \pm 0.010$, and the experimental number of Auger K electrons to be 58 ± 2, a total number of 906 ± 165 K captures is obtained, which is less than a number of vacancies obtained from the transition intensities, even if it is assumed that there are no transitions to the Yb^{173} ground level. This may be due either to the comparatively large L capture, or to the inaccuracy in determination of the Auger-electron yield.

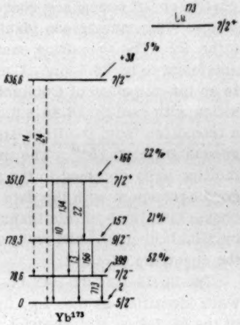

FIG. 2. Decay scheme of Lu^{173}.

The spectrum of the long-lived isotopes produced from source 1 disclosed a series of lines not belonging to Lu^{173}, shown upon repeated measurements to have diverse half lives, all different from the half life of Lu^{173}. Table III lists energies of these lines. Two lines were observed in the region of the L lines of the 78.6-kev γ transition with energies 66.47 and 67.53 kev, identified as $L_I + L_{II}$ and L_{III}. M and K lines of the same transition were also found. The K-L energy distance indicates that the conversion occurs in an atom with Z = 70. Table IV gives a comparison of the experimental and theoretical ratios of the

TABLE III. Energies of lines connected with the decays of Lu^{174*} and Lu^{174}

No. of line	Identification of line	Line energy, kev	No. of line	Identification of line	Line energy, kev
1	$K\gamma$ 76.5	15.10	8	$L_{II}\gamma$ 59.0	—
2	$L_I\gamma$ 44.7	33.79	9	$L_{III}\gamma$ 59.0	49.75
3	$L_{II}\gamma$ 44.7	34.27	10	$M\gamma$ 59.0	—
4	$L_{III}\gamma$ 44.7	—	11	$N\gamma$ 59.0	58.56
5	$M\gamma$ 44.7	42.14	12	$L_I + L_{II}\gamma$ 76.5	66.47
6	$N\gamma$ 44.7	44.06	13	$L_{III}\gamma$ 76.5	67.53
7	$L_I\gamma$ 59.0	48.14	14	$M\gamma$ 76.5	74.34

TABLE IV. Comparison of experimental and theoretical ratios of internal-conversion coefficients for the 76.5-kev γ transition of Lu^{174}

	Experiment	$E1$	$E2$	$E3$	$M3$
$K:L$	0.23±0.06*	5.7	0.263	0.012	0.42
$L_I+L_{II}:L_{III}$	1,05±0.03	3.34	1.01	1.06	0.745
$L:M$	3,6±0.1	—	—	—	—

*The correction for absorption in the source is neglected.

coefficient of secondary conversion for this transition. The comparison identifies the transition to be E2. The transition energy was measured and found to be 76.5 kev. Chupp et al. observed in an investigation of Coulomb excitations[7] a transition with energy 76.46 ± 0.01 kev, identified as a transition from the first excited state to the ground state of Yb^{174}. The transition energy and multipolarity obtained in the present work are in good agreement with the data of Chupp et al.[7] The conversion lines of this transition were observed by Mihelich et al.[8] and were also associated with the spectrum of Lu^{174}.

The 33.79-, 34.27-, 42.14- and 44.06-kev lines were identified as the L_I, L_{II}, M, and N lines of the 44.7-kev γ transition. The distance between the L_I and M lines is 8.35 kev. A comparison with the distance between L_I and M as obtained by x-ray data[9] [Z = 70 (8.09 kev), Z = 71 (8.38 kev), Z = 72 (8.68 kev)] indicates that the conversion takes place in an atom with Z = 71. The ratios $L_I:L_{II}:L_{III} = 1:(0.156 \pm 0.004):(0.038 \pm 0.007)$ obtained indicate unequivocally that the transition is of the M1 type. The theoretical value for the M1 transition is $L_I:L_{II}:L_{III} = 1:0.093:0.013$. If there is an E2 admixture, it does not exceed 1% (approximately 0.75% for $L_I/L_{II}/$ and approximately 0.3% for L_{III}/L_I).

Lines 7, 8, 9, 10 and 11 in Table III have been identified as L, M, and N lines. It is difficult to determine the Z of the atom in which the conversion takes place directly from the L-M energy distance, since the M line falls on the KLM Auger lines. To obtain a better value of Z we measured the distance between the L_I and L_{III} lines. The source was isolated from the housing of the spectrometer and a certain voltage was applied to it. With a constant field in the spectrometer, we plotted the lines L_I and L_{III} several times while varying the voltage. The distance between the lines was read from the plot directly in volts and was found to be 1631 ± 12 v. The x-ray data for different Z yield the following values:

	Tm	Yb	Lu	Hf
Z	69	70	71	72
Distance between lines, v	1460	1544	1625	1716

Thus, the distance obtained between the L_I and L_{III} lines is in good agreement with the distance in the atom with Z = 71. The transition energy is $E_\gamma = 59.0$ kev. The experimentally obtained ratio $L_I:L_{II}:L_{III} = (0.49 \pm 0.02):(0.07 \pm 0.01):1$ is close to the tabulated one for the M3 transition ($L_I:L_{II}:L_{III} = 0.46:0.060:1$). For comparison, we give the theoretical value of the L-shell secondary conversion coefficient for transitions with a different multipolarity (Z = 71, k = 0.10, where k is the energy in m_0c^2 units):

$E4$ $L_I:L_{II}:L_{III} = 0.02:0.99:1$
$E5$ $L_I:L_{II}:L_{III} = 0.02:0.01:1$
$M4$ $L_I:L_{II}:L_{III} = 0.15:0.02:1$
$M5$ $L_I:L_{II}:L_{III} = 0.08:0.01:1$

To obtain more exact values of the half-lives of the intensities of the conversion lines, two series of measurements were made with source 2, and three series of measurements with source 1. Each series consisted of two measurements. The first series with source 2 was performed 2.5 to 3 years after the preparation of the source, while the second was performed 150 days after the first. In the case of source 1, the first series of measurements was made 300 days after separation, the second was made 100 days after the first, and the third 100 days after the second. In measurements with source 2, the half-lives of the lines in the Lu^{173} spectrum were found to be approximately 160 days. The intensity of the lines $L\gamma$ 44.7 kev was found to be so low as to require special measurement. A rough estimate of the half-lives, based on the data of Bobrov et al.[1] and on our measurements, yields a half-live of about 100 days for $L\gamma$ 44.7 kev. The $L\gamma$ 59.0 kev lines cannot be separated from the stronger KMM Auger lines in these measurements. The lines $L\gamma$ 76.5 kev and $L\gamma$ 78.6 kev are very close to each other, and therefore the combined area of the two lines was measured. The half-life of the entire group is approximately the same as for the Lu^{173} lines. The half-life of $M\gamma$ 76.5 kev does not differ greatly from that of the Lu^{173} lines, and is perhaps somewhat shorter. A rough estimate of the half-life of $M\gamma$ 76.5 kev, from the data of Bobrov et al.[1] and our measurements, yields a value of approximately 200 to 250 days.

The measurements with source 1 were performed three times. Since the measurement conditions (the aperture of the instrument) varied, it is impossible to calculate the half-life directly from these measurements, and it has become necessary to determine it from its ratio to $T_{1/2}$ for Lu^{173}, the value of which (107 days) was taken from reference 1 (our measurements with source 2 gave nearly the same value). Taking the $L\gamma$ 78.6-kev line of Lu^{173} as a reference, the half-lives of the remaining lines were found to be:

Line	$T_{1/2}$
$K\gamma$ 78.6 kev Lu^{173}	195 days
$L_I\gamma$ 44.7 kev	97 days
$K\gamma$ 100.6 kev	166 days
$L_{III}\gamma$ 59.0 kev	87 days
$L\gamma$ 76.5 kev	309 days
$M\gamma$ 76.5 kev	271 days
$M\gamma$ 78.6 + $N\gamma$ 76.5 kev	182 days

The lines of Lu^{173} have nearly the same half-life as the reference line $L\gamma$ 78.6 kev ($T_{1/2}$ = 170 days). The half-life of $L_I\gamma$ 44.7 kev and $L_{III}\gamma$ 59.0 kev are ralatively close to each other ($T_{1/2}$ ~ 85 — 95 days). The half-life of the γ 76.5-kev lines amounts to 250 — 300 days and is clearly much greater than that of the reference line. The 44.7- and 59.0-kev γ transitions belong to the same isotope. This is confirmed by the fact that they occur in an atom having the same value of Z, that their lines have nearly equal half-lives, and that they have practically the same intensity:

$$I_{\text{tot}}\ (\gamma\ 59.0\ \text{kev}) : I_{\text{tot}}\ (\gamma\ 44.7\ \text{kev}) = 0.94 \pm 0.03.$$

An attempt can be made to establish the particular lutetium isotope to which these transitions belong. Lutetium has a large number of known isotopes with different half-lives.[10] The isotopes Lu^{169}, Lu^{170}, Lu^{171}, and Lu^{172} are obviously eliminated, for once the nucleus goes over from the isomer state to the ground state, the decay has a relatively small half-life, and the strongest transitions following the decay of these isotopes would have been observed. The level schemes of Lu^{173}, Lu^{175}, and Lu^{177} have been investigated and do not contain such transitions. This leaves only Lu^{174} and Lu^{176}. The isotope Lu^{176} is found in the natural isotope mixture (2.6%) and decays with $T_{1/2} \approx 2.1 \times 10^{10}$ years[10] to high-spin Hf^{176} levels. The spin of the ground state of Lu^{176} is 7.[11] Rotational levels with spins 8 and 9 have been obtained above the ground state by Coulomb excitation, with values $3\hbar^2/J \approx 66$ kev. In addition to the Lu^{176} in the ground state, an isomer state with $T_{1/2}$ = 3.7 hours is known. No transition from the isomer state to the ground state has been observed. Lu^{176*} decays to the 0^+ and 2^+ levels of Hf^{176}. Its spin is small (it is assumed to be 1). The energy difference between the ground and excited states of Lu^{176} (based on the energies of the β^- decay) amounts to approximately 170 kev. It is thus seen that the low-lying excited levels of Lu^{176} have been sufficiently well investigated, but the levels corresponding to the transitions we observed did not appear. In addition, compounds obtained by bombardment with fast protons do not display, as a rule, sufficiently large amounts of neutron-excess isotopes.

It is most probable that the transitions belong to Lu^{174}. One of the possible versions of the decay scheme, which would agree with all the measured values of the half-lives, is shown in Fig 3. To reconcile the half-lives of $M\gamma$ 76.5 kev in the measurements with the various sources, it is necessary to assume that when the lutetium fraction is first liberated it contains more Lu^{174*} than Lu^{174}. Then the amount of Lu^{174} in the ground state (γ-line intensity 76.5 kev) will first increase to a maximum (approximately 150 days from the instant of irradiation) and will then decrease. By the time measurements with source 1 were performed (300 to 500 days after irradiation), the apparent half-life of Lu^{174} should have been approximately 210 to 250 days. In the measurements with source 2 (approximately 1000 days after irradiation), the apparent half-life was close to the real one (obviously, 160 to 170 days). Wilkinson and Hicks[12] give a value $T_{1/2}$ = 165 ± 5 days for the half life of Lu^{174}.

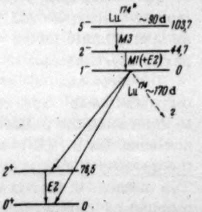

FIG. 3. Proposed decay scheme of Lu^{174*}.

The possible spins of the ground state of ${}_{71}\mathrm{Lu}^{174}_{103}$ can be obtained by considering the neighboring odd nuclei. The neighboring nucleus, ${}_{70}\mathrm{Yb}^{173}_{103}$, has spin and parity $5/2^-$ in the ground state, and $7/2^+$ in the first excited state ($E_\gamma = 351.0$ kev). The spin and parity of ${}_{71}\mathrm{Lu}^{175}_{104}$ are $7/2^+$ in the ground state and $5/2^+$ in the first excited state ($E_\gamma = 343$ kev). Thus, the characteristics of the ground state of Lu^{174} can be either 6^- or 1^-. The characteristics of the excited states are 7^+, 0^+, 5^-, and 0^-. Of the two possible ground-state characteristics, it is apparently 1^- which is realized, since decay to the first rotational level 2^+ of Yb^{174} is observed. A search for a transition from the second excited level of Yb^{174} to the first level produced no results. The intensity of this transition amounts to not more than 2% of the total intensity of the γ transition, 76.5 kev.

If the ground state of Lu^{174} is 1^-, then for the resultant multipolarities M1 and M3 the excited states have characteristics 2^- and 5^-. The Lu^{174*} goes from the isomer state through an intermediate level (2^-) to the ground state. It remains unclear why the M3 transition is so greatly hindered and why there are no transitions to the rotational levels of Yb^{174} with spin 4^+ or 6^+ directly from the isomer state (the M3 transition is hindered by an approximate factor 2×10^7 compared with single-particle estimates).

The first excited level of Lu^{174} (2^-) can be interpreted as the first rotational level. It is possible to determine the moment of inertia of the odd-odd nucleons Lu^{174}. (It is more convenient to deal with the quantity $3\hbar^2/J$.) In this case $3\hbar^2/J = 67.2$ kev. The moment of inertia of Lu^{174} is greater than the moment of inertia of the neighboring nuclei with odd A. The energy of the second rotational level is 112 kev, i.e., the level should lie above that with the level with characteristics 5^- and does not appear in this case.

Recently Dillman et al.[13] indicated that an 84-kev transition was observed in the spectrum of Lu^{174}. This transition is interpreted as one from the first excited state of Hf^{174} to the ground state. They did not notice any conversion lines corresponding to such a transition. If this transition exists, its intensity is considerably greater than that of the 76.5-kev γ transition, namely, $K\gamma$ 76.5 kev : $K\gamma$ 84 kev ≥ 5.

Assuming the scheme shown in Fig. 3 and values of 59.0 and 76.5 kev for the relative intensities of the γ transitions, the intensity of the transitions to the ground and first-excited states of Yb^{174} can be estimated by considering that the majority of transitions are to these levels (several transitions with greater energy were observed in reference 13, but their total intensity is less than the total intensity of the 76.5-kev γ transitions). The number of β^- decays to the levels of Hf^{175}, as indicated earlier,[11] amounts to approximately 20%. Under these conditions, an estimate shows that the number of transitions to the ground state of Yb^{174} is approximately 4 times the number of transitions to the first excited state: log ft ~ 8.4 and ~ 9.0 respectively (at $\Delta E = 1.5$ Mev).

The ratio of the intensity of the K x-rays to the intensity of the 76.5-kev γ transition is found to be approximately 50, which agrees, within the limits of errors, with the results given in reference 13.

The authors express their sincere gratitude to Professor V. M. Kel'man for interest in the work and for valuable remarks made in the discussion of the results.

---

[1] Bobrov, Gromov, Dzhelepov, and Preobrazhenskiĭ, Izv. Akad. Nauk SSSR, Ser. Fiz. **21**, 940 (1957), Columbia Tech. Transl. p. 942.

[2] Dzhelepov, Preobrazhenskiĭ, and Sergienko, ibid. **22**, 795 (1958), transl. p. 789.

[3] Gorodinskiĭ, Murin, Pokrovskiĭ, and Preobrazhenskiĭ, ibid. **22**, 818 (1958), transl. p. 812.

[4] L. A. Sliv and I. M. Band, Таблицы коэффициентов внутренней конверсии γ-излучения, ч. 1, *K*-оболочка, (Tables of Gamma-Ray Internal-Conversion Coefficients), Acad. Sci. Press, 1956-1958.

[5] Bichard, Mihelich, and Harmatz, Bull. Am. Phys. Soc., ser. II, **3**, 358 (1958).

[6] P. R. Gray, Phys. Rev. **101**, 1306 (1956).

[7] Chupp, Du Mond, Gordon, Jopson, and Mark, Phys. Rev. **112**, 518 (1958).

[8] Mihelich, Harmatz, and Handley, Phys. Rev. **108**, 989 (1957).

[9] K. Siegbahn, Beta- and Gamma-Ray Spectroscopy, Amsterdam, 1955.

[10] Strominger, Hollander, and Seaborg, Revs. Modern Phys. **30**, 585 (1958).

[11] N. I. Kaliteevskiĭ and M. P. Chaĭka, Dokl. Akad. Nauk SSSR **126**, 57 (1959), Soviet Phys.-Doklady **4**, 594 (1959); Elbek, Olesen, and Skilbreid, Nucl. Phys. **10**, 294 (1959).

[12] G. Wilkinson, H. G. Hicks, Phys. Rev. **81**, 540 (1951).

[13] Dillman, Henry, Gove, and Becker, Phys. Rev. Lett. **2**, 27 (1959).

Translated by J. G. Adashko
206

SOVIET PHYSICS JETP VOLUME 11, NUMBER 4 OCTOBER, 1960

INVESTIGATION OF THE RELATIVE INTENSITIES OF SOME CONVERSION LINES OF THE SPECTRUM OF NEUTRON-DEFICIENT LUTETIUM ISOTOPES

M. G. IODKO, V. V. TUCHKEVICH, V. A. ROMANOV, and O. M. KRESIN

Leningrad Physico-Technical Institute, Academy of Sciences, U.S.S.R.

Submitted to JETP editor August 7, 1959

J. Exptl. Theoret. Phys. (U.S.S.R.) **38**, 1027-1030 (April, 1960)

A prism spectrometer was employed to investigate a number of the more intense lines in the conversion spectrum of neutron-deficient lutetium isotopes. The relative intensities and energies of the lines were determined, and the multiplicities of the corresponding γ transitions were derived from the relation between the L-subshell intensities.

SOME of the more intense lines in the conversion spectrum of neutron-deficient isotopes of lutetium were investigated. The measurements were made with a prism spectrometer having a transmission ~ 0.1% and an instrument half width ~ 0.1%.[1,2] It must be noted that the widths of the conversion lines were greater than the instrument width, owing to the finite source thickness.

Two sources were used, comprising isotopes of the lutetium fraction separated from a tantalum target bombarded by fast protons (660 Mev). The first source was used to measure the energies and intensities of the 66, 70, and 75.85-kev conversion line in the spectrum of Lu^{171} ($T_{1/2} \sim 8$ days), and of the 78.70- and 90.55-kev lines in the spectrum of Lu^{172} ($T_{1/2} \sim 6.7$ days). The second source was used to determine the relative intensities of the γ 84.19-kev L lines in the spectrum of Lu^{170} ($T_{1/2} \sim 2$ days), of the γ 87.30-kev L lines in the spectrum of Lu^{169} ($T_{1/2} \sim 2$ days), and also the relative intensities of the γ 181.4-kev L lines in the spectrum of Lu^{172} (reference 3). The second source was considerably thicker than the first, and consequently the conversion lines were greatly smeared and hence difficult to separate. The data obtained with this source are consequently merely tentative.

The line energy was measured by the bias method.[4] By using a constant magnetic field in the spectrometer and varying the voltage applied between the source and the case of the spectrometer, it is possible to plot small portions of the spectrum. This method can be used to determine with great accuracy the energy distance between the conversion lines, and by measuring the energy distance between a line of known energy and the investigated line it is possible to determine accurately the energy of the latter. In our case the measurement of the energy of the conversion lines was facilitated by the fact that the lutetium fraction contained Yb^{169}, of which the spectrum has been thoroughly investigated and the energies of the γ transitions measured by the crystal-diffraction method.[5,16]

The reference line employed was $K\gamma$ (109.78 ± 0.02) kev. The binding energy of Tm on the K shell [$E_K = (59.40 \pm 0.01)$ kev] was calculated from the data of reference 6. The binding energies on the L subshells were taken from the tables (see reference 7). The bias method was used to measure directly, in volts, the energy distance from the reference line to the investigated line, and to calculate the energy of the γ transition from the values of the electron binding energies in the atom. The distance between the conversion lines was determined accurate to several volts.

Table I lists the values obtained for the energies of the conversion lines and the calculated transition energies. The energy of the 130.52 ± 0.03 and 93.60 ± 0.03 kev γ transitions in the spectrum of Yb^{169}, calculated in this manner, coincide with the values of the energy obtained with a curved-crystal spectrometer:[5] 130.53 ± 0.03

TABLE I

Line energy, kev	Identification and γ-transition energy, kev
50.38±0.02	$K\gamma$ (109.78±0.02)* in Tm
56.75±0.02	$L_{II}\gamma$ (66.74±0.02) in Yb
66.94±0.03	$L_{III}\gamma$ (75.89±0.03) in Yb
69.79±0.03	$L_{III}\gamma$ (78.74±0.03) in Yb
71.12±0.03	$K\gamma$ (130.52±0.03) in Tm
81.71±0.03	$L_{III}\gamma$ (90.66±0.03) in Yb
83.50±0.03	$L_{I}\gamma$ (93.62±0.03) in Tm

***The energy of this transition is taken from reference 5.**

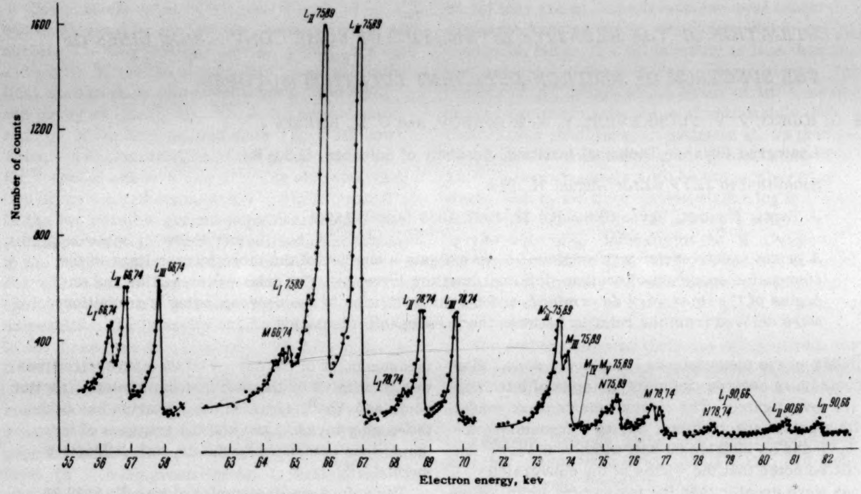

and 93.60 ± 0.04 kev respectively.

The diagram shows the conversion lines of the spectrum of the neutron-deficient isotopes of Lu, obtained with the first source (the instrument spectrum, without correction for Hρ and for decay). The spectrum was plotted by bias, in sections 4 — 6 kev wide, over approximately 12 days.

The ratio of the intensities of the conversion lines for the transitions from the L subshells make it possible to establish the multipolarity of the transitions with a great degree of certainty.

Table II lists the ratios of the intensities of the L-conversion lines of the 66.74- and 75.89-kev transitions in the spectrum of Lu^{171}. Both transitions occur between levels of the main rotational band of Yb^{171}. The spin of the ground state of Yb^{171} is one-half.[8] The sequence of the levels was unambiguously established in reference 9. The 66.74-kev transition is mixed (68% M1 + 32% E2). The Sliv and Band tables[10] were used to calsulate the E2 admixture, both from the L_{II}/L_I ratio and from the L_{III}/L_I ratio, accurate to ±2% (this includes the errors connected with the inaccuracy in the calculated internal-conversion coefficients). The 75.89-kev transition is of the E2 type. The intensity ratio on the L subshells excludes with great certainty all transitions with the exception of E2 and E3. The measured L_I/L_{III} ratio indicates that the transition is of the E2 type. The multipolarity of this transition was determined as E2 in reference 11, and as E3 in references 12 and 13.

The intensity ratio on the M_I, M_{II}, and M_{III} subshells is close to the ratio on the L_I, L_{II}, and L_{III} subshells. For the 66.74-kev γ transition, $M_I:M_{II}:M_{III} = 1:1.29:1.55$, while for the 75.89-kev γ transition $M_I + M_{II}:M_{III}:M_{IV} + M_V = 0.89:1:0.06$. It is interesting to compare the ratio of the intensities of the M lines of the 75.89-kev γ transition with the calculated ratios of the coefficients of internal conversion on the M subshells, given in reference 14. The calculated ratios are $M_I + M_{II}:M_{III}:M_{IV} + M_V = 0.96:1:0.032$ and $1.08:1:0.113$ for the E2 and E3 transitions respectively.

Table III lists the ratio of the intensities of the conversion lines from the L subshells for three transitions in the spectrum of Lu^{178}. The 78.74-

TABLE II

E_γ, kev	$L_I:L_{II}:L_{III}$			$L:M$
	Experiment	Theory, from E2	Theory, from E3	Experiment
66.74	1 : (2.00±0.04) : (2.02±0.02)	1 : 25.5 : 27.9	—	2.8
75.89	(0.050±0.003) : (0.97±0.01) : 1	0.053 : 0.95 : 1	0.018 : 1.04 : 1	3.1

TABLE III

ε_γ, kev	$L_I : L_{II} : L_{III}$		
	Experiment	**Theory, from E2**	**Theory, from M1**
78.74	$(0.09\pm0.02) : (0.97\pm0.04) : 1$	$0.06 : 0.96 : 1$	
90.66	$(0.28\pm0.01) : (1.11\pm0.03) : 1$	$0.09 : 1.01 : 1$	$1 : 0.091 : 0.013$
181.4	$0.52 : 1.27 : 1$	$0.57 : 1.32 : 1$	—

and 181.4-kev transitions are E2, and represent the transitions of the principal rotation band of the even-even nucleus Yb^{172}. The L_I line of the 78.74-kev transition is somewhat too high, owing to the presence of the long-lived Lu^{173} in the source. The 78.74-kev L_I γ line in the spectrum of Lu^{172} coincides with one of the strongest lines in the spectrum of Lu^{173} (L_I γ, 78.6 kev). It is very difficult to separate these lines. The 90.66-kev transition in the spectrum of Lu^{172} is one of the transitions between the upper excited states. From the intensity ratio of the L lines one can calculate the value of the mixture of the different multipolarities (assuming that the mixture is M1 + E2). The transition was found to be 30% M1 + 70% E2. The 84.19-kev transition in the spectrum of Lu^{170} is of type E2 and is a transition from the first excited state to the ground state of the even-even nucleus Yb^{170} (reference 15). The experimental value of the $L_I : L_{II} : L_{III}$ ratio is $0.09 : 0.97 : 1$, against the theoretical $0.07 : 0.98 : 1$. The 87.30-kev transition in the spectrum Lu^{169} has an intensity ratio $L_I : L_{II} : L_{III} = 1 : 0.08 : 0.28$. The calculated admixtures of E2)assuming a M1 +E2 mixture) give 9%and 4% for L_{III}/L_I and L_{II}/L_I respectively. It is obvious that the E2 admixture does not exceed 10%, although the exact value of the mixture cannot be established, for in the region of L lines of this transition there are many lines of other longer-lived isotopes, which are difficult to separate.

---

[1] Kel'man, Kaminskiĭ, and Romanov, Izv. Akad. Nauk SSSR, Ser. Fiz. **18**, 209 (1954).

[2] Kel'man, Metskhvarishvili, Preobrazhenskiĭ, Romanov, and Tuchkevich, JETP **37**, 639 (1959), Soviet Phys. JETP **10**, 456 (1960).

[3] Kel'man, Metskhvarishvili, Preobrazhenskiĭ, Romanov, and Tuchkevich, JETP **35**, 1309 (1958), Soviet Phys. JETP **8**, 914 (1959).

[4] V. A. Romanov, Izv. Akad. Nauk SSSR, Ser. Fiz. **22**, 191 (1958), Columbia Tech. Transl. p. 188.

[5] Hatch, Boehm, Mormier, and Du Mond, Phys. Rev. **104**, 745 (1956).

[6] Chupp, Du Mond, Gordon, Jopson, and Mark, Phys. Rev. **112**, 1183 (1958).

[7] K. Siegbahn, Beta- and Gamma-Ray Spectroscopy, Appendix VI, Amsterdam, 1955.

[8] A. H. Cooke and J. G. Park, Proc. Phys. Soc. **A69**, 282 (1956).

[9] Elbek, Nielsen, and Olesen, Phys. Rev. **108**, 406 (1957).

[10] L. A. Sliv and I. M. Band, Таблицы коэффициентов внутренней конверсии гамма-излучения, ч. 2, *L*-оболочка, (Table of Gamma-Ray Internal-Conversion Coefficients part 2, L Shell) Acad. Sci. Press, 1958.

[11] Bobrov, Gromov, Dzhelepov, and Preobrazhenskiĭ, Izv. Akad. Nauk SSSR, Ser. Fiz. **21**, 940 (1957), Columbia Tech. Transl. p. 942.

[12] J. W. Mihelich and B. Harmatz, Phys. Rev. **106**, 1232 (1957).

[13] Mihelich, Harmatz, and Handley, Phys. Rev. **108**, 989 (1957).

[14] M. E. Rose, Internal Conversion Coefficients, Amsterdam, 1958.

[15] J. W. Mihelich and E. L. Church, Phys. Rev. **85**, 690 (1952).

[16] Chupp, Du Mond, Gordon, Jopson, and Mark, Phys. Rev. **112**, 518 (1958).

Translated by J. G. Adashko
207

SOVIET PHYSICS JETP VOLUME 11, NUMBER 4 OCTOBER, 1960

LARGE COSMIC-RAY INTENSITY FLUCTUATIONS IN THE STRATOSPHERE

A. N. CHARAKHCH'YAN, V. F. TULINOV, and T. N. CHARAKHCH'YAN

P. N. Lebedev Physics Institute, Academy of Sciences U.S.S.R.; Nuclear Physics Institute, Moscow State University

Submitted to JETP editor August 25, 1959

J. Exptl. Theoret. Phys. (U.S.S.R.) 38, 1031-1036 (April, 1960)

The energy spectrum of an abnormally large proton flux, more than 20 times normal, was derived from stratospheric measurements. The exponent of the differential spectrum is equal to 6.0 in the 120 — 170 Mev energy range. It is suggested that these protons are due to corpuscular beams with frozen-in magnetic fields, emitted during the solar chromospheric flare on May 10, 1959.

On May 11, 1959, large fluctuations in the cosmic-ray intensity were registered in the atmosphere, and continued, to a varying extent, until May 15, 1959. On May 12, the cosmic-ray intensity at 64° geomagnetic latitude and at high altitudes was approximately 20 times normal.

The measurements were carried out using a radio probe raised to the atmosphere by balloons.[1] The number of discharges in a single counter, and the number of double coincidences in a telescope consisting of two Geiger-Müller counters, were measured.

EFFECTS OBSERVED AT 64° LATITUDE

The evaluation of the measurements at the Loparskaya station on the morning of May 11 (operation of the apparatus was started at 10:10 a.m.) has shown that the cosmic-ray intensity at high altitudes is much greater than the normal one. The results of the measurements are shown in Fig. 1.

On the same day, at 1:00 p.m., a second balloon was sent up and measured mainly double coincidences. During short time intervals, information on the number of particles detected by single counters was also obtained. Data up to the atmospheric pressure $p = 40\ g/cm^2$ were obtained, and these confirmed the results obtained in the morning.

Two measurements were also carried out on May 12. The first (instrument started at 10:05 a.m.) was done by means of one counter, and the second (instrument started at 3:00 p.m.) by means of a telescope and a single counter. The measured number of discharges in the single counter are shown in the same Fig. 1. As can be seen from the figure, at low pressures ($p < 50\ g/cm^2$), the cosmic-ray intensity remained roughly the same on May 12 as on May 11. However, at higher pressures, the number of detected particles was less than normal.

The decrease in cosmic-ray intensity, also observed at sea level, was related to the strong magnetic storm which began on May 11 at about 11:00 p.m. World Time.

The results of the measurements on May 13 (start 10:00 a.m.) are also shown in Fig. 1. At the time of these measurements, the cosmic-ray intensity was considerably less than on May 11, as a result of which an excessive number of particles was observed only at sufficiently high altitudes. An increase in the number of particles at high altitudes in the stratosphere was also detected on May 14 (start at 3:00 p.m.) and on May 15 (start at 3:02 p.m.). On May 16 and 17 the intensity at high altitudes in the stratosphere was already back to normal.

Thus, the increase in cosmic-ray intensity at high altitudes at 64° latitude detected on May 11 continued, to a greater or lesser extent, for about five days.

RESULTS OF THE MEASUREMENTS AT 51° AND 41° LATITUDE

Simultaneously with the measurements at 64° latitude, measurements were also carried out at latitudes of 51 and 41°, where no increase in the cosmic-ray intensity was observed. It follows from this that the additional primary particles at 64° latitude could not have been photons. On May 12, the number of particles was 12% less than normal at 51° latitude and 8% less than normal at 41° latitude (in the maxima of the intensity curves). The intensity decrease at these latitudes on the

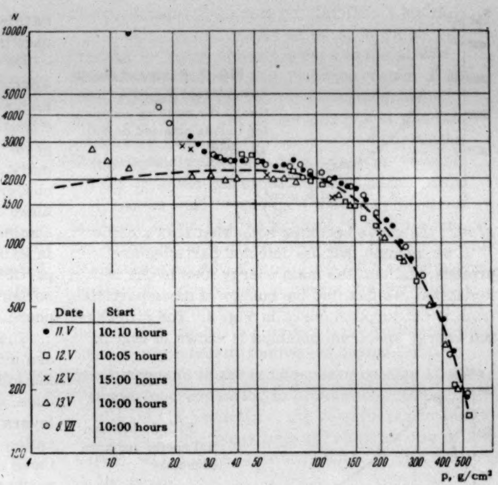

FIG. 1. Variation of the number of pulses per minute N with the atmospheric pressure from data obtained on May 11–13, 1959, and on July 8, 1958 (Moscow time). The dashed line represents a normal intensity, according to the data of May 4, 5, and 7, 1959.

following days was also roughly within the same limits.

NATURE AND SPECTRUM OF PRIMARY PARTICLES

It can be seen from Fig. 1 that an increase in cosmic-ray intensity occurred on May 11 at pressures $p = 100 - 200\ \mathrm{g/cm^2}$. The same result was obtained during the fluctuations observed on July 8, 1958.[2] Therefore, the results obtained at $100 - 200\ \mathrm{g/cm^2}$ cannot be considered accidental.

As can be seen from the results of the measurements on May 11 (Fig. 1) a very sharp rise in the number of particles occurred in the range of low pressures, while the increase was considerably smaller in the range of high pressures. It seems, therefore, that the spectrum of primary particles consists of two different branches, corresponding respectively to low-energy particles absorbed in $10 - 20\ \mathrm{g/cm^2}$ of matter and to particles of relatively high energies, with a range of $100 - 200\ \mathrm{g/cm^2}$. Moreover, it has to be kept in mind that the particle-absorption curve in the atmosphere is related to altitude effects, and not to time variations.

It follows from Fig. 1 that the fluctuations observed on July 8, 1958 and on May 11, 1959 are practically identical. Such a coincidence of the data obtained for two fluctuations which have occurred at different times is astonishing. Similar results can be obtained only if the spectrum of the primary particles remains stable for at least several hours, preferably for ten hours. It can therefore be assumed that the observed variations in the number of particles are related not to time fluctuations but to the altitude effect.

The analysis of the absorption curve at high altitudes obtained from the measurements of the single counter (May 11) shows that the intensities obtained can be explained to the same extent either by assuming a proton nature for the primary particles with energies from 100 to 300 Mev, or by assuming that the detected particles are bremsstrahlung photons produced by electrons in the range 100 — 200 kev. However, the data obtained from the measurements using a telescope with a 7 mm aluminum absorber cannot be attributed to γ rays produced by electrons in the above-mentioned energy range.

The spectrum of the primary particles is best studied from the measurements made on May 12 by means of the telescope. On that day, the radiosonde reached an altitude of 35 km. Low-pressure data and the corresponding differences between the measured and normal intensities, are shown in Fig. 2. (The numbers to the left and to the right of the y axis represent the number of particles per minute and the ratio of the additional intensity to the normal one, respectively.) It can be seen from the figure that the number of particles increases sharply with the altitude. In the range of $15 - 7\ \mathrm{g/cm^2}$, the number of particles increases by a factor of almost 8. At pressures less than 7

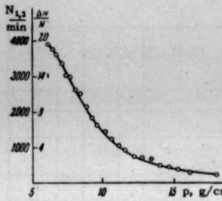

FIG. 2. Number of double coincidences $N_{1,2}$ as a function of the pressure according to data obtained on May 12, 1959.

g/cm², the curve becomes somewhat less steep.

If we assume that the detected particles are protons, and that the main energy loss is due to ionization, we can find the energy of these particles from the absorption curve in Fig. 2. The differential energy spectrum obtained is shown in Fig. 3.

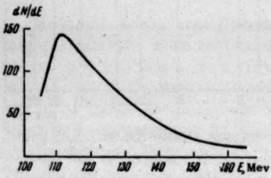

FIG. 3. Differential energy spectrum of protons

In the 120 — 170 Mev range the curve can be approximated by a power function with an exponent equal to 6.0. The spectrum has a maximum at an energy corresponding to the critical energy of primary protons at this latitude (100 — 120 Mev).

Before the present article had been prepared for publication, P. T. Kellog and later J. R. Winckler were kind enough to inform us that on May 12 they detected, by means of emulsions, in the latitude of Minneapolis, a large number of protons with energies in the 110 — 220 Mev range. The proton energy spectrum in the 110 — 220 Mev energy range observed by them had an exponent $\gamma = 4.8$.

Anderson,[3] by means of an ionization chamber and a telescope consisting of Geiger-Müller counters recorded, on August 22, 1958 and at an altitude corresponding to a pressure of 10 g/cm², a ten-fold increase in the cosmic-ray intensity. This, as shown by his analysis, was due to protons having energies of about 170 Mev.

The question whether a cut-off exists in the primary proton spectrum is of great interest. For such a steep spectrum, assuming that it continues in the same manner in the low-energy range, the flux of primary protons at extreme northern latitudes will be exceptionally great. However, data pointing to a cut-off in the proton spectrum can most probably be obtained from measurements carried out by means of artificial satellites during chromospheric flares.

On May 12, measurements with a single counter were carried out at high latitudes, practically simultaneously with the telescope readings. The total intensity of the protons at pressures of 22 and 24 g/cm² was calculated, using the spectrum of primary protons obtained. The cosmic-ray intensity observed by the single-counter measurements at these latitudes was found to be twice the intensity obtained by the above calculation. Consequently, in addition to protons detected by the telescope, particles with a range less than 7 mm Al (absorber in the telescope) are present in the stratosphere.

The origin of these short-range particles, which are most probably electrons, can be explained in the following manner. The primary protons produce, with a certain probability, stars in the upper layers of the atmosphere, and thus produce evaporation neutrons. The absorption mean free path of these neutrons is considerably greater than the range of primary protons, and thus the neutrons reach greater depths. The evaporation neutrons produce hard γ rays in inelastic collisions with the nuclei of the atmospheric atoms. The energy of these γ rays is, however, not high enough to produce electrons that can be detected efficiently with a telescope containing a 7 mm Al absorber.[4] Preliminary estimates show that the above-mentioned difference between the cosmic-ray intensity measured on May 12 with a single counter and the expected intensity under the assumption that the additional particles are protons can only be due to effects produced by evaporation neutrons. From this point of view, it is natural to assume that this increase in the number of particles detected on July 8, 1958 and on May 11, 1959 by means of single counters at 100 — 200 g/cm² is primarily due to the short-range electrons. In such a case, the assumption that the primary proton spectrum has a "kink" is no longer necessary.

DISCUSSION OF RESULTS

It should be noted that the increase in cosmic-ray intensity studied by us had a very long duration, and that its amplitude was practically constant for many hours. These features did not characterize the cosmic-ray fluctuations previously observed on earth, e.g., on February 23, 1956.

The fluctuations in cosmic-ray intensity observed on May 11 — 15 were evidently due to a large chromospheric flare which occurred on May 10, 1959. The Research Institute for Terrestrial Magnetism, Ionosphere, and Radio-Wave Propagation of the U.S.S.R. Academy of Sciences has supplied us with information obtained on chromospheric flares and magnetic storms during May 1959. Some data referring to the observations during the period from May 10 to May 15, 1959 are shown in Fig. 4. The height and base of the top rectangles represent the intensity and duration of the chromospheric flare, respectively. The top rectangles (double shading) refer to the region of heliographic coordinates $\varphi = +15°$ and $l = -50°$; the unshaded rectangles refer to other heliographic coordinates.

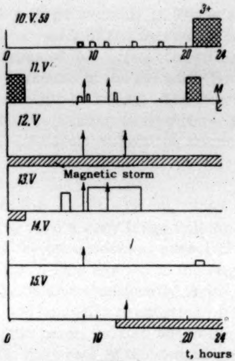

FIG. 4

The lower rectangles (single shading) refer to magnetic storms. The arrows indicate the time of the measurement when an increase in cosmic-ray intensity was observed in the stratosphere at 64° latitude.

As can be seen from Fig. 4, the first data about the increased cosmic-ray intensity were obtained 11 hours after the beginning of the chromospheric flare on the sun on May 10. For the given case, it is impossible to draw any conclusions about the decay of the arrival of cosmic rays relative to the chromospheric flare on the sun. Better data on this subject are available for the flare of July 8, 1958. The increase in cosmic-ray intensity detected on July 8, 1958 was preceded by a chromospheric flare on the sun on July 7, 1958 of intensity 3^+ and duration from 0:58 a.m. to 4:14 a.m. World Time.[5] However, measurements carried out on July 7, 1958 at high altitudes in the stratosphere at 8:30 a.m. World Time did not show an increase in cosmic-ray intensity. Consequently, the delay in the arrival of cosmic rays relative to the chromospheric flare was greater than 4 hours.

Winckler et al.[6] report an event in which an increased intensity of cosmic rays in the stratosphere at 55° latitude was observed on March 26, 1958, about three days after a chromospheric flare on the sun. The authors interpret this fact as showing that particles accelerated during the chromospheric flare are kept either in the solar corona or in the gas clouds ejected from the sun.

It can be seen from Fig. 4 that a very strong magnetic storm has set in about 27 hours after the chromospheric flare (intensity 3^+, heliographic coordinates $\varphi = +15°$ and $l = -50°$) which began on May 10. The letter M in the plot for May 11 shows the beginning of the decrease in cosmic-ray intensity on the earth. As has been explained, the cosmic-ray intensity decreased during the first measurements in the stratosphere on May 12 at altitudes corresponding to pressures > 100 g/cm^2 (while, at the same time, the cosmic-ray intensity remained anomalously high at relatively low pressures), which is in agreement with the observations on the earth.

The decrease in cosmic-ray intensity during very strong magnetic storms can be explained satisfactorily by the influence on the cosmic rays of the frozen-in magnetic fields carried by solar corpuscular streams.[7,8] While the earth is submerged in the corpuscular stream, the frozen-in magnetic fields scatter cosmic particles, which leads to the observed decrease in cosmic-ray intensity.

As can be seen from Fig. 4, two measurements were carried out at high altitudes before the onset of the magnetic storm on May 11, and two measurements were made on May 12 during the magnetic storm. In spite of this, data on the cosmic-ray intensity at high altitudes are practically identical for May 11 and May 12. It seems as if the magnetic storms led to a decrease in the intensity of high-energy cosmic rays, but had no effect on those primary protons having considerably lower energies. In order to resolve the contradiction between these two facts, it is necessary to assume that the solar corpuscular streams carrying the frozen-in magnetic field are themselves sources of fast protons. Due to magnetic fields in the solar corpuscular streams, fast protons are trapped in them, and then fall upon the earth both during and before the time when the earth is submerged in the corpuscular stream. This assumption is strengthened by the great intensity of cosmic-ray flares and their delay relative to the chromospheric flare.

It seems that the study of cosmic-ray flares in the stratosphere offers new experimental possibilities for the study of electromagnetic properties of solar corpuscular streams.

In conclusion, the authors express their thanks to I. K. Marshanov and to Yu. N. Komarov for carrying out the measurements.

---

[1] Vernov, Tulinov, and Charakhch'yan, Dokl. Akad. Nauk SSSR **122**, 788 (1958), Soviet Phys.—Doklady **3**, 980 (1959).

[2] Rymko, Tulinov, and Charakhch'yan, JETP **36**, 1687 (1959), Soviet Phys. JETP **9**, 1202 (1959).

[3] K. A. Anderson, Phys. Rev. Lett. **1**, 335 (1958).

[4] A. N. Charakhch'yan and T. N. Charakhch'yan, JETP **35**, 1088 (1958), Soviet Phys. JETP **8**, 761 (1959).

[5] Солнечные данные 1958 г., Бюллетень №7, (Solar Data for 1958, Bulletin No. 7), Academy of Sciences, U.S.S.R.

[6] Freier, Ney, and Winckler, Journal of Geophysical Research **64**, 685 (1959).

[7] H. Alfvén, Cosmical Electrodynamics (Clarendon Press, Oxford, 1950).

[8] L. I. Dorman, Вариации космических лучей, (Cosmic Ray Variations), Moscow 1957.

Translated by H. Kasha
208

SOVIET PHYSICS JETP VOLUME 11, NUMBER 4 OCTOBER, 1960

ANOMALIES IN THE MODULUS OF ELASTICITY AND IN INTERNAL FRICTION IN THE ALLOY Fe_3Pt

G. I. KATAEV and Z. D. SIROTA

Moscow State University

Submitted to JETP editor August 31, 1959

J. Exptl. Theoret. Phys. (U.S.S.R.) **38**, 1037-1041 (April, 1960)

Results are presented of measurement of the temperature dependence of Young's modulus and of internal friction of a disordered alloy with a composition close to that of Fe_3Pt. A very large anomaly in Young's modulus and a sharp internal friction peak are observed in the vicinity of the ferromagnetic Curie point (71° C). On application of a magnetic field, two types of ΔE effect (of different sign) are produced, due to the domain structure and to a decrease in the dynamic Young's modulus near the Curie point as a result of intradomain spin ordering. The experimental variation of Young's modulus is compared with the corresponding temperature dependence of the modulus, deduced on the basis of magnetic data from relaxation thermodynamic theory.

1. Alloys of the Fe-Pt system, close to Fe_3Pt in composition, have a very large volume magnetostriction by the paraprocess, especially in the disordered state.[1] This has led to the suggestion that there should be an exceptionally large anomaly in the elastic and inelastic properties of such alloys near the Curie point, related not to the ordering of the magnetic moments of the domains when a load is applied, but to the ordering of the spins within the domains.[2] The aim of the present work was to study such anomalies in the alloy Fe_3Pt.

2. The measurements were made on the same 58 wt % Pt, 42 wt % Fe specimen as before,[1] i.e., on a 3 mm diameter rod, 187 mm long, produced by drawing the melt out of an induction furnace in a quartz tube under vacuum. The specimen was homogenized before the measurements by heating at 1020° C, followed by quenching in water to fix the disordered state (the Kurnakov point of this alloy is between 900 and 1000° C).

Young's modulus E and the logarithmic decrement δ, proportional to the internal friction, were measured at frequencies between 1200 and 1300 cps, corresponding to the third flexural mode of vibration of the specimen; we have described previously[3] the apparatus for measuring the relative modulus to 0.004% and the decrement to 1%.

3. The variation of Young's modulus with temperature for the alloy in the disordered state is shown in Fig. 1. An anomalous increase in modulus with temperature is found up to 220° C, but the steepest part of the curve is in the region of the Curie point (71° C).

The anomaly at room temperature is 31.4% of the value of E_0 at that temperature, i.e., of the modulus when the effect of ferromagnetic interaction is discounted (the value of E_0 is derived by extrapolating the linear part of the curve, in the paramagnetic state, down to room temperature). It can be seen that the anomaly, $E_0 - E_1$ tends to increase further below room temperature. So large an anomaly of the elastic modulus, which does not disappear in a saturating field, has not been observed before in ferromagnets, and is comparable in magnitude only with the anomaly in the oxide antiferromagnets NiO and CoO.[4] The "technical" saturation magnetic field reduces the anomaly, but only very little — to 29.7% of E_0; from this it follows that the predominant part of the anomaly is due to the volume magnetostriction by the paraprocess. This is the same phenomenon observed (but less clearly) by Engler[5] in a 42% Ni, 58% Fe alloy and by Belov et al.[2] in elinvar-type alloys. The temperature variation of the logarithmic decrement in the unmagnetized alloy is also shown in Fig. 1. The decrement has a fairly sharp and high peak a few degrees below the Curie point. Similar, but lower and broader peaks were found near the Curie point in elinvar-type alloys.[2]

4. Figure 2 shows the temperature dependence of the ΔE-effect for five magnetic field values between 8.4 and 839 oe. The usual ΔE-effect, due

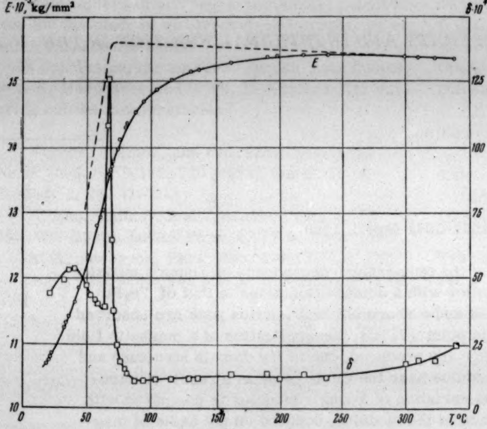

FIG. 1. Temperature dependence of Young's modulus E and logarithmic decrement δ for the disordered alloy 58 wt % Pt, 42 wt % Fe in the unmagnetized state. The dashed curve shows E, calculated from magnetic data.

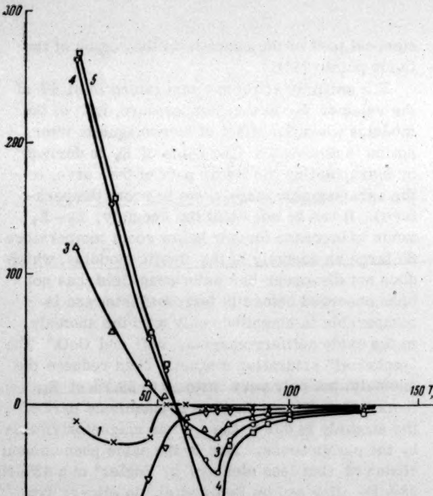

FIG. 2. Temperature dependence of the change in Young's modulus as a function of field, for various magnetic fields: 1 – 8.4, 2 – 84, 3 – 252, 4 – 503, 5 – 839 oe.

to the alteration of the domain structure in a magnetic field is observed at 19–55°C. The normal saturation of the ΔE-effect occurs if fields of 500–800oe, but the ΔE-effect is negative in fields below 100 oe. The latter phenomenon, i.e., the reduction in Young's modulus in weak fields, was observed in alloys, but only at room temperature, by Williams et al.[6] and also by several Japanese workers (see, for example, Yamamoto and Taniguchi[7]), but has not yet been explained.

The non-saturating reduction in the modulus ΔE for all fields in the immediate vicinity of the Curie point (in the paraprocess region) has a relaxation character, as has been shown earlier.[2] Its dependence on the angular frequency of the specimen, ω, is given by the relation:

$$\frac{1}{\Delta E} = \frac{3\beta\rho}{\gamma^2 E_0^2} + \frac{\omega^2\beta^{1/3}\rho}{3\gamma^2 k^2 E_0^2 H^{4/3}} \tag{1}$$

where β is the thermodynamic coefficient in the expansion for the specific thermodynamic potential of the ferromagnet near the Curie point (in powers of the magnetization and the elastic stresses), γ is the magnetostriction constant (in the paraprocess region), k is a kinetic coefficient that determines the rate at which the ferromagnet reaches the equilibrium state of magnetization, and ρ is the density (12.2 g/cm^3). It can be seen from Fig. 3 that at 73° C the experimental points for ΔE, plotted as $(\Delta E)^{-1}$ vs. $H^{-4/3}$, fit a straight line well.

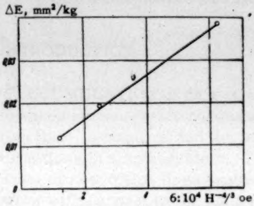

FIG. 3. Dependence of $(\Delta E)^{-1}$ on $H^{-4/3}$ near the Curie point (73°C).

5. The following relations were derived previously[2] from the theory of second-order phase transitions and the thermodynamics of irreversible processes, taking account of relaxation:

$$E = E_0[1 - \Delta_E/(1+\omega^2\tau^2)], \tag{2}$$

$$\delta = \pi\Delta_E\omega\tau/(1+\omega^2\tau^2), \tag{3}$$

$$\tau = 1/k[(H/\sigma) + 2\beta\sigma^2], \tag{4}$$

$$\Delta_E = E_0\gamma^2\sigma^2/\rho[(H/\sigma) + 2\beta\sigma^2], \tag{5}$$

where τ is the relaxation time, Δ_E the degree of relaxation of Young's modulus, and σ the equilibrium magnetization.*

Equations (1) to (5) are derived on the assumption of a one-domain specimen and for $\Delta_E \ll 1$. It is easy to show that to apply these expressions to an alloy with a large anomaly in the modulus it is better to replace Δ_E by

$$\Delta_E' = \Delta_E/(1+\Delta_E).$$

The thermodynamic coefficients α, β, γ, and the equilibrium magnetization σ are calculated from the experimental data of reference 1. Figure 4 shows this temperature dependence (the Curie point, Θ = 71° C, is determined from the condition $\alpha = 0$, cf. reference 8).

In order to calculate the relaxation time τ from Eq. (4) one must know the kinetic coefficient k. This was determined at the temperature of the maximum decrement T_{max} = 66.5° C by two means: a) from the slope of the line in Fig. 3 and Eq. (1), since this slope is almost the same at 73° C as at 66.5° C; b) from the relation

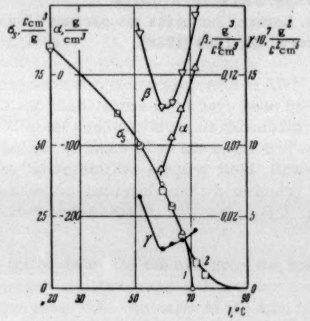

FIG. 4. Temperature dependence of spontaneous magnetization σ_s and thermodynamic coefficients α, β, γ: $1-\sigma_s$ calculated from the thermodynamic coefficients, $2-\sigma_s$ from data on the paraprocess magnetostriction.

$$\Theta - T_{max} = \omega / 2k\alpha_\Theta', \tag{6}$$

which follows from (4) for H = 0 and under the condition for maximum internal friction, $\omega\tau = 1$, taking $\beta\sigma^2 = -\alpha = \alpha_\Theta'(\Theta - T)$ (see Belov[8]); from the plot of δ in Fig. 1 we obtain $\Theta - T_{max} = 4.5°$. The kinetic coefficient derived by both means comes out as 72 cm^3/g-sec.

This value was used to calculate the temperature variation of E near the Curie point, shown by the dashed line in Fig. 1. The calculated curve for E reaches the value $E = E_0$ at the Curie point. Instead of this, the experimental curve shows a relatively steep rise above the Curie point up to 220° C. This may be explained as the existence of a tail of the spontaneous magnetization of the structurally disordered specimen, which spreads out the ferromagnetic transition, and also as the influence of short-range order, which is not considered in the present theory. The decrement in the region of the maximum, calculated from Eq. (3), is one order of magnitude larger, and the maximum is somewhat broader, than that observed, which cannot yet be explained satisfactorily.

---

*Equations (1) and (5) differ from the corresponding expressions of reference 2 in the inclusion of the factor ρ (the density) which was omitted there; because of this, the jump in Young's modulus at the Curie point, as calculated in that paper (dotted curve in Fig. 1a), should be reduced by a factor equal to ρ (about 8).

In conclusion it is a pleasure to express our thanks to Professor K. P. Belov for his interest in the present work.

---

[1] K. P. Belov and Z. D. Sirota, JETP **36**, 1058 (1959), Soviet Phys. JETP **9**, 752 (1959).

[2] Belov, Kataev, and Levitin, JETP **37**, 938 (1959), Soviet Phys. JETP **10**, 670 (1960).

[3] G. I. Kataev, Заводская лаборатория (Plant Laboratory) **24**, 1258 (1958).

[4] R. Street and B. Lewis, Nature **168**, 1036 (1951).

[5] O. Engler, Ann. Physik **31**, 145 (1938).

[6] Williams, Bozorth, and Christensen, Phys. Rev. **59**, 1005 (1941).

[7] M. Yamamoto and S. Taniguchi, Sci. Repts. Research Inst. Tôhoku Univ. **A7**, 34 (1955).

[8] K. P. Belov, Usp. Fiz. Nauk **65**, 207 (1958).

Translated by R. Berman
209

SOVIET PHYSICS JETP VOLUME 11, NUMBER 4 OCTOBER, 1960

INVESTIGATION OF THE LINE WIDTH AND SHAPE IN THE PARAMAGNETIC RESONANCE SPECTRUM OF THE Cr^{+++} ION IN CORUNDUM SINGLE CRYSTALS

A. A. MANENKOV and V. B. FEDOROV

P. N. Lebedev Physics Institute, Academy of Sciences, U.S.S.R.

Submitted to JETP editor September 15, 1959

J. Exptl. Theoret. Phys. (U.S.S.R.) 38, 1042-1046 (April, 1960)

The broadening of the fine-structure lines in the paramagnetic resonance spectrum of Cr^{+++} in single crystals of Al_2O_3 has been studied. The width and shape of the lines have been investigated for different electronic transitions and for different concentrations of chromium. The experimental results can be qualitatively interpreted on the basis of an assumption of a broadening mechanism and of a local inhomogeneity in the crystalline electric field. However, quantitative comparison of the experimental data with the theory of dipole broadening of paramagnetic resonance lines does not yield satisfactory agreement.

INTRODUCTION

ACCUMULATION of data on the broadening of electron paramagnetic resonance (e.p.r.) absorption lines is required for the study of internal interactions in a spin-system. The shape and the width of absorption lines enable us to draw conclusions with respect to the nature and the magnitude of these interactions.

In the present work we have studied the width and the shape of e.p.r. absorption lines of a Cr^{+++} ion in the corundum (Al_2O_3) lattice at room temperature. The samples were in the form of single crystals of $Al_2O_3 \cdot Cr_2O_3$ with chromium content from 10^{-5} to 10^{-2} (the concentration was determined as the ratio of the number of paramagnetic chromium ions, which had isomorphically replaced the diamagnetic aluminum ions, to the number of aluminum ions). The broadening of the lines of the "parallel" spectrum was studied (the trigonal symmetry axis of the crystal was parallel to the constant applied magnetic field). This spectrum is described by the spin Hamiltonian

$$\hat{\mathcal{H}} = -\sum_i D_i \hat{S}_{zi}^2 + g_\parallel \beta H \sum_i \hat{S}_{zi} + \sum_{i,k} \hat{W}_{ik}, \tag{1}$$

where the summation indices i and k denote the paramagnetic chromium ions; H is a constant magnetic field; $\hat{S}_{zi}$ is the operator for the component of the spin of the i-th chromium ion in the direction of the constant magnetic field; $2D_i$ is the splitting of the energy levels in the crystalline electric field for the i-th chromium ion; $g_\parallel$ is the spectroscopic splitting factor for the "parallel" orientation of the sample; β is the Bohr magneton; $\hat{W}_{ik}$ is the operator for the energy of the spin-spin interaction between the i-th and the k-th chromium ions. The constants of the spin Hamiltonian have been measured in references 1.

The investigations were made at a frequency of $\nu = 9375$ Mcs. The "parallel" e.p.r. spectrum of the ion consists of three lines corresponding to the transitions

$$M_1 = {}^3/_2 \rightarrow {}^1/_2, \qquad M_2 = -{}^1/_2 \rightarrow {}^1/_2, \qquad M_3 = {}^1/_2 \rightarrow {}^3/_2,$$

observed respectively for the following values of the constant magnetic field:

$$H_1 = (2D_i - h\nu)/g_\parallel\beta, \qquad H_2 = h\nu/g_\parallel\beta,$$
$$H_3 = (2D_i + h\nu)/g_\parallel\beta. \tag{2}$$

Here M_i are the magnetic quantum numbers corresponding to the operator $\hat{S}_z$; $\hbar$ is Planck's constant.

EXPERIMENTAL RESULTS AND QUALITATIVE DISCUSSION

Our experiments show that the width of the e.p.r. absorption lines of the Cr^{+++} ion in corundum does not vary on cooling the samples from 300° to 77°K. Therefore, the spin-lattice interaction does not affect the line width.

We have also found that the anisotropic broadening of absorption lines is negligibly small for all samples, owing to the imperfections in the single crystals investigated. This conclusion follows from the experimental fact that the lines corresponding to the ${}^1/_2 \rightarrow {}^3/_2$ and ${}^3/_2 \rightarrow {}^1/_2$ transitions have the same width. Had anisotropic broadening taken place, the ${}^1/_2 \rightarrow {}^3/_2$ line would be considerably broader than the $^3/_2 \rightarrow {}^1/_2$ line, for if the crystal symmetry axis deviates from the parallel orientation by as little as 1° or 2° the shift of the resonance frequency of the $^1/_2 \rightarrow {}^3/_2$ transition is comparable with the line width, while it is negligibly small for the $^3/_2 \rightarrow {}^1/_2$ transition.

Thus, the broadening of the spectrum lines is apparently due only to the magnetic dipole interactions between the spins (cf. later with respect to the effect of the exchange interactions).

We have measured the concentration dependence of the width, the peak intensity, and the shape of the lines for different electronic transitions. The concentration dependence of the width and the peak intensity is shown for different transitions in Figs. 1 and 2. The width and the shape of the line are the same for the $^3/_2 \rightarrow {}^1/_2$ and the $^1/_2 \rightarrow {}^3/_2$ transitions, so that in all subsequent discussions the data are given for only one of these two transitions. The measurements were carried out by comparing different samples under identical experimental conditions, so that the relative accuracy of the results is sufficiently high. A comparison of the line shapes for different transitions among themselves and also with the Gaussian

$$G(x) = (\sigma\sqrt{2\pi})^{-1}\exp(-x^2/2\sigma^2)$$

and the Lorentz

$$L(x) = a/\pi(x^2 + a^2)$$

curves was made by using the values of the ratios $I\Delta/S$ and Δ/Δ' which have the characteristic values:

$I\Delta/S = 0.936$, $\Delta/\Delta' = 1.175$ for the Gaussian curve,
$I\Delta/S = 0{,}637$, $\Delta/\Delta' = 1.734$ for the Lorentz curve.

Here I is the peak line intensity, Δ the line width at the I/2 level, Δ' the line width taken between points of maximum slope, and S the area of the absorption line.

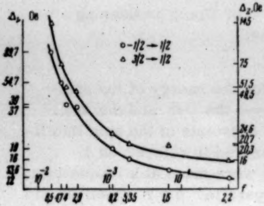

FIG. 1. Dependence of the width of e.p.r. absorption lines of the Cr+++ ion in corundum on chromium concentration for two electron transitions in the "parallel" spectrum.

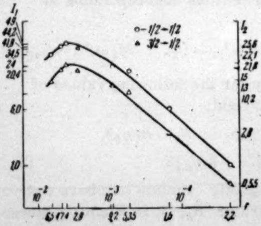

FIG. 2. Dependence of the peak intensity of of e.p.r. absorption lines of the Cr+++ ion in corundum on chromium concentration for two electron transitions in the "parallel" spectrum (the peak intensity is expressed in relative units).

The results of the measurements are given in the table. The table also gives the values of the concentration of chromium in the samples investigated determined from the area of the absorption line. The index 1 denotes quantities which refer to the transition $-^1/_2 \rightarrow {}^1/_2$, the index 2 denotes the transition $^3/_2 \rightarrow {}^1/_2$. From the experimental data exhibited it can be seen that a) the line corresponding to the $^3/_2 \rightarrow {}^1/_2$ electronic transition is broader than the line corresponding to the $-^1/_2 \rightarrow {}^1/_2$ transition; b) at low concentrations ($\sim 10^{-5}$) the line widths for both transitions tend to constant values; c) the peak intensity for both lines has an absolute maximum within the given range of concentrations; d) the ratios of the widths and the ratios of the peak intensities for lines corresponding to two transitions are approximately constant and begin to increase at the highest of the concentrations investigated; e) the line shape for both transitions at high dilutions is approximately Gaussian and varies little with concentration, changing towards the Lorentz curve only at the maximum concentrations studied; f) the line shapes for the two transitions differ insignificantly (there is a small difference always in the direction of greater similarity to the Lorentz curve for the line shape of the $^3/_2 \rightarrow {}^1/_2$ transition compared with the line corresponding to the $-^1/_2 \rightarrow {}^1/_2$ transition); g) the chromium concentrations in the corundum, determined from the areas of the absorption lines agree with the results of optical measurements.

We have not succeeded in explaining the observed large difference in the line widths for the two transitions by means of the single mechanism of dipole interactions. As shown by theoretical calculations (cf. below), $\sigma_1 > \sigma_2$ (σ_2 is the second moment of the absorption curve). But from the experimental data it can be seen that the line shapes are approximately the same for both transitions. Therefore, the contribution to the line width from the dipole spin-spin interactions is greater for the $-^1/_2 \rightarrow {}^1/_2$ transition, while experimentally it gives a narrower absorption line. The greater line width for the $^3/_2 \rightarrow {}^1/_2$ transition can be qualitatively explained by the spatial inhomoge-

Cr concentration in Al_2O_3 (from line areas)	I_1/I_2	Δ_2/Δ_1	$I_1\Delta_1/S_1$	$I_2\Delta_2/S_2$	Δ_1/Δ_1'	Δ_2/Δ_2'
$2.2\cdot10^{-5}$	1.85	1.32	0.89	0.87	0.91	0.89
$1.5\cdot10^{-4}$	2.13	1.50	0.89	0.85	1.0	1.22
$5.35\cdot10^{-4}$	2.0	1.30	1.0	0.86	1.06	1.18
$9.2\cdot10^{-4}$	1.84	1.30	0.815	0.77	1.12	1.21
$2.9\cdot10^{-3}$	1.93	1.30	0.88	0.80	1.11	1.27
$4\cdot10^{-3}$	1.91	1.32	0.79	0.74	1.19	1.23
$4,7\cdot10^{-3}$	2.0	1.37	0.85	0.79	1.16	1.31
unknown	2.14	1.43	0.86	0.78	—	—
$6.5\cdot10^{-3}$	2.30	1.65	0.81	0.71	1.17	1.46

neity of the electric crystalline field. This inhomogeneity is associated with local distortions of the crystal lattice, which lead to different initial splitting of the spin levels for the Cr^{+++} ions situated at different points of the sample. This effect appears in the spin Hamiltonian as a fluctuation of the constant D and, in accordance with (2), contributes only to the line widths of the $3/2 \rightarrow 1/2$ transition.

Local distortions of the crystalline field can arise for two reasons. Firstly, the isomorphic introduction of chromium into the corundum lattice distorts the lattice somewhat. Secondly, distortions are due to the large mechanical stresses in the corundum crystals containing chromium (single crystals of chromium-containing corundum are grown from a melt at high temperatures). The fact that the ratio of the widths Δ_2/Δ_1 does not vary at first with increasing chromium concentration shows that at low concentrations the introduction of chromium does not add anything to the stresses that are present in the pure Al_2O_3 lattice. An increase in the ratio Δ_2/Δ_1 in samples with higher concentrations shows that the introduction of a large quantity of chromium into the corundum lattice introduces additional local distortions of the crystalline field compared with the pure corundum lattice.

The existence of a residual line width for the $-1/2 \rightarrow 1/2$ transitions at high magnetic dilutions can be explained by magnetic dipole interactions of the Cr^{+++} ions with the Al^{27} nuclei.

Let us consider the dependence of the peak intensity of the lines for the two transitions on the concentration of the solid solution $Al_2O_3\cdot Cr_2O_3$. The maximum in the peak intensity of the line for the $-1/2 \rightarrow 1/2$ transition observed experimentally in the range of concentrations investigated can be explained in the following manner. For high chromium concentrations (~ 1%) not all the chromium ions are properly situated in the lattice. Some are situated in an entirely different crystalline field. These ions give no contribution to the intensity of the absorption line, but broaden the lines by interacting with the ions which are responsible for the resonance absorption corresponding to the transition being observed. The decrease in I_2 with increasing concentration is relatively more rapid than the decrease in I_1, since the width Δ_2 increases more rapidly than Δ_1, also because of the increase in the inhomogeneity of the crystalline field.

COMPARISON OF EXPERIMENTAL DATA WITH THE THEORY OF DIPOLE BROADENING

We have compared the experimental line width for the $-1/2 \rightarrow 1/2$ transition, for which the dipole contribution must be the principal one, with the theoretical value obtained by using the calculated dipole broadening of the second moment of the absorption curve.

The formulas for the second moment of the absorption curves have been given by Pryce and Stevens[2] for the case when the ion spectrum consists of several lines, while Kittel and Abrahams[3] have taken into account the effect of the concentration of the paramagnetic ions in the solid solution on the dipole broadening. In our case the formula for the second moment has the form

$$\overline{\langle\Delta\nu^2\rangle} = X/N\,(2S+1),$$

$$\begin{aligned} X = \sum_{i,k} [&|\langle 1,1|\hat{W}_{ik}|1,1\rangle - \langle 2,1|\hat{W}_{ik}|2,1\rangle \\ &- \langle 2,1|\hat{W}_{ik}|1,2\rangle|^2 + |\langle 1,2|\hat{W}_{ik}|1,2\rangle - \langle 2,2|\hat{W}_{ik}|2,2\rangle \\ &+ \langle 2,1|\hat{W}_{ik}|1,2\rangle|^2 + |\langle 1,3|\hat{W}_{ik}|1,3\rangle \\ &- \langle 2,3|\hat{W}_{ik}|2,3\rangle|^2 + |\langle 1,3|\hat{W}_{ik}|3,1\rangle - \langle 2,3|\hat{W}_{ik}|3,2)|^2 \\ &+ |\langle 1,4|\hat{W}_{ik}|1,4\rangle - \langle 2,4|\hat{W}_{ik}|2,4\rangle|^2 \\ &+ |\langle 1,4|\hat{W}_{ik}|4,1\rangle - \langle 2,4|\hat{W}_{ik}|4,2\rangle|^2], \end{aligned} \qquad (3)$$

with $\nu_{12} \neq \nu_{23} \neq \nu_{34}$ (the superior bar denotes an average). Here N is the number of paramagnetic ions, the spin is $S = 3/2$, the indices $j = 1, 2, 3, 4$ denote the energy levels of the paramagnetic ion, and ν_{12} is the frequency of the transition for which the second moment of the absorption curve is calculated. In our case this is the $-1/2 \rightarrow 1/2$ transition.

On substituting for $\hat{W}_{ik}$ the Hamiltonian for the dipole interaction between the spins

$$\hat{W}_{ik} = g^2 \beta^2 r_{ik}^{-3} [\hat{S}_i\hat{S}_k - 3r_{ik}^{-2} (\hat{S}_i\hat{r}_{ik})(\hat{S}_k\hat{r}_{ik})]$$

and on evaluating the matrix elements in formula (3), we obtain for the line corresponding to the $-1/2 \rightarrow 1/2$ transition

$$h^2 \overline{\langle \Delta\nu^2 \rangle} = f \sum_k \tfrac{81}{8} \varkappa_{ik}^2, \quad \varkappa_{ik} = g_\parallel^2 \beta^2 r_{ik}^{-3} \left[\tfrac{3}{2} \gamma_{ik}^2 - \tfrac{1}{2}\right]; \qquad (4)$$

f is the concentration of the chromium in the corundum, and γ_{ik} is the cosine of the angle between the radius-vector $\mathbf{r}_{ik}$ and the z symmetry axis. We note that for the $3/2 \rightarrow 1/2$ transition

$$h^2 \overline{\langle \Delta\nu^2 \rangle} = f \sum_k \tfrac{69}{8} \varkappa_{ik}^2,$$

which is smaller than the second moment of the absorption curve for the $-1/2 \rightarrow 1/2$ transition (we have made use of this fact in the preceding section). On evaluating the lattice sums we obtain, for $M = -1/2 \rightarrow 1/2$, $\sigma_1 = 3960\sqrt{f}$ oe. For $f = 5 \times 10^{-3}$ we have $\sigma_1 = 280$ oe, while for $f = 2 \times 10^{-5}$ we have $\sigma_1 = 18$ oe. If we take into account the fact that for the Gaussian curve $\Delta/\sigma = 2.35$, for the Lorentz curve cut off at $x = 10a$ the ratio is $\Delta/\sigma = 0.86$, while the observed line shape is intermediate between the Gaussian and the Lorentz curves (being closer to the Gaussian curve), then the calculated line widths exceed the experimental ones by a factor of several fold for all the investigated concentrations.

We have also evaluated the contribution made to the line width by the interaction of the chromium ions with the aluminum nuclei. This contribution turns out to be ~ 4.5 oe (for $\Delta = 2.35\,\sigma$), which is less than the minimum observed width of 12 oe in a sample with $f = 2 \times 10^{-5}$.

CONCLUSION

Thus, analysis of the experimental data on the broadening of absorption lines in the "parallel" e.p.r. spectrum in chromium-containing corundum shows that we can qualitatively explain the experimental data on the basis of the dipole interaction mechanism and of the assumption of local inhomogeneity of the crystalline electric field. However, we have not succeeded in obtaining quantitative agreement between the experimental widths of the transitions with those calculated theoretically by evaluating the second moment of the absorption curve. The experimentally observed values of the line width are smaller by a factor of several fold than those calculated theoretically on the basis of the dipole mechanism. This suggests that the difference might be due to exchange interactions. However, exchange interactions in such highly magnetically-dilute samples of chromium-containing corundum as we have investigated could hardly have any appreciable effect on the absorption line widths.

The authors express their gratitude to A. S. Bebchuk, R. P. Bashuk, and L. M. Kharitonova for providing the samples of chromium-containing corundum and for optical measurements of chromium concentrations.

---

[1] A. A. Manenkov and A. M. Prokhorov, JETP **28**, 762 (1955), Soviet Phys. JETP **1**, 611 (1955). A. A. Manenkov, Thesis, Physics Institute, Academy of Sciences, U.S.S.R., 1955.

[2] M. H. L. Pryce and K. W. H. Stevens, Proc. Phys. Soc. **A63**, 36 (1950).

[3] C. Kittel and E. Abrahams, Phys. Rev. **90**, 238 (1953).

Translated by G. Volkoff
210

SOVIET PHYSICS JETP VOLUME 11, NUMBER 4 OCTOBER, 1960

*INTERNAL CONVERSION PAIRS IN THE DECAY OF NEUTRAL π MESONS**

Yu. A. BUDAGOV, S. WIKTOR, V. P. DZHELEPOV, P. F. ERMOLOV, and V. I. MOSKALEV

Joint Institute for Nuclear Research

Submitted to JETP editor September 18, 1959

J. Exptl. Theoret. Phys. (U.S.S.R.) 38, 1047-1052 (April, 1960)

Twenty seven charge-exchange scattering events with subsequent decay $\pi^0 \rightarrow e^- + e^+ + \gamma$ were recorded in a hydrogen-filled diffusion cloud chamber located in a magnetic field and operating in 128-Mev and 162-Mev negative pion beams. The probability for this decay relative to that for the usual decay is found to be 0.0117 ± 0.0015. Results of measurements of the momenta and angles of the electron-positron pairs are presented. The experimental energy characteristics of the pairs and angular distributions are in satisfactory agreement with theory.

INTRODUCTION

THE decay of a neutral pion into an electron-positron pair and a photon

$$\pi^0 \rightarrow e^- + e^+ + \gamma \tag{1}$$

was first discussed theoretically by Dalitz.[1] This alternate decay mode may be interpreted as internal conversion of one of the photons in the field of the other. Dalitz, and later Kroll and Wada,[2] used quantum electrodynamics to calculate the internal conversion coefficient and the principal energy and angle characteristics of such decays. The results of these calculations depend only weakly on the form of the meson theory. Kerimov et al.[3] recently calculated the probability for the decay (1) taking into account the spin states (longitudinal polarization) of the electron-positron pair and the photon. Experimentally this decay was studied by a number of authors,[4-7] but with comparatively low accuracy. It was therefore considered important to study the reaction (1) further with the purpose of obtaining more accurate results.

We report here on data based on the study of 27 events representing the $\pi^0 \rightarrow e^- + e^+ + \gamma$ decay, found in a diffusion cloud chamber operating in 128-Mev and 162-Mev negative pion beams. The results of a preliminary analysis of 14 such decays were reported by us previously.[8]

The chamber was filled with hydrogen at a pressure of 25 atmos and placed in a constant magnetic field of 9000 gauss. The experimental setup, the operating conditions in the negative pion beams, and the method of analysis have already been described in more detail previously.[9,10] The neutral pions were obtained by charge-exchange scattering. The indicated 27 cases of the decay (1) were found after scanning twice approximately 90,000 stereo photographs and were identified by π^- meson tracks ending in the gas inside the chamber and accompanied by the emission of an electron-positron pair. Photographs of two such cases are shown in Fig. 1. It should be noted that all the pairs found were assumed to be due to internal conversion, since as a result of the low stopping power of gaseous hydrogen the probability for the appearance of one pair in the present experiment, produced by a photon from the $\pi^0 \rightarrow 2\gamma$ decay, at a distance less than 1 mm from the decay point (external conversion) amounts to 7×10^{-5}.

DETERMINATION OF THE INTERNAL CONVERSION COEFFICIENT

The relative probability for the decay mode (1) for a neutral pion is given by the expression

$$2\rho_0 = \frac{w(\pi_0 \rightarrow e^- + e^+ + \gamma)}{w(\pi^0 \rightarrow 2\gamma)} = \frac{2\alpha}{3\pi}\left[\ln\left(\frac{m_{\pi^0}^2}{m_e^2}\right) - \frac{7}{2}\right] = 0.0118, \tag{2}$$

where α is the fine structure constant. The results of experimental determinations of the coefficient $2\rho_0$ are collected in Table I. The data on $2\rho_0$ of Daniel et al.[4] and Anand[5] were obtained by scanning nuclear emulsions exposed to cosmic rays, where the number of neutral pions produced in a star could not be determined with sufficient accuracy. The value for $2\rho_0$ found by Lindenfeld et al.[6] using counters is also of comparatively low accuracy. Sargent et al.[7] obtained the internal

---

*Reported at the VI session of the Scientific Council of the Joint Institute for Nuclear Research (May 1959) and at the Kiev Conference on High-Energy Physics (July 1959).

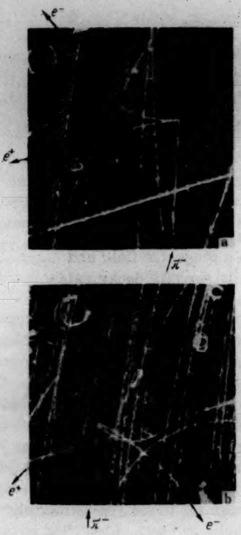

FIG. 1. Photographs of $\pi^- + p \rightarrow \pi^0 + n$ followed by the decay $\pi^0 \rightarrow e^- + e^+ + \gamma$ obtained with a hydrogen diffusion chamber: a – pair No. 3, b – pair No. 6.

TABLE I

$2\rho_0$	Author
0.020 ± 0.006	Daniel et al.[4]
$0{,}013 \pm 0.004$	Anand[5]
$0.0145 \pm^{0.0080}_{0.0045}$	Lindenfeld et al.[6]
0.0106 ± 0.0017	Sargent et al[7]
$0{,}0117 \pm 0.0015$	This work

conversion coefficient by working with slow π^- mesons, which stopped in a hydrogen diffusion chamber. The main difficulty in determining $2\rho_0$ by this method lies in the identification of the pairs due to the π^0 decay and the internal conversion pairs from the reaction $\pi^- + p \rightarrow n + \gamma$. Furthermore, the quantity $2\rho_0$ was found in that work under the assumption that the Panofsky ratio P is 0.94. If one takes for P the value 1.5 – 1.8, as determined more recently,[11] then the value of the coefficient $2\rho_0$, calculated from the data of Sargent et al., will be in disagreement with its theoretical value and other experimental data.

The method for determining the internal conversion coefficient adopted in this work makes use of fast negative pions, when the number of pairs due to internal conversion of photons from the reaction $\pi^- + p \rightarrow n + \gamma$ amounts to only 1% of the number of $\pi^0 \rightarrow e^- + e^+ + \gamma$ decays. Therefore the contribution from such pairs may be neglected in the computation of the coefficient $2\rho_0$. In addition the number of π^0 mesons decaying in the usual way (into two photons) can be accurately determined from the number of elastic scattering events and the known ratio of elastic and charge-exchange scattering cross sections. The direct determination of the number of charge-exchange events is extremely difficult in a diffusion chamber due to local insensitive regions and edge effects.

The coefficient $2\rho_0$ is determined from the formula

$$2\rho_0 = \frac{N_{\text{pair}}}{N_{\text{el}}} \frac{\sigma_{\text{el}}}{\sigma_{\text{total}} - \sigma_{\text{el}}} \frac{\eta_{\text{el}}}{\eta_{\text{pair}}}, \tag{3}$$

where N_{pair} and N_{el} are the number of decay and elastic scattering events respectively; σ_{total} is the total cross section for the $\pi^- p$ interaction; σ_{el} is the total elastic $\pi^- p$ scattering cross section; η_{pair} and η_{el} are the efficiencies for the observation of events corresponding to the decay (1) and to elastic scattering.

The same selection criteria were applied to the pairs from π^0 decays as were used for elastic $\pi^- p$ scattering.[10] These criteria were satisfied by 26 pairs and 1285 elastic scattering events. A correction was made in the number of elastic scattering events connected with Coulomb scattering and the interference between Coulomb and nuclear scattering. For σ_{total} and σ_{el} entering into Eq. (3) we took the average values of total $\pi^- p$-interaction cross sections[12] and total elastic cross sections,[10] weighted by the number of elastic scattering events at 128 Mev and 162 Mev.

The detection efficiency for elastic $\pi^- p$ scattering events was determined from missed events, whose tracks lie in a plane close to the vertical, and was found to be 90%; the pair detection efficiency was assumed to be the same. The relative probability for the decay (1), as calculated from Eq. (3) with the above remarks taken into account, was found to be $2\rho_0 = 0.0117 \pm 0.0015$, and the internal conversion coefficient for photons from the π^0 decay was found to be $\rho_0 = 0.0058 \pm 0.0008$, where the indicated errors are statistical probable errors. This value for $2\rho_0$ is in good agreement with the theoretical value (2).

ANGLE AND ENERGY CHARACTERISTICS OF THE PAIRS

Table II shows the results of the analysis of the 27 electron-positron pairs found in this work. The total energy of the electron, the positron, and the pair are listed in the first three columns of the table. In the following columns are listed the cor-

VOL II 4

TABLE II

Pair No.	E^-, Mev	E^+, Mev	$E=E^-+E^+$, Mev	α, degrees (l.s.)	θ, degrees (l.s.)	θ*, degrees (c.m.s.)
1	—	—	—	2.5	118	128
2	>192	46	>238	16	50	60
3	19	41	60	36	95	107
4	148	>74	>222	7	91	103
5	20	111	131	8	145	151
6	27	6	33	22	117	127
7	89	67	156	6	50	60
8	>14	>96	>110	5	100	111.5
9	—	—	—	2	110	121
10	75	105	180	53	140	147
11	39	>152	>191	3	99	111
12	10	24	34	38	86	98
13	166	20	186	28	65	75
14	22	27	49	46	118.5	128.5
15	33	40	73	25	76	88
16	25	>51	>76	20	101	112.5
17	7.3	52	59.3	5	119	129
18	23	>122	>145	2	89	101
19	79	27	106	29	44	53
20	42	14	56	17.5	97	108
21	—	32	>32	25	90	102
22	16	187	203	13	92	104
23	45	47	92	32.5	62	73
24	>67	79	>146	5	91	103
25	21	65	86	74	93	105
26	39	29	68	10.5	54	64
27	63	41	104	8	141	148

relation angles α (i.e., the angle between the positron and the electron) in the laboratory frame, and also the angle θ between the direction of the total momentum of the pair and the direction of motion of the π^- meson in the laboratory system (l.s.) and the corresponding angle θ* in the center-of-mass system (c.m.s.). Momenta (energies) were measured with an accuracy of ~10%, whereas angles were measured with an accuracy of 1°. In the case of very short tracks only lower limits for the corresponding energies are listed in the table. Events 1 and 9 were found in emulsions exposed without the magnetic field.

It is interesting to compare these experimental data with the results of the calculations by Dalitz and by Kroll and Wada.

1. The experimental distribution of pairs n (α) in correlation angles α is shown in Fig. 2. The solid line in Fig. 2 represents the theoretical form for this distribution as obtained by Dalitz (private communication) in the rest system of the π^0. For angles $\alpha > 2°$ this distribution is of the form $n(\alpha)\,d\alpha \sim d\alpha/\alpha$. If the velocity of the π^0 meson is taken into account the distribution is shifted only insignificantly in the direction of smaller angles and it therefore follows from Fig. 2 that the experimental distribution is not in contradiction with theory.

In the rest frame of the neutral pion, half of the pairs should be emitted with a correlation angle less than $\alpha_{1/2} = 18.1°$ (according to Dalitz). In this work we found for $\alpha_{1/2}$ the value 16°.

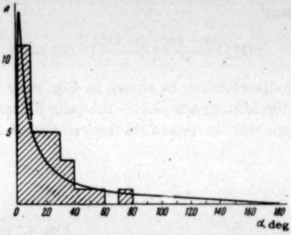

FIG. 2. The distribution of pairs from the decay $\pi^0 \to e^- + e^+ + \gamma$ in correlation angle α (l.s.). The solid curve refers to the theoretical distribution in the π^0 rest frame as obtained by Dalitz (private communication)

2. The distribution of the pairs in the parameter

$$y = |p_{e^-} - p_{e^+}| / |\mathbf{p}_{e^-} + \mathbf{p}_{e^+}|, \tag{4}$$

where $\mathbf{p}_{e^-}$ and $\mathbf{p}_{e^+}$ are the momenta of the electron and positron in the laboratory frame, is shown in Fig. 3 in the form of a histogram. This parameter characterizes the division of energy between the particles of a pair. The smooth curve represents the theoretical distribution in the parameter y in the rest frame of the neutral pion, as obtained by Kroll and Wada. The parameter y depends only weakly on the velocity of the π^0 meson. It is seen from the figure that the distribution of pairs in the parameter y is in agreement with theory and there is no tendency for the particles in a pair to share the energy equally, as suggested by the results of Sargent et al.[7] and particularly strongly by the results of Anand.[5]

3. An important theoretical characteristic of

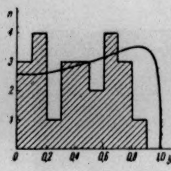

FIG. 3. The distribution of pairs in the parameter y. The solid curve refers to the theoretical distribution.[2]

the pairs from the decay (1) is their distribution in the parameter

$$x = (E^- + E^+)^2 - (\mathbf{p}_{e^-} + \mathbf{p}_{e^+})^2, \qquad (5)$$

where E^-, E^+, $\mathbf{p}_{e^-}$, and $\mathbf{p}_{e^+}$ are the total energies and momenta of the electrons and positrons. The parameter x is an invariant and can be interpreted as the degree to which the intermediate photon, which converts into the pair, is virtual, or as the square of the "rest mass" of the virtual photon. On the assumption that the linear dimensions of the currents responsible for the electromagnetic radiation in the decay of the π^0 are small compared to $2\hbar/m_\pi c$, the following distribution was obtained by Dalitz:[1]

$$f(x) = \frac{x + 2m_e^2}{x^2}\left(\frac{x - 4m_e^2}{x}\right)^{1/2}(m_\pi^2 - x)^3. \qquad (6)$$

This distribution is shown in Fig. 4 by the solid curve; the histogram shows the pair distribution in the parameter x based on the results of this work.

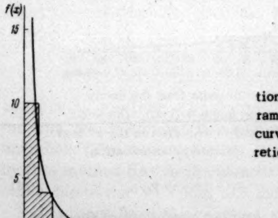

FIG. 4. The distribution of pairs in the parameter x. The solid curve refers to the theoretical distribution.[1,2]

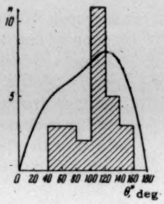

FIG. 5. Angular distribution of the pairs relative to the direction of of the π^- mesons in the π^--p center-of-mass system. The solid curve refers to the angular distribution $\sin\theta^* \, d\sigma/d\Omega$ (in an arbitrary scale) of photons from the decay of neutral pions produced in the reaction $\pi^- + p \to \pi^0 + n$ by 150-Mev π^- mesons.[13]

It can be seen that the majority of pairs has small values of x. This means that the intermediate photon is virtual to a small degree only, i.e., the characteristics of the internal conversion pairs from the decay (1) should not be very different from the characteristics of pairs produced by real photons (external conversion). Consequently the angular distribution of the pairs should practically coincide with the angular distribution of photons from the decay $\pi^0 \to 2\gamma$. In Fig. 5 we show in the form of a histogram the angular distribution of pairs in the angle θ^* in the π^--p center-of-mass frame obtained in this work. It is seen that this distribution is not in contradiction with the solid curve which represents $(d\sigma/d\Omega)\sin\theta^*$ (arbitrary scale) and corresponds to the photon angular distribution from the decay of π^0 mesons obtained from the reaction $\pi^- + p \to \pi^0 + n$ with 150 Mev π^- mesons.[13]

The total energies of the pairs $E = E^- + E^+$ are, as was to be expected, contained in the interval 17 — 270 Mev, corresponding to the limits of the calculated energy spectrum of photons from the decay of neutral pions produced by the charge-exchange process.

In conclusion, it should be noted that in the scanning of the photographs one event was found corresponding to the decay of a π^0 according to the mode $\pi^0 \to e^- + e^+ + e^- + e^+$.[9] Not one of the 27 pairs has kinematics in agreement with the decay mode $\pi^0 \to e^- + e^+$, the relative probability of which is of order 10^{-7} according to estimates by Drell.[14]

The authors are grateful to Prof. R. Dalitz for communicating some unpublished theoretical calculations.

---

[1] R. H. Dalitz, Proc. Phys. Soc. **A64**, 667 (1951).

[2] N. M. Kroll and W. Wada, Phys. Rev. **98**, 1355 (1955).

[3] Kerimov, Mukhtarov, and Gadzhiev, JETP **37**, 575 (1959), Soviet Phys. JETP **10**, 407 (1960).

[4] Daniel, Davies, Mulvey, and Perkins, Phil. Mag. **43**, 753 (1952).

[5] B. M. Anand, Proc. Roy. Soc. **A220**, 183 (1953).

[6] Lindenfeld, Sachs, and Steinberger, Phys. Rev. **89**, 531 (1953).

[7] Sargent, Cornelius, Rinehart, Lederman, and Rogers, Phys. Rev. **98**, 1349 (1955).

[8] Budagov, Viktor, Dzhelepov, Ermolov, and Moskalev, JETP **35**, 1575 (1958), Soviet Phys. JETP **8**, 1101 (1959).

[9] Budagov, Viktor, Dzhelepov, Ermolov, and Moskalev, JETP **36**, 1080 (1959), Soviet Phys. JETP **9**, 767 (1959).

[10] Budagov, Viktor, Dzhelepov, Ermolov, and Moskalev, Reported by Pontecorvo at the Confer-

ence on High Energy Physics, Kiev, July 1959; JETP 38, 734 (1960), Soviet Phys. JETP 11, 531 (1960).

[11] Fischer, March, and Marshall, Phys. Rev. 109, 533 (1958); E. L. Koller and A. M. Sachs, Bull. Am. Phys. Soc. 4, 24 (1959).

[12] Klepikov, Meshcheryakov, and Sokolov, Conference on High Energy Physics, Kiev, July 1959.

[13] Ashkin, Blaser, Feiner, and Stern, Phys. Rev. 101, 1149 (1956).

[14] S. D. Drell, Nuovo cimento 11, 693 (1959).

Translated by A. M. Bincer
211

SOVIET PHYSICS JETP VOLUME 11, NUMBER 4 OCTOBER, 1960

IONIZATION OF GASES BY NEGATIVE IONS

Ya. M. FOGEL', A. G. KOVAL', and Yu. Z. LEVCHENKO

Physico-Technical Institute, Academy of Sciences, Ukrainian S.S.R.

Submitted to JETP editor September 29, 1959

J. Exptl. Theoret. Physics (U.S.S.R.) **38**, 1053-1060 (April, 1960)

The total cross sections for positive-ion formation in collisions of H^- ions (10 to 50 kev) with the atoms He, Ne, Ar, Kr and Xe and the molecules H_2, N_2 and O_2 have been measured; the same cross sections have been measured for O^- ions with the same energy in collisions with inert gas atoms and H_2 and O_2. The ionization cross sections for H^- and H^+ are compared.

INTRODUCTION

BECAUSE of the great amount of work[1-16] carried out in recent years, chiefly by N. V. Fedorenko and his co-workers, a number of the characteristic features of the ionization of gases by positive ions have been established. One of the results of this work is an understanding of the differences in the ionization of gases by positive ions and by electrons. It is also of interest to compare ionization processes in gases when ionization is caused by ions of the same type with opposite charge.

A comparison of this kind can be useful in establishing the role of the sign of the charge of heavy particles with the same mass and atomic number. In H^+ and H^- there is a sharp difference in the structure of the electron shell: one is a bare nucleus while the other has a closed shell, similar to that in helium. Another important difference in ionization caused by positive and negative ions should be kept in mind. Ionization by positive ions is accompanied by a competing process, capture of a single electron (single-electron charge exchange). Ionization by negative ions is not accompanied by this process. The chief competing process in this case is the one in which a single electron is detached from the negative ion.

It follows that a comparison of the ionization of gases by positive and by negative ions should furnish certain data concerning ionization of gases by heavy particles. However, such a comparison is not possible because of the complete lack of experimental data on the ionization of gases by negative ions. The present work has been undertaken in order to obtain these data and to compare them with data on ionization cross sections for positive ions. For a number of reasons, ionization of gases by H^- is of greatest interest. To clarify the role of ion mass, we have also measured ionization cross sections for D^-. In addition, to determine the effect of the atomic number and electron-shell structure of the ion, we have measured ionization cross sections for O^- ions.

METHOD OF MEASUREMENT

When negative ions move through a gas the following inelastic processes can occur:

I. $A^- + B \rightarrow A^- + B^*$ — **excitation**
II. $A^- + B \rightarrow A^- + B^{k+} + ke$ — **ionization** $(1 < k < Z_B)$;
III. $A^- + B \rightarrow A^{(k-1)+} + ke + B$ — **stripping** $(1 < k < Z_A + 1)$;
IV. $A^- + B \rightarrow A + B^-$ — **charge exchange**

(the last process is possible if particle B has a positive electron affinity).

If the gas is molecular the molecules can dissociate into positive and negative ions. In an atomic gas traversed by a beam of negative ions, slow positive ions are formed only by ionization. Thus, the total cross section for positive-ion formation, σ_i^+, can be measured by a potential method; the method used here is essentially that described in references 1, 3, and 6.

A magnetic field parallel to the plane of the measurement electrode is used to suppress secondary electron emission from this electrode; this method has also been used earlier.[6]

The cross section σ_i^+ is computed for single collisions from the formula

$$\sigma_i^+ = i_H^+ / I_0^- nL, \qquad (1)$$

where i_H^+ is the positive current at the measurement electrode with the magnetic field on, I_0^- is the current of the primary beam, n is the number of gas particles per cm^3, and L is the length of the measurement electrode.

The total cross section for the formation of electrons and slow negative ions, σ^-, is determined from the formula

$$\sigma^- = i^-/I_0^- nL, \tag{2}$$

where i^- is the negative current at the measurement electrode in the absence of the magnetic field. The value of σ^- computed from Eq. (2) is somewhat high because of the secondary emission from the negatively charged plate of the measurement capacitor. If the secondary emission coefficient for this plate is small, the following relation holds:

$$\sigma^- = \sigma_i^+ + \sum_{k=0}^{Z_A} (k+1)\,\sigma_{-1k} + \sigma_i^-, \tag{3}$$

where σ_{-1k} is the cross section for the detachment of $k+1$ electrons from the negative ion and σ_i^- is the cross section for the formation of slow negative ions.

If

$$\sigma_i^- \ll \sigma_i^+ + \sum_{k=0}^{Z_A} (k+1)\,\sigma_{-1k},$$

we have

$$\sigma^- = \sigma_i^+ + \sum_{k=0}^{Z_A} (k+1)\,\sigma_{-1k}. \tag{4}$$

The cross section σ_i^- is determined from the expression

$$\sigma_i^- = i_H^-/I_0^- nL, \tag{5}$$

where i_H^- is the negative current at the measurement electrode in the presence of the magnetic field.

The following remarks should be made with regard to σ_i^+. Actually, σ_i^+ represents the sum $\sum_{k=1}^{Z_A} k\sigma_i^{k^+}$ where $\sigma_i^{k^+}$ is the cross section for ionization with detachment of k electrons from the gas particle. $\sigma_i^{k^+}$ can be determined from the relative intensity of the peaks in the charge spectrum characteristic of the slow positive ions as obtained by an auxiliary mass spectrometer. In turn, each $\sigma_i^{k^+}$ represents the sum of the cross sections for ionization without change of charge of the negative ion and with detachment of one, two, or more electrons from the negative ion.

APPARATUS

A diagram of the apparatus used for measuring the cross sections for ionization of gases by negative ions is shown in Fig. 1.

The negative-ion source is the negative-ion injector of the charge-exchange electrostatic accelerator being built at the Physico-Technical Institue, Academy of Sciences, Ukrainian S.S.R. The design of this injector and its characteristics have been described by us in detail earlier[17] and will not be considered further in the present paper.

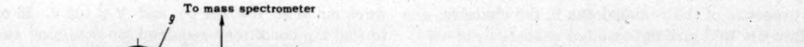

FIG. 1. Diagram of the apparatus.

A monoenergetic beam of negative ions of a given kind is selected by the magnetic mass monochromator 1 and focused by the electrostatic quadrupole lens 2 on the slit (2 × 4 mm). The beam is then deflected through an angle of 10° by the electric field of the plane capacitor 4 and strikes the input slit 5 of the collision chamber 6. The axis of the collision chamber is inclined with respect to the beam axis in front of the capacitor 4 by an angle of 10° (not shown in the sketch). By means of the deflection capacitor it is possible to select neutral atoms and positive ions produced by collisions of ions of the beam with molecules of the residual gas in the space between the magnetic analyzer and the collision chamber.

The primary beam enters the collision chamber through an input slit (0.5 × 1 mm), traverses the input channel (4 × 6 mm and 25 mm long) and leaves through an exit channel (5.5 × 8.5 mm and 15 mm long). In order to supress secondary electron emission from its edges, the input slit is insulated from the frame of the collision chamber and is maintained at a positive potential of 300 v. The measurement volume is formed by the five plane capacitors 7 consisting of electrodes with an area of 50 × 50 mm which are spaced every 30 mm. The four coils 8 wound directly on the frame are used to produce a longitudinal magnetic field in the chamber. The gas pressure in the collision chamber is measured with a Knudsen gauge. When the trap 9 is filled with liquid air the pressure of the residual gas in the chamber is 7 or 8×10^{-6} mm Hg.

The current in the primary beam is measured with a Faraday cylinder 11. The beam transmission through the collision chamber is monitored by a Faraday cylinder 10. Both Faraday cylinders are furnished with magnetic control. At the residual gas pressure indicated above the chamber transmission is 100%; at a pressure of 1×10^{-4} mm Hg the transmission is reduced to 85 or 90%.

The primary beam current is measured with a mirror galvanometer with a sensitivity of 1×10^{-10} amp per division. The primary beam current varies from 1.5×10^{-7} to 1×10^{-8} amp. The current at the measurement electrode (plate of the fourth capacitor) is measured with a string electrometer with a sensitivity of 1×10^{-12} amp per division. The currents I_0^- and i_H^+ are measured simultaneously in order to avoid errors due to random fluctuations in the primary beam current.

An auxiliary mass spectrometer is connected to the collision chamber; this instrument is used to make mass spectrometer analyses of the slow ions formed in the gas by passage of the negative ions.

Differential pumping for the collision chamber is realized by means of an MM-1000 diffusion pump which pumps through two ports, 12 and 13. Liquid-air traps are used to prevent vapors of the organic materials in the pump from reaching the apparatus.

The energy of the negative ions is determined from the potential difference traversed by these ions. In the case of H^- resulting from $H_2^+ \rightarrow H^-$, the energy is computed from the formula $E = e[\frac{1}{2}V_{ext} + V_{acc}]$; for H^- and O^- resulting from $H^+ \rightarrow H^-$ and $O^+ \rightarrow O^-$ the energy is computed from the formula $E = e[V_{ext} + V_{acc}]$. The extraction and acceleration potentials V_{ext} and V_{acc} are measured with S-96 electrostatic voltmeters. The random error in the measurements, as estimated from the spread in the results, is ±10%; the error in the energy measurements is ±3%.

RESULTS OF THE MEASUREMENTS

Before the measurements were made, a number of $i_H^+/I_0^- = f(H)$ and $i_H^+/I_0^- = F(V)$ characteristic curves were obtained to determine the magnetic field H required for suppression of secondary emission from the measurement electrode and the electrode potential V required for obtaining a saturation current. Subsequently all measurements were made at $H = 140$ oe and $V = 100$ v. In order to find the conditions required for obtaining single collisions, the dependence of i_H^+/I_0^- on gas pressure p in the collision chamber is determined. The cross sections σ_i^+ and σ^- are determined from the slope of the linear portion of this curve.

To check the accuracy of the overall method, the total cross sections for the positive-ion formation by protons in hydrogen and argon were measured. The cross sections obtained this way agree, within the error limits of the measurements, with the data available in the literature.[6,14,15]

In addition, measurements were made to determine the total cross sections for free-electron formation in hydrogen and argon by H^- ions. The relation $\sigma^- = \sigma_{-10} + 2\sigma_{-11} + \sigma_i^+$ should hold for H^- ions [cf. Eq. (4)]. This relation was found to hold fairly well, as can be seen from Fig. 2, where we show the dependence of σ^- and $\sigma_{-10} + 2\sigma_{-11} + \sigma_i^+$ on v. The values of σ_{-10} for argon and hydrogen were taken from the work of Stedeford and Hasted[18] and Stier and Barnett[19] respectively; the value of σ_{-11} was taken from reference 20. For hydrogen

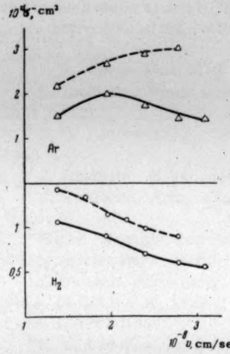

FIG. 2. The dependence of σ^- (solid curve) and $\sigma_{-10} + 2\sigma_{-11} + \sigma_i^+$ (dashed curve) on v for argon and hydrogen.

the quantities σ^- and $\sigma_{-10} + 2\sigma_{-11} + \sigma_i^+$ are in agreement, within the experimental errors; in argon, however, at velocities greater than 2×10^8 cm/sec, the second quantity is somewhat greater than the first.

The results of measurements of σ_i^+ for H^- ions with energies from 10 to 50 kev for five inert gases and three molecular gases are shown by the $\sigma_i^+(v)$ curves in Fig. 3.

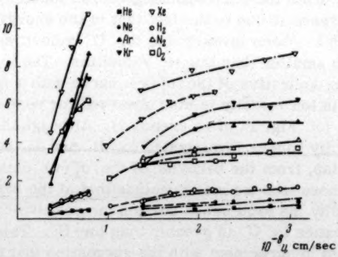

FIG. 3. The function $\sigma_i^+(v)$ for H^- (dot-dashed curves), D_1^- (dashed curves) and O_1^- (solid curves) for five inert gases and three molecular gases.

The dependence of σ_i^+ on ion velocity is the same for all gases: initially σ_i^+ increases as the velocity increases; then the $\sigma_i^+(v)$ curve reaches a plateau which extends up to the end of the velocity range which has been studied. σ_i^+ varies somewhat from one gas to another. In inert gases it increases with the atomic number of the gas while in molecular gases it increases in the order H_2, O_2, N_2.

To determine the effect of ion mass on σ_i^+ (all other conditions remaining the same) we have measured this cross section for D^- ions with energies from 10 to 50 kev in hydrogen, oxygen, neon, and xenon. The $\sigma_i^+(v)$ curves for H^- and D^- are compared in Fig. 3. As is apparent from the figure, σ_i^+ is the same for H^- and D^-, within the limits of the experimental errors, for the velocity range investigated; thus, the ion mass does not affect σ_i^+.

As has been indicated above, it is of interest to compare ionization caused by protons and by negative hydrogen ions. It is obvious that σ_i^+ for H^- must be compared with σ^-, the total cross section for the formation of free electrons by H^+. In Fig. 4 this comparison is made for inert gases. The data for argon are taken from reference 15 while the data for the other gases have been kindly furnished to us by N. V. Fedorenko from his publications. It is apparent from Fig. 4 that $\sigma_i^+(v)$ and $\sigma^-(v)$ vary in the same way and that the absolute values of the cross sections are approximately the same. However, the ionization cross section curves for heavy particles and electrons differ markedly. The reasons for this difference have been discussed many times in papers published by Fedorenko and his co-workers and will not be considered here. A similar situation obtains for the molecular gases. Thus, H^+, H^- and D^- yield ionization cross sections which are approximately the same, in spite of the differences in the sign of the charge, mass, and electron-shell structure. In order to clarify the effect of the nuclear charge it would seem desirable in the future to compare σ_i^+ in H^-, He, and Li^+.

We have already indicated that in collisions of H^- with gas molecules ionization of the gas particle and detachment of electrons from the ion (stripping) are competing processes. The stripping probability for the H^- depends on the sum $\sigma_{-10} + \sigma_{-11}$, the sum of the cross section for stripping of one and two electrons from the fast ion. The total probability for transition of electrons into the continuum of the system comprised of the two colliding atomic particles is given by the sum $\sigma_{-10} + \sigma_{-11} + \sigma_i^+$. In Fig. 4 we compare the functions $\sigma_i^+(v)$, $\sigma_{-10} + \sigma_{-11} = f(v)$ and $\sigma_{-10} + \sigma_{-11} + \sigma_i^+ = F(v)$ for inert gases. The values of σ_{-10} are taken from reference 18 while the values of σ_{-11} are taken from reference 20.

The following conclusions follow from an analysis of the curves in Fig. 4: 1) the cross section σ_i^+ is much smaller than the sum of the cross sections $\sigma_{-10} + \sigma_{-11}$ (20 – 25% of this sum for xenon, krypton, and argon and approximately 12% for neon and helium); 2) the quantities σ_i^+, $\sigma_{-10} + \sigma_{-11}$ and $\sigma_{-10} + \sigma_{-11} + \sigma_i^+$ increase monotonically with the atomic number of the gas; 3) the behavior of the

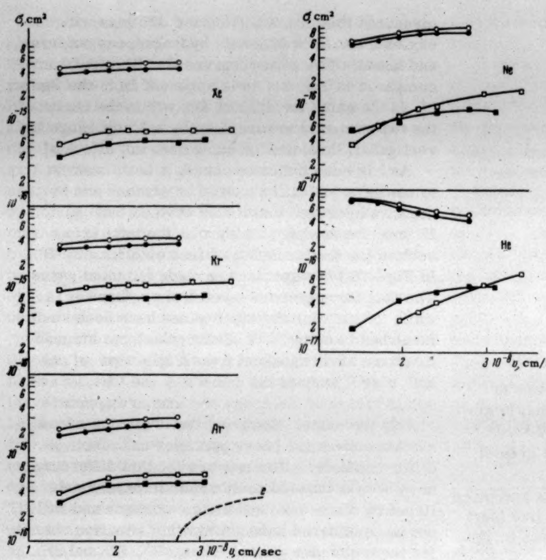

FIG. 4. □ – cross section for ionization by protons, ■ – cross section for ionization by H_1^-, ● – sum of the cross sections $\sigma_{-10} + \sigma_{-11}$, ○ – sum of the cross sections $\sigma_{-10} + \sigma_{-11} + \sigma_i^+$, the dashed curve is the electron ionization cross section.

functions $\sigma_i^+(v)$, $\sigma_{-10} + \sigma_{-11} = f(v)$ and $\sigma_{-10} + \sigma_{-11} + \sigma_i^+ = F(v)$ is the same for all gases except helium. These conclusions would seem to be incompatible with the notion of competition between ionization and stripping in atomic collisions; according to this interpretation, $\sigma_{-10} + \sigma_{-11} + \sigma_i^+$ should be a weak function of the atomic number of the gas while the σ_i^+ and $\sigma_{-10} + \sigma_{-11}$ should vary in opposite directions as the atomic number of the gas varies. These quantities should also vary in opposite directions as the ion velocity varies. Actually, both vary in the same direction as the atomic number of the gas and the velocity of the ion; moreover, $\sigma_{-10} + \sigma_{-11} + \sigma_i^+$ increases appreciably with the atomic number of the gas. This last finding would seem to indicate that the total probability for transition of electrons from bound states in the colliding atomic particles into states in the continuum depends on the number of electrons in the electron shell of the colliding particles and increases as this number increases.

The data obtained in measurements of the cross sections σ_i^+ for O^- ions with energies from 10 to 50 kev in five inert gases and in hydrogen and oxygen are shown in Fig. 3 in the form of $\sigma_i^+(v)$ curves.

A characteristic feature of the $\sigma_i^+(v)$ curves for O^- is the rapid increase in σ_i^+ with ion velocity; in this feature these curves differ essentially from the corresponding curves for H^-. This difference is due to the fact that in the energy range which has been investigated the O^- velocities are much smaller than the H^- velocities. The increase in the derivative of the $\sigma_i^+(v)$ curve with a reduction in ion velocity is also observed for positive ions (cf. Fig. 11 of reference 7). Although the velocity ranges investigated for H^- and O^- do not overlap, from the behavior of the $\sigma_i^+(v)$ curves for these ions we may conclude that at the same velocity the total cross section for positive-ion formation by O^- is greater than for H^-. This result is in agreement with the suggestion that the cross section for transition of electrons into a state in the continuum increases as the number of electrons in the electron shells of the colliding particles increases. A more detailed analysis of the results presented in the present paper will be made after completion of the second stage of this work, which will consist of an investigation of the slow-ion charge spectrum and the determination of the cross sections for ionization with detachment of one, two, or more electrons.

In conclusion, we wish to take this opportunity to express our gratitude to Professor A. K. Val'ter for his continued interest in this work, to L. P. Rekova and A. F. Khodyachikh who participated in

the measurements, and to Technician P. A. Chudnyĭ for construction of the collision chamber.

---

[1] J. P. Keene, Phil. Mag. **40**, 369 (1949).

[2] E. Lindholm, Proc. Phys. Soc. (London) **A66**, 1068 (1953).

[3] N. B. Fedorenko, J. Tech. Phys. (U.S.S.R.) **24**, 1950 (1954).

[4] E. Lindholm, Z. Naturforsch. **9a**, 535 (1954).

[5] E. Lindholm, Arkiv Fysik **8**, 257 (1954); **8**, 433 (1954).

[6] Fogel', Krupnik, and Safronov, JETP **28**, 589 (1955), Soviet Phys. JETP **1**, 415 (1955).

[7] Fedorenko, Afrosimov, and Kaminker, J. Tech. Phys. (U.S.S.R.) **26**, 1929 (1956), Soviet Phys.-Tech. Phys. **1**, 1861 (1957).

[8] N. V. Fedorenko and V. V. Afrosimov, J. Tech. Phys. (U.S.S.R.) **26**, 1941 (1956), Soviet Phys.-Tech. Phys. **1**, 1872 (1957).

[9] D. E. Moe, Phys. Rev. **104**, 694 (1956).

[10] V. V. Afrosimov and N. V. Fedorenko, J. Tech. Phys. (U.S.S.R.) **27**, 2557 (1957), Soviet Phys.-Tech. Phys. **2**, 2378 (1958).

[11] V. V. Afrosimov and N. V. Fedorenko, J. Tech. Phys. (U.S.S.R.) **27**, 2573 (1957), Soviet Phys.-Tech. Phys. **2**, 2391 (1958).

[12] H. B. Gilbody and J. B. Hasted, Proc. Roy. Soc. (London) **A240**, 382 (1957).

[13] E. Blauth, Z. Physik **147**, 228 (1957).

[14] Afrosimov, Il'in, and Fedorenko, JETP **34**, 1398 (1958), Soviet Phys. JETP **7**, 968 (1958).

[15] Afrosimov, Il'in, and Fedorenko, J. Tech. Phys. (U.S.S.R.) **28**, 2266 (1958), Soviet Phys.-Tech. Phys. **3**, 2080 (1959).

[16] D. E. Moe and O. H. Petsch, Phys. Rev. **110**, 1358 (1958).

[17] Fogel', Koval', and Timofeev, J. Tech. Phys. (U.S.S.R.) **29**, 1381 (1959), Soviet Phys.-Tech. Phys. **4**, 1270 (1960).

[18] J. B. H. Stedeford and J. B. Hasted, Proc. Roy. Soc. (London) **A227**, 466 (1955).

[19] P. M. Stier and C. F. Barnett, Phys. Rev. **103**, 896 (1956).

[20] Fogel', Ankudinov, and Slabospitskiĭ, JETP **32**, 453 (1957), Soviet Phys. JETP **5**, 382 (1957).

Translated by H. Lashinsky
212

SOVIET PHYSICS JETP VOLUME 11, NUMBER 4 OCTOBER, 1960

THE ISENTROPIC COMPRESSIBILTY OF ALUMINUM, COPPER, LEAD, AND IRON AT HIGH PRESSURES

L. V. AL'TSHULER, S. B. KORMER, M. I. BRAZHNIK, L. A. VLADIMIROV, M. P. SPERANSKAYA, and A. I. FUNTIKOV

Submitted to JETP editor October 7, 1959; resubmitted January 3, 1960

J. Exptl. Theoret. Phys. (U.S.S.R.) 38, 1061-1073 (April, 1960)

A method is described for measuring the speed of propagation of weak disturbances behind the front of strong shock waves. The existence of two sound velocities, corresponding to the elastic and plastic states of the material, has been detected. With the aid of the techniques which have been developed, the sound velocities and isentropic compression moduli of aluminum, copper, iron, and lead have been determined in the pressure range 0.4 to 3.5 × 10^6 atmos. On the basis of the experimental results so obtained, the magnitudes of the thermal energy, the temperatures of the shock compression, and the Gruneisen coefficients have been estimated.

INTRODUCTION

THE new methods of studying the properties of matter at high pressures are based on the use of strong shock waves.[1,2] A determination of two of the wave parameters — its velocity of propagation and the velocity of the mass of material behind the front — permits the pressure and density in the shock compression to be found.

A third important kinematic parameter of a shock wave is the speed of sound within the material compressed by the shock. Its value characterizes the speed with which small disturbances (weak shocks and relaxation waves) are propagated through the compressed material. A knowledge of the speed of sound, in this sense, is of undoubted interest, not only for geophysical investigations, but also for other investigations connected with the propagation of sound and shock waves, and in particular for properly setting up experiments to determine dynamic compressibility.

Measurements of sound velocity play a large part in the study of the equation of state. It is well known that a shock compression increases the internal energy of a body by the amount $\Delta E = \frac{1}{2} P_\Gamma (v_0 - v)$, where P_Γ is the pressure in the shock, v_0 is the initial specific volume, and v is the specific volume behind the shock wave front. On the diagram of pressure vs specific volume (Fig. 1), ΔE is equal to the area of the triangle OAB. The energy thus acquired is partly spent in overcoming the elastic repulsive forces, increasing the elastic potential of the lattice by an amount equal to the area of the curvilinear triangle O_1DA.

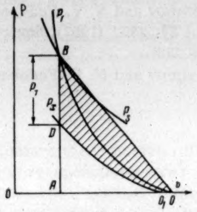

FIG. 1

The remaining part, represented by the shaded area in the diagram, is liberated in the form of thermal energy, heating up the material and increasing its entropy. As a result, the points on the dynamic adiabatic lie on different isentropics P_S above the curve for elastic or cold compression P_X. Through the relation $-v^2 (\partial P/\partial v)_S = C^2$, measurements of the speed of sound behind the front of a strong shock wave determine the slope of the isentropics — in other words, the isentropic compressibility of the material — in the extreme high pressure region of hundreds of thousands or millions of atmospheres.

In the present study we present methods of measuring the speed of sound behind the front of strong shock waves, and the results of measurements on aluminum, copper, lead, and iron in the range of pressure from 4 × 10^5 to 3.5 × 10^6 atmos. On the basis of the experimental results obtained, the isentropic derivatives have been calculated and the thermal energies and temperatures in the shock have been estimated. The Grüneisen coefficients have also been estimated, with somewhat less accuracy.

1. MEASUREMENTS OF THE SPEED OF SOUND BY THE LATERAL RELAXATION METHOD

By definition, the speed of sound is the speed of propagation of small disturbances with respect to the moving material. Since at the wave front $C + U > D$ (U being the bulk velocity of the material behind the shock wave front and D the velocity of the front), it follows that any disturbance originating behind the shock wave front will overtake the front, and will produce changes in all the parameters, including the kinematic parameters U and D themselves. This permits measurements to be made of the velocity of propagation of acoustic disturbances, since it registers their arrival at the shock wave front.

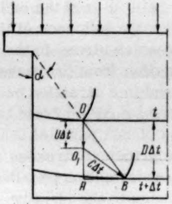

FIG. 2

In the method of lateral relaxation, the shock wave moves along a cylindrical sample with a stepped shape (Fig. 2). The surface of the shoulder acts as a source of rarefaction waves. Expansion waves propagate with the speed of sound through the shock in the metal and overtake the shock wave front, causing a reduction of pressure in the peripheral zone of the sample.

Let us consider the two positions of the shock wave front at the instants t and $t + \Delta t$. Let the point O separate the relaxed portion of the front from the unrelaxed part. After the time Δt the shock wave has progressed a distance $D\Delta t$, and the metal particles which were originally at point O have been displaced along behind the front for a distance $U\Delta t$. After the same interval Δt the relaxation waves will have reached a sphere of radius $C\Delta t$ with its center at O_1. Since the motion of the rarefaction waves caused when a shock wave passes around an internal angle is self similar, the trajectory of the boundary point is a straight line, making a constant angle of relaxation α with the direction of propagation of the shock wave. In the right-angled triangle O_1AB we have $AB = \sqrt{(C\Delta t)^2 - (D-U)^2\Delta t^2}$. The same leg in the triangle AOB is $AB = D\Delta t \tan\alpha$. Equating, we obtain the following expressions for the tangent of the relaxation angle and the speed of sound:

$$\tan\alpha = \sqrt{(C/D)^2 - [(D-U)/D]^2}, \tag{1}$$

$$C = D\sqrt{(\tan\alpha)^2 + [(D-U)/D]^2}. \tag{2}$$

Thus, for measurements of the speed of sound by the lateral relaxation method, if the parameters D and U for the shock wave are known, the tangent of the relaxation angle α must be determined experimentally.

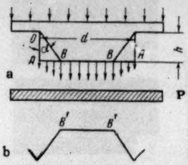

FIG. 3. a – Scheme of experiment for determining the relaxation angle. b – Front of the flying material.

The general scheme of the experiment for measuring the angle α is evident from Fig. 3. Until the instant when the shock wave emerges from the sample slab, the relaxation waves create a region of reduced pressures and lower throw-off speeds on the wave-front surface. The velocity of the free surface of the sample therefore falls off from point B toward point A, as shown schematically by the lengths of the arrows. The boundary of the unrelaxed region is found by measuring the throw-off velocities, or (which amounts to the same thing) the difference in the time of flight of the metal to a Plexiglas plate P fixed a short distance away from the sample. The process of the collision of the thrown-off surface with the Plexiglas surface is determined with a double-objective slit photo-chronograph with a type SFR-3 rotating mirror[3] having a sweep speed up to 6 km/sec. A break in the profile of the flying material (see points B′ in the sketch of the photochronogram, Fig. 3) determines the boundary of the unrelaxed region. Knowing the diameter of the shoulder d, the height h of the sample, the scale of the photograph k, and the distance B′B′ measured on the film, we find the quantity of interest to us from the formula

$$\tan\alpha = (d - kB'B')/2h. \tag{3}$$

where k is the ratio of the dimensions in nature to the dimensions on the film.

The shock wave parameters necessary to evaluate the speed of sound from (2) are determined in separate experiments. If the dynamic adiabatic is known, it is sufficient to measure a single parameter of the shock wave, for example its velocity D.

2. RELAXATION WAVES – ELASTIC AND PLASTIC

At pressures of 300 to 500 × 10^3 atmos, the photochronograms recording the time differences in the shock along the indicator surface differ fundamentally in nature for materials having different mechanical properties. With water, for example, the photograph records a sharp bend at the boundary of the unrelaxed zone (see Fig. 4a). On the other hand, with a steel sample the curve has a rounded contour without sharply defined boundaries to mark off the region of the relaxation waves (Fig. 4b).

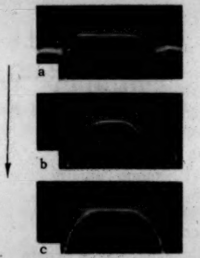

FIG. 4. Experimental photochronograms. Velocity of travel of the light across the film is 6 mm/microsec. Direction of motion is shown by the arrow.

On the basis of the pictures obtained, it can be assumed that for rigid materials the more slowly moving particles of the peripheral zone retard the neighboring portions of the unrelaxed region, which originally received the maximum momentum. In practice, if a thin layer of water or alcohol is applied to the metal surface to receive the momentum of the free surface, it permits the distribution of velocities across the sample diameter to be recorded more clearly, and the boundary of the unrelaxed zone to be determined with high precision (see Fig. 4c). Nonetheless, the difference in flight time for different parts of the liquid layer confirms in basic outline the picture derived above of a gradual decrease of velocity in the relaxed zone, and a large relaxation angle.

Table I gives the results of relaxation angle measurements for water, copper, and iron at relatively small shock pressures. The sound velocities C^* and the corresponding compressibility moduli $\rho_0 C^{*2}$ have been calculated from the observed relaxation angles. In Table I these quantities are compared with the values of the derivatives of the dynamic adiabats $dP_\Gamma/d\sigma$, which for low pressures characterize the isentropic compressibilities of the materials with reasonable accuracy. For water the experimentally measured modulus $\rho_0 C^{*2}$ is somewhat smaller than the derivative of the dynamic adiabat, in agreement with the theory of the subject; for copper and iron it is considerably greater — approximately 1.5 times.

The data given in the table prove beyond doubt that in the metals under consideration there are wave systems propagating with speeds greatly exceeding the isentropic velocity of acoustic waves of volume compression.

In order to understand their origin, let us consider the variation in the state of stress of a metal which has been compressed by a shock wave, when a plane relaxation wave acts upon it. The elastoplastic properties of an isotropic medium are characterized by three constants: the Young's modulus E, the Poisson ratio μ, and the critical shear stress σ_k. Under the influence of the relaxation wave the compressive stress in the direction normal to the relaxation front decreases by some amount ΔP_n, and in a direction parallel to the front it decreases by ΔP_τ. From the symmetry conditions in the planes parallel to the relaxation front, two of the principal stresses are equal, and there will be no deformation parallel to the front. This condition leads to the identity

$$\Delta P_\tau - \mu(\Delta P_\tau + \Delta P_n) = 0,$$

which enables us to connect the intensity of the relaxation wave

$$\Delta P_n = [(1-\mu)/(1-2\mu)](\Delta P_n - \Delta P_\tau)$$

with the difference between the principal stresses. As long as

$$\Delta P_n \leqslant [(1-\mu)/(1-2\mu)]\, 2\sigma_k,$$

the medium behaves like an elastic body, with a velocity of propation for longitudinal elastic waves $C^* = \sqrt{(K_s + \frac{4}{3}G)/\rho}$. In this expression, $K_s = E/3(1-2\mu)$ is the isentropic modulus of volume compression, and $G = E/2(1+\mu)$ is the shear modulus. When

$$\Delta P_n > [(1-\mu)/(1-2\mu)]\, 2|\sigma_k|$$

the medium changes to a state of plastic flow, for which the shear modulus is taken to be zero. Under these conditions the speed of the "plastic" relaxation waves $C = \sqrt{K/\rho}$, just as in the case of

TABLE I

Material	α, deg	D.km/sec	U.km/sec	C*.km/sec	$\rho_0 C^{*2}$, 10^{10} d/cm²	$dP_\Gamma/d\sigma$, 10^{10} d/cm²	μ	ν
Water	47.5	4.42	1.52	5,60	31.4	34.2	—	—
Copper	41	5,24	0,87	6.33	357.8	288.8	0.34	0.82
Iron	46.5	5.34	0,98	7.15	401.3	298.2	0.28	0,77

liquids, is determined by the isentropic modulus of volume compression K_s. The velocity ratio

$$C/C^* = \nu = \sqrt{(1+\mu)/3(1-\mu)}. \quad (4)$$

depends only on the Poisson ratio.

The existence of two speeds, "elastic" and "plastic," under the experimental conditions of Fig. 3 leads to the appearance of two concentric zones of relaxation on the wave front surface — an inner "elastic" zone of weak relaxation and an external "plastic" zone.

Making use of the relation (4), we can calculate from C^* the value of the isentropic modulus $K_s = \rho_0 C^2 = \rho_0 C^{*2}\nu^2$. For both metals the values so obtained, $K_s \approx 240 \times 10^{10}$ d/cm², are somewhat smaller than $dP_\Gamma/d\sigma$, confirming the theory proposed above for the phenomenon.

The elastic relaxation zone is weakly developed in materials such as lead which have a large Poisson ratio and a small value of critical shear stress. Because σ_k decreases with temperature, it would seem at first sight that the high temperatures in a strong shock should lead to the disappearance of the elastic relaxation wave for all materials. However, this is countered by the high pressures, which increase the melting temperature[4] and raise the critical shear stress. Thus, according to Bridgman's data,[5] the application of pressures of 25×10^3 and 50×10^3 atmos increases $2\sigma_k$ for soft iron from 1200 kg/cm² to 6600 and 12000 kg/cm² respectively. For copper at these pressures $2\sigma_k$ is equal to 1050, 3000, and 4900 kg/cm² respectively. In view of these statements, it is quite possible that longitudinal elastic waves will exist at shock pressures of 10^6 atmos and above.

In relation to the method, the presence of an elastic zone makes the accurate determination of the boundary of the "plastic" relaxation much more difficult. The method described in the following section does not have this drawback.

3. THE OVERTAKING-RELAXATION METHOD

In the overtaking-relaxation method we study the collision between a plate and a sample, made of materials with known dynamic adiabats. In the simplest variant of the method, the plate and sample are made of the same material. From the surface of impact, shock waves OB and OA travel through the sample and the moving plate (see the x, t diagram, Fig. 5). At the instant the shock wave emerges from the rear surface of the plate (point A) a centered rarefaction wave is set up which overtakes the shock wave and weakens it. The occurrence of the first α-characteristic on the shock wave trajectory takes place at a distance

$$l = [(1+M)/(1-M)]\,\Delta, \quad (5)$$

where Δ is the thickness of the striker plate and $M = (D-U)/C$ is the Mach number. The relation (5) enables one to find M, provided that there actually is an overtaking, and consequently to find C also, if $D_1 - U_1$ is known. This form of the method was proposed by E. I. Zababakhin in 1948.

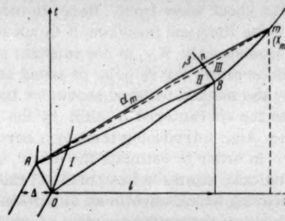

FIG. 5

Since the determination of the distance l, where the wave begins to slow down because of the presence of the faster elastic relaxation wave, is beset with considerable experimental error, it is expedient to change the form of the method and find the time t_m of arrival of the shock wave at a given point m, already known to lie on the relaxed portion of the shock wave trajectory. In this way one finds the slope of the α-characteristic $W_{\alpha m} = U_m + C_m$ that passes through the origin of the x, t diagram and the point m, whose coordinates are x_m and t_m. Then by measuring the material velocity U_m at the same point directly, or by determining it from a known shock adiabatic equation, we find the velocity of sound $C_m = W_{\alpha m} - U_m$ from the speed of the shock wave. In an expanded form, it is not difficult to show that

$$C_m = \frac{x_m + (2-\sigma_1)\,\Delta/\sigma_1}{D_1 t_m - \Delta}\, D_1 - U_m, \quad (6)$$

where $\sigma_1 = D_1/(D_1 - U_1)$ and D_1 are the parameters for the unrelaxed region.

Thus, the measurement of the velocity of sound by the overtaking-relaxation method reduces to the experimental determination of the shock wave trajectory in x, t coordinates, plus a measurement of the material velocity at one or a number of points on this trajectory.

The whole of the above treatment is valid under the assumption that the α-characteristics are straight lines everywhere in the region OAm, with a slope $W_a = U + C = \text{const}$. Let us go into this question in more detail. When two similar materials collide, three regions of flow can be distinguished in the x, t plane (see Fig. 5): I — the region OAB; II — ABn; and III — Bnm. In regions

I and II the flow is isentropic, since in region I the value of W_α is constant over the whole region, and in II it is constant over each α-characteristic. In region III the flow is not isentropic, since the intensity of the shock wave (and consequently also the entropy of the material behind its front) decreases beyond the point B, where the relaxation wave traveling from point A first overtakes the shock wave front. Here, in contrast to region II, the Riemann invariant β is not constant, and consequently W_α is not constant either.

Having determined the velocity of sound at the point m by the method outlined above, we then approximate the characteristic Anm by the straight line Am, introducing thereby a certain inaccuracy. In order to estimate the error, some numerical calculations have been made of the motion of a decaying shock wave in an aluminum test piece. In this calculation the equation of state

$$P - P_x = (n - 1)\, v^{-1} (E - E_x), \qquad P_x = a\,[(v_0 / v)^n - 1],$$

was used, taking into account not only the elastic terms but also the thermal terms in the pressure and energy. Different values of n from 1.67 to 4 were used in the computations, corresponding to a variation of the Grüneisen coefficient from $\frac{2}{3}$ to 3.

The calculations showed that in aluminum at plastic shock velocities of 5.6 km/sec, at distances of ten or more times the thickness of the plate, the maximum error in the sound velocity did not exceed 1.5%. At this point the pressure at the front of a decaying wave amounts to about one half of its original value. The error is smaller the closer the measuring region is to the portion of the shock wave not reached by the relaxation. A similar calculation has also been carried out for lead with the same results, using the equation of state taken from reference 6.

For a collision between plates of unlike materials, we must know not only the shock adiabatic for the striker plate but also the relation between the material velocity and the sound velocity in the rarefaction wave. In this case the computation of results is somewhat more complicated, since at the collision boundary there is a discontinuity at which the α-characteristics are refracted as they pass.

There are two possible cases of collision: when the material of the test piece is "softer" and when it is "harder" than the material of the striker plate. By the terms "softer" and "harder" we mean a flatter or steeper slope of the Hugoniot adiabat for the given material in P, U coordinates. In both cases the refraction of the α-characteristics can easily be taken into account with the aid of the x, t and P, U diagrams.

4. EXPERIMENTAL RESULTS

A determination of the speed of sound behind the front of strong shock waves presupposes a knowledge of the dynamic adiabats. In working out the experimental data of the present investigation, the dynamic adiabats given in reference 6 for aluminum, copper, lead, and iron were used.

In the first series of experiments the decay curves of shock waves were recorded in test pieces of aluminum, copper, lead, and iron when struck by a 2 mm aluminum plate. The speed of the plate was 5.60 km/sec. In order to record the trajectory of the shock wave in the test piece, which was made up of several plates, electrical contact pickups were introduced through small drill-holes. The successive short-circuiting of the pickups by the shock wave was recorded on a single-sweep cathode ray oscillograph. The

TABLE II

Metal	D_{Al}, km/sec	x_m, mm	t_m, msec	D_m, km/sec	P_m, 10^{10}d/cm^2	σ_m	C_m, km/sec
Aluminum	9,13	—	—	9.13*	69,3*	1,442*	—
		14.20	1.558	8.52	54,5	1.383	8,84
		19.16	2.205	7.92	41.2	1.320	8.13
Copper	10,45	—	—	6.69*	108.7*	1.374*	—
		10,95	1.697	5.92	69.2	1.284	6.32
		14.94	2.399	5,54	52.4	1,237	5.95
Lead	10,34	—	—	4.91*	105.2*	1.626*	—
		6.47	1.373	4.16	65.6	1.502	4.24
		9,45	2,133	3.72	46.4	1.420	3,85
Iron	10,31	—	—	7.01*	104.5*	1.374*	—
		10.93	1.656	5.76	54,2	1,263	6.70
		14.90	2.374	5.34	41.5	1.228	6.12

*The marked states are in the unrelaxed region.

TABLE III

Metal	D_{Fe}, km/sec	x_m, mm	t_m, msec	U_m, km/sec	P_m, 10^{10}d/cm²	σ_m	C_m, km/sec
Aluminum		—	—	3.77*	107.2*	1.561*	—
	7.06	12.50	1.194	3.54	97.5	1,534	9,76
Copper		—	—	2.77*	200.6*	1.519*	—
	8.67	8.00	0.992	2.47	169.2	1.475	7.78
		11,00	1.398	2.12	135.2	1,422	7.13
		15.00	1.981	1.77	104.6	1.365	6.71
Lead		—	—	2.82*	197.3*	1.842*	—
	8.61	6.00	0,988	2,34	146.7	1.734	5.16
		9,00	1,572	1.84	100.8	1.616	4.62
		12,00	2.225	1,56	78.0	1.545	4.29
Iron		—	—	2.86*	191.4*	1.502*	—
	8.54	8,00	0.940	2.62	168,0	1.472	8.49
		11,0	1.329	2.12	122,3	1.405	7.85

*See footnote to Table II.

states in the striker plate and in the first thin screening plate were found graphically, from the intersection of the Hugoniot adiabat for aluminum with the adiabatic for the test piece on the pressure-velocity diagram. From the time delays found experimentally and the distance between the pickups, the trajectory of the shock wave was constructed and the wave velocities in the different portions of the trajectory were determined. In each experiment the recording was carried out over several base-lines.

The results of the measurements are given in Table II. Here t_m is the time from the instant of collision, and x_m is the distance from the collision surface. In the second column of the table are shown the speeds of the shock waves passing through the aluminum plate after the collision.

In the second series of experiments the amplitude of the unrelaxed wave was increased to 1.0 × 10^6 atmos for aluminum and to 1.8 × 10^6 atmos for the other metals. A 1.5-mm steel plate was used as the striker, moving at 5.71 km/sec. In order to make the decay curves observable, a thin aluminum film was applied to the surface of the test piece parallel to the collision surface. When the shock wave emerged at the boundary of the film and the test piece, the film was torn away from the test piece and was projected with a velocity W_{Al} characterizing the amplitude of the wave at that cross section of the sample. The time (and consequently also the velocity with which the film moved) was recorded on a velocity photochronograph by the illumination from the shock wave in the air. The illumination was produced at the instant of the first movement of the film, and stopped as soon as it collided with a Plexiglas barrier, placed at a distance of 8 – 12 mm from the test sample. The transition from the speeds of motion of the aluminum film to the material velocities behind the shock wave front was accomplished with the aid of special calibrating experiments, in which measurements were made of the velocity acquired by an aluminum film under the influence of shock waves of known amplitudes. The decay curves U (x) for the four metals under investigation are shown in Fig. 6, together with the experimental reference points. A knowledge of the U (x) curve makes it possible, with the aid of the known D, U relationships, to proceed successively to the D (x) curve and the curve t (x) $= \int_0^x dx/D$. The subsequent treatment of the experiment in the second series was identical with the treatment of the experiments in the first series. The results so obtained are shown in Table III.

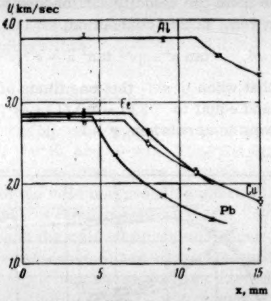

FIG. 6

The chief difference in the experiments of the third series (Table IV) consisted in a further increase of the projection velocity of the steel striker. Here the speed of sound was measured at pressures exceeding 1.5 × 10^6 atmos for aluminum and 3.5 × 10^6 atmos for copper, lead, and iron.

TABLE IV

Metal	P_m, 10^{10}d/cm^2	σ_m	C_m, km/sec
Aluminum	195.5 160.0	1.761 1.701	11.74 11.23
Copper	379.6 311.7	1.694 1.638	9.48 8.93
Lead	385.0 279.5	2.177 2.003	6.56 5.92
Iron	347.8 284.9	1.650 1.600	9.98 9.53

The experimental values of the sound velocities made it possible to find the dependence of the Mach number, $(D-U)/C$, and the tangent of the relaxation angle, $\tan\alpha$, on the degree of compression. The Mach number, as is well known, expresses the relative velocity of the relaxation wave and the shock wave. In its turn, $\tan\alpha$ defines the region of the shock wave which has been reached by the relaxation wave produced when the wave front meets a source of perturbation. Both these quantities can be calculated either from the propagation velocity C of the compressional waves, or from the velocity C* of longitudinal elastic waves. In this connection,

$$M^* = \nu M, \qquad \tan\alpha^* = [\nu^{-2}\tan^2\alpha + \sigma^{-2}(\nu^{-2}-1)]^{1/2}.$$

Note that when $\sigma = 1$ the magnitude of $\tan\alpha^*$ is finite and equal to $\sqrt{2(1-2\mu)/(1+\mu)}$, whereas $\tan\alpha$ drops to zero when $\sigma = 1$.

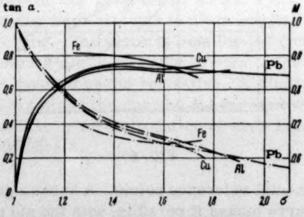

FIG. 7. Dependence of Mach number (dot-dash curves) and $\tan\alpha$ (full curves) on the degree of compression.

Figure 7 shows the experimental values of M and $\tan\alpha$ for the four metals. The values of $\tan\alpha$ for very high pressures lie in an extremely narrow interval from 0.66 to 0.73, regardless of the fact that these metals have different compressibilities. Even more striking is the fact that the same values of $\tan\alpha$ at high values of compression are also possessed by water, paraffin, and Plexiglas, according to measurements by the authors. Apparently it is possible to use the value $\tan\alpha \approx 0.7$ for very strong shocks waves in other materials also.

It is essential to know the values of the Mach numbers and relaxation angles in order to set up experiments for investigation of dynamic compressibilities in a proper manner. It has been shown above that during the collision of the striker with the test piece the Mach number, through the relation (5), determines how far the shock wave propagates up to the time when the relaxation wave reaches it; i.e., in other words it determines the permissible value of the base line for measuring D. In its turn, $\tan\alpha$ imposes conditions on the ratio between the diameter of the test sample d and its height h. In order to preserve a region near the axis of the sample cylinder which is not affected by lateral relaxation, where the shock wave parameters can be measured, the condition

$$d > 2h \tan\alpha^*$$

must be fulfilled.

For high degrees of compression and correspondingly high pressures, the amplitude of the relaxation shock wave becomes negligibly small in comparison with the pressures under study. This permits the use of the values M and $\tan\alpha$ in place of M* and $\tan\alpha^*$ in calculating sample dimensions. The above considerations were taken into account in setting up the experiments whose results are given in references 1 and 2.

5. THE ISENTROPIC COMPRESSIBILITY OF METALS

Let us generalize the results so far obtained by expressing the modulus of isentropic compression in the form of a power series:

$$K_s = \rho_0 C_\Gamma^2 = \sum_{k=1}^{n} b_k(\sigma-1)^{k-1}. \tag{7}$$

Integrating (7) leads to the function

$$I(\sigma) = \sum_{k=1}^{n} b_k k^{-1}(\sigma-1)^k. \tag{8}$$

At $P = 0$ and $\sigma = 1$, $I(\sigma)$ has a contact of the third order with the isentropic which passes through the origin of coordinates, and a second order contact with the Hugoniot adiabat. This circumstance determines the relations between the first three coefficients of (8) and the coefficients in the expression for the dynamic adiabatic:

$$P_\Gamma = \sum_{k=1}^{n} a_k(\sigma-1)^k.$$

It is easy to show that $b_1 = a_1$, $b_2 = 2a_2$, and $b_3 = 3a_3 - \frac{1}{2}\gamma_{p0}(a_1 + a_2)$, where γ_{p0} is the value of the Grüneisen coefficient for the lattice under nor-

TABLE V

Metal	b_k, 10^{10} d/cm²					
	k=1	2	3	4	5	6
Aluminum	73.1	305.4	194.8	—444	519	—106
Copper	137.0	543.4	266.8	4037	—11745	9650
Lead	41.4	203.4	184.2	248	—439	167
Iron	196.3	—157.0	3862.2	—5448	3077	—

mal conditions ($P = 0$; $T = 20°C$). The values of the coefficients a_1, a_2, and a_3 are borrowed from reference 6. For aluminum, copper, and lead γ_{p0} is taken equal to 2.09, 1.98, and 2.46 respectively. The coefficients b_4, b_5, and b_6 are chosen to fit the experimental data. The numerical values of the coefficients are shown in Table V. For iron, the chosen coefficients determine the isentropic modulus in the interval $1.20 < \sigma < 1.8$. These coefficients are not related to the parameters of iron under the initial conditions, since at $\sigma = 1.22$, according to Bancroft[2] there is a break in the compressibility curve caused by a phase transition.

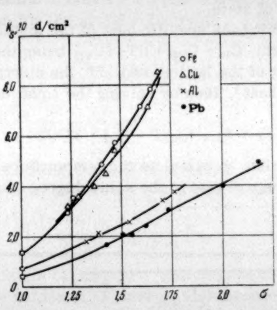

FIG. 8. Dependence of isentropic compression modulus K_s on the degree of compression. □ – initial value of $K_s = \rho_0 C_0^2$.

Figure 8 shows the variation of the isentropic modulus with the degree of shock compression. The isentropic modulus increases rapidly with the amplitude of the shock wave. Thus, for lead at $\sigma = 2.1$ and $P_\Gamma = 3.2 \times 10^{12}$ d/cm² it exceeds its initial value by more than ten times.

The experimental dependence of the speed of sound $C_\Gamma = \sqrt{K_s/\rho_0}$ on the degree of shock compression is shown in the left-hand side of Table VI for the four metals under investigation.

6. UPPER LIMIT OF THE CURVES OF "COLD" COMPRESSION. ESTIMATES OF THERMAL ENERGIES AND TEMPERATURES

Let us assume that the total pressure is the sum of the "cold" and thermal pressures: $P_\Gamma = P_X + P_T$. Inasmuch as $(\partial P_T/\partial \rho)_s > 0$, it is possible to establish unconditionally that $C_X^2(\sigma) < C_\Gamma^2(\sigma, T)$, where $C_X(\sigma)$ is the speed of sound at $T = 0$. Hence it follows that

$$P_x(\sigma) < \int_{\sigma_k}^{\sigma} \rho_0 C_\Gamma^2 d\sigma = I(\sigma) - I(\sigma_k) = I(\sigma, \sigma_k), \qquad (9)$$

where $\sigma_k = \rho/\rho_k$, and ρ_k is the density of the material at $T = 0°K$ and $P = 0$. Thus the function $I(\sigma, \sigma_k)$ appears as the upper limit of the possible positions of the cold compression curve. The relative positions of the dynamic adiabatic, the function $I(\sigma, \sigma_k)$, and the cold compression curve $P_X(\sigma)$ taken from reference 6, are illustrated in Figs. 9 and 10. Comparison shows that the curves $P_X(\sigma)$ are located below $I(\sigma, \sigma_k)$, in agreement with the above. It is characteristic of all the metals that $I(\sigma, \sigma_k)$ is considerably closer to $P_X(\sigma)$ than to P_Γ. The presence of a difference $P_\Gamma - I(\sigma, \sigma_k)$ was the first experimental evidence, ten years ago, of the large part played by thermal pressure in the shock compression of solid bodies.

TABLE VI

σ	C_Γ (km/sec) from ref. 7				C_Γ (km/sec), calculated*		
	Al	Cu	Pb	Fe	Al	Cu	Pb
1.1	6.23	4.70	2.37		6.16	4.67	2.34
1.2	7.17	5.53	2.83		7.04	5.46	2.80
1.3	8.03	6.36	3.29	6.91	7.87	6.21	3.24
1.4	8.81	7.12	3.74	7.83	8.67	6.98	3.70
1.5	9.57	7.83	4.18	8.70	9.52	7.80	4.15
1.6	10.34	8.59	4.60	9.54	10.31	8.73	4.60
1.7	11.10	9.67	4.98	10.40	11.04	9.80	4.98
1.8			5.34				5.32
1.9			5.67				5.58
2.0			5.98				5.82
2.1			6.26				6.13

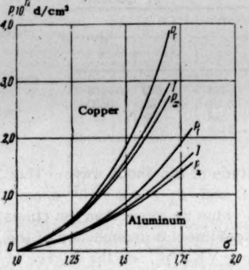

FIG. 9

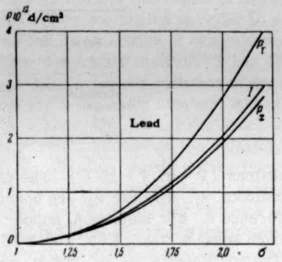

FIG. 10

The thermal energy of the shock compression is

$$E_{\text{T}}-E_0=\tfrac{1}{2}P_\Gamma(\sigma-1)/\rho_0\sigma-\int\limits_{\sigma_{\text{K}}}^{\sigma}(P_x/\rho_0\sigma^2)d\sigma. \quad (10)$$

Let us find the lower bound of the value $E_T - E_0$, by replacing P_X in the integrand of (10) by the function $I(\sigma, \sigma_k)$, considered as a first approximation to $P_X(\sigma)$. The thermal energies calculated in this way are shown in Table VII. They are very close to the true values, since for small degrees of compression P_Γ, P_X, and $I(\sigma, \sigma_k)$ are close together, while at high compressions the major role in (10) is played by the first term, with the result that the relative error due to the substitution of the function $I(\sigma, \sigma_k)$ for the true curve $P_X(\sigma)$ is very small. It should be emphasized that the upper limit of the position of the compression curve at the absolute zero of temperature and the values of the thermal energy have been obtained directly from experimental measurements of the dynamic and isentropic compressibilities, without appealing to any one form or another of the equation of state.

Assuming the specific heat of the metals to be of the form $C_V = C_{Vp} + \beta T$ (C_{Vp} being the specific heat of the lattice, and βT the electronic specific heat), then by solving the equation

$$E_{\text{T}}=E_0+C_{vp}(T-T_0)+\beta T^2/2 \qquad (11)$$

it is possible to calculate the temperature of the shock compression to the same degree of approxi-

TABLE VII

σ	1.1	1.2	1.3	1.4	1.5	1.6	1.7	1.8	1.9	2.0	2.1
Aluminum											
$E_{\text{T}}-E_0$, 10^{10} erg/g	0.043	0.164	0.449	1.027	2.086	3.817	6.331	9.616			
T, 10^3 deg K	0.34	0,48	0.78	1.40	2.46	4.18	6,47	9.25			
T from ref. 6, 10^3 °K	0.35	0.49	0.82	1.48	2.64	4.41	6.79	9.67			
γ_p					1.1	1.1	1.1	1.1			
γ_p from ref. 6					1.44	1.43	1,39	1.30			
Copper											
$E_{\text{T}}-E_0$, 10^{10} erg/g	0.026	0.103	0.315	0.752	1.514	2.882	5.069				
T, 10^3 deg K	0.36	0.56	1.11	2.20	4.29	7.24	11.97				
T from ref. 6, 10^3 °K	0.36	0,58	1.15	2.30	4.35	7.53	12.42				
γ_p					1.2	1,2	1.2				
γ_p from ref. 6					1,55	1.53	1.54				
Lead											
$E_{\text{T}}-E_0$, 10^{10} erg/g	0.042	0.067	0.127	0.265	0,505	0.884	1.432	2.139	3.005	3.985	5.138
T, 10^3 deg K	0.36	0.55	0.99	1.92	3.43	5.54	8,23	11.30	14.64	18.05	21.70
T from ref. 6, 10^3 °K	0,36	0.56	1.04	2.00	3.55	5.73	8.48	11.59	15.00	18.47	22.15
γ_p					1.5	1,4	1,3	1.25	1.15	1.0	0,9
γ_p from ref. 6					1.77	1.69	1,60	1.48	1.35	1.21	1,07

mation.* As can be seen from Table VII, the temperatures calculated in this way differ very little from the temperatures obtained in reference 6.

Replacing P_x by $I(\sigma, \sigma_k)$ makes it possible also to obtain a lower limit for the values of the Grüneisen coefficients, if the pressures on the Hugoniot adiabatic and the shock wave temperatures T, found above, are substituted into the equation for the dynamic adiabat:[6]

$$P_\Gamma = P_x + \rho_0\sigma C_{vp}\gamma_p[T - T_0 + E_0/C_{vp}] + \tfrac{1}{4}\rho_0\sigma\beta T^2. \quad (12)$$

Equation (12), apart from quantities which have already been mentioned, involves the quantities $\beta = \beta_0\sigma^{1/2}$, β_0 being the coefficient of electronic specific heat at $\sigma = 1$, and T_0 and E_0 being the temperature and internal energy under normal conditions. The observed γ_p are about 20 – 25% smaller than the values calculated in reference 6 (see Table VII).

Finally, let us use the measured sound velocity data, and the approximate values of T and γ_p which have been obtained, to determine the slopes of the dynamic adiabats. To this end we write the expression for the sound velocity at the Hugoniot adiabat:

$$\rho_0 C_\Gamma^2 = \frac{dP_x}{d\sigma} + \left[1 + \frac{d\ln\gamma_p}{d\ln\sigma} + \frac{C_{vp}\gamma_p}{C_{vp}+\beta T}\right]\rho_0 C_{vp}\gamma_p T + \frac{1}{2}\left[\frac{4\gamma_p C_{vp}+\beta T}{C_{vp}+\beta T} + \frac{1}{2}\right]\rho_0\beta T^2. \quad (13)$$

Differentiating (12) and eliminating $dP_x/d\sigma$ with the aid of (13), we arrive at the relation†

$$\frac{dP_\Gamma}{d\sigma} = \frac{\rho_0 C_\Gamma^2 - (P_\Gamma/2\sigma)[\gamma_p(1-\beta T/C_{vp}) + \beta T/2C_{vp}]}{1 - (\sigma - 1)[\gamma_p(1-\beta T/C_{vp}) + \beta T/2C_{vp}]/2}. \quad (14)$$

An estimate of $dP_\Gamma/d\sigma$ with the aid of the approximate values of T and γ_p by means of (14) is considerably more accurate than an estimate from the results of dynamic measurements because of the inevitable inaccuracies in recording the coordinates, which are sufficiently trustworthy to fix the location of the Hugoniot adiabat in the field of the P, σ diagram, but not its slope. In deriving the equation of state for the high pressure region, the original experimental data in references 6 and 8 are the results of dynamic compressibility measurements, in the form of an equation for the dynamic adiabatic $P_\Gamma = \sum_{k=1}^{n} a_k(\sigma-1)^k$. The equation of state obtained by this method, according to (14), can represent the actual slope of the isentropic correctly only in case the original analytical expression for the Hugoniot adiabatic describes the true values of the derivatives with sufficient accuracy over the entire length of the adiabat. Taking this fact into account made it possible to obtain, in reference 6, an equation of state suitable for calculating the speed of sound. As Table VI shows, the discrepancy between the experimental and calculated values of C_Γ does not exceed 2%.

The present work was begun under the initiative of Academician Ya. B. Zel'dovich in 1948. A number of valuable proposals were made by Corresponding Member of the Academy of Sciences (U.S.S.R.) E. I. Zababakhin. K. K. Krupnikov, B. N. Ledenev, and A. A. Bakanova contributed to the success of the investigation by their studies on the shock compression of metals, and also by taking part in the discussions. The authors received assistance on questions of apparatus and methods from Prof. V. A. Tsukerman and his coworkers, I. Sh. Model' and M. A. Kanunov. Individual measurements which contributed to the work were obtained by V. I. Borodulin. In carrying out the experiments, N. S. Tenigin, A. N. Kolesnikova, L. N. Gorelova, and M. S. Shvetsov took part, along with the authors.

To all these comrades the authors express their profound gratitude.

[1] Al'tshuler, Krupnikov, Ledenev, Zhuchikhin, and Brazhnik, JETP **34**, 874 (1958), Soviet Phys. JETP **7**, 606 (1958).

[2] Al'tshuler, Krupnikov, and Brazhnik, JETP **34**, 886 (1958), Soviet Phys. JETP **7**, 614 (1958).

[3] A. S. Dubovik, Ж. научн. прикл. фотогр. и кинематогр. (J. Sci. and Appl. Photogr. and Cinematog.) **2**, 293 (1957).

[4] J. J. Gilvarry, Phys. Rev. **102**, 317 (1956).

[5] P. V. Bridgman, Study of Large Plastic Deformations and Rupture (Russ. transl.) IIL (1955).

[6] Al'tshuler, Kormer, Bakanova, and Trunin, JETP **38**, 790 (1960), Soviet Phys. JETP **11**, 573 (1960).

[7] Bankroft, Peterson, and Minshall, J. Appl. Phys. **27**, 291 (1956).

[8] Walsh, Rice, McQueen, and Yarger, Phys. Rev. **108**, 196 (1957).

Translated by D. C. West
213

---

*In these calculations we have used the values given in reference 6 for E_0, T_0, C_{vp}, and β.

†The derivation of (14) given here is due to Yu. M. Shustov; in its general form, the relation between the Grüneisen coefficient and the derivatives of the two intersecting curves in the field of the P-ρ diagrams was previously given by K. K. Krupnikov.

SOVIET PHYSICS JETP VOLUME 11, NUMBER 4 OCTOBER, 1960

ENERGY SPECTRUM OF MESONS FROM NUCLEAR DISINTEGRATIONS PRODUCED BY 9-Bev PROTONS

Yu. T. LUKIN, Zh. S. TAKIBAEV, and E. V. SHALAGINA

Kazakh State University

Submitted to JETP editor October 28, 1959

J. Exptl. Theoret. Phys. (U.S.S.R.) **38**, 1074-1077 (April, 1960)

The energy of secondary shower particles in stars produced by 9-Bev protons in photographic emulsions was determined. The mean total energy of secondary π mesons has been found to be equal to (0.78 ± 0.10) Bev, and the mean transverse momentum equal to (0.19 ± 0.03) Bev/c. It has been found that (40 ± 5) % of the primary proton energy is spent in meson production.

In the study of the mechanism of interaction of high-energy particles and nuclei with nucleons and atomic nuclei, the spectrum of secondary relativistic particles, the majority of which are mesons, is of considerable interest. The knowledge of the energy spectrum of the mesons and, consequently, their average energy, makes it possible to compute the inelasticity coefficient and to solve the question as to whether one or another meson production theory is applicable.

For this purpose, we have determined the energy of secondary shower particles in stars produced by 9 Bev protons on emulsion nuclei. The energy was determined from multiple Coulomb scattering. Tracks (longer than 2.5 mm) for which the grain density g satisfied the condition $g \leq 1.4\, g_0$, where g_0 is the grain density in a primary proton track, were chosen for the measurements. Out of 101 stars, 62 stars were selected, in which 95 tracks suitable for scattering measurements were found.

Scattering was measured for three cells simultaneously, and the momentum of the particles was determined as in the experiment of Chasnikov et al.[1] according to the formula

$$p\beta = K t_1^{3/2} \left(\frac{64D_1^2 + D_4^2 - 16D_2^2}{D_1^2 D_4^2 - D_2^4} \right)^{1/2}, \qquad (1)$$

where D_1, D_2, and D_4 are second differences of coordinates on the cells with the length of t_1, $2t_1$, and $4t_1$ respectively, and K is the scattering constant of the emulsion, whose numerical values for the various cell lengths are taken from the article of Fichtel and Friedländer.[2] Equation (1) was obtained under the assumption that the measured second difference of the ordinates

$$D^2 = D_{\text{coul}}^2 + n^2, \qquad (2)$$

where $n = \sqrt{D_f^2 + D_n^2}$ is the sum of the "false" scattering and of the measurement "noise." Moreover, the value of n for cell t_1 is then determined from the equation (see reference 1)

$$n_1 = (8D_1^2 - D_2^2) / \sqrt{64D_1^2 + D_4^2 - 16D_2^2}. \qquad (3)$$

The correctness of the method of measurement used was checked on the tracks of primary protons, for which the sum n_1 of "false" scattering and of "noise," as determined according to Eq. (3), was compared with the value of n determined according to Eq. (2). In the latter case, D_{Coul} corresponded to an energy of 9 Bev. It was found that, for all primary protons, both equations give the same values of n coinciding with the values of n obtained from the tracks of secondary particles.

Using the above method, which we call the "multiple-cell method," we found the energy of primary protons to be (9.0 ± 0.8) Bev. This provides the basis for considering the multiple-cell method useful for excluding the "false" scattering and "noise" in the measurements of the scattering of relativistic particles. The measurements have also shown that "false" scattering for the type of emulsion used varies with the cell length (in the range of cell lengths from 0.25 mm to 2 mm) according to the law t^x, where $x = 1$.

The particles were identified from the well-known curves of the variation of ionization with $p\beta$.[3] In all doubtful cases, the track was identified as a meson or a proton track following the method of Kalbach et al.[3] As a result of the analysis, it was found that 60 tracks belong to π mesons and 35 to protons.

The energy spectrum of investigated π mesons in the laboratory system of coordinates is shown in Fig. 1. The x axis represents the kinetic energy,

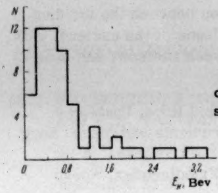

FIG. 1. Energy spectrum of π mesons in the laboratory system.

and the y axis the number of mesons per given energy interval. The mean meson kinetic energy is (0.88 ± 0.11) Bev.

The measurements of scattering and grain density along the track showed that all protons were emitted at angles $\theta \leq 25°$. In this range of angles, for particles whose momentum was measured, the ratio of the number of π mesons to the number of protons was found to be equal to 1.32. In the following discussion, it is assumed that, for angles $\theta \leq 25°$, such a ratio is correct for all shower particles, including also those which could not be identified because of the small track length. It was found that the total number of relativistic particles in that angle interval was equal to 151 for 62 stars. Hence, it follows that 65 tracks belonged to fast protons (on the average 1.05 protons per star).

The angular distribution of mesons whose momentum has been determined differs from the angular distribution of all shower particles in the same stars. From the angular distribution of all shower particles, the contribution due to protons has been excluded. It was assumed that, in each angle interval, the ratio of the number of π mesons to the number of protons is the same as for particles with measured momentum. Using this corrected angular distribution for π mesons, and the variation of the kinetic energy with the angle of emission as determined by us, it was found that the mean total energy of mesons is equal to (0.78 ± 0.10) Bev.

If we take into account that the mean number of secondary shower particles in stars selected for measurements is equal to 4.14, and that there are 1.05 protons per star, then the number of charged and neutral π mesons equals 4.6. The energy fraction of the primary protons spent for meson production is then equal to (40 ± 5)%. This value is in agreement with the results of references 4 — 7, within the limits of experimental errors.

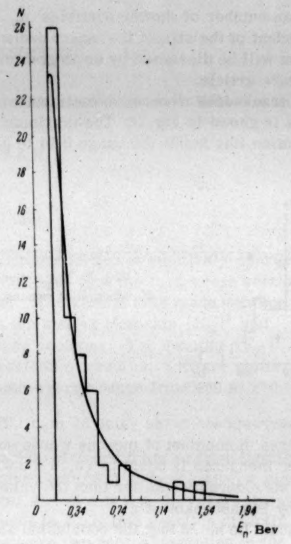

FIG. 2. Energy spectrum of π mesons in the c.m.s.

The differential energy spectrum of mesons in the c.m.s. is shown in Fig. 2. The x axis represents the total meson energy, and the y axis the number of mesons in a given energy range. The energy is recalculated from the laboratory system to the c.m.s. under the assumption of a nucleon-nucleon interaction and of an isotropic angular distribution of produced particles in the c.m.s. The histogram shows the experimental results. The solid line represents the energy spectrum for nucleon-nucleon interactions, calculated according to the Heisenberg theory and normalized for the total number of investigated particles. The maximum in the experimentally-obtained distribution occurs for mesons with an energy of about 0.25 Bev, and the mean meson energy is equal to (0.38 ± 0.05) Bev, which is in agreement both with the results obtained for nucleon-nucleon interactions at an energy of 9 Bev,[6] and with the results of Fretter and Hansen[8] pertaining to the interaction of nucleons with light nuclei, the mean energy of the primary particles being of the order of 100 Bev. It can be seen from Fig. 2 that the experimental spectrum of mesons produced in the interaction of protons with the emulsion nuclei agrees with the theoretical spectrum calculated under the assumption of a nucleon-nucleon interaction. We find these results very interesting. They may clearly indicate the fact that almost all mesons are produced in a single nucleon-nucleon interaction. The same result is reached from an analysis of data presented in references 6 and 7, from which it follows that the mean number of shower particles n_s is almost independent of the size of the target nucleus. This problem will be discussed by us in greater detail in a future article.

The transverse momentum distribution of the mesons is shown in Fig. 3. The maximum of this distribution lies inside the range 0.11 to 0.16 Bev/c, which corresponds to the value of $m_\pi c$. The mean transverse momentum of mesons whose scattering has been measured is equal to (0.19 ± 0.03) Bev/c, i.e., is considerably smaller than the value obtained by Barashenkov et al.[7]

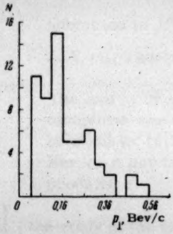

FIG. 3. Transverse momentum distribution of mesons.

It should be noted that the conclusion about the cascade character of the nucleon-nucleus interaction[7] is in agreement with the results obtained by us earlier[9] in the analysis of the energy spectrum of protons with ionization from 1.4 g_0 to 6.8 g_0 from stars produced by cosmic-ray particles with a mean energy on the order of 10 Bev. The development of the nucleon cascade inside the nucleus does not exclude the possibility that all mesons are produced in a single interaction between the incident nucleon and one of the nucleons of the nucleus, with the ensuing collisions between nucleons and mesons possibly being elastic.

---

[1] Chasnikov, Takibaev, and Boos, Приборы и техника эксперимента (Instruments and Meas. Engg.) 1, 54 (1959).

[2] C. Fichtel and M. W. Friedlaender, Nuovo cimento 10, 1032 (1958).

[3] Kalbach, Lord, and Tsao, Phys. Rev. 113, 330 (1959).

[4] Bayatyan, Gramenitskiĭ, Nomofilov, Podgoretskiĭ, and Skrzypczak, JETP 36, 690 (1959), Soviet Phys. JETP 9, 483 (1959).

[5] Zhdanov, Markov, Strel'tsov, Tret'yakova, Cheng, and Shafranova, JETP 37, 611 (1959), Soviet Phys. JETP 10, 433 (1960).

[6] V. I. Veksler, Paper presented at the 9th Conference on High-Energy Particle Physics, Kiev, 1959.

[7] Barashenkov, Belyakov, Wang, Glagolev, Dalkhazhav, Kirillova, Lebedev, Mal'tsev, Markov, Tolstov, Tsyganov, Shafranova, and Yao, Joint Institute for Nuclear Research, preprint P-331, 1959.

[8] V. Fretter and I. Hansen, Paper presented at the International Cosmic-Ray Conference, Moscow, 1959.

[9] Yu. T. Lukin and Zh. S. Takibaev, Вестник АН КазССР (News of the Academy of Science of Kazakh S.S.R.) 1, 78 (1959).

Translated by H. Kasha
214

SOVIET PHYSICS JETP VOLUME 11, NUMBER 4 OCTOBER, 1960

PHOTOPRODUCTION OF CHARGED PIONS NEAR THRESHOLD

M. I. ADAMOVICH, É. G. GORZHEVSKAYA, V. G. LARIONOVA, V. M. POPOVA, S. P. KHARLAMOV, and F. R. YAGUDINA

P. N. Lebedev Physics Institute, Academy of Sciences, U.S.S.R.

Submitted to JETP editor November 4, 1959

J. Exptl. Theoret. Phys. (U.S.S.R.) 38, 1078-1083 (April, 1960)

We have measured the differential cross section for the photoproduction of positively-charged π mesons on hydrogen at photon energies 153 — 175 Mev. We also give the total cross section for the photoproduction of negative π mesons on deuterium. A comparison is made between the experimental and theoretical values for the squares of the matrix elements $|K_p|^2$ and $|K_n|^2$ for the photoproduction of π^+ and π^- mesons on free nucleons. The quantity $|K_n|^2$ is compared with the Panofsky ratio and with the meson-nucleon interaction S-phase shifts. The value of the ratio σ^-/σ^+ has been obtained in the photon-energy range from 153 to 175 Mev.

INTRODUCTION

A large number of experiments have been done on the photoproduction of charged π mesons on nucleons. In most of these the quantity measured was the cross section for meson production at large photon energies. Up to the present time, no measurements have been made on the differential cross section for the photoproduction of π mesons for photon energies in the range 150 to 170 Mev. At these energies, only the total cross section for the photoproduction of positively charged π mesons on hydrogen has been measured.[1] The photoproduction of negative π mesons on deuterium has been studied with nuclear emulsions doped with heavy hydrogen.[2]

A comparison of the experimental data with the results of theoretical calculations[3] has yielded the squares of the matrix elements for the photoproduction of π^- mesons on free neutrons for photon energies in the 153 — 188 Mev range. Extrapolation of these data to lower energies leads to a value for the square of the matrix element at threshold. The method used was that employed by Beneventano et al.[4] to find the threshold value for the square of the matrix element for the photoproduction of π^+ mesons on protons. It is based on an empirical rule valid in the 170 — 250 Mev energy range, and also on the experimental data on photoproduction near threshold obtained by Leiss et al.[1] In a succeeding paper these authors have noted that their earlier results were wrong.[5]

In principle, the threshold value for the square of the matrix element for photoproduction of π^- mesons can be obtained from an investigation of the radiative capture of slow negative π mesons by protons, $\pi^- + p \rightarrow n + \gamma$. However, it would be very difficult to study this reaction directly, because there are two neutral particles in the final state. For this reason it is customary to measure the Panofsky ratio, i.e., the ratio of the probability of scattering with charge exchange to that of radiative capture of negative π mesons. It is uniquely connected with the threshold value of the square of the matrix element for photoproduction of π^- mesons on neutrons, $|K_n|^2$, through the limit of the quantity $|\alpha_3 - \alpha_1|/\eta$ as $\eta \rightarrow 0$. Here α_1 and α_3 are the S-phase shifts for the scattering of mesons in the states with isotopic spin $1/2$ and $3/2$, respectively, and η is the meson momentum in the center-of-mass system.

As is well known,[3] the threshold value of $|K_n|^2$, obtained by extrapolation or from the difference between the S-phase shifts $|\alpha_3 - \alpha_1| = 0.28\eta$,[6] disagrees with the directly-measured Panofsky ratio.[7,8] Baldin[3] attempted to explain this discrepancy by assuming the existence of a neutral π_0^0 meson, an isotopic spin singlet. However, it was later shown experimentally that an isotopic scalar meson does not exist. Cini et al.[9] then pointed out that in the extrapolation of Beneventano et al.[4] no account was taken of the direct interaction between the electromagnetic field and the meson current. This contribution to the amplitude for meson photoproduction is described by the so-called "retarded term" and it has a significant effect in the analysis of the experimental data on the photoproduction of charged mesons near threshold. In particular, this "retarded term" contradicts the extrapolation employed and can improve the agreement between data on the photoproduction of π mesons and the Panofsky ratio. To check these aspects of meson theory, it is necessary to measure the cross section for the photoproduction of π^+ mesons near threshold and to improve the statistical accuracy of measurements on the cross section for photoproduction of π^- mesons on deuterium. Good measurements of these quantities would also lead to a value for the ratio of probabilities for production of π^- and π^+ mesons on free nucleons near threshold.

EXPERIMENT

The purpose of the experiment was to find the cross sections for the photoproduction of charged π mesons near threshold:

$$\gamma + p \rightarrow \pi^+ + n, \tag{1}$$

$$\gamma + n \rightarrow \pi^- + p. \tag{2}$$

These reactions were investigated on the synchrotron of the Academy of Sciences Physis Institute. The methods used to study the reaction (1) depended on the energy range. To measure the differential cross section of this reaction for photon energies in the 153 — 161 Mev range, a polyethylene film of thickness 0.00905 g/cm^2 was used as a target. Data for hydrogen were obtained by subtracting the background due to photoproduction of π^+ mesons on carbon. To do this, we irradiated a carbon target of thickness 0.0129 g/cm^2 simultaneously with the polyethylene film. This technique was feasible because the Coulomb field inside the carbon nucleus sharply inhibits the production of low energy π^+ mesons. Since we were interested in slow π^+ mesons, thin films had to be used, which eliminated the necessity for making corrections for scattering and energy loss of mesons in the target.

The photon beam was obtained by bremsstrahlung of 263-Mev electrons. The mesons from the target were detected by NIKFI K-400μ nuclear emulsions. Both the emulsions and the targets were in vacuum. The entrance window (100μ Al) was 1 m from the targets and the plates. A magnetic field inside the vacuum chamber was used to filter out electrons from the beam. Lead and carbon blocks shielded the chamber from externally scattered γ rays.

The plates were scanned twice. The average efficiency for detecting mesons was 90%. The total number of π^+ mesons was found by counting the number of the $\pi \rightarrow \mu$ decays for which the μ-meson track ended in the emulsion. The energy of each π^+ meson was found by measuring its residual range; the other quantity measured was the angle between its direction of motion and the photon beam.

The geometry of the experiment was such that the plates would register mesons in the energy range 0.5 to 6 Mev and at angles to the photon beam ranging from 60° to 120° in the laboratory frame of reference. To find the cross section in the center-of-mass system, all the events were sorted out into energy and angle intervals. The values of the cross section were obtained from mean values taken in these intervals.

The table shows the cross section for photon energies in the ranges 152.9 — 158.3 Mev and 158.3 — 161 Mev, and for a c.m.s. mean angle $\theta = 120°$.

To measure the differential cross section of reaction (1) at higher photon energies, the target used was liquid hydrogen in a foamed polystyrol vessel. The π^+-meson detectors were layers of unbacked type NIKFI P-400μ emulsion. The placing of the emulsions depended on the π meson energy.

To detect mesons produced by photons of energy 160 — 165 Mev, the emulsion stack was placed in a small vacuum chamber in the vessel with the hydrogen. The entrance window of the chamber was a brass foil 30μ thick, 6 mm from the axis of the beam. The average angle between the mesons detected and the beam was 78° in the laboratory frame of reference. The target was irradiated by a photon

E_γ, Mev	$10^{30} \frac{d\sigma^+}{d\Omega}$ (120°), cm^2/sr (c.m.s.)	$10^{29}\, \sigma_d^-$, cm^2 (l.s.)	$f^2_{\pi^+}$	$f^2_{\pi^-}$
150		1.07 ± 0.25		
156.5	3.4 ± 0.6	4.01 ± 0.57	0.078 ± 0.013	0.077 ± 0.011
159.5	4.2 ± 1.7			
162.5	6.7 ± 1.5		0.089 ± 0.011	
163.5		6.97 ± 0.79		0.082 ± 0.009
167.5	5.94 ± 0.97 ($\theta = 103°$)		0.081 ± 0.009	
170.5		8.98 ± 1.09		0.087 ± 0.01
172.5	7.50 ± 0.58		0.090 ± 0.007	
181		6.68 ± 0.69 ($E_\pi \leqslant 30$ Mev)		0.085 ± 0.009

beam obtained by stopping 180-Mev electrons.

To measure the differential cross section in the 165 — 175 Mev energy range, the mesons were detected by emulsions placed right in the liquid hydrogen, 2 cm from the axis of the photon beam. The mean angle between the π mesons and the beam was 90°. In this case the energy spectrum of the photons had a maximum at 200 Mev. The plates were scanned and measured as described above.

The table gives the measured values of the differential cross section for the photoproduction of π^+ mesons on hydrogen in the center-of-mass system for mean photon energies 162.5, 167.5, and 172.5 Mev.

In all experiments on reaction (1), the photon energy was measured with an ionization chamber calibrated against the thick-walled graphite chamber used to measure photon intensities.[2]

Data on reaction (2) were obtained by studying the reaction

$$\gamma + d \rightarrow \pi^- + p + p \tag{3}$$

using nuclear emulsions doped with deuterium and irradiated in the photon beam of the synchrotron of the Academy of Sciences Physics Institute. The experiment has been described in detail previously.[2] For the present investigation, the statistical accuracy was increased and several non-essential improvements were made. In particular, the following were taken into account: 1) the detection efficiency (96%)[2]; 2) the increase in the concentration of ordinary water in the heavy water after each doping of the emulsion (this increased the calculated cross sections by 5%); 3) the low efficiency with which the upper 20 and bottom 100μ of the doped emulsion registered the reaction studied.[2]

The table shows the total cross section for reaction (3) for photons in the energy intervals 153 — 160, 160 — 167, 167 — 174 and 174 — 188 Mev. The statistical accuracy here is significantly higher for the more energetic photons, than that previously quoted.[4]

DISCUSSION OF THE RESULTS

Figure 1 shows the experimentally derived values for the squares of the matrix element for photoproduction of π^+ mesons:

$$|K_p|^2 = (\pi / W)\, d\sigma^+ / d\Omega.$$

As usual,

$$W = \eta\omega / (1 + \omega / M)(1 + \nu / M),$$

where η and ω are the c.m.s. momentum and total energy of the meson, ν is the photon energy, and M is the nucleon mass. The same figure shows the experimental data obtained by Barbaro et al.[10] with the Illinois betatron.

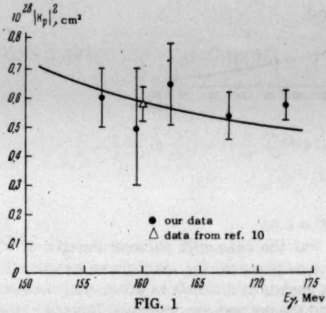

FIG. 1

The solid curve on the figure is the theoretical curve $|K_p|^2 = (\pi/W)\, d\sigma^+/d\Omega$ for photoproduction of π^+ mesons near threshold (taking into account S states and the direct π-meson photo effect:

$$\frac{d\sigma^+}{d\Omega}\frac{\pi}{W} = \frac{2\pi e^2 f^2}{\mu^2}\frac{1}{\nu\omega}\left[1 - \frac{\eta^2}{2\nu^2}\frac{\sin^2\theta}{(1-\eta\cos\theta)^2} - \frac{g_n + g}{M}\,\omega\left(1 - \frac{\eta^2}{2}\right)\right], \tag{4}$$

where μ is the meson mass, and the meson-nucleon coupling constant f^2 is taken to be 0.08.

As is evident from the figure, in the photon energy range 155.6 — 172.3 Mev the experimental data agree with the supposition that the π^+ meson is formed primarily in an S state. The statistical accuracy of the experimental data is not great enough to distinguish between the solid curve and a constant value for $|K_p|^2$, so it is difficult to conclude whether the experimental data agree with the theory or not. However, if we compare the old Illinois data[4] in the 170 — 250 Mev energy range with Barbaro's data[10] and our own, then it appears that in the 156 — 250 Mev range the experimental values of $|K_p|^2$ increase with decreasing photon energy. This agrees qualitatively with the theoretical prediction, but it is too early to speak of quantitative agreement.

The data on reaction (3) and Baldin's calculations yield the total cross section for photoproduction of π^- mesons on neutrons:

$$\sigma_n = \frac{1}{\pi}\,|K_n|^2\, W,$$

where $|K_n|^2$ is the square of the matrix element. Figure 2 shows the experimental values of $|K_n|^2$. The solid curve on this figure is a theoretical one, calculated from the formula

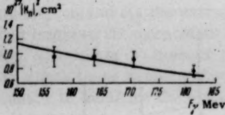

FIG. 2

$$|K_n|^2 = 4\pi^2 \frac{2e^2f^2}{\mu^2}\frac{1}{\nu\omega}\Big[1-\Big(\frac{1}{2\nu^2\eta}\ln\frac{1+\eta}{1-\eta}-\frac{1}{\nu^2}\Big) + \frac{g_n+g_p}{M}\,\omega\Big(1-\frac{\eta^2}{2}\Big)\Big] \qquad (5)$$

with $f^2 = 0.08$.

As was the case with photoproduction of π^+ mesons on protons, the inadequate statistical accuracy makes it difficult to discuss agreement between theory and experiment. However, the experimental points do tend to follow the theoretical curve, but do not contradict a constant $|K_n|^2$ in this energy range. At the same time, an extrapolation to the threshold with $|K_n|^2 = \text{const}$ leads to a contradiction between the threshold value of $|K_n|^2$ and the Panofsky ratio. If the experimental data in Fig. 1 were extrapolated to the threshold with formula (5), then the threshold value of $|K_n|^2$ would become 1.16×10^{-27} cm², which agrees with the measured value of the Panofsky ratio.[7,8] The departure from linearity of the S phase as a function of meson momentum is taken into account.[9] It is clear that to really check the theory it is necessary to have experimental data at energies close to threshold and high statistical accuracy. The same applies to the photoproduction of π^+ mesons on protons.

The table shows the meson nucleon coupling constant f^2 obtained from hydrogen (column 4) and deuterium (column 5). As is clear from the table, the values of the constant agree with each other within experimental error. In particular, the mean value of f^2 found from the experiment on the photoproduction of π^+ mesons on protons is 0.085 ± 0.005, while the mean value found from negative mesons is 0.083 ± 0.005. The uncertainties quoted are statistical.

Using the experimental value of the constant for π^+ and π^- mesons, we obtain the following value for the ratio σ^-/σ^+ in the 153 — 175 Mev photon-energy range.

$$\sigma^-/\sigma^+ = 1.3 \pm 0.15.$$

This value of the ratio of the cross sections for formation of negative and positive π mesons on free nucleons agrees well with the theoretical prediction.[11]

In an earlier paper[2] we quoted a value of 1.34 for the ratio σ^-/σ^+ at photon energy very near the threshold for production of π mesons. This was obtained by extrapolating to the threshold the data of Beneventano et al.[4] regarding the photoproduction of π^+ mesons on hydrogen and our data on π^- mesons, the extrapolations being made according to the same law. The value of σ^-/σ^+ quoted in the present paper is free of uncertainties in the calibration of the photon beam. It should be noted that the threshold value of σ^-/σ^+ does not depend on the nature of the extrapolation.

In conclusion, the authors express their gratitude to A. M. Baldin for useful discussions, to I. N. Usova and Yu. I. Krutov for help in measuring the beam intensity, and to É. I. Bakhtinskaya, L. G. Samokhvalova, I. D. Bannikova, L. I. Ivanova, V. A. Kuznetsova, N. P. Nayashkova, N. G. Shvedova, V. D. Paramonova, R. G. Dikaya, R. A. Kozlova, and L. G. Kasparova for scanning the emulsions.

---

[1] Leiss, Robinson, and Penner, Phys. Rev. 98, 201 (1955).

[2] Adamovich, Kyz'micheva, Larionova, and Kharlamov, JETP 35, 27 (1958), Soviet Phys. JETP 8, 21 (1959).

[3] A. M. Baldin, Nuovo cimento 8, 569 (1958).

[4] Beneventano, Bernardini, Carlson-Lee, Stoppini, and Tau, Nuovo cimento 4, 323 (1956).

[5] J. E. Leiss and S. Penner, Bull. Am. Phys. Soc. 4, 273 (1959).

[6] Nagle, Hildebrand, and Plano, Phys. Rev. 105, 718 (1957).

[7] Cassels, Fidecaro, Wetherell, and Wormald, Proc. Phys. Soc. (London) A70, 405 (1957).

[8] Kuehner, Merrison, and Tornabene, Proc. Phys. Soc. (London) A73, 545 (1959).

[9] Cini, Gatto, Goldwasser, and Ruderman, Nuovo cimento 10, 243 (1958).

[10] Barbaro, Goldwasser, and Carlson-Lee, Bull. Am. Phys. Soc. 4, 23 (1959).

[11] Chew, Goldberger, Low, and Nambu, Phys. Rev. 106, 1345 (1957).

Translated by R. Krotkov
215

SOVIET PHYSICS JETP VOLUME 11, NUMBER 4 OCTOBER, 1960

THE $Al^{27} \to Na^{24}$, $Co^{59} \to Mn^{56}$, *AND* $P^{31} \to Na^{24}$ *REACTIONS IN THE 260-Mev GAMMA-RAY ENERGY RANGE*

A. N. GORBUNOV, F. P. DENISOV, and V. A. KOLOTUKHIN

P. N. Lebedev Physics Institute, Academy of Sciences, U.S.S.R.

Submitted to JETP editor November 4, 1960

J. Exptl. Theoret. Phys. (U.S.S.R.) **38**, 1084-1087 (April, 1960)

The dependence of the yield of a number of photonuclear reactions on the peak bremsstrahlung energy from the synchrotron was measured by the induced-radioactivity method. The differential cross sections were computed from the yield curves by the "photon-differences" method. The form of the energy dependence of the effective cross sections indicates that photonuclear reactions at photon energies above 60 – 80 Mev proceed mainly without the formation of an intermediate nucleus.

THE purpose of the present experiments was to obtain information about the character of the interaction of photons and nuclei in the 30- to 260-Mev energy range. Three photonuclear reactions, giving rise to radioactive isotopes, were investigated:

$$Al^{27} \to Na^{24}, \quad Co^{59} \to Mn^{56}, \quad P^{31} \to Na^{24}.$$

The experiments were performed with the 260-megavolt synchrotron of the Physical Institute of the Academy of Sciences. The peak energy of the synchrotron is known within ± 2%. Intermediate values of the energy were established with the same precision. The targets were prepared from sufficiently pure substances, so that the reactions with the impurities could be neglected. The activity of the samples was measured with three identical 4π arrays of beta counters. The efficiency of the arrays was monitored in the course of the experiment against a radium standard within a precision of ± 1%. The radioactive isotopes were identified by their half-lives.

The Al, P, and Co samples were simultaneously irradiated within an identical geometry. To introduce corrections for the nonuniformity of the intensity, its time distribution during irradiation was measured by an ionization chamber with a flux integrator. The intensity integrated over the time of irradiation (~ 40 minutes) was measured by means of the $C^{12}(\gamma, n)C^{11}$ reaction, whose absolute yield was measured as a function of the peak bremsstrahlung energy up to 260 Mev by Barber et al.[1] In all, we carried out 48 irradiations for 15 values of the synchrotron energy. The spread of the irradiation results, carried out at the same nominal energy value but at different times, did not exceed the experimental error, which was determined mainly by the statistical accuracy of each reading and by the energy instability of the synchrotron.

The yield of the reaction investigated

$$B_x(E_0) = \int_0^{E_0} \sigma_x(E_0)\,\eta(E,\ E_0)\,dE$$

is expressed in terms of the yield of the $C^{12}(\gamma, n)C^{11}$ reaction

$$B_C(E_0) = \int_0^{E_0} \sigma_C(E_0)\,\eta(E\ \ E_0)\,dE$$

and in terms of the quantities measured during the experiment as follows:

$$B_x(E_0) = B'_x(E_0)\,B_C(E_0),$$

where E_0 is the peak value of the bremsstrahlung energy spectrum, E is the energy of the photon, $\sigma_X(E)$ is the effective cross section of the investigated reaction, $\sigma_C(E)$ is the effective cross section of the $C^{12}(\gamma, n)C^{11}$ reaction, $\eta(E, E_0)$ is the spectrum of the bremsstrahlung and $B'_X(E_0)$ is the ratio of the number of active nuclei, produced as a result of the investigated reaction and the $C^{12}(\gamma, n)C^{11}$ reaction with carbon, reduced to equal numbers of irradiated nuclei. We obtained this ratio from measurements of the activities of the investigated samples by introducing corrections for the decay, the registration efficiency, and for the differing number of irradiated nuclei.

The values of $B_X(E_0)$ and $B'_X(E_0)$ are given in Fig. 1. We have plotted the errors connected with the energy instability of the synchrotron along the abscissa, and the statistical errors along the ordinate axis. The precision with which the absolute values of the yields were determined is

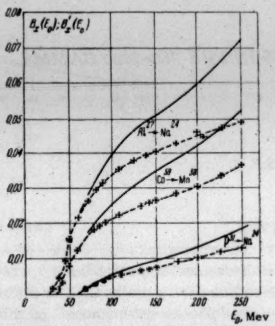

FIG. 1. Active yields of the $Al^{27} \rightarrow Na^{24}$, $Co^{59} \rightarrow Mn^{56}$, and $P^{31} \rightarrow Na^{24}$ reactions as a function of the peak bremsstrahlung energy. The values of $B'_X(E_0)$ are given by the continuous curves, of $B_X(E_0)$ – by the dashed curves [the values of $B_X(E_0)$ are given in arbitrary units].

about 20%. The main part of the errors is connected with the inaccuracy in determining the absolute β activities of the samples.

The differential effective cross sections σ were calculated from the yield curves by the "photon differences" method.[2] The results obtained are shown in Figs. 2 – 4.

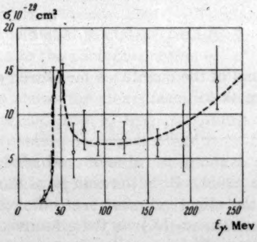

FIG. 2. Effective cross section for the $Al^{27} \rightarrow Na^{24}$ reaction.

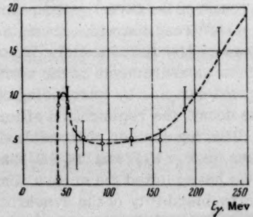

FIG. 3. Effective cross section for the $Co^{59} \rightarrow Na^{24}$ reaction.

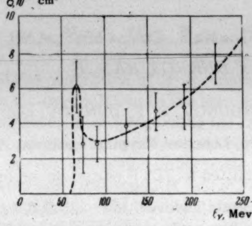

FIG. 4. Effective cross section for the $P^{31} \rightarrow Na^{24}$ reaction.

The reactions $Al^{27} \rightarrow Na^{24}$ and $Co^{59} \rightarrow Mn^{56}$ can result from three different processes [(γ, He^3), (γ, Dp), and $(\gamma, 2pn)$] whose thresholds, calculated with account of the Coulomb barrier, are 23, 29, and 31 Mev for Al^{27}, and 34, 41, and 43 Mev for Co^{59}, respectively. Since the registration of the corresponding activities of Al and Co begins at energies around the threshold of the (γ, Dp) and $(\gamma, 2pn)$ reactions, it is obvious that, of the three, the two latter processes play the most substantial part in both elements.

The reaction $P^{31} \rightarrow Na^{24}$ is the result of a large number of processes of which the energetically most convenient (γ, Be^7) has a threshold of about 40 Mev; the energetically least convenient process $(\gamma, 4p3n)$ has a threshold of about 90 Mev. The experimental threshold of the Na^{24} yield from P^{31} is in the neighborhood of 60 Mev. This indicates that in this reaction processes involving emission of bound nucleons, i.e., of the type $(\gamma, He^4, 2pn)$, play a substantial part.

However, regardless of the relation between the discussed processes, the effective cross sections for the production of Na^{24} and Mn^{56} should have a resonance character if the reactions proceed with the formation of an intermediate nucleus.[4] The presence of various processes should only lead to an increase in the resonance width. The experimentally-obtained effective cross sections do indeed have a maximum in the energy range of ~ 10 Mev above threshold. However, they do not fall off to zero after the maximum, as expected according to the intermediate-nucleus model, but after reaching approximately half their maximum value, they remain constant in the Al and Co reactions, and even increase in the P reaction. This fact can be explained in two ways. One can assume that at large energies interactions involving the formation of an intermediate nucleus play the main part, but that the effective cross sections of the investigated reactions remain constant, owing to the increase in the effective cross section for photon absorption. However, available experimental data indicate that the effective cross sections for photon absorption by nuclei in the 60- to 130-Mev energy range increase very slowly,[5] and consequently such an explanation is unsatisfactory. The following explanation is more probable. At photon energies exceeding 60 Mev the interaction between photons and nuclei does not lead to the formation of an intermediate nucleus. The energy and momentum of the photon are absorbed not by the nucleus as a whole, but by a group of nucleons which leaves the nucleus, transferring to it only a part of the energy. One such mechanism is probably the much-discussed "quasi-neutron mechanism."[6] In such an interaction it may turn out that the probability of transferring to the nucleus a given portion of energy varies little with the energy of the incident particle, and consequently the effective cross section for the production of a given isotope will also vary little.

Thus, the variation of the effective cross sections which we have obtained permits us to assume that at energies above 60 — 80 Mev the interaction of photons with nuclei proceeds mainly without the formation of an intermediate nucleus, via photon absorption by a group of intranuclear nucleons. This conclusion and also the experimental results are in agreement with those obtained in analogous experiments with heavy particles.[7]

The authors thank Professor P. A. Cerenkov for his interest in this work, and the synchrotron crew for the high quality of their work.

---

[1] Barber, George, and Reagan, Phys. Rev. **98**, 73, (1955).

[2] L. Katz and A. G. W. Cameron, Canad. J. Phys. **29**, 518 (1951).

[3] L. I. Schiff, Phys. Rev. **83**, 252 (1951).

[4] J. M. Blatt and V. F. Weisskopf, Theoretical Nuclear Physics, Wiley, New York 1952.

[5] D. M. Lebedev, Dissertation, Physics Institute, U.S.S.R. Academy of Sciences, 1952.

[6] J. S. Levinger, Phys. Rev. **84**, 43 (1951).

[7] N. M. Hintz and N. F. Ramsey, Phys. Rev. **88**, 19 (1952).

Translated by Z. Barnea
216

SOVIET PHYSICS JETP VOLUME 11, NUMBER 4 OCTOBER, 1960

PIEZOMAGNETISM IN THE ANTIFERROMAGNETIC FLUORIDES OF COBALT AND MANGANESE

A. S. BOROVIK-ROMANOV

Institute of Physical Problems, Academy of Sciences, U.S.S.R.

Submitted to JETP editor November 6, 1959

J. Exptl. Theoret. Phys. (U.S.S.R.) **38**, 1088-1098 (April, 1960)

A special magnetic balance and press were constructed to observe piezomagnetism experimentally. In agreement with theoretical predictions, piezomagnetic moments m_l^p were found to appear in CoF_2 and MnF_2 on applying shear stresses σ_{ik}. The values of the piezomagnetic modulus are $\sim 10^{-3}$ gauss $(kg/cm^2)^{-1}$ for CoF_2 and 10^{-5} gauss $(kg/cm^2)^{-1}$ for MnF_2. A detailed analysis of the results obtained is made in terms of the thermodynamic theory. Together with the piezomagnetic moment perpendicular to the direction of sublattice magnetization, which is equivalent to the well-studied weak transverse ferromagnetism, a moment was observed parallel to the sublattice magnetization, which is equivalent to a weak longitudinal ferromagnetism not previously observed.

1. INTRODUCTION

THE possibility in principle of a piezomagnetic effect has long been discussed. As early as 1928, Voight[1] considered all the crystallographic classes in which, according to his view, a piezomagnetic effect was possible from symmetry considerations, i.e., the appearance of a spontaneous magnetic moment on applying elastic stresses. However, his treatment was erroneous, since he did not take into account the additional symmetry element, R, for magnetic crystals, which involves a change of sign of the magnetic moments on inversion.[2] The symmetry group of any paramagnetic crystal contains the transformation R, and therefore the appearance of a spontaneous moment different from zero is impossible here. In substances possessing magnetic structure (ferromagnets and antiferromagnets), the transformation R, enters only in combination with other symmetry elements; it follows that in principle such substances can be piezomagnetic.[3,4] Naturally, the greatest interest lies in the study of the piezomagnetic effect in antiferromagnets, which do not under normal conditions possess macroscopic spontaneous moments. Dzyaloshinskiĭ,[5] from considerations of magnetic symmetry, indicated a number of actual antiferromagnets in which the piezomagnetic effect should be observed. More recently, Tavger[6] and Le Corre[7] determined the piezomagnetic tensors for antiferromagnets of all magnetic structure classes.

The piezomagnetic effect in antiferromagnets is closely connected with the appearance of weak ferromagnetism, which has been experimentally studied in detail in α-Fe_2O_3,[8] and $MnCO_3$ and $CoCO_3$.[9,10] A theoretical consideration of these phenomena[11,12] showed that in many cases, in the same crystallographic structure, different types of antiferromagnetic ordering with different magnetic symmetries are possible. Thus, magnetic symmetry in some types does not permit a spontaneous ferromagnetic moment, whilst in other types antiferromagnetism is accompanied by weak ferromagnetism. It follows that if, on the application of stress to a crystal not possessing a spontaneous moment, the crystal deforms in such a way that its magnetic symmetry changes, then a ferromagnetic moment can arise in it.

We have already communicated the discovery of the piezomagnetic effect in the fluorides of cobalt and manganese.[13] These compounds transform into the antiferromagnetic state in a temperature region convenient for study: MnF_2 at $T_N = 66.5°K$,[14] CoF_2 at $T_N = 37.7°K$.[15] So, even at 20°K, the magnetization of the sub-lattices in them is almost saturated. Both substances have a simple tetragonal lattice (group D_{4h}^{14}).[16] In the antiferromagnetic state the spins of the ions at the centers of the crystallographic cells are antiparallel to the spins of the ions at the corners of the cells[17] — as shown in Fig. 1. Dzyaloshinskiĭ has shown[5,18] that in these compounds a piezomagnetic moment should be observed along all three axes,*

---

*In Dzyaloshinskiĭ paper[5] a term was omitted in the expression for the thermodynamic potential responsible for the appearance of a piezo-magnetic moment along the z axis. A complete analysis of this problem was given in his dissertation.[18]

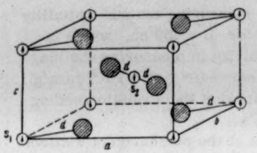

FIG. 1. The magnetic structure of MnF$_2$ and CoF$_2$. Open circles – Mn, Co; shaded circles – F.

but only on applying shear stresses

$$m_x^p = \Lambda_1\sigma_{yz}, \qquad m_y^p = \Lambda_1\sigma_{xz}, \qquad m_z^p = \Lambda_2\sigma_{xy}. \qquad (1)$$

In a previous paper[13] we described the discovery of the "transverse" piezomagnetic moment ($\Lambda_1\sigma_{xz}$). In the present paper a more detailed description is given of the results of these experiments, and experiments demonstrating the "longitudinal" piezomagnetic moment ($\Lambda_2\sigma_{xy}$).

2. APPARATUS AND SPECIMENS

Considering the smallness of the expected piezomagnetic effect, we decided on the balance method of measuring magnetic moments as the most sensitive of known methods. A diagram of the apparatus we used is shown in Fig. 2. The specimen under study, 1, situated in tube 2 of press 3, lay in the inhomogeneous field of the electromagnet 4, 5.

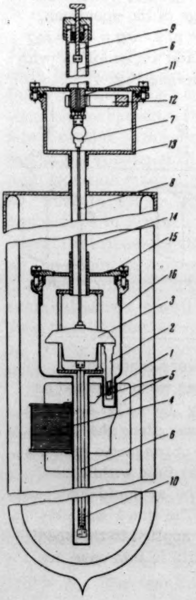

FIG. 2. Diagram of the magnetic torsion balance.

The use of a small electromagnet situated directly inside the Dewar excluded all effects involving the magnetization of the material from which the press was made.

If the specimen possesses a magnetic moment m, then the force

$$F_z = CmH,$$

acts on it, where the constant $C = H^{-1}dH/dz$ depends on the position of the specimen relative to the poles of the magnet. For a magnet of small dimensions, C changes markedly, even for small changes of specimen position. Before the start of each series of measurements the specimen was placed in the region where C had its maximum value. Then a displacement of the specimen by ±0.1 mm caused the constant C to diminish by $\sim 0.5\%$. By using a photocompensator device, we were able to maintain the specimen position constant with an accuracy of ±0.03 mm.

To measure the force F acting on the specimen, the press 3 was suspended on vertical tungsten wires 6, with a diameter of $50\,\mu$ and length of 10 cm. The lower wire was fixed directly to the press and the upper to plate 7, which was rigidly connected to the press by means of quartz rod 8. The upper end of the upper wire was fixed to the movable stem 9. Rotation of the stem enabled the zero correction of the system to be made, and, by lowering it, it was possible to arrest the balance. Spring 10 maintained a constant tension in the wires. The measurements were made by a compensation method. A compensating moment was created by passing a current through coil 11, which rotated in the gap of permanent horseshoe magnet 12. The current was fed to the coil through the two tungsten wires.

The entire torsional balance was situated in a vacuum jacket, 13, 14, 15, and 16.

An essential part of the apparatus was the press, with the aid of which stresses were created in the specimen. A detailed diagram of the press is given in Fig. 3. Using a suggestion by P. L. Kapitza, the press, suspended on the fine wires, was controlled by a bellows. To bellows 17 were soldered upper and lower rigid plates 18 and 19. After this the bellows was evacuated through capillary 20. The capillary was squeezed off and soldered up. The external atmospheric pressure thus compressed the bellows with a force of ~2.5 kg. The lower cap of the bellows lay on supporting frame 21, fixed to the body of the press, 22. On lowering the pressure in the space surrounding the press, elastic forces started to straighten out the compressed bellows. The pressure thus arising was

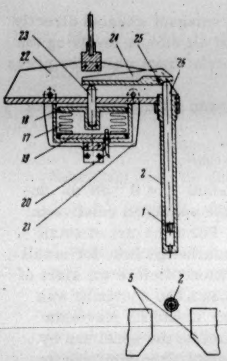

FIG. 3. Diagram of the press and bellows (the numbering of the components follows that of Fig. 2).

transferred through rod 23 to the long arm of lever 24, oscillating about shaft 25, which was fixed to the body of the press. The other lever arm (the ratio of the arms was 1 : 6) bore on rod 26, by means of which the pressure was transmitted to the specimen, 1. The specimen was at the end of tube 2, screwed into the body of the press. The dependence of the pressure created in the press on the pressure of the helium gas surrounding the press was determined with a wire strain gauge fixed to the side surface of the tube and previously calibrated by using a direct load on rod 26. This dependence was not completely linear, owing to the non-linearity of the bellows compression and small deformations of the lever. Thus, the maximum force acting on the specimen (~ 7 kg) was smaller than calculated.

The magnetic balance had a photocompensator (used also in our previous work), which automatically maintained the current through compensating coil 11, such that an optical beam reflected from a mirror fixed to plate 7 remained in the null position (with a displacement accuracy dictated by the photocompensator control circuit). In the photocompensator amplifier a differentiating circuit was included which ensured damping of the magnetic balance.*

The parameters of the compensating system were such that a moment of 1 dyne-cm was created by a current of 830 μa. The uncertainty of the balance reading was approximately ± 0.3 μa. The sensitivity can thus be estimated at 4×10^{-4} dyne-cm. For a specimen of weight 10 mg this gave a sensitivity in measuring the susceptibility of $\sim 2 \times 10^{-6}$ emu/g for H = 400 oe, which is equivalent to a sensitivity in measuring the magnetic moment in the same field of $\sim 10^{-3}$ emu/g. However, the calibration of the absolute reading was not better than 5%.

All measurements of the piezomagnetic effect were performed at the temperature of liquid hydrogen (T = 20.4° K).

Single crystals of MnF_2 and CoF_2 were used; they were grown by N. N. Mikhaĭlov and O. S. Zaĭtsev from a melt subjected to an atmosphere of HF vapor. Small pieces of the crystals, of arbitrary shape and dimensions (0.3 cm³), were oriented in the necessary way by an x-ray goniometer. They were then ground by hand to produce a rectangular parallelepiped of dimensions 1 × 1 × 2 mm. The end of this parallelepiped was glued to the lower end of the rod with BF-2 glue. Then the rod was held in a special mandrel, and the other end of the specimen was ground strictly perpendicular to the axis of the rod. A small layer of vacuum grease ensured a close contact between the specimen and the end of the tube. On applying a pressure p to the specimen thus mounted, homogeneous stresses arose in it: a) $\sigma_{ii} = p$ $(\sigma_{kk} = \sigma_{ll} = \sigma_{ik} = \sigma_{il} = \sigma_{kl} = 0)$, if the i axis was along the long edge of the specimen, and b) $\sigma_{ik} = p/2$ $(\sigma_{ii} = \sigma_{kk} = p/2,\ \sigma_{ll} = \sigma_{il} = \sigma_{kl} = 0)$, if the i and k axes made angles of 45° with the long edge of the specimen (see Fig. 4).

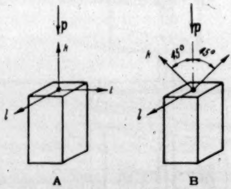

FIG. 4. Orientation of the specimens for investigations on piezomagnetism: A – shear stresses absent, B – a shear stress $\sigma_{ik} = p/2$ arises.

3. RESULTS

The main measurements were made with a CoF_2 crystal in which the axes were directed as follows: i → x, k → z, l → y (see Fig. 4, B). In this case the magnetic field was along the y axis. Figure 5 shows the variation of magnetic moment m_y with field, on changing the field within the limits of −1.1 koe to +1.1 koe at liquid-hydrogen temperature (T = 20.4° K). The line 1 was obtained when no pressure was applied to the specimen. The experimental results in this case are described by the equation

---

*The author is very grateful to V. I. Ozhogin for constructing the photocompensator circuit, and also to A. N. Vetchinkin for a number of valuable discussions on the choice of the photocompensator circuit.

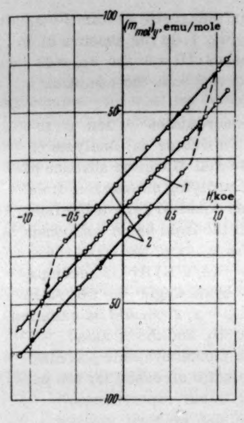

FIG. 5. Variation of molar magnetic moment m_y of CoF_2 with magnetic field: 1 – in the absence of stress, 2 – under a stress $\sigma_{xz} = 340\ kg/cm^2$.

$$m_y = m_y^0 + \chi_y^0 H,$$

where $\chi_y^0 = 56 \times 10^{-3}$ emu/mole and $m_y^0 = -1$ emu/mole. On applying to this specimen the maximum pressure obtained, $p = 680\ kg/cm^2$, the experimental points are described by two straight lines (2 in Fig. 5)

$$m_y = \pm m_y^p + \overset{\circ}{\chi}{}_y^p H. \qquad (2)$$

The value of the spontaneous moment $m_y^p = 16$ emu/mole and does not depend on the field. In weak fields (up to 500 oe) the direction of the moment remains unchanged. For large fields in the opposite direction to the moment m_y^p, the magnetization of the specimen reverses. The reversal of magnetization takes place comparatively slowly. For a field of 810 oe, ~ 40% reversal of magnetization occurs in 5 minutes. Further change is very slow. On increasing the field further to 980 oe, almost complete reversal of magnetization takes place in 7 minutes. The results on magnetization reversal were not well reproducible; we have therefore limited ourselves to a qualitative study, and in Fig. 5 the region of magnetization reversal is tentatively shown by broken lines.

The results obtained in Fig. 5, and additional measurements at two intermediate pressures, show that within the limits of accuracy of our experiments the paramagnetic susceptibility χ_y does not change on applying pressure. Therefore, we studied the variation of piezomagnetic moment m_y^p on pressure by measuring the change of the total moment m_y in a constant magnetic field, H = 1.1 koe, while changing the pressure on the specimen. The results of these measurements are given in Fig. 6, from which it is seen that m_y^p varies linearly with pressure, with

$$m_y^p = 5.1 \cdot 10^{-2} \sigma_{xz}\ \text{emu/mole} = 2.1 \cdot 10^{-3} \sigma_{xz}\ \text{gauss}$$
$$(\sigma_{xz}\ \text{in kg/cm}^2).$$

Measurements were made on the same crystal of the magnetic moment along the [101] direction, where the field was perpendicular to the y axis. As in the previous case, a small residual moment $m^0 = 1.1$ emu/mole was observed. On applying pressure its value changed only by 30%.

FIG. 6. Variation of transverse piezomagnetic moment per unit volume m_y^p for CoF_2 on the value of the applied shear stress σ_{xz}.

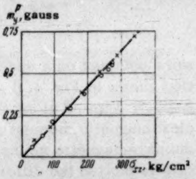

Analogous results were obtained on a specimen in which the axes were directed as follows: i → x, k → y, l → z. During measurements of the magnetic moment m_z (the field H was along the z axis), curves were obtained analogous to those shown in Fig. 5. In this case

$$\chi_z^0 = \chi_z^p = 13 \cdot 10^{-3}\text{emu/mole}, \quad m_z^0 = 1.2\text{emu/mole}.$$

On applying pressure a piezomagnetic moment m_z^p appears, which also varies linearly with pressure (Fig. 7):

$$m_z^p = 1.9 \cdot 10^{-2} \sigma_{xy}\ \text{emu/mole} = 0.8 \cdot 10^{-3} \sigma_{xy}\ \text{gauss}$$
$$(\sigma_{xy}\ \text{in kg/cm}^2).$$

FIG. 7. Variation of the longitudinal piezomagnetic moment per unit volume m_z^p for CoF_2 on the value of the applied shear stress σ_{xy}.

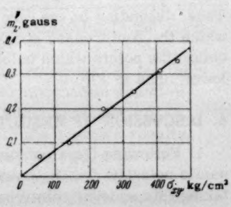

During magnetic measurements along the [110] axis we also observed a small residual moment, $m^0 = 0.8$ emu/mole which changed by 30% on applying the maximum pressure.

A specimen was also studied with axes orientated as shown in Fig. 4,A (i → x, k → y, l → z). In this specimen also, residual moments $m_x^0 = 1$ emu/mole, $m_z^0 = 1.3$ emu/mole were observed, which changed on applying the maximum pressure by 30 and 20%.

A piezomagnetic effect was also discovered in the MnF_2 crystal. The results shown in Fig. 8 were obtained on a specimen having the orientation shown in Fig. 4, B ($i \to x$, $k \to z$, $l \to y$, the field H applied along the y axis). Because the piezomagnetic moment amounted to only ~1% of the paramagnetic moment χH, on the abscissa axis is plotted the difference of moments measured under pressure ($p = 520$ kg/cm²), and without pressure, $\Delta m = m_y^p - m_y^0$. The results obtained show that under a pressure $p = 520$ kg/cm², a piezomagnetic moment $m_y^p = 0.12$ emu/mole $= 5 \times 10^{-3}$ gauss appears in the specimen. Together with this a slight (~0.2%) decrease in the susceptibility occurs. We found that the direction of the piezomagnetic moment remains unchanged on applying a field in the opposite direction of a magnitude up to the maximum we used −1.1 koe. The direction of the piezomagnetic moment could only be changed if the compressed specimen was cooled in the magnetic field from a temperature above the Néel point ($T_N = 67.5$°K) to hydrogen temperature. The direction of the piezomagnetic moment was always coincided with the direction of the field in which the specimen was cooled. This direction was then always preserved during repeated pressure removals and applications of opposing fields. Thus, depending on the direction of the field in which the compressed specimen was cooled, we obtain the points which belong to the upper and lower lines in Fig. 8.

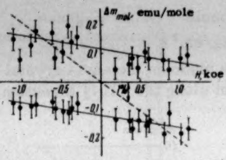

FIG. 8. The piezomagnetic effect in MnF_2. The broken curve corresponds to a susceptibility change of 1%.

4. DISCUSSION OF RESULTS

1) Following Dzyaloshinskiĭ,[5,12] the thermodynamic potential for the investigated fluorides, taking into account relativistic terms linear in the stress σ_{ik} and in the magnetic moment $\mathbf{m} = \mathbf{s}_1 + \mathbf{s}_2$, and invariant with respect to transformations of the group D_{4h}^{14}, can be written in the following form:

$$\tilde{\Phi} = \tfrac{1}{2} a(\gamma_x^2 + \gamma_y^2) + \tfrac{1}{2} B\mathrm{m}^2 + \tfrac{1}{2} bm_z^2 + e(\gamma_x m_y + \gamma_y m_x) + \lambda_1 (m_x \sigma_{yz} + m_y \sigma_{xz})\gamma_z + \eta_1 (\gamma_y \sigma_{yz} + \gamma_x \sigma_{xz})\gamma_z + \lambda_2 m_z \gamma_z \sigma_{xy} + \eta_2 \gamma_x \gamma_y \sigma_{xy} - \mathrm{mH}, \tag{3}$$

where γ_x, γ_y, γ_z are the components of a unit vector along the antiferromagnetic vector $\mathbf{l} = \mathbf{s}_1 - \mathbf{s}_2$. As is seen from Fig. 1, in the absence of an external field and stresses ($H = 0$ and $\sigma_{ik} = 0$) $\gamma_x = \gamma_y = 0$. To this corresponds the condition $a' = a - e^2/B > 0$.

We shall use polar coordinates θ and φ to label the directions of the vector γ. Analysis of the thermodynamic potential (3) in the absence of stresses shows that on applying an external field H, the angle θ remains equal to zero if the field is along the z axis. If the field has a component $H_\perp$ perpendicular to the z axis, the appearance of a magnetization $m_\perp = (a/a'B) H_\perp$ is accompanied by a rotation of $\mathbf{l}$ by an angle $\theta = eH_\perp/a'B$. Here the condition $\psi + \varphi = \pi/2$ should be satisfied (ψ is the angle between $H_\perp$ and the x axis).

We shall analyze the thermodynamic potential (3) in the presence of elastic stresses for the particular cases occurring in our experiments.

2) For the first specimen we have $\sigma_{xy} = \sigma_{yz} = 0$, $\sigma_{xz} \neq 0$. In this case minimization of the potential in the absence of a field gives*

$$\theta = |\sigma_{xz}| (\eta_1 B - e\lambda_1)/(aB - e^2) \tag{4a}$$

and $\varphi = 0$ or π depending on the sign of σ_{xz}. Thus, in agreement with the result obtained by Dzyaloshinskiĭ,[5] a spontaneous moment arises along the y axis:

$$m_y^p = \sigma_{xz} (e\eta_1 - a\lambda_1)/(aB - e^2). \tag{4b}$$

In this way the application of a stress σ_{xz} causes, as is shown schematically in Fig. 9, the magnetization of the sublattices to be no longer strictly antiparallel, and by rotating in the zy plane they include an angle $\pi - 2\beta$, where $\beta = m_y^p/l$. This is accompanied by the rotation of the antiferromagnetic vector as a whole through an angle θ in the xz plane. This picture agrees completely with what was observed in previously studied antiferromagnets with weak transverse ferromagnetism.

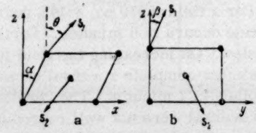

FIG. 9. Rotations of the magnetic moments of the sublattices in the transverse piezomagnetic effect: a – in the xz plane, and b – in the yz plane.

The application of a magnetic field along the y axis increases the angle θ by $eH_y/a'B$; the following expression is obtained for the magnetic moment in this case:

---

*In all the calculations which follow we assume that in the initial state $\theta_0 = 0$. If we take the initial value $\theta_0' = \pi$, then the expression for θ' will have the form $\theta' = \pi - \theta$; piezomagnetic moments change sign on inversion.

$$m_y = m_y^p + (a / a'B) H_y. \tag{5}$$

This conclusion of the theory is in complete agreement with what we observed in experiment [see Fig. 5 and Eq. (2)]. The experimental data we obtained allow the evaluation of the rotation angle of the sublattices and some of the coefficients of the expression. For further calculation we will neglect the difference between a and a′ (taking $e^2/B \ll a$). Then, in the case of CoF_2* we have $B = 1/\chi_\perp = 0.5 \times 10^3$; assuming that both terms in (4b) give approximately equal contributions, we obtain an estimate for the coefficient $\lambda_1 \sim 0.5$ (in any case $\lambda_1 \leq 1$). On applying the stress $\sigma_{xz} = 500$ kg/cm², we obtain the following estimates for the angles: $\alpha = \sigma_{xz}/G \sim 2 \times 10^{-3}$ (the shear modulus G was here taken to be 0.25×10^{-6} kg/cm²); $\beta = m_y^p/l \sim 5 \times 10^{-3}$. To evaluate θ it does not suffice to know the coefficients e and a. If it is assumed that the value of the relativistic terms amounts to $\sim 10^{-3}$ of the exchange energy, then for the angle θ the value $\sim 10^{-3}$ is obtained, i.e., all three angles are of the same order of magnitude.

If the applied field is directed perpendicular to the y axis, minimization of the potential (3) gives the following solution for the components of the moment:

$$m_x = (a/a'B) H_x, \qquad m_y = m_y^p, \qquad m_z = H_z/(B + b),$$

which also agrees with our measurements of the moments along the [101] axis — in this direction the magnetic properties do not depend on pressure and the crystal does not display ferromagnetism (we shall return to the weak parasitic moment). The angle θ is changed by the field also, as in the previous case, whilst the angle φ does not remain constant, but increases gradually and tends in large fields ($eH_x \gg B\eta_1\sigma_{xz}$) to $\varphi = \pi/2$.

3) Special interest attaches to the case $\sigma_{xz} = \sigma_{yz} = 0$; $\sigma_{xz} \neq 0$. In this case, in the absence of a field, the direction of the spontaneous magnetization vector is not changed on applying pressure ($\theta = 0$). A piezomagnetic moment, as already shown,[12] is obtained along the z axis:

$$m_z^p = \lambda_2\sigma_{xy} / (B + b).$$

Thus there arises here weak longitudinal ferromagnetism, which has not been previously observed. In distinction from the transverse, the longitudinal weak ferromagnetism is caused by the difference in the values of the magnetic moments of the ions in the two sublattices. As is seen from Fig. 10, the ions 1 and 2, which are equivalent before deformation with respect to symmetry of the crystalline field, after shear deformation in the xy plane, cease to be equivalent. It is apparent that, if the change of the angle between the x and y axes from $\pi/2$ causes such a change of the crystalline field, while the size of the magnetic moments changes linearly with deformation, then the signs of these changes in both sublattices should be opposite. The microscopic nature of the different changes of the crystalline fields for different ions is connected with the different signs of the changes in distance to nearest fluoride ions, as seen from Fig. 10.

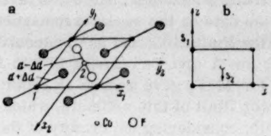

FIG. 10. The longitudinal piezomagnetic effect: a – the change of symmetry of the crystalline fields, b – the change of the sublattice magnetic moments.

On applying a magnetic field the angles φ and θ change, to a first approximation, just as they do in the undeformed crystal, and for the magnetic moments the solution is obtained

$$m_\perp = (a / a'B) H_\perp,$$
$$m_z = H_z / (B + b) + \lambda_2\sigma_{xy} / (B + b). \tag{6}$$

This result also agrees completely with what we observed in the experiments with the second CoF_2 specimen. From the experimental data the value $\lambda_2 = 1.6$ is found directly.

4) The crystallographic symmetry of the fluorides is such that the thermodynamic potential only contains terms for shear stresses σ_{ik} ($i \neq k$). This agrees with the negative results obtained on the third CoF_2 crystal, where we provided only compressive stresses (σ_{ii}).

5) During measurements on all the specimens we encountered a weak ferromagnetic moment even in undeformed crystals. The size of this moment varied within limits of up to 1½ times in different specimens, and was approximately 10 times smaller than the piezomagnetic moments we observed. In distinction from the latter, this moment was practically isotropic. The size of the observed parasitic moment was such that it could be caused by a susceptibility decrease of ~ 2% on changing from a field of 1 koe to a field of 10 koe.

---

*Below all quantities are given in the cgs emu system calculated for 1 cm³ of substance. The pressures are given in kg/cm².

It should be pointed out that a variation of χ on H in CoF_2 of such an order has also been observed by other workers.[19,20] It is possible that the parasitic moment is caused by a piezomagnetic effect due to inhomogeneous internal stresses in the specimens studied. However, an anneal we carried out on one of the specimens did not change the value of the moment.

6) The thermodynamic theory naturally cannot predict the size of the piezomagnetic effect. Dzyaloshinskiĭ,[18] from very crude premises, has given a formula to estimate the size of the piezomagnetic modulus:

$$\Lambda \sim \sqrt{a\chi / \Theta E},$$

where Θ is the Néel temperature in energy units and E is Young's modulus. The ratio a/Θ, according to the data on the weak ferromagnetism, lies within the limits 10^{-2} and 10^{-5}. Accordingly, an estimate for Λ gives a value of 10^{-3} to 10^{-4}. The result for MnF_2 gave a value an order smaller than the lower limit of this estimate, which is not unreasonable, considering the crudity of the estimate. The smallness of the piezomagnetic effect in MnF_2 is easily explained if it is assumed that the weak ferromagnetism is caused by spin-orbital and not dipole interactions.* For the Mn^{++} ion in the S state, the spin-orbital interaction should be very small. Most favorable in this respect is the Co^{++} ion. The particular splitting of its ground state by the crystalline field[22,23] means that the effect of spin-orbital interaction in it should be the greatest of all the transition element ions. With this is apparently associated the anomalously large size of the piezomagnetic effect. In particular this refers to the longitudinal effect, which is entirely due to the effect of the crystalline fields.

7) From the thermodynamic discussion given above, it follows that for the same sign of σ_{ik} the direction of the piezomagnetic moment is uniquely connected with the direction of the antiferromagnetic vector ($m_y^p \sim \sin\theta$; $m_z^p \sim \cos\theta$, where the angle θ lies within the limits 0 and π). Therefore, a reversal of the piezomagnetic moment by an external field should be accompanied by a rotation of the antiferromagnetic vector $\boldsymbol{l}$ through 180°. The two states with $\theta = 0$ and $\theta = \pi$ are divided by a potential barrier with a height of the order of the anisotropy energy $a \sim 10^7$ erg/cm^3. In our experiments we showed that in the same crystal repeatedly cooled, the spontaneous moment observed in the absence of a field was always in the same direction. This indicates two facts: a) in the crystals studied a single-domain antiferromagnetic structure is formed, b) the direction of the antiferromagnetic vector in a given crystal is always the same, for which some imperfection of the crystal is responsible, causing the energetic preference of one of the states. The energy difference can be estimated from the size of the magnetic energy required for magnetization reversal. In our experiments magnetization reversal was observed for $mH \sim 5 \times 10^2$ erg/cm^3. We established that this value decreased somewhat (by ~30%) after an anneal of one of the specimens. It should be emphasized that the energy indicated is four orders smaller than the height of the potential barrier. It can be assumed, therefore, that the observed magnetization reversal time (in our experiments $\tau \sim 30$ sec) is associated with the lifetime of the sublattices. However, to obtain quantitative conclusions, it is necessary to develop the theory of magnetization reversal kinetics, and perform further experiments in this area.

8) In view of the low accuracy in orienting the crystals, the values we obtained for $\chi_\perp$ and $\chi_\parallel$ at T = 20.4°K can contain significant errors — up to 10% of the difference $\chi_\perp - \chi_\parallel$. Up to the present only the difference of susceptibilities[19] has been measured in CoF_2 single crystals. Our data, $\chi_\perp - \chi_\parallel = 43 \times 10^{-3}$ emu/mole, agree within the limits of accuracy indicated above, with the value 48×10^{-3} emu/mole obtained by Stout and Mataresse.[19] In this connection, attention should be turned to the fact that in the case of CoF_2 the susceptibility $\chi_\parallel$ does not apparently tend to zero as $T \to 0°K$.

In conclusion, the author expresses his deep gratitude to Acad. P. L. Kapitza for constant interest in the work, N. N. Mikhaĭlov and O. S. Zaĭtsev for making the MnF_2 and CoF_2 single crystals, I. E. Dzyaloshinskiĭ for useful discussions, and also V. I. Kolokol'nikov for assistance in carrying out the experiments.

Note added in proof (March 9, 1960). Moriya, in a recently published paper [T. Moriya, J. Phys. Chem. Solids **11**, 73 (1959)], by considering the change of potential of the crystalline field during compression in the [110] direction, evaluated the quantity $\Lambda_2 = 4 \times 10^{-3}$ gauss/(kg/cm^2), which is only eight times greater than our experimental result.

---

*This has been shown for rhombohedral structures by Bertaut;[21] analogous calculations confirm this effect for the fluorides also.

[1] W. Voight, Lehrbuch der Kristallphysik, Leipzig (1928).

[2] L. D. Landau and E. M. Lifshitz, Статистическая физика (Statistical Physics), GITTL, (1951).

[3] B. A. Tavger and V. M. Zaïtsev, JETP **30**, 564 (1956), Soviet Phys. JETP **3**, 430 (1956).

[4] L. D. Landau and E. M. Lifshitz, Электродинамика сплошных сред (Electrodynamics of Continuous Media), Gostekhizdat (1957).

[5] I. E. Dzyaloshinskiĭ, JETP **33**, 807 (1957), Soviet Phys. JETP **6**, 621 (1958).

[6] B. A. Tavger, Кристаллография **3**, 342 (1958), Soviet Phys.-Crystallography **3**, 344 (1959).

[7] Y. Le Corre, J. phys. radium **19**, 750 (1958).

[8] L. Néel and R. Pauthenet, Compt. rend. **234**, 2172 (1952). L. Néel, Revs. Modern Phys. **25**, 58 (1953).

[9] A. S. Borovik-Romanov and M. P. Orlova, JETP **31**, 579 (1956), Soviet Phys. JETP **4**, 531 (1957).

[10] A. S. Borovik-Romanov, JETP **36**, 766 (1959), Soviet Phys. JETP **9**, 539 (1959).

[11] I. E. Dzyaloshinskiĭ, JETP **32**, 1547 (1957), Soviet Phys. JETP **5**, 1259 (1957).

[12] I. E. Dzyaloshinskiĭ, JETP **33**, 1454 (1957), Soviet Phys. JETP **6**, 1120 (1958).

[13] A. S. Borovik-Romanov, JETP **36**, 1954 (1959), Soviet Phys. JETP **9**, 1391 (1959).

[14] J. W. Stout and H. E. Adams, J. Amer. Chem. Soc. **64**, 1535 (1942).

[15] J. W. Stout and E. Catalano, Phys. Rev. **92**, 1575 (1953).

[16] R. W. G. Wyckoff, The Structure of Crystals, N.Y. (1931).

[17] R. A. Erickson, Phys. Rev. **90**, 779 (1953).

[18] I. E. Dzyaloshinskiĭ, Dissertation, Moscow (1957).

[19] J. W. Stout and L. M. Mataresse, Revs. Modern. Phys. **25**, 338 (1953).

[20] W. J. de Haas and B. H. Schultz, Physica **6**, 481 (1939).

[21] F. Bertaut, Compt. rend. **246**, 3335 (1958).

[22] A. Abragam and M. H. L. Pryce, Proc. Roy. Soc. **A206**, 173 (1951).

[23] T. Nakamura and H. Taketa, Progr. Theor. Phys. **13**, 129 (1955).

Translated by K. F. Hulme
217

SOVIET PHYSICS JETP VOLUME 11, NUMBER 4 OCTOBER, 1960

ELASTIC SCATTERING OF 240 —330 Mev π^- MESONS BY HYDROGEN

V. G. ZINOV and S. M. KORENCHENKO

Joint Institute for Nuclear Research

Submitted to JETP editor November 13, 1959

J. Exptl. Theoret. Phys. (U.S.S.R.) **38**, 1099-1105 (April, 1960)

Results of measurements of differential cross sections for the elastic scattering of π^- mesons of energies 240, 270, 307 and 333 Mev by hydrogen are given.

STUDY of the scattering of π^+ mesons by hydrogen in the energy region up to 360 Mev[1-3] has made it possible to establish the main features of the interaction of π mesons with nucleons in the states with isotopic spin $T = 3/2$. Until recently, very little was known about the interaction of π mesons with nucleons in the $T = 1/2$ states. The state with $T = 1/2$ enters only into scattering of negative π mesons. Determination of the contribution of these states in the energy region near resonance is practically impossible because of the overwhelming contribution of the interaction in $T = 3/2$, $j = 3/2$ states. It might be hoped that more specific information about the interaction in $T = 1/2$ states could be obtained at high energies. In connection with this, the authors carried out a systematic study of the interaction of π^- mesons with hydrogen in the energy range 240 — 330 Mev on the synchrocyclotron of the Joint Institute, using scintillation counters.

Preliminary results of this work have been given earlier.[4-7]

1. EXPERIMENTAL ARRANGEMENT

A detailed description of the apparatus and liquid-hydrogen target used has already been given by the authors.[8] Therefore, we limit ourselves to only a few remarks here.

The geometry of the experiment is shown in the figure. The beam of π^- mesons falling on the hydrogen target is detected by counters 1 and 2, connected in coincidence. The π mesons scattered at various angles are counted by two "angular" telescopes consisting of counters 3, 4 and 5, 6 connected in coincidence with counters 1, 2. In order to cut down the number of spurious coincidences, the counters 1 — 6 were connected in anticoincidence with counter 7, placed behind the target. This made it possible to decrease the background of random coincidences by a factor of 15 or 20, so that the number of random coincidences did not exceed 4 to 7% of the scatterings from hydrogen. A special control was established so that the working intensity of the synchrocyclotron did not fluctuate more than 10% relative to the mean level. Therefore, the error in measurements arising from fluctuation in the background of random coincidences did not exceed ± 0.7%.

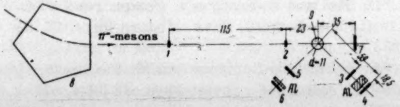

Geometry of the elastic-scattering experiment: 1, 2 – scintillation counters (6 × 6 cm); 3, 4, 5, 6 – scintillation counters (12.6 × 11.5 cm); 7 – anticoincidence counter (12.6 × 11.5 cm); 8 – deflecting magnet; 9 – liquid hydrogen.

In the following, where four-fold coincidences 1234 or 1256 are referred to, coincidences of the type $1234\overline{7}$ and $1256\overline{7}$ are implied.

In measurement of the differential cross sections at 30, 45 and 60°, aluminum filters were placed in front of counters 4 and 6 to absorb recoil protons; the thicknesses of these filters at the various energies are given in Table I. In measurements at other angles, filters of thickness 5.4 g/cm^2 were always placed in front of counters 4 and 6 in order to decrease the background from low-energy particles.

2. MEASUREMENT OF THE DIFFERENTIAL CROSS SECTIONS FOR ELASTIC SCATTERING OF π^- MESONS OF ENERGIES 240, 270, 307 AND 333 Mev BY HYDROGEN

The angular distributions of π^- mesons scattered elastically by hydrogen were determined by measuring the ratios of four-fold coincidences Q in counters 1, 2, 3, 4 and 1, 2, 5, 6 to the two-fold coincidences D in counters 1 and 2. The measurements were carried out at 30, 45, 60, 80, 100, 125 and 150° in the l.s.

TABLE I. Thicknesses of aluminum filters for absorption of recoil protons (g/cm^2)

Angle in l.s., deg	240 Mev	270 Mev	307 Mev	333 Mev
30	16.2	21.6	28.4	31.0
45	10.8	14.8	20.2	21.6
60	5.4	8.1	9.4	10.8

All of the measurements were carried out in several series. Some of them were made simultaneously with the study of charge-exchange scattering of the π^- mesons. The measurements of a given series of the ratios Q/D for 240-Mev π^- mesons are given in Table II. The variation in observed values with change in energy is illustrated by the analogous Table III for 333 Mev. From Tables II and III it can be seen that at some angles the effect from hydrogen is two or more times smaller than the background from scattering of mesons off the walls of the target and counters.

TABLE II. Values of the ratio Q/D, observed at 240 Mev in one of the series of measurements

Angle in l.s., deg	(Q/D) × 10^6 with H	(Q/D) × 10^6 without H	Difference
30	144.3 ± 4.28	133.2±3.6	31.1±5.6
45	63.1 ± 2.0	36.5±1.5	26.6±2.5
60	47.5 ± 1.8	23.0±1.4	24.5±2.3
80	24.7 ± 1.6	10.8±1.1	13.9±2.0
100	23.1 ± 1.0	10.0±0.7	13.1±1.3
125	29.8 ± 1.6	13.0±0.7	16.6±2.0
150	48.0 ± 1.7	30.6±1.5	17.4±2.3

TABLE III. Values of the ratio Q/D, observed at 333 Mev in one of the series of measurements

Angle in l.s., deg	(Q/D) × 10^6 with H	(Q/D) × 10^6 without H	Difference
30	102.3 ± 3.3	73.5±3.2	28.7±4.6
45	53.1 ± 1.7	29.3±1.3	23.8±2.1
60	45.6 ± 2.1	27.3±1.7	18.3±2.7
80	29.6 ± 0.9	15.4±0.9	14.2±1.3
100	19.2 ± 1.2	10.4±1.1	8.8±1.6
125	21.0 ± 1.2	8.0±0.8	13.0±1.5
150	35.0 ± 2.2	26.0±2.1	9.0±3.0

Before beginning each series, the energy of π^- mesons in the beam was determined and the working of the apparatus was checked.

The differential cross sections were determined from the formula

$$\left(\frac{d\sigma}{d\Omega}\right)_{\text{lab}} = \frac{(Q/D)_{\text{diff}} - n_{\pi^0}}{N\Omega f h} \cdot 10^{-6}, \qquad (1)$$

where $(Q/D)_{\text{diff}} = (Q/D)_{\text{with H}} - (Q/D)_{\text{without H}}$ is the effect per 10^6 counts of the monitor (mean weighted value for all of the series of measurements) with corrections to the observed values of Q/D for erroneous counts in the coincidences 1, 2; n_{π^0} is the effect produced by electrons and positrons from the decay of π^0 mesons (per 10^6 counts of the monitor); N is the mean number of hydrogen atoms per cm^2, this number being 0.447×10^{24} to an accuracy of ±1% for all energies; Ω is the solid angle subtended by the angular telescope; f is a correction to the observed cross section which is independent of scattering angle and h is a correction depending on angle of scattering.

The values of all terms in Eq. (1) are given in Tables IV — VII.

The n_{π^0} effect is composed of two parts. The main part is from electrons and positrons produced by conversion of γ rays from π^0 decays in hydrogen, walls of the target and counters 3 and 5. From measurements of exchange scattering, the effect of γ-ray conversion in a lead convertor of thickness 7.4 g/cm^2 is known at each angle. Knowing the cross sections for conversion and Compton effect in lead, carbon and hydrogen,[9,10] we can determine the number of electrons falling on the angular telescope to a sufficient accuracy. The counts produced by these electrons constituted 3.3 ± 1% of the counts observed in the same conditions with a lead convertor. In addition to electrons coming from conversion of γ rays, electrons produced[11] in ~ 1.6% of π^0 decays, $\pi^0 \rightarrow e^+ + e^- + \gamma$, were taken into account. In determining the n_{π^0} corrections, the absorption of electrons in the aluminum filters[10,12] placed between counters 3 and 4, and between 5 and 6, was taken into consideration.

The correction f, which did not depend on scattering angle, included corrections for the admixture of μ mesons in the beam and absorption of π^- mesons in counter 2, the front wall of the target, and in the hydrogen. The correction h, which depended upon angle, came mainly from the absorption of π mesons in the aluminum filter placed between the counters of the angular telescope. The magnitude of the absorption was determined experimentally by measuring Q/D with and without the aluminum filter. The measurements were carried out in the direct π^- beam with decreased intensity. The energies of the π^- mesons were chosen to correspond to those of π mesons scattered at the corresponding angle.

In addition to this main effect, the correction h also takes into account:

(a) absorption of the scattered π^- mesons in

TABLE IV. Differential cross sections for the elastic scattering of 240-Mev π^- mesons by hydrogen

Angle in l.s., deg	Ω, sr	$(Q/D)_{\text{diff}}$	n_{π^0}	f	h	$10^{27}(d\sigma/d\Omega)_{\text{l.s.}}$ cm²/sr	Angle in l.s., deg	$10^{27}(d\sigma/d\omega)$ in c.m.s., cm²/sr
30	0.0287	26.6±2.1	3.4	0.920	0.804	2.44±0.24	39.9	1.48±0.15
45	0.0342	25.8±1.7	3.0	0.920	0.848	1.91±0.17	58.7	1.30±0.12
60	0.0414	20.6±1.4	2.8	0.920	0.893	1.21±0.11	76.3	0.953±0.087
80	0.0414	13.4±1.3	1.5	0.920	0.900	0.779±0.090	97.8	0.763±0.088
100	0.0411	11.8±0.8	1.0	0.920	0.902	0.707±0.062	117.1	0.856±0.076
125	0.0410	15.3±0.9	0.9	0.920	0.904	0.945±0.078	138.6	1.44±0.12
150	0.0414	17.4±1.4	1.0	0.920	0.895	1.075±0.106	158.1	1.92±0.19

TABLE V. Differential cross sections for the elastic scattering of 270-Mev π^- mesons by hydrogen

Angle in l.s., deg	Ω, sr	$(Q/D)_{\text{diff}}$	n_{π^0}	f	h	$10^{27}(d\sigma/d\Omega)_{\text{l.s.}}$ cm²/sr	Angle in l.s., deg	$10^{27}(d\sigma/d\omega)$ in c.m.s. cm²/sr
30	0.0287	22.6±1.7	2.9	0.925	0.756	2.20±0.22	40.6	1.30±0.13
45	0.0342	21.2±1.6	2.8	0.925	0.811	1.60±0.15	59.6	1.07±0.10
60	0.0414	16.9±1.2	1.8	0.925	0.892	0.990±0.093	77.3	0.775±0.073
80	0.0414	9.8±1.1	1.0	0.925	0.899	0.574±0.071	98.8	0.563±0.073
100	0.0411	10.0±0.8	0.7	0.925	0.900	0.608±0.061	117.9	0.748±0.074
125	0.0410	11.1±0.8	0.7	0.925	0.905	0.678±0.057	139.3	1.06±0.09
150	0.0414	13.5±1.2	0.7	0.925	0.909	0.819±0.086	158.4	1.51±0.16

TABLE VI. Differential cross sections for the elastic scattering of 307-Mev π^- mesons by hydrogen

Angle in l.s., deg	Ω, sr	$(Q/D)_{\text{diff}}$	n_{π^0}	f	h	$10^{27}(d\sigma/d\Omega)_{\text{l.s.}}$, without correction for meson production cm²/sr	Correction to $10^{27}(d\sigma/d\Omega)_{\text{l.s.}}$ for meson production, cm²/sr	Angle in c.m.s. deg	$10^{27}(d\sigma/d\omega)$ in c.m.s. cm²/sr
30	0.0340	27.5±2.6	3.4	0.934	0.724	2.34±0.27	0.052±0.040	41.3	1.31±0.16
45	0.0413	24.3±2.3	2.0	0.934	0.774	1.67±0.19	0.053±0.040	60.6	1.06±0.13
60	0.0413	16.8±1.2	1.3	0.934	0.865	1.04±0.106	0.066±0.050	78.5	0.752±0.091
80	0.0513	11.5±0.9	0.8	0.934	0.909	0.548±0.048	0.043±0.028	100.0	0.500±0.056
100	0.0513	10.4±0.9	0.5	0.934	0.895	0.515±0.054	0.017±0.017	119.0	0.625±0.072
125	0.0513	11.4±1.1	0.4	0.934	0.893	0.574±0.065	0.002±0.002	140.0	0.923±0.105
152	0.0494	11.4±1.0	0.5	0.934	0.893	0.594±0.062	0	160.3	1.15±0.12

TABLE VII. Differential cross sections for the elastic scattering of 333-Mev π^- mesons by hydrogen

Angle in l.s., deg	Ω, sr	$(Q/D)_{\text{diff}}$	n_{π^0}	f	h	$10^{27}(d\sigma/d\Omega)_{\text{l.s.}}$ without correction for meson production cm²/sr	Correction to $10^{-27}(d\sigma/d\Omega)_{\text{l.s.}}$ for meson production, cm²/sr	Angle in c.m.s. deg	$10^{27}(d\sigma/d\omega)$ in c.m.s. cm²/sr
30	0.0340	27.1±1.5	3.2	0.939	0.728	2.30±0.24	0.12±0.06	41.9	1.22±0.14
45	0.0413	22.8±1.3	2.3	0.939	0.799	1.48±0.12	0.13±0.06	61.3	0.874±0.093
60	0.0413	16.2±1.3	1.4	0.939	0.871	0.985±0.084	0.11±0.05	79.2	0.675±0.076
80	0.0511	12.8±0.8	0.9	0.939	0.919	0.604±0.046	0.093±0.03	100.8	0.508±0.055
100	0.0511	9.47±0.75	0.4	0.939	0.900	0.470±0.038	0.056±0.028	119.7	0.527±0.060
125	0.0511	11.7±0.9	0.4	0.939	0.883	0.595±0.057	0.017±0.007	140.6	0.954±0.096
150	0.0511	9.32±1.13	0.3	0.939	0.896	0.468±0.052	0.004±0.002	159.2	0.914±0.104

hydrogen (mainly because of charge-exchange scattering), scattering of π^- mesons in the walls of the target and counters 3 and 5; the size of this correction was 2 – 4%.

(b) random coincidences in counters 1, 2, 3, 4 and 1, 2, 5, 6 of the type of coincidences 123 of the recoil proton accompanied by a spurious particle traversing counter 4 (this correction did not exceed 1% of that from the hydrogen).

(c) a geometrical factor – a small (not larger than 1.2%) change in the observed cross section as compared with the true one, coming from the finite dimensions of the counters, which means that the measured cross section was averaged over an angle of 13 – 15°.

At 307 and 333 Mev it was already necessary to take into account processes in which charged mesons are produced by the π^- mesons. The contribution from these processes at 80° in the l.s. was determined experimentally.[8] For the other angles, corrections for this effect were made under the following schematic assumptions: the angular distribution of mesons participating in inelastic processes is isotropic in the c.m.s.; the energy spectrum of these mesons has the form of an isosceles triangle. The corrections to the differential cross section in the l.s., calculated under these assumptions, are given in Tables VI and VII.

The errors in the differential cross sections, shown in Tables IV – VII, include, in addition to statistical errors, errors in the determination of terms which enter into Eq. (1). The contributions from individual effects to these errors for 270 Mev are given in Table VIII. At different energies, the errors differ only little from those given in this table.

The c.m.s. angles and differential cross sections are given in the two last columns of Tables IV – VII.

Additional measurements of the cross section for π^- elastic scattering were carried out at 80° in the l.s. at 270, 307 and 333 Mev using the method of conjugate telescopes, i.e., the scattered π^- meson was detected in coincidence with the recoil proton. Because of this, the background was a factor of about five less than the scattering from hydrogen. In processing these results, practically the same corrections as in the processing of data obtained by the usual means were made. The only difference was that, instead of corrections for the conversion of γ rays, a correction was introduced into h for absorption of recoil protons (1.4 – 1.9%) in the hydrogen and in the walls of the target. The production of mesons by mesons obviously does not have to be taken into account.

The results of these measurements and the corrections carried out are given in Table IX. The differential cross section in the c.m.s., obtained by averaging the results of measurements carried out in the usual way and by the method of conjugate telescopes, is given in the last column.

3. CONCLUSIONS

We represent now the angular distribution of elastically scattered mesons in the c.m.s. as a sum of three Legendre polynomials:

$$\frac{d\sigma}{d\omega} = A_0^- + A_1^- P_1(\cos\vartheta) + A_2^- P_2(\cos\vartheta). \qquad (2)$$

The values of the coefficients A_l^- (in cm^2 sr^{-1})

TABLE VIII. Individual effects (in percentages of the differential cross section) entering into the errors in the differential cross sections at 270 Mev

Angle in l.s., deg	Δn_{π°	Correction for the Al filter	Geometrical factor	Effect of anticoincidence	Random coincidence	Absorption of the beam in the walls of the target and counter 2	False counts in the coincidences 1, 2	Inhomogeneity of the beam and inaccuracies in the determination of the solid angles	Absorption in counters 4 and 6 and in the walls of the target	Total error
30	4.2	3	1	1	1	0.5	1	3	0.5	6.3
45	4.4	2.5	1	1	1	0.5	1.5	3	0.8	6.4
60	3.5	2.5	1	1	1	0.5	1.5	3	0.8	5.8
80	3.3	2	1	1	1	0.5	1.5	3	0.8	5.6
100	2.3	2	1	1	1	0.5	1.5	3	0.8	5.0
125	2.1	2	1	1	1	0.5	1.5	3	0.5	4.9
150	1.8	2	1	1	1	0.5	1	3	0.5	4.8

TABLE IX. Differential cross sections for elastic π^--meson scattering by hydrogen at 80° l.s. and 270, 307 and 333 Mev, obtained by the method of conjugate telescopes

Energy of π^- mesons, Mev	Ω, sr	$(Q/D)_{\text{diff}}$	f	h	$10^{27}(d\sigma/d\Omega)_{\text{l.s.}}$, cm^2/sr	Angle in c.m.s., degrees	$10^{27}(d\sigma/d\omega)_{\text{c.m.s.}}$, obtained by the method of conjugate telescopes, cm^2/sr	$10^{27}(d\sigma/d\omega)_{\text{c.m.s.}}$, mean value, cm^2/sr
270	0.0344	7.66±0.72	0.925	0.879	0.613±0.065	98.8	0.601±0.065	0.585±0.053
307	0.0417	7.91±0.30	0.934	0.894	0.508±0.038	100.0	0.502±0.038	0.501±0.032
333	0.0417	8.03±0.31	0.939	0.907	0.506±0.037	100.8	0.503±0.037	0.505±0.032

TABLE X. Coefficients of the angular distribution of π^- mesons (10^{-27} sr^{-1})

Energy of π^- mesons, Mev	A_0^-	A_1^-	A_2^-	M	M_0, expected	$\sigma_{\pi^- \to \pi^+} = 4\pi A_0^-$, 10^{-27} cm^2
240	1.20 ± 0.06	0.17 ± 0.11	0.89 ± 0.15	5.67	4	15.1 ± 0.8
270	0.99 ± 0.05	0.21 ± 0.09	0.74 ± 0.12	2.80	4	12.4 ± 0.6
307	0.91 ± 0.06	0.38 ± 0.11	0.72 ± 0.11	2.09	4	11.4 ± 0.8
333	0.82 ± 0.05	0.32 ± 0.06	0.57 ± 0.10	4.54	4	10.3 ± 0.6

calculated by the least squares method, are given in Table X. These coefficients give the minimum value of the sum of weighted squares of deviations

$$M = \sum \left(\frac{\sigma_i - f_i}{\epsilon_i} \right)^2, \qquad (3)$$

where f_i is the differential cross section at the i-th angle calculated from Eq. (2), σ_i is the experimental value of the differential cross section, and ϵ_i is the error in the measured differential cross section.

According to the theory of errors,[13,14] with the correct relation between experimental points, the most probable value of M is roughly equal to the difference between the number of experimental points and the number of parameters fitted. In our case, this number is four at all energies. Comparison of the expected values of M and those obtained (Table X) shows that the experimental values of the differential cross sections satisfy the dependence Eq. (2) sufficiently well.

Integrating the angular distribution of Eq. (2), one obtains the total cross section for elastic scattering of π^- mesons by protons. Integration leads to the expression

$$\sigma_{\pi^- \to \pi^-} = 4\pi A_0^-.$$

The magnitudes of the total cross sections obtained in this way are given in the last column of Table X.

---

[1] Mukhin, Ozerov, and Pontecorvo, JETP **31**, 371 (1956), Soviet Phys. JETP **4**, 237 (1957).

[2] A. I. Mukhin and B. Pontecorvo, JETP **31**, 550 (1956), Soviet Phys. JETP **4**, 373 (1957).

[3] E. L. Grigor'ev and N. A. Mitin, JETP **32**, 445 (1957), Soviet Phys. JETP **5**, 378 (1957).

[4] V. G. Zinov and S. M. Korenchenko, JETP **33**, 335 (1957), Soviet Phys. JETP **6**, 260 (1958).

[5] V. G. Zinov and S. M. Korenchenko, JETP **33**, 1308 (1957), Soviet Phys. JETP **6**, 1007 (1958).

[6] V. G. Zinov and S. M. Korenchenko, JETP **33**, 1307 (1957), Soviet Phys. JETP **6**, 1006 (1958).

[7] V. G. Zinov and S. M. Korenchenko, JETP **36**, 618 (1959), Soviet Phys. JETP **9**, 429 (1959).

[8] V. G. Zinov and S. M. Korenchenko, JETP **34**, 301 (1958), Soviet Phys. JETP **7**, 210 (1958).

[9] I. L. Lawson, Phys. Rev. **75**, 433 (1949).

[10] De Wire, Ashkin, and Beacher, Phys. Rev. **83**, 505 (1951).

[11] Lindenfeld, Sachs, and Steinberger, Phys. Rev. **89**, 531 (1953).

[12] Davies, Bethe, and Maximon, Phys. Rev. **93**, 788 (1954).

[13] I. V. Dunin-Barkovskiĭ and N. V. Smirnov, Теория вероятностей и математичемкая статистика в технике (Theory of Probability and Mathematical Statistics in Technology) Gostekhizdat, 1955.

[14] M. E. Rose, Phys. Rev. **91**, 610 (1953).

Translated by G. E. Brown
218

SOVIET PHYSICS JETP VOLUME 11, NUMBER 4 OCTOBER, 1960

INVESTIGATION OF THE DECAY SCHEME OF As^{76} *BY THE* γ-γ *COINCIDENCE METHOD*

N. N. DELYAGIN and A. A. SOROKIN

Institute of Nuclear Physics, Moscow State University

Submitted to JETP editor November 18, 1959

J. Exptl. Theoret. Phys. (U.S.S.R.) **38**, 1106-1110 (April, 1960)

The decay scheme of As^{76} was investigated with a scintillation coincidence spectrometer. Excited states of Se^{76} were found at 0.56, 1.21, 1.76, 2.42, 2.63 and ~ 2.85 Mev. Thirteen γ transitions between these levels were detected and their relative intensities were determined.

1. INTRODUCTION

THE decay scheme of As^{76} (T = 26.7 hours) has been investigated by many authors. In reference 1, where the available experimental data are analyzed and an extensive bibliography is provided, Gustova and Chubinskiĭ have shown that the generally accepted decay scheme of As^{76} (see reference 2, for example) is very incomplete and have proposed a new decay scheme, which takes the most recent data into account.[1,3,4] These data are, however, insufficient to determine the decay scheme unambiguously. Excited states of Se^{76}, according to the scheme proposed in reference 1, are so located that gamma transitions with identical or almost identical energies can occur between different levels. Such transitions cannot be resolved in the observed gamma spectrum, which is therefore not amenable to an unambiguous interpretation. The decay scheme given in reference 1 includes levels and transitions that lack direct and reliable experimental confirmation. The relative intensities of many transitions are based only on indirect data (intensity balance), which cannot be regarded as reliable since the intensities of the partial beta transitions have not been definitely determined.

Earlier results obtained by means of γ-γ coincidence studies[5-7] were actually only qualitative since the coincidence spectra were not analyzed and the results were interpreted on the basis of a simplified decay scheme.[2] The γ-γ coincidences studied in the present work have enabled us to establish unambiguously the existence of several excited Se^{76} states and of γ transitions between them. The relative intensities of the transitions were determined through a quantitative analysis of the spectra.

2. APPARATUS, SOURCE, AND EXPERIMENTAL PROCEDURE

We used a coincidence scintillation spectrometer, which was a modification of the instrument described in reference 8. The gamma rays were registered by NaI(Tl) crystals, measuring 4 cm in both thickness and diameter, in conjuction with a FEU-13 photomultiplier. The spectrometer resolution was 9.5% in the analyzing channel and 10.5% in the control channel for the 662-kev γ line of Cs^{137}. Pulses from the single-channel pulse-height analyzer in the control channel and from the integrating discriminator in the analyzing channel were fed to a coincidence scheme with a resolution time $2\tau = 1.5 \times 10^{-7}$ sec. Pulses from the photomultiplier of the analyzing channel were simultaneously fed to a 100-channel analyzer (AI-100-1) triggered by the coincidence circuit.

The efficiency calibration of the spectrometer was based on the total efficiency curves of NaI(Tl) crystals, which were computed in reference 9, and on the experimental ratios of the photopeak area to the area of the entire spectrum for certain gamma emitters with a simple decay scheme in the 150 — 2620 kev region. The resulting photoefficiency curve was verified by measurements with a number of isotopes for which the relative intensities of gamma transitions are well known. These measurements showed that the curve could be used to determine such relative intensities with 5 — 10% accuracy in not too complex spectra. The spectra were resolved with the aid of characteristic curves, from which the line shape for a gamma transition of given energy could be determined. The method of plotting these curves is described in reference 10.

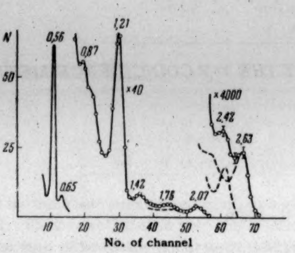

FIG. 1. Gamma-ray spectrum of As^{76}. Energies are given in Mev. Statistical errors for energies under 2.2 Mev are smaller than the size of the circles. Resolution of the hard part of the spectrum is represented by dashed curves. The ordinates are counting rates in arbitrary units.

The As^{76} source was prepared by irradiating arsenic metal with thermal neutrons in a reactor for a period of 40 hours, after which the arsenic was evaporated at about 500° C. Control measurements were performed with a source in which the bombarded arsenic was converted into AsH_3, thus completely eliminating the activity of Sb^{124}, which amounted to less than 1% impurity in the bombarded arsenic.

For coincidence measurements the source was placed between two NaI (Tl) crystals 15 cm apart. A lead absorber 2 mm thick was placed before the crystal of the control channel. Single gamma rays were measured with large distances between the source and crystal (up to 60 cm) in order to eliminate the possible summation of pulses from cascade gamma rays.

3. RESULTS

The gamma spectrum. Figure 1 shows the gamma-ray spectrum of As^{76} which was measured with 50 cm distance between the source and crystal. This spectrum was used to determine the relative intensities of nine gamma lines, which are given in Table I. The 0.56-Mev line was taken as 100.

TABLE I

Energy, Mev	Relative intensity
0,56	100
0,65	13.6±1.5
0.87	0.46±0.09
1.21	12.8±0.7
1,42	1.15±0.10
1,76	0.76±0.11
2.07	1.7±0.15
2.42	0.09±0.03
2,63	0.11±0.03
>2.70	<0.01

Our results for the relative intensities are in good agreement with references 4 and 1. The greatest discrepancies are found in the cases of the 1.42- and 2.63-Mev lines, although the results still agree within experimental error. It should be noted that in references 1 and 4 the existence of a few more weak gamma lines is indicated. We did not detect these lines, but we are not absolutely certain of their nonexistence because it is difficult to resolve the spectra with the required degree of accuracy.

As already mentioned in the introduction, some of the relative intensities in Table I do not correspond to actual gamma-transition intensities since certain lines may include contributions from transitions of equal or nearly equal energy between different levels of Se^{76}, as has been confirmed by investigation of the γ-γ coincidence spectrum.

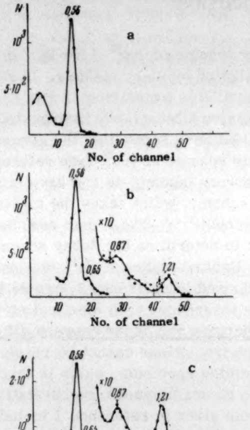

FIG. 2. γ–γ coincidence spectra. Energy ranges defined by the control analyzer window are: a – 2.0 – 2.2 Mev, b = 1.6 – 1.76 Mev, c = 1.4 – 1.5 Mev, d = 1.1 – 1.3 Mev.

γ-γ coincidences. Figure 2 shows the γ-γ coincidence spectra for four window positions of the control channel analyzer. In Fig. 2a the 2.07-Mev transition is in cascade only with the 0.56-Mev transition. Figure 2b shows peaks representing transitions with the energies 0.56, 0.65, 0.87, and 1.21 Mev. Comparison with the preceding spectrum showed that the 0.56-Mev photopeak may be entirely attributed to the 2.07 — 0.56 Mev cascade. Thus the 1.6 — 1.8 Mev gamma rays are in cascade with 0.65-, 0.87-, and 1.21-Mev gamma rays. Figure 2c shows the same peaks with a different intensity distribution. Taking Fig. 2b into account, it can be shown that the 0.87-Mev photopeak results entirely from the 0.87 — 1.76 Mev cascade, and that the 1.42-Mev gamma ray is in cascade with 0.56-, 0.65- and 1.21-Mev transitions. Figure 2d shows photopeaks at 0.56, 0.65, 1.21, 1.42 and ~ 1.64 Mev, all of which represent transitions in cascade with the 1.21-Mev transition.

In addition to the spectra in Fig. 2 we measured coincidences while the analyzer window was set for the 0.56-Mev photopeak. These results confirmed the preceding measurements; specifically, no 0.56 — 1.76 Mev cascade was observed.

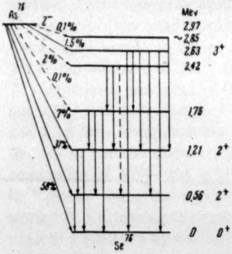

FIG. 3. Decay scheme of As^{76}.

The observed noncoincidence and coincidence spectra can be completely accounted for on the basis of the Se^{76} level scheme in Fig. 3, which will be discussed in the following section. In accordance with this scheme the relative intensities of the 0.87-, 1.42-, 1.76-, 2.07-, and 2.63-Mev transitions can be determined directly from the noncoincidence spectrum; the corresponding lines cannot be accounted for by superposed transitions with nearly identical energies.

When the decay scheme in reference 1 was constructed it was most difficult to determine the 0.56-, 0.65- and 1.21-Mev intensity distribution. These intensities were found by comparing the photopeak areas in the coincidence spectra, using noncoincidence line intensities. For example, by comparing the areas of the 1.21- and 1.42-Mev peaks in Fig. 2d we determined the relative intensity of the 1.21-Mev transition between the 1.21- and 2.42-Mev levels. Similarly, the spectrum in Fig. 2c (using the results in Fig. 2b) yielded the intensity ratio of the direct transition (1.21 Mev) to the 0.65 — 0.56 Mev cascade transition from the 1.21-Mev level to the ground state of Se^{76}; this ratio was found to be 0.85 ± 0.15.

The intensity of the 0.66-Mev transition between the 2.42- and 1.76-Mev levels was obtained from the spectrum in Fig. 2b by comparing the areas of the 0.66- and 0.87-Mev peaks. The relative intensities of other transitions were determined similarly by comparing the photopeaks in the coincidence spectra. For a number of transitions the intensities could be determined by different independent methods, thus providing an additional check on the correctness of the results. Table II shows the relative intensities that we obtained by the described procedure.

4. DISCUSSION

The decay scheme which we propose for As^{76} is shown in Fig. 3. In addition to the previously well known levels of Se^{76} at 0.56, 1.21, and 2.63 Mev (see reference 2, for example) we have introduced levels at 1.76, 2.42, and ~ 2.85 Mev. The 2.85-Mev level is required to account for the observed 1.21 — 1.64 Mev cascade. There is no additional evidence for the existence of this level, from which no ground-state transition was observed. The existence of the 2.42-Mev level is shown by the direct 2.42-Mev transition and the 1.21 — 1.21 and 0.66 — 1.76 Mev cascades. The 1.76-Mev level provides a reasonable explanation

TABLE II

Energy, Mev	Levels, Mev		Relative intensity	Energy, Mev	Levels, Mev		Relative intensity
	initial	final			initial	final	
0.56	0.56	0	100	0.66	2.42	1.76	1.5±0.4
0.65	1.21	0.56	12.1 ± 1.6	1.21	2.42	1.21	3.1 ± 1.0
1.21	1.21	0	10.3 ± 2.1	2.42	2.42	0	0.09 ± 0.03
0.55	1.76	1.21	1.5 ± 0.8	0.87	2.63	1.76	0.46 ± 0.09
1.20	1.76	0.56		1.42	2.63	1,21	1.15 ± 0.10
1.76	1.76	0	0.76 ± 0.11	2.07	2.63	0.56	1.7 ± 0.15
				2.63	2.63	0	0.11 ± 0.03

for the 0.87 — 1.76 and 0.66 — 1.76 Mev cascades without introducing additional levels between 0.56 and 1.21 Mev.

The Se^{76} levels in Fig. 3 enable us to account for all transitions observed by us and for their relative intensities. Our measurements do not indicate the existence of the 2.07-Mev level introduced by Gustova and Chubinskiĭ.[1] Nevertheless, an effort was made to process the data under the assumption that such a level exists. The measurements could not be accounted for when the existence of this level was assumed. If transitions associated with a 2.07-Mev level do exist their intensities are much smaller than the intensities of the transitions represented by the same energies which are shown in Table II.

The experimental data were inadequate to determine the relative intensities of the 0.55- and 1.2-Mev transitions from the 1.76-Mev level. Only their combined intensity could be determined, but the existence of at least one of the two transitions is shown by coincidences between 0.87- and 1.21-Mev photons.

The partial beta intensities in Fig. 3 were not obtained directly in the present work but were computed from the intensity balance of gamma transitions using reliable data for the two hardest components of the As^{76} beta spectrum. The combined intensity of the softer beta transitions obtained in this manner does not disagree with the available very inaccurate experimental data.

The authors wish to thank V. S. Shpinel' for his interest, and Cheng Tsung-Shuang and V. I. Anikin for assistance with the measurements.

[1] L. V. Gustova and O. V. Chubinskiĭ, JETP **35**, 1369 (1958), Soviet Phys. JETP **8**, 957 (1958).

[2] Strominger, Hollander, and Seaborg, Revs. Modern Phys. **30**, 585 (1958).

[3] Grigor'ev, Gustova, Zolotavin, Kratsik, Poleshchuk, and Chubinskiĭ, Вестник ЛГУ (Bulletin, Leningrad State University), Phys. and Chem. Series **10**, 37 (1957).

[4] Dzhelepov, Prikhodtseva, Feoktistov, and Khol'nov, Izv. Akad. Nauk SSSR, Ser. Fiz. **20**, 1361 (1956), Columbia Tech. Transl. p. 1245.

[5] J. J. Kraushaar and M. Goldhaber, Phys. Rev. **89**, 1081 (1953).

[6] Kurbatov, Murray, and Sakai, Phys. Rev. **98**, 674 (1955).

[7] E. G. Funk and M. L. Wiedenbeck, Phys. Rev. **109**, 922 (1958).

[8] Delyagin, Sorokin, Forafontov, and Shpinel', Izv. Akad. Nauk SSSR, Ser. Fiz. **20**, 913 (1956), Columbia Tech. Transl. p. 828.

[9] A. L. Stanford and W. K. Rivers, Rev. Sci. Instr. **29**, 406 (1958).

[10] Éstulin, Kalinkin, and Melioranskiĭ, JETP **32**, 979 (1957), Soviet Phys. JETP **5**, 801 (1957).

Translated by I. Emin
219

SOVIET PHYSICS JETP VOLUME 11, NUMBER 4 OCTOBER, 1960

RESONANCE SCATTERING OF GAMMA RAYS BY Se^{76}

N. N. DELYAGIN

Institute of Nuclear Physics, Moscow State University

Submitted to JETP editor November 18, 1959

J. Exptl. Theoret. Phys. (U.S.S.R.) **38**, 1111-1114 (April, 1960)

The lifetime of the first excited state of Se^{76} (0.56 Mev) was measured through the resonance scattering of gamma rays from a gaseous As^{76} source in the form AsH_3. $(1.3 \pm 0.2) \times 10^{-11}$ sec was obtained for the lifetime. The absence of resonance scattering of 1.21-Mev quanta, representing the ground-state transition from the second excited state of Se^{76}, indicates that the corresponding partial lifetime of the second excited Se^{76} state is greater than 6×10^{-12} sec.

1. INTRODUCTION

RECENT investigations[1,2] have shown that the beta decay of As^{76} is accompanied by gamma radiation corresponding to transitions between at least seven levels of Se^{76}. More than 90% of these beta decays go to the ground level and first two excited levels of Se^{76} (0.56 and 1.21 Mev). Both excited states have the spin and parity assignment 2^+, and electric quadrupole transitions are observed from these levels to the ground level of Se^{76} (see the decay scheme of As^{76} in the preceding article[2]). The end-point energies of the beta transitions to the 0.56- and 1.21-Mev levels of Se^{76} are 2.41 and 1.76 Mev, respectively. Favorable conditions thus exist for the observation of the resonance scattering of 0.56- and 1.21-Mev gamma rays by Se^{76} nuclei using the method of cascade transitions.[3-5] Following the beta decay of As^{76}, gamma rays are emitted by excited Se^{76} recoil nuclei which are in motion. The Doppler effect changes the magnitude of the emitted quanta, a certain fraction of which are increased by the amount of energy required to compensate for recoil losses during emission and absorption; this is a necessary condition for the observation of resonance scattering. In this type of experiment, it is usually necessary to use gaseous sources of gamma rays to insure a sufficiently long mean free time for the recoil nuclei. Otherwise, following the beta decay, collisions with neighboring atoms of the source material would slow the recoil nuclei down before radiating and the described compensation mechanism could not come into play.

The resonance scattering cross section is associated with the width of the excited level; observation of this process therefore enables us to determine the width and, consequently, the lifetime of the level. Temmer and Heydenburg,[6] as well as Alkhazov et al.[7] have obtained 1.7×10^{-11} sec and 1.3×10^{-11} sec, respectively, for the first excited level (0.56 Mev) of Se^{76} by means of Coulomb excitation. Coulomb excitation has led to conflicting values for the partial lifetime of the second excited state (for the direct transition to the ground state of Se^{76}). Reference 7 gives 2.5×10^{-12} sec, while the preliminary result given in reference 8 is of the order 10^{-11} sec.

2. RESONANCE GAMMA-RAY SCATTERING PROBABILITY

The calculation of the resonance scattering probability resembles earlier calculations by the present author[5] and by Metzger.[9] The resonance scattering probability can be expressed as a function of the excited level width. Constants are determined from the characteristics of the As^{76} decay scheme and from the parameters of the scatterer. The total scattering probability for a given experimental geometry is obtained by numerical integration over the volume of the scatterer. It is necessary to know the energy distribution N(E) of the gamma rays and its density at the resonance value of E.

The decay-scheme data which are required for the calculation are given in the preceding paper;[2] the uncertainties in the decay scheme have no essential effect.

$N(E_p)$ depends on the type of beta interaction. Despite recent progress in the study of beta decay, we have advanced no specific hypothesis regarding the type of interaction. The resulting uncertainty is included in the overall experimental error.

3. EXPERIMENTAL PROCEDURE

As already mentioned, the observation of resonance scattering requires the use of a gaseous gamma-ray source. It would be simplest for this purpose to use metallic arsenic containing As^{76}, which sublimes at a relatively low temperature. However, in arsenic vapor As_4 molecules are formed, so that the recoil atoms resulting from beta decay are not, strictly speaking, free. Although the energy of the recoil atoms considerably exceeds the atomic binding energy in the As_4 molecule, in some instances the bonds might not be broken (for example, when the recoil atom is moving toward the center of the molecule). Recoil energy may also be partially lost through other processes such as molecular rotation. Since such processes cannot be taken into account exactly, the gaseous source must either be a monatomic gas or a compound of As and a very light element such as hydrogen. In the latter case the molecular mass would be practically that of the As atom and the uncertainty associated with the chemical bonds would be unimportant.

In the present work arsine (AsH_3) was used as the gaseous source. About 5 mg arsenic metal was irradiated with thermal neutrons in a reactor for a period of 40 hours and was then used to prepare the alloy As_2Zn_3. The arsine produced by the interaction between this alloy and 30% sulfuric acid was collected in a 9-cm^3 glass ampoule and was solidified by cooling with liquid air. During this process the ampoule was evacuated and then sealed. Evacuation was required since collisions between recoil atoms and air molecules would otherwise reduce the resonance scattering effect. The pressure of the AsH_3 source gas did not exceed 0.02 atm, thus entirely excluding the possibility that collisions would affect the experimental results. The total activity of the source was of the order 10 mC, but only about 35% and 5% of the total number of decays is accompanied by the emission of 0.56-Mev and 1.21-Mev gamma rays, respectively.

The experimental geometry and the method of determining the resonance scattering cross section are described in reference 5. The scatterer was a hollow thin-walled aluminum cylinder filled with 99.5% pure selenium powder. The cylinder was 13.5 cm long and had an outside diameter of 30 cm. The selenium formed a layer 1.45 cm thick with a total weight of 6185 g. An arsenic scatterer of similar dimensions was used for comparison; the two scatterers were interchanged every 2 minutes. Similar measurements were also performed with a solid As^{76} source whose activity was equal to that of the gaseous source. When the solid source was used the counting rate of scattered radiation was identical for both scatterers. In conjunction with the gaseous source the counting rate for the selenium scatterer increased due to resonance scattering by Se^{76}. The experimental results were corrected for decay during the 70-hour period of continuous measurements.

Preliminary measurements were obtained with a source in the form of arsenic metal vapor produced by heating to ~ 500° C. Comparison with the results obtained with the AsH_3 source shows that the above-mentioned chemical-bond effect actually occurs; the resonance scattering cross section was 10 – 15% less in the first case. The experimental results that are discussed in the following section were obtained with the gaseous AsH_3 source alone.

4. RESULTS AND DISCUSSION

The average counting rate of resonance-scattered 0.56-Mev gamma rays was 0.52 ± 0.02 pulse/sec. This was 6% of the total counting rate, which represented mainly the laboratory background and elastic nonresonance gamma-ray scattering. A multichannel pulse-height analyzer was used to measure the scattering spectrum shown in the figure. Scattering by arsenic is represented by a smoothly falling curve while scattering by selenium exhibits a resonance peak at 0.56 Mev. The lifetime of the first excited Se^{76} state was found to be $(1.3 \pm 0.2) \times 10^{-11}$ sec, which is in excellent agreement with the Coulomb excitation value of 1.32×10^{-11} sec given in reference 7. The difference between these two results and 1.7×10^{-11} sec, which is given in reference 6 on the basis of Coulomb excitation, is within experimental error.

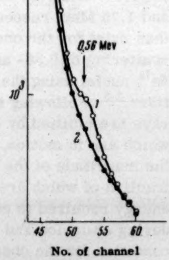

Gamma-ray scattering spectrum. 1 – Se scatterer; 2 – As scatterer; N – pulse counting rate in arbitrary units.

We did not observe resonance scattering of 1.21-Mev gamma rays, corresponding to the ground-state transition from the second excited state. In any event the counting rate of resonance scattering was under 0.002 pulse/sec, thus making it possible to measure only the lower limit of the lifetime. The partial lifetime of the second excited Se^{72} state for direct ground-state transitions must therefore be greater than 6×10^{-12} sec. This disagrees with the 2.5×10^{-12} sec lifetime given in reference 7, but agrees with reference 8, where a lifetime of the order 10^{-11} sec was obtained.

When we used the intensity ratio of the direct and cascade transitions from the second excited Se^{76} state, which is given in the preceding paper, we found that the partial lifetime for the cascade transition is also greater than 6×10^{-12} sec.

In references 6 and 7 Coulomb excitation was used to determine the reduced probabilities for electric quadrupole transitions from the first excited states of even-even selenium isotopes with mass numbers A = 76, 78, and 80. A relationship is found between these reduced probabilities and the excitation energies similar to that previously noted in references 5, 10 and 11 for even-even isotopes of several elements; an increase of excitation energy is always accompanied by a decrease of the reduced transition probability.

The author wishes to thank V. S. Shpinel' for directing this work, and V. I. Anikin for assistance with the preparation of the sources and with the measurements.

Note added in proof (March 4, 1960). New measurements of the lifetimes of excited Se^{76} states produced by Coulomb excitation were published after the present paper had gone to press. Alkhazov, Andreev, Grinberg, Erokhina, and Lemberg obtained 1.8×10^{-11} sec for the lifetime of the first excited Se^{76} state (Abstracts of the Tenth Conference on Nuclear Spectroscopy, Moscow, 1960, p. 95). The review article by Van Patter [Nuclear Phys. **14**, 42 (1959)] gives results obtained by McGowan and Stelson: $(1.62 \pm 0.15) \times 10^{-11}$ sec for the lifetime of the first excited state and $(1.2 \pm 0.4) \times 10^{-11}$ sec for the partial lifetime of the second excited state. These results are in agreement with our present work.

---

[1] L. V. Gustova and O. V. Chubinskiĭ, JETP **35**, 1369 (1958), Soviet Phys. JETP **8**, 957 (1959).

[2] N. N. Delyagin and A. A. Sorokin, JETP **38**, 1106 (1960), this issue, p. 799

[3] F. R. Metzger, Phys. Rev. **101**, 286 (1956); **103**, 983 (1956).

[4] N. N. Delyagin and V. S. Shpinel', Izv. Akad. Nauk SSSR, Ser. Fiz. **22**, 861 (1958), Columbia Tech. Transl. p. 855.

[5] N. N. Delyagin, JETP **37**, 1177 (1959), Soviet Phys. JETP **10**, 837 (1960).

[6] G. M. Temmer and N. P. Heydenburg, Phys. Rev. **104**, 967 (1956).

[7] Alkhazov, Gangrskiĭ, and Lemberg, Report at IX All-Union Conference on Nuclear Spectroscopy, Kharkov, 1959.

[8] P. H. Stelson and F. K. McGowan, Bull. Am. Phys. Soc. Ser. II, **4**, 232 (1959).

[9] F. R. Metzger, Phys. Rev. **110**, 123 (1958).

[10] P. H. Stelson and F. K. McGowan, Phys. Rev. **110**, 489 (1958).

[11] N. N. Delyagin, JETP **37**, 849 (1959), Soviet Phys. JETP **10**, 605 (1960).

Translated by I. Emin
220

SOVIET PHYSICS JETP VOLUME 11, NUMBER 4 OCTOBER, 1960

FRAGMENT PRODUCTION BY 100-Mev PROTONS

U. R. ARIFKHANOV, M. M. MAKAROV, N. A. PERFILOV, and V. P. SHAMOV

Radium Institute, Academy of Sciences, U.S.S.R.

Submitted to JETP editor November 26, 1959

J. Exptl. Theoret. Phys. (U.S.S.R.) 38, 1115-1122 (April, 1960)

The production of multiply charged fragments by 100-Mev protons incident on photoemulsion nuclei was investigated. The cross section for the fragmentation was found to be (1.93 ± 0.64) mb for heavy emulsion nuclei and (1.16 ± 0.36) mb for light nuclei. Energy and angle characteristics of the process are presented. A number of arguments are given in favor of the hypothesis that the multiply charged fragments are produced at 100 Mev by quasielastic scattering on nucleon clusters in the nucleus.

1. INTRODUCTION

THE study of the process of emission of many-nucleon structures (nuclei of He, Li, Be, etc.) from nuclei under the influence of bombardment by high-energy particles has recently become of considerable interest.

A study of this phenomenon throws light on the subject of nuclear structure, and also provides us with a better understanding of the mechanism of nuclear reactions. The Brueckner[1] model of strongly correlated particles provides an additional stimulus for the study of the fragmentation process.

Despite the large number of papers devoted to the study of this phenomenon, there exists as yet no unified point of view as to the mechanism of production of many-nucleon structures, or fragments, in nuclear reactions.

In this paper we study the production of fragments in photoemulsion nuclei by 100-Mev protons. The choice of energy was dictated by two considerations. First, at this value of E_p the nuclear cascade is not yet very well developed, and secondly, fragmentation takes place at an energy below the meson production threshold. All these circumstances simplify the study of the fragmentation process.

2. EXPERIMENTAL METHOD

In this work we used fine-grain nuclear type P-9 (ch) photoplates, sensitive to protons with energies up to 100 Mev. The emulsion used made it possible to detect all charged products of nuclear disintegrations and to separate by visual means multiply charged particles with $Z > 2$ from α particles and protons.

The irradiation by 100-Mev protons was performed at the synchrocyclotron of the Joint Institute for Nuclear Research. A decrease in the energy of the accelerated protons was accomplished by slowing them down in a copper block. The geometry of the experiment excluded from the beam the admixture of higher energy protons and of background neutrons.

In the scanning process stars with dense cone-like tracks of fragments with $Z > 2$ were selected. The number of fragments with charge $Z = 3$ might have been somewhat underestimated, because the tracks of α particles and Li nuclei were separated from each other visually and some Li fragments may have been missed. The charge was determined only for those fragments whose tracks formed with the emulsion plane an inclination angle (prior to development) of less than 35° and whose range was longer than 18μ. The separation of fragments by their charge was accomplished by track thickness measurements.[2] Then a distribution of individual events was constructed as a function of the track width, utilizing the last 18μ of the range. The hammerlike tracks of Li^8 and Be^8 were used for calibration. As a result charges were determined for 86 fragments from among the 295 fragments found. These data include also events consisting of the emission of two α particles with approximately equal energies in a narrow cone (< 3°), which could be identified as the decay in flight of a Be^8 nucleus.

We discuss next the method used for separating stars formed from light (C, N, O) and heavy (Ag, Br) emulsion nuclei. To that end the Coulomb barrier criterion was used: stars containing α-particle tracks with a range less than 50μ ($E_\alpha \leq 9$ Mev) but more than 4μ (which corresponds to the maximum range of the recoil nucleus), as well as stars containing tracks of two protons with ranges less than 120 μ ($E_p \leq 4$ Mev), were considered to be due to disintegrations of light nuclei. The validity of such a classification by "infrabarrier" particles, repeatedly verified for normal (without fragments) disintegrations of emulsion nuclei, was confirmed in the following manner. An analysis of the distribution in the number of prongs of stars with fragments produced from light nuclei showed, on one hand, good agreement with the corresponding distribution for normal stars also produced from light nuclei,[3,4] and, on the other hand, a difference from the distribution of stars with fragments produced in the disintegrations of heavy emulsion nuclei. As a final test the distribution in the number of prongs was analyzed for those stars with fragments which contained also a recoil nucleus and therefore must have been due to the disintegration of a heavy nucleus. It was found that the distributions of stars with fragments and stars with fragments and recoil nuclei were the same which testifies to the validity of the adopted criterion.

In this manner, 169 stars were classified as disintegrations of heavy nuclei and 126 stars as disintegrations of light nuclei. All these were subjected to a detailed analysis.

3. EXPERIMENTAL RESULTS

a) Cross section and character of the disintegrations. An estimate was obtained for the cross section for production of fragments from light and heavy emulsion nuclei. The proton flux was determined from the number of stars with prong number $n \geq 2$. The cross section for production of stars with $n \geq 2$ was taken to be equal to 139 mb.[5] In this manner the fragmentation cross section was found to be (1.93 ± 0.64) mb for Ag and Br nuclei and (1.16 ± 0.36) mb for C, N, and O nuclei.

A comparison with the data on fragment production cross sections by higher energy protons[6] is possible only for fragments with $Z \geq 4$ and with ranges $l > 15\,\mu$. In our case these cross sections are (0.81 ± 0.29) and (0.44 ± 0.16) mb respectively for heavy and light emulsion nuclei. Figure 1 shows data taken from reference 6 together with the results of this work. As can be seen, the fragment production cross section from heavy nuclei continues to fall with decreasing proton energy E_p. The light nuclei fragmentation cross section also falls with decreasing E_p, but considerably more slowly. However, the latter conclusion may be influenced by the inadequacy of the method used for identification of light and heavy nuclei in this work and in reference 6.

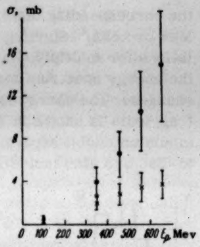

FIG. 1. Fragment production cross section σ as a function of the proton energy E_p: ● – from heavy nuclei, × – from light nuclei.

Disintegrations of heavy nuclei with fragment production are accompanied by a release of more energy than in normal disintegrations, as was also observed at other proton energies.[6] The average number of prongs in stars with fragments produced from heavy emulsion nuclei is equal to three, whereas in normal disintegrations it is equal to two (we use the average of the data of Hodgson[3] and Lees et al.[4]).

At the same time we obtained the relative probability for fragment emission from heavy nuclei as a function of the number of prongs in the star. The results of this analysis are given in Fig. 2 and show that the probability in question has a maximum.

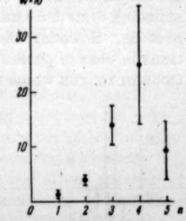

FIG. 2. Relative probability W of fragment emission as a function of the number n of prongs in the star (for heavy nuclei).

For stars due to light nuclei the large statistical errors make it impossible to draw any definite conclusions about the behavior of the corresponding probability.

b) Fragment distribution in charge, energy and range. Charges were determined for 49 fragments produced in disintegrations of Ag and Br nuclei, and for 37 fragments produced in disintegrations of C, N, and O nuclei. The results of the measurements are given in the table.

We note that the distribution in charge for fragments from Ag and Br nuclei is very similar to

Nuclei	Fragments		
	Li	Be	B
Ag, Br	30	14	5
C, N, O	20	12	5

the corresponding distribution obtained with 660 Mev protons.[6] Starting from the range-energy relations for multiply charged ions,[7] we constructed the energy spectrum for fragments with identified charges. The energy spectrum for Li and Be fragments is shown in Fig. 3 for light and heavy emulsion nuclei separately. Events corresponding to Be^8 are also included in the Be spectrum.

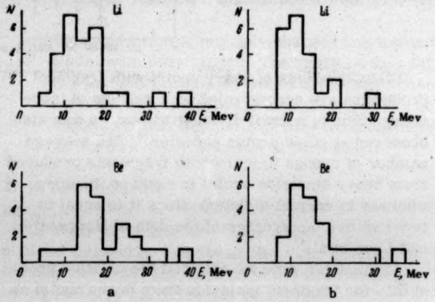

FIG. 3. Energy distribution of Li and Be fragments: a – for heavy nuclei, b – for light nuclei.

Poor statistics make it impossible to compare the fragment energy distributions with the corresponding distributions obtained with higher energy protons. However, the similarity of the distributions in charge permits a comparison of the distributions in ranges which is shown in Fig. 4. As can be seen the most probable range is approximately the same at different proton energies, despite the considerable difference in the distributions at large range values.

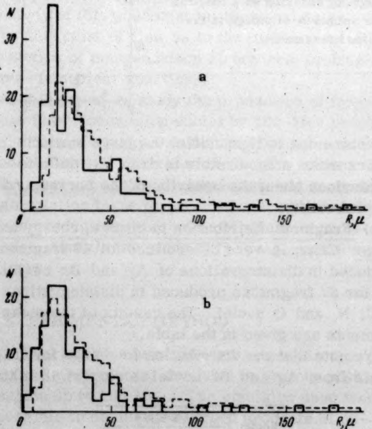

FIG. 4. The distribution of fragments in range R: a – for heavy nuclei, b – for light nuclei. The dashed line refers to the E_p = 660-Mev data.[6]

c) Angular distribution of the fragments. As can be seen from Fig. 5 a substantial asymmetry exists in the angular distribution of fragments obtained from the disintegrations of heavy and light emulsion nuclei. The ratio of the number of fragments in the forward hemisphere (with respect to the direction of the proton beam) to that in the backward hemisphere is equal to 9.0 ± 2.7 in the case of heavy emulsion nuclei. This is significantly larger than at higher proton energies (3.1 ± 0.5 at E_p = 350 Mev[6]). The asymmetry in the angular distribution of fragments from light nuclei is 24 : 1 and this value, too, is considerably larger than that obtained with 660-Mev protons. The previously obtained data[6,8] on the dependence on the incident proton energy of the asymmetry in the disintegrations of heavy emulsion nuclei are shown in Fig. 6. These data show quite unambiguously that as E_p increases the fragment distribution becomes more and more isotropic.

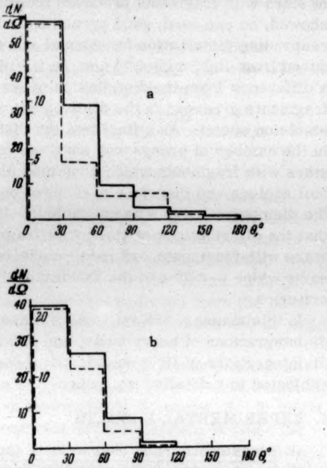

FIG. 5. Angular distribution of fragments produced on light (a) and heavy (b) emulsion nuclei. The solid line refers to all fragments, the dashed line refers to fragments with $l > 25\mu$ for light, and with $l > 40\mu$ for heavy, emulsion nuclei

4. DISCUSSION OF RESULTS

We must first discuss the very fact that fragments are produced at energies below the meson

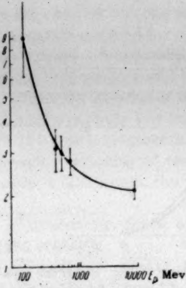

FIG. 6. The dependence of the asymmetry of fragment production in the disintegrations of heavy nuclei on the proton energy E_p. Along the ordinate is plotted the ratio of the number of fragments emitted in the forward and backward directions.

production threshold. In a number of radiochemical investigations (see, e.g., Friedlander et al.[9]) the production of fragments with masses ~ 10 — 40 was associated with intense meson production and absorption in the nucleus. It is, of course, not possible to put an equality sign between the reaction products studied by us and those obtained by Friedlander et al.,[9] but it does follow from our work that multiply-charged fragments can be produced also without meson participation. Consequently it is quite likely that at least some of the fragments produced in the bombardment of nuclei by high-energy (~ 1 Bev) protons are of the same origin as the fragments studied by us.

It is of interest to discuss the production of multiply-charged fragments by 100-Mev protons from the point of view of fission, evaporation, and nuclear cascade processes.

The possibility of fragment production as the result of asymmetric fission was studied in detail by Lozhkhin and Perfilov,[6] who showed that asymmetric fission fails to explain satisfactorily many of the experimental facts of fragmentation: for example, it is rather difficult to relate asymmetric fission and the appearance of fragments with energy in excess of the Coulomb repulsion.

It has been suggested by some authors (see, in particular, Hodgson[10] and Skjeggestad and Sorensen[11]) that fragments might be produced in the process of evaporation from a strongly excited nucleus. It appears to us that in this case, too, there are significant contradictions with experiment, of which the most important is the pronounced asymmetry in the fragment distribution. In the evaporation model the asymmetry is due to translational motion and is given by the ratio $(u + v)/(u - v)$, where u is the speed of the "evaporating" particle and v is the speed of the nucleus. This ratio is equal to 1.16, in disagreement with the experimental value of 9 for the asymmetry.

However, a certain fraction of the fragments might, apparently, be produced in the evaporation process. Indeed, of the 169 fragments found in the disintegrations of heavy nuclei, 17 were emitted into the backward hemisphere relative to the direction of the beam. Let us suppose that these fragments were produced in the evaporation process from the Ag and Br nuclei. Then, making use of the value of the asymmetry expected for the evaporation process (1.16), we come to the conclusion that only 37 fragments can be due to evaporation.

The probability for the emission of various particles relative to the probability for proton emission may be obtained from the evaporation theory developed by Hagedorn and Macke.[12] The calculation of the relative probability of evaporation of Be^9 fragments from Ru^{100} nuclei (Ru is between Ag and Br), using the values 2.58 Mev for the parameter T and 18.8 Mev for V, gives a result in good agreement with experiment if it is assumed that 37 fragments are due to evaporation.

Consequently it may be assumed that the evaporation process is responsible for the production of at most one fifth of all fragments.

The possibility that multiply charged fragments are produced by the nuclear cascade process is evident already from their anisotropic distribution. It may be supposed that the fragments are emitted from the nucleus as a result of quasielastic interactions of the incident nucleon with strongly bound nucleon clusters in the nucleus.[13] Indeed, there exist a number of reasons for the belief[14] that when a nucleus is traversed by a nucleon not only nucleon-nucleon interactions are possible, but also interactions between the nucleon and a cluster formed as a consequence of a shortlived nuclear matter fluctuation.[15] The experiments of Meshcheryakov et al.[14] showed that the existence of such clusters (type d) is possible; in all probability the cascade α particles detected in photoemulsion experiments[16] are also due to such shortlived clusters. The similarity of a majority of the characteristics of the knock-out processes of fast α particles and of heavier fragments should be noted. It is therefore plausible to assume that occasionally also larger structures of the light nuclei type can be formed in a nucleus and it is with these structures, as a whole, that the incident particle interacts. If fragment emission is due to quasielastic scattering of protons by nucleon clusters in the nucleus then there should exist a correlation between the directions of emission of the multiply charged fragments and the fast recoil proton. A search for such a correlation was carried out for all disintegrations with fragments. The number of disintegrations with two cascade protons did not exceed 4%. Consequently in almost all disintegrations we measured one spatial angle between the direction of emission of the fragment and of the proton with an energy in excess of 20 Mev. The angular distribution so obtained is shown in Fig. 7 for the disintegrations of heavy emulsion nuclei (the picture was analogous for fragments from light nuclei). As can be seen from the figure, a pronounced correlation exists between the directions of emission of the fragment and the fast proton. The dotted line in the figure refers to the calculated distribution in the angles between the fragments and cascade protons derived from the angular distributions of the fragments and the protons. Figure 7 shows that the discovered correlation is not accidental.

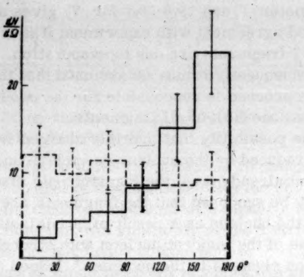

FIG. 7. Correlation between fragments and cascade protons (for heavy nuclei). The dashed line refers to calculated accidental correlation. Along the abscissa is plotted the angle between the directions of the fragment and the proton (E > 20 Mev).

Starting from the hypothesis of a collision mechanism for fragment production, we can discuss the dependence of the fragment energy on its emission angle according to the formulas for elastic collisions. Figure 8 shows curves calculated for the interaction of a 100-Mev proton with nuclei of mass 7 and 9, and also the experimental points. These experimental points are rather widely scattered and fall significantly below the calculated curve. This circumstance suggests that for 100-Mev protons the fragments are knocked out not by the primary, but by secondary, nucleons produced in the branching out process of the nuclear cascade and having a significantly lower energy. Indeed, if we construct curves for elastic collisions in such a manner that the deviations towards larger and smaller angles are approximately equal, we find that these curves correspond to protons with energies between 30 and 60 Mev, in agreement with the results obtained for the knockout of cascade α particles.[17] The scatter of the points relative to the calculated curves might be explained by the momentum distribution of the fragments in the nucleus.

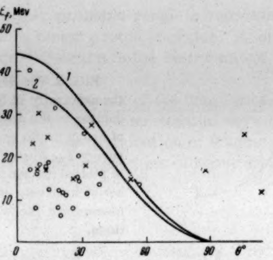

FIG. 8. The dependence of fragment energy E_f on the emission angle θ. The curves refer to calculations for elastic collisions: 1 – for fragments with mass M = 7 (Li); 2 – for M = 9 (Be). ● – experimental points for Li; × – for Be.

We conclude therefore that multiply-charged fragments are produced at $E_p = 100$ Mev mainly by quasielastic knock-out of nucleon clusters from the peripheral region of the nucleus by secondary nucleons, arising from a branched-out cascade.

The available data, unfortunately, do not allow a more precise determination of what part of the fragments under study is due to the nuclear cascade and what part is due to evaporation, although it seems to us that in such an approach to the fragmentation process the influence of the evaporation mechanism could have been only overemphasized, and that basically fragments are produced on heavy emulsion nuclei in the process of a branched-out nuclear cascade.

In the above discussion we have said little about fragmentation of light emulsion nuclei. The basic experimental results on fragment production are the same for light and heavy nuclei. The different energy dependence of the cross section and of the anisotropy are apparently related to a different degree of development of the cascade process. Indeed, calculations on the nuclear cascade process using the Monte Carlo method[18] show that for light nuclei the number of cascade nucleons changes slowly with proton energy, which explains the comparatively weak energy dependence of the cross section and anisotropy. In the fragmentation process of light nuclei the collision mechanism should operate almost exclusively, since the term "evaporation" is not applicable to light nuclei, and fragment production as residual nuclei is in contradiction with the angular distribution. Thus, in the case of nucleus pulverization the ratio of fragments emitted forward and backward should not exceed 1.5 and consequently no more than 10% of the fragments could be produced in this manner.

Thus the results of this work are evidence that at comparatively low incident proton energies (~100 Mev) fragments are produced by quasi-elastic scattering of secondary nucleons on moving nucleon clusters in the nucleus.

---

[1] Brueckner, Eden, and Francis, Phys. Rev. **98**, 1445 (1955).

[2] Nakagawa, Tamai, Huzita, and Okudaira, J. Phys. Soc. Japan **11**, 191 (1956).

[3] P. E. Hodgson, Phil. Mag. **45**, 190 (1954).

[4] Lees, Morrison, Muirhead, and Rosser, Phil. Mag. **44**, 304 (1953).

[5] L. S. Germain, Phys. Rev. **82**, 596 (1951).

[6] O. V. Lozhkin and N. A. Perfilov, JETP **31**, 913 (1956), Soviet Phys. JETP **4**, 790 (1957); O. V. Lozhkin, Thesis, Radium Inst. Acad. Sci., 1957.

[7] A. Papineau, Compt. rend. **242**, 2933 (1956).

[8] Perfilov, Ivanova, Lozhkin, Makarov, Ostroumov, Solov'eva, and Shamov, JETP **38**, 345 (1960), Soviet Phys. JETP **11**, 250 (1960).

[9] Friedlander, Miller, Wolfgang, Hudis, and Baker, Phys. Rev. **94**, 727 (1954).

[10] P. E. Hodgson, Phil. Mag. **42**, 207 (1951).

[11] P. Skjeggestad and S. O. Sorensen, Phys. Rev. **113**, 1115 (1959).

[12] R. Hagedorn and W. Macke, Kosmische Strahlung, Berlin, 1953, p. 201.

[13] G. A. Leksin, JETP **32**, 440 (1957), Soviet Phys. JETP **5**, 371 (1957).

[14] Azhgireĭ, Vzorov, Zrelov, Meshcheryakov, Neganov, and Shabudin, JETP **33**, 1185 (1957), Soviet Phys. JETP **6**, 911 (1958).

[15] D. I. Blokhintsev, JETP **33**, 1295 (1957), Soviet Phys. JETP **6**, 995 (1958).

[16] Ostroumov, Perfilov, and Filov, JETP **36**, 367 (1959), Soviet Phys. JETP **9**, 254 (1959).

[17] V. I. Ostroumov and R. A. Filov, JETP **37**, 643 (1959), Soviet Phys. JETP **10**, 459 (1960).

[18] Metropolis, Bivins, Storm, Turkevich, Miller, and Friedlander, Phys. Rev. **110**, 185 (1958).

Translated by A. M. Bincer
221

SOVIET PHYSICS JETP VOLUME 11, NUMBER 4 OCTOBER, 1960

THE EXISTENCE OF NEW ISOTOPES OF LIGHT NUCLEI AND THE EQUATION OF STATE OF NEUTRONS

Ya. B. ZEL'DOVICH

Submitted to JETP editor October 22, 1959

J. Exptl. Theoret. Phys. (U.S.S.R.) 38, 1123-1131 (April, 1960)

The limits of stability (relative to nucleon emission) of light nuclei are considered. The existence (in the sense of stability against decay with emission of a nucleon) of the following nuclei is predicted: He^8, Be^{12}, O^{13}, $B^{15,17,19}$, C^{16-20}, N^{18-21}, Mg^{20}. The problem of the possibility of existence of heavy nuclei composed of neutrons only is considered. The problem is reduced to that of a Fermi gas with a resonance interaction between the particles. The energy of such a gas is proportional to $\omega^{2/3}$, where ω is its density. The accuracy of the calculations is not sufficient to determine the sign of the energy and answer the question as to the existence of neutron nuclei.

THE problem of the possible isotopes has been treated by Nemirovskii[1,2] for $8 \le Z \le 84$, and by Baz'[3] for the region $17 \le A \le 40$. The former uses the one-particle approximation, with an attempt to find the dependence of the parameters of the well on the numbers of neutrons and protons. For nuclei with an excess of protons Baz' bases his discussion on the experimental data on the mirror nuclei (with excess of neutrons) and on the well-known expression for the Coulomb energy. For nuclei with an excess of neutrons he extrapollates the binding energy in series of nuclei with constant isotopic spin.

These papers predict the existence of many as yet unknown β-active isotopes. In the table given below the isotopes so predicted are enclosed in dashed-line squares. One of them has very recently been observed experimentally.[4]

In the present paper (Sec. 1) we make additional predictions in the region of the lightest nuclei; the isotopes so predicted are enclosed in solid-line squares in the table. We point out particularly the conclusion that there is a large probability that He^8 exists. For nuclei with an excess of neutrons the writer has tried to take the effect of shells and the pair interaction of neutrons into account as accurately as possible.

In Sec. 2 the question is raised of the existence of nuclei composed solely of neutrons. In the limiting case of a large number of neutrons, by using the data on resonance in the ^1S scattering, one can find the general form of the dependence of the energy on the density of the nuclear matter, but the accuracy of the first approximation obtained in this paper is insufficient to give a definite answer to the question of the existence of such nuclei.

1. LIGHT NUCLEI

Following the method of Baz',[3] one easily convinces oneself that there must exist a nucleus O^{13} with a proton binding energy not smaller than 1.2 Mev and with β^+-decay energy 16 to 17 Mev. Using the data[4] on the mass of O^{20}, we conclude that the mirror nucleus Mg^{20} must exist with proton binding energy not less than 2.7 Mev and β^+-decay energy about 7 Mev. The existence of O^{12}, Ne^{16}, and Mg^{19} is not excluded (empty spaces in the table);* the corresponding mirror isotopes Be^{12}, C^{16}, and N^{19} are predicted in this paper (see later argument), but their energies cannot be predicted with enough accuracy to give a definite conclusion about O^{12}, Ne^{16}, and Mg^{19}. The isotopes Ne^{17}, Na^{19}, Mg^{21}, and Mg^{22} are predicted by Baz'.

Regarding all the other nuclei in the upper right-hand part of the table we can assert with assurance that they are unstable against emission of a proton, i.e., they do not exist, which is shown in the table by the minus signs in all the upper cells.

Let us turn to the nuclei with an excess of neutrons. A nucleus with an excess of neutrons does not exist in the case in which all the discrete levels are already filled up with neutrons. An important point here is that the nuclear forces fall off rapidly with distance, and therefore the number of levels in the field of the nuclear forces is limited (in

---

*These nuclei may be unstable with respect to the emission of two protons at once. On the other hand, at the limit of stability the expression for the Coulomb energy of the last proton, $1.2(Z-1)A^{-1/3}$, gives too large a result; for example, in the pair Li^8-B^8 we have for Li^8 the binding energy $Q_n = 2$ Mev and for B^8 the value $Q_p = 0.2$ Mev, so that the difference is 1.8 Mev, whereas by the formula we would get $1.2 \times 4 \times 7^{-1/3} = 2.5$ Mev.

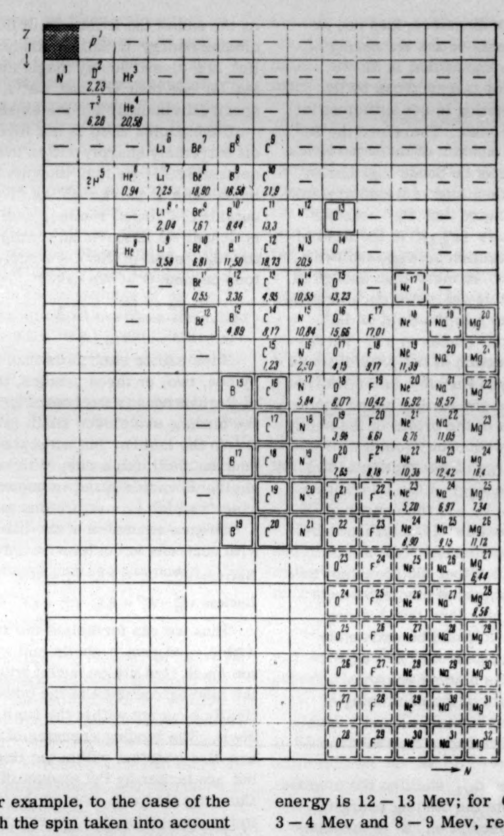

▨	p^1	—	—	—	—	—	—	—	—	—	—	—
N^1	D^2 2.23	He^3	—	—	—	—	—	—	—	—	—	—
—	T^3 6.28	He^4 20.58	—	—	—	—	—	—	—	—	—	—
—	—	—	Li^6	Be^7	B^8	C^9	—	—	—	—	—	—
	?H^5	He^6 0.94	Li^7 7.25	Be^8 18.90	B^9 18.58	C^{10} 21.9	—		—	—	—	—
		—	Li^8 2.04	Be^9 1.67	B^{10} 8.44	C^{11} 13.3	N^{12}	O^{13}	—	—	—	—
		He^8	Li^9 3.58	Be^{10} 6.81	B^{11} 11.50	C^{12} 18.73	N^{13} 20.9	O^{14}	—		—	—
		—	—	Be^{11} 0.55	B^{12} 3.36	C^{13} 4.95	N^{14} 10.55	O^{15} 13.23	—	Ne^{17}	—	
		—		Be^{12}	B^{13} 4.89	C^{14} 8.17	N^{15} 10.84	O^{16} 15.66	F^{17} 17.01	Ne^{18}	Na^{19}	Mg^{20}
				—		C^{15} 1.23	N^{16} 2.50	O^{17} 4.15	F^{18} 9.17	Ne^{19} 11.39	Na^{20}	Mg^{21}
					B^{15}	C^{16}	N^{17} 5.84	O^{18} 8.07	F^{19} 10.42	Ne^{20} 16.92	Na^{21} 18.57	Mg^{22}
				—		C^{17}	N^{18}	O^{19} 3.96	F^{20} 6.61	Ne^{21} 6.76	Na^{22} 11.05	Mg^{23}
					B^{17}	C^{18}	N^{19}	O^{20} 7.63	F^{21} 8.18	Ne^{22} 10.36	Na^{23} 12.42	Mg^{24} 16.4
				—		C^{19}	N^{20}	O^{21}	F^{22}	Ne^{23} 5.20	Na^{24} 6.97	Mg^{25} 7.34
					B^{19}	C^{20}	N^{21}	O^{22}	F^{23}	Ne^{24} 8.90	Na^{25} 9.15	Mg^{26} 11.12
								O^{23}	F^{24}	Ne^{25}	Na^{26}	Mg^{27} 6.44
								O^{24}	F^{25}	Ne^{26}	Na^{27}	Mg^{28} 8.58
								O^{25}	F^{26}	Ne^{27}	Na^{28}	Mg^{29}
								O^{26}	F^{27}	Ne^{28}	Na^{29}	Mg^{30}
								O^{27}	F^{28}	Ne^{29}	Na^{30}	Mg^{31}
								O^{28}	F^{29}	Ne^{30}	Na^{31}	Mg^{32}

contradistinction, for example, to the case of the Coulomb field). With the spin taken into account the number of levels is always even; therefore if a nucleus exists containing an odd number of neutrons $(2n + 1)$, then there is also a place for a subsequent $(2n + 2)$-nd neutron. On account of the mutual attraction of a pair of neutrons the binding energy of the $(2n + 2)$-nd neutron is always larger than that of the preceding $(2n + 1)$-st neutron.

In each cell of the table that corresponds to an experimentally known isotope there is written the binding energy of the last neutron. It is easily verified that in all cases $E_{2n+2} > E_{2n+1}$. Therefore the existence of the nuclei Be^{12} and C^{16} definitely follows from the existence of Be^{11} and C^{15}. As a rough estimate, the binding energy of a neutron in Be^{12} is about 2 — 3 Mev, and the β-decay energy is 12 — 13 Mev; for C^{16} these values are 3 — 4 Mev and 8 — 9 Mev, respectively.

It is much harder to settle the existence of other isotopes. Extrapolation for fixed isotopic spin[3] T is not reliable, since it involves comparison of neutrons that are in different shells.

For the lightest nuclei the idea of a smooth dependence of the parameters of the well on N and Z[1,2] does not take sufficient account of the individual peculiarities of the shells. We shall try to make maximum use of the experimental data. It is known from the scattering of neutrons by He^4 that for the partial wave $P_{3/2}$ there is a resonance at the energy +1.0 Mev (i.e., in the continuous spectrum) with width 0.55 Mev (which corresponds to an He^5 lifetime of 10^{-21} sec). The nucleus He^5 does not exist, and consequently there is no discrete bound state of a neutron in the field of He^4.

In the same sense, the dineutron does not exist, since from experiments on the scattering of neutrons by protons it is known that in the ^1S state, which is allowed for two neutrons by the Pauli principle, the attraction is not sufficient for the formation of a bound state. Therefore the He^6 nucleus is a remarkable system of three particles $(n + n + He^4)$, which cannot be bound together in pairs, but all three together form a bound system. Quite crudely we can imagine that He^6 consists of two neutrons in the state $(P_{3/2})^2$ in the field of He^4. The energy of interaction between the two neutrons (about -3 Mev) is more than enough to compensate for the positive energy of each neutron in the state $P_{3/2}$ (+1 Mev) in the field of He^4.

The $P_{3/2}$ shell has four places in all. Therefore we can raise the question of the possibility of He^7 and He^8. According to Kurath,[5] in the limit of small range of the forces and weakly bound nucleons, and for large radius of the orbits of the shell ($r_0 \ll r_1$, $L = 3K$, in his notation), one gets a simple result: if the energy of interaction of two neutrons is B, then the energy of the interaction of three neutrons is also B, and the energy of the interaction of four neutrons is 2B, i.e., the neutrons combine in pairs, as it were. From this there follows the conclusion that He^7 does not exist, but He^8 exists; the expected binding energy of a neutron in 0.8 — 0.5 Mev, and the β-decay energy is about 12 Mev. It would be extremely desirable to verify the existence of He^8 experimentally and determine its binding energy.

How accurately the rule of the combining of neutrons in pairs in a single shell around a doubly magic (closed) core holds experimentally can be seen from two examples.[*]

1) The filling up of the $d_{5/2}$ shell on the closed O^{16} (see table). We quote the binding energies (in megavolts). The subscript on E is the number of neutrons in the $d_{5/2}$ shell (the upper index is the atomic weight):

$$E_1^{17} = 4.15, \quad E_2^{18} = 8.07, \quad E_3^{19} = 3.96, \quad E_4^{20} = 7.65.$$

There are no data on E_5 and E_6, which finish the filling of the shell; the nuclei O^{21} and O^{22} have not yet been observed.

2) The filling up of the $f_{7/2}$ shell on Ca^{40}, which has closed shells (this example has been treated partially by Nemirovskiĭ[2]). The binding energies are:

E_1^{41}	E_2^{42}	E_3^{43}	E_4^{44}	E_5^{45}	E_6^{46}	E_7^{47}	E_8^{48}
8.3	11.4	8.0	11.4	7.4	11.0 (?)[†]	6.8 ?[†]	10.8

At the end of the filling-up of the $f_{7/2}$ shell the binding energy E falls sharply: $E_9^{49} = 5.1$. Since He^4 is a closed doubly magic nucleus (and an even stabler one than O^{16} and Ca^{40}), these examples speak convincingly for the existence of He^8.

If the proton shell is not filled, then E drops off extremely sharply within the range of the given neutron shell; we may imagine that the first neutrons unite in pairs with the "free" protons (those outside the closed shells), and later neutrons can no longer do this. As an example let us consider the $d_{5/2}$ shell of Ne^{18} — a nucleus with two protons beyond O^{16}. We have:

E_1^{19}	E_2^{20}	E_3^{21}	E_4^{22}	E_5^{23}	E_6^{24}
11.4	16.9	6.8	10.4	5.2	8.9

If the proton shell falls short of being closed by one, two, or three protons, the binding energy of the neutrons is decreased as compared with the binding to a closed shell (cf. C^{15}, N^{16}, and O^{17} in the table). But within the limits of a given neutron shell (on a core with holes in the proton shell) E varies little, in contradistinction to the case in which excess protons are present.

We give examples of the filling of the $f_{7/2}$ shell with neutrons in nuclei with unfilled proton shells:

Nucleus K_{19}^{39}: $E_1^{40} = 7.9$, $E_2^{41} = 10.0$, $E_3^{42} = 7.4$, $E_4^{43} = 10.8$.

Nucleus Ar_{18}^{38}: $E_1^{39} = 6.7$, $E_2^{40} = 9.7$, $E_3^{41} = 6.1$.

Thus we can formulate the rule that on nuclei with closed proton shells and with holes in the proton shell (but not on nuclei with excess protons), the binding energies of the odd neutrons are practically constant within the limits of a given neutron shell. The binding energies of the even neutrons are also constant within the limits of a given shell, but are larger by the amount of the pairing energy. Carrying this rule over to the $d_{5/2}$ shell, we come to the conclusion that the experimental fact of the existence of bound $d_{5/2}$ states in the nuclei C^{15} and N^{16}, N^{17} guarantees the possibility of filling up the entire $d_{5/2}$ shell, to C^{20} and N^{21}, respectively.

An examination of the binding energies of neutrons in the table reveals a regular increase of E in each row, with increase of the number of protons (the single exception is the pair $Li^8 - Be^9$, which is due to the special structure of Be^8). Extrapolation of E to the left along the rows makes probable the existence of B^{15}, and from this — by the principle of the constancy of the binding energy in a shell — of B^{17} and B^{19}. The existence of the nuclei with odd numbers of neutrons, B^{14}, B^{16}, B^{18}, remains questionable. With considerable assurance we can assert that the odd (in n) nuclei Be^{13}, Be^{15}, Be^{17}, Li^{10}, He^9 do not exist.

---

[*] The mass data are taken from review articles.[6–8]

[†] The nucleus Ca^{46} has not been studied, so that one knows experimentally only the sum $E_6^{46} + E_7^{47} = 17.8$; the separate terms in the table are obtained by interpolation.

On the whole, however, the assertions that can be made reliably about nuclei with excess neutrons not known to exist are extremely scanty. From studies of scattering only the nonexistence of n^2 and He^5 is quite accurately proved. From principles of the pair interaction of neutrons it is obvious that n^3 and He^7 do not exist. There is no longer such certainty regarding H^5 (H^5 is entered in the table with a question mark), and the hypothesis that it is stable has been suggested.[9] We note that if n^4 and H^5 existed, then there would be isotopically similar quasi-stable systems H^4 with $T = 2$ and He^5 with $T = 3/2$, which would manifest themselves in the scattering of n by T and of n by He^4; this situation has been examined in detail in a separate note.[10] At present there are no experimental data in the required range of neutron energies.

Unlike the upper right-hand part of the table, which is almost solidly filled with minus signs ("does not exist"), in most of the cells of the lower left-hand part we can put neither a minus nor the symbol of a nucleus ("exists"). The obscurity of the problem of the limits of existence of isotopes with excess neutrons is a consequence of the fact that the limiting case is not clear; it is not known whether a heavy nucleus composed solely of neutrons could exist.

2. THE NEUTRON LIQUID

The problem of the limiting number of neutrons that can adhere to a heavy nucleus has been considered by Wheeler;[11] he came to the conclusion that for $Z \sim 90-100$ the maximum mass number is $A_{max} \sim 500-600$. Wheeler used the Weizsäcker formula; Nemirovskiĭ[2] correctly critizes this formula near the limits of existence, and therefore Wheeler's conclusions are not reliable.

Let us consider the extreme case of a very large nucleus consisting of neutrons alone. If it does exist, it surely does so only with a density much smaller than that of ordinary nuclei. Let us first examine the properties of a neutron liquid of small density; these properties are determined by the pair interactions of the neutrons at small energies (up to a few Mev). In this region only the interaction of pairs of neutrons in the ^1S state is of importance, and here this interaction is completely determined by the scattering length* (cf., e.g., reference 12)

$$a = -(d \ln \varphi / dr)^{-1} = -19 \cdot 10^{-13} \text{ cm};$$

the sign corresponds to the absence of a bound state, and the quantity a corresponds to the so-called energy of a virtual level (μ is the reduced mass, equal to $M/2$):

$$E_v = \hbar^2/2\mu a^2 = 0.11 \text{ Mev}.$$

We cite here the well-known calculation[13,14] of the energy of interaction of particles in the continuous spectrum, confining ourselves at once to the S wave. As usual, we consider first a spherical box for $\mathbf{r} = \mathbf{r}_1 - \mathbf{r}_2$, where $\mathbf{r}_1$ and $\mathbf{r}_2$ are the coordinates of the two particles, i.e., we set $\psi(\mathbf{r}) = 0$ at $|\mathbf{r}| = R$. Without interaction the normalized S-wave function in such a box is

$$\psi = \sin(n\pi r/R) / r\sqrt{2\pi R}.$$

With an interaction corresponding to scattering with the phase shift α we have

$$\psi = \sin[\alpha + R^{-1}(n - \alpha/\pi)\pi r] / r\sqrt{2\pi R},$$

which corresponds to a change of the energy of the n-th state given by

$$\Delta E_n = -\hbar^2 n\pi\alpha / \mu R^2.$$

Let us eliminate the auxiliary quantities R and n from the expression for ΔE_n. The state under consideration is characterized by the momentum of the relative motion

$$p_n = \hbar n\pi / R$$

and the density at the origin of coordinates in the unperturbed motion

$$\rho_n(0) = \psi^2(0) = \pi n^2 / 2R^3.$$

Let us express ΔE_n in terms of p and $\rho(0)$; after this we can set $R \to \infty$, $n \to \infty$, and forget about n. We get

$$\Delta E = -2\pi\hbar^3\alpha\rho(0) / \mu p. \tag{1}$$

We express the phase in terms of the scattering length:

$$\alpha = -\tan^{-1}(ap/\hbar).$$

For $E \ll E_V$, $ap \ll \hbar$ we have

$$\alpha = ap/\hbar, \qquad \Delta E = -2\pi\hbar^2 a\rho(0) / \mu; \tag{2}$$

for $E \gg E_V$, $ap \gg \hbar$ we get

$$\alpha = \pi/2, \qquad \Delta E = -\pi^2\hbar^3\rho(0) / p\mu. \tag{3}$$

Let us apply the expressions (2) and (3) to a Fermi gas consisting of neutrons only with mean density ω. We single out one neutron with a definite spin direction. At the point where this neutron is located, the density of other neutrons with the same spin direction is zero by the Pauli principle; if there were no interaction, the density of the other neutrons with antiparallel spins would not differ from that of those with parallel spins on the average over all space; that is, $\omega(0) = \omega/2$. We recall that ω is the total density of neutrons with both spin directions and that the formula for ΔE contains just the density in the state without interaction.*

---

*For pp scattering $a = -17.2$, and for np scattering $a = -23.7$; we assume that a depends linearly on the product of the magnetic moments.

We still have to take into account the fact that the change of energy ΔE relates to a system of two particles; in order not to include the interaction of each pair twice, we recall that the decrease of the energy of one particle is $\Delta E/2$. We finally find that if for a pair of particles in the ^1S state $\Delta E = k\rho(0)$, where k is a coefficient that depends on the momentum, then the change of the energy of all the gas in unit volume on account of the interaction is

$$U = \omega^2 \bar{k}/4; \tag{4}$$

here k is averaged over the Fermi distribution.

The Fermi distribution is characterized by the boundary momentum p_f, the boundary energy E_f, and the total kinetic energy $\mathcal{E}$ of all the gas in unit volume; as is well known

$$\mathcal{E} = \omega\bar{E} = \tfrac{3}{5}\omega E_f, \qquad E_f = p_f^2/2M,$$
$$\omega = p_f^3/3\pi^2\hbar^3, \qquad \mathcal{E} = p_f^5/10\pi^2\hbar^3 M. \tag{5}$$

When we average k we get a result which depends on the ratio of E_f to the energy E_v of the virtual level. For $E_f < E_v$ the quantity k is constant and $(\mu = M/2)$

$$U = -\pi\hbar^2 \alpha\omega^2/2\mu. \tag{6}$$

In the limiting case $E_f \gg E_v$ we must average over the Fermi distribution p^{-1}, where p is the momentum of the relative motion of two particles. We have

$$\mathbf{p} = \mu(\mathbf{v}_1 - \mathbf{v}_2) = \tfrac{1}{2}M(\mathbf{v}_1 - \mathbf{v}_2) = \tfrac{1}{2}(\mathbf{p}_1 - \mathbf{p}_2). \tag{7}$$

Using the electrostatic analogy† we easily find

$$\overline{|\mathbf{p}_1 - \mathbf{p}_2|^{-1}} = 6/5p_f, \qquad \overline{p^{-1}} = 12/5p_f \tag{8}$$

and finally

$$U = -3\pi^2\hbar^3\omega^2/5\mu p_f = -2p^5/15\pi^2\hbar^3 M = -\tfrac{4}{3}\mathcal{E}. \tag{9}$$

This is a remarkable result: the interaction energy is a constant multiple of the kinetic energy.

If we take these results literally, we get the following physical conclusions about the dependence on the density of the average energy of a neutron, $E_1(\omega) = (\mathcal{E} + U)/\omega$: at small density, in the limit

$$E_1 = \tfrac{3}{5}E_m > 0, \qquad E_1 \sim \omega^{2/3}, \tag{10}$$

the interaction is proportional to a higher power of ω (higher than the first power); at the density ω_0 that corresponds to $E_f = 5E_v$, the energy E_1 goes to zero, and then changes sign and at larger densities

$$E_1 = -\tfrac{1}{3}E_m < 0, \qquad E_1 \sim \omega^{2/3}. \tag{11}$$

This expression holds for* $\omega > \omega_0 \approx a^{-3}$. From this it follows that a nucleus can exist that consists of neutrons only, with a binding energy given by $-E_1$.

This treatment does not give the equilibrium density, since according to Eq. (11) as the density increases E_1 continues to decrease (E_1 is negative and its absolute value increases). To find the equilibrium density and the binding energy at this density we must bring in the effective range of nuclear forces and the interaction in states with $l \neq 0$. Qualitatively, however, the fact of the existence of neutron nuclei itself follows just from the change of sign of E_1, which is obtained from a calculation at the density $\omega_0 = a^{-3}$. Since a is extremely large, we have $\omega_0 \approx 0.001\,\omega_n$, where ω_n is the density of ordinary nuclei. In a state corresponding to the density ω_0 for which $E_1 = 0$ the boundary kinetic energy E_f is about 0.5 Mev, so that the contribution from $l \neq 0$ and the influence of the effective range are negligible; thus the assumptions about the interaction of the neutrons that were the basis for the calculation are very well satisfied at $\omega = \omega_0$. We note that if the existence of a range of values of ω in which $E_1 < 0$ is confirmed, then the surface tension of the neutron liquid will give a definite critical size of the neutron droplet, i.e., a minimum number of neutrons for which the existence of a neutron nucleus is possible. Therefore if it is proved that bound states n^4, n^6, or n^8 do not exist, this does not by itself exclude the existence of heavier neutron nuclei.

---

*Another possible approach is based on the fact that the statistical weights of the triplet and singlet are in the ratio 3 : 1; a given neutron interacts with only ¼ of the others. But in the singlet state without scattering the density at the origin of coordinates is twice as large as the average density throughout the volume, since in the singlet state only even angular momenta l are possible, and therefore the S state, the only one that contributes to $\rho(0)$, makes up twice as large a fraction of all singlet states as in the case of different particles. We finally find (1 is the index for the singlet) $\omega(0) = 2\bar{\omega}_1 = 2(\omega/4) = \omega/2$, which agrees with the result obtained in the text.

†For any body

$$\overline{r_{12}^{-1}} = \iint r_{12}^{-1}\,dv_1 dv_2 = \int \varphi_1 dv_1 = \bar{\varphi},$$

where φ is the potential for unit charge density, which satisfies the equation $\Delta\varphi = -4\pi$ inside the body and $\Delta\varphi = 0$ outside the body.

*A consistent calculation on the assumptions made above gives a value of the coefficient very close to unity.

Nevertheless the main result — the change of sign of E_1 — is by no means to be regarded as established, since only the pair interaction of the neutrons has been considered and no account has been taken of the influence of the other neutrons on the wave functions of the interacting pair. The result is doubly unreliable because for $\omega > \omega_0$ the desired quantity E_1 is the small difference of two nearly equal quantities:

$$E_1 = \overline{E} + U_1, \qquad \overline{E} = \tfrac{3}{5} E_f, \qquad U_1 = -\tfrac{4}{5} E_f = -\tfrac{4}{3} \overline{E}. \tag{12}$$

For $\omega > \omega_0$, $E_f \gg E_V$, the scattering does not depend on the length a, and we can set $a = \infty$, $a^{-1} = 0$, i.e., consider resonance scattering. Then the problem contains no dimensionless parameters. From dimensional considerations it follows that in this region

$$E_1 \sim U_1 \sim \overline{E} \sim E_f \sim \omega^{2/3}. \tag{13}$$

The formula (11) for E_1 is in agreement with this requirement. But then the correction to E_1 because of the influence of a third neutron on the wave functions of a given pair is also proportional to E_f, i.e., depends on the same power of the density and can differ from E_f and E_1 only by a numerical coefficient. This case is not like the usual one; in the Fermi gas at absolute zero with resonance scattering one cannot expand in a series of powers of the density.

We have not found the corrections for the interactions of three and more particles; it is quite possible that they will change the sign of E_1 in the region $\omega > \omega_0$. We know that $E_1 > 0$ for $\omega < \omega_0$. On the other hand, for values of ω approaching the density of ordinary nuclei it is to be expected that the energy will lie above that calculated from the resonance S scattering.* Therefore, if from an exact solution of the problem of the Fermi gas with resonance interaction it is found that $E_1 > 0$, this will mean that the existence of nuclei composed of neutrons only is impossible.

We note that the expression (11) for E_1 found by using the pair interaction is not the mathematical expectation of the energy, calculated with the unperturbed functions of the problem without interaction (otherwise we could assert that the true E_1 could only be lower than that so found); in the calculation of the interaction the change of the wave functions was taken into account from the very start (see beginning of Sec. 2). Actually the calculation of the energy of the pair interaction includes within itself the change of the wave function at the origin. We recall that $\rho(0)$ is the density that would exist in the absence of interaction; in the presence of the interaction we get for small r

$$\Psi \sim r^{-1}, \;\; \rho = {}^{1}\!/_{4}\, \pi^2 (h^2/pr)^2 \rho(0).$$

It is obvious that the change of the density and the wave function (and consequently also of the momentum spectrum) affects the interaction of the pair under consideration with other particles. We note that with a finite change of the total energy in this way of treating the pair interaction the mathematical expectations of the kinetic and potential energies are infinite and of opposite signs.

Resonance scattering with a singular potential that is nonvanishing in a small region gives in the limit zero interaction in the first order, second order, and so on, in perturbation theory; a finite result is given only by the sum of an infinite number of terms (for details see reference 15). The expression for E_1 given above is not the first approximation of perturbation theory for a Fermi gas with pair interaction between the neutrons. E_1 is the result of including in a definite way a chosen infinite succession of the terms of the perturbation-theory series, and therefore it is not clear what is the sign of the correction to E_1. The assertion of Yang and Lee[16] that not only in a Bose gas, but also in a Fermi gas any attraction always leads to a condensation seems not to be well founded.

I take this occasion to express my gratitude to A. I. Baz', V. I. Gol'danskiĭ, L. D. Landau, A. B. Migdal, and P. É. Nemirovskiĭ for discussions, and to D. V. Grigor'ev for help in the preparation of this article.

---

*By the method described above we would get for nuclear matter consisting of equal numbers of neutrons and protons, with the Coulomb interaction neglected, the result $U_1 = -4\overline{E}$; for the ordinary nuclear density this would give a binding energy ~ 60 Mev, many times the experimental value.

[1] P. É. Nemirovskiĭ, JETP **36**, 889 (1959), Soviet Phys. JETP **9**, 627 (1959).

[2] P. É. Nemirovskiĭ, JETP **33**, 746 (1957), Soviet Phys. JETP **6**, 573 (1958).

[3] A. I. Baz', Атомная энергия (Atomic Energy) **6**, 571 (1959).

[4] N. Jarmie and M. G. Silbert, Phys. Rev. Letters **3**, 50 (1959).

[5] D. Kurath, Phys. Rev. **88**, 804 (1952).

[6] F. Ajzenberg-Selove and T. Lauritsen, Nuclear Phys. **11**, 1 (1959).

[7] P. M. Endt and J. C. Kluyver, Revs. Modern Phys. **26**, 95 (1954).

[8] D. M. Van Patter and W. Whaling, Revs. Modern Phys. **26**, 402 (1954).

[9] C. H. Blanchard and R. G. Winter, Phys. Rev. **107**, 774 (1957).

[10] Ya. B. Zel'dovich, JETP **38**, 278 (1960), Soviet Phys. JETP **11**, 202 (1960).

[11] J. A. Wheeler, in Niels Bohr and the Development of Physics (Russian Translation), IIL, 1958.

[12] H. Bethe and P. Morrison, Elementary Nuclear Theory (Russian Translation) IIL, 1958.

[13] L. D. Landau and E. M. Lifshitz, Статистическая физика (Statistical Physics), Gostekhizdat, 1951.

[14] K. Huang and C. N. Yang, Phys. Rev. **105**, 767 (1957).

[15] Ya. B. Zel'dovich, JETP **38**, 278 (1960), Soviet Phys. JETP **11**, 202 (1960).

[16] T. D. Lee and C. N. Yang, Phys. Rev. **105**, 1119 (1957).

Translated by W. H. Furry
222

SOVIET PHYSICS JETP VOLUME 11, NUMBER 4 OCTOBER, 1960

MULTIPLE PRODUCTION OF JET PARTICLES IN PERIPHERAL COLLISIONS

Yu. A. ROMANOV and D. S. CHERNAVSKIĬ

P. N. Lebedev Physics Institute, Academy of Sciences, U.S.S.R.

Submitted to JETP editor May 25, 1959

J. Exptl. Theoret. Phys. (U.S.S.R.) 38, 1132-1139 (March, 1960)

Peripheral collisions of high energy nucleons ($E_{lab} > 10^{12}$ ev) are considered. The Weizsäcker-Williams method was used to classify the peripheral collisions and to describe the peculiarities of each type of interaction.[5] One of the simplest cases (peripheral single-meson interaction) is calculated by perturbation methods.

THE interest in the peripheral collisions of high energy nucleons has increased considerably in recent times. This is mainly due to the fact that stars with anomalous "two hump" angular distributions have been registered and described.[1] These stars can only be interpreted as the result of a peripheral collision with formation of two excited states. The kinematics of such a process have been discussed repeatedly in the literature.[2-4] At the present moment it seems appropriate to us to consider possible versions of this interaction, assuming that the excitation of the nucleons is caused by the exchange of π mesons.

1. CALCULATION BY THE WEIZSÄCKER-WILLIAMS METHOD

In this method (which we shall call the WW method) the problem of the peripheral interaction of two nucleons is solved in two stages. In the first stage one calculates the probability for a head-on collision of a nucleon with the π meson belonging to another nucleon (or of two π mesons belonging to two different nucleons). These processes lead to the formation of an excited system with mass M*. In the second stage one computes the decay of the excited system into secondary particles.

The following processes may take place as a result of the peripheral interaction of two nucleons.

1. One-meson interaction. Only one of the nucleons gives up its meson which undergoes a central collision with the other nucleon. The recoil and the excitation of the first nucleon are neglected, i.e., it is assumed that the excitation of the first nucleon is small ($\sim \mu c^2$).

2. Single virtual $\pi\pi$ interaction. The meson belonging to one nucleon collides with the meson of the other nucleon.

3. Two-meson interaction. Each of the nucleons undergoes a central collision with the π meson of the other nucleon.

4. Double collision of virtual π mesons (for short, double $\pi\pi$ collision). The meson belonging to one of the nucleons interacts with one of the peripheral π mesons of the nucleon which it meets in its path. The other π meson of the second nucleon goes through an analogous process.

For the description of these processes by the WW method we write the function $\rho(\epsilon, \gamma, b)$ in the form*

$$\rho(\varepsilon, \gamma, b) = A^2 K_0^2\left(b\sqrt{1+(\varepsilon/\gamma)^2}\right),$$
$$\hbar = c = \mu = 1. \tag{1}$$

For $b \gtrsim r_0$ (r_0 is the smallest possible value of the impact parameter, which has the meaning of the core radius of the nucleon) this function can be approximated by the simpler function

$$\rho(\varepsilon, \gamma, b) = \begin{cases} A^2 e^{-2b}/b, & \varepsilon < \gamma \\ 0, & \varepsilon > \gamma \end{cases}. \tag{2}$$

The constant A^2 is determined (as it is usually done in the WW method[6]) by the condition of normalization to the total energy of the nucleon:†

$$\int_0^\infty\!\!\int \rho(\varepsilon, \gamma, b)\, \varepsilon d\varepsilon\, 2\pi b db = E_0 = M\gamma, \tag{3}$$

from where we have $A^2 = 2M/\gamma\pi$, where M is the mass of the nucleon and E_0 its energy in the center-of-mass system (c.m.s.).

---

*The function $\rho(\varepsilon, \gamma, b)$ has the meaning of the probability that a meson of energy ε hits a unit area which is at a distance b from a nucleon moving with velocity γ. Expression (1) has been used repeatedly in the literature.[5,6] It can be obtained by taking the meson field of the nucleon in its rest system in the form of a Yukawa potential.

†It should be noted that the WW method has an arbitrariness in this respect. The point is that neither in the form (1) nor in the form (2) can the function $\rho(\varepsilon, \gamma, b)$ be extrapolated to the region of small $b \ll r_0$. However, this region is very important in the normalization. The estimates of the cross sections for the various types of collisions obtained below, therefore, are correct only in order of magnitude.

Let us consider the one meson collision with the help of the WW method. The probability of the collision of one nucleon with the peripheral meson of another nucleon with energy ϵ (momentum $k \sim \epsilon$) is equal to

$$dw = \int_{r_0}^{\infty} 2\pi b\, db\, \rho(\varepsilon, \gamma, b)\, \sigma(\pi, N)\, d\varepsilon.$$

Assuming that the cross section of the purely inelastic interaction of the π meson with the nucleon, $\sigma(\pi, N)$, is independent of the energy, we find

$$dw = 2M\gamma^{-1} e^{-2r_0} \sigma(\pi, N)\, d\varepsilon.$$

It is easily seen that the mass of the excited state $M^* = \sqrt{E^2 - p^2} = \sqrt{(E_0 + \epsilon)^2 - (p-k)^2}$ is equal to $M^* = 2\sqrt{\epsilon E_0}$ (here E_0 and p are the energy and the momentum of the nucleon in the c.m.s.). The probability for the formation of this state is

$$dw = \sigma(\pi, N)\, \gamma^{-2} e^{-2r_0} M^* dM^*.$$

The maximal value of M^* is $M^*_{\max} = 2\gamma\sqrt{M}$. The total cross section for the process is

$$\sigma = \int_0^{2\gamma\sqrt{M}} M^* dM^* \gamma^{-2} \sigma(\pi, N)\, e^{-2r_0} = 2Me^{-2r_0} \sigma(\pi, N). \qquad (4)$$

The angular distribution of the secondary particles in a one-meson collision should be symmetric in the rest system of the excited state (in the following we shall call this system the M^* system). In order to transform the angular distribution from the M^* system to the center-of-mass system of the colliding nucleons we must know the relative velocity of these systems γ_r.

The momentum of the excited state in the c.m.s. is equal to

$$p = p_0 - \varepsilon = M^* \gamma_r.$$

The energy ϵ is related to the excitation energy M^* by $\epsilon = (M^*/2)^2/M\gamma$. From this we find

$$p = M[\gamma - (M^*/2M)^2 \gamma^{-1}].$$

It should be noted that the second term on the right hand side is always considerably smaller than the first term; even for $M^* = M^*_{\max} = 2\gamma\sqrt{M}$ it amounts to 1/M of the magnitude of the first term. Therefore $p \sim p_0$. The required velocity (or, more precisely, the quantity $\gamma_r = (1 - v_r^2)^{-1/2}$) is equal to

$$\gamma_r = p / M^* = (M / M^*)\{\gamma - (M^*/2M)^2 \gamma^{-1}\}. \qquad (5)$$

The corresponding half angle of secondary particles (i.e., the angle into which half of the total number of particles are emitted) in the c.m.s. is $\theta_{1/2} = 1/\gamma_r$.

We can estimate the order of magnitude of the angle in the c.m.s. into which the excited nucleon is emitted, whereafter it decays into the secondary particles; it will be equal to $\vartheta \sim p_\perp/p$, where $p_\perp$ is the perpendicular component of the momentum. According to the uncertainty relation we have $p_\perp \approx 1/b \approx 1/\mu$ (b is the impact parameter for a peripheral collision). The maximal value of the angle ϑ is equal to

$$\vartheta_{\max} = 1 / b_{\min} p = 1 / r_0 p \approx 2\mu / p_0.$$

2. CALCULATION OF ONE-MESON COLLISIONS IN THE PERTURBATION THEORY

Let us compare the results obtained by the WW method with those obtained in the calculation of peripheral one-meson collisions by perturbation theory, assuming that the excitation is caused by the exchange of a single π meson (see reference 7, and also reference 8). The graph for this process is shown in Fig. 1. The quantities p_{01} and p_{02} are the 4-momenta of the free nucleons, q_i and p_i are the momenta of the secondary particles, and M_1 and M_2 are the masses of the intermediate excited states.

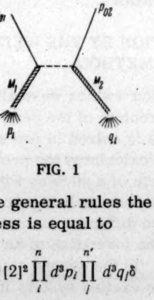

FIG. 1

According to the general rules the total probability for the process is equal to

$$dw = \sum_{n,n'} \int \frac{1}{(k^2+\mu^2)^2} [1]^2 [2]^2 \prod_i^n d^3p_i \prod_j^{n'} d^3q_j\, \delta \times \left(p_{01} + p_{02} - \sum^n p_i - \sum^{n'} q_j \right), \qquad (6)$$

where $k = p_{01} - \Sigma p_i = -(p_{02} - \Sigma q_j)$; [1] and [2] are matrix elements of the interaction of the meson with the nucleon, leading to the formation of n and n′ secondary particles, respectively. The probability dw can also be expressed in the form

$$dw = \sum_{n,n'} \int \frac{1}{(k^2+\mu^2)^2} d^4P_1 [1]^2 [2]^2 \prod_i^n d^3p_i \prod_j^{n'} d^3q_j \times \delta\left(p_{02} + k - \sum q_j\right) \delta\left(p_{01} - k - \sum p_i\right), \qquad (7)$$

where $P_1 = \Sigma p_i$. Now

$$\sum_{n}\int [1]^2 \prod_{i}^{n} d^3p_i\delta\left(p_{01} - k - \sum p_i\right) = w_{\pi N}(-k,\ p_{01}),$$

$$\sum_{n'}\int [2]^2 \prod_{j}^{n'} d^3q_j\delta\left(p_{02} + k - \sum q_j\right) = w_{\pi N}(k,\ p_{02}), \qquad (8)$$

where $w(k, p_{01})$ is the total probability of the interaction of the π meson with the nucleon. In general the quantity $w(k, p_{01})$ depends on the energy of the colliding particles in the c.m.s.; the sum of their energies is equal to the mass of the excited state M_1 (or M_2). Hence $w(k, p_{02}) = w(M_2)$.

We shall assume further that these quantities are constant for large energies (M_1 or $M_2 \gg M$) and independent of M_1 and M_2. Then

$$dw \sim d^4P_1\, w_{\pi N}^2 / (k^2 + \mu^2)^2. \qquad (9)$$

It is easily shown that

$$d^4P_1 = (P_1/2E_0)\, d\Omega_{P_1} M_1 dM_1 M_2 dM_2, \qquad (10)$$

where $d\Omega_{P_1} = \sin\vartheta\, d\vartheta\, d\varphi$ and ϑ is the angle between P_1 and p_{01}.

Let us examine the denominator of (9) in the c.m.s. of the colliding nucleons. For sufficiently large energies, when $E_{01} = E_{02} \gg M_1, M_2, M$, we can expand all quantities into a series in powers of M/E, which yields

$$k^2 + \mu^2 = 4\,\{\mu^2/2 + E_{01}E_1(1 - \cos\vartheta) + \varkappa/2\}^2,$$

where*

$$\varkappa = (M_1^2 - M^2)(M_2^2 - M^2) / 4E_{01}^2$$
$$+ (M_1^2 + M_2^2)\, M_1^2 M_2^2 / (2E_{01})^4.$$

We note that $\kappa \ll \mu^2$ for M_1, $M_2 \ll \mu E_{01}/M$. We then obtain for the probability†

$$dw \sim \frac{w_{\pi N}^2 2\pi \sin\vartheta\, d\vartheta\, M_1 dM_1 M_2 dM_2 P_1}{8\,\{\mu^2/2 + E_{01}E_1(1 - \cos\vartheta) + \varkappa/2\}^2 E_{01}}. \qquad (9a)$$

In the region of small angles, $(1 - \cos\vartheta) \ll \mu^2/2E_{01}^2$, expression (9a) is large because the denominator is small ($\sim\mu^2$); as the angle increases the expression (9a) decreases rapidly, approximately like ϑ^{-3}. This is the region of peripheral collisions, as the perpendicular component of the momentum transfer is here of the order μc.

In the region of large angles, $(1 - \cos\vartheta) \gg \mu^2/2E_{01}^2$, the above calculation is not valid, since one cannot restrict oneself any longer to first order perturbation theory. Integrating over the region of small angles from zero to $\vartheta \sim \mu/p_{01}$, we obtain

$$dw \sim w_{\pi N} \frac{{}_1dM_1 M_2 dM_2 P_1 \mu^2}{p_{01}^2 E_{01}(2\mu^4 + 3\varkappa\mu^2 + \varkappa^2)}. \qquad (11)$$

Let us investigate the denominator of this expression. We have

$$2\mu^4 + 3\mu^2\varkappa + \varkappa^2 = (\mu^2 + \varkappa)(2\mu^2 + \varkappa). \qquad (12)$$

We note that, when the excitations M_1 and M_2 are of the same order of magnitude, expression (12) increases rapidly, starting from

$$M_1 \sim M_2 = (2E_{01}^2\mu^2)^{1/4} \approx \sqrt{M\mu\gamma}. \qquad (13)$$

The quantity (13) is considerably smaller than $M^*_{\max}$, which appears in the WW method.

Let us now consider the case when one of the nucleons is not excited at all ($M_1 = M$), whereas the other is strongly excited ($M_2 \gg M$). It is seen that the denominator of (11) stays almost constant up to

$$M_2 = [16E_{01}^2(\mu/M)^2]^{1/4}$$

and then increases very rapidly as M_2 increases. Therefore the quantity $M_{2\,\max}$ (defined in the same way as $M^*_{\max}$ in the WW method) is equal to

$$M_{2\,max} = 2E_{01}\sqrt{\mu/M} = 2\gamma\sqrt{M\mu}$$

and agrees with $M^*_{\max}$ of the WW method. We note that we obtain the same result in the case when the excitation of the first nucleon is not equal to zero, but small, i.e., when $M_1 - M \sim \mu$.

It is seen from the preceding discussion that the perturbation calculation on the basis of the graph of Fig. 1 is not completely equivalent to the WW method. The point is that in the WW method one always assumes that one of the nucleons gives up its meson and the other nucleon captures it. One should therefore expect that the investigation of the matrix element corresponding to the graph of Fig. 2, where $t_1 < t_2$ always, is more closely related to the WW method. Indeed, the probability for the strong excitation of the nucleon with the

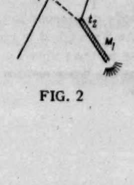

FIG. 2

---

*In the last term we made use of $M \ll M_1 + M_2$, i.e., we have assumed that one of the nucleons is excited appreciably.

†We use the sign $\sim$ in front of this expression, since we do not intend to determine the total cross section for the peripheral collisions, but are interested only in its dependence on M_1, M_2, and ϑ.

momentum p_{02} calculated on the basis of this graph has the denominator $E_{01} - E_1 - \sqrt{\mu^2 + (p_{01} - p_0)^2}$, which increases rapidly as soon as the excitation of the first nucleon $(M_1 - M)$ becomes greater than μ. This can be seen easily by calculating the matrix element of graph 2 in the rest system of the first nucleon. Thus any strong symmetric excitation of the nucleons is in this case not very probable. The same can be said about the graph in which $t_1 > t_2$ always. However, the matrix element corresponding to the graph of Fig. 1, which was considered above, is the sum of the matrix elements for the graph 2 (where $t_1 < t_2$) and for the analogous graph with $t_1 > t_2$. The probability equals the sum of the component probabilities plus an interference term. This term makes possible the excitation of the two nucleons up to $M_1 \sim \sqrt{M\mu\gamma}$. However, when one nucleon is excited more strongly than the other, the interference term appears to be unimportant. It is essential that the interference is not taken account of in the WW method, so that the symmetric excitation of the nucleons cannot be treated by the WW method.

The simple virtual $\pi\pi$ collision can be described in perturbation theory by the graph of Fig. 3. The analog of this process in electrodynamics is the pair formation by an electron on a nucleus.* However, it is more convenient to consider this process with the help of the WW method and not by perturbation theory.

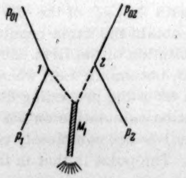

FIG. 3

The probability for this interaction is

$$w = \int \sigma(\pi, \pi)\, \rho_1(\varepsilon_1, \gamma, b_1)\, \rho_2(\varepsilon_2, \gamma, b_2)\, d\varepsilon_1\, d\varepsilon_2\, dS,$$

where the integration goes over the plane perpendicular to the line of motion of the nucleons, excluding the regions where b_1 and b_2 are smaller than r_0; b_1 and b_2 are the distances from a given point to the centers of the nucleons. Using the approximation (2) we find

$$w = \frac{2M^2}{\pi} \left\{ e^{-4r_0} + (1 - 4r_0)\, \mathrm{Ei}\,(4r_0) \right\} \sigma(\pi, \pi). \tag{14}$$

The probability for the production of an excited state with proper energy $M^* = 2\sqrt{\epsilon_1 \epsilon_2}$ is equal to

$$\begin{aligned} dw(M^*) &= f \int_0^\gamma \sigma(\pi, \pi)\, (2M / \pi\gamma)^2\, \varepsilon_1^{-1}\, d\varepsilon_1\, M^*\, dM^* \\ &= \sigma(\pi, \pi)\, (2M^2/\pi^2\gamma^2) \ln \gamma \cdot M^*\, dM^*\, f, \end{aligned} \tag{15}$$

where

$$f = \int dS e^{-2(b_1 + b_2)} / b_1 b_2 = \frac{\pi}{2} [e^{-4r_0} + (1 - 4r_0)\, \mathrm{Ei}\,(4r_0)].$$

It should be emphasized that the production of two strongly excited systems is impossible in one-meson collisions; this can occur only through the exchange of two mesons.

A two-meson collision takes place when a peripheral meson belonging to one of the nucleons interacts with the other nucleon and at the same time the meson of the second nucleon interacts with the first one. The Feynman graph corresponding to this process is shown in Fig. 4. The calculation of this process by the WW method was done in reference 5; here we shall quote only some of the results.

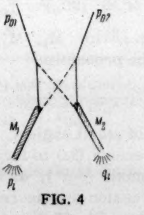

FIG. 4

1. The probability for the double interaction is somewhat smaller than the probability for the simple interaction, but is still of the same order of magnitude (their ratio is ½).

2. The probability that the excitation of the nucleons in a double πN interaction is the same (and, hence, the angular distribution of the secondary particles is symmetric in the c.m.s.) depends weakly on the energy and is equal to about ½ in the energy region (in the laboratory system) $E_{\mathrm{lab}} \approx 10^{12} - 10^{14}$ ev.

---

*Pair production in the collision of an electron with a nucleus can be calculated by the WW method in two ways. One can expand the field of the electron in terms of quanta and then use the known cross section for pair production by a quantum on a nucleus, $\sigma(\gamma, N)$. Or one can expand the fields of the electron and of the nucleus in terms of quanta and then use the cross section for pair production in the collision of two quanta, $\sigma(\gamma, \gamma)$. The results of these two calculations must be identical, since both methods correspond to the same graph (Fig. 3). In the first case the WW method is employed in the point 1, and in the second case in the points 1 and 2. The calculation presented above [using the cross section $\sigma(\pi, \pi)$] corresponds to the second method.

3. The angular distribution of the secondary particles in the c.m.s. consists of two parts (corresponding to the two excited nucleons). However, if the decay of the excited nucleons conforms to the Landau theory, both these angular distributions are quite smeared out, so that their separation is practically impossible.

4. The coefficient of anelasticity for collisions of this type should be of order unity.

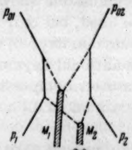

FIG. 5

The double $\pi\pi$ interaction (see Fig. 5) is different from the preceding case both in principle and in practice. Firstly, it can occur only if the amplitude of the two-meson state is represented in the peripheral field of the nucleon with sufficiently large weight. The frequency with which these cases occur, therefore, gives information not only about the average strength of the meson field at the periphery of the nucleon, but also about the functional form of this field. Secondly, the coefficient of anelasticity for these collisions must be considerably smaller than for a head-on or double πN collision; the maximal value occurs when the first nucleon gives up to mesons having the maximal energy $\epsilon \sim \gamma\mu$ in the c.m.s. In this case* $K_{max} \approx 2\mu/M \approx 0.3$. These cases should be observed in the form of "stars" having a small coefficient of anelasticity with an angular distribution which has two maxima† (i.e., the function $dN/d\lambda$, $\lambda = -\ln \tan \theta$, contains two maxima).

It should be noted that the interpretation of these "stars" is considerably more complicated than in the case of "stars" with a large coefficient of anelasticity even in the case of a symmetric angular distribution it is here in general not possible to determine the energy of the primary particle from the angular distribution of the secondary ones.

In order to predict the number of secondary particles and their angular distribution in the c.m.s., one must adopt some hypothesis for the mechanism of their creation. In our case the use of the Fermi-Landau theory is less justified than in the case of NN and πN interactions.* Therefore, the question whether one should use some other model (for example, the Heisenberg model, which assumes maximal energy dissipation) or the Fermi-Landau model can be decided only by experiment. Some experimental data quoted in reference 2 were evaluated in reference 9. It follows from these data that in the case of the double $\pi\pi$ interaction the process is apparently described more adequately by the Heisenberg theory than by the Landau theory.

Finally, it is appropriate to make some remarks on the manner in which the peripheral meson field of the nucleon affects the collision of a nucleon with a nucleus. This problem has been considered by one of the authors,[5] who found the following results:

1. Owing to the presence of the peripheral field, a strong excitation of the nucleus is possible, much stronger than the excitation studied by Heitler and Terraux.[11] The probability for this excitation decreases with increasing energy.

2. If the meson present in the peripheral field of the nucleon has sufficient energy, it will interact independently of the nucleon, which will give rise to the appearance of an accompanying shower. The shower as a whole will become asymmetric: a large part of the particles will fly "backwards" in the c.m.s., i.e., in the opposite direction of the primary nucleon.†

It was found in reference 5 that: a) the number of particles in the accompanying shower, N_{acc}, is on the average one half of that in the main shower, N_{main}, and b) the half angle of the accompanying shower, $\theta_{1/2\,acc}$, (in the laboratory system) is on the average four times larger than $\theta_{1/2\,main}$. The latter means that in the coordinates $dN/d\lambda$, λ the maxima of the angular distributions are located at a distance $\Delta\lambda = \log 4 = 0.6$.

---

*The average value of the coefficient of anelasticity is $K \sim 0.5\, K_{max} \sim 0.15$. However, under the experimental conditions, the average value for the observed stars should be somewhat smaller.

†If the energy of the colliding mesons is the same in the c.m.s., the double $\pi\pi$ interaction gives an angular distribution with only one maximum. In this case it is impossible to differentiate it from the one-meson interaction.

*The point is that the Fermi-Landau theory is appropriate for the description of classical processes. For a head-on collision of two nucleons and propagation along their impact waves (according to reference 10) we have for the action $S \approx p\Delta = M\gamma(1/\mu\gamma) = M/\mu \gg 1$.

This process can therefore be considered classical and there is no objection to the application of the Fermi-Landau theory in this case. For a head-on πN collision the action is of the same order of magnitude as for an NN collision. However, it can be easily shown that for a $\pi\pi$ collision (when it is also treated hydrodynamically) the magnitude of the action is smaller: $S = 1$. This indicates that the $\pi\pi$ interaction is a quantum process and can therefore follow different laws than the NN or πN interactions.

† In view of the asymmetry of the angular distribution, the energy can in this case not be determined by the angles. The shower has to be symmetrized first, i.e., the accompanying shower has to be separated out. The observation of asymmetric showers and the problem of their symmetrization has been discussed earlier by Takibaev.[12]

We quote here the results of a comparison of these estimates with the experimental data.[12,13] The data of Gurevich, Mishakova, Nikol'skiĭ, and Surkova[13] indicate that the probability for a strong excitation of the nucleus does indeed decrease as the energy goes up. The portion (α) of stars caused by nucleons and containing more than 10 black and gray tracks is for different intervals of the energy E_{lab} equal to

E_{lab}, Mev =	$10^{10} - 10^{11}$	$10^{11} - 10^{12}$	$10^{12} - 10^{13}$
$\alpha =$	0.8	0.43	0.4

For a comparison of the theoretical data on the accompanying collisions with experiment we made use of the summed histograms of six stars of reference 13 (147 tracks; see Fig. 6) and of six stars of reference 12 (139 tracks; see Fig. 7). All these stars are the result of collisions of energetic nucleons ($E_{lab} \sim 10^{12}$ ev) with nuclei (the stars contained black and gray tracks).

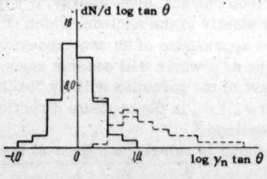

FIG. 6

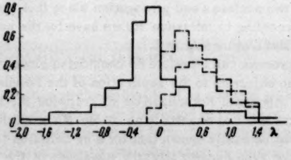

FIG. 7

The symmetrization and separation of the accompanying showers was carried out in the following way. It was assumed that the maximum of the histogram (in the $dN/d\lambda$, λ coordinates) coincides with the maximum of the main shower. The total number of particles in the main shower was taken to be twice the number of particles lying to the left of the maximum. The solid line in Figs. 6 and 7 represents the histogram of the collisions, whereas the dashed line refers to the accompanying collisions. It follows from these histograms that $N_{main}/N_{acc} = 2.3$ (reference 13) and $= 1.8$ (reference 12). The distance between the maxima is $\Delta\lambda = 0.8$ (reference 13) and 0.7 (reference 12). In our opinion, these data are in satisfactory agreement with the theoretical estimates.

It should be noted that the comparison above is not sufficiently accurate for the following reasons: a) not all asymmetric showers obtained in reference 13 were used, but only those which have a clearly defined asymmetry; b) we used summed histograms, and additional asymmetries may have been introduced in their composition because the position of the maximum could not be determined accurately.

In conclusion the authors take this opportunity to express their gratitude to Prof. E. L. Feĭnberg for fruitful discussions and interest in this work and to Prof. I. I. Gurevich and his collaborators for showing us their data.

---

[1] Cick, Danysz, Gierula, Jurak, Miesowicz, Perneger, Vrana, and Wolter, Nuovo cimento **6**, 1409 (1957); Cick, Cogen, Gierula, Holinski, Jurak, Miesowicz, Saniewska, and Perneger, Nuovo cimento **10**, 741 (1958).

[2] E. L. Feĭnberg and D. S. Chernavskiĭ, Doklady Akad. Nauk SSSR **81**, 795 (1951).

[3] S. Takagi, Prog. Theoret. Phys. **7**, 123 (1952).

[4] W. J. Kraushaar and J. J. Marx, Phys. Rev. **93**, 326 (1954).

[5] D. S. Chernavskiĭ, Nuovo cimento Suppl. **8**, 775 (1958).

[6] W. Heitler and H. W. Peng, Proc. Roy. Irish Acad. **A49**, 101 (1943).

[7] G. Chew, preprint.

[8] L. B. Okun' and I. Ya. Pomeranchuk, JETP **36**, 300 (1959), Soviet Phys. JETP **9**, 207 (1959).

[9] D. S. Chernavskiĭ, Postepy Fizyki **9**, 653 (1958).

[10] S. Z. Belen'kiĭ and G. A. Milekhin, JETP **29**, 20 (1955), Soviet Phys. JETP **2**, 14 (1956).

[11] W. Heitler and Ch. Terraux, Proc. Phys. Soc. **A66**, 929 (1953).

[12] Zh. S. Takibaev, Transactions of the Institute of Nuclear Physics, Academy of Sciences, Kasakh SSR **1**, (1957).

[13] Gurevich, Mishakova, Nikol'skiĭ, and Surkova, JETP **34**, 265 (1958), Soviet Phys. JETP **7**, 185 (1958).

Translated by R. Lipperheide
223

SOVIET PHYSICS JETP VOLUME 11, NUMBER 4 OCTOBER, 1960

THE THERMODYNAMIC AVERAGE OF FUNCTIONS OF THE DISPLACEMENT OF ATOMS IN A NON-IDEAL CRYSTALLINE LATTICE

V. I. PERESADA

Khar'kov State University

Submitted to JETP editor July 8, 1959

J. Exptl. Theoret. Phys. (U.S.S.R.) 38, 1140-1147 (April, 1960)

It is necessary to obtain the thermodynamic average of the function $\exp i(\mathbf{q}\cdot\mathbf{u_R})$, where $\mathbf{q}$ is a constant vector and $\mathbf{R}$ the displacement of the $\mathbf{R}$-th atom from its equilibrium position, when one studies the scattering of x rays or slow neutrons by atomic systems. In the case of small oscillations the thermodynamic average of any function $F((\mathbf{q}\cdot\mathbf{u_R}))$ is uniquely determined by the mean-square fluctuation $D(\mathbf{n}, \mathbf{R}, T)$ of the displacement of the $\mathbf{R}$-th atom in the direction of the vector $\mathbf{n} = \mathbf{q}/q$ (T is the temperature of the system). A method is given for the evaluation of the quantity $D(\mathbf{n}, \mathbf{R}, T)$ for an infinite perfect lattice with a finite number of localized defects. We have obtained an asymptotic expression for the function $D(\mathbf{n}, \mathbf{R}, T)$ at large distances from the defects. This asymptotic value is determined by the lattice and the nature of the defects. This method of evaluation can also be applied to other problems.

WHEN considering problems connected with small vibrations of crystal lattices it is usually necessary to take the time average of several functions of the displacement of a given atom of the lattice in thermal equilibrium from its equilibrium position. If, for instance, we study the scattering of x rays (or slow neutrons) by a crystal lattice, we must find the time average of the quantity $\exp i(\mathbf{q}\cdot\mathbf{u_R})$, where $\mathbf{q} = (\mathbf{p}-\mathbf{p}')/h$ ($\mathbf{p}$ and $\mathbf{p}'$ are respectively the momenta of the incident and the scattered waves, h is Planck's constant divided by 2π), $\mathbf{u_R}$ is the displacement of the $\mathbf{R}$-th atom in the lattice from its equilibrium position, $\mathbf{R}$ is the radius vector of the equilibrium position of the atom. Another example would be the evaluation of the dispersion of the displacement of the atom from its equilibrium position.

If we use the distribution function for the displacements from its equilibrium position for a one-dimensional oscillator (Bloch,[1] see also reference 2) which is in thermodynamic equilibrium with the surrounding medium, and also use the fact that the motion of any atom can be written as a linear combination of normal vibrations when the atoms in the system execute small vibrations, we can show that the thermodynamic average of any function $F(\mathbf{q}\cdot\mathbf{u_R})$ which depends on the dot product of the constant vector $\mathbf{q}$ and the displacement, $\mathbf{u_R}$, of the $\mathbf{R}$-th atom in the system which executes small vibrations, can be expressed by the formula

$$\langle F(\mathbf{q}\mathbf{u_R})\rangle = \pi^{-1/2}\int_{-\infty}^{\infty} F(xq\sqrt{2}\,D(\mathbf{n}, \mathbf{R}, T))\,e^{-x^2}\,dx, \qquad (1)$$

where $q = |\mathbf{q}|$, $\mathbf{n} = \mathbf{q}/q$, T is the absolute temperature, and $D(\mathbf{n}, \mathbf{R}, T)$ is the mean-square fluctuation of the displacement of the $\mathbf{R}$-th atom in the direction of the vector $\mathbf{n}$. It is thus sufficient to find the quantity $D(\mathbf{n}, \mathbf{R}, T) = \langle(\mathbf{n}\cdot\mathbf{u_R})^2\rangle^{1/2}$ for the evaluation of $\langle F(\mathbf{q}\cdot\mathbf{u_R})\rangle$ or, in particular, of the quantity $\langle\exp i(\mathbf{q}\cdot\mathbf{u_R})\rangle$.

It is very difficult to evaluate the quantity $D(\mathbf{n}, \mathbf{R}, T)$ for the case of an imperfect crystal lattice. Among the deformations of a crystalline lattice there is, however, one form of deformation which enables us to overcome the difficulties in the calculation of the quantity $D(\mathbf{n}, \mathbf{R}, T)$. We have in mind the so-called localized lattice defects which can be described by a method developed and effectively used by I. M. Lifshitz[3-9] in several of his papers. This method makes it possible to consider such important lattice defects as the substitution of an atom in the lattice by a foreign atom, the occurrence of a vacancy or of the displacement of an atom in the lattice, and other localized irregularities.

In connection with the proposed use of averages of functions of the form $F(\mathbf{q}\cdot\mathbf{u_R})$ (in particular, in the problem of the elastic scattering of slow neutrons by a mixture of light isotopes), we give in the present paper the evaluation of the mean-square fluctuation $D(\mathbf{n}, \mathbf{R}, T)$ of the displacements of atoms in a given direction $\mathbf{n}$ for an infinite crystal lattice with a finite number of localized defects.

The local character of the perturbations enables us to choose the normal coordinates of the infinite unperturbed lattice in such a special way that they can be divided into two sets, one of which is not changed by the presence of the perturbation. The method of calculation makes use of this fact and can also be used for other problems connected with vibrations of imperfect lattices.

The small-oscillations equation of any system of atoms can be written in the form

$$m_{\mathbf{R}}\frac{d^2 u_{\mathbf{R}}}{dt^2} = -\sum_{\mathbf{R}',\sigma'} A_{\mathbf{RR}'}^{\sigma\sigma'} u_{\mathbf{R}'}^{\sigma'}, \tag{2}$$

where $m_{\mathbf{R}}$ is the mass of the $\mathbf{R}$-th atom in the lattice, $u_{\mathbf{R}}^{\sigma}$ the component of the displacement of the $\mathbf{R}$-th atom from its equilibrium position along the σ-th axis of a Cartesian system of coordinates, and $A_{\mathbf{RR}'}^{\sigma\sigma'}$ the coefficients of the interaction between the atoms in the system in the linear approximation. The general solution of the set of differential equations (2) is a superposition of normal vibrations $\xi_{\lambda\rho}\chi_{\lambda\rho}(\mathbf{R})$

$$u_{\mathbf{R}} = (m_{\mathbf{R}})^{-1/2}\sum_{\lambda\rho}\xi_{\lambda\rho}\,\chi_{\lambda\rho}(\mathbf{R}), \tag{3}$$

where the $\xi_{\lambda\rho}$ are normal coordinates, satisfying the equations

$$d^2\xi_{\lambda\rho}/dt^2 + \lambda\xi_{\lambda\rho} = 0$$

($\lambda = \omega_{\lambda}^2$ are the squares of the eigen frequencies of the system); the $\chi_{\lambda\rho}(\mathbf{R})$ form a complete orthonormal set of eigenfunctions of the equation

$$L\chi = \lambda\chi; \tag{4}$$

L is a Hermitian operator defined by its matrix elements

$$L_{\mathbf{RR}'}^{\sigma\sigma'} = A_{\mathbf{RR}'}^{\sigma\sigma'}(m_{\mathbf{R}}\,m_{\mathbf{R}'})^{-1/2}. \tag{5}$$

The squares of the eigen frequencies of the system are the eigenvalues of the operator L.

Using Eq. (3) and the fact that the distribution function of the displacements of a one-dimensional oscillator in thermodynamic equilibrium with its surrounding medium is a Gaussian distribution (Bloch[1]), we can write the expression for the square of the fluctuation $D^2(\mathbf{n}, \mathbf{R}, T)$ of the displacement of the $\mathbf{R}$-th atom of the system in the form

$$D^2(\mathbf{n}, \mathbf{R}, T) = m_{\mathbf{R}}^{-1}\sum_{\lambda\rho} f(\lambda, T)\,|\,\mathbf{n}\chi_{\lambda\rho}(\mathbf{R})\,|^2, \tag{6}$$

where

$$f(\lambda, T) = (h/2\sqrt{\lambda})\coth(h\sqrt{\lambda}/2kT) \tag{7}$$

is the square of the mean square fluctuation of the Gaussian distribution, T the absolute temperature, and k Boltzmann's constant. We note that Eq. (6) for D^2 can be written in the form

$$D^2(\mathbf{n}, \mathbf{R}, T) = m_{\mathbf{R}}^{-1}\sum_{\sigma\sigma'}\{f(L, T)\}_{\mathbf{RR}'}^{\sigma\sigma'}\,n^{\sigma}n^{\sigma'}, \tag{8}$$

where the $\{f(L, T)\}_{\mathbf{RR}'}^{\sigma\sigma'}$ are the matrix elements of the operator $f(L, T)$.

The spectrum of the operator L consists for an infinite perfect crystal lattice of several finite sections of the real axis, and every point of the spectrum of the operator L is infinitely degenerate. In that case we can rewrite Eq. (6) as follows

$$D^2(\mathbf{n}, \mathbf{R}, T) = \frac{1}{m_{\mathbf{R}}}\int f(\lambda, T)\,\{\sum_{\rho}|\,\mathbf{n}\psi_{\lambda\rho}(\mathbf{R})\,|^2\}\,d\lambda. \tag{9}$$

Following Lifshitz,[3,4] we call a localized lattice deformation any defect that can be taken into account in the small-oscillations equations (2) by adding some finite-dimensional Hermitean operator Λ to the operator L of the unperturbed lattice. A whole series of actually existing defects (substitution of an atom of the basic lattice by a foreign one, vacancies, interstitials, and so on) are defects of this kind. It has been shown[4] that when the operator L is bounded and has a continuous spectrum and the operator Λ has a finite number of dimensions, the spectrum of the perturbed operator $\tilde{L} = L + \Lambda$ can differ from the spectrum of L only in a finite number of isolated points. Let $\lambda_1, \lambda_2, \ldots, \lambda_n$ be all the points of the discrete spectrum of the operator $\tilde{L} = L + \Lambda$. If we denote all quantities referring to the perturbed operator $\tilde{L}$ by a tilde, (~) we can, according to (9), write down for the quantity $\tilde{D}^2$ of the perturbed problem the following expression

$$\tilde{D}^2(\mathbf{n}, \mathbf{R}, T) = m_{\mathbf{R}}(\tilde{m}_{\mathbf{R}})^{-1}D^2(\mathbf{n}, \mathbf{R}, T) + (m_{\mathbf{R}})^{-1}S(\mathbf{n}, \mathbf{R}, T), \tag{10}$$

$$S(\mathbf{n}, \mathbf{R}, T) = \int f(\lambda, T)\,\{\sum_{\rho}|\,\mathbf{n}\tilde{\psi}_{\lambda\rho}(\mathbf{R})|^2 - \sum_{\rho}|\mathbf{n}\psi_{\lambda\rho}(\mathbf{R})\,|^2\}\,d\lambda + \sum_{\lambda_k} f(\lambda_k, T)\,|\,\mathbf{n},\ \tilde{\psi}_{\lambda_k}(\mathbf{R})\,|^2, \tag{11}$$

where the $\tilde{\psi}_{\lambda\rho}$ and $\tilde{\psi}_{\lambda_k}$ are the eigenfunctions of the operator $\tilde{L}$ corresponding respectively to the continuous and the discrete spectra, and $\tilde{m}_{\mathbf{R}}$ is the mass of the $\mathbf{R}$-th atom of the perturbed lattice.

It is necessary, according to (10), to evaluate the quantity $S(\mathbf{n}, \mathbf{R}, T)$ in order to find the quantity $\tilde{D}^2$. It appears that to do this it is necessary to know the complete set of the eigenfunctions of the operator $\tilde{L}$. Since the perturbing operator Λ has a finite number of dimensions, however, the problem of finding the quantity $\tilde{D}^2(\mathbf{n}, \mathbf{R}, T)$ simplifies considerably.

Let us denote by H_λ the eigen-subspace of the operator L corresponding to the spectral point λ. We separate from this subspace the subspace H''_λ spanned by the functions ψ_λ satisfying the equation $\Lambda\psi_\lambda = 0$. It is clear that any solution of the equation $(L-\lambda)\psi_\lambda = 0$ corresponding to the subspace H''_λ is at the same time a solution of the perturbed equation $(\widetilde{L}-\lambda)\psi_\lambda = 0$. We denote by H'_λ the subspace orthogonal to H''_λ which with H''_λ makes up the eigen-subspace H_λ. We consider also subspaces H' and H'' which are the closures respectively of the subspaces H'_λ and H''_λ with all possible λ (it is evident that any space H is the orthogonal sum of subspaces H'_λ and H''_λ).

Let L' and L'' be the operators produced by the operator L in the subspaces H' and H'', respectively. Let $\widetilde{L}'$ and $\widetilde{L}''$ be similarly the operators produced by the operator $\widetilde{L}$, also in the subspaces H' and H''. One shows easily that $\widetilde{L}'' = L''$ and $\widetilde{L}' = L' + \Lambda$. This last fact enables us to conclude that all physical consequences caused by the localized perturbation Λ must be describable in terms of the subspace H'. In our particular case this means that we can consider in Eq. (11) for $S(\mathbf{n}, \mathbf{R}, T)$ the summation over ρ to extend only over the eigenfunctions of the operators L' and $L' + \Lambda$ defined in H'. One sees easily that the degree of degeneracy of the spectrum of the operators L' and $L' + \Lambda$ is finite.

It will be found convenient to choose as the basis in H' a complete set of eigenfunctions of the operator L'. We obtain such a basis by constructing a base in the eigen-subspaces H'_λ of the operator L'. To do this we consider the eigenfunctions $\mathbf{g}_i(\mathbf{R})$ of the operator Λ, i.e., let $\Lambda\mathbf{g}_i = \gamma_i\mathbf{g}_i$, where the γ_i are the non-zero eigenvalues of the operator Λ. The number of functions $\mathbf{g}_i$ is equal to the rank r of the operator Λ. We shall assume that the functions $\mathbf{g}_i$ are normalized to $[\mathbf{g}_i\mathbf{g}_k] = \delta_{ik}$ (here and henceforth the square brackets indicate the scalar product in the atomic-displacements space: $[\mathbf{g}_i\mathbf{g}_k] = \sum_{\sigma,\mathbf{R}} g_i^\sigma(\mathbf{R})\overline{g_k^\sigma(\mathbf{R})}$.

If we choose for the eigenfunctions of the operator L the usual representation

$$\chi_{\mathbf{k},s}(\mathbf{R}) = \mathbf{e}_{\mathbf{k},s}\exp[i\mathbf{k}\mathbf{R}] \tag{12}$$

[here $\mathbf{e}_{\mathbf{k},s}$ is the polarization vector, $\mathbf{k}$ a reciprocal-lattice vector multiplied by 2π, and s the number of the vibration mode; the eigenvalues of the operator L in this representation are functions of $\mathbf{k}$ and s: $\lambda = \lambda_s(\mathbf{k})$], we can write the vectors $\mathbf{g}_i(\mathbf{R})$ in the form

$$\mathbf{g}_i(\mathbf{R}) = \int \varphi_{\lambda,i}(\mathbf{R})\,d\lambda, \tag{13}$$

$$\varphi_{\lambda,i} = \sum_s \int \frac{[\mathbf{g}_i\chi_{\mathbf{k},s}]\chi_{\mathbf{k},s}(\mathbf{R})\,d\Omega}{|\nabla\lambda_s(\mathbf{k})|}. \tag{14}$$

The integrals in (14) [and also those in (17) below] are taken over the surfaces $\lambda_s(\mathbf{k}) = \lambda$.

One can show that the space spanned by all functions $\varphi_{\lambda,i}$ with a given value of λ completely exhausts the subspace H'_λ. From this it follows that the closure of the linear envelope of the functions $\varphi_{\lambda,i}$ with all possible λ and i contains within itself the subspace H'. The functions

$$\phi_{\lambda\rho} = \sum_i c_{\rho i}(\lambda)\varphi_{\lambda,i} \tag{15}$$

with the $c_{\rho i}(\lambda)$ satisfying the conditions

$$\sum_{ij} c_{\rho i}(\lambda)\overline{c_{\rho' j}(\lambda)}\alpha_{ij}(\lambda) = \delta_{\rho\rho'}, \tag{16}$$

where

$$\alpha_{ij}(\lambda) = \sum_s \int \frac{[\mathbf{g}_i\chi_{\mathbf{k},s}][\mathbf{g}_j\chi_{\mathbf{k},s}]\,d\Omega}{|\nabla\lambda_s(\mathbf{k})|}, \tag{17}$$

form thus an orthonormal basis for the space H'.

We shall look for solutions of the perturbed equation $(L' + \Lambda - \lambda)\widetilde{\psi}_\lambda = 0$ in the form of an expansion in terms of the eigenfunctions of the operator L'; to do this we write

$$(L' - \lambda)\widetilde{\phi}_\lambda = -\Lambda\widetilde{\phi}_\lambda. \tag{18}$$

Since $\Lambda\widetilde{\psi}_\lambda$ belongs to the subspace of the functions $\mathbf{g}_i$,

$$(L' - \lambda)\widetilde{\phi}_\lambda = \sum_i c_i(\lambda)\,\mathbf{g}_i = \sum_i c_i(\lambda)\int \varphi_{\mu i}\,d\mu.$$

We have thus for the eigenfunctions of the operator $L' + \Lambda$

$$\widetilde{\phi}_\lambda = \sum_i c_i(\lambda)\left\{\fint \frac{\varphi_{\mu i}\,d\mu}{\mu - \lambda} + A(\lambda)\phi_{\lambda,i}\right\}. \tag{19}$$

The symbol $\fint$ indicates here the principal-value integral. $A(\lambda)$ is a regularizing function, which depends on λ and which must be determined together with the coefficients $c_i(\lambda)$. It is clear that for the discrete spectrum of the operator $L' + \Lambda$, the integrals in (19) are taken in the usual sense and $A(\lambda) \equiv 0$.

To determine the functions $c_i(\lambda)$ and $A(\lambda)$, we apply to both sides of Eq. (19) the operator Λ and multiply the result by $\mathbf{g}_j$. This leads to a set of r homogeneous linear equations for the $c_i(\lambda)$:

$$\sum_i c_i(\lambda)\left[A(\lambda)\alpha_{ij}(\lambda) + \fint \frac{\alpha_{ij}(\mu)}{\mu - \lambda}\,d\mu + \delta_{ij}/\gamma_j\right] = 0. \tag{20}$$

If λ belongs to the spectrum of the operator L, the condition that the set (20) be solvable leads to an algebraic equation for $A(\lambda)$ of degree not greater than r (if λ does not belong to the spectrum of the operator L, this condition gives us an equation for the points of the discrete spectrum of the perturbed operator $L' + \Lambda$). Let $A_\rho(\lambda)$ be the solutions of this equation, and let the $c_{\rho i}(\lambda)$ be the corresponding solutions of the set (20). It is clear that $c_{\rho i}(\lambda)$ with different values of ρ are orthogonal to one another in the metric defined by the matrix $\| \alpha_{ij}(\lambda) \|$ and that they can thus be chosen to satisfy Eq. (16). If we substitute in (19) the values obtained for $A_\rho(\lambda)$ and for the $c_{\rho i}(\lambda)$, normalized according to (16), we find the eigenfunctions of the continuous spectrum of the perturbed problem

$$\tilde{\phi}_{\lambda\rho} = N_\rho(\lambda)\left\{A_\rho(\lambda)\sum_i c_{\rho i}(\lambda)\varphi_{\lambda i} + \sum_i c_{\rho i}(\lambda)\int \frac{\varphi_{\mu i}\, d\mu}{\mu - \lambda}\right\}, \tag{21}$$

where $N_\rho(\lambda)$ is a normalization factor. One can show* that

$$N_\rho(\lambda) = [A_\rho^2(\lambda) + \pi^2]^{-1/2}.$$

If we put

$$\theta_{\lambda\rho} = \frac{1}{\pi}\sum_i c_{\rho i}(\lambda)\int \frac{\varphi_{\mu i}}{\mu - \lambda}\, d\mu, \tag{22}$$

and introduce the function

$$\zeta_\rho(\lambda) = \cot^{-1}(\pi^{-1} A_\rho(\lambda)), \tag{23}$$

we can therefore rewrite Eq. (21) as follows

$$\tilde{\phi}_{\lambda\rho} = \cos\zeta_\rho(\lambda)\,\phi_{\lambda\rho} + \sin\zeta_\rho(\lambda)\,\theta_{\lambda\rho}, \tag{24}$$

where the functions $\psi_{\lambda\rho}$ are given by Eq. (15).

Comparison shows the functions $\zeta_\rho(\lambda)$, defined by Eq. (23) and by the equation for $A_\rho(\lambda)$, to be the same as the shift functions, first obtained by a slightly different method by I. M. Lifshitz for the one-dimensional[4] and the many-dimensional[6] cases. Lifshitz showed (see also a paper by Kreĭn[11]) that if we know the functions $\zeta_\rho(\lambda)$ we can find the difference of the traces of two operators such as $f(L + \Lambda)$ and $f(L)$, where $f(x)$ is one of a very large class of functions. One can show from the asymptotic behavior of the functions $\tilde{\psi}_{\lambda\rho}$ and $\psi_{\lambda\rho}$ at large distances from the lattice defect that the functions $\zeta_\rho(\lambda)$ also determine the phase shift of the wave scattered by the localized defect. This conclusion is a generalization of Lifshitz' result[12] to problems that are not spherically symmetric.

One can use the properties of the functions $\psi_{\lambda\rho}$, $\theta_{\lambda\rho}$, and $\zeta_\rho(\lambda)$ to show that the functions $\tilde{\psi}_{\lambda\rho}$ form a complete orthonormal set of eigenfunctions of the operator $L' + \Lambda$ in the continuous spectrum.

To find the functions $\tilde{\psi}_{\lambda_k}$ of the discrete spectrum of the operator $L' + \Lambda$ we must put $A(\lambda) = 0$ in Eqs. (19) and (20) and write integrals in the usual sense instead of principal-value integrals. The condition that Eqs. (20) be solvable gives us an equation for the eigenvalues λ_k of the operator $L' + \Lambda$ in the discrete spectrum. The expressions for the $\tilde{\psi}_{\lambda_k}$ and the corresponding normalization conditions can easily be obtained and are therefore omitted here.

Having found the eigenfunctions (15) and (24) of the operators L' and $L' + \Lambda$, we can use (11) to evaluate $S(\mathbf{n}, \mathbf{R}, T)$ and thus also $\tilde{D}^2(\mathbf{n}, \mathbf{R}, T)$ from (10). We get for $S(\mathbf{n}, \mathbf{R}, T)$ the following expression

$$S(\mathbf{n}, \mathbf{R}, T) = \frac{h}{2}\int \coth\left(\frac{h\sqrt{\lambda}}{2kT}\right) F(\lambda, \mathbf{R})\frac{d\lambda}{\sqrt{\lambda}} + \frac{h}{2}\sum_{\lambda_i}\coth\left(\frac{h\sqrt{\lambda_i}}{2kT}\right)\frac{1}{\sqrt{\lambda_i}}(\mathbf{n}\tilde{\phi}_{\lambda i}(\mathbf{R}))^2; \tag{25}$$

$$F(\lambda, \mathbf{R}) = \sum_\rho \{\sin^2\zeta_\rho(\lambda)\,[|\mathbf{n}\theta_{\lambda\rho}(\mathbf{R})|^2 - |\mathbf{n}\phi_{\lambda\rho}(\mathbf{R})|^2] + \tfrac{1}{2}\sin 2\zeta_\rho(\lambda)\,[(\mathbf{n}\theta_{\lambda\rho}(\mathbf{R}))\overline{(\mathbf{n}\phi_{\lambda\rho}(\mathbf{R}))} + \overline{(\mathbf{n}\theta_{\lambda\rho}(\mathbf{R}))}(\mathbf{n}\phi_{\lambda\rho}(\mathbf{R}))]. \tag{26}$$

Knowing the value of $\tilde{D}^2(\mathbf{n}, \mathbf{R}, T)$ for the perturbed problem we can easily use Eq. (1) to evaluate the time average of any function $F(\mathbf{q}\cdot\mathbf{u_R})$ when localized defects are present in the crystal lattice. We obtain in that way the complete solution of the problem posed in the present paper.

Expression (25) derived for $S(\mathbf{n}, \mathbf{R}, T)$, along with Eq. (10) for the square of the mean-square fluctuation of the displacements of the atoms of a crystal lattice with a finite number of defects, can be used to draw some conclusions about the behavior of the quantity $\tilde{D}^2$ at large distances from the defects. A detailed analysis of Eqs. (25) and (26) shows that at large distances R from a defect the asymptotic behavior of Eq. (25) for S is determined solely by the long-wave part of the spectrum, so that we can neglect in the expression for S the contribution from the optical modes of vibrations and the contribution from the vibrations corresponding to the discrete spectrum. One can evaluate the asymptotic behavior in the general case of an arbitrary lattice and of any localized defect. We shall not perform here the fairly cumbersome and tiresome calculation, but only quote the general result.

---

*The proof of this statement, as of some other statements about the functions $\tilde{\psi}_{\lambda\rho}$, is omitted here because it is cumbersome. These proofs are based upon a consideration of the asymptotic behavior of the functions $\tilde{\psi}_{\lambda\rho}$ at large distances from the localized defect. Their asymptotic behavior can be found, if one knows the asymptotic behavior of the functions $\varphi_{\lambda i}$. The functions $\varphi_{\lambda i}$ are by (14) expressed as a sum of integrals. Lifshitz[5] and Lifshitz and Peresada[10] have evaluated the asymptotic behavior of similar integrals in connection with other problems.

For large values of R the asymptotic behavior of S is the sum of a finite number of terms of the form

$$A_i \frac{T}{\Theta}\left(\frac{b}{R}\right)^2 \coth\left(B_i \frac{RT}{b\Theta}\right),$$

where the quantities A_i and B_i can be evaluated in closed form for each given crystal and each given perturbation. They depend on the direction of the radius vector **R** at the point of observation, on the differential properties of the surfaces $\lambda_i(\mathbf{k}) = \lambda$ as $\lambda \to 0$, and on the type of the lattice defect. Θ is some characteristic temperature similar to the Debye temperature, and b is a characteristic length of the same order of magnitude as the dimensions of the elementary crystal cell.

It follows from the expression given here for S that at crystal temperatures T and at distances R such that $RT \ll b\Theta$ the asymptotic form of S is

$$A\left(\frac{b}{R}\right)^3 + B\left(\frac{T}{\Theta}\right)^2 \frac{b}{R}$$

where for a given lattice and a given perturbation A and B depend only on the vector $\mathbf{R}/R$. In particular, $S \sim A(b/R)^3$ when $T = 0$, i.e., at absolute zero the extra term in the fluctuation of the displacement decreases in inverse proportion to the cube of the distance from the defect. When $RT \gg b\Theta$ this extra term decreases as $1/R^2$.

Summarizing the results of this paper we can reach the following conclusions:

1. The time average of any function of the dot product of a constant vector **q** and the displacement from the equilibrium position $\mathbf{u}_\mathbf{R}$ of the **R**-th atom of any system of atoms which executes small vibrations and which is in thermodynamic equilibrium with the surrounding medium is uniquely determined by the mean square fluctuation D(**n**, **R**, T) of the displacements of the **R**-th atom in the direction of the vector $\mathbf{n} = \mathbf{q}/|\mathbf{q}|$.

2. One can evaluate the fluctuation D(**n**, **R**, T) in closed form in the case of an arbitrary infinite perfect crystal lattice in which there is a finite number of localized defects such as foreign atoms substituted for an atom, interstitials, vacancies, and so on, provided one knows the spectral properties of the corresponding perfect lattice without defects and provided one knows the finite-dimensional operator Λ which describes these defects.

Although the determination of D(**n**, **R**, T) can be reduced to the evaluation of the trace of an operator, it turns out to be impossible to apply here Lifshitz' results[6] on the evaluation of the difference between traces, since in this case one cannot write the operator whose trace determines the value of D(**n**, **R**, T) as some function of the operator L.

3. The change in the square of the function D(**n**, **R**, T), caused by the presence of localized deformations in the crystal lattice, is determined, according to (10), by the function S(**n**, **R**, T); we suggested in this paper a special method of evaluating this function. This method is based upon the fact that, in the case of localized lattice deformations described by adding a finite-dimensional operator Λ to the operator L, it turns out to be possible to split off from the space H, on which the operator L is determined, a subspace H′ such that all physical consequences caused by the perturbation Λ can be described in terms of the subspace H′. This makes it possible to obtain the closed Eq. (25) for S(**n**, **R**, T).

4. As expected, the quantities $\zeta_\rho(\lambda)$, first defined by Lifshitz[6] for the case of a three-dimensional lattice and called by him "shifts," occur in the expression for S(**n**, **R**, T). These quantities determine the phase shifts of the waves scattered by a localized inhomogeneity of the crystal.

5. In the general case of an arbitrary infinite perfect crystal with a finite number of localized defects, one can find the asymptotic behavior of the function at large distances from the defects. The asymptotic expression for S includes the dependence on the form of the localized irregularity of the lattice. The difference between the mean-square fluctuations $\tilde{D}^2$ and D^2 of the perturbed and the unperturbed lattices at absolute zero decreases with the distance R as R^{-3}. At sufficiently low temperatures, there is a region in the crystal where $(\tilde{D}^2 - D^2) \sim AR^{-3} + T^2R^{-1}$. Outside this region $(\tilde{D}^2 - D^2) \sim TR^{-2}$ as $R \to \infty$.

In conclusion, I express my deepest gratitude to Professor I. M. Lifshitz for his constant interest in this paper, for valuable advice, and for discussing the results obtained.

---

[1] F. Bloch, Z. Physik **74**, 295 (1932).

[2] L. D. Landau and E. M. Lifshitz, Статистическая физика (Statistical Physics) Gostekhizdat, 1951 [Engl. Transl., Pergamon Press, 1958].

[3] I. M. Lifshitz, JETP **12**, 117, 137 (1942).

[4] I. M. Lifshitz, JETP **17**, 1017, 1076 (1947).

[5] I. M. Lifshitz, JETP **18**, 293 (1948).

[6] I. M. Lifshitz, Usp. Mat. Nauk 7, 171 (1952).

[7] I. M. Lifshitz and G. I. Stepanova, JETP 30, 938 (1956), Soviet Phys. JETP 3, 656 (1956).

[8] I. M. Lifshitz and G. I. Stepanova, JETP 31, 156 (1956), Soviet Phys. JETP 4, 151 (1957).

[9] I. M. Lifshitz and G. I. Stepanova, JETP 33, 485 (1957), Soviet Phys. JETP 6, 379 (1958).

[10] I. M. Lifshitz and V. I. Peresada, Ученые записки ХГУ (Scientific Notes of the Khar'kov State University) 64, Proc. Phys. Division of the Phys.-Math. Faculty 6, 37 (1955).

[11] M. G. Kreĭn, Матем. сб Math. Symposium 33, 597 (1953).

[12] I. M. Lifshitz, loc. cit. ref. 10, 37, Proc. Phys. Division of the Phys.-Math. Faculty 1, 105 (1943).

Translated by D. ter Haar

224

SOVIET PHYSICS JETP VOLUME 11, NUMBER 4 OCTOBER, 1960

POLARIZATION EFFECTS IN THE SCATTERING OF ELECTRONS BY DEUTERONS

G. V. FROLOV

Radium Institute, Academy of Sciences, U.S.S.R.

Submitted to JETP editor July 8, 1959

J. Exptl. Theoret. Phys. (U.S.S.R.) 38, 1148-1152 (April, 1960)

The differential cross section and the change of polarization of the electrons are calculated for the process of disintegration of polarized deuterons by polarized electrons, with the electromagnetic form factors of the nucleons taken into account. An expression is also obtained for the polarization of recoil deuterons from the elastic scattering of polarized electrons by unpolarized deuterons.

In a previous paper[1] the differential cross section and the change of polarization of the electrons were calculated for the elastic scattering of polarized electrons by polarized deuterons. In the present paper we consider the differential cross section and the change of the polarization of the electrons in the disintegration of polarized deuterons by polarized electrons, and also obtain formulas for the polarization of the recoil deuterons from the elastic scattering of polarized electrons by unpolarized deuterons. The deuterons are assumed to be nonrelativistic, and the admixture of D wave in the ground state of the deuteron is neglected.

Treating the interaction of an electron with a deuteron as the interaction with the bound neutron and proton, as was done in reference 1, we have for the matrix element of the interaction:

$$S_{if} = e^2 q^{-2} \langle \chi_f | S | \chi_i \rangle. \tag{1}$$

Here $q = p_1 - p_2$ is the change of the four-momentum of the electron, χ_f and χ_i are the spin functions of the final and initial states of the deuteron,

$$S = A + \mathbf{B}(\boldsymbol{\sigma}_1 + \boldsymbol{\sigma}_2)/2 + \mathbf{C}(\boldsymbol{\sigma}_1 - \boldsymbol{\sigma}_2)/2,$$

$$A = I_1(g_4 - i\mathbf{g}\mathbf{q}/2M) - \mathbf{I}_2\mathbf{g}/2M, \qquad \mathbf{B} = I_3[\mathbf{q}\times\mathbf{g}],$$

$$\mathbf{C} = I_4[\mathbf{q}\times\mathbf{g}], \qquad g_\mu = (\bar{u}_2\gamma_\mu u_1), \tag{2}$$

u_2 and u_1 are spinors for the electron,

$$I_1 = \int \varphi_{\varkappa t}^* (a_p e^{i\mathbf{q}\mathbf{r}/2} + a_n e^{-i\mathbf{q}\mathbf{r}/2}) \varphi_d \, d\mathbf{r},$$

$$\mathbf{I}_2 = 2\int \varphi_{\varkappa t}^* (a_p e^{i\mathbf{q}\mathbf{r}/2} - a_n e^{-i\mathbf{q}\mathbf{r}/2}) \nabla\varphi_d \, d\mathbf{r},$$

$$I_3 = \frac{1}{2M}\int \varphi_{\varkappa t}^* [(a_p + b_p) e^{i\mathbf{q}\mathbf{r}/2} + (a_n + b_n) e^{-i\mathbf{q}\mathbf{r}/2}] \varphi_d \, d\mathbf{r},$$

$$I_4 = \frac{1}{2M}\int \varphi_{\varkappa s}^* [(a_p + b_p) e^{i\mathbf{q}\mathbf{r}/2} - (a_n + b_n) e^{-i\mathbf{q}\mathbf{r}/2}] \varphi_d \, d\mathbf{r},$$

a_p, a_n and b_p, b_n are the electric and magnetic form factors of the proton and neutron,[2] $\mathbf{r}$ is the relative coordinate of the nucleons, $\boldsymbol{\sigma}_1$ and $\boldsymbol{\sigma}_2$ are the spin operators of the proton and neutron, $\varphi_{\kappa t}$ and $\varphi_{\kappa s}$ are the coordinate functions of the triplet and singlet states of the two nucleons, φ_d is the coordinate function of the deuteron, and M is the mass of a nucleon.

The initial state is described by a density matrix which is the direct product of the density matrices of the electron and deuteron:

$$\rho_0 = \rho_e \times \rho_d,$$

where

$$\rho_e = \tfrac{1}{2}(1 + i\gamma_5\hat{\zeta}_1)\eta^{(+)}(p_1),$$

$$\rho_d = \tfrac{1}{4}[1 + \tfrac{1}{3}\boldsymbol{\sigma}_1\boldsymbol{\sigma}_2 + \boldsymbol{\alpha}(\boldsymbol{\sigma}_1 + \boldsymbol{\sigma}_2) + \beta_{im}(\sigma_{1i}\sigma_{2m} + \sigma_{2i}\sigma_{1m})],$$

$\eta^{(+)}(p) = (i\hat{p} - m)\gamma_4/2\epsilon$ is the projection operator that selects positive-energy states. The four-vector $\zeta_\mu = (\boldsymbol{\zeta}, \zeta_4)$ characterizes the polarization of the electron.

In the rest system $\zeta_\mu = (\boldsymbol{\zeta}^0, 0)$; in an arbitrary reference system

$$\boldsymbol{\zeta} = \boldsymbol{\zeta}_t^0 + \boldsymbol{\zeta}_l^0 \varepsilon/m, \qquad \zeta_4 = i\,\mathbf{p}\boldsymbol{\zeta}^{(0)}/m,$$

where $\boldsymbol{\zeta}_t^0$ and $\boldsymbol{\zeta}_l^0$ are the transverse and longitudinal components of the vector $\boldsymbol{\zeta}^0$; $\mathbf{p}$ is the momentum, ϵ the energy, and m the mass of the electron; $\boldsymbol{\alpha}$ and β_{im} characterize the polarization of the deuteron; $\beta_{im} = \beta_{mi}$; $\mathrm{Sp}\,\beta_{im} = \beta_{ii} = 0$. In the present case the concept of polarization also includes what is ordinarily called alignment.

THE DIFFERENTIAL CROSS SECTION FOR INELASTIC SCATTERING

The differential cross section for disintegration of the deuteron which corresponds to the relative momentum κ of the nucleons in the final state has the following form:

$$\frac{d\sigma}{d\Omega} = \frac{1}{4}\left(\frac{e^2}{4\pi}\right)^2 \frac{\mathrm{Sp}\,\{\eta^{(+)}(p_2)\, S\rho_0 S^+\}}{[1 + \xi\sin^2(\vartheta/2)]\,\varepsilon_1^2 \sin^4(\vartheta/2)} \frac{d\varkappa}{(2\pi)^3}. \tag{3}$$

Here ϑ is the angle of scattering of the electron, and $\xi = \epsilon_1/M$.

For a prescribed scattering angle the energy spectrum of the electrons has a sharp peak. Therefore for the range of energies that makes the main contribution to the cross section, q does not change to any important extent. Regarding q as constant, one can easily carry out the integration over κ, using in an approximate way the completeness of the functions $\varphi_{\kappa s}$ and $\varphi_{\kappa t}$. Performing also the summation over the spin variables of the nucleons and the electron, we have

$$\int \frac{d\varkappa}{(2\pi)^3}\,\mathrm{Sp}\,\{\eta_i^{(+)}(p_2)\;S\rho_0 S^+\} = \overline{|I_1|^2}\cos^2\frac{\vartheta}{2} - \frac{m\overline{I_1 I_3}}{\varepsilon_1\varepsilon_2} - [(\boldsymbol{\alpha}\boldsymbol{\zeta})\,\mathbf{q}^2 - (\boldsymbol{\alpha}\mathbf{q})\,(\boldsymbol{\zeta}\mathbf{q})] + \frac{\mathbf{q}^2}{3}\Big(1+\sin^2\frac{\vartheta}{2}\Big)(2\overline{|I_3|^2} + \overline{|I_4|^2})$$

$$+ \frac{im}{2\varepsilon_1\varepsilon_2}(\overline{|I_3|^2} + \overline{|I_4|^2})\,(\boldsymbol{\alpha}\mathbf{q})\,[\zeta_4\mathbf{q}^2 - i\,(\varepsilon_1-\varepsilon_2)\,(\boldsymbol{\zeta}\mathbf{q})] + \frac{(\overline{|I_3|^2} - \overline{|I_4|^2})}{\varepsilon_1\varepsilon_2}\,\beta_{lm}\,\Big\{\varepsilon_1\varepsilon_2\cos^2\frac{\vartheta}{2}\,(p_{1l}p_{2m} + p_{2l}\,p_{1m})$$

$$-\,\varepsilon_2\Big(\varepsilon_2 + \varepsilon_1\sin^2\frac{\vartheta}{2}\Big)p_{1l}p_{1m} - \varepsilon_1\Big(\varepsilon_1 + \varepsilon_2\sin^2\frac{\vartheta}{2}\Big)p_{2l}p_{2m}\Big\}.$$

Here

$$\overline{|I_1|^2} = \int\frac{d\varkappa}{(2\pi)^3}|I_1|^2 = a_p^2 + a_n^2 + 2a_p a_n f(2q) - (a_p+a_n)^2 f^2(q), \qquad \overline{I_1 I_3} = \int\frac{d\varkappa}{(2\pi)^3}\,\mathrm{Re}\,(I_1 I_3^*) = \frac{1}{2M}\{a_p(a_p+b_p) + a_n(a_n+b_n)$$

$$+ [a_p(a_n+b_n) + a_n(a_p+b_p)]\,f(2q) - (a_p+a_n)\,(a_p+a_n+b_p+b_n)\,f^2(q)\},$$

$$\overline{|I_3|^2} = (2M)^{-2}\{(a_p+b_p)^2 + (a_n+b_n)^2 + 2\,(a_p+b_p)\,(a_n+b_n)\,f(2q) - (a_p+a_n+b_p+b_n)^2 f^2(q)\},$$

$$\overline{|I_4|^2} = (2M)^{-2}\{(a_p+b_p)^2 + (a_n+b_n)^2 - 2\,(a_p+b_p)\,(a_n+b_n)\,f(2q)\}. \tag{4}$$

The form factor of the deuteron is

$$f(q) = \int|\varphi_d|^2 e^{i\mathbf{qr}/2}\,d\mathbf{r} = \int_0^\infty u^2\frac{\sin(qr/2)}{qr/2}\,dr,$$

where $\varphi_d = u/(4\pi)^{1/2} r$. In particular, if $\psi_d = (\gamma/2\pi)^{1/2} e^{-\gamma r}/r$, the form factor is

$$f(q) = \frac{4\gamma}{q}\,\tan^{-1}\frac{q}{4\gamma}.$$

From these expressions it can be seen that the difference $\overline{|I_3|^2} - \overline{|I_4|^2}$ involves only terms containing $f^2(q)$ and $f(2q)$. These quantities are small for the changes of momentum that are of interest here, and therefore the contribution to the cross section from the "tensor" polarization is also small.

The final expression for the differential cross section for disintegration accompanied by scattering of the electron by the angle ϑ can be conveniently written with the following choice of coordinate axes:

$$\mathbf{k} = \mathbf{p}_1/|\,\mathbf{p}_1\,|, \qquad \mathbf{n} = [\mathbf{p}_1\times\mathbf{p}_2]/|[\mathbf{p}_1\times\mathbf{p}_2]\,|, \qquad \mathbf{l} = [\mathbf{k}\times\mathbf{n}]. \tag{5}$$

We get

$$d\sigma/d\Omega = (d\sigma/d\Omega)_0\,(1 - N/N_0), \tag{6}$$

where

$$N_0 = \overline{|I_1|^2} + \frac{\mathbf{q}^2}{3}\Big(1 + 2\tan^2\frac{\vartheta}{2}\Big)(2\overline{|I_3|^2} + \overline{|I_4|^2}), \qquad N = 2\overline{I_1 I_3}\,(\boldsymbol{\zeta}_1^0\mathbf{k})\tan\frac{\vartheta}{2}\,[(\boldsymbol{\alpha}\mathbf{k})\,\varepsilon_2\sin\vartheta - (\boldsymbol{\alpha}\mathbf{l})\,(\varepsilon_1 - \varepsilon_2\cos\vartheta)]$$

$$+ (\overline{|I_3|^2} + \overline{|I_4|^2})\tan\frac{\vartheta}{2}\,(\boldsymbol{\zeta}_1^0\mathbf{k})\,(\varepsilon_1+\varepsilon_2)\,[(\boldsymbol{\alpha}\mathbf{k})\,(\varepsilon_1 - \varepsilon_2\cos\vartheta) + (\boldsymbol{\alpha}\mathbf{l})\,\varepsilon_2\sin\vartheta]$$

$$+ (\overline{|I_3|^2} - \overline{|I_4|^2})\sin^2\frac{\vartheta}{2}\,\beta_{im}\Big\{k_i k_m\Big(1+\tan^2\frac{\vartheta}{2}\Big)(\varepsilon_1^2 + 2\varepsilon_1\varepsilon_2 + \varepsilon_2^2\cos^2\vartheta) + 4l_i l_m\varepsilon_2\Big(\varepsilon_1 + \varepsilon_2\sin^2\frac{\vartheta}{2}\Big)$$

$$+ 4l_i k_m\varepsilon_2\tan\frac{\vartheta}{2}\,(\varepsilon_1 - \varepsilon_2\cos\vartheta)\Big\}. \tag{7}$$

The differential cross section for unpolarized particles is

$$\Big(\frac{d\sigma}{d\Omega}\Big)_0 = \frac{1}{4}\Big(\frac{e^2}{4\pi}\Big)^2\frac{N_0\cos^2(\vartheta/2)}{[1+\xi\sin^2(\vartheta/2)]\;\varepsilon_1^2\sin^4(\vartheta/2)}. \tag{8}$$

It has been assumed everywhere in the calculations that

$$\varepsilon_1 \gg m, \qquad \vartheta \gg m/\varepsilon_1.$$

The formula (8) goes over into the expression obtained by Jankus[3] for point nucleons if in the expression for N_0 we neglect $f(2q)$ and in the term with q^2 we also neglect $f^2(q)$.

From the expressions that have been obtained it can be seen that the differential cross section does not depend on the transverse component of the polarization of the electrons. If the electrons are not polarized, only the last term remains in (7). In this case the cross section differs little from $(d\sigma/d\Omega)_0$.

THE CHANGE OF POLARIZATION OF THE ELECTRONS IN INELASTIC SCATTERING

The basic expression for the final polarization $\boldsymbol{\zeta}_2$ of the electrons from disintegration of polarized deuterons by electrons of polarization $\boldsymbol{\zeta}_1$ is as follows:

$$\zeta_2 = \frac{i\,(\varepsilon_2/m)\,\mathrm{Sp}\,\{\gamma\gamma_4\gamma_5\eta^{(+)}(p_2)\,Sp_0S^{+}\eta^{(+)}(p_2)\}d\varkappa}{\mathrm{Sp}\,\{\eta^{(+)}(p_2)\,Sp_0S^{+}\}\,d\varkappa}. \tag{9}$$

To determine the polarization of those electrons that have been scattered through the angle ϑ, independent of the final state of the nucleons, we must carry out an integration over κ. This is done in just the same way as before.

We present the result:

$$\begin{aligned}\zeta_2^0 = \mathbf{k}\,[&C_{11}(\zeta_1^0\mathbf{k}) + C_{12}(\zeta_1^0\mathbf{n}) + C_{13}(\zeta_1^0\mathbf{l}) + D_{11}(\boldsymbol{\alpha}\mathbf{k}) + D_{13}(\boldsymbol{\alpha}\mathbf{l})]\\ &+ \mathbf{n}\,[C_{22}(\zeta_1^0\mathbf{n}) + C_{23}(\zeta_1^0\mathbf{l})] + \mathbf{l}\,[C_{31}(\zeta_1^0\mathbf{k}) + C_{32}(\zeta_1^0\mathbf{n})\\ &+ C_{33}(\zeta_1^0\mathbf{l}) + D_{31}(\boldsymbol{\alpha}\mathbf{k}) + D_{33}(\boldsymbol{\alpha}\mathbf{l})].\end{aligned} \tag{10}$$

The coefficients appearing in the formula (10) have the following values:

$$\begin{aligned}C_{11} = \frac{\cos\vartheta}{N_0 - N}\Big\{&\overline{|I_1|^2} + \frac{\mathbf{q}^2}{3}\big(2\overline{|I_3|^2} + \overline{|I_4|^2}\big)\Big(1 + 2\tan^2\frac{\vartheta}{2}\Big)\\ &- 2\varepsilon_2\tan^2\frac{\vartheta}{2}\,\overline{\big(|I_3|^2 - |I_4|^2\big)\beta_{im}}\Big[l_ik_m\sin\vartheta\,(\varepsilon_1 - \varepsilon_2\cos\vartheta)\\ &+ 2k_ik_m\Big(\varepsilon_1 - \frac{1}{4}\varepsilon_2\sin^2\vartheta\Big) + 2l_il_m\cos^2\frac{\vartheta}{2}\Big(\varepsilon_1 + \varepsilon_2\sin^2\frac{\vartheta}{2}\Big)\Big]\Big\},\end{aligned}$$

$$\begin{aligned}C_{22} = \frac{1}{N_0 - N}\Big\{&\overline{|I_1|^2} + \frac{\mathbf{q}^2}{3}\big(2\overline{|I_3|^2} + \overline{|I_4|^2}\big)\\ &- 2\varepsilon_2\tan^2\frac{\vartheta}{2}\big(\overline{|I_3|^2} - \overline{|I_4|^2}\big)\beta_{im}\Big[2k_ik_m\Big(\varepsilon_1 + \frac{1}{4}\varepsilon_2\sin^2\vartheta\Big)\\ &+ 2l_il_m\Big[\varepsilon_1\Big(1 + \sin^2\frac{\vartheta}{2}\Big) - \frac{1}{4}\varepsilon_2\sin^2\vartheta\Big]\\ &- l_ik_m\sin\vartheta\,(\varepsilon_1 - \varepsilon_2\cos\vartheta)\Big]\Big\},\end{aligned}$$

$$\begin{aligned}C_{23} = \frac{2\varepsilon_2\tan(\vartheta/2)\,\big(\overline{|I_3|^2} - \overline{|I_4|^2}\big)\beta_{im}}{N_0 - N}\Big\{&2n_il_m\Big[\varepsilon_1\Big(1 + \sin^2\frac{\vartheta}{2}\Big)\\ &- \varepsilon_2\cos^2\frac{\vartheta}{2}\Big] - n_ik_m\sin\vartheta\,(\varepsilon_1 + \varepsilon_2)\Big\},\end{aligned}$$

$$\begin{aligned}D_{11} = -\frac{\cos\vartheta\tan(\vartheta/2)}{N_0 - N}\Big\{&2\overline{I_1I_3}\varepsilon_2\sin\vartheta + \big(\overline{|I_3|^2} + \overline{|I_4|^2}\big)\\ &\times\tan\frac{\vartheta}{2}(\varepsilon_1 + \varepsilon_2)(\varepsilon_1 - \varepsilon_2\cos\vartheta)\Big\},\end{aligned}$$

$$\begin{aligned}D_{13} = \frac{2\cos\vartheta\tan(\vartheta/2)}{N_0 - N}\{&\overline{I_1I_3}(\varepsilon_1 - \varepsilon_2\cos\vartheta) - \big(\overline{|I_3|^2} + \overline{|I_4|^2}\big)\\ &\times\sin^2\frac{\vartheta}{2}\varepsilon_2(\varepsilon_1 + \varepsilon_2)\};\end{aligned}$$

$$C_{13} = C_{22}\sin\vartheta, \qquad C_{12} = -C_{23}\sin\vartheta, \qquad C_{31} = -C_{11}\tan\vartheta,$$

$$D_{33} = -D_{13}\tan\vartheta, \qquad C_{33} = C_{22}\cos\vartheta, \qquad C_{32} = -C_{23}\cos\vartheta,$$

$$D_{31} = -D_{11}\tan\vartheta.$$

From these expressions it can be seen that the "tensor" polarization of the deuteron gives a small contribution to the polarization of the scattered electron. It is more convenient to express the final polarization in the coordinate system connected with the scattered electron:

$$\zeta_{2l} = (\zeta_2\mathbf{p}_2)/|\mathbf{p}_2|, \qquad \zeta_{2t}^{\perp} = (\zeta_2\mathbf{n}), \qquad \zeta_{2t}^{\parallel} = (\zeta_2[\mathbf{p}_2\times\mathbf{n}])/|\mathbf{p}_2|;$$

ζ_{2l} is the longitudinal component; $\zeta_{2t}^{\perp}$ is the transverse component perpendicular to the plane of the reaction; $\zeta_{2t}^{\parallel}$ is the transverse component in the plane of the reaction. For the incident electron

$$\zeta_{1l} = (\zeta_1\mathbf{k}), \qquad \zeta_{1t}^{\perp} = (\zeta_1\mathbf{n}), \qquad \zeta_{1t}^{\parallel} = (\zeta_1\mathbf{l}).$$

In this notation the result can be written in the following way:

$$\begin{aligned}\zeta_{2l}^0 &= [C_{11}\zeta_{1l}^0 + (\boldsymbol{\alpha}\mathbf{k})D_{11} + (\boldsymbol{\alpha}\mathbf{l})D_{13}]/\cos\vartheta,\\ \zeta_{2t}^{0\perp} &= C_{22}\zeta_{1t}^{0\perp} + C_{23}\zeta_{1t}^{0\parallel},\\ \zeta_{2t}^{0\parallel} &= C_{22}\zeta_{1t}^{0\parallel} - C_{23}\zeta_{1t}^{0\perp}.\end{aligned}$$

It can be seen that in the scattering the longitudinal and transverse components change independently of each other. If the deuteron is originally unpolarized, we get

$$\begin{aligned}\zeta_{2l}^0 &= \zeta_{1l}^0,\\ \zeta_{2t}^{0\parallel} &= \zeta_{1t}^{0\parallel}\{1 - 2\mathbf{q}^2\tan^2(\vartheta/2)\,\big(2\overline{|I_3|^2} + \overline{|I_4|^2}\big)/3N_0\},\\ \zeta_{2t}^{0\perp} &= \zeta_{1t}^{0\perp}\{1 - 2\mathbf{q}^2\tan^2(\vartheta/2)\,\big(2\overline{|I_3|^2} + \overline{|I_4|^2}\big)/3N_0\}.\end{aligned}$$

In this case the longitudinal component of the polarization of the electron does not change in the scattering, and both transverse components change in the same way. If the electron is originally unpolarized, we have

$$\zeta_{2l}^0 = [(\boldsymbol{\alpha}\mathbf{k})D_{11} + (\boldsymbol{\alpha}\mathbf{l})D_{13}]/\cos\vartheta, \qquad \zeta_{2t}^{0\perp} = \zeta_{2t}^{0\parallel} = 0.$$

Longitudinally polarized electrons are produced.

Comparison of these expressions with experimental data can give additional information about the form factors of nucleons.

POLARIZATION OF THE RECOIL DEUTERONS FROM ELASTIC SCATTERING

The following expressions are obtained for the quantities α and β_{im} that characterize the polarization of the recoil deuterons from elastic scattering of polarized electrons by unpolarized deuterons:

$$\begin{aligned}(\boldsymbol{\alpha}\mathbf{k}) = -\frac{4\varepsilon_2\sin^2(\vartheta/2)\,(a_p + a_n + b_p + b_n)}{3MR_0}(\zeta_1^0\mathbf{k})\Big\{&a_p + a_n\\ &- \frac{\varepsilon_1(a_p + a_n + b_p + b_n)}{4M}\Big(2\tan^2\frac{\vartheta}{2} + \xi\sin^2\frac{\vartheta}{2}\Big)\Big\},\end{aligned}$$

$$\begin{aligned}(\boldsymbol{\alpha}\mathbf{l}) = \frac{2\varepsilon_2\sin^2(\vartheta/2)\tan(\vartheta/2)\,(a_p + a_n + b_p + b_n)}{3MR_0}(\zeta_1^0\mathbf{k})\Big\{&(a_p + a_n)\\ &\times(2 + \xi) + \frac{\varepsilon_1(a_p + a_n + b_p + b_n)}{2M}\Big(2 - \xi\sin^2\frac{\vartheta}{2}\Big)\Big\},\end{aligned}$$

$$\begin{aligned}\beta_{im}k_ik_m = \frac{\mathbf{q}^2(a_p + a_n + b_p + b_n)^2}{12M^2R_0}\Big[&\sin^2\frac{\vartheta}{2} - \frac{1}{3}\Big(1 + 2\tan^2\frac{\vartheta}{2}\Big)\\ &- \xi\sin^4\frac{\vartheta}{2}\Big],\end{aligned}$$

$$\begin{aligned}\beta_{im}l_il_m = \frac{\mathbf{q}^2(a_p + a_n + b_p + b_n)^2}{12M^2R_0}\Big[&\frac{1}{3}\Big(\tan^2\frac{\vartheta}{2} - 1\Big)\\ &- \sin^2\frac{\vartheta}{2} + \xi\sin^4\frac{\vartheta}{2}\Big].\end{aligned}$$

$$\beta_{im}l_ik_m = -\frac{\mathbf{q}^2(a_p + a_n + b_p + b_n)^2}{24M^2R_0}\tan\frac{\vartheta}{2}\sin^2\frac{\vartheta}{2}(2 + \xi\cos\vartheta),$$

$$\beta_{im}n_in_m = -\beta_{im}k_ik_m - \beta_{im}l_il_m.$$

Here

$$R_0 = (a_p + a_n)^2 - \frac{\mathbf{q}^2(a_p + a_n + b_p + b_n)^2}{6M^2}\Big(1 - \frac{2}{\cos^2(\vartheta/2)}\Big).$$

The other notations are the same as before.

From these expressions it can be seen that the average value $\frac{1}{2}\alpha$ of the spin of the recoil deuteron lies in the plane of the scattering. α is zero if the incident electrons are unpolarized, but the quantities β_{im} are different from zero even in this case.

Therefore experiments to determine the "tensor" polarization of the recoil deuterons are in a certain sense the simplest of the polarization experiments on the elastic scattering of electrons by deuterons.

[1] G. V. Frolov, JETP **37**, 522 (1959), Soviet Phys. JETP **10**, 369 (1960).

[2] Akhiezer, Rozentsveĭg, and Shmushkevich, JETP **33**, 765 (1957), Soviet Phys. JETP **6**, 588 (1958).

[3] V. Z. Jankus, Phys. Rev. **102**, 1586 (1956).

Translated by W. H. Furry
225

SOVIET PHYSICS JETP VOLUME 11, NUMBER 4 OCTOBER, 1960

RESONANCE ABSORPTION OF HIGH-FREQUENCY SOUND ENERGY BY SEMICONDUCTOR CURRENT CARRIERS IN A MAGNETIC FIELD

E. P. POKATILOV

Kishinev State University

Submitted to JETP editor July 27, 1959

J. Exptl. Theoret. Phys. (U.S.S.R.) 38, 1153-1159 (April, 1960)

The absorption coefficient of ultrasound in a semiconductor is estimated with account of quantization of the electron energy in a magnetic field.

IN a number of papers published in recent years,[1-3] the results of experimental and theoretical investigations of the absorption of ultrasonic energy by current carriers in a magnetic field has been reported for the case of ultrasonic frequencies ω that are less than or equal to the collision frequency of the electrons $1/\tau$ (τ is the relaxation time).

The case of higher ultrasonic frequencies, for which the inequality

$$\omega \geqslant \omega_0 > 1/\tau, \tag{1}$$

where ω_0 = cyclotron frequency of the electron, is satisfied, has been investigated theoretically by the author.[4] This inequality is the inverse of that used in the papers mentioned above. However, the calculation[4] was made in the classical approximation $\lambda_s > \lambda_{el}$ for the special case $\kappa_z = 0$ (κ_z is the component of the wave vector of the ultrasonic wave in the direction of the magnetic field).

1. Inasmuch as the absorption of ultrasonic energy has a resonance character,[4] we shall make use of a variant of the Wigner-Weisskopf theory of quantum processes. The Schrödinger equation for electrons interacting in a magnetic field with phonons and lattice impurities has the form

$$i\hbar\partial\Psi/\partial t = (H_0 + H_{int})\Psi, \tag{2}$$

where

$$H_0 = (2m^*)^{-1}\left[\left(p_x + \frac{e\mathcal{H}}{c}y\right)^2 + p_y^2 + p_z^2\right] + H_{\rm phon} \tag{3}$$

is the sum of Hamiltonian operators for the motion of an electron in a magnetic field, and of the acoustic phonons of the lattice, $H_{\rm phon}$;

$$H_{int} = H_{1\,int} + H_{2\,int} + H_{3\,int} \tag{4}$$

is the energy of interaction of the electron with the ultrasound ($H_{1\,\rm int}$), the acoustic vibrations of the lattice ($H_{2\,\rm int}$), and the impurities ($H_{3\,\rm int}$).

At low temperatures, for which the resonance effects under consideration can be measured, the optical vibrations do not have an appreciable value. The interaction operators $H_{1\,\rm int}$ and $H_{2\,\rm int}$ are chosen in the forms

$$H_{1\,int} = a\,\mathrm{div}\,\mathbf{u} = V_\varkappa e^{i\varkappa\mathbf{r}} + V_\varkappa^* e^{-i\varkappa\mathbf{r}}, \qquad V_\varkappa = \tfrac{1}{2} ia\mathbf{u}_0\varkappa e^{-i\omega t}; \tag{5}$$

$$H_{2\,int} = a\sum_{\varkappa' j}\mathrm{div}\,\mathbf{u}(\varkappa', j). \tag{6}$$

In Eqs. (5) and (6), the quantity a is the constant of interaction of the electron with the lattice vibrations, $\mathbf{u}_0$ is the vector of the amplitude of the ultrasonic wave, κ and ω are the wave vector and the frequency of the ultrasound, respectively, while κ' and j are the wave vector and the polarization of the acoustic vibrations. We have no need here for the explicit form of the operator $H_{3\,\rm int}$.

We express the solution of (2) as a superposition of wave functions that are solutions of the equation

$$i\hbar\partial\Psi/\partial t = H_0\Psi, \tag{7}$$

$$\Psi = \sum_\lambda b_\lambda \exp(-iE_\lambda t/\hbar)\,\psi_{n,\,k_x,\,k_z}\,\Phi_{N_\varkappa}\prod\Phi_{N_{\varkappa'}}, \tag{8}$$

where

$$\psi_{n,\,k_x,\,k_z} = C_n \exp\{i(k_x x + k_z z) - \tfrac{1}{2}\alpha(y - y_0)^2\}\,H_n(\sqrt{\alpha}(y - y_0)) \tag{9}$$

is the normalized wave function of the free electron in a magnetic field, $\alpha = |e|\mathcal{H}/c\hbar$ and the remaining notation is the same as that in the book by Landau and Lifshitz;[5] Φ_{N_K} is the oscillator wave function describing the ultrasonic vibration of the lattice; $\Pi\Phi_{N_{K'}}$ is the product of the oscillator wave functions of the acoustical vibrations of the lattice

$$E_\lambda = \varepsilon_\parallel(k_z) + \hbar\omega_0(n + \tfrac{1}{2}) + \hbar\omega(N_\varkappa + \tfrac{1}{2}) + \sum\hbar\omega_{\varkappa'}(N_{\varkappa'} + \tfrac{1}{2}). \tag{10}$$

In (10), $\epsilon_\parallel$ is the kinetic energy of motion of the electron along the direction of the magnetic field; $\hbar\omega_0(n+\frac{1}{2})$ is the energy of motion in the plane x, y; $\hbar\omega(N_K+\frac{1}{2})$ is the ultrasonic energy; $\sum_{\kappa'}\hbar\omega_{\kappa'}(N_{\kappa'}+\frac{1}{2})$ is the energy of the acoustic vibration; λ is an index denoting the total set of quantum numbers of the system. In the sum (8), one of the amplitudes b_{λ_0} is equal to unity at the initial instant of time while the other is equal to zero. The indices λ and λ_0 differ in the quantum numbers of the electron states, and also by the occupation numbers of the phonon levels; in the state λ these occupation numbers differ from their initial values by unity or by zero.

Applying the Wigner-Weisskopf method,[6] we find the equation for b_λ, the transition-probability amplitude, and for $\gamma_n(k_z)$, the reciprocal of the mean lifetime of the electron in the state n, k_z:

$$b_\lambda = -H_{int}(\lambda,\lambda_0)[\exp\{i(E_\lambda-E_{\lambda_0}) \times t/\hbar - \gamma t/2\}\hbar/(E_\lambda-E_{\lambda_0})+i\gamma/2], \quad (11)$$

$$\gamma_n = -\frac{2}{\hbar^2}\sum_\lambda |H_{int}|^2[1-\exp\{i(E_{\lambda_0}-E_\lambda)t/\hbar+\gamma t/2\}] \times[i(E_{\lambda_0}-E_\lambda)/\hbar+\gamma/2]^{-1}. \quad (12)$$

To find the transition probabilities under the action of ultrasound, it is necessary to compute $H_{1\,int}(\lambda,\lambda_0)$. The phonon part of the wave function (8) contributes the following factor to the square of the modulus of the matrix element:

$$\left|\int\Phi_{N_\varkappa-1}V_\varkappa\Phi_{N_\varkappa}du\right|^2=\left|\int\Phi_{N_\varkappa+1}V_\varkappa^*\Phi_{N_\varkappa}du\right|^2\approx\frac{1}{16}a^2\varkappa^2u_0^2. \quad (13)$$

In (13) the number of ultrasonic phonons N_K, which is assumed to be much larger than unity, is approximately expressed by the ultrasonic amplitude.

We now compute the electron part of the matrix element. In accord with the work of Zil'berman,[7]

$$\int\exp\{-\tfrac{1}{2}\alpha(y-y_0')^2\}H_{n'}(\sqrt{\alpha}(y-y_0') \times\exp\{i\varkappa_y y-\tfrac{1}{2}\alpha(y-y_0)^2\}H_n(\sqrt{\alpha}(y-y_0))dy$$
$$=\exp\{i\varkappa_y y_0+i\beta(\varkappa_y,y_0-y_0')\}\int\exp\{-\alpha y'^2 +i\varkappa_\rho y'\}H_{n'}(\sqrt{\alpha}y')H_n(\sqrt{\alpha}y')dy'. \quad (14)$$

The form of the phase $\beta(\kappa_y, y_0-y_0')$ is given in reference 7. We use here the notation $\kappa_\rho^2 = (k_x'-k_x)^2+\kappa_y^2$, $y' = y-y_0$. The integral in (14) is given by

$$\sqrt{\pi/\alpha}\,2^{n_1}(i\varkappa_\rho/\sqrt{\alpha})^{n_2-n_1}n_1!\,L_{n_1}^{n_2-n_1}(\varkappa_\rho^2/2\alpha)\exp\{-\varkappa_\rho^2/2\alpha\}; \quad (15)$$

n_2 and n_1 are the largest and smallest of the numbers n and n′, respectively, and L_n^m is the Laguerre polynomial.

As a result of these calculations we get for the probability of transition of an electron (under the action of ultrasound) from the state n, k_z, k_x into the state n′, k_z', k_x',

$$|b_\lambda|^2=(2\pi)^2\frac{1}{16}(a\varkappa u_0)^2\lambda_\rho^{n_2-n_1}e^{-\lambda_\rho}[L_{n_1}^{n_2-n_1}(\lambda_\rho)]^2 \times[(n_1+1)\ldots n_2]^{-1}|[\exp\{i(E_\lambda-E_{\lambda_0})t/\hbar-\gamma t/2\} -1]/[(E_\lambda-E_{\lambda_0})/\hbar+i\gamma/2]|^2\delta(-k_z'+k_z\pm\varkappa_z), \quad (16)$$

where $\lambda_\rho = \kappa_\rho^2/2\alpha$ is a dimensionless parameter that determines the ratio of the radius of the orbit of the electron in the state n = 0 to the projection of the ultrasonic wave in the direction perpendicular to the magnetic field. In obtaining (16), $|H_{1\,int}|^2$ was integrated over k_x'; as a result, κ_ρ^2 became equal to $\kappa_x^2+\kappa_y^2$. The plus sign in the δ function in front of κ_z corresponds to a transition with absorption of sound energy, while the minus sign corresponds to a transition with radiation.

2. The ultrasonic absorption coefficient Γ is obtained from the formula

$$\Gamma = U/c_0E_{so}, \quad (17)$$

where c_0 is the sound velocity, $E_{so} = \rho u_0^2\omega^2/2$ is the sound energy density, and U is the energy absorbed per second per unit volume by the current carriers of the semiconductor. Calculation of Γ thus reduces to calculation of U. Below we shall introduce formulas for U under different assumptions relative to the state of the electron gas.

It is easy to obtain, using the Pauli principle, a formula for the mean number of transitions from the level n, k_z to the level n′, k_z',

$$\gamma_n(k_z)f_n(k_z)(1-f_{n'}(k_z'))|b_\lambda(\infty)|^2; \quad (18)$$

$f_n(k_z)$ is the distribution function of the electrons. If we substitute $|b_\lambda|^2$ from (16) in (18), taking the case of absorption of a phonon, and then integrate over k_z', k_z, sum over n, n′, and multiply the resultant expression by $2g = |e|\mathcal{H}/\pi\hbar c$ (the density of states with the given quantum numbers n and k_z), then we obtain the number of electron transitions with absorption of ultrasonic phonons per unit time. In similar fashion, we find the number of transitions with radiation of ultrasonic phonons. Multiplying these numbers of transitions by $\hbar\omega$ and $-\hbar\omega$, respectively, and adding, we obtain, finally, the unknown value of U:

$$U=2g\hbar\omega\Big\{\sum_{n,n'}\int\gamma_nf_n(k_z) \times[1-f_{n'}(k_z+\varkappa_z)]|b_\lambda(k_z+\varkappa_z,\infty)|^2dk_z -\sum_{n',n}\int\gamma_nf_n(k_z)[1-f_{n'}(k_z-\varkappa_z)]|b_\lambda(k_z-\varkappa_z,\infty)|^2dk_z\Big\}. \quad (19)$$

The results of calculation of γ_n by (12) will be published separately; in the present paper we shall assume γ to be constant. We introduce in (19) the new summation indices $\Delta n = n_2 - n_1$ and $n = n_1$, and substitute the expression for $|b_\lambda|^2$; we get, finally,

$$U = g\left(\frac{a\varkappa u_0}{4}\right)^2 \frac{\gamma\omega}{\pi\hbar} \sum_{\Delta n,\, n=0}^{\infty} \lambda_\rho^{\Delta n} e^{-\lambda_\rho}$$
$$\times [(n+1)\ldots(n+\Delta n)]^{-1} [L_n^{\Delta n}(\lambda_\rho)]^2$$
$$\times \left\{ \int \frac{[f_n(k_z) - f_{n+\Delta n}(k_z+\varkappa_z)]\, dk_z}{(\Delta n\omega_0 - \omega + [\varepsilon_\parallel(k_z+\varkappa_z) - \varepsilon_\parallel(k_z)]/\hbar)^2 + \gamma^2/4} \right.$$
$$\left. + \int \frac{[f_{n+\Delta n}(k_z) - f_n(k_z+\varkappa_z)]\, dk_z}{(\Delta n\omega_0 + \omega + [\varepsilon_\parallel(k_z) - \varepsilon_\parallel(k_z+\varkappa_z)]/\hbar)^2 + \gamma^2/4} \right\}. \tag{20}$$

We shall now consider certain special cases of Eq. (20).

Nondegenerate Semiconductor

a) $\kappa_z = 0$. As a consequence of the large value of the denominator of the second integral in (20), this term can be neglected. Substituting in (20)

$$f \sim \exp\{-[\varepsilon_\parallel + \hbar\omega_0(n + \tfrac{1}{2}) - \mu]/\Theta\}, \tag{21}$$

We can sum in it over n. Eliminating $e^{\mu/\Theta}$ from (20) by means of the formula for the electron concentration

$$N = \frac{g}{\pi} e^{\mu/\Theta} [1 - e^{-\hbar\omega_0/\Theta}]^{-1} \int e^{-\varepsilon_\parallel/\Theta}\, dk_z \tag{22}$$

we get an expression for U containing only a summation over Δn:

$$U = 2N\left(\frac{a\varkappa u_0}{4}\right)^2 \frac{\omega}{\hbar} \sum_{\Delta n=0}^{\infty} \frac{\operatorname{sh}(\Delta n\hbar\omega_0/2\Theta)}{(\Delta n\omega_0 - \omega)^2 + \gamma^2/4}$$
$$\times \exp\{-\lambda_\rho (1 + e^{-\hbar\omega_0/\Theta})(1 - e^{-\hbar\omega_0/\Theta})^{-1}\}$$
$$\times I_{\Delta n}(2\lambda_\rho e^{-\hbar\omega_0/2\Theta} [1 - e^{-\hbar\omega_0/\Theta}]^{-1}). \tag{23}$$

Here $I_{\Delta n}$ is the Bessel function of imaginary argument.

In the derivation of Eq. (23), nondegeneracy was assumed; therefore we can assume that $\hbar\omega_0/\Theta < 1$ and

$$\exp\{-\hbar\omega_0/\Theta\} - 1 \sim \hbar\omega_0/\Theta. \tag{24}$$

To go to the classical limit, we must assume $\lambda_\rho \ll 1$. Substituting (24) in (22), and setting $(\omega/\omega_0)^2 \Theta/m^* c_0^2 = x$, we find an approximate expression for U:

$$U \approx \frac{N}{\Theta}\left(\frac{a\varkappa u_0}{4}\right)^2 \gamma\omega \sum_{\Delta n=1}^{\infty} \Delta n\omega_0 e^{-x} I_{\Delta n}(x)/[(\Delta n\omega_0 - \omega)^2 + \gamma^2/4], \tag{25}$$

which is very close to Eq. (10) of reference 4, obtained by classical means. The fundamental difference between (10) of reference 4 and (25) is that instead of $1/\tau^2$ in the denominator of the classical formula, we here have $\gamma^2/4$. A formula that agrees exactly with the classical can be obtained if we use, in place of the probability (16), the square of the modulus of the matrix element of the Dirac theory of quantum transitions, averaged over time by means of the factor $e^{-t/\tau}$. The numerical calculations and the consequences of (25) were discussed in reference 4. A graph is given there, too, from which the resonance character of the ultrasonic absorption is clearly evident.

b) $\kappa_z \neq 0$. We substitute f from (21) in (20) and sum over n:

$$U = g\left(\frac{a\varkappa u_0}{4}\right)^2 \frac{\omega\gamma}{\pi\hbar} \sum_{\Delta n} (1 - e^{-\hbar\omega_0/\Theta})^{-1}$$
$$\times \exp\left\{-\lambda_\rho \frac{1 + e^{-\hbar\omega_0/\Theta}}{1 - e^{-\hbar\omega_0/\Theta}} + \frac{\hbar\omega_0\Delta n}{2\Theta}\right\}$$
$$\times I_{\Delta n}(2\lambda_\rho e^{-\hbar\omega_0/\Theta}/[1 - e^{-\hbar\omega_0/\Theta}])\, e^{\mu/\Theta}$$
$$\times \left\{ \int \frac{\exp(-\varepsilon_\parallel/\Theta) - \exp\{-\Delta n\hbar\omega_0/\Theta - \varepsilon_\parallel(k_z+\varkappa_z)/\Theta\}}{[\Delta n\omega_0 - \omega + (\varepsilon_\parallel(k_z+\varkappa_z) - \varepsilon_\parallel(k_z))/\hbar]^2 + \gamma^2/4}\, dk_z \right.$$
$$\left. + \int \frac{\exp(-\varepsilon_\parallel/\Theta) - \exp\{\Delta n\hbar\omega_0/\Theta - \varepsilon_\parallel(k_z+\varkappa_z)/\Theta\}}{[\Delta n\omega_0 + \omega + (\varepsilon_\parallel(k_z) - \varepsilon_\parallel(k_z+\varkappa_z))/\hbar]^2 + \gamma^2/4}\, dk_z \right\}. \tag{26}$$

It is of interest to note that in both cases a) and b) of the nondegenerate state of the current carrier, the energy U is proportional to the number of particles N.

Metal

We shall make an approximate estimate of U for $\kappa_z = 0$. We neglect the second integral in (20) and take the mean value of the positive expression $[L_n^{\Delta n}]^2 \lambda_\rho^{\Delta n} e^{-\lambda_\rho} [(n+1)\ldots(n+\Delta n)]^{-1}$ outside the summation over n. We obtain

$$U \sim (g/m^*)(a\varkappa u_0/4)^2 (\gamma\omega\Delta n\hbar\omega_0 N/\omega_0\mu); \tag{27}$$

μ is the chemical potential of the electron gas. Equation (27) shows that only a comparatively small part $\Delta n\hbar\omega_0/\mu$ of all of the electrons plays a role in the process of absorption of ultrasonic energy in metals.

Semiconductor in which the Current Carriers are in a Degenerate State

For those comparatively high magnetic field intensities that guarantee satisfaction of the inequality $\omega_0 > 1/\tau$, the states of the electron with energy $\epsilon_\parallel + \hbar\omega_0(n + \frac{1}{2})$ are strongly degenerate. The multiplicity of the degeneracy 2g at $\mathcal{H} \sim 10^3$ oe is very large (of the order 10^{10}). Such strong degeneracy causes only a small number of the low-lying quantum levels to be filled. For example, for $N \sim 10^{17}$ cm^{-3} and $\omega_0 \sim 10^{10}$, the number of the highest filled discrete level is of the order of 10. Therefore, the coefficient of absorption can be computed by direct summation of several non-vanishing terms in (20). As before, we shall consider two cases.

a) $\kappa_Z = 0$. We introduce a new integration variable

$$(\hbar/2\pi)\,dk_z = [(2m^*/\varepsilon_\parallel)^{1/2}/2\pi\hbar]\,d\varepsilon_\parallel. \tag{28}$$

We substitute (28) in (20) and, using the notation

$$F_{-1/2}\left(\mu-\hbar\omega_0\left(n+\frac{1}{2}\right)\right) = \int\frac{d\varepsilon_\parallel}{\varepsilon_\parallel^{1/2}\,[\exp\{(\varepsilon_\parallel+\hbar\omega_0(n+1/2)-\mu)/\Theta\}+1]}$$

— the Fermi integral with index $-\frac{1}{2}$, we obtain

$$U = (g/2\pi^2\hbar^2)(a\varkappa u_0/4)^2\,\gamma\omega\,(2m^*)^{1/2}\sum_{\Delta n,\,n}\frac{\lambda_\rho^{\Delta n}\,[L_n^{\Delta n}]^2\,e^{-\lambda_\rho}\,\{F_{-1/2}(\mu-(n+1/2)\hbar\omega_0)-F_{-1/2}(\mu-(n+\Delta n+1/2)\hbar\omega_0)\}}{(n+1)\ldots(n+\Delta n)\,[(\Delta n\omega_0-\omega)^2+\gamma^2/4]}. \tag{29}$$

The numerical value of Γ can be found from the tables for $F_{-1/2}$ (see, for example, reference 8).

b) $\kappa_Z \neq 0$. In this case, too, there will be comparatively few non-vanishing terms in the sum over n. If $\hbar\omega_0 \gg \Theta$, the gas can be considered strongly degenerate. Calculation of the integrals in (20) leads to the following formula for the ultrasonic absorption:

$$\begin{aligned}\Gamma = \frac{gm^*a^2}{16\pi\rho c_0^2\hbar^2}&\sum_{\Delta n}(\lambda_\rho^0)^{\Delta n}\frac{\sin^{2\Delta n}\vartheta}{\cos\vartheta}\sum_n\frac{2e^{-\lambda_\rho}}{(n+1)\ldots(n+\Delta n)}\left[L_n^{\Delta n}\right]^2\\
&\times\Big\{\tan^{-1}\Big[\frac{\omega_0}{\gamma}\Big(\lambda_\rho^0\Big[\cos^2\vartheta+2k_z\\
&\times\Big(\mu-\hbar\omega_0\Big(n+\frac{1}{2}\Big)\Big)\frac{\cos\vartheta}{\varkappa}\Big]+2\Big(\Delta n-\frac{\omega}{\omega_0}\Big)\Big)\Big]\\
&-\tan^{-1}\Big[\frac{\omega_0}{\gamma}\Big(\lambda_\rho^0\Big[\cos^2\vartheta-2k_z\\
&\times\Big(\mu-\hbar\omega_0\Big(n+\frac{1}{2}\Big)\Big)\frac{\cos\vartheta}{\varkappa}\Big]+2\Big(\Delta n-\frac{\omega}{\omega_0}\Big)\Big)\Big]\\
&-\tan^{-1}\Big[\frac{\omega_0}{\gamma}\Big(\lambda_\rho^0\Big[\cos^2\vartheta+2k_z\\
&\times\Big(\mu-\hbar\omega_0\Big(n+\Delta n+\frac{1}{2}\Big)\Big)\frac{\cos\vartheta}{\varkappa}\Big]+2\Big(\Delta n-\frac{\omega}{\omega_0}\Big)\Big)\Big]\\
&+\tan^{-1}\Big[\frac{\omega_0}{\gamma}\Big(\lambda_\rho^0\Big[\cos^2\vartheta-2k_z\\
&\times\Big(\mu-\hbar\omega_0\Big(n+\Delta n+\frac{1}{2}\Big)\Big)\frac{\cos\vartheta}{\varkappa}\Big]\\
&+2\Big(\Delta n-\frac{\omega}{\omega_0}\Big)\Big)\Big]+\ldots\Big\}.\end{aligned} \tag{30}$$

Here $\lambda_\rho^0 = \hbar\omega^2/2m^*\omega_0c_0^2$, $k_Z\,[\mu-\hbar\omega_0(n+\frac{1}{2})]$ is the Fermi value of the wave number for an electron in the n-th discrete level. The dots take the place of the sum of an additional four arctangents similar to those written down, with the parameter $2(\Delta n+\omega/\omega_0)$ in place of $2(\Delta n-\omega/\omega_0)$. In (30), ϑ is the angle between the direction of propagation of the ultrasound and the intensity of the magnetic field.

The calculation of Γ has been carried out according to Eq. (30) for ϑ in the interval from 0 – 90°, and a graph has been constructed of the dimensionless quantity $\Gamma\cdot 16\pi\rho c_0^2\hbar^2/gm^*a^2$. The following numerical values of parameters were chosen for the calculation: $\omega/\omega_0 = 2$; $\lambda_\rho^0 = 0.2$, $c_0 = 5\times10^5$ cm/sec. The chemical potential μ we set equal to $3.75\,\hbar\omega$, which corresponds to an electron concentration $N \approx 5\times10^{16}$ cm^{-3}. Summation in (30) was carried out over n from 0 to 3 for two values $\Delta n = 1, 2$. For $\Delta n > 2$, the term $(\lambda_\rho^0)^{\Delta n}$ becomes a very small quantity in our example.

The dashed lines in the drawing indicate graphs of the individual terms of the sum in (30) with $\Delta n = 1$ and n = 0, 1, 2. Each of these has a maximum for intermediate values of ϑ, which describes the resonance of electrons found in the discrete level with n = 0, 1, 2. In this resonance process, part of the energy of the phonon (in the given example, $\frac{1}{2}$) is used up to change the translational motion of the electron in the direction of the magnetic field. From the laws of conservation of energy and momentum, it is easy to obtain an equation for ϑ for which a particular type of resonance sets in. This resonance is determined by the zeros of the arctangents in (30):

$$\lambda_\rho^0(\cos^2\vartheta\pm2k_z\cos\vartheta/\varkappa)+2(\Delta n-\omega/\omega_0)=0. \tag{31}$$

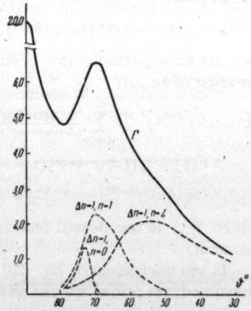

Dependence of the sound absorption Γ (in units of gm*a²/16πρc₀²ħ²) on angle ϑ. The contribution of the different terms of the sum (30) corresponding to different values of n and Δn is shown by the dashed lines.

The deeper the level n, the larger the resonance angle ϑ. This circumstance is excellently illustrated by the given graphs.

The resonance effect under consideration can be of interest in the following connection. The absorption of phonons with $\kappa_z \neq 0$ leads to a change of the momentum of the electrons by $\hbar\kappa_z$. In unit time, $U/\hbar\omega$ phonons are absorbed, and, consequently, the rate of change of the projection of the momentum of the electrons on the z axis is equal to $\dot{P}_z = \kappa_z U/\omega$. It is easy to estimate the current flowing in the direction of the magnetic field,

$$j_z \approx e\tau\varkappa_z E_{s0}\Gamma / m^* \omega, \tag{32}$$

or the intensity of the electric field inside the bounded semiconductor:

$$E_z \sim e\tau\varkappa_z E_{s0}\Gamma / m^* \omega\sigma, \tag{33}$$

σ is the electrical conductivity of the semiconductor.r

3. Experiments on ultrasonic resonance of current carriers required low temperatures of the order of 1°K and high ultrasonic frequencies $\sim 10^{10}$, 10^{11} cps. At the present time, ultrasonic technology has come close to this range of frequencies. Thus, for example, Baranskii[9], and Bömmel and Dransfeld[10] have obtained frequencies $\sim 2.5 \times 10^9$ cps, while Jacobson[11] has reached 10^{10} cps. Recently results have been published of the measurement of ultrasonic absorption in silicon, germanium, etc, for frequencies close to 10^9, and at temperatures of about $-150°$C.[12] If the results of experiments are roughly extrapolated to the region of much lower temperatures $\sim 1°$K and much higher frequencies $\omega \sim 10^{10}, 10^{11}$, then one can assume that the lattice absorption should under these conditions be of the order of 10^2 cm^{-1}, while the electronic part estimated by Eq. (25) is $\Gamma_{el} \sim 10$ cm^{-1} (for values of the parameters $N = 10^{12}$ cm^{-3}, $a = 15 \times 10^{-12}$ ev, $c_0 \sim 10^5$ cm/sec, $x \sim 1$, $\omega \sim 10^{11}$, $\gamma^{-1}\omega_0 \sim 1$) although an order lower is sufficiently large for experimental observation. It is also necessary to remark that the measurement of the electric field produced by the effect of "amplification" of the electrons along the magnetic lines of force [which, by (31), (32), is proportional to the electronic part of the absorption coefficient], can be shown to be a much easier problem than the separation of the contribution of the electronic absorption from the general absorption of the semiconductor.

In conclusion, I want to express my gratitude to Yu. E. Perlin for useful discussions and to V. L. Gurevich for a discussion of the fundamental aspects of the problem and valuable comments.

---

[1] H. Bömmel, Phys. Rev. **108**, 1094 (1957).

[2] Morse, Bohm, and Gavenda, Phys. Rev. **109**, 1394 (1958).

[3] A. Pippard, Phil. Mag. **2**, 1147 (1957).

[4] E. P. Pokatilov, JETP **36**, 5 (1959), Soviet Phys. JETP **9**, 1037 (1959).

[5] L. D. Landau and E. M. Lifshitz, Квантовая механика, (Quantum Mechanics), Gostekhizdat, 1948 [Engl. Pergamon, 1958].

[6] W. Heitler, Quantum Theory of Radiation, Oxford, 1959.

[7] A. E. Zil'berman, JETP **23**, 49 (1952).

[8] P. Rhodes, Proc. Roy. Soc. (London) **A204**, 396 (1950).

[9] K. N. Baranskiĭ, Dokl. Akad. Nauk SSSR **114**, 517 (1957), Soviet Phys.-Doklady **2**, 237 (1957).

[10] H. Bömmel and K. Dransfeld, Phys. Rev. Lett. **1**, 234 (1958).

[11] D. Jacobson, Phys. Rev. Lett. **2**, 249 (1959).

[12] Lamb, Redwood, and Steinshleifer, Phys. Rev. Lett. **3**, 28 (1959).

Translated by R. T. Beyer
226

SOVIET PHYSICS JETP VOLUME 11, NUMBER 4 OCTOBER, 1960

SCATTERING OF ELECTRONS BY NUCLEI ACCORDING TO THE α-PARTICLE MODEL

E. V. INOPIN and B. I. TISHCHENKO

Physico-Technical Institute, Academy of Sciences, Ukrainian S.S.R.

Submitted to JETP editor August 12, 1959

J. Exptl. Theoret. Phys. (U.S.S.R.) **38**, 1160-1166 (April, 1960)

Elastic and inelastic (including excitation of rotational levels) scattering of high-energy electrons by Be^9, C^{12}, and O^{16} nuclei is considered on the basis of the α-particle model. The calculated differential cross sections for elastic scattering on these nuclei, and also the inelastic scattering with excitation of the 2.43- and 6.8-Mev levels in Be and the 4.43-Mev level in C^{12} are in good agreement with the experiments. It is also shown that elastic scattering on C^{12} with excitation of the 9.61-Mev level can be explained within the framework of the model under consideration if one ascribes spin and parity 3^- to this level.

1. INTRODUCTION

A number of experimental facts obtained in the last few years indicate the correctness of the description, in the case of several nuclei at least, in terms of the α-particle model. Thus, for example, Baz' noted[1] that the curve of neutron separation energies has, as function of atomic number A, a sawtoothed shape in the region $4 \leq A \leq 40$, such that each nucleus of type $A = 4n$ corresponds to a maximum in this curve, and each nucleus of type $A = 4n + 1$, to a minimum.

In experiments[2] on capture of high-energy neutrons, rather detailed information about the momentum distribution of nucleons in He^4, Be^9, and C^{12} was obtained. These experiments succeeded in separating off the contribution in the distribution for Be^9 coming from the weakly-bound ($E_B \cong 1.5$ Mev) external nucleon, so as to give the distribution for the Be^8 core. All three of the distributions obtained were very similar; this is easy to explain, using the α-particle model, since this model leads directly to identical distributions, aside from effects from the relatively slow movement of α particles in these nuclei.

Results of experiments on (p, α) reactions by high-energy protons (see reference 3; references to other work on the same subject are given there) are also of great interest. It turned out that particular features of this process gave a direct indication of the existence of strongly-correlated α-particle groups in both light and heavy nuclei.

In connection with further study of the existence of strong α correlations in nuclei, it is of interest to consider other experiments from this point of view. Experiments on elastic and inelastic scattering of high-energy electrons by nuclei would contribute greatly to this.

In the present work, expressions are obtained on the basis of the α-particle model for elastic and inelastic scattering of electrons, and experimental data relating to Be^9, C^{12}, and O^{16} is analyzed.

2. CROSS SECTIONS FOR ELASTIC AND INELASTIC SCATTERING OF ELECTRONS BY Be^9, C^{12}, AND O^{16}

In connection with the basic assumption that a class of nuclei with a clear α-particle structure exists, we shall assume that the target nucleus can be represented by a system of α particles, the positions of which are fixed relative to each other. This system can begin to rotate as a whole because of the action of the field of the incident electron. The rotational states will, as usual, be characterized by quantum numbers I and K (I is the angular momentum of the rotational state, K the projection on the axis of maximum symmetry of the system considered). The problem consists in calculating $\sigma_{IK}(\theta)$, the cross section for the process in which the electron is scattered through an angle θ and the nucleus goes into the rotational state I, K. Here, the only transitions considered are those in which the internal structure of the α particle is preserved.

Calculations in the Born approximation, which is adequate for treating the scattering of electrons by light nuclei, can be carried through in all of the cases considered below. The cross section for elastic scattering on α particles, $\sigma_\alpha(\theta)$, enters, of course, as a multiplicative factor into the expression for the derived cross section. It can be written as $\sigma_\alpha(\theta) = \sigma_\alpha^C(\theta)\,F_\alpha(q)$, where σ_α^C is the cross section for Coulomb scattering by a point α particle. According to the data of Hofstadter et al.,[4] the form-factor for the α particle is $F_\alpha(q) = \exp(-q^2a^2/6)$ with a mean-square radius $a = 1.61$ f.

Be^9. The simplest α-particle nucleus, Be^8, is unstable; however, our considerations can be applied to Be^9, which can be viewed as consisting of two α particles and an external neutron. The latter is a neutral particle, and does not affect the scattering directly. However, the presence of the neutron influences the rotational functions of the nucleus and, in this way, the results of interaction of the electron with the nucleus.

The spin of Be^9 is $I_0 = 3/2$; therefore it follows that we should take $K_0 = 3/2$. Excited states will be characterized by the quantum numbers $K = K_0 = 3/2$ and $I = 5/2$, $7/2$, etc. Denoting the distance between α particles by 2d, we obtain the following expressions for the cross sections for elastic and inelastic scattering with excitation of the $I = 5/2$ and $I = 7/2$ levels:

$$\sigma_{3/2,\,3/2}(\theta) = 4\sigma_\alpha(\theta)\,[j_0^2(qd) + j_2^2(qd)], \tag{1}$$

$$\sigma_{5/2,\,3/2}(\theta) = \frac{72}{7}\sigma_\alpha(\theta)\,[j_2^2(qd) + \frac{1}{6} j_4^2(qd)], \tag{2}$$

$$\sigma_{7/2,\,3/2}(\theta) = \frac{40}{7}\sigma_\alpha(\theta)\,[j_2^2(qd) + \frac{9}{5} j_4^2(qd)], \tag{3}$$

where j_l is the spherical Bessel function and q is the momentum transfer. For electron energies below ~ 200 Mev, the terms involving j_4 in Eqs. (2) and (3) are small, and, therefore, we can write, with good accuracy,

$$\sigma_{5/2,\,3/2}(\theta) = \frac{9}{5}\sigma_{7/2,\,3/2}(\theta). \tag{4}$$

We consider now the corresponding experimental data. In the work of McIntyre et al.,[5] the angular distributions of elastic and inelastic scattering, with excitation of the 2.5- and 6.8-Mev levels of Be^9, were measured at angles of 60 — 90° with 190-Mev electrons. The 2.5-Mev level appears[6] to have spin and parity $5/2^-$; the 6.8-Mev level must be $7/2^-$ if it is to be in the same rotational band. Such an assumption is confirmed by the ratio of energies, 6.8 : 2.5 = 2.7, which is near to the value of 12 : 5 = 2.4 obtained from the formula

$$E_I = (\hbar^2/2J)\,[I(I+1) - I_0(I_0+1)].$$

Comparison of calculated and experimental data is shown in Fig. 1. In so far as absolute values were not measured, the choice of the general scale is made by setting the calculated value equal to the experimental point for elastic scattering at $\theta = 60°$. The best value for d turned out to be d = 1.9 f. We see that there is good agreement with experiment. A noticeable divergence occurs only in the case of curve 2 for $\theta = 90°$. The preliminary character of the experimental data makes it difficult to decide what importance to attribute to this difference.

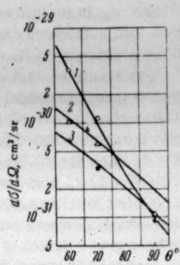

FIG. 1. Differential cross sections for elastic and inelastic scattering of 190-Mev electrons by beryllium: 1 – calculated curve for elastic scattering; 2 – inelastic scattering with excitation of the 2.5-Mev level; 3 – calculated curve for inelastic scattering with excitation of the 6.8-Mev level; ○, △, ● – experimental values for the corresponding processes.

If we choose d = 1.9 f, we obtain a = 2.48 f for the mean-square radius of Be^9, in reasonable agreement with the value a = 2.2 ± 0.2 f given by Hofstadter in his last review.[7] For the intrinsic quadrupole moment we obtain $Q_0 = 8d^2 = 0.29$ barn, from which

$$Q = Q_0 I_0 (2I_0 - 1)/(I_0 + 1)(2I_0 + 3) = 0.058 \text{ barn}.$$

Unfortunately, no reliable data on the quadrupole moment of Be^9 exists. In references 8 and 9, rough estimates give $|Q| = 0.02$ barn.

Thus, the existing experimental data on Be^9 does not contradict the proposed treatment; however, it would be desirable to have more detailed and accurate experimental points for both the elastic and inelastic scattering of electrons by this nucleus.

C^{12}. We will consider the carbon nucleus as consisting of three α particles, which form an isosceles triangle. The axis of maximum symmetry is, clearly, a line going through the center of the triangle and perpendicular to its plane.

Since the symmetry axis of this system is not of infinite order, not only rotational states with K = 0 can exist, but also those with K > 0. Invariance of this system under rotations through $2\pi/3$ limits the acceptable values of K to K = 3n, where n is an integer. The parity Π of the rotational levels is connected with K by the relation $\Pi = (-1)^K$. The energy of the rotational level is determined by the formula

$$E_K^I = \frac{\hbar^2}{2J_1} I(I+1) + \frac{\hbar^2}{2}\left(\frac{1}{J_2} - \frac{1}{J_1}\right) K^2, \tag{5}$$

where J_1 is the moment of inertia relative to the two-fold symmetry axis and J_2 is the moment of inertia relative to the three-fold symmetry axis..

The levels of carbon have been analyzed with the α-particle model by Glassgold and Galonsky.[10] The carbon levels 0^+ ($E = 0$) and 2^+ ($E = 4.43$ Mev) can be related to the rotational band with $K = 0$; then the 3^- level (first level in the band with $K = 3$) is obtained at 5.53 Mev. Since this 5.53-Mev level has not been observed to date, this conclusion was considered by these authors to be a grave defect of this theory.

It should be noted, however, that this conclusion is based on a classical calculation of the moment of inertia: the α particles were considered to be points, so that $J_1 = J_2/2$. It is known from the study of the rotational spectra of heavy nuclei that J_{rigid} is often several times larger than the effective moment of inertia J. The situation may be similar in our case, leading to a strong decrease in J_2 compared to its classical value. Then the 3^- level would appear substantially higher. One can, in particular, assume this level to be the 9.61-Mev level.

The existing experimental data do not contradict this assumption. From the fact that the 9.61-Mev level decays into Be^8 and α particles, it follows that the spin and parity of this level should be either both even or both odd. It is clear that this requirement is satisfied by the assignment 3^-. The stripping reaction $B^{11}(d, n)$ with excitation of the 3^- level of C^{12} should give the value $l = 2$. This value was obtained in reference 11. It should be noted that these data, while not contradicting the value 3^-, also are consistent with the value 1^-.

The following expressions are obtained for the cross sections for elastic scattering and excitation of 2^+ and 3^- levels:

$$\sigma_{00}(\theta) = 9\sigma_\alpha(\theta)\, j_0^2(x), \quad \sigma_{20}(\theta) = \frac{45}{4}\sigma_\alpha(\theta)\,[3j_1(x)/x - j_0(x)]^2,$$
$$\sigma_{33}(\theta) = \frac{315}{16}\sigma_\alpha(\theta)\, j_3^2(x), \qquad x = 2qd/\sqrt{3}. \tag{6}$$

Comparison of cross sections calculated from Eq. (6) with the experimental data of Fregeau are shown in Fig. 2, for an electron energy of 187 Mev. The best value of the parameter d was $d = 1.5$. We see that the calculated curves for the elastic scattering and for the inelastic scattering with excitation of the 4.43-Mev level agree well with experiment. The curve describing the inelastic scattering with excitation of the 9.61-Mev level is in generally satisfactory agreement with experiment. It diverges in the small-angle ($\theta \leq 50°$) region; however, the experimental data in this region are not reliable. This can be seen both from the irregular trend of the experimental points for $\theta = 35$, 45, and 50°, and from the form of the energy spectra at small angles given in reference 12. The data on the elastic scattering of 420 Mev electrons is compared with calculations (which used the same value $d = 1.5$ f) on Fig. 3.

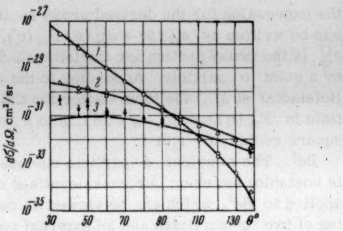

FIG. 2. Differential cross sections for elastic and inelastic scattering of 187-Mev electrons on carbon: 1 – calculated curve for elastic scattering; 2 – inelastic scattering with excitation of the 4.43-Mev level; 3 – inelastic scattering with excitation of the 9.61-Mev level; ○, ▲, ● – experimental values for the corresponding processes.

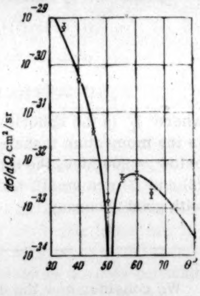

FIG. 3. Calculated curve and experimental values of the differential cross section for elastic scattering of 420-Mev electrons by carbon.

We see that the agreement between theory and experiment is good even for large values of the momentum transfer q. It should be noted that the vanishing of the cross section at $\theta = 51°$ comes from the incorrectness of the Born approximation in the region of a diffraction minimum — an accurate calculation should lead to a nonzero value of the cross section.

O^{16}. Dennison[13] was successful in showing that the position and characteristics of many of the levels of the oxygen atom could be explained by application of the α-particle model to this nucleus. If we consider this nucleus to be composed of α particles forming a tetrahedron, we obtain the following expression for the elastic-scattering cross section:

$$\sigma_{00}(\theta) = 16\,\sigma_\alpha(\theta)\, j_0^2\left(\sqrt{3/2}\, qd\right). \tag{7}$$

Comparison with the experiment of Hofstadter[7] (see Fig. 4) shows that the theoretical curve reproduces the experimental data well (using d = = 1.6 f) aside from the region of the diffraction minimum, where the Born approximation is inapplicable.

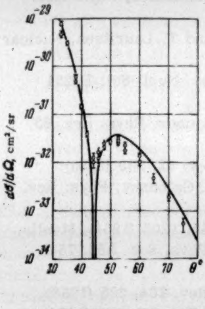

FIG. 4. Calculated curve and experimental values of the differential cross section for elastic scattering of 420-Mev electrons by oxygen.

3. CONCLUDING REMARKS

All in all, one can assert that the α-particle model is successful in explaining the existing experimental data on the scattering of electrons by Be^9, C^{12}, and O^{16}. Further experiments are necessary for definitive conclusions about the applicability of the α-particle model to these nuclei. In particular, a reliable experimental determination of the spin and parity of the 9.61-Mev level in C^{12} would be of great interest, since the existence of a 3^- state in nuclei consisting of three α particles is a very characteristic feature of such a model. It would also be important to establish the spin and parity of the 6.8-Mev level in Be^9.

In the preceding, we applied the terminology of the α-particle model in its most primitive form. However, it should be emphasized that the results obtained are independent of a number of assumptions characteristic of the primitive α-particle model. In particular, the α-particle groups entering into the composition of the nuclei considered do not have to be considered to be true α particles, preserving their individuality in the nucleus. For the considerations given here, only the type of density distribution is of basic importance. Thus, the symmetry D_{3h} assumed for C^{12} completely determines the rotational spectrum of this nucleus (0^+, 2^+, 3^-, etc.) and it is clear that to determine the rotational spectrum it is not necessary to resort to arguments connected with α particles that obey Bose statistics. From a mathematical point of view, this is connected with the fact that the group D_{3h} is isomorphous with the group formed by rearrangements of the isosceles triangle. Thus, the proposed considerations do not exclude the possibility of exchange of nucleons between the α-particle groups. From this point of view, the root mean square radius of the α-particle group a should be considered to be a parameter entering into the theory, and the result that the value of a obtained is close to the root mean square radius of the α particle should indicate that the deviation of the mean density in the α-particle group from that of the density of the free α particle is small.

It should be noted that the theoretical interpretation of the data on the scattering of electrons by the nuclei considered has been treated in a number of articles. Thus, Morpurgo[14] calculated the form-factor for the excitation of the 4.43-Mev state in C^{12}, using shell-model functions, in both the L-S and j-j coupling. His results gave too small an inelastic cross section (by a factor of two in the L-S coupling, and of six in the j-j coupling). Calculations for Be^9 and C^{12} were also carried out in intermediate coupling in the shell model,[15,16] but no satisfactory agreement with experiment was obtained there. Ferrell and Visscher[17] have shown that the data on C^{12} could be explained by adding an appropriate amount of the state corresponding to collective motion of the nucleus.

In the light of these results, the results obtained here appear to deserve attention, since, on the basis of a simple model, they give a very unambiguous (in so far as the data on elastic scattering already completely determine the parameters of the model) explanation of the experimental data on both elastic and inelastic scattering of several nuclei.

It is interesting to follow up how several of the conclusions of the α-particle model agree with conclusions of the shell model. It is well known that for p-shell nuclei, the shell model leads to a charge density

$$\rho(r)=\frac{2}{\pi^{3/2}a_0^3(2+3\alpha)}\left(1+\alpha\frac{r^2}{a_0^2}\right)\exp\left(-\frac{r^2}{a_0^2}\right), \qquad (8)$$

where $\alpha = (Z-2)/3$ and a_0 is a parameter. It is also well known[7] that this distribution fits well the data on elastic scattering of electrons by C^{12} ($a_0 = 1.64$) and O^{16} ($a_0 = 1.77$).

It is of interest to compare this distribution with that obtained by averaging the α-particle density over all orientations of the nucleus. The elastic scattering on the α-particle nucleus is obviously the same as that on a spherical one possessing just that density. A straightforward calculation leads to the following result for this density:

$$\rho(r) = \sqrt{\frac{3}{8\pi^3}}\,\frac{1}{abr}\exp\left[-\frac{3}{2a^2}(r^2+b^2)\right]\sinh\frac{3rb}{a^2}, \quad (9)$$

where a is the root mean square radius of the α particle (a = 1.61 f), and b is the distance from the center of gravity of the nucleus to the center of the α particle ($b = 2d/\sqrt{3}$ for C^{12} and $b = \sqrt{3/2}\,d$ for O^{16}).

The distributions calculated from Eqs. (8) and (9) for C^{12} and O^{16} are given in Fig. 5. We see that the distributions given by the shell model and the α-particle model coincide almost completely.

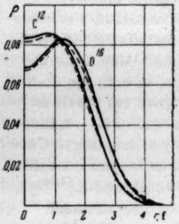

FIG. 5. Shape of the charge distribution (proton charge/f^3) in C^{12} and O^{16}, calculated from the α-particle model (solid curves) and from the shell model model (dashed curves).

Mention should be made in this connection of the work by Perring and Skyrme,[18] who have shown that it is possible here to construct wave functions for the ground states of Be^8, C^{12}, and O^{16} which, when antisymmetrized, turn out to be identical with the wave functions of the shell model.

---

[1] A. I. Baz', JETP **31**, 831 (1956), Soviet Phys. JETP **4**, 704 (1957).

[2] W. Selove, Phys. Rev. **101**, 231 (1956); S. Glashow and W. Selove, Phys. Rev. **102**, 200 (1956).

[3] P. E. Hodgson, Nuclear Phys. **8**, 1 (1958).

[4] R. Hofstadter, Revs. Modern Phys. **28**, 214 (1956).

[5] McIntyre, Hahn, and Hofstadter, Phys. Rev. **94**, 1084 (1954).

[6] F. Ajzenberg-Selove and T. Lauritsen, Nuclear Phys. **11**, 1 (1959).

[7] R. Hofstadter, Ann. Rev. Nucl. Sci. **7**, 231 (1957).

[8] Hatton, Rollin, and Seymour, Phys. Rev. **83**, 672 (1951).

[9] W. D. Knight, Phys. Rev. **92**, 539 (1953).

[10] A. E. Glassgold and A. Galonsky, Phys. Rev. **103**, 701 (1956).

[11] A. Graue, Phil. Mag. **45**, 1205 (1954); Maslin, Calvert, and Jaffe, Proc. Phys. Soc. **A69**, 754 (1956).

[12] J. H. Fregeau, Phys. Rev. **104**, 225 (1956).

[13] D. M. Dennison, Phys. Rev. **96**, 378 (1954).

[14] G. Morpurgo, Nuovo cimento **3**, 430 (1956).

[15] M. K. Pal and S. Mukherjee, Phys. Rev. **106**, 811 (1957).

[16] M. K. Pal and M. A. Nagarajan, Phys. Rev. **108**, 1577 (1957).

[17] R. A. Ferrell and W. M. Visscher, Phys. Rev. **104**, 475 (1956).

[18] J. K. Perring and T. H. Skyrme, Proc. Phys. Soc. **A69**, 600 (1956).

Translated by G. E. Brown
227

SOVIET PHYSICS JETP VOLUME 11, NUMBER 4 OCTOBER, 1960

ALLOWANCE FOR THE MEDIUM IN RADIATION CORRECTIONS TO COULOMB SCATTERING

M. L. TER-MIKAELYAN

Physics Institute, Academy of Sciences, Armenian S.S.R.

Submitted to JETP editor August 25, 1959

J. Exptl. Theoret. Phys. (U.S.S.R.) **38**, 1167-1169 (April, 1960)

Radiation corrections to electron scattering are treated with allowance for the "density effect." When condition (5) holds, the corrections due to the medium become important and are given by formula (4).

As already pointed out by the author,[1] the polarization effect in bremsstrahlung must affect the calculation of radiation corrections to Coulomb scattering. The reason for this effect can be easily understood from the following considerations. Experimentally the sum of two cross sections is always measured — the elastic Coulomb cross section, and the bremsstrahlung cross section for quanta of energy lower than some specified energy $\hbar\omega_{\min}$ determined by the resolving power of the experimental apparatus.

Taking this circumstance into account enables us to avoid in the theoretical calculations the difficulties associated with the infrared divergence, which renders invalid the calculation of a purely elastic scattering cross section. However, the bremsstrahlung formulas for relativistic particles undergo considerable changes, due both to multiple scattering and to the polarization of the medium. It is evident that these changes in the bremsstrahlung cross section will also affect the calculation of radiation corrections to Coulomb scattering, since, as just noted, we actually always have to calculate the sum of two cross sections. Simple addition of the new bremsstrahlung cross section and of the purely elastic scattering cross section (with the radiation corrections evaluated for the case of vacuum) would be inconsistent.

Obviously, it is necessary to take into account the effect of the medium also in evaluating the radiation corrections themselves. Let us investigate the effect of the polarization of the medium. In the case of elastic scattering which is of interest to us there are no photons both at the beginning and at the end of the process, so that the whole effect of the polarization of the medium reduces to a change in the photon propagator.

In contrast to the vacuum case, a photon moving in a medium undergoes repeated absorptions and emissions. To obtain the altered propagator we have to sum a number of Feynman diagrams in which each succeeding diagram differs from the preceding one by an additional absorption and emission of the photon with no change of frequency. In this way we obtain a geometric progression whose sum yields the desired propagator. The results of calculations using such an altered propagator must then be averaged over the states of all the atoms. This procedure of calculation can be given a simple graphic interpretation by noting that such a method of calculation is in a certain sense equivalent to the transition from the microscopic to the macroscopic Maxwell's equations.[2] To obtain the rules for writing down the matrix elements, taking the effect of the medium into account, it is convenient to utilize the following formal method.* We write the macroscopic Maxwell's equations for the potentials in four-dimensional invariant form (we shall write them in the Mandel'shtam-Tamm form which is completely equivalent to the usual one)

$$\varepsilon^{ik}\varepsilon^{lm}\partial^2 A_k / \partial x^l \partial x^m = J^i, \qquad \varepsilon^{lm}\partial A_l / \partial x^m = 0. \qquad (1)$$

$\epsilon^{ik} = \epsilon^{ki}$ is the dielectric permittivity and magnetic permeability tensor introduced by Mandel'shtam and Tamm, with non-zero components $\epsilon^{00} = \epsilon\sqrt{\mu}$ and $\epsilon^{\alpha\alpha} = -1/\sqrt{\mu}$ in the rest system of the medium ($\alpha = 1, 2, 3$); $\epsilon^{ik} = 0$ for $i \neq k$. The transition to the vacuum case consists of replacing the tensor ϵ^{ik} by the metric tensor g^{ik} ($g^{00} = 1$;

---

*Ryazanov[3] has utilized similar rules for writing down the matrix elements on the basis of quantization of the macroscopic Maxwell's equations. However, as has been brought out in a discussion with K. M. Polievktov-Nikoladze, E. L. Feĭnberg and M. I. Ryazanov, quantum electrodynamics in a medium must be used with a certain amount of caution, and in each specific case must be justified on the basis of the microscopic quantum equations.

$g^{\alpha\alpha} = -1$ $(\alpha = 1, 2, 3)$; $g^{ik} = 0$ for $i \neq k$).

Following Feynman's arguments[4] we arrive at the conclusion that the change that must be introduced in order to take into account the effect of the medium reduces to replacing the photon propagator by $D = -ihc/(2\pi)^4 \epsilon^{lm} k_l k_m$. The ends of the internal photon line will now correspond to the matrices $ie\gamma^i$ and $ie\epsilon^{-1}_{\mu i}\gamma^\mu$. Let us make use of this formal method for evaluating the electron self-energy. From physical considerations it follows that an electron in a medium will polarize the material. Moreover, the use of the ordinary dielectric constant will lead to the damping of the initial electron wave function due to energy losses. If we represent the electron wave function in the form $\exp(iEt/h - \gamma t/2)$, then we obtain for the quantity $i(E - E_V)/h - \gamma/2$ (where E_V is the electron self-energy in vacuum) the expression (for $v \ll c$):

$$\gamma = -\frac{e^2}{2\pi^2 hv} \operatorname{Im} \int_0^{k_{max}} \frac{dk}{k} \int_0^{kv} \frac{d\omega}{\varepsilon(\omega)},$$

$$\Delta E = -\frac{e^2}{4\pi^2 v} \int_0^{k_{max}} \frac{dk}{k} \int_{-kv}^{+kv} d\omega \left(\frac{1}{\varepsilon(\omega)} - 1\right). \qquad (2)$$

From the quantity γ we can easily obtain the energy losses of a nonrelativistic particle by multiplying the integrand by $h\omega$. The quantity ΔE is the polarization energy of the medium (cf. reference 5). It is also necessary to note that the use of the usual value of $\epsilon(\omega)$ is justified for distances larger than interatomic distances. Therefore γ determines the energy losses for "distant" collisions. It is natural that in order that the method of summation of diagrams should be equivalent to the method using macroscopic equations we must make the same approximation in the former method of calculation.

We return to the problem of the radiation corrections to scattering by a Coulomb field. By following the usual calculation procedure we must, in order to avoid the infrared catastrophe, also consider the bremsstrahlung cross section for soft quanta of frequency ω. The latter formula can be easily obtained if we evaluate the emission of radiation for a given deflection of the electron classically. The scattering probability is given by the Coulomb scattering cross section $d\sigma_C$. The formula has the form

$$d\sigma = d\sigma_C \frac{2\alpha}{\pi\sqrt{\varepsilon}} \{2\Phi \coth 2\Phi - 1\} \frac{d\omega}{\omega},$$

$$\sinh \Phi = \frac{v}{c}\sqrt{\varepsilon} \frac{\sin(\theta/2)}{\sqrt{1 - \varepsilon v^2/c^2}}; \qquad (3)$$

θ denotes the scattering angle of the electron. In evaluating the elastic scattering cross section up to terms of order e^6 we must take the absolute value of the square of the sum of the matrix elements of second and fourth order with respect to e. It should be noted that in evaluating the second-order matrix element (simple Coulomb scattering) we can neglect the effect due to the neighboring atoms, since the scattering occurs in the region inside the atom. Since the correction terms contain the fourth-order matrix element linearly, we can use in the matrix elements the photon propagator averaged over the states of the system, which for small momenta (large distances) coincides with the Green's function for Eq. (1). The infrared divergence in the corrections cancels the integral in (3) over ω from $\omega = 0$ to $\omega = \omega_{min}$. We assume that $\omega_{min} \gg \omega_{atom}$ and utilize the limiting value $\epsilon(\omega) = 1 - 4\pi NZe^2/m\omega^2$. The change in the radiation corrections in the medium will be associated with formula (3) in which, in spite of the fact that $\epsilon \approx 1$, it is necessary to take the medium into account when $1 - v^2/c^2 \approx 4\pi NZe^2/m\omega^2$. Finally, an additional term will appear in the radiation corrections to Coulomb scattering which is associated with the effect under consideration. The formula for the scattering cross section in second order perturbation theory has the form

$$d\sigma = d\sigma_V(\omega_{min}) - d\sigma_C \frac{4\alpha}{\pi} \ln^2 \frac{m^{3/2} c^2 \omega_{min}}{E\sqrt{4\pi NZe^2}}, \qquad (4)$$

where $d\sigma_V$ is the ordinary differential scattering cross section including radiation corrections in the case of vacuum. Formula (4) is valid for scattering angles

$$\theta > \sqrt{1 - v^2/c^2 + 4\pi NZe^2/m\omega^2}$$

and under the condition

$$\omega_{min} \ll \sqrt{4\pi NZe^2/m}\, E/mc^2. \qquad (5)$$

In the opposite case the effect of the medium is unimportant. It is possible to neglect the effect of multiple scattering on the calculation under discussion.

---

[1] M. L. Ter-Mikaelyan, Izv. Akad. Nauk SSSR, Ser. Fiz. **19**, 657 (1955), Columbia Tech. Transl. p. 595.

[2] V. B. Berestetskii, JETP **8**, 148 (1938).

[3] M. I. Ryazanov, JETP **32**, 1244 (1957), Soviet Phys. JETP **5**, 1013 (1957).

[4] R. P. Feynman, Phys. Rev. **76**, 769 (1949).

[5] J. Lindhard, Niels Bohr and the Development of Physics, edited by W. Pauli, (Russ. Transl.), 1958, p. 244.

Translated by G. Volkoff
228

SOVIET PHYSICS JETP VOLUME 11, NUMBER 4 OCTOBER, 1960

POLARIZATION OF DEUTERONS ELASTICALLY SCATTERED ON ZERO-SPIN NUCLEI

G. M. BUDYANSKIĬ

Submitted to JETP editor September 20, 1958

J. Exptl. Theoret. Phys. (U.S.S.R.) 38, 1170-1175 (April, 1960)

The most general form of the transition matrix is presented. The dependence of the transition matrix parameters on experimentally observed quantities is established. The general and explicit expressions are derived for the double scattering cross section and vector and tensor polarization, in which account is made of the mixing of the different waves. It is shown that by a choice of a special form of the potential (such as that employed in the optical model) phase shifts, and hence a description of the scattering, can be obtained. Calculations performed in the Born approximation are compared with the experimental results.

A large number of experimental and theoretical researches have been devoted to the study of polarized nucleons. In these researches attempts have been made to draw up a complete phase analysis and to establish the amplitudes of nucleon-nucleon scattering with the aim of investigating spin-dependent interactions.[1-4] Detailed information on the character of the nuclear forces can also be obtained from experiments on scattering of particles with spin 1 on zero spin targets. In this case the results can be obtained at energies of several Mev and the quantity of experiments necessary for completing the phase analysis is not large.

Consideration of the polarization of deuterons has attracted considerably less attention in the literature.[1-4] Expressions were derived in the research of Cheĭshvili[2] for the cross section and the polarization, which were obtained by use of projection operators; however, in this case the possibility of transitions with a change in the orbital momentum was not taken into account.

Extension of the method developed by Vol'fenshteĭn et al. for describing particles with spin $\frac{1}{2}$ (which is based on the use of the transition matrix M and the density ρ) to the case under consideration makes it possible to obtain results both in general form and in a form suitable for application. Calculation of transitions with change of orbital momentum does not raise any difficulties.

The most general form of the transition matrix is defined by the requirement that it be invariant under spatial rotations and reflections and under time reversal:

$$M = A(\vartheta, \varphi) + B_i(\vartheta, \varphi) S_i + C_{ij} S_{ij}. \qquad (1)$$

Denoting the unit vectors in the directions of the incident and scattered beams by $\mathbf{k}_i$ and $\mathbf{k}_f$, and introducing the mutually-orthogonal vectors

$$\mathbf{P} = (\mathbf{k}_i + \mathbf{k}_f)/|\mathbf{k}_i + \mathbf{k}_f|,$$
$$\mathbf{K} = (\mathbf{k}_i - \mathbf{k}_f)|\mathbf{k}_i - \mathbf{k}_f|, \quad \mathbf{N} = [\mathbf{k}_i, \mathbf{k}_f]/|[\mathbf{k}_i, \mathbf{k}_f]|, \qquad (1')$$

we can write M in the form

$$M = A + BS_N + C(S_P^2 + S_K^2 - \tfrac{4}{3}\delta_{ij}) + D(S_P^2 - S_K^2). \qquad (1a)$$

Making use of these expressions for the transition matrix, we derive the vector and tensor polarizations for the cross section in the general form of the following formula:

$$I_0 = \tfrac{1}{3}(3AA^* + 2B_i B_i^* + C_{ij} C_{ij}^*),$$
$$I_0 P_n = \tfrac{1}{3}[4\,\mathrm{Re}(AB_n^*) + 2\,\mathrm{Re}(C_{ni} B_i^*) - \mathrm{Im}(B_i B_j^* \varepsilon_{ijn}) - \mathrm{Im}(C_{ik} C_{jk} \varepsilon_{ijn})],$$
$$I_0 T_{mn} = \tfrac{1}{3}[2\,\mathrm{Re}(AC_{mn}^*) + \mathrm{Re}(B_m B_n^*) - \tfrac{1}{3} B_i^* B_i \delta_{mn} - \mathrm{Re}(C_{mi} C_{in}^*) + \tfrac{1}{3} C_{ij} C_{ji} \delta_{mn} - \mathrm{Im}(C_{mi} B_j \varepsilon_{ijn}) - \mathrm{Im}(B_i C_{jn} \varepsilon_{mij})] \qquad (2)$$

and accordingly in the chosen set of coordinates

$$I_0 = \tfrac{1}{3}\{3|A|^2 + 2|B|^2 + \tfrac{2}{3}|C|^2 + 2|D|^2\},$$
$$I_0 P_N = \tfrac{4}{3}\,\mathrm{Re}[(A - \tfrac{1}{3}C)B^*],$$
$$I_0(T_P T_K + T_K T_P) = -\tfrac{4}{3} i\,\mathrm{Re}\,BD^*, \qquad (2a)$$
$$I_0 T_N = \tfrac{1}{3}\{2|A|^2 + 2|B|^2 + \tfrac{2}{9}|C|^2 + 2|D|^2 - \tfrac{4}{3}\,\mathrm{Re}\,AC^*\}.$$

In this case, if the y axis is perpendicular to the plane of the first scattering, or if the direction of motion of the beam of deuterons between the two collisions coincides with the z axis, the angular distribution of deuterons undergoing double scattering can be written in the form

$$I(\vartheta'\varphi') = I_0(\vartheta')[1 + \tfrac{1}{2}\alpha\alpha' + \tfrac{3}{2}(\beta\beta' + \gamma\gamma')\cos\varphi' + \tfrac{3}{2}\delta\delta'\cos 2\varphi'], \qquad (3)$$

where ϑ and ϑ' are the angles of first and second scattering, respectively, φ' is the angle between the planes of the scattering.

The parameters α, β, γ, and δ are determined by the relations

$$I_0\alpha = -\tfrac{1}{3}|B|^2 + \tfrac{1}{9}|C|^2 - \tfrac{1}{3}|D|^2 + \tfrac{2}{3}\operatorname{Re} AC^* + 2\cos\vartheta \operatorname{Re}[D^*(A - \tfrac{1}{3}C - iB\tan\vartheta)],$$

$$I_0\beta = \tfrac{4}{3}\operatorname{Re}[B^*(A - \tfrac{1}{3}C)],$$

$$I_0\gamma = \tfrac{4}{3}\cos\vartheta \operatorname{Re}\{D^*[iB - (A + \tfrac{1}{3}C)\tan\vartheta]\},$$

$$I_0\delta = \tfrac{1}{3}(-|B|^2 + \tfrac{1}{3}|C|^2 - |D|^2 + 2\operatorname{Re} AC^*) + \tfrac{2}{3}\cos\vartheta \operatorname{Re}[D^*(-A + \tfrac{1}{3}C + iB\tan\vartheta)], \tag{3a}$$

while the parameters α', β', γ', and δ' differ from these only by the fact that all the quantities are replaced by the corresponding values for the second scattering.

With the help of the well-known formula of Blatt and Biedenharn for the amplitude of the scattered waves[5]

$$\psi = i\lambda \frac{\exp(ikr)}{r} \sum_{m_{s'}} \chi_{m_{s'}} \sum_{m_s} M_{m_s m_{s'}} a_{m_s} = i\lambda \frac{\exp(ikr)}{r} \sum_{m_{s'}} \chi_{m_{s'}} \times \sum_{J,l,l'} i^{l-l'} \pi^{1/2}(2l+1)^{1/2}(l, s, 0, m_s | l, s, J, m_s) \times (l', s', \mu, m_{s'} | l', s', J, m_s)(\delta_{l',l} - S^J_{l',l}) Y_{l',\mu}$$

The explicit form of the dependence of the matrix M on the angle of scattering and phase shifts can be established:

$$M = \begin{pmatrix} a & b\exp(-i\varphi) & c\exp(-2i\varphi) \\ d\exp(i\varphi) & f & -d\exp(-i\varphi) \\ c\exp(2i\varphi) & -b\exp(i\varphi) & a \end{pmatrix}. \tag{4}$$

Here

$$a = \frac{i\lambda}{2\sqrt{2}} \sum_J \Big\{\sqrt{\frac{J}{2J+3}}\,[\sqrt{J}\,(1 - S^J_{J+1,J+1}) + \sqrt{J+1}\,S^J_{J+1,J-1}]\,P_{J+1,0} + \sqrt{\frac{J+1}{2J-1}}\,[\sqrt{J}\,S^J_{J-1,J+1} + \sqrt{J+1}\,(1 - S^J_{J-1,J-1})] \times P_{J-1,0} + \sqrt{2J+1}\,[1 - \exp(2i\delta_J)]\,P_{J,0}\Big\},$$

$$b = \frac{i\lambda}{2} \sum_J \Big\{\sqrt{\frac{J+2}{2J+3}}\,[-\sqrt{J+1}\,(1 - S^J_{J+1,J+1}) + \sqrt{J}\,S^J_{J+1,J-1}]\,P_{J+1,-1} + \sqrt{\frac{J-1}{2J-1}}\,[-\sqrt{J+1}\,S^J_{J-1,J+1} + \sqrt{J}\,(1 - S^J_{J-1,J-1})]\,P_{J-1,-1} - \sqrt{\frac{2J+1}{J(J+1)}}\,[1 - \exp(2i\delta_J)]\,P_{J,-1}\Big\},$$

$$c = \frac{i\lambda}{2\sqrt{2}} \sum_J \Big\{\sqrt{\frac{(J+2)(J+3)}{2J+3}}\Big[\sqrt{\frac{J}{J+1}}\,(1 - S^J_{J+1,J+1}) + S^J_{J+1,J-1}\Big]\,P_{J+1,2} + \sqrt{\frac{(J-2)(J-1)}{2J-1}} \Big[S^J_{J-1,J+1} + \sqrt{\frac{J+1}{J}}\,(1 - S^J_{J-1,J-1})\Big]\,P_{J-1,2} - \sqrt{\frac{(2J+1)(J-1)(J+2)}{J(J+1)}}\,[1 - \exp(2i\delta_J)]\,P_{J,2}\Big\},$$

$$d = \frac{i\lambda}{2} \sum_J \Big\{\sqrt{\frac{J(J+2)}{2J+3}}\Big[-\sqrt{\frac{J}{J+1}}\,(1 - S^J_{J+1,J+1}) - S^J_{J+1,J-1}\Big]\,P_{J+1,1} + \sqrt{\frac{(J-1)(J+1)}{2J-1}}\Big[S^J_{J-1,J+1} + \sqrt{\frac{J+1}{J}}\,(1 - S^J_{J-1,J-1})\Big]\,P_{J-1,1}\Big\}.$$

$$f = \frac{i\lambda}{\sqrt{2}} \sum_J \Big\{\sqrt{\frac{J+1}{2J+3}}\Big[\sqrt{J+1}\,(1 - S^J_{J+1,J+1}) - \sqrt{J}\,S^J_{J+1,J-1}\Big]\,P_{J+1,0} - \sqrt{\frac{J}{2J-1}}\Big[\sqrt{J+1}\,S^J_{J-1,J+1} - \sqrt{J}\,(1 - S^J_{J-1,J-1})\Big]\,P_{J-1,0}\Big\},$$

where $S^J_{l',l}$ are the elements of the scattering matrix which has the form

$$S = \begin{pmatrix} \cos^2\varepsilon\exp(2i\Phi_{J-1}) + \sin^2\varepsilon\exp(2i\Phi_{J+1}) & \tfrac{1}{2}\sin 2\varepsilon\,[\exp(2i\Phi_{J-1}) - \exp(2i\Phi_{J+1})] \\ \tfrac{1}{2}\sin 2\varepsilon\,[\exp(2i\Phi_{J-1}) - \exp(2i\Phi_{J+1})] & \sin^2\varepsilon\exp(2i\Phi_{J-1}) + \cos^2\varepsilon\exp(2i\Phi_{J+1}) \end{pmatrix}$$

in the case under consideration.[5] Here ϵ is the so-called mixing parameter, $\Phi_{J\pm1}$ is the phase shift of waves with orbital momentum $l = J \pm 1$.

As a consequence of the invariance of the matrix M relative to time reversal, the additional condition

$$(a - c - f)/\cos\vartheta = \sqrt{2}\,(b + d)/\sin\vartheta \tag{5}$$

is placed on its elements.

By making use of the explicit form of the spin operators, it is possible to establish the dependence of the cross section, and also the vector and tensor polarization, on the scattering angle and, on the phase shifts. For example,

$$I_0 = \tfrac{1}{3}\operatorname{Sp} MM^* = \tfrac{2}{3}(|a|^2 + |b|^2 + |c|^2 + |d|^2 + \tfrac{1}{2}|f|^2),$$

$$I_0 = P_N = \tfrac{1}{3}\operatorname{Sp} MM^* S_N = \tfrac{2}{3}\sqrt{2}\,i \operatorname{Im}[(a - c)d^* + bf^*],$$

$$I_0(T^2_P + T^2_K - \tfrac{4}{3}\delta_{ik}) = \tfrac{1}{3}\{\tfrac{1}{3}|a|^2 - \tfrac{2}{3}|b|^2 + \tfrac{1}{3}|c|^2 - \tfrac{2}{3}|d|^2 - \tfrac{1}{3}|f|^2 + 2\operatorname{Re} ac^*\}. \tag{6}$$

One can also develop an explicit expression for the parameters entering into the expression for the cross section of the doubly scattered beam of deuterons:

$$I_0\alpha = -\tfrac{1}{3}[|a|^2+|b|^2+|c|^2+4|d|^2+2|f|^2]+\cos^2(\vartheta/2)[|a|^2+|b|^2+|c|^2]+\sin^2(\vartheta/2)[-|b|^2+2|d|^2+|f|^2$$
$$+2\,\mathrm{Re}\,ac^*]+\sqrt{2}\sin\vartheta\,\mathrm{Re}(ad^*+bf^*-cd^*),\qquad I_0\beta=\tfrac{2}{3}\sqrt{2}\,i\,\mathrm{Im}[(a-c)d^*+bf^*],$$
$$I_0\gamma=\tfrac{1}{3}\sin\vartheta[|a|^2+2|b|^2+|c|^2-2|d|^2-|f|^2-2\,\mathrm{Re}\,ac^*]-\tfrac{2}{3}\sqrt{2}\cos\vartheta\,\mathrm{Re}(ad^*+bf^*-cd^*),$$
$$I_0\delta=\tfrac{1}{3}\{-|b|^2-2|d|^2-|f|^2-2\,\mathrm{Re}\,ac^*+\sin^2(\vartheta/2)(|a|^2+|b|^2+|c|^2)+\cos^2(\vartheta/2)(2|d|^2+|f|^2-|b|^2+2\mathrm{Re}\,ac^*)$$
$$-\sqrt{2}\sin\vartheta\,\mathrm{Re}(ad^*+bf^*-cd^*)\}. \qquad (7)$$

We note that these formulas can be obtained from Eqs. (2a) and (3a) by determining the coefficients in explicit form in dependence on M and the mean value of the spin operators

$$A=\tfrac{1}{3}\mathrm{Sp}\,M=\tfrac{1}{3}(2a+f),\ B=\tfrac{1}{2}\mathrm{Sp}\,MS_N=i(b-d)/\sqrt{2},$$
$$C=\tfrac{3}{2}\mathrm{Sp}\,M(S_P^2+S_K^2-\tfrac{4}{3}\delta_{ik})=\tfrac{1}{2}(a-f)+\tfrac{3}{2}c,$$
$$D=\tfrac{1}{2}\mathrm{Sp}\,M(S_P^2-S_K^2)=(a-c-f)/2\cos\vartheta$$
$$=\sqrt{{}^1\!/_2}(b+d)/\sin\vartheta.$$

Thus, to carry out phase analysis and to establish the scattering amplitude of deuterons on a zero-spin nucleus, it is necessary to determine four parameters from experiment. Measurement of the differential cross section of the doubly-scattered beam of deuterons makes it possible to determine three quantities: the coefficients for $\cos 2\varphi$, $\cos\varphi$ and the free term. Only one additional experiment is necessary. Consequently, the study of double scattering makes it possible to solve the problem that has been presented.

Another, and in a certain sense opposite, approach to this problem is also possible. Assuming a certain definite form for the interaction potential as, for example, is the case for the optical model, and setting

$$V=V_0\frac{1+i\zeta}{1+\exp[(r-r_0)/t]}$$
$$-\frac{2\xi}{tr_0}V_0(1+i\zeta)\frac{\exp[(r-r_0)/t]}{\{1+\exp[(r-r_0)/t]\}^2}(\mathbf{SL})$$
$$+\begin{cases}(3r_0^2-r^2)(Ze^2/2r_0^3) & \text{for } r<r_0\\ Ze^2/r & \text{for } r>r_0\end{cases} \qquad (8)$$

(ξ is the constant of spin-orbit coupling, and $r_0 = 1.28\,A^{1/3}\times 10^{-13}$ cm), one can find the phase shift of the different waves and thus describe the elastic scattering. In this case, the spin-orbit Coulomb interaction is not taken into account, since it is small in comparison with the spin-orbit nuclear interaction. For an exact solution, numerical calculations are necessary which can be completed only on electronic computing machines. An explicit expression for the amplitude of the scattered wave can be written down in the WKB approximation:

$$f=-\frac{\lambda\eta_1}{2\mu^2}\exp[-i\eta_1\ln\mu^2]+\sum_l{}' k^{-1}(2l+1)\exp[i(2\eta_{i_l}+\Delta_l)]$$
$$\times\sin\Delta_l P_l(\cos\vartheta)+\sum_{m_{s'}}\chi_{m_{s'}}\sum_{m_s}\dot{M}_{m_s m_{s'}}(\vartheta,\varphi)a_{m_s}. \qquad (9)$$

Here the phase shifts are determined by the potential (under the assumption V ≪ E) in the following fashion:

$$\Phi_l=\frac{m}{(kh)^2}\int_{\varkappa}^{\infty}\frac{V_l(\tau)\tau d\tau}{[\tau^2-\varkappa^2]^{1/2}}\qquad\left(\tau=kr_0,\ \varkappa=l+\frac{1}{2}\right),$$

while the phase shift satisfying the Coulomb scattering,

$$\Delta_l=-\eta_1\ln\left[\tau+\sqrt{\tau^2-\varkappa^2}+\eta_1\sqrt{\tau^2-\varkappa^2}\left\{\frac{3}{2\tau}-\frac{\tau+2\varkappa^2}{\sigma\tau^3}\right]\right\},$$

where

$$\eta_{i_l}=\arg\Gamma(l+1+i\eta_1),\qquad \eta_1=\frac{mZe^2}{h^2k},\qquad \mu=\sin\frac{\vartheta}{2}.$$

However, for the form of potential chosen, only numerical methods are applicable, and at high energies, one must consider a large number of waves ($l_{\max}\approx kr_0$) and the computations become cumbersome. Only in the Born approximation are the calculations carried out in elementary fashion.

According to the results of Fernbach, Heckrotte, and Lepore,[6] an interaction of type (8) is obtained if the nuclear potential is regarded as the result of an average pair interaction of the nucleons. Then V_d can be regarded as the sum of V_n and V_p. If the y axis is directed along the vector **N**, the parameters in the formula for the cross section of the doubly scattered beam take the form

$$\alpha=\delta=-\frac{1}{3}\frac{|H|^2}{|G|^2+{}^2\!/_3|H|^2},\qquad i\beta=-\frac{4i}{3}\frac{\mathrm{Im}(GH^*)}{|G|^2+{}^2\!/_3|H|^2}. \qquad (10)$$

while the differential cross section for unpolarized deuterons is of the form

$$I_0=\left(\frac{2M}{h}\right)^2\left(\frac{4\alpha_1}{q}\right)^2\left(\tan^{-1}\frac{q}{4\alpha_1}\right)\left\{|G|^2+\frac{2}{3}|H|^2\right\},$$
$$G(\vartheta)=\frac{2V_0(1+i\zeta)}{q}\int_0^\infty J_1(qr)\frac{\partial\rho(r)}{\partial r}r^2dr+\frac{3}{2}\frac{Ze^2}{r_0}\left\{\frac{1}{q^3}\sin qr_0\right.$$
$$\left.-\frac{r_0}{q^2}\cos qr_0+\frac{r_0^2}{q^2}\left(1+\frac{2}{(qr_0)^2}\right)\right\}J_1(qr_0),$$
$$H(\vartheta)=\frac{2\xi V_0(1+i\zeta)}{q}k^2\sin\vartheta\int J_1(qr)\frac{\partial\rho(r)}{\partial r}r^2dr,\quad q=2k\sin\frac{\vartheta}{2}. \qquad (11)$$

In the work of Chamberlain et al.,[4] 156-Mev deuterons undergo double scattering on carbon. At scattering angle $\vartheta = \vartheta' = 20°$, the following dependence of the differential cross section on the azimuthal angle φ was obtained experimentally:

$$I(20, \varphi) = u + v\cos\varphi + w\cos 2\varphi,$$

and the values of the parameters (in mb/sr) amounted to

$$u = 50.3 \pm 2.2, \quad v = 15.3 \pm 1.9, \quad w = -1.8 \pm 3.6.$$

The statistical errors for the ratios u : v : w are given.

Calculations carried out by these authors in the momentum approximation, and calculations with a square well, lead to results that differ several fold from the experimental. In the calculation with the potential (8), under the assumption that

$$\xi = 3.3 \cdot 10^{-27}\ \text{cm}^2, \quad t = 0.7 \cdot 10^{-13}\ \text{cm},$$

$$r_0 = 1.28 A^{1/3} \cdot 10^{-13}\ \text{cm}, \quad V_0 = 42\ \text{Mev}, \quad \zeta = 0.3,$$

the following values were obtained for the parameters:

$$u = 42.6, \quad v = 10.9, \quad w = 6.6\ \text{mb/sr}$$

and if we put $V_0 = 30$ Mev and $\zeta = 0.4$, then they are shown to be equal to

$$u = 20.6, \quad v = 8.4, \quad w = 3.25\ \text{mb/sr}$$

Both the absolute values and the ratios of the values of the parameters that were obtained agree with the experimental data better than in the researches previously mentioned. Further divergence from the experimental values can evidently be eliminated by application of a more accurate method of calculation and consideration of the breakdown of the deuteron.

---

[1] W. Lakin, Phys. Rev. **98**, 139 (1955).

[2] O. D. Cheĭshvili, JETP **30**, 1147 (1956), Soviet Phys. JETP **3**, 974 (1957).

[3] H. P. Stapp, Phys. Rev. **107**, 607 (1957).

[4] Baldwin, Chamberlain, Segrè, Tripp, Wiegand, and Ypsilantis, Phys. Rev. **95**, 1104 (1954); **103**, 1502 (1956).

[5] J. M. Blatt and L. C. Biedenharn, Revs. Modern Phys. **24**, 258 (1952).

[6] Fernbach, Heckrotte, and Lepore, Phys. Rev. **97**, 1059 (1955).

Translated by R. T. Beyer
229

SOVIET PHYSICS JETP VOLUME 11, NUMBER 4 OCTOBER, 1960

ON THE QUANTUM-MECHANICAL CALCULATIONS OF THE PRESSURE IN SOLIDS

G. M. GANDEL'MAN and E. S. PAVLOVSKIĬ

Submitted to JETP editor September 29, 1959

J. Exptl. Theoret. Phys. (U.S.S.R.) 38, 1176-1182 (April, 1960)

A quantum-mechanical formula which is a generalization of the virial theorem is derived, for the pressure in a solid at zero temperature. A more detailed examination is made of the application of this formula in the approximation of spherical cells.

INTRODUCTION

In the treatment of solid substances the usual problem is the calculation of the energy of cohesion in the normal state, and also the determination of the compressibility curve, i.e., the dependence of the pressure on the density. The pressure at a prescribed density is calculated (at zero temperature) as the derivative of the energy of the substance with respect to its volume,

$$p = -dE/dV. \tag{1}$$

Thus to determine the pressure in a given state one must know the energy also in a neighboring state, which is a considerable inconvenience. As is well known (cf. e.g., reference 1), in the Thomas-Fermi statistical method one can calculate the pressure directly in terms of the Thomas-Fermi potential or in terms of the density of electrons at the boundary of a cell in the given state, without differentiation. But the Thomas-Fermi method does not give negative pressures and for this reason does not describe the cohesion of solids. Inclusion of exchange and quantum corrections gives a zero pressure at a finite density, but in a region in which these effects cannot be treated as corrections.

A quantum-mechanical approach to the calculation of the energy and the pressure not only gives the fact of the cohesion of solids and the correct order of magnitude of the cohesion energy, but also can give a number of features of the compressibility curve that are caused by changes of the structure of the electron shells during compression. An example of this is the phase transition observed in cesium, for which Sternheimer[2] has proposed an explanation in terms of a calculation. In connection with this there is the interesting question of how one can express the pressure in terms of the quantum-mechanically described state of a solid. Feynman[3] has considered an analogous problem. He found the forces with which the nuclei in a molecule can be held at a prescribed distance in terms of the wave function of the electrons in a stationary state (with the prescribed position of the nuclei).

The problem of the pressure in a solid is much more complicated. This is due to the fact that in molecules the electron wave functions vanish at infinity together with their derivatives, whereas in the case of a solid one considers either an infinite body with a given density or else a body of a fixed finite volume (in a sense that will be stated later) with a prescribed pressure on its surface, so that the system is not closed.

It would be possible to express the pressure in terms of the quantum-mechanical stress tensor,[4] part of which is due to the electric interaction (the electromagnetic tensor). This part has to be included, despite the electric neutrality of the atoms taken as a whole, since although the mean electric field (and the total electric volume force) acting on an atom is zero, it nevertheless contributes to the surface forces, to the pressure. This is expressed by the fact that the electric field appears quadratically in the electromagnetic tensor. The necessity of taking the electromagnetic tensor into account brings with it a number of difficulties; because of this we shall not derive the formula for the pressure in terms of the stress tensor.

DERIVATION OF THE QUANTUM-MECHANICAL FORMULA FOR THE PRESSURE

The energy of a solid body in which the nuclei are regarded as fixed at the points $\mathbf{R}_\alpha$ ($\alpha = 1, 2, \ldots, N$, where N is the number of nuclei) is given by the following formula:

$$\hat{E} = \int \Psi^*(q)\, \hat{H}\, \Psi(q)\, dq + E_{\mathrm{NN}},$$

$$E_{\mathrm{NN}} = \tfrac{1}{2} \sum_{\beta \neq \alpha} Z^2 e^2 / |\mathbf{R}_\alpha - \mathbf{R}_\beta|, \tag{2}$$

where $\hat{H}$ is the Hamiltonian of the system of electrons (relativistic effects are everywhere neglected):

$$\hat{H}(q) = -\frac{\hbar^2}{2m}\sum_i \Delta_i - Ze^2 \sum_{i,\alpha} \frac{1}{|\mathbf{r}_i - \mathbf{R}_\alpha|} + \frac{e^2}{2} \sum_{i,\, k \neq i} \frac{1}{r_{ik}}. \quad (3)$$

The summation over i is taken over all electrons; q is the set of space and spin coordinates of all the electrons. In the stationary state determined from the condition that the energy be a minimum, $\Psi(q)$ satisfies the Schrödinger equation

$$\hat{H}(q)\Psi(q) = E_0\Psi(q) \quad (4)$$

and the normalization condition

$$\int \Psi^*(q)\Psi(q)\,dq = 1. \quad (4a)$$

Strictly speaking the integrals in Eqs. (2) and (4a) must be extended over an infinite volume, but in this case we would have to include in the system considered also the body that bounds the volume. We shall replace it by a rigid wall, and at the boundary of the volume V shall postulate the boundary condition $\Psi = 0$. Thus the concept of the volume of the body is sharply defined. Now we can assume that the integrals in Eqs. (2) and (4a) are taken over the volume V.

The energy (2) depends on a parameter, on the volume V or, what is the same thing, on the average internuclear distance R_0. For the calculation of the pressure we differentiate the energy with respect to this parameter. In doing so we note that when R_0 changes there are changes of the wave function and of the volume of integration

$$\frac{dE}{dR_0} = \int\left(\frac{\partial\Psi^*(q)}{\partial R_0}\hat{H}\Psi(q) + \Psi^*\hat{H}\frac{\partial\Psi}{\partial R_0}\right)dq + \int\Psi^*\frac{\partial\hat{H}}{\partial R_0}\Psi\,dq + \frac{dE_{\mathbf{NN}}}{dR_0} + \frac{\partial' E}{\partial R_0}.$$

Here in the last term $\partial'/\partial R_0$ denotes differentiation with constant Ψ and H (with respect to the "upper limit"). In the first integral we add and subtract $(\partial\Psi/\partial R_0)(\hat{H}\Psi)^*$, and then use the Schrödinger equation (4). We get

$$\frac{dE}{dR_0} = E_0\left\{\frac{\partial'}{\partial R_0}\int\Psi^*\Psi\,dq + \int\frac{\partial}{\partial R_0}(\Psi^*\Psi)\,dq\right\} + \int\Psi^*\frac{\partial\hat{H}}{\partial R_0}\Psi\,dq + \frac{dE_{\mathbf{NN}}}{dR_0} + \int\left[\Psi^*\hat{H}\frac{\partial\Psi}{\partial R_0} - \frac{\partial\Psi}{\partial R_0}(\hat{H}\Psi)^*\right]dq.$$

The expression in curly brackets is equal to zero because of the preservation of the normalization (4a) under the change of volume. Accordingly we have

$$\frac{dE}{dR_0} = \int\Psi^*\frac{\partial\hat{H}}{\partial R_0}\Psi\,dq + \frac{dE_{\mathbf{NN}}}{dR_0} + \int\left[\Psi^*\hat{H}\frac{\partial\Psi}{\partial R_0} - \frac{\partial\Psi}{\partial R_0}(\hat{H}\Psi)^*\right]dq. \quad (5)$$

Equation (5) differs from the Feynman formula[3] by the last term, which arises because of the fact that the system considered here is not closed. It is not hard to convince oneself that for a finite volume of the body this term does not vanish, as it would for a free molecule. Equation (5) is convenient in that it contains only quantities of the same order of magnitude as the quantity dE/dR_0 that is being calculated. The larger terms of the order of E/R_0 are automatically excluded. In calculating the pressure p directly from Eq. (1) by first calculating the energy E(V) as a function of the volume and then differentiating with respect to V one would have to find small differences of large quantities, since the energy of compresssion (or the energy of cohesion) is much smaller than the total energy E of the body. For practical purposes, however, formula (5) is unsuitable, because the region near the surface of the body makes substantial contributions to all the integrals although the region itself can be made arbitrarily small in comparison with the whole volume of the body. This is due to the fact that $\partial\Psi/\partial R_0$ and $\partial H/\partial R_0$ are proportional near the surface to the linear dimensions of the body. To prove this let us write the boundary condition $\Psi = 0$ at the surface of the body, $\mathbf{r} = \mathbf{R}$, for a variation of R_0:

$$\Psi + \delta R_0 \partial\Psi/\partial R_0 = 0 \text{ at } \mathbf{r} = \mathbf{R} + \delta\mathbf{R},$$

from which we get on the boundary

$$\frac{\partial\Psi}{\partial R_0} = -\frac{\partial\Psi}{\partial\mathbf{r}}\frac{\partial\mathbf{R}}{\partial R_0} = -\frac{\partial\Psi}{\partial\mathbf{r}}\frac{\mathbf{R}}{R_0}. \quad (6)$$

The proof is similar for $\partial H/\partial R_0$.

Thus, although the formula (5) is correct, it cannot be used in practice because of the finite contribution of the region near the surface of the body. Just to make this situation clearer, we have considered a body of finite volume, and not an infinite body with a prescribed density. In the following section a formula for the pressure will be obtained that is free from this shortcoming.

GENERALIZATION OF THE VIRIAL THEOREM

As is well known, the virial theorem $E + E_K = 0$ holds in the quantum mechanics of a stationary system of particles interacting by the Coulomb law; E and E_K are respectively the total energy and kinetic energy of the system. The usual way of proving this theorem is to introduce into the formula for the energy a scale factor λ, and then set the derivative of the energy with respect to the parameter λ equal to zero for $\lambda = 1$, because of the stationary property of the system (the energy must be a minimum for $\lambda = 1$).

By exactly the same method we obtain in this section a generalization of the virial theorem for a quantum-mechanical system of nuclei and electrons in a stationary state with a prescribed finite value of its volume V (the nuclei, as before, are regarded as fixed); this theorem provides a possibility of calculating the pressure.

We shall start from the Hartree-Fock (H-F) approximation, which we are going to use in what follows. The theorem so obtained can, however, be extended to a more general case without difficulty.

We write down the energy in the H-F approximation:[5,6]

$$E = -2\frac{\hbar^2}{2m}\sum_{k=1}^{ZN/2}\int \psi_k^*(\mathbf{r})\,\Delta\psi_k(\mathbf{r})\,d\mathbf{r} - 2Ze^2\sum_k\sum_\alpha\int\frac{|\psi_k(\mathbf{r})|^2}{|\mathbf{r}-\mathbf{R}_\alpha|}\,d\mathbf{r}$$

$$+\,2e^2\sum_{i,\,k}\int\frac{1}{r_{12}}\,|\psi_i(\mathbf{r}_1)^2|\,\psi_k(\mathbf{r}_2)|^2\,d\mathbf{r}_1\,d\mathbf{r}_2$$

$$-\,e^2\sum_{i,\,k}\int\frac{1}{r_{12}}\,\psi_i^*(\mathbf{r}_1)\,\psi_k(\mathbf{r}_1)\,\psi_k^*(\mathbf{r}_2)\,\psi_i(\mathbf{r}_2)\,d\mathbf{r}_1\,d\mathbf{r}_2 + E_{\mathbf{NN}}$$

$$\equiv E_\mathrm{K} + E_{\mathbf{eN}} + E_{\mathbf{ee}} + A_{\mathbf{ee}} + E_{\mathbf{NN}} \tag{7}$$

Here $\psi_i(\mathbf{r})$ are the spatial parts of the one-electron wave functions from which the Fock determinant is constructed. Equation (7) is written for the case in which there is a pair of electrons with opposite spins for each spatial state ψ_i (this means that ferromagnetic substances are excluded from this treatment). The summation over i and k is taken over all different spatial functions; the summation over the spins has already been done.

The requirement that the energy be a minimum with respect to arbitrary variations of the ψ_i that preserve the orthonormality of the system of functions ψ_i leads to the system of H-F equations (λ_{ik} are variation parameters):

$$\left(-\frac{\hbar^2}{2m}\Delta - \sum_\alpha\frac{Ze^2}{|\mathbf{r}-\mathbf{R}_\alpha|} + 2e^2\sum_i\int\frac{|\psi_i(\mathbf{r}')|^2}{|\mathbf{r}-\mathbf{r}'|}\,d\mathbf{r}'\right)\psi_k(\mathbf{r})$$

$$-\,e^2\sum_i\int\frac{\psi_i^*(\mathbf{r}')\,\psi_i(\mathbf{r})\,\psi_k(\mathbf{r}')}{|\mathbf{r}-\mathbf{r}'|}\,d\mathbf{r}' = \sum_i \lambda_{ki}\,\psi_i(\mathbf{r}). \tag{8}$$

To derive the virial theorem we take as the unit of length the average internuclear distance R_0 and introduce a changed form of the wave functions:

$$\boldsymbol{\rho} = \mathbf{r}/R_0, \qquad \psi_i(\mathbf{r}) = R_0^{-3/2}\varphi_i(\boldsymbol{\rho}).$$

Here it must be remembered that the $\varphi_i(\rho)$ have further dependence on R_0 as a parameter. We express the energy E in terms of the φ_k:

$$E = -2\frac{\hbar^2}{2m\,R_0^2}\sum_k\int\varphi_k^*\,\Delta_\rho\,\varphi_k\,d\boldsymbol{\rho} - \frac{2Ze^2}{R_0}\sum_{k,\,\alpha}\int\frac{|\varphi_k(\boldsymbol{\rho})|^2}{|\boldsymbol{\rho}-\mathbf{R}_\alpha/R_0|}\,d\boldsymbol{\rho}$$

$$+\,\frac{2e^2}{R_0}\sum_{i,\,k}\int\frac{1}{\rho_{12}}\,|\varphi_i(\boldsymbol{\rho}_1)|^2\,|\varphi_k(\boldsymbol{\rho}_2)|^2\,d\boldsymbol{\rho}_1\,d\boldsymbol{\rho}_2$$

$$-\,\frac{e^2}{R_0}\sum_{i,\,k}\int\frac{1}{\rho_{12}}\,\varphi_i^*(\boldsymbol{\rho}_2)\,\varphi_k(\boldsymbol{\rho}_2)\,\varphi_k^*(\boldsymbol{\rho}_1)\,\varphi_i(\boldsymbol{\rho}_1)\,d\boldsymbol{\rho}_1\,d\boldsymbol{\rho}_2$$

$$+\,\frac{Z^2e^2}{2R_0}\sum_{\alpha,\,\beta\neq\alpha}\left|\frac{\mathbf{R}_\alpha}{R_0}-\frac{\mathbf{R}_\beta}{R_0}\right|^{-1}. \tag{7a}$$

There are corresponding changes in the H-F equations. Let us differentiate Eq. (7a) with respect to R_0. Here, just as in the preceding section, we make use of the H-F equations for φ_k, first adding and subtracting a term

$$2\,\frac{\hbar^2}{2mR_0^2}\sum_k\int\frac{\partial\varphi_k}{\partial R_0}\,\Delta_\rho\,\varphi_k^*\,d\boldsymbol{\rho},$$

in E_K. We note that in the differentiation there is no need to take into account the dependence of $\mathbf{R}_\alpha/R_0$ on R_0, since the change of the mutual distribution of the nuclei with a change of R_0 occurs in second order. We get:

$$\frac{dE}{dR_0} = -\frac{1}{R_0}\left(2E_\mathrm{K} + E_{\mathbf{eN}} + E_{\mathbf{ee}} + A_{\mathbf{ee}} + E_{\mathbf{NN}}\right)$$

$$-\,\frac{\hbar^2}{mR_0^2}\sum_k\int\left(\varphi_k^*\,\Delta_\rho\frac{\partial\varphi_k}{\partial R_0} - \frac{\partial\varphi_k}{\partial R_0}\,\Delta_\rho\,\varphi_k^*\right)d\boldsymbol{\rho}$$

$$+\,2\sum_{i,\,k}\int d\boldsymbol{\rho}\left(\lambda_{ki}\,\frac{\partial\varphi_k^*}{\partial R_0}\,\varphi_i + \lambda_{ki}^*\,\frac{\partial\varphi_k}{\partial R_0}\,\varphi_i^*\right).$$

The last term is equal to zero, as is easily seen if we recall the self-adjoint property of the matrix λ_{ki} and the preservation of the orthonormality of the functions φ_k under the change of volume. Using Eq. (1) and the relation $V \sim R_0^3$, we get the virial theorem in the following form

$$3pV = E_\mathrm{K} + E + \frac{\hbar^2}{mR_0}\sum_k\int\left(\varphi_k^*\,\Delta_\rho\frac{\partial\varphi_k}{\partial R_0} - \frac{\partial\varphi_k}{\partial R_0}\,\Delta_\rho\varphi_k^*\right)d\boldsymbol{\rho}. \tag{9}$$

In Eq. (9), unlike Eq. (5), the contribution of the region near the surface of the body can obviously be made arbitrarily small as the number of cells N goes to infinity, since the boundary conditions on the φ_k are fixed for a value of ρ that does not depend on R_0. The origin of the last term in Eq. (9) is the same as for Eq. (5). Let us transform this term to a more convenient form. To do this we break up the integral with respect to ρ over the entire volume into a sum of integrals over the individual cells V_α and note that the integrand can be put in the form of the divergence of a vector. Accordingly the volume integral over

V_α can be reduced to an integral over the surface S of the cell:

$$3pV = E_\kappa + E + \frac{\hbar^2}{mR_0}\sum_{k,\alpha}\oint_{S_\alpha}\left(\varphi_k^*\nabla_\rho\frac{\partial\varphi_k}{\partial R_0} - \frac{\partial\varphi_k}{\partial R_0}\nabla_\rho\varphi_k^*\right)_n dS. \tag{10}$$

By means of the boundary conditions the derivatives of φ_k with respect to R_0 on the cell surfaces that appear in Eq. (10) can always be expressed in terms of the values of the functions themselves and their derivatives at the boundary, in a manner similar to the way this was done in the preceding section [Eq. (6)]. This will be done concretely a bit later [cf. Eq. (12)] for the Bloch conditions in the Wigner-Seitz method of spherical cells.

In concluding this section we remark that the extension of the result of Eq. (9) or Eq. (10) obtained in the H-F approximation to the general case is trivial. We give the result:

$$3pV = E_\kappa + E + \frac{\hbar^2}{2mR_0}\sum_i\int\left(\Phi^*(\rho)\,\Delta_{\rho_i}\frac{\partial\Phi}{\partial R_0} + \frac{\partial\Phi}{\partial R_0}\Delta_{\rho_i}\Phi^*\right)d\rho,$$

$$E_\kappa = -\frac{\hbar^2}{2mR_0^2}\sum_i\int\Phi^*(\rho)\,\Delta_{\rho_i}\Phi\,d\rho =$$

$$-\frac{\hbar^2}{2m}\sum_i\int\Psi^*(q)\,\Delta_i\,\Psi(q)\,dq,$$

$$E = \int\Psi^*(q)\,\hat{H}\,\Psi(q)\,dq + E_{NN},$$

$$\Phi(\rho) = R_0^{3n/2}\,\Psi(q), \quad \rho = q/R_0.$$

The summation is taken over all electrons; n is the number of electrons.

THE PRESSURE IN THE WIGNER-SEITZ APPROXIMATION

Ordinarily calculations of the energy of cohesion of solids are made by means of the sperical alcell method of Wigner and Seitz.[7] In this case the parameter R_0 is the radius of a cell. At the boundary of the cell $\rho = 1$. The wave function φ_k of an electron with the quasi-momentum **k** obeys the Bloch conditions, which in the case of spherical cells take the form[8]

$$\varphi_k(\rho, \pi-\theta) = \exp\{-2ikR_0\cos\theta\}\,\varphi_k(\rho, \theta),$$

$$\partial\varphi\;(\rho, \pi-\theta)/\partial\rho$$

$$= -\exp\{-2ikR_0\cos\theta\}\,\partial\varphi_k(\rho, \theta)/\partial\rho \text{ at } \rho = 1. \tag{11}$$

Here θ is the angle between the quasi-momentum **k** and the radius vector **r**. Differentiating the expressions (11) with respect to R_0, let us substitute them in Eq. (10), first breaking the integral in Eq. (10) into two identical integrals and replacing θ by $(\pi-\theta)$ in one of them.

After this we use the conditions (11) and their complex conjugates. We get

$$3pv = E_\kappa + E + \frac{\hbar^2}{mR_0}\sum_k\int ik\cos\theta\left\{\left(\varphi_k^*\frac{\partial\varphi_k}{\partial\rho} - \frac{\partial\varphi_k^*}{\partial\rho}\varphi_k\right)\right\}_{\rho=1} d\Omega. \tag{12}$$

Here E and E_K are the total and kinetic energies belonging on the average to one cell, and v is the volume of a cell. For the case of the simple boundary conditions $\varphi_k = 0$ or $\partial\varphi_k/\partial\rho = 0$ at $\rho = 1$ the last term in Eq. (12) is zero.

Equation (12) can be written in terms of the ψ_k:

$$3pv = E_\kappa + E + \frac{\hbar^2R_0^3}{m}\sum_k\int ik\cos\theta\left|\left(\psi_k^*\frac{\partial\psi_k}{\partial r} - \frac{\partial\psi_k^*}{\partial r}\psi_k\right)\right|_{r=R_0} d\Omega. \tag{12a}$$

In the cell method the wave function ψ_k is written in the form of a series

$$\psi = \sum_l A_l(k)\,R_l(E, r)\,P_l(\cos\theta)\cdot \tag{13}$$

R_l satisfies the radial Schrödinger equation with the potential U(r). The function (13) must satisfy the Bloch conditions; this gives an infinite system of homogeneous equations for the A_l, which in practice is broken off at a finite number of equations and unknowns; by equating the determinant of the system to zero one can find the eigenvalue E for a given R_0.[8]

After the functions ψ_k are found, the total energy E and the kinetic energy E_K are found by calculating integrals [cf. Eq. (7)]. Here in the spherical-cell approximation all the integrals except the exchange integral reduce to integrals over the individual cells. In the calculation of the exchange integral, however, the interaction of several neighboring cells is important, and this leads to well known difficulties in the practical use of Eq. (12).

We note that the solution of the one-electron Schrödinger equation (14) (sic) with the boundary conditions (11) gives the functions ψ_k approximately, because the system of H-F equations does not break up exactly into separate equations of the type of Eq. (14). The H-F equations can be reduced to the form (14) by means of the modification of the H-F approximation proposed by Slater,[9] with subsequent introduction of an effective potential U(r) that is the same for all electrons. It is most expedient to use for U(r) the statistical Thomas-Fermi potential.

The formula (12), which it is most convenient to use, was derived by applying one-electron functions of the Bloch type in the H-F method (to each spatial function satisfying the Bloch conditions there corresponds a pair of electrons with opposite spins).

Therefore the question arises as to the accuracy of the H-F approximation as applied to a metal. It is well known that for the case of an unfilled band, when the H-F method does not coincide with the Heitler-London method, the H-F method can be extremely inaccurate at small densities of the substance because of the neglect of the effect of Coulomb correlation between the electrons.[6,10] Therefore calculation of the cohesion energy by the H-F method without the introduction of correlation corrections can give incorrect results. In spite of this we can hope for good accuracy of the H-F approximation in the calculation of the pressure in compressed substances. In any case, however, it is always necessary to estimate the importance of correlation effects.

In conclusion the writers express their sincere gratitude to Ya. B. Zel'dovich for a deep analysis of questions touched on in this paper and for helpful advice and suggestions, and also to N. A. Dmitriev and V. N. Mokhov for helpful discussions.

[1] P. Gombas, Die statistische Theorie des Atoms und ihre Anwendungen, Springer, 1949.

[2] R. Sternheimer, Phys. Rev. **78**, 235 (1950).

[3] R. P. Feynman, Phys. Rev. **56**, 340 (1939).

[4] W. Pauli, Die allgemeinen Prinzipien der Wellenmechanik (Russian translation), Gostekhizdat, Moscow-Leningrad, 1947.

[5] V. A. Fock, Z. Physik **61**, 126 (1930).

[6] F. Seitz, The Modern Theory of Solids (Russian translation), Gostekhizdat, Moscow-Leningrad, 1949.

[7] E. P. Wigner and F. Seitz, Phys. Rev. **43**, 804 (1933).

[8] H. Brooks, Nuovo cimento Supplement **7**, 186 (1958).

[9] J. C. Slater, Phys. Rev. **81**, 385 (1951).

[10] N. F. Mott, Nuovo cimento Supplement **7**, 312 (1958).

Translated by W. H. Furry
230

SOVIET PHYSICS JETP VOLUME 11, NUMBER 4 OCTOBER, 1960

COHERENT ELECTRON RADIATION IN A SYNCHROTRON. III

M. S. RABINOVICH and L. V. IOGANSEN

P. N. Lebedev Physics Institute, Academy of Sciences, U.S.S.R.

Submitted to JETP editor September 30, 1959

J. Exptl. Theoret. Phys. (U.S.S.R.) 38, 1183-1187 (April, 1960)

The electromagnetic interaction of electrons in a synchrotron is considered with the shielding effect of the chamber walls taken into account for bunches of arbitrary shape. The effect of these forces on the phase motion of the electrons and on the dimensions of a bunch are evaluated.

In earlier papers[1,2] we have considered the coherent radiation forces in a synchrotron and have evaluated the effect of these forces on the phase motion of the electrons. However, in this earlier work the shielding effect of the walls of the synchrotron vacuum chamber was neglected; furthurmore, it was assumed that the bunch moves in an infinite free space. In the present paper we consider the same problems but take the shielding effect into account. The shielding effect of the walls is introduced as an approximation: it is assumed that the bunch moves close to an infinite ideally conducting plane or between two such planes. Under these conditions it is convenient to use the method of images.

In particular, the force which acts on a single electron rotating at a distance b above a shielding plane is equal to the force exerted by a "positron" which rotates in synchronism with the electron at a distance b below the plane. With the method which we have developed earlier[1] it is an easy matter to find the interaction forces in a dipole of this kind. We assume that $p \equiv b/a \ll 1$, where a is the radius of the orbit and expand these forces in powers of p^2. Then, for the tangential force we have

$$f_\tau \approx \frac{2}{3}\frac{e^2}{a^2}\gamma^4(1-2p^2\gamma^4\ldots) \qquad (p \ll 1/\gamma^2), \tag{1}$$

$$f_\tau \approx \frac{e^2}{a^2}\left(\frac{\sqrt{3}}{4}\frac{1}{\gamma^2 p^3} - \frac{\sqrt{3}}{10}\frac{1}{p}\cdots\right) \qquad (p \gg 1/\gamma^2); \tag{2}$$

for the vertical force

$$f_z \approx -\frac{e^2}{\gamma a^2}\frac{1}{(2p)^2} \qquad (p \ll 1/\gamma^2), \tag{3}$$

$$f_z \approx -\frac{e^2}{a^2}\frac{3^{3/4}}{8p^{3/2}} \qquad (p \gg 1/\gamma^2), \tag{4}$$

$$\gamma = (1-\beta^2)^{-1/2}, \quad \beta = v/c.$$

The force given by (1) is balanced by radiation dissipation so that when $p \ll 1/\gamma^2$, i.e., when $b \ll a/\gamma^2$, there is essentially no radiation from the dipole. At first glance this result may appear strange. It would appear that the dipole does not radiate when the distance between the charges, 2b, is small compared with the wavelength at which maximum radiation occurs: $ƛ_{\text{max}} = 2a/3\gamma^3$. Actually, because of the directivity of the radiation this effect comes into play earlier. As is well known, the radiation at the n-th harmonic is concentrated in a cone with opening angle $\alpha \sim n^{-1/3}$. Hence the difference in the path length of waves which emanate from the electron and the positron is $\Delta \sim b\alpha \sim bn^{-1/3}$. For a given value of b, all harmonics with wavelengths $\lambda \gg \lambda_b \equiv b\sqrt{b/a} \equiv ap^{3/2}$ cancel because the charges are of opposite sign. Since $ƛ_{\text{max}} = 2a/3\gamma^3$, all harmonics cancel when $b \ll a/\gamma^2$, i.e., when $p \ll \gamma^{-2}$.

We now consider the interaction forces in a bunch. The coherent radiation force which acts on an individual electron in an unshielded bunch is given approximately by the following expression[1]

$$f_{\tau\,\text{coh}}(\psi) \approx -\frac{2}{3^{1/3}}\frac{Ne^2}{a^2}\frac{d}{d\psi}\int_0^\infty \frac{\varphi(\psi-x)}{x^{1/3}}\,dx, \tag{5}$$

$$1 \gg \vartheta_0 \gg 1/\gamma^3, \qquad \vartheta_0^{4/3} \gg (\sigma_0/a)^2. \tag{6}$$

Here ϑ_0 is the effective angular dimension of the bunch; σ_0 is the effective cross sectional radius of the bunch; N is the number of electrons in a bunch; ψ is the phase (azimuth) of the electron being considered; $\varphi(\psi)$ is the phase distribution of the electrons in the bunch. In the derivation of Eq. (5) we consider only the interaction of the electron in question with the part of the bunch which is behind it. The interaction with charges in front of the electron can be neglected. This procedure is valid because the interaction forces are not symmetrical forward and backward since the radiation is highly directive. The maximum value of the force (5) is of order $Ne^2/a\vartheta_0^{4/3}$.

Using the same method as that employed in the derivation of Eq. (5), we find that the coherent radiation force acting on an individual electron in a bunch which rotates over a single shielding plane is given approximately by

$$f_{\tau\,\mathrm{coh}}(\psi, p) \approx \frac{2}{3^{1/3}} \frac{Ne^2}{a^2} p^2 \frac{d^2}{d\psi^2} \int\limits_0^\infty \frac{\varphi(\psi - x)}{x^{1/3}}\, dx. \tag{7}$$

In the derivation of Eq. (7) it is assumed that

$$1 \gg \vartheta_0 \gg 1/\gamma^3, \qquad 1 \gg p \gg 1/\gamma^2, \qquad \vartheta_0^{4/3} \gg p^2, \qquad \sigma_0/a \ll p. \tag{8}$$

It is further assumed that the phase distribution of electrons in the bunch $\varphi(\psi)$ is a smooth function. The smoothness criterion is given below. As in the derivation of Eqs. (5) and (7), account is taken only of the interaction between the electron being considered and the charges behind it. Hence, Eqs. (7) and (5) cannot be used behind the bunch.

The condition $1 \gg p \gg 1/\gamma^2$ can be written in the form $a \gg \lambda_b \gg ƛ_{max}$ which implies that the short wave radiation of each individual electron must be unshielded. The condition $\vartheta_0^{4/3} \gg p^2$ means that the dimension of the bunch $a\vartheta_0$ must be large compared with $\lambda_b \equiv ap^{3/2}$. The coherent radiation of a small unshielded bunch is concentrated in the region of wavelengths which are of the order of the dimensions of the bunch; hence, the condition $a\vartheta_0 \gg \lambda_b$ means that the shielding is strong, i.e., that a large part of the coherent radiation is shielded. The ratio $p^2/\vartheta_0^{4/3}$ characterizes the fraction of unshielded coherent radiation.

In Fig. 1 we show the dependence of the force (7) on azimuth ψ for a bunch of Gaussian shape. It is assumed that the bunch moves to the right. The maximum value of this force is of order $Ne^2p^2/a^2\vartheta_0^{8/3}$.

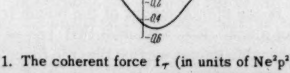

FIG. 1. The coherent force f_τ (in units of $Ne^2p^2/a^2\vartheta_0^{8/3}$, acting on a single electron of a Gaussian shielded bunch as a function of azimuth ψ (in units of ϑ_0). The dashed curve shows the phase distribution of particles in the bunch.

The power expended by the forces (5) and (7) in acting on the bunch is equal to the power of the coherent radiation (with opposite sign) of the unshielded bunches respectively. Integrating (5) and (7) over a bunch we find that these powers are of order $N^2e^2c/a^2\vartheta_0^{4/3}$ and $N^2e^2cp^2/a^2\vartheta_0^{8/3}$ respectively. In the particular case in which the bunch is Gaussian, using Eq. (7) we obtain an expression for the power which coincides exactly with that obtained by Schiff;[3] Schiff's result is obtained by a phase analysis and summation of the intensities of the harmonics in the spectrum.

The Coulomb part of the total tangential force which acts on a single electron in a bunch differs from the corresponding expression for Coulomb force in an unshielded bunch[1] only in the logarithmic term which contains the shielding parameter $p \equiv b/a$; this component is approximately

$$f_{\tau\,\mathrm{Coul}}(\psi, p) \approx -\frac{2}{\gamma^2} \frac{Ne^2}{a^2} \ln\left(2e\,\frac{b}{\sigma}\right) \varphi'(\psi), \tag{9}$$

where σ is the cross sectional radius of the bunch. Hence, shielding is less important for the Coulomb force than for the coherent radiation force.

Although shielding acts mainly to reduce the coherent force, the Coulomb force can be smaller than the coherent force when $\gamma \gg 1$. From a comparison of the orders of magnitude of the quantities in (7) and (9) it follows that the Coulomb force can be neglected (as compared with the coherent force) if

$$(p\gamma)^2 \gg \vartheta_0^{2/3} \ln(b/\sigma). \tag{10}$$

Equation (7) applies only when a bunch is smooth; it cannot be used if a bunch has highly irregular sections or sharp ends. Hence we consider the case of a rectangular bunch separately:

$$\varphi(\psi) = \begin{matrix} 1/4\,\vartheta_0, & |\psi| < 2\vartheta_0; \\ 0, & |\psi| > 2\vartheta_0. \end{matrix}$$

We will not derive general expressions for the forces and radiation power because these expressions are not particularly illuminating, but shall only give certain results. The coherent forces for a rectangular bunch over a single shielding plane for the case $p = 0.1$ and $\vartheta_0 = \pi/8$ are shown in Fig. 2. It is assumed that the bunch moves to the right. It is apparent that the regions close to the ends of the bunch are the most important.

The force which acts on an inner portion of order $b\sqrt{b/a} \equiv ap^{3/2}$ close to the front of the bunch is given approximately by

$$f_\tau \approx -\frac{Ne^2}{a^2} \frac{1}{4\vartheta_0} \frac{3}{2(\sqrt{3}\,p)^{1/2}}. \tag{11}$$

At a distance $a\eta$ from the end, inside the bunch, the force is

$$f_\tau \approx -\frac{Ne^2}{a^2} \frac{1}{4\vartheta_0} \frac{2}{|6\eta|^{1/3}} \qquad (0 < \eta < p^{3/2}). \tag{12}$$

The same situation obtains for a bunch between two shielding plates; the power expended by these forces in acting on the end portions of a bunch of

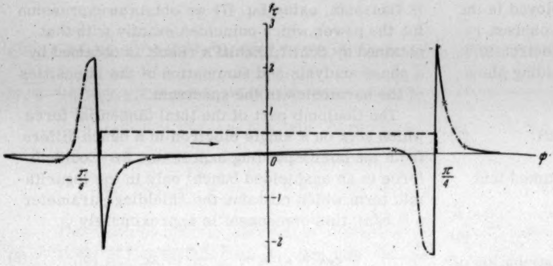

FIG. 2. The coherent force f_τ (in units of Ne^2/a^2) acting on an individual electron in a rectangular bunch as a function of azimuth ψ for the particular case $\vartheta_0 = \pi/8$, $p = 0.1$. The dashed line shows the phase distribution of particles in the bunch.

width of order λ_b is

$$W_{\text{coh}} \approx \frac{N^2e^2c}{a^2}\frac{\sqrt{3}\,p}{(4\vartheta_0)^2}. \tag{13}$$

This result is in agreement with that obtained by Schwinger (cited by Nodvick and Saxon);[4] Schwinger's expression is obtained by summation of the wave-zone radiation over the entire spectrum. The Schwinger method, however, cannot be used to compute the effect of individual portions of the bunch in the general expression for the radiation power. Nodvick and Saxon[4] assume that the Schwinger expression (13) can be applied to a bunch of arbitrary shape. Actually, however, this procedure is not valid because the radiation (13) comes from the ends of the bunch; the radiation is in fact due to the existence of sharp ends in the bunch.

A bunch may be assumed smooth if there is no marked variation in charge density in a distance large compared with $\lambda_b \equiv b\sqrt{b/a}$. Under these conditions Eq. (7) can be used. If this condition is not satisfied the expressions for the forces in a rectangular bunch can be used as an approximation.

In practice, because of the coherent forces it is probable that there are considerable charge-density gradients near the front of a bunch. However, because of the same forces high density gradients cannot exist for long at the rear of the bunch; any sharp density variation is spread out so that the bunch always has a smeared-out tail. In what follows it will be assumed that the bunch is smooth and that Eq. (7) can be used.

We now estimate the effect of the coherent forces (5) and (7) on the phase motion of electrons in a "cumulative" system. This effect is intensified to the extent that the angular dimension of a bunch is reduced because of the usual incoherent radiation damping of the phase oscillations. Hence the coherent forces limit the dimension to which a bunch can be compressed without an external agency. The minimum angular dimension of a bunch due to a force such as (5) when there is no shielding is of the following order of magnitude:[2]

$$\vartheta_0 \sim (2\pi Ne/aV)^{3/7}, \tag{14}$$

where V is the peak value of the radio-frequency voltage. Equation (14) is easily obtained from the condition that close to the rear of the bunch the phasing electric force is comparable with the coherent force which tends to disturb phase stability.

Similarly, when shielding is taken into account, i.e., when the forces in (7) are considered, this dimension is of the order of

$$\vartheta_0 \sim (2\pi Nep^2/aV)^{3/11}. \tag{15}$$

The estimates in (14) and (15) apply for the same conditions as Eqs. (5) and (7) respectively.

Substituting in Eq. (14) $a = 50$ cm, $V = 10$ kev, and assuming $N = 10^{13}$, we find $\vartheta_0 \sim 3.5$. This result means that because of the coherent radiation force a bunch will not be small in the absence of a shielding wall; however, in this case (14) does not apply. Substituting the same parameters in (15) and assuming that $p = 0.05$, we find $\vartheta_0 \sim 0.4$.

The vertical force due to the shielding planes is directed toward the planes and leads to an instability. In the case of a closed current ring this force is given approximately by

$$f_z \approx \frac{Ne^2}{a^2}\frac{z}{a}\left\{\frac{1}{\gamma^2}\frac{\pi}{8p^2} + \beta^2 \ln\frac{1}{p}\right\}, \tag{16}$$

where z is the displacement of the bunch from the median plane. It is assumed that $|z| \ll b$. Using reasonable values we find that the force in (16) is considerably smaller than the magnetic focusing force and need not be considered in practice.

---

[1] L. V. Ioganesen and M. S. Rabinovich, JETP **37**, 118 (1959), Soviet Phys. JETP **10**, 83 (1960).

[2] L. V. Ioganesen, JETP **37**, 299 (1959), Soviet Phys. JETP **10**, 211 (1960).

[3] L. Schiff, Rev. Sci. Instr. **17**, 6 (1946).

[4] J. S. Nodvick and D. S. Saxon, Phys. Rev. **96**, 180 (1954).

Translated by H. Lashinsky
231

SOVIET PHYSICS JETP VOLUME 11, NUMBER 4 OCTOBER, 1960

QUANTUM OSCILLATIONS OF THE PHOTOELECTRIC YIELD OF METALS IN A MAGNETIC FIELD

G. E. ZIL'BERMAN and I. O. KULIK

Khar'kov Military Institute of Aviation Engineering; Khar'kov State University

Submitted to JETP editor October 9, 1959

J. Exptl. Theoret. Phys. (U.S.S.R.) 38, 1188-1200 (March, 1960)

The quantum oscillations of the volume (external) photoelectric effect in metals in a magnetic field are investigated in the ultraviolet region of the spectrum for electrons obeying an arbitrary dispersion law. The expression for the photocurrent contains, besides oscillations of the de Haas-van Alphen type, some new terms which are also characteristic of other optical phenomena. It is shown that a study of the photocurrent oscillations and the photoelectron energy distribution function permits one, in principle, to determine the shape of the Fermi surface as well as the arrangement of the separate electron groups in the reciprocal lattice and also to determine the shape of the isoenergetic surfaces lying below the Fermi surface. The calculation is carried out for the case where the magnetic field is perpendicular to the surface. The influence of collisions between photoelectrons prior to exit from the metal on the oscillations of the photoelectron yield is investigated.

1. INTRODUCTION

THE investigations of recent years, starting with the work of Lifshitz, Kosevich, and Pogorelov,[1] have brought out that it is very important to study the quantum oscillation effects if one of the basic problems of the electron theory of metals, the determination of the dispersion law for the conduction electrons in actual metals, is to be solved.*

The best known of these effects are the de Haas-van Alphen effect (oscillations of the magnetic susceptibility of metals in a varying magnetic field) and the related Shubnikov-de Haas effect (oscillations of the electric resistance). A careful experimental study of the de Haas-van Alphen effect carried out by Verkin, Lazarev, and co-workers in the U.S.S.R.[3] and by Shoenberg (cf. reference 4 and others) in England has already led to the determination of the shape of the Fermi surface in a number of actual cases.

In the present paper we consider the external photoelectric effect in metals in a magnetic field in the ultraviolet region of the spectrum. The magnetic field is directed perpendicular to the surface, so that the electrons reach the anode freely. Under these conditions the photoelectron current contains, besides the a component which changes monotonically with H, several oscillatory components. One of these is due to the same oscillations of the number of states of the electrons in the magnetic field which give rise to the de Haas-van Alphen effect. The periods are in this case determined by the extremal[1] (or limiting[5]) cross sections of the Fermi surface.

The second component is due to the periodic dependence of the transition matrix element on the magnetic field. It has nothing to do with the number of states and represents a new oscillatory effect which is common to all optical phenomena connected with transitions between bands. The study of this effect allows us, in principle, to determine the arrangement of separate regions of the Fermi surface in the reciprocal lattice. This possibility of determining the location of the separate groups, which did not exist previously, is due to the presence of a new parameter in the optical effects: the frequency of light. The third component represents the interference effect.

Another new piece of information which may be obtained from photoelectric experiments (measuring the energy distribution of the emitted electrons) is the shape of the isoenergetic surfaces lying below the Fermi surface. Finally, it is an interesting feature of photoelectric experiments that they permit us, in principle, to study in relatively weak fields large electron groups, whose oscillations are washed out under the usual conditions on account of the domain structure.[1] In photoelectric experiments one can use a narrow light beam which takes in only one domain.

---

*The study of the resonance effects serves the same purpose (cf. Azbel' and Kaner[2]).

In conclusion we note the important circumstance that the effect under consideration, just as the de Haas-van Alphen effect, depends practically only on the dispersion law and not on its genesis (the wave functions).

2. THE VOLUME PHOTOEFFECT IN A METAL

It is known that the absorption of light by a conduction electron near the surface, as a result of which the electron leaves the metal (surface photoeffect[6,7]), is possible only if the energy conservation law is fulfilled, whereas the extra momentum can be transferred to the surface. This effect occurs for the frequencies $\omega \geq \omega_g$, where $\omega_g = W/\hbar$ (W is the work function).

For a light frequency ω which surpasses the second photoelectric threshold, $\omega \geq \omega_g'$ the so-called volume photoeffect becomes possible,[6,8,9] in which the electron first goes from the conduction band to a higher lying band and then leaves the metal. The photoelectrons are thus not excited in a thin surface layer, but in a volume of metal of thickness δ (δ is the penetration depth of the light in the metal, $\delta \gg a$). The yield of the volume photoeffect is therefore in general much greater than the yield of the surface effect.

Usually the maxima of the spectral distribution curves of the yield for these two types of the photoeffect do not overlap, since ω_g, as a rule, lies in the visible or near the ultraviolet region, while ω_g' lies in the more remote ultraviolet.* In the following we shall consider the photoeffect in the ultraviolet region of the spectrum, assuming that it can be separated from the surface effect. The energy of the electrons in this case is sufficiently large, so that one can neglect the reflection of the electrons from the surface potential barrier and from the distortions of the periodic potential near the surface. The calculation of the current of emitted electrons reduces then to the calculation of the current towards the surface inside the metal.

All oscillatory effects are observed only at very low temperatures and in pure metals, and the penetration depth of light in the metal, δ, is small ($\delta \sim 10^{-5}$ to 10^{-6} cm). Collisions of the photoelectrons with the phonons (or impurities) do not play any role (besides, they do not change the energy of the electron to any appreciable extent). The collisions of the photoelectron with the other electrons lead, however, to a great loss of energy. As is known (see, for example, reference 13), these losses can be divided into losses due to the excitation of plasma oscillations and losses due to collisions with separate screened electrons.

The free path length for the first interaction (the collective one) is equal to a few lattice constants; however, the excitation of plasma oscillations is possible only after the photoelectron has reached a certain minimal energy E_p. From the experimental data on the characteristic losses of electrons[13,14] it is known that this energy is equal to 20 to 25 ev for many metals. We can therefore choose a metal in which the photoelectrons do not excite plasma oscillations.

As to the losses of the second type (the individual losses), it appears that the corresponding free path length is very great on account of the effective screening. According to reference 15, this length is 100 or more times greater than the lattice constant for slow electrons (photoelectrons) in alkali metals. The calculation of l for the screened Coulomb interaction[13,16,17] of free electrons with account of the exclusion principle gives a value which is several times smaller. However, the band structure of the spectrum either forbids or lowers the probability for a number of transitions which are possible for free electrons, which leads to an increase in l. In the case where the photoelectron with the wave vector $\mathbf{k}_1$ remains in the upper band after the collision while the conduction electron stays in the lower band, the time of free flight can be shown[21] to be equal to

$$\tau = \tau_B (15\pi/8)(\alpha/k_1)^4 D^{-2}.$$

Here $\tau_B = \hbar^3/me^4$ is the characteristic Bohr time, α^{-1} is the screening radius (according to the estimate of references 6 and 13, $\alpha^{-1} \gtrsim 10^{-8}$ cm), and D^{-2} is a factor which depends on the wave functions in both bands, $D^2 < 1$. If $\mathbf{k}_1$ is small, for example, $|\mathbf{k}_1| = \alpha/4$ (here $D^2 = 1/3$), $\tau \approx 10^4 \tau_B$, i.e., the time of flight is large. If both electrons appear in the lower band after the collision, which is possible if k_1 and the width of the forbidden band are small, then

$$\tau = \tau_B (3\pi/8)(a^2 + \lambda)^2 k_0^{-3} \lambda^{-1/2} D^{-2},$$

where λ is the width of the conduction band (multiplied by $m/\hbar^2$). In this case D^2 is always small (for example, of order 10^{-2} to 10^{-4}), so that τ is large again.

The collisions lead to a decrease of the oscillation amplitude [according to reference 18, by a factor $\exp(h/\tau\mu H)$] without change in the period. Since τ depends critically on the band structure of the metal, it may occur that oscillations of the photocurrent are observable in one metal and inobservable in another. It is evidently convenient to conduct the experiments in metals with large $\mu = e\hbar/m^*c$ in strong fields ($H \sim 10^5$ oersted). Here the energy of the photoelectron must be below the level of the discrete (plasma) losses.

---

*This is not true for all metals.[10] Contrary to previous acceptance,[6,7] it has recently been suggested[9,11,12] that the photoeffect in alkali metals in the region 500 to 300 mμ is also predominantly a volume effect.

In conclusion we note that the ultraviolet radiation of the metal causes not only transitions from the conduction band to the higher lying band, but also transitions from the narrow bands below the conduction band into states immediately below the barrier.[19] The two kinds of photoelectrons are easily separated since they have completely different energies after leaving the metal.

3. CALCULATION OF THE PHOTOCURRENT

The Hamiltonian of the electron in a metal placed in a magnetic field can be written in the form

$$\hat{H} = \hat{H}^{(0)} + \hat{V},$$

where

$$\hat{H}^{(0)} = \frac{1}{2m}\left(\frac{\hbar}{i}\nabla - \frac{e}{c}\mathbf{A}^0\right)^2 + V_p(\mathbf{x}); \qquad (1)$$

$$\hat{V} = -\frac{e}{mc}\mathbf{A}\left(\frac{\hbar}{i}\nabla - \frac{e}{c}\mathbf{A}^0\right). \qquad (2)$$

Here $V(\mathbf{x})$ is the periodic potential; $\mathbf{A}^0(-Hy, 0, 0)$ is the vector potential of the constant magnetic field $H = H_z$; $\mathbf{A}$ is the vector potential of the light wave, and is equal to

$$\mathbf{A} = (cF/i\omega)\,\mathbf{a}\exp\{i\varkappa\mathbf{x} - i\omega t\}$$

(F is the amplitude of the electric vector; $\mathbf{a}$ is the polarization vector; $|\mathbf{a}| = 1$).

To solve the Schrödinger equation $\hat{H}\Psi = i\hbar\,\partial\Psi/\partial t$ we must first find the eigenfunctions of the unperturbed problem. Using the results of a previous paper,[20] we write down the orthonormal eigenfunctions of the electron obeying an arbitrary dispersion law in the magnetic field:*

$$\Psi_{k_1nk_3}(\mathbf{x}) = \frac{1}{\sqrt{L}}e^{ik_1x}\frac{1}{\sqrt{L}}e^{ik_3z}$$
$$\times\int g_n(k_2, k_3)\exp\{ik_2(y + \alpha_0^2k_1)\}\,v\left(k_1 + \frac{y}{\alpha_0^2}, k_2, k_3; x, y, z\right)dk_2, \qquad (3)$$

where $v(\mathbf{k}; \mathbf{x})$ is a periodic Bloch function normalized in the "region of periodicity" of volume L^3 according to

$$L^{-3}\int|v|^2\,d\tau = 1.$$

In formula (3) $g_n(k_2, k_3)$ is the eigenfunction of the electron in the magnetic field in the $\mathbf{k}$ representation. It is given by

$$g_n(k_2, k_3) = \frac{\hbar A}{\pi\sqrt{m}}\left|\frac{\partial E}{\partial\varkappa_1}\right|^{-1/2}\exp\{-i\alpha_0^2\varkappa_{10}(k_2 - k_{20})\}\cos\left(\alpha_0^2S_n(k_2) - \frac{\pi}{4}\right). \qquad (4)$$

The trajectory of the electron in the reciprocal space (Fig. 1) is given by the intersection of the isoenergetic surface $E(\mathbf{k}) = E$ with the plane $k_3 = \text{const}$; correspondingly, the equation of the trajectory $\kappa_1 = \kappa_1(k_2)$ is found from the relation $E(\kappa_1, k_2, k_3) = E$; $\alpha_0 = (\hbar c/eH)^{1/2}$ is the radius of the lowest quantum mechanical orbit of the free electron, $a/\alpha_0 \ll 1$ (a is the lattice constant); the meaning of the area $S_n(k_2)$ is clear from Fig. 1.

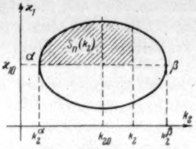

FIG. 1

For the sake of generality, we consider an arbitrary group of electrons whose center (κ_{10}, k_{20}) does not coincide with the origin of a cell of the reciprocal lattice. The dimensionless constant A is found from the normalization condition:

$$2\pi\int|g_n(k_2, k_3)|^2\,dk_2 = 1.$$

The corresponding wave function for the total Hamiltonian $\hat{H}$ is sought in the form

$$\Psi(\mathbf{x}, t) = \psi_{k_1nk_3}(\mathbf{x})\exp\{-iE_n(k_3)t/\hbar\} + \Phi(\mathbf{x}, t),$$

where $\Phi(\mathbf{x}, t)$ is the perturbation term. The expansion of Φ in terms of the complete orthonormal system of functions has the form

$$\Phi(\mathbf{x}, t) = \sum_{n'}\int dk_1'dk_3'\,C_{k_1'n'k_3'}\,\psi'_{k_1'n'k_3'}(\mathbf{x})\exp\left\{-\frac{iE'_{n'}(k_3')t}{\hbar}\right\}$$

[the prime characterizes functions of the electron in the upper band; $v'(\mathbf{k}; \mathbf{x})$ is a Bloch function for the upper band; $g'_{n'}(k_2, k_3)$ has a form analogous to (4)]. The usual perturbation theory leads to the following expression for the coefficients $C_{k_1'n'k_3'}$:

---

*We neglect the effect of the boundary of the metal. The wave function for the finite metal differs from the wave function (3) by an additional exponentially decreasing (at a distance ~ a from the boundary) term. Since in the calculation of the transition probability we are interested in the overlap integral of the eigenfunctions of the initial and final states ψ and ψ' (cf. below), the exponentially decreasing term can be neglected (this cannot be done in the calculation of the surface effect, where the basic integral without account of the boundary reduces to zero in virtue of the orthonormality).

$$C_{k_1' n' k_3'} = \left(\frac{L}{2\pi}\right)^2 \frac{\pi e F}{m\omega} M^{k_1' n' k_3'}_{k_1 n k_3} \delta(E' - E - \hbar\omega), \tag{5}$$

where the matrix element for the transition is equal to

$$M^{k_1' n' k_3'}_{k_1 n k_3} = \int \psi^{*'}_{k_1' n' k_3'}(\mathbf{x})\, \mathbf{a}\left(\frac{\hbar}{i}\nabla - \frac{e}{c}\mathbf{A}^0\right)\psi_{k_1 n k_3}(\mathbf{x})\, d\tau$$

(in this formula we neglect the factor $e^{i\boldsymbol{\kappa}\cdot\mathbf{x}}$, since the wave vector of the photon $\boldsymbol{\kappa}$ is much smaller than the wave vector of the electron $\mathbf{k}$: $\kappa \ll k$). With the help of formula (3) we write this expression in the form

$$M^{k_1' n' k_3'}_{k_1 n k_3} = \int g^{*'}_{n'}(k_2', k_3')\, \chi(\mathbf{k}', \mathbf{k})\, g_n(k_2, k_3)\, dk_2\, dk_2', \tag{6}$$

where

$$\chi(\mathbf{k}', \mathbf{k}) = \frac{\hbar L}{a} \delta_{k_1 k_1'} \delta_{k_3 k_3'} \sum_{m=-\infty}^{\infty} \sigma_m(k_2, k_3)\, \delta_{k_2', k_2 + ma/\alpha_0^2}. \tag{7}$$

Here the σ_m are certain dimensionless coefficients (which depend weakly on the magnetic field) which can be expressed in terms of the Bloch functions of the conduction band and the higher lying band. Substituting (7) in (6) we obtain the matrix element for the transition in the form

$$M^{k_1' n k_3'}_{k_1 n k_3} = \frac{2\pi\hbar}{a} S_{nn'}(k_3)\, \delta_{k_1 k_1'}\, \delta_{k_3 k_3'}, \tag{8}$$

where

$$S_{nn'}(k_3) = \sum_m \int g^{*'}_{n'}(k_2 + ma/\alpha_0^2, k_3)\, \sigma_m(k_2, k_3)\, g_n(k_2, k_3)\, dk_2.$$

Using the condition $a/\alpha_0 \ll 1$ and formula (4) for the eigenfunctions $g_n(k_2, k_3)$ we transform $S_{nn'}$ to the form

$$S_{nn'}(k_3) = \int g^{*'}_{n'}(k_2, k_3)\, \sigma(k_2, k_3)\, g_n(k_2, k_3)\, dk_2, \tag{9}$$

where

$$\sigma(k_2, k_3) = \sum_m \sigma_m(k_2, k_3) \exp\{ima\,\varkappa_1(k_2)\}$$

is a quantity which depends smoothly on the magnetic field. As was mentioned already, we must know the exact eigenfunctions of the electron in the metal (Bloch functions) in order to calculate $\sigma(k_2, k_3)$. However, a number of effects in the magnetic field, in particular, the oscillations of the photoelectric current with the magnetic field, do not depend on the actual form of these functions. These oscillations are determined by the functions $g_n(k_2, k_3)$ and $g'_{n'}(k_2, k_3)$, which depend only on the dispersion law. The exact wave functions are needed only for the calculation of the amplitude of the oscillations. But since σ is a dimensionless quantity of order unity, one can estimate the order of magnitude of the amplitudes.

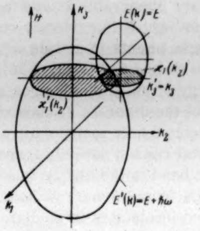

FIG. 2

Thus the oscillatory properties of the transition depend on the dispersion law for the electrons in the metal and not on its genesis.

It is seen from formulas (5) and (8) that the transitions considered above obey the following selection rules:

$$k_3' = k_3, \quad E'_{n'}(k_3') = E_n(k_3) + \hbar\omega$$

(the condition $k_1' = k_1$ implies, moreover, that the "center of rotation" does not change during the transition). The trajectories of the electron in the initial $[\kappa_1(k_2)]$ and final $[\kappa_1'(k_2)]$ states are shown in Fig. 2. Here $E(\mathbf{k})$ and $E'(\mathbf{k})$ determine the dispersion law for the electron in the conduction band and the upper band, respectively. Since the functions $g_n(k_2, k_3)$ decrease very fast (exponentially) outside the region of classical motion of the electron (see reference 20), the quantities $S_{nn'}(k_3)$ and the matrix element for the transition will be different from zero only if the trajectories $\kappa_1(k_2)$ and $\kappa_1'(k_2)$ intersect each other (Fig. 2). Otherwise the matrix element for the transition is negligibly small, and the photon yield from this group of electrons is zero.

Knowing the perturbed wave function, we can find the current of emitted electrons according to the known quantum mechanical formula

$$j_z(n, k_3) = \frac{ieh}{2m}\left(\Phi \frac{\partial \Phi^*}{\partial z} - \Phi^* \frac{\partial \Phi}{\partial z}\right);$$

$j_z(n, k_3)$ represents the current corresponding to a given initial state n, k_3. To find the total current J_z we must sum this quantity over all electrons in the metal, which gives

$$J_z = \frac{L^3}{2\pi^2\alpha_0^2} \sum_n \int \frac{1}{\exp\{(E - \zeta)/\theta\} - 1} \bar{j}_z(n, k_3)\, dk_3, \tag{10}$$

where $\bar{j}_z(n, k_3)$ denotes the average value of the current density. It is easily seen that the function $\psi_{k_1 n k_3}(\mathbf{x})$ [formula (3)] corresponds to the current

$$\breve{j}_z = (e/\hbar L^3)\,\partial E_n(k_3)/\partial k_3.$$

We calculate the current $\bar{j}_z(n, k_3)$ with the help of (5) and (8) and substitute it in formula (10). Taking account of $\delta_{k_1k_1'}$, $\delta[E_{n'}'(k_3') - E_n(k_3) - \hbar\omega]$, and $\delta_{k_3k_3'} = (2\pi/L)\,\delta(k_3 - k_3')$ in the integration over dk_1', dk_3', and dk_3, respectively, we obtain

$$J_z = \frac{\pi e^3\hbar F^2 L}{m^2a^2\omega^2\alpha_0^2}\sum_{n,n'}\left(e^{(E-\zeta)/\theta}+1\right)^{-1}|S_{nn'}(k_3)|^2\left|\frac{\partial H_{nn'}}{\partial k_3}\right|^{-1},$$

$$H_{nn'}(k_3) = E_{n'}'(k_3') - E_n(k_3) - \hbar\omega. \qquad (11)$$

Up to this point we have not taken into account the attenuation of the light wave in the metal, as a consequence of which the photocurrent appeared to be proportional to the thickness of the cathode L. It can be shown that the consideration of the damping leads to the replacement of the quantity L in formula (11) by δ, the penetration depth of the field in the metal (we assume $\delta \gg a$). Then the photocurrent per unit area of the surface ceases to depend on the thickness of the cathode, if $L > \delta$.

To change the summation in formula (11) to an integration, we use the Poisson summation formula:

$$\sum_{n=0}^{\infty} f(n) = \frac{1}{2}f(0) + \sum_{p=-\infty}^{\infty}\int_0^{\infty} e^{2\pi ipn}f(n)\,dn,$$

and apply it to the summation over n and n′. We also introduce the following notations. For the calculation of the quantities $S_{nn'}$ we must use the method of steepest descent, and it will turn out (see below) that $S_{nn'}$ has in the general case the form

$$|S_{nn'}(k_3)|^2 = \left(\frac{a}{\alpha_0}\right)^2\sum_{\alpha}\vartheta_{nn'}^{(\alpha)}(k_3)\cos\left(\alpha_0^2\sigma_\alpha(E, k_3) + \gamma_\alpha\right), \qquad (12)$$

where the $\vartheta_{nn'}^{(\alpha)}$ are certain coefficients which depend smoothly on the magnetic field, and the $\sigma_\alpha(E, k_3)$ are areas which determine the oscillations of the matrix element of the transition; the γ_α are certain phases, $\sigma_0 = 0$, $\gamma_0 = 0$; $\vartheta_{nn'}^{(0)}$, represents the non-oscillatory term.

In this way we transform (11) to the form

$$J_z = \sum_{\alpha}\sum_{p,q=-\infty}^{\infty} e^{-i\pi p - i\pi q}\int dk_3\int dS\,\frac{\Lambda^{(\alpha)}(S,k_3)}{\exp\{(E-\zeta)/\theta\}+1}\exp\{ip\alpha_0^2S\}$$

$$\times\exp\{iq\alpha_0^2S'(E, k_3)\}\cos[\alpha_0^2\sigma_\alpha(E, k_3) + \gamma_\alpha], \qquad (13)$$

where

$$\Lambda^{(\alpha)} = \frac{e^3\hbar F^2\delta}{4\pi m^2\omega^2}\left(\frac{\partial S'}{\partial k_3}\right)_S\vartheta_{nn'}^{(\alpha)}(k_3)\left|\frac{\partial H_{nn'}}{\partial k_3}\right|^{-1} \qquad (14)$$

is a quantity which depends smoothly on the magnetic field. J_z in formula (13) represents the photocurrent from the given electron group. The total current is obtained by summing over all groups in the conduction band.

Changing the integration over dS in formula (13) to an integration over the energy, with the help of the formula for the semiclassical quantization of the energy levels of the electron in the magnetic field,[1,20]

$$S(E, k_3) = 2\pi\left(n + \tfrac{1}{2}\right)/\alpha_0^2,$$

we can write the photocurrent J_z in the form of a sum:

$$J_z = J_z^0 + J_z^1 + J_z^2 + J_z^{12}, \qquad (15)$$

$$J_z^0 = \int_0^{\infty}\frac{dE}{\exp\{(E-\zeta)/\theta\}+1}\int dk_3\,\frac{\partial S}{\partial E}\,\Lambda^{(0)}(E, k_3), \qquad (16)$$

$$J_z^1 = 2\,\mathrm{Re}\sum_{p=1}^{\infty} e^{-i\pi p}\int_0^{\infty}\frac{dE}{\exp\{(E-\zeta)/\theta\}+1}\int dk_3\,\frac{\partial S}{\partial E}\,\Lambda^{(0)}(E, k_3)$$

$$\times\exp\{ip\alpha_0^2S(E, k_3)\}, \qquad (17)$$

$$J_z^2 = \mathrm{Re}\sum_{\alpha\neq 0}\int_0^{\infty}\frac{dE}{\exp\{(E-\zeta)/\theta\}+1}\int dk_3\,\frac{\partial S}{\partial E}\,\Lambda^{(\alpha)}(E, k_3)$$

$$\times\exp\{i\alpha_0^2\sigma_\alpha(E, k_3) + i\gamma_\alpha\}. \qquad (18)$$

Here J_z^0 is the non-oscillatory part of the current; J_z^1 is the oscillatory part of the current due to the periodic dependence of the number of states on the magnetic field (analogous to the de Haas-van Alphen effect); J_z^2 is the oscillatory part of the current due to the periodic dependence of the matrix element of the transition on the magnetic field; J_z^{12} is the oscillatory part of the current corresponding to the interference of parts 1 and 2, which we shall not write down explicitly.

In the case of the volume photoeffect we therefore have to do with two types of oscillations of the photoyield with the magnetic field: 1) oscillations connected with the number of states (J_z^1), analogous to the de Haas-van Alphen and Shubnikov-de Haas effects etc., and 2) oscillations connected with the matrix element for the transition (J_z^2), which are characteristic for all optical phenomena (volume photoeffect, absorption of light in metals, etc.) related to transitions between different energy bands.

4. THE OSCILLATORY PARTS OF THE CURRENT

1. The oscillatory part of the current connected with the number of states is given by formula (17). The integrals in (17) can be evaluated by the method of steepest descent, so that the final answer will contain the extremal Fermi cross sections $S_m(\zeta)$, just as in the case of the de Haas-van Alphen effect.[1] We find

$$J_z^1 = \frac{2\sqrt{2\pi}}{\alpha_0^3}\Lambda^{(0)}(\zeta, k_{3m})\left|\frac{\partial^2 S}{\partial k_3^2}\right|_m^{-1/2}\sum_{p=1}^{\infty}p^{-1/2}\frac{z}{\operatorname{sh} pz}\sin\left[p\alpha_0^2S_m(\zeta) - \pi p \pm \frac{\pi}{4}\right], \qquad (19)$$

where

$$z = 2\pi^2\theta/\mu^* H,\ \mu^* = e\hbar/m^* c,\ m^* = (\hbar^2/2\pi)\,\partial S_m/\partial\zeta. \quad (20)$$

In the limiting cases of weak and strong magnetic fields ($z \gg 1$ and $z \ll 1$) we have:

for $z \gg 1$,

$$J_z^1 = \frac{2\,(2\pi)^{3/2}\theta}{\alpha_0}\,\Lambda^{(0)}(\zeta,\ k_{3m})\,\frac{\partial S_m}{\partial\zeta}\left|\frac{\partial^2 S}{\partial k_3^2}\right|_m^{-1/2}\exp\left\{-2\pi^2\frac{\theta}{\mu^* H}\right\}$$
$$\times\sin\left[\alpha_0^2 S_m(\zeta) - \pi \pm \frac{\pi}{4}\right]; \quad (21)$$

for $z \ll 1$,

$$J_z^1 = \frac{2\,(2\pi)^{1/2}}{\alpha_0^3}\,\Lambda^{(0)}(\zeta,\ k_{3m})\left|\frac{\partial^2 S}{\partial k_3^2}\right|_m^{-1/2}\sum_{p=1}^{\infty} p^{-3/2}$$
$$\times\sin\left[p\alpha_0^2 S_m(\zeta) - \pi p \pm \frac{\pi}{4}\right]. \quad (22)$$

Let us estimate the relative magnitude of the oscillatory terms as compared with the non-oscillatory term J_z^0, assuming that by order of magnitude

$$J_z^0 = \int_0^{\zeta} dE \int dk_3\,\frac{\partial S}{\partial E}\,\Lambda^{(0)}(E,\ k_3) \sim \zeta\bar{\Lambda}^{(0)}\,\frac{2\pi m}{\hbar^2}\left(\frac{2m\zeta}{\hbar^2}\right)^{1/2}.$$

We find

$$J_z^1/J_z^0 \sim \frac{4\pi}{\sqrt{2}}\left(\frac{\mu H}{\zeta}\right)^{1/2}\frac{\theta}{\zeta}\,\frac{m^*}{m}\,\bar{\Lambda}_s^{(0)}/\bar{\Lambda}^{(0)},\quad z \gg 1; \quad (23)$$

$$J_z^1/J_z^0 \sim \frac{1}{\pi\sqrt{2}}\left(\frac{\mu H}{\zeta}\right)^{3/2}\bar{\Lambda}_s^{(0)}/\bar{\Lambda}^{(0)},\quad z \ll 1. \quad (24)$$

Here $\bar{\Lambda}_s^{(0)}$ is the average value of $\Lambda^{(0)}(E,\ k_3)$ for the given (s-th) group, and $\bar{\Lambda}^{(0)}$ is the analogous quantity for the basic group; m is the mass of the free electron; $\mu = e\hbar/mc$ [here the oscillatory part of the current J_z^1 refers to the given electron group (which is small, for example), while the non-oscillatory part J_z^0 refers to the basic (large) group].

For an estimate of the ratio $\Lambda_s^{(0)}/\Lambda^{(0)}$ we assume that approximately

$$\bar{\Lambda}_s^{(0)}/\bar{\Lambda}^{(0)} \sim \bar{\vartheta}_{nn's}^{(0)}/\bar{\vartheta}_{nn'}^{(0)}$$

[cf. formula (14)], which leads to the very crude estimate

$$\bar{\Lambda}_s^{(0)}/\bar{\Lambda}^{(0)} \sim (n_0/n)^{1/3},$$

where n_0 is the density of the electrons of the basic group, and n that of the given group.

2. The oscillatory part of the current connected with the matrix element of the transition is given by formula (18). The calculation of J_z^2 is analogous to that of J_z^1; as a result we have

$$J_z^2 = \frac{(2\pi)^{1/2}}{\alpha_0^3}\sum_{\alpha\neq 0}\Lambda^{(\alpha)}(\zeta,\ k_{3m})\left|\frac{\partial^2\sigma_\alpha}{\partial k_3^2}\right|^{-1/2}\frac{\partial S(\zeta,\ k_{3m}^{\alpha}),\partial\zeta}{\partial\sigma_\alpha^m/\partial\zeta}\,\frac{z_\alpha}{\sinh z_\alpha}$$
$$\times\sin\left[\alpha_0^2\sigma_\alpha^m(\zeta) + \gamma_\alpha \pm \frac{\pi}{4}\right], \quad (25)$$

where

$$z_\alpha = 2\pi^2\theta/\mu_\alpha^* H,$$
$$\mu_\alpha^* = e\hbar/m_\alpha^* c,\quad m_\alpha^* = (\hbar^2/2\pi)\partial\sigma_\alpha^m/\partial\zeta \quad (26)$$

[$\sigma_\alpha^m(\zeta)$ is the extremal value of the area σ_α; $k_3 = k_{3m}^{\alpha}$ is the extremal point]. In the limiting cases $z_\alpha \gg 1$ and $z_\alpha \ll 1$ formula (25) gives:

for $z_\alpha \gg 1$

$$J_z^2 = \frac{(2\pi)^{3/2}\theta}{\alpha_0}\sum_{\alpha\neq 0}\Lambda^{(\alpha)}(\zeta,\ k_{3m}^{\alpha})\,\frac{\partial S(\zeta,\ k_{3m}^{\alpha})}{\partial\zeta}\left|\frac{\partial^2\sigma_\alpha}{\partial k_3^2}\right|_m^{-1/2}$$
$$\times\exp\left\{-2\pi^2\frac{\theta}{\mu_\alpha^* H}\right\}\sin\left[\alpha_0^2\sigma_\alpha^m(\zeta) + \gamma_\alpha \pm \frac{\pi}{4}\right]; \quad (27)$$

for $z_\alpha \ll 1$

$$J_z^2 = \frac{(2\pi)^{1/2}}{\alpha_0^3}\sum_{\alpha\neq 0}\Lambda^{(\alpha)}(\zeta,\ k_{3m}^{\alpha})\left|\frac{\partial^2\sigma_\alpha}{\partial k_3^2}\right|_m^{-1/2}\frac{\partial S(\zeta,\ k_{3m}^{\alpha})/\partial\zeta}{\partial\sigma_\alpha^m/\partial\zeta}$$
$$\times\sin\left[\alpha_0^2\sigma_\alpha^m(\zeta) + \gamma_\alpha \pm \frac{\pi}{4}\right]. \quad (28)$$

The period of the oscillations is in this case equal to

$$\Delta(1/H) = 2\pi e/\hbar c\sigma_\alpha^m(\zeta). \quad (29)$$

The order of magnitude of the oscillation amplitudes is estimated in the same way as under point 1. We have

$$z_\alpha \gg 1:\quad J_z^2/J_z^0 \sim \frac{2\pi}{\sqrt{2}}\,g_\alpha\left(\frac{\mu H}{\zeta}\right)^{1/2}\frac{\theta}{\zeta}\,\frac{m^*}{m}\,\bar{\Lambda}_s^{(\alpha)}/\bar{\Lambda}^{(0)}, \quad (30)$$

$$z_\alpha \ll 1:\quad J_z^2/J_z^0 \sim \frac{g_\alpha}{2\pi\sqrt{2}}\left(\frac{\mu H}{\zeta}\right)^{3/2}\frac{m^*}{m_\alpha^*}\,\bar{\Lambda}_s^{(\alpha)}/\bar{\Lambda}^{(0)}, \quad (31)$$

where $g_\alpha = (1/2\pi)\,|\partial^2\sigma_\alpha/\partial k_3^2|_m^{-1/2}$. As before, $\bar{\Lambda}_s^{(\alpha)}/\bar{\Lambda}^{(0)} \sim (n_0/n)^{1/3}$. The meaning of the quantities $\sigma_\alpha^m(\zeta)$, m_α^*, and g_α will be explained below (point 4).

3. The oscillatory component due to interference J_z^{12} has in general a very complicated form. It contains oscillatory terms of the type

$$\sin\left[\alpha_0^2(pS + qS' \pm \sigma_\alpha) + \delta\right]$$

(and a few others). However, if we are interested only in low frequency oscillations corresponding to small groups and in weak fields ($z \gg 1$), we can restrict ourselves to the term $\sin[\alpha_0^2(S - \sigma_\alpha) + \delta]$. The quantity $S - \sigma_\alpha = \sigma'_\alpha$ represents the area complementary to σ_α (see Fig. 3).

4. For the calculation of the amplitudes $\vartheta_{nn'}^{(\alpha)}(k_3)$ and the areas $\sigma_\alpha(E,\ k_3)$ we turn to the formulas (12) and (9). The integral (9) is computed by the method of steepest descent. The saddle points are given by the intersections of the trajectory of the electron in the initial and final bands, t_1 and t_2. $\sigma_\alpha(E,\ k_3)$ represents the shaded area in Fig. 3 [the final answer contains the extremal Fermi value of this area $\sigma_\alpha^m(\zeta)$].

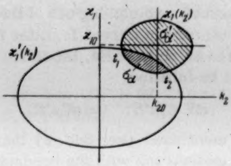

FIG. 3

As already mentioned, it is necessary for the occurence of a photoyield from the given (for example, small) electron group that the isoenergetic surfaces $E(\mathbf{k}) = \zeta$ and $E'(\mathbf{k}) = \zeta + \hbar\omega$ intersect. The low frequency oscillations corresponding to a small electron group (J_Z^1 and J_Z^2) will therefore be confined to some narrow interval of frequencies,

$$\omega_0 - \Delta\omega \leqslant \omega \leqslant \omega_0 + \Delta\omega_0,$$

where, in order of magnitude, $\Delta\omega/\omega_0 \sim 2(n/n_0)^{1/3}$ (see Fig. 4; the isoenergetic surfaces of the upper band are schematically represented by spheres). The position of the center of this interval, ω_0, is determined by the arrangement of the small electron group in the reciprocal lattice.

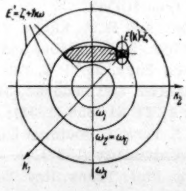

FIG. 4

In the investigation of the oscillations of the photoelectric yield (and also of the coefficient of the absorption of light and of some other optical quantities) we can therefore not only determine the shape of the Fermi surface, as in the oscillation effects of the type of the de Haas-van Alphen effect, but also the location of the centers of the groups.

Let us consider the spectral distribution of the oscillation frequencies $\Omega = 2\pi/\Delta(1/H)$:

$$\Omega(\omega) = (\hbar c/e)\,\sigma_\alpha^m(\zeta, \omega). \tag{32}$$

The function $\Omega(\omega)$ has the characteristic behavior shown in Fig. 5, where the $\omega_0^{(k)}$ correspond to the centers of the groups which alternately intersect the surface $E' = \zeta + \hbar\omega$ as the frequency changes. Near the limits of the frequency interval in which the photoyield of the given group occurs, $\sigma_\alpha^m(\zeta, \omega)$, $m_\alpha^*(\omega)$, and $g_\alpha(\omega)$ become very small, so that the oscillation amplitude increases [see formulas (30) and (31)]. Away from the limits of this interval we have, in order of magnitude, $\sigma_\alpha^m \lesssim S_m$, $m_\alpha^* \leq m^*$, and $g_\alpha \sim 1$.

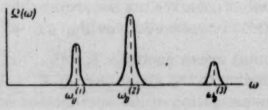

FIG. 5

5. ENERGY DISTRIBUTION OF THE PHOTOELECTRONS

To find the energy distribution of the emitted electrons $Z(E) = dJ_Z/dE$ we turn to the formulas (15) to (18). We have

$$Z(E) = Z^0(E) + Z^1_{\text{osc}}(E) + Z^2_{\text{osc}}(E) + Z^{12}_{\text{osc}}(E);$$

$$Z^0(E) = \frac{1}{\exp\{(E_1 - \zeta)/\theta\} + 1}\int \frac{\partial S}{\partial E_1}\Lambda^{(0)}(E_1, k_3)\,dk_3, \tag{33}$$

$$Z^1_{\text{osc}}(E) = \frac{1}{\exp\{(E_1 - \zeta)/\theta\} + 1}$$

$$\times\ 2\,\mathrm{Re}\sum_{p=1}^{\infty} e^{-i\pi p}\int \frac{\partial S}{\partial E_1}\Lambda^{(0)}(E_1, k_3)\exp\{ip\alpha_0^2 S(E_1, k_3)\}\,dk_3, \tag{34}$$

$$Z^2_{\text{osc}} = \frac{1}{\exp\{(E_1 - \zeta)/\theta\} + 1}\,\mathrm{Re}\sum_{\alpha \neq 0}\int \frac{\partial S}{\partial E_1}\Lambda^{(\alpha)}(E_1, k_3)$$

$$\times\exp\{i\alpha_0^2\sigma_\alpha(E_1, k_3) + i\gamma_\alpha\}\,dk_3, \tag{35}$$

where $E_1 = E - \hbar\omega$ is the energy of the electron before the transition. Here $Z^0(E)$ is the non-oscillatory part of the distribution function; $Z^1_{\text{osc}}(E)$ is the oscillatory part of the energy distribution function of the photoelectrons connected with the number of states; $Z^2_{\text{osc}}(E)$ is that part connected with the matrix element of the transition.

The calculation of the integrals (34) and (35) by the method of steepest descent leads to the expressions

$$Z^1_{\text{osc}}(E) = \frac{1}{\exp\{(E_1 - \zeta)/\theta\} + 1}\,\frac{2(2\pi)^{1/2}}{\alpha_0}\Lambda^{(0)}(E_1, k_{3m})\left|\frac{\partial^2 S}{\partial k_3^2}\right|_m^{-1/2}\frac{\partial S_m}{\partial E_1}$$

$$\times\sum_{p=1}^{\infty} p^{-1/2}\cos\left[p\alpha_0^2 S_m(E_1) - \pi p \pm \frac{\pi}{4}\right], \tag{36}$$

$$Z^2_{\text{osc}}(E) = \frac{1}{\exp\{(E_1 - \zeta)/\theta\} + 1}\,\frac{(2\pi)^{1/2}}{\alpha_0}$$

$$\times\sum_{\alpha \neq 0}\Lambda^{(\alpha)}(E_1, k_{3m}^\alpha)\,\frac{\partial S(E_1, k_{3m}^\alpha)}{\partial E_1}\left|\frac{\partial^2\sigma_\alpha}{\partial k_3^2}\right|_m^{-1/2}\cos\left[\alpha_0^2\sigma_\alpha^m(E_1)\right.$$

$$\left.+\ \gamma_\alpha \pm \frac{\pi}{4}\right]. \tag{37}$$

In contrast to the saturation current J_Z, the oscillations of the energy distribution function of the photoelectrons are not determined by the extremal Fermi cross sections $S_m(\zeta)$, $\sigma_\alpha^m(\zeta)$, but by the extremal cross sections $S_m(E_1)$, $\sigma_\alpha^m(E_1)$ corresponding to the given energy $E_1 = E - \hbar\omega$.

The investigation of the oscillations of the energy distribution function of the photoelectrons with the magnetic field permits us, in principle, to determine any arbitrary isoenergetic surface besides the Fermi surface $E(\mathbf{k}) = \zeta$.

Let us now consider the function

$$J_z(E) = \int_0^E Z(E)\,dE.$$

This function is connected with the current-voltage characteristic of the photoelement $J(V)$, i.e., the dependence of the photocurrent on the voltage V at the anode of the photoelement, through the relation $J(V) = J_z - J_z(-eV)$ (here $J_z = J_z(\infty)$ is the saturation current). With the help of formulas (36) and (37) we obtain

$$J_z^1 = \frac{2(2\pi)^{1/2}}{\alpha_0^3}\Lambda^{(0)}(E_1, k_{3m})\left|\frac{\partial^2 S}{\partial k_3^2}\right|_m^{-1/2}\sum_{p=1}^{\infty} p^{-3/2}\sin\left[p\alpha_0^2 S_m(E_1) - \pi p \pm \frac{\pi}{4}\right], \tag{38}$$

$$J_z^2 = \frac{(2\pi)^{1/2}}{\alpha_0^3}\sum_{\alpha\neq 0}\Lambda^{(\alpha)}(E_1, k_{3m}^\alpha)\left|\frac{\partial^2\sigma_\alpha}{\partial k_3^2}\right|_m^{-1/2}\frac{\partial S(E_1, k_{3m}^\alpha)/\partial E_1}{\partial\sigma_\alpha^m/\partial E_1} \times \sin\left[\alpha_0^2\sigma_\alpha^m(E_1) + \gamma_\alpha \pm \frac{\pi}{4}\right]. \tag{39}$$

The order of magnitude of the amplitudes of the oscillatory terms are estimated in analogy to what we did before (Sec. 3, point 4):

$$J_z^1(E)/J_z^0(E) \sim (1/\pi\sqrt{2})(\mu H/E_1)^{3/2}\,\overline{\Lambda}_s^{(0)}/\overline{\Lambda}^{(0)}, \tag{40}$$

$$J_z^2(E)/J_z^0(E) \sim (g_\alpha/2\pi\sqrt{2})(\mu H/E_1)^{3/2}(m^*/m_\alpha^*)\,\overline{\Lambda}_s^{(\alpha)}/\overline{\Lambda}^{(0)}. \tag{41}$$

The $J_z(E)$ oscillate with the magnetic field with the same frequencies as $Z(E)$. However, the function $J_z(E)$ not only oscillates for variations of the magnetic field, but also for variations of E. This leads to oscillations of the current-voltage characteristic of the photoelement $J(V)$ as a function of the voltage at the anode V. The period of these oscillations is equal to

$$\Delta E = 2\pi\alpha_0^{-2}\Big/\frac{\partial S_m}{\partial E_1} = \mu^* H. \tag{42}$$

Correspondingly

$$\Delta V = \mu H\gamma/e, \tag{43}$$

where $\gamma = m/m^*$ for $J_{osc}^1(V)$ and $\gamma = m/m_\alpha^*$ for $J_{osc}^2(V)$. For $H = 10^4$ we have $\Delta V = 10^{-4}\gamma V$.

The instability of the potential at the anode, δV, the non-nonochromatic nature of the light, $\delta\omega$, and collisions of the photoelectrons before leaving the metal can lead to a smoothing out of the oscillations of the current-voltage curve. In order for these oscillations to be observable, the following conditions must be fulfilled:

$$e\delta V \ll \mu^* H; \quad \hbar\delta\omega \ll \mu^* H.$$

We already mentioned (see Sec. 2) that the collisions of photoelectrons with the conduction electrons may give rise to a lowering of the amplitude of the oscillations of the total photocurrent. In the investigation of the oscillations of the energy distribution of the photoelectrons another effect will superpose itself on this effect: the "intermingling" of the electrons as a consequence of the collisions.

The experimentally observed oscillations can be enhanced by applying a variable saw-tooth voltage on the anode of the photoelement and including a resonant circuit tuned to the frequency $\nu = fV_0/\Delta V$, where f and V_0 are the frequency and the amplitude of the sawtooth voltage.

The authors express their gratitude to I. M. Lifshitz and M. I. Kaganov for comments on this work.

---

[1] I. M. Lifshitz and A. M. Kosevich, JETP **29**, 730 (1958), Soviet Phys. JETP **2**, 636 (1959). I. M. Lifshitz and A. V. Pogorelov, Dokl. Akad. Nauk SSSR **98**, 1143 (1954).

[2] M. Ya. Azbel' and E. A. Kaner, JETP **30**, 811 (1956), Soviet Phys. **3**, 772 (1956) and JETP **32**, 896 (1957), Soviet Phys. JETP **5**, 730 (1957).

[3] Verkin, Lazarev, and Rudenko, JETP **20**, 93 and 995 (1950); JETP **21**, 658 (1951); JETP **25**, 471 (1953). B. I. Verkin, Doctoral Dissertation, Khar'kov State University (1957).

[4] D. Shonberg, Phil. Trans. Roy. Soc. London **A425** No. 1 (1952).

[5] G. E. Zil'berman, JETP **34**, 243 (1958), Soviet Phys. JETP 7, 169 (1958).

[6] I. E. Tamm and S. P. Shubin, Z. Physik **68**, 97 (1931).

[7] K. Mitchell, Proc. Roy. Soc. **A146**, 442 (1934).

[8] H. Y. Fan, Phys. Rev. **68**, 43 (1945).

[9] H. Mayer and H. Thomas, Z. Physik **147**, 419 (1957).

[10] R. J. Cashman and E. Bassoe, Phys. Rev. **55**, 63 (1939).

[11] H. Thomas, Z. Physik **147**, 395 (1957).

[12] S. Methfessel, Z. Physik **147**, 442 (1957).

[13] D. Pines, Revs. Modern Phys. **28**, 184 (1956).

[14] Characteristic Electron Energy Losses in Solids, Collection of Transl. Papers, IIL (1959).

[15] S. Methfessel, Helv. Phys. Acta **31**, 303 (1958).

[16] P. A. Wolff, Phys. Rev. **95**, 56 (1954).

[17] M. L. Goldberger, Phys. Rev. **74**, 1269 (1948).

[18] R. B. Dingle, Proc. Roy. Soc. A211, 517 (1952).

[19] H. E. Hinteregger, Phys. Rev. 96, 538 (1954).

[20] G. E. Zil'berman, JETP 32, 296 (1957), Soviet Phys. JETP 5, 208 (1957).

[21] G. L. Zil'berman and I. O. Kulik, Физика металлов и металловедение (Physics of Metals and Metallurgy), in press.

Translated by R. Lipperheide
232

SOVIET PHYSICS JETP VOLUME 11, NUMBER 4 OCTOBER, 1960

THE EFFECT OF AN EXTERNAL ELECTRIC FIELD ON THE SHAPE OF THE INTRINSIC ABSORPTION EDGE IN NON-CONDUCTING CRYSTALS

D. S. BULYANITSA

Leningrad State University

Submitted to JETP editor October 17, 1959

J. Exptl. Theoret. Phys. (U.S.S.R.) **38**, 1201-1204 (April, 1960)

The problem stated in the title is solved using many-electron wave functions. The external electric field is taken into account exactly, but the Coulomb interactions of the electrons and holes are neglected. In the region of the intrinsic absorption edge, the absorption coefficient is obtained for all values of the electric field and frequencies of the absorbed light.

THE change in the shape of the intrinsic absorption edge of non-conducting crystals has been considered by Keldysh.[1] He used the approximate wave functions obtained by Houston[2] for the electron moving in the periodic and uniform fields. As a result, Keldysh concludes that there is a shift of the absorption edge in the red direction. An explicit form was obtained for the absorption coefficient as a function of electric field E and the frequency of the absorbed light ω, for frequencies sufficiently far from the limiting frequency ω_0 of intrinsic absorption without any external field (or for a sufficiently weak electric field). A previous paper by the author[3] was devoted to the same problem; however, it referred only to the case of forbidden transitions and did not contain the bases of the method used.

In the present paper we give a more general discussion. The result obtained for the absorption coefficient holds for all values of E and ω. In the limiting case $E \rightarrow 0$ it goes over to the known expression for the intrinsic absorption by the crystal without an external field.[4]

We assume that our crystal contains N valence electrons and an optical transition involves this system as a whole. The conduction and valence bands we take as simple and non-degenerate. Electron spin is not taken into account. Further, we use single-electron orthogonal localized Wannier functions of the valence band (cf. the review by Haken[5]):

$$a(\mathbf{n}, \mathbf{r}) = N^{-1/2}\sum_{\mathbf{k}} e^{i\mathbf{k}\mathbf{r}} f(\mathbf{k}, \mathbf{r}). \tag{1}$$

where $f(\mathbf{k}, \mathbf{r})$ is the Bloch function of the valence band corresponding to the wave vector $\mathbf{k}$, and the sum is taken over the first Brillouin zone. Wannier functions for the conduction band $\tilde{a}(\mathbf{n}, \mathbf{r})$ are constructed in a similar way.

We write the wave function of the initial ground state of the crystal in the form

$$\Psi_0(\mathbf{r}_1, \mathbf{r}_2, \ldots, \mathbf{r}_N) = A(0; \mathbf{r}_1, \ldots, \mathbf{r}_N) = N^{-1/2} \det|(\mathbf{n}_\alpha, \mathbf{r}_\beta)|. \tag{2}$$

The index $\alpha = 1, 2, \ldots, N$, labels the Wannier functions. The index $\beta = 1, 2, \ldots, N$, labels the electrons. The wave function of the final excited state are taken in the form

$$\Psi(\mathbf{r}_1, \ldots, \mathbf{r}_N) = \sum_{\mathbf{mn}} c(\mathbf{m}, \mathbf{n}) A(\mathbf{m}, \mathbf{n}; \mathbf{r}_1, \ldots, \mathbf{r}_N). \tag{3}$$

The determinant $A(\mathbf{m}, \mathbf{n})$ entering into (3) is similar to the determinant $A(0)$, except that the valence-band Wannier function numbered $\mathbf{m}$ is changed into the conduction-band Wannier function numbered $\mathbf{n}$. The wave function (3) describes the excited state of the crystal, where in the absence of an external field the coefficients $c(\mathbf{m}, \mathbf{n})$ are determined from the Wannier equation.[5] We shall show that the presence of an external electric field only affects the equation for $c(\mathbf{m}, \mathbf{n})$ if the process of direct transfer of electrons by the field into higher bands is considered as improbable. Then the optical transition from the state $\Psi_0(\mathbf{r}_1, \ldots, \mathbf{r}_N)$ to the state $\Psi(\mathbf{r}_1, \ldots, \mathbf{r}_N)$, when the function $c(\mathbf{m}, \mathbf{n})$ corresponds to the continuous spectrum of the Wannier equation, also gives the intrinsic absorption of light by the crystal.

We calculate the matrix element of the transition. The perturbation operator has the form

$$H = \frac{e}{mc}\sum_{i=1}^{N} \mathbf{p}_i \mathbf{A}(\mathbf{r}_i), \tag{4}$$

$\mathbf{r}_i$, $\mathbf{p}_i$ are the coordinate and momentum of the i-th electron and $\mathbf{A}(\mathbf{r})$ is the vector potential field of the light wave. Using (2), (3), and the relation between the Bloch and Wannier functions, we can obtain

$$(\Psi \mid H \mid \Psi_0) = -\frac{ieh}{mc}\mathbf{A}_0 \sum_{\mathbf{mn}} e^{i\varkappa\mathbf{n}} c^*(\mathbf{m},\ \mathbf{n}) \sum_{\mathbf{k}} e^{i(\mathbf{k},\,\mathbf{n}-\mathbf{m})}\mathbf{M}(\mathbf{k}), \tag{5}$$

κ is the wave vector of the photon; $\mathbf{A}_0$ is the amplitude of the vector potential. Here

$$\mathbf{M}(\mathbf{k}) = \int \tilde{u}^*(\mathbf{k},\ \mathbf{r})\,\nabla u(\mathbf{k},\ \mathbf{r})\,d\mathbf{r}, \tag{6}$$

$u(\mathbf{k}, \mathbf{r})$, $\tilde{u}(\mathbf{k}, \mathbf{r})$ are the periodic factors of the Bloch functions of the valence and conduction bands. The integral is taken throughout one cell.

We now obtain an equation for the functions $c(\mathbf{m}, \mathbf{n})$. We assume that $c(\mathbf{m}, \mathbf{n})$ changes little in a distance of the order of the lattice constant, so that it is possible to transfer from discrete vector arguments $\mathbf{m}$ and $\mathbf{n}$ to continuous $\mathbf{r}_2$ and $\mathbf{r}_1$, which correspond to the coordinates of holes in the valence band and electrons in the conduction band. We do not take into account their interaction. If there were no external field, the equation would contain only terms corresponding to the free motion of electrons and holes. Its solution $c(\mathbf{r}_1, \mathbf{r}_2)$ would be a product of plane waves, and (3) would give the usual band states. The absorption coefficient calculated thus by our method will agree with that obtained in reference 4. We will now include the external field. It is not difficult to find in our system the matrix element of the interaction operator of the electrons with the electric field using the functions $A(\mathbf{m}, \mathbf{n})$:

$$\left(\mathbf{m},\ \mathbf{n} \left| \left(\sum_{i=1}^{N} \mathbf{E}\mathbf{r}_i\right) \right| \mathbf{m}',\ \mathbf{n}'\right) = \delta_{\mathbf{mm}'} \int \tilde{a}^*(\mathbf{n},\ \mathbf{r})\,(\mathbf{E}\mathbf{r})\,\tilde{a}(\mathbf{n}',\ \mathbf{r})\,d\mathbf{r}$$
$$-\,\delta_{\mathbf{nn}'} \int a^*(\mathbf{m}',\ \mathbf{r})\,(\mathbf{E}\mathbf{r})\,a(\mathbf{m},\ \mathbf{r})\,d\mathbf{r}. \tag{7}$$

Finally, under the assumptions made, the equation for the functions $c(\mathbf{r}_1, \mathbf{r}_2)$ takes the form (field along the z axis):

$$\left(-\frac{h^2}{2m_1}\nabla_1^2 - \frac{h^2}{2m_2}\nabla_2^2 + eEz_1 - eEz_2\right) c(\mathbf{r}_1,\ \mathbf{r}_2) = \varepsilon c(\mathbf{r}_1,\ \mathbf{r}_2). \tag{8}$$

Here m_1 and m_2 are the effective masses of electrons and holes.

By transforming to relative coordinates $\mathbf{R}$ and $\mathbf{r}$, it is easy to separate the motion of the center of gravity and the relative motion in the plane transverse to the field

$$c(\mathbf{R},\ \mathbf{r}) = L^{-3/2} e^{i\mathbf{K}\mathbf{R}}\, L^{-1} e^{i\lambda_1 x + i\lambda_2 y}\, \varphi(z). \tag{9}$$

Here K is the wave vector of the center of gravity, λ_1 and λ_2 are the components of the two-dimensional wave vector of the relative motion in the transverse plane, and L is the side of the normalization cube. The solution of the equation then remaining, normalized in the energy interval, is well known:[6]

$$\varphi(z) = A\Phi(q), \qquad q = (z - \varepsilon_2 / eE)\,(2\mu eE / h^2)^{1/3},$$
$$A = (2\mu)^{1/3} / \pi^{1/2} (eE)^{1/6} h^{2/3}, \tag{10}$$

ϵ_2 is the energy of the relative motion along the field, μ is the reduced mass of the electron and hole, and Φ is the Airy function.[7]

We consider here the case of allowed optical transitions when

$$\mathbf{M}(0) = \mathbf{M}_0 \neq 0. \tag{11}$$

Using the properties of the sum over $\mathbf{k}$ in (5), it is easy to show that the many-electron matrix element of the optical transition in this case is equal to the product of the usual one-electron matrix elements in the value of the function $c(\mathbf{R}, \mathbf{r})$ at the point $\mathbf{r} = 0$. The probability of the transition is determined from the known formula of quantum mechanics by summing the square of the matrix elements over all possible states. We introduce the expression thus obtained into the usual formula for the optical absorption coefficient:[8]

$$\alpha = 4\pi h\omega w / n\mathscr{E}^2, \tag{12}$$

where w is the probability of an optical transition in unit volume and unit time, n is the refractive index and $\mathscr{E}$ is the electric field of the light wave.

We will express the Airy function entering into (10) in terms of Bessel functions of order $^1/_3$.[7] After carrying out the calculation indicated, we obtain the following results.

In the region $\omega < \omega_0$, in which the crystal is transparent in the absence of external field, the absorption is now different from zero and is given by the formula

$$\alpha = \frac{4\mu e^2}{\pi n m^2 c\omega} \,|\,\mathbf{e}\mathbf{M}_0\,|^2 \frac{(\mu eE)^{1/3}}{(3h)^{2/3}} \int_{x_0}^{\infty} \xi^{1/3} K_{1/3}^2(\xi)\,d\xi,$$
$$x_0 = (2\sqrt{2\mu} / 3heE)\,(h\omega_0 - h\omega)^{3/2}. \tag{13}$$

Here $\mathbf{e}$ is the polarization vector of the light and K is the MacDonald function. For sufficiently large values of $\omega_0 - \omega$ an asymptotic formula can be given:

$$\alpha = \frac{2\mu e^2}{n m^2 c\omega} \,|\,\mathbf{e}\mathbf{M}_0\,|^2 \frac{(\mu eE)^{1/3}}{(3h)^{2/3}} \int_{x_0}^{\infty} \xi^{-2/3} e^{-2\xi}\,d\xi. \tag{14}$$

If it is assumed that in this case the exponential is the most important, formula (14) is close to the corresponding formula in Keldysh's paper. For $\omega = \omega_0$ the absorption coefficient is equal to

$$\alpha_0 = \frac{4}{\pi}\frac{\mu e^2}{n m^2 c\omega} \,|\,\mathbf{e}\mathbf{M}_0\,|^2 \frac{(\mu eE)^{1/3}}{(3h)^{2/3}} \int_{0}^{\infty} \xi^{1/3} K_{1/3}^2(\xi)\,d\xi. \tag{15}$$

In the range $\omega > \omega_0$ the absorption coefficient takes the form

$$\alpha = \alpha_0 + \frac{4\pi}{3}\frac{\mu e^2}{nm^2c\omega}\,|\mathbf{eM}_0|^2\frac{(\mu eE)^{1/3}}{(3h)^{2/3}}\int_0^{y_0}\xi^{1/3}[J_{-1/3}(\xi) + J_{1/3}(\xi)]^2\,d\xi,$$

$$y_0 = (2\sqrt{2\mu}\,/\,3heE)\,(h\omega - h\omega_0)^{3/2}. \qquad (16)$$

We will now take our formula to the limit $E \to 0$. Then $x_0 \to \infty$, and it is seen from (13) that the absorption tends to zero for $\omega < \omega_0$. From (15) it is apparent that α_0 is also zero in this case and the absorption starts at the limiting frequency ω_0. By substituting into (16) the asymptotic expression for the Bessel functions, we verify that it is possible to select the terms tending to zero with the external field and the terms not depending on the field. These latter terms give the correct value of the absorption coefficient for allowed band transitions without an external field

$$\alpha = \frac{4\sqrt{2}}{n}\frac{\mu^{3/2}e^2}{m^2hc\omega}\,|\mathbf{eM}_0|^2\,(h\omega - h\omega_0)^{1/2}. \qquad (17)$$

Expression (17) agrees exactly with the result obtained by Bardeen, Blatt, and Hall.[4] Similarly, it is possible to show that the usual band formula is true also for sufficiently large $\omega - \omega_0$, which agrees with Keldysh's conclusion.

We shall not present here the results for the case of forbidden transitions (they are given in reference 3). The basis of the method used there follows from a consideration of formula (5) of the present paper. The matrix element in this case will contain the derivatives of the function $c(\mathbf{r}_1, \mathbf{r}_2)$ at the point $\mathbf{r}_1 = \mathbf{r}_2$. We note that the formulae thus obtained contain several integrals more complicated than Bessel functions of order $1/3$. The absorption coefficient is different from zero for $\omega < \omega_0$, depends on the polarization of the incident light relative to the electric field, and for $E \to 0$ transforms to the usual band expression varying with frequency as $(\omega - \omega_0)^{3/2}$.[4]

In conclusion I express my deep gratitude to Professor P. P. Pavinskii for interest in the work and discussion.

---

[1] L. V. Keldysh, JETP **34**, 1138 (1958), Soviet Phys. JETP **7**, 788 (1958).

[2] V. W. Houston, Phys. Rev. **58**, 184 (1940).

[3] D. S. Bulyanitsa, Вестник ЛГУ (Bull. Leningrad Univ.), No. 10, 20 (1959).

[4] Bardeen, Blatt, and Hall, Photoconductivity Conference, Atlantic City (November, 1954), New York (1956).

[5] H. Haken, Fortschr. Physik **6**, 271 (1958).

[6] L. D. Landau and E. M. Lifshitz, Квантовая механика, (Quantum Mechanics), Gostekhizdat, (1948), (Transl., Pergamon Press, 1959).

[7] V. A. Fock, Таблицы функций Эйри (Tables of Airy Functions) M. (1946).

[8] D. L. Dexter, Photoconductivity Conference, Atlantic City (November, 1954), New York (1956).

Translated by K. F. Hulme
233

SOVIET PHYSICS JETP VOLUME 11, NUMBER 4 OCTOBER, 1960

ON THE BUILD-UP OF ELECTROMAGNETIC WAVES IN A PLASMA MOVING IN A NON-DISPERSIVE DIELECTRIC IN THE PRESENCE OF A CONSTANT MAGNETIC FIELD

G. G. GETMANTSEV and V. O. RAPOPORT

Radio-Physics Institute, Gor'kiĭ State University

Submitted to JETP editor October 20, 1959

J. Exptl. Theoret. Phys. (U.S.S.R.) **38**, 1205-1211 (April 1960)

We have obtained a dispersion relation that determines the propagation of plane electromagnetic waves in a plasma beam moving in a fixed plasma along the lines of force of a constant and uniform magnetic field. We have found the damping (or build-up) coefficients of the rarefied plasma moving along the magnetic field in a non-dispersive dielectric.

RECENTLY several papers have been published on the propagation of electromagnetic waves in interpenetrating moving media, in particular in plasma beams moving in a fixed plasma or in a non-dispersive dielectric.[1-3] The range of problems for which suitable solutions have been given in sufficient completeness and for which expressions have been obtained for the damping (or build-up) coefficients of the waves is all the same very limited. We attempt in the present paper to remedy this situation partly by solving the problem of the build-up (damping) coefficient of plane electromagnetic waves propagating in a plasma moving in a non-dispersive medium along the lines of force of a constant and uniform magnetic field.

We shall determine the damping coefficients of the waves by a phenomenological method proposed earlier.[2] The main point of this method is that we first find the phenomenological equations that relate the electromagnetic fields in the interpenetrating media. By combining these equations with the Maxwell equations describing the propagation of plane electromagnetic waves, we can obtain a dispersion relation of the form $f(\omega, \mathbf{k}) = 0$, where ω is the frequency of the electromagnetic wave and $\mathbf{k}$ its wave vector. Solving the dispersion relation we find the required damping coefficients for the wave.

We shall derive the dispersion relation for the case where a non-magnetic, anisotropic, and gyrotropic medium I moves in a fixed non-magnetic medium II, which is also anisotropic and gyrotropic. (A plasma in a constant magnetic field has such properties.) The medium II is at rest in the laboratory frame of reference, and its electrical properties are characterized by its dielectric-constant tensor ϵ_{ij}. The medium I, which is related to a frame of reference K', moves uniformly with respect to the medium II and in a straight line along the x axis of the frame K with a velocity v, so that the x and the x' axes coincide and are parallel to the lines of force of the external magnetic field **H**, while the y' and z' axes are parallel to the y and z axes.

The electrical properties of medium I in the frame K' are characterized by the tensor ϵ'_{ij}.[*] Since we have assumed that media I and II are gyrotropic, the tensors ϵ_{ij} and ϵ'_{ij} are Hermitian and thus $\epsilon_{ij} = \epsilon^*_{ji}$ and $\epsilon'_{ij} = \epsilon'^*_{ji}$. As we have in view a plasma in a constant external magnetic field, we shall also assume[4] that $\epsilon_{12} = \epsilon_{13} = \epsilon'_{13} = \epsilon'_{12} = 0$.

Once we know the tensors ϵ_{ij} and ϵ'_{ij}, we can determine the tensors of the moments (the polarization and magnetization tensors) $M_{ij}(II, K)$ and $M_{ij}(I, K')$ in the fixed and the moving media. The components of the electromagnetic fields **D**, **B**, **E**, and **H** which are defined in the frame of reference K, enter, of course, also into the tensor $M_{ij}(II, K)$, and into the tensor $M_{ij}(I, K')$ the components of the fields **D'**, **B'**, **E'**, and **H'** in the frame of reference K', which are found from the unprimed fields by a Lorentz transformation. Using a Lorentz transformation to transform the tensor of the moments $M_{ij}(I, K')$ to the frame of reference K, we can find the resulting tensor of the moments in the frame K

$$M_{ij}(\mathrm{I}, \mathrm{II}, K) = M_{ij}(\mathrm{II}, K) + M_{ij}(\mathrm{I}, K) = (H_{ij} - F_{ij})/4\pi, \qquad (1)$$

---

[*] We assume that the effective electrical field in the presence of two media is equal to the average macroscopic field, since the polarizations are additive only in that case. It is well known that the effective and the average macroscopic fields are equal in a plasma and also in any other sufficiently rarefied medium.[4]

where H_{ij} and F_{ij} are the electromagnetic field tensors in the frame of reference K (refrence 5; cf. footnote on preceding page).

After substituting into the Maxwell equations which contain the curl operator the expressions for plane waves, these equations become

$$\mathbf{D} = -n[\nu\times\mathbf{H}], \qquad \mathbf{B} = n[\nu\times\mathbf{E}], \tag{2}$$

where n is the refractive index of the medium in the frame of reference K, and ν is a unit vector in the direction of propagation of the wave. The condition that there be a nontrivial simultaneous solution of the algebraic equations (1) and (2) for the 12 components of the electromagnetic field vectors means that the determinant of the set (1) and (2) must vanish. The 12-th order determinant easily reduces to a 4-th order one. Writing the latter out in detail we can get, after straightforward, though tedious transformations, the following dispersion relation

$$\begin{aligned}&(\varepsilon_{11} + \dot{\varepsilon}_{11} - 1)\,[(\varepsilon_{22} + \dot{\varepsilon}_{22}\gamma^2 - n^2\cos^2\theta)(\varepsilon_{33} + \dot{\varepsilon}_{33}\gamma^2 - n^2)\\ &\quad + (\varepsilon_{23} + \dot{\varepsilon}_{23}\gamma^3)^2] - n^2\sin^2\theta\,[(\varepsilon_{22} + \dot{\varepsilon}_{22} - \beta^2\varepsilon_{22}\dot{\varepsilon}_{22})\\ &\quad \times(\varepsilon_{33} + \dot{\varepsilon}_{33}\gamma^2 - n^2) + (\varepsilon_{23} + \dot{\varepsilon}_{23}\gamma)^2\\ &\quad - \beta^2(\dot{\varepsilon}_{22}\varepsilon_{23}^2 + \varepsilon_{22}\dot{\varepsilon}_{23}^2\gamma^2)] = 0;\\ &\dot{\varepsilon}_{ii} = (\varepsilon'_{ii} - 1)/(1-\beta^2), \qquad \dot{\varepsilon}_{23} = \varepsilon'_{23}/(1-\beta^2),\\ &\gamma = 1 - n\beta\cos\theta, \qquad \beta = v/c.\end{aligned} \tag{3}$$

The most interesting case of propagation of electromagnetic waves, which can be studied by using Eq. (3), is the case where a plasma moves in a fixed plasma along the lines of force of a constant and uniform magnetic field. In the following, however, we study the simpler case where the plasma moves along the magnetic field in a non-dispersive dielectric. The dispersion relation (3) simplifies then considerably and one can obtain relatively simple solutions after a few additional assumptions.

Assuming that the fixed medium is a non-dispersive dielectric ($\epsilon_{23} = 0$, $\epsilon_{ij} = \epsilon$), we get by rearranging the terms in (3)*

$$\begin{aligned}&\varepsilon(\varepsilon - n^2)^2 + \dot{\varepsilon}_{22}(\varepsilon - n^2)(\varepsilon\gamma^2 + \chi) + \gamma^2\chi(\dot{\varepsilon}_{22}^2 + \dot{\varepsilon}_{23}^2)\\ &\quad + \dot{\varepsilon}_{11}[(\varepsilon - n^2)(\varepsilon - n^2\cos^2\theta + \dot{\varepsilon}_{22}\gamma^2)\\ &\quad + \dot{\varepsilon}_{22}\gamma^2(\varepsilon - n^2\cos^2\theta + \dot{\varepsilon}_{22}\gamma^2) + \dot{\varepsilon}_{23}^2\gamma^4] = 0;\end{aligned} \tag{4}$$

where

$$\begin{aligned}&\dot{\varepsilon}_{11} = \varepsilon'_{11} - 1 = -\omega_0^2(1-\beta^2)/(\omega - \widetilde{\omega})^2,\\ &\dot{\varepsilon}_{22} = -\omega_0^2/\left((\omega - \widetilde{\omega})^2 - \dot{\omega}_H^2\right),\\ &\dot{\varepsilon}_{23} = -i\omega_0^2\dot{\omega}_H/(\omega - \widetilde{\omega})\left[(\omega - \widetilde{\omega})^2 - \dot{\omega}_H^2\right],\\ &\dot{\omega}_H = \omega_H\sqrt{1-\beta^2}, \qquad \chi = \varepsilon\gamma^2 - n^2\sin^2\theta\,(1 - \varepsilon\beta^2),\\ &\tilde{\omega} = kv\cos\theta = \omega n\beta\cos\theta.\end{aligned}$$

The dispersion relation (4) establishes a connection between the frequency ω of the electromagnetic wave and its wave vector **k**. In order to establish the presence of damped (or growing) waves and to find the damping coefficient it is necessary to solve Eq. (4) for ω with real wave numbers k. The presence of plane electromagnetic waves which are damped in time is indicated in this procedure by the existence of complex solutions for ω.*

We study in the following the solutions of the dispersion relation (4) for a rarefied plasma beam, i.e., under the condition that the plasma frequency $\omega_0 = (4\pi e^2 N/m)^{1/2}$ is small compared with the frequency of the wave ω and compared with the characteristic frequencies $\widetilde{\omega} = kv\cos\theta$ and ω_N^*. When, however, we go over to the limiting case of no magnetic field ($\omega_H^* = 0$), we shall assume that $\omega_0 \ll \omega, \widetilde{\omega}$. In solving Eq. (4) we must distinguish between two cases. In the first case none of the denominators in the expressions for the ϵ_{ij}^* tends to zero as $\omega_0 \to 0$, while in the second case at least one of the denominators in the ϵ_{ij}^* tends to zero as $\omega_0 \to 0$. We study first the character of the solutions of Eq. (4) for the first case.

We look for the solution by the method of successive approximations, writing for the refractive index $n = \sqrt{\epsilon} + \Delta n$. Substituting this expression into (4) we find

$$\begin{aligned}&4\varepsilon^2(\Delta n)^2 - 2\sqrt{\varepsilon}\,[\dot{\varepsilon}_{22}(\varepsilon\gamma^2 + \chi) + \dot{\varepsilon}_{11}\varepsilon\sin^2\theta]\,\Delta n\\ &\quad + \gamma^2\chi(\dot{\varepsilon}_{22}^2 + \dot{\varepsilon}_{23}^2)\\ &\quad + \dot{\varepsilon}_{22}\dot{\varepsilon}_{11}\gamma^2\varepsilon\sin^2\theta + \dot{\varepsilon}_{23}^2\dot{\varepsilon}_{11}\gamma^4 = 0.\end{aligned}$$

---

*The expressions for ϵ_{11}^*, ϵ_{22}^*, and ϵ_{23}^* were obtained by taking into account the fact that in going to the system of reference K′, which moves with the plasma, we must substitute in the expression for the components of the tensor ϵ'_{ij} the frequency ω' transformed according to the Doppler formula $\omega' = \omega(1 - n\beta\cos\theta)/\sqrt{1-\beta^2}$. The frequency $\omega_H^* = \omega_H\sqrt{1-\beta^2}$ is the gyro frequency in the plasma beam from the point of view of an observer in the frame of reference K. The occurrence of the factor $\sqrt{1-\beta^2}$ is connected with the Lorentz transformation of the time.

*If we solve the dispersion relation for k for real values of ω, as was done in reference 3, the solutions for k can in principle also be complex. For the case of infinite media, considered here, the selection of solutions with complex k which correspond to a true build-up is difficult, since complex solutions for k can result from the "entrainment" of waves by the moving medium.

If we separate explicitly the factor containing ω_0 from the coefficients of $(\Delta n)^2$, of Δn, and of the constant term, this equation becomes

$$a_2\Delta n^2 + 2a_1\omega_0^2\Delta n + a_0\omega_0^4 = 0,$$

where the coefficients a_0, a_1, and a_2 no longer contain the parameter ω_0. The solution of this equation, which is quadratic in Δn, is such that $\Delta n \sim \omega_0^2$. Since ω, n, and the wave number k, which we fix and assume to be real, are connected through the relation $\omega n = kc$, we can assert that the correction to the frequency ω of the wave, due to the presence of a plasma beam, must also be of the order ω_0^2.

We shall show in the following that in the second case, when the denominators in the ϵ_{ij}^* tend to zero as $\omega_0 \to 0$, i.e., when some peculiar resonance takes place, we obtain a correction to the frequency of the order ω_0, or an even more appreciable one. This means that if the solutions of the first kind include complex solutions, the damping of the waves determined by them will for rarefied plasma beams be negligibly small compared with the damping of the waves as determined by solutions of the second kind. When solving the dispersion relation (4) for resonances in the ϵ_{ij}^*, we must again distinguish between two different cases.

1. The case of strong perturbations. a) Putting $\omega - \widetilde{\omega} = \xi$, we assume that ξ, $\omega_0 \ll \omega$, ω_H^* and we retain in the dispersion relation (4) terms without ω_0 and terms containing ω_0^2/ξ^2, dropping all other terms, since they are small compared with the terms retained. Then Eq. (4) becomes

$$\varepsilon(\varepsilon - n^2) - \omega_0^2\xi^{-2}(1-\beta^2)(\varepsilon - n^2\cos^2\theta) = 0. \tag{5}$$

Solving Eq. (5) for ξ and taking into account that $n\beta\cos\theta = 1$, we find*

$$\xi = \pm\omega_0\left(\frac{(1-\beta^2)(1-\varepsilon\beta^2)}{\varepsilon(1-\varepsilon\beta^2\cos^2\theta)}\right)^{1/2}\cos\theta. \tag{6}$$

It follows from (6) that the correction to the frequency turns out to be of the order ω_0. If $\epsilon\beta^2 > 1$ and $\epsilon\beta^2\cos^2\theta < 1$, the quantity ξ turns out to be imaginary, which indicates the occurrence of waves that are damped or are building up in time. There is instability outside the cone determined by the Cerenkov condition $\epsilon\beta^2\cos^2\theta = 1$. This case and the two next cases discussed below could perhaps be called cases of strong perturbations, as the difference $\epsilon - n^2$ is generally speaking not small and does not tend to zero as $\omega_0 \to 0$. That $\epsilon - n^2$ does not tend to zero as $\omega_0 \to 0$ is, of course, a consequence of neglecting in all expressions given above the corrections necessitated by taking into account thermal motion in the plasma beam. It is physically evident that when thermal motion is taken into account the refractive index n must tend to $\sqrt{\epsilon}$ when the concentration in the plasma beam is reduced. We shall formulate the condition for the validity of the results given here, which are obtained by neglecting thermal motion, at the end of the paper.

b) In the limiting case of no magnetic field ($\omega_H^* = 0$) we put, as before, $\omega - \widetilde{\omega} = \xi$ and assume that ξ, $\omega_0 \ll \omega$. Retaining in the dispersion relation (4), as before, terms without ω_0 and terms with ω_0^2/ξ^2, and dropping all other terms which are small compared with the ones retained, we get

$$\varepsilon(\varepsilon - n^2) - \omega_0^2\xi^{-2}[(1-\beta^2)(\varepsilon - n^2\cos^2\theta) - n^2\sin^2\theta(1-\varepsilon\beta^2)] = 0. \tag{7}$$

Solving Eq. (7) for ξ under the condition $n\beta\cos\theta \fallingdotseq 1$ we find

$$\xi = \pm\omega_0[(1-\varepsilon\beta^2)(1-\beta^2\cos^2\theta)/\varepsilon(1-\varepsilon\beta^2\cos^2\theta)]^{1/2}. \tag{8}$$

The correction to the frequency is found to be of the order ω_0, as in the preceding case, and instability occurs when $\epsilon\beta^2 > 1$ and $\epsilon\beta^2\cos^2\theta < 1$, i.e., outside the Cerenkov cone. We note also that the solution (8), as is the case for the solution (6), is not valid in the neighborhood of the Cerenkov cone ($\epsilon\beta^2\cos^2\theta \to 1$), for then $\xi \to \infty$.

c) We assume now that the resonance occurs at frequencies near $\widetilde{\omega} \pm \omega_H^*$ and we put $\omega - \widetilde{\omega} \pm \omega_H^* = \xi$. Proceeding as in the preceding cases, we get from the dispersion relation (4)

$$\varepsilon(\varepsilon - n^2) - \omega_0^2(\varepsilon\gamma^2 + \chi)/(\omega - \widetilde{\omega} \mp \omega_H^*)\xi = 0 \tag{9}$$

and hence

$$\xi = \omega_0^2(\varepsilon\gamma^2 + \chi)/\varepsilon(\varepsilon - n^2)(\omega - \widetilde{\omega} \mp \omega_H^*). \tag{10}$$

The correction to the frequency turns out to be real and proportional to ω_0^2. There is therefore no instability in this case. The solution found here is invalid when $\epsilon - n^2 \approx 0$, i.e., when $\epsilon\beta^2 \times \cos^2\theta \approx n^2\beta^2\cos^2\theta \approx \widetilde{\omega}^2/(\widetilde{\omega} \mp \omega_H^*)^2$. The solution when $\epsilon - n^2 \to 0$ is studied below.

2. The case of weak perturbations combines the solutions of the dispersion relation (4) under the condition $\epsilon - n^2 \to 0$ as $\omega_0 \to 0$.

a) We put $\omega - \widetilde{\omega} = \xi$ and assume as before that ξ, $\omega_0 \ll \omega$, ω_H^*. Under the condition $\epsilon\beta^2 \times \cos^2\theta = 1$, which is the same as the condition for Cerenkov radiation of a single charged particle,

$$n^2 = \frac{n^2\omega^2\beta^2\cos^2\theta}{\omega^2\beta^2\cos^2\theta} = \frac{\varepsilon\widetilde{\omega}^2}{\omega^2} = \varepsilon\frac{\widetilde{\omega}^2}{(\widetilde{\omega}+\xi)^2}$$

---

*The equation $n\beta\cos\theta = 1$ follows immediately from the condition $\xi/\omega \ll 1$ since $\omega - \widetilde{\omega} = \omega(1 - n\beta\cos\theta) = \xi$.

or

$$\varepsilon - n^2 = \varepsilon\,(1 - \tilde{\omega}^2/(\tilde{\omega} + \xi)^2) \approx \varepsilon 2\xi/\tilde{\omega}.$$

The dispersion relation (4) is then appreciably simplified

$$2\varepsilon^2\xi/\tilde{\omega} - \omega_0^2\xi^{-2}(1 - \beta^2)(\varepsilon - n^2\cos^2\theta) = 0. \tag{11}$$

Solving Eq. (11) for ξ and assuming that $n^2 \approx \epsilon$ we find

$$\xi = (\omega_0^2\tilde{\omega}\,(1 - \beta^2)\sin^2\theta/2\varepsilon)^{1/3}. \tag{12}$$

It follows from (12) that the correction to the frequency $\xi \sim \omega_0^{2/3}$ turns out to be larger than in the preceding cases. ξ tends to 0 more slowly than ω_0, as $\omega_0 \to 0$. When we evaluate the root in (12), two values turn out to be complex, one of which corresponds to a wave that builds up in time.

b) Putting the external magnetic field equal to zero ($\omega_H^* = 0$) we assume as before $\omega - \tilde{\omega} = \xi$ and $\epsilon\beta^2\cos^2\theta = 1$, so that $n^2 = \epsilon\tilde{\omega}^2/(\tilde{\omega} + \xi)^2$. Upon suitable obvious simplification, the dispersion relation (4) becomes

$$2\varepsilon^2\xi/\tilde{\omega} - \omega_0^2\xi^{-2}[(1 - \beta^2)(\varepsilon - n^2\cos^2\theta) - n^2(1 - \varepsilon\beta^2)\sin^2\theta] = 0. \tag{13}$$

Using the equation $n^2 \approx \epsilon$ and eliminating β^2, we can write the solution of Eq. (13) in the form

$$\xi = (\omega_0^2\tilde{\omega}\,(\varepsilon - 1)\tan^2\theta/2\varepsilon^2)^{1/3}, \tag{14}$$

which shows the existence of increasing waves. Equation (14) has been obtained earlier.[2] It was shown then that it determines the build-up of an electromagnetic wave, which has a component of the electrical field parallel to the velocity of the plasma beam, i.e., a wave such as occurs in the Cerenkov effect for a single charged particle.

c) As in the case of strong perturbations, we now assume that $\xi = \omega - \tilde{\omega} - \omega_H^*$ and $\xi \ll \omega$, ω_H^*. In order that $\epsilon - n^2$ tend to zero as $\omega_0 \to 0$ it is necessary, as already noted, to put $\epsilon\beta^2\cos^2\theta = \tilde{\omega}^2/(\tilde{\omega} + \omega_H^*)^2$. The result is

$$n^2 = \varepsilon\,(\tilde{\omega} + \dot{\omega}_H)^2/(\tilde{\omega} + \dot{\omega}_H + \xi)^2,\quad (\varepsilon - n)^2 \approx 2\varepsilon\xi/(\tilde{\omega} + \dot{\omega}_H),$$

and the dispersion relation is, after the usual simplifications, of the form*

$$2\varepsilon^2\xi/(\tilde{\omega} + \dot{\omega}_H) - \omega_0^2(\varepsilon\gamma^2 + \chi)/\xi(\omega - \tilde{\omega} + \dot{\omega}_H) = 0. \tag{15}$$

Solving Eq. (15) for ξ we find

$$\xi = \pm\omega_0[\dot{\omega}_H/2\varepsilon(\tilde{\omega} + \dot{\omega}_H) - (\tilde{\omega} + \dot{\omega}_H)(1 - \varepsilon\beta^2)\sin^2\theta/4\varepsilon\dot{\omega}_H]^{1/2} \tag{16}$$

Equation (16) is obtained under the condition $\epsilon\beta^2 \times \cos^2\theta = \tilde{\omega}^2/(\tilde{\omega} + \omega_H^*)^2 < 1$. When the velocity of the plasma beam exceeds that of light, $\epsilon\beta^2 > 1$, the expression under the square root sign is positive, and the correction to the frequency is a real quantity indicating that there is no build-up in the case under consideration.

d) If $\xi = \omega - \tilde{\omega} + \omega_H^*$ and $\epsilon\beta^2\cos^2\theta = \tilde{\omega}^2/(\tilde{\omega} - \omega_H^*)^2$, the sign of ω_H^* changes in the dispersion relation. The solution of Eq. (15) then becomes

$$\xi = \pm\omega_0[-\dot{\omega}_H/2\varepsilon(\tilde{\omega} - \dot{\omega}_H) + (\tilde{\omega} - \dot{\omega}_H)(1 - \varepsilon\beta^2)\sin^2\theta/4\varepsilon\dot{\omega}_H]^{1/2}. \tag{17}$$

When $\sqrt{\epsilon}\,\beta\cos\theta > 1$, $\omega_H^* < \tilde{\omega}$, we have $\epsilon\beta^2 > 1$, and the correction to the frequency turns out to be imaginary showing the existence of increasing waves. It follows from (16) and (17) that the criterion for instability is in this case the inequality $\sqrt{\epsilon}\,\beta\cos\theta > 1$. This criterion was formulated by Zheleznyakov.[1]

If the inequality $\sqrt{\epsilon}\,\beta\cos\theta > 1$ is satisfied, the component of the beam velocity along the direction of propagation of the wave turns out to be larger than the phase velocity of the wave. An interpretation of the phenomena that occur then and are connected with the build-up of the electromagnetic wave is contained in the cited paper by Zheleznyakov. We note that the instability determined by Eq. (17) occurs also for $\theta = 0$, i.e., for a wave propagated in the direction of motion of the plasma beam.

It was noted in the foregoing that we did not take into account the thermal motion in the plasma beam when deriving the dispersion relation. One can obtain a criterion for the validity of the solutions found here. Zheleznyakov[1] found in the nonrelativistic approximation a dispersion relation for the case of interpenetrating plasma beams, taking thermal motion into account. The form of this dispersion relation is such that the thermal correction remains inessential, as long as an inequality of the kind

$$(\omega - \tilde{\omega} \pm \omega_H)/kv_T \gg 1, \tag{18}$$

where v_T is the velocity of the thermal motion of the electrons in the plasma, is satisfied. The meaning of inequality (18) becomes clear if one takes into account that the required correction to the frequency $\xi = \omega - \tilde{\omega} \pm \omega_H$ and that when there is thermal motion the parameter $\tilde{\omega} = kv\cos\theta$ is spread over a range $\Delta\tilde{\omega} \approx kv_T$. It is clear that the thermal motion can be neglected if $\xi = \omega - \tilde{\omega} \pm \omega_H \gg \Delta\tilde{\omega} \approx kv_T$, i.e., just when inequality (18) is satisfied.

---

*If the plasma beam moves along a constant magnetic field in vacuo ($\varepsilon = 1$), Eq. (15) for the case of the propagation of a wave along the direction of motion of the plasma beam ($\theta = 0$) goes over into the dispersion relation studied in a paper by Twiss.[6]

In the case of weak perturbations considered above, when $\epsilon - n^2 \approx \epsilon\xi/\tilde{\omega}$, the inequality $\Delta\tilde{\omega}/\xi \ll 1$ can easily be shown to lead to the inequality $|c/\sqrt{\epsilon} - c/n| \gg v_T$. (This was pointed out by V. V. Zheleznyakov.) This means that the difference between the velocity of propagation of an electromagnetic wave in a dielectric without a plasma and the velocity of a wave when a plasma beam is present must be much larger than the velocity of the thermal motion in the plasma.

The authors are grateful to V. V. Zheleznyakov for discussing the results obtained here.

---

[1] V. V. Zheleznyakov, Изв. высш. уч. завед., Радиофизика (News of the Colleges, Radio Physics) **2**, 14 (1959).

[2] G. G. Getmantsev, JETP **37**, 843 (1959), Soviet Phys. JETP **10**, 600 (1960).

[3] Ya. B. Faĭnberg and V. S. Tkalich, J. Tech. Phys. (U.S.S.R.) **29**, 491 (1959), Soviet Phys.-Tech. Phys. **4**, 438 (1959).

[4] Al'pert, Ginzburg, and Feĭnberg, Распространение радиоволн (Propagation of Radio Waves) Gostekhizdat, 1953.

[5] R. Becker, Theory of Electrons (Russ. Transl.) Gostekhizdat, 1936.

[6] R. Q. Twiss, Phys. Rev. **84**, 448 (1951).

Translated by D. ter Haar
234

SOVIET PHYSICS JETP VOLUME 11, NUMBER 4 OCTOBER, 1960

A RELATIVISTIC TRANSPORT EQUATION FOR A PLASMA. II*

Yu. L. KLIMONTOVICH

Moscow State University

Submitted to JETP editor October 24, 1959

J. Exptl. Theoret. Phys. (U.S.S.R.) 38, 1212-1221 (April, 1960)

We use the chain of equations for the relativistic distribution functions which we obtained earlier[1] to derive a relativistic transport equation in second approximation for a plasma. We derive first a transport equation in which only the retarded interaction of charged particles is taken into account. This equation is in a particular case the same as the one obtained in a paper by Belyaev and Budker.[2] We consider a relativistic Fokker-Planck equation for a plasma in which the retarded interaction between charged particles and the excitation of plasma oscillations by non-equilibrium charged particles is taken into account.

1. THE SECOND-APPROXIMATION TRANSPORT EQUATION FOR A RELATIVISTIC PLASMA

WE use in this section the results of reference 1 to derive a second-approximation classical transport equation for a plasma; this is the relativistic analogue of the equation obtained by Bogolyubov. Belyaev and Budker[2] considered as a special case of this the equation where radiation and pair production were neglected. It becomes the same as Landau's equation as $c \to \infty$.

We first derive the transport equation neglecting radiation. We can obtain this, for instance, as follows.

We start from Eqs. (12) and (13) of reference 1 for the random functions $N_{q_i p_i}$ and F_{ik}, with this difference, however, that we take instead of Eqs. (13) for the tensor F_{ik} the equations for the four-potential A_i

$$u_i \partial N_{q_i p_i} / \partial q_i + \frac{e}{c} F_{ik} u_k \partial N_{q_i p_i} / \partial p_i = 0, \qquad (1)$$

$$\nabla^2 A_i - \frac{1}{c^2} \partial^2 A_i / \partial t^2 = -\frac{4\pi e}{c} \int u_i N_{q_i p_i} d^4 p, \ \partial A_i / \partial q_i = 0. \qquad (2)$$

We assume that there is a positive-charge background of ions. For the sake of simplicity, we shall write sometimes N_{x_i} instead of $N_{q_i p_i}$, where x_i indicates the eight-vector (q_i, p_i).

As we intend to obtain an approximate transport equation neglecting radiation, we can write the solution of Eq. (2) in the form

$$A_i(q_i) = \frac{ec}{2\pi^3} \iint_{t_0}^{t} u_i' N_{q_i' p_i'} e^{-i\mathbf{k}(\mathbf{q}-\mathbf{q}')} \omega_k^{-1} \sin \omega_k (t - t') \, d^3 k \, d\Omega' \qquad (3)$$

We can let the lower limit tend to $-\infty$, provided the time needed to establish statistical equilibrium τ and the characteristic dimensions l of the system are such that $1/c \ll \tau$. $d\Omega' = d^4 q' d^4 p'$ in Eq. (3).

Using Eq. (3) to eliminate the potential A_i from Eq. (1) and writing

$$L_{il} = \frac{e^2}{2\pi^2} \int \left\{ \frac{\partial}{\partial q_l} (u_i' e^{-i\mathbf{k}\mathbf{q}} \omega_k^{-1} \sin \omega_k t) - \frac{\partial}{\partial q_i} (u_l' e^{-i\mathbf{k}\mathbf{q}} \omega_k^{-1} \sin \omega_k t) \right\} d^3 k, \qquad (4)$$

we get the following equation for the function $N_{q_i p_i}$

$$u_l \partial N_{q_i p_i} / \partial q_l + \iint_{t_0}^{t} L_{il}(q_i - q_i', p_i') N_{q_i' p_i'} d\Omega' u_l \partial N_{q_i p_i} / \partial p_i = 0. \qquad (5)$$

Using (5) we can find a chain of equations for the moments of the random function $N_{q_i p_i}$. We get the first equation for $\overline{N_{q_i p_i}}$ by a straight averaging of (5). To obtain the equation for the second moment $\overline{N_{x_i} N_{x_i'}}$ for $t \neq t'$ and $q \neq q'$, we multiply (5) by $N_{x_i'}$ and average

$$u_l \partial \overline{N_{x_i} N_{x_i'}} / \partial q_l + \iint_{t_0}^{t} L_{il} u_l \frac{\partial}{\partial p_i} (\overline{N_{x_i} N_{x_i'} N_{x_i''}}) d\Omega'' = 0, \qquad (6)$$

where $d\Omega'' = d^4 q'' d^4 p''$. By interchanging the variables $q_i \rightleftarrows q_i'$ and $p_i \rightleftarrows p_i'$ we can obtain another equation for the second moment which is the same as the first.

It is sometimes more convenient to use equations for the corresponding distribution functions instead of the chain of equations for the moments of the random functions $N_{q_i p_i}$. We have given in reference 1 the equations which connect the moments of the random functions N_{qp} with the distribution functions for the variables **q**, **p**, and t. One can write down the corresponding equations for the functions $N_{q_i p_i}$ of eight variables. For instance,

---

*The present paper is a direct continuation of reference 1 by the author.

$$\overline{N_{x_l} N_{x'_l}} = N(N-1) f_2 + N \int \delta(x_i - x'_i(s'))\, ds' f_1(x_i)$$

and similar equations for higher moments.

Subsituting these equations into the equations for the moments, and taking into account that $L_{il}(q_i, q_i) = 0$, we get the following two equations as the first of a chain of equations for relativistic distribution functions

$$u_l \frac{\partial f_1}{\partial q_l} + N \iint_{t_0}^{t} L_{il} u_l \frac{\partial f_2}{\partial p_i}\, d\Omega' = 0, \tag{7}$$

$$u_l \frac{\partial f_2}{\partial q_l} + \int_{t_0}^{t} \int L_{il} u_l \frac{\partial f_2}{\partial p_i} \delta(x''_i - x'_i(s'))\, d\Omega'' ds'$$
$$+ N \int_{t_0}^{t} \int L_{il} u_l \frac{\partial f_3}{\partial p_i}\, d\Omega'' = 0, \quad t \neq t' \tag{8}$$

and a similar second equation for f_2.

We denote by μ the parameter that characterizes the weakness of the interaction. Let $\mu \sim e$. We cut off the chain of Eqs. (7) and (8) by putting

$$f_2 = f_1 f_1 + \mu^2 g, \quad f_3 = f_1 f_1 f_1. \tag{9}$$

Here $g = g(x_i, x'_i)$ is the relativistic correlation function.

The approximate set of equations for f_1 and g becomes, after integration over q''_i and p''_i,

$$u_i \frac{\partial f_1}{\partial q_i} + N \int_{t_0}^{t} \int L_{il} u_i f_1 d\Omega' \frac{\partial f_1}{\partial p_i} + N \iint_{t_0}^{t} L_{il} u_l \frac{\partial}{\partial p_i} g\, d\Omega' = 0, \tag{10}$$

$$u_i \frac{\partial}{\partial q_i} g + \int_{t_0}^{t} L_{il} u_l \frac{\partial f_1}{\partial p_i} f_1(q'_i(s'), p'_i(s'))\, ds' = 0. \tag{11}$$

The correlation function which determines the connection between different positions of particles at different times enters into Eq. (10) for f_1. It follows from Eq. (11) that the correlation function itself is determined by the distribution function of the first particle at time t and by the distribution function of the second particle at all times, within the limits $t \geq t' \geq t_0$, i.e., by the complete motion of the second (primed) particle in that time interval. The dependence of the right-hand side of the equation on q_i manifests itself in that the second particle is during its motion at the point q′ in the time t′.

In Eq. (11) for g we take thus only the influence of the motion of the second particle on the first one into account. The reaction of the first particle on the second one is described by the correlation function satisfying the second equation. This one is obtained from Eq. (11) by the substitution $x_i \rightleftarrows x'_i$ and has the following form

$$u'_i \frac{\partial}{\partial q_i} g + \int_{t_0}^{t} L_{il}(q'_i - q_i, p_i)\, u'_l \frac{\partial f_1}{\partial p'_i} f_1(q_i(s), p_i(s))\, ds = 0. \tag{11'}$$

The distribution function of the first particle at times $t_0 \leq t \leq t'$ occurs in the right-hand side of Eq. (11). Because the particles are identical, we must substitute into the right-hand side of Eq. (10) a symmetrical combination of solutions of Eqs. (11) and (11′).

We write Eq. (11) explicitly, substituting into it Eq. (4) for L_{il}

$$u_i \frac{\partial g}{\partial q_l} = -\frac{e^2}{2\pi^2} \iint_{t_0}^{t} \Big\{ \frac{\partial}{\partial q_i} (v'_l e^{-i\mathbf{k}(\mathbf{q}-\mathbf{q}')} \omega_k^{-1} \sin \omega_k (t - t'))$$
$$- \frac{\partial}{\partial q_l} (v'_i e^{-i\mathbf{k}(\mathbf{q}-\mathbf{q}')} \omega_k^{-1} \sin \omega_k (t - t') \Big\}$$
$$\times u_l \frac{\partial f_1}{\partial p_i} f_1(q'_i(\tau), p'_i(\tau))\, d\tau d^3k. \tag{12}$$

In this equation $v'_k = u'_k/\gamma'$, $d\tau' = ds'\gamma'$, $q' = q'(\tau)$, $t' = t'(\tau) = \tau$, and $\gamma' = \epsilon'/m_0c^2$. There is a similar equation for the second correlation function.

As the interaction is weak, one can determine the trajectory of the second particle in the right-hand side of Eq. (12) by the method of successive approximations. As we wish to obtain the transport equation up to terms of order μ^4, we must restrict ourselves to the zeroth approximation when solving the equations of motion. In that approximation $\mathbf{q}(\tau) = \mathbf{v}\tau + \mathbf{C}$ and $\mathbf{q}'(\tau) = \mathbf{v}'\tau + \mathbf{C}'$. We determine the constants **C** and **C′** from the conditions $\mathbf{q}(\tau) = \mathbf{q}(t) \equiv \mathbf{q}$ at $\tau = t$, and $\mathbf{q}'(\tau) = \mathbf{q}'(t') \equiv \mathbf{q}'$ at $\tau = t'$. We therefore have $\mathbf{C} = \mathbf{q} - \mathbf{v}t$ and $\mathbf{C}' = \mathbf{q}' - \mathbf{v}'t'$. We get thus

$$\mathbf{q}(\tau) = \mathbf{v}(\tau - t) + \mathbf{q}, \quad \mathbf{q}'(\tau) = \mathbf{v}'(\tau - t') + \mathbf{q}'. \tag{13}$$

Using Eqs. (13) and the fact that

$$f_1(q' - v'(t' - \tau), \tau, p'_l) \approx f_1(q', t', p'_i),$$

we can write Eq. (12) as follows

$$u_l \frac{\partial g}{\partial q_i} = -\frac{e^2}{2\pi^2} \int_{t_0}^{t} \int \Big\{ \frac{\partial}{\partial q_i} (v'_l \exp\{-i\mathbf{k}(\mathbf{q} - \mathbf{q}' - \mathbf{v}'(\tau - t'))\}$$
$$\times \omega_k^{-1} \sin \omega_k (t - \tau) - \frac{\partial}{\partial q_l} (v'_i \exp\{-i\mathbf{k}$$
$$\times (\mathbf{q} - \mathbf{q}' - \mathbf{v}'(\tau - t'))\}$$
$$\times \omega_k^{-1} \sin \omega_k (t - \tau)) \Big\} u_l \frac{\partial f_1}{\partial p_i} f_1(q'_i p'_i)\, d\tau d^3k \tag{14}$$

and a similar second equation for the function of g.

Making in Eq. (14) a change of variables $t - \tau = t^*$, letting $t_0 \rightarrow -\infty$, and integrating over t^*, we get in this case the following equations for g

$$u_l \frac{\partial g}{\partial q_l} = \frac{e^2}{2\pi^2} \int \frac{k_i' v_l' - k_l' v_i'}{\omega_k^2 - (\mathbf{k}\mathbf{v}')^2}$$

$$\times \sin \mathbf{k} [\mathbf{q} - \mathbf{q}' - \mathbf{v}' (t - t')] d^3 k u_l \frac{\partial f_1}{\partial p_i} f_1 (p_i'),$$

$$u_l' \frac{\partial g}{\partial q_l'} = \frac{e^2}{2\pi^2} \int \frac{k_i v_l - k_l v_i}{\omega_k^2 - (\mathbf{k}\mathbf{v})^2}$$

$$\times \sin \mathbf{k} [\mathbf{q}' - \mathbf{q} - \mathbf{v} (t' - t)] d^3 k u_l' \frac{\partial f_1}{\partial p_i'} f_1 (p_i). \qquad (15)$$

In these equations k_i and k_i' are wave four-vectors with components $\mathbf{k}$, $i(\mathbf{k}\cdot\mathbf{v})/c$ and $\mathbf{k}$, $i(\mathbf{k}\cdot\mathbf{v}')/c$ respectively.

The solution of these equations for time intervals which are larger than the correlation time, so that one can neglect the initial values of the functions g, can be written in the form

$$g = \frac{e^2}{2\pi^2 \gamma} \int_0^\infty \int \frac{k_i' v_l' - k_l' v_i'}{\omega_k^2 - (\mathbf{k}\mathbf{v}')^2} \sin \mathbf{k} [\mathbf{q} - \mathbf{q}' - \mathbf{v}' (t - t') - (\mathbf{v} - \mathbf{v}') \tau]$$

$$\times u_l (\partial f_1 / \partial p_i)_{\mathbf{q} \rightarrow \mathbf{q} - \mathbf{v}\tau} f_1 (q_i' p_i') \, d^3 k d\tau \qquad (16)$$

with a corresponding expression for the second correlation function. When obtaining Eq. (16) we have used the fact that $u_i k_i' = \gamma (\mathbf{k}\cdot\mathbf{v} - \mathbf{k}\cdot\mathbf{v}')$.

Using (16) to eliminate g from Eq. (10), we get the required relativistic transport equation in second approximation. It is the same in the nonrelativistic approximation as Eq. (10.18) of Bogolyubov's paper.[3]

From the second-approximation transport equation obtained here we can obtain the relativistic generalization of the well-known Landau equation. To do this we consider the case of a distribution function which varies so slowly in space-time that one can consider it to be constant over a region defined by the correlation radius and the corresponding correlation time.

In that case we can drop in Eq. (16) the derivatives with respect to the coordinates, i.e., we can assume

$$(\partial f_1 / \partial p_i)_{\mathbf{q} \rightarrow \mathbf{q} - \mathbf{v}\tau} = \partial f_1 / \partial p_i.$$

Substituting the expression for g into Eq. (10), integrating over q_i', and assuming the function $f_1(q_i')$ to be independent of q_i' we get the following transport equation

$$u_i \frac{\partial f_1}{\partial q_i} = \frac{\partial}{\partial p_i} \int \mathscr{E}_{il} (p_i, p_i') \left\{ \frac{\partial f_1}{\partial p_l} f_1 - \frac{\partial f_1}{\partial p_l'} f_1 \right\} d^4 p'. \qquad (17)$$

The components of the $\mathscr{E}_{il}$ tensor are defined by the equation

$$\mathscr{E}_{il} = 2e^4 N (u_n u_n')^2 \int \frac{k_i k_l}{(\omega_k^2 - \omega^2)^2} \delta (k_j u_j) \delta (k_j u_j') d^3 k d\omega. \qquad (18)$$

We can write Eq. (18) in a different form

$$\mathscr{E}_{il} = \frac{e^2 N}{32\pi^4 c^2} \int k_i k_l (A_j u_j)^2 d^3 k d\omega,$$

where the $A_j(\mathbf{k}, \omega)$ are the Fourier components of the 4-potential produced by the charged particle in the independent-motion approximation.

We can integrate over $\mathbf{k}$ and ω in Eq. (18). If we use the fact that the tensor $\mathscr{E}_{il}$ is symmetric in u_i and u_i' and that $u_i \mathscr{E}_{il} = 0$ and $u_i' \mathscr{E}_{il} = 0$, we need only find the trace of the tensor $\mathscr{E}_{il}$ to determine the $\mathscr{E}_{il}$. As a result we get the following equation

$$\mathscr{E}_{il} = 2\pi e^4 N (u_n u_n')^2 c^{-5} L [(u_n u_n')^2 c^{-4} - 1]^{-3/2}$$

$$\times \{[c^{-4} (u_n u_n')^2 - 1] \delta_{il} - c^{-2} (u_i u_l + u_i' u_l')$$

$$- c^{-4} (u_n u_n') (u_i u_l' + u_i' u_l)\}. \qquad (19)$$

$L = \int dk/k$ is the Coulomb logarithm.

Equation (17) is the same as the transport equation obtained in Belyaev and Budker's paper.[2]

It is often more convenient to use a transport equation for the usual distribution function $F_1(\mathbf{q}, \mathbf{p}, t)$. Taking into account the connection between f_1 and F_1 (see references 1 and 2)

$$f_1 (p_i) = F_1 (\mathbf{q}, \mathbf{p}, t) \delta (\varepsilon - c \sqrt{m_0^2 c^2 + p^2}) m_0 c^2 / \varepsilon \qquad (20)$$

substituting Eq. (20) into Eq. (17), and integrating over ϵ, we get the following equation

$$\frac{\partial F_1}{\partial t} + \mathbf{v} \frac{\partial F_1}{\partial \mathbf{q}}$$

$$= \frac{\partial}{\partial p_\alpha} \int \mathscr{E}_{\alpha\beta}^{\bullet} \left\{ \frac{\partial F_1}{\partial p_\beta} F_1 - \frac{\partial F_1}{\partial p_\beta'} F_1 \right\} d^3 p'; \quad \alpha, \beta = 1, 2, 3. \qquad (21)$$

In this equation

$$\mathscr{E}_{\alpha\beta}^{\bullet} = 2e^4 N (v_n v_{n'})^2 \int \frac{k_\alpha k_\beta \delta (\mathbf{k}\mathbf{v} - \mathbf{k}\mathbf{v}')}{[\omega_k^2 - (\mathbf{k}\mathbf{v})^2]^2} d^3 k, \quad v_n = u_n / \gamma. \qquad (22)$$

If one uses Eq. (9) of reference 1 instead of Eq. (1) for the random function $N_{\mathbf{qp}}(t)$, one can derive Eq. (21) directly.

The relativistic Maxwell distribution, which for particles of constant mass can be written in the form

$$f_1 (q_i, p_i) = C \delta (p_i^2 + m_0^2 c^2) \exp (p_i \bar{u}_i / \varkappa T), \qquad (23)$$

satisfies the transport Eq. (17). In Eq. (23) C is a normalizing factor, $\bar{u}_i$ the average velocity four-vector in the equilibrium state, and T the temperature.

When one substitutes (23) into Eq. (17), one must take into account the fact that $k_l\bar{u}_l = 0$ because of the equation of continuity, and that $k_l u_l = k_l u_l' = 0$, because of the occurrence of the δ functions in the expression for the tensor $\mathscr{E}_{il}$.

In the system of coordinates in which the average electron velocity vanishes Eq. (23) for the usual distribution function $F^{(0)}(\mathbf{p})$ is of the form

$$F^{(0)}(\mathrm{p}) = C\exp\{-c\sqrt{m_0^2c^2 + p^2}/\varkappa T\}. \qquad (24)$$

The transport equation (17) which we have obtained is incomplete even in the chosen approximation $\sim e^4$. This is due to the following facts. The derivation of Eq. (17) was based upon the use of Eq. (5), from which the variables characterizing the state of the electromagnetic field were completely eliminated. Indeed, in Eq. (5) we took only the retarded interaction between the particles into account.

We have seen that the transport equation obtained in this manner is not completely satisfactory, as it contains a divergent integral over the wave numbers, the "Coulomb" logarithm $\int dk/k$. A similar situation arose also when the corresponding nonrelativistic Landau transport equation was derived.[4]

The divergence difficulty was avoided in the nonrelativistic case by choosing an upper limit for the integral at large $k \sim 1/a$, where $a = e^2/m_0v^2$, and a lower limit at small $k \sim 1/r_d = k_d$, where r_d is the Debye radius. In a paper by Temko[5] the integration domain at small k in the derivation of the Fokker-Planck equation for a plasma is limited because the Debye screening is taken into account.

Both in this and in other cases, the interaction corresponding to small $k < 1/r_d$ is neglected in the derivation of the transport equation, which therefore takes only the screened interaction between the electrons in the plasma into account.

It is, however, well known[6,7] that the screened interaction accounts for only a part of the interaction energy of the electrons. The other part of the interaction, corresponding to small values of k, can be expressed in terms of the plasma oscillation variables. To obtain the complete transport equation one must thus take into account the interaction of non-equilibrium electrons with the plasma oscillations. One possible solution of this problem was considered by the author in reference 8.

We saw that a similar situation also arises in the derivation of a relativistic transport equation. This indicates that it is only possible to restrict oneself to taking retarded interactions between particles into account in the wave-number range $k > k_d$. It is thus impossible to eliminate the field variables completely. In order to choose the dividing value k_d, one must consider a suitable expression for the relativistic correlation function.

To conclude the present section, we note another possible way to derive a relativistic transport equation. One can use the fact that the interaction is weak to express approximately the second double-time distribution function which occurs in Eq. (7) in terms of the single-time distribution function. In that case one can reduce the problem not to the solution of Eqs. (14) and (15) for the double-time correlation functions, but to the solution of an equation for the single-time correlation function, which can also be obtained from Eq. (5).

2. A RELATIVISTIC FOKKER-PLANCK TRANSPORT EQUATION FOR A PLASMA WITH ACCOUNT OF THE EMISSION OF PLASMA WAVES

One can consider the distribution of the charged particles in a plasma to be in equilibrium when fast particles pass through a plasma, provided the number of fast (non-equilibrium) charged particles is small. The transport equation for the plasma is in that case the Fokker-Planck equation. One obtains it in the relativistic case from Eqs. (17) and (21) for the functions f_1 and F_1 by replacing in these equations the functions dependent on the primed momenta by the corresponding expressions for the equilibrium state. The relativistic Fokker-Planck transport equation for the function F_1 has thus, for instance, the following form

$$\frac{\partial F_1}{\partial t} + \mathbf{v}\frac{\partial F_1}{\partial \mathbf{q}} = \frac{\partial}{\partial p_\alpha} D_{\alpha\beta}\frac{\partial F_1}{\partial p_\beta} + \frac{\partial}{\partial p_\alpha}(A_\alpha F_1). \qquad (25)$$

The coefficients $D_{\alpha\beta}$ and A_α are defined by the expressions

$$D_{\alpha\beta} = \int \mathscr{E}^*_{\alpha\beta}(\mathbf{p}, \mathbf{p}')\, F^{(0)}(\mathbf{p}')\, d^3p',$$

$$A_\alpha = -\int d^3p' \mathscr{E}^*_{\alpha\beta}(\mathbf{p},\mathbf{p}')\, \partial F^{(0)}(\mathbf{p}')/\partial p'_\beta, \qquad (26)$$

where $F^{(0)}(\mathbf{p})$ is the relativistic Maxwell distribution (24), while the tensor $\mathscr{E}^*_{\alpha\beta}$ is defined by Eq. (22).

We consider now briefly the derivation of the relativistic Fokker-Planck equation with account of diffusion processes and of the systematic friction processes caused by the excitation of plasma oscillations.

We turn to Eqs. (1) and (2). We expand the vector potential in a Fourier series

$$A_i = \sqrt{4\pi c^2 / V} \sum_k \{A_i^{(1)}(k) \sin \mathbf{kq} + A_i^{(2)}(k) \cos \mathbf{kq}\}.$$

The equations for the Fourier coefficients have the form

$$\ddot{A}_i^{(j)} + \omega_k^2 A_i^{(j)} = \sqrt{4\pi / V} e \int N_{q_i p_i} \genfrac{}{}{0pt}{}{\sin \mathbf{kq}}{\cos \mathbf{kq}} d^3k d^4p, \quad j = 1,\ 2. \tag{27}$$

We eliminate, as before, the vector potential from the equations for $N_{q_i p_i}$, but we do this now only for the components of the vector potential with wave numbers $k > k_d$. The equation for the function $N_{q_i p_i}$ has in that case the form

$$u_i \partial N_{x_i} / \partial q_i + \frac{e}{c} F_{il} u_l \partial N_{x_i} / \partial p_i + \iint\limits_{-\infty}^{t} L_{il} N_{x'_i} d\Omega' u_l \partial N_{x_i} / \partial p_l = 0, \quad x_i = (q_i,\ p_i). \tag{28}$$

In F_{il} we have here

$$A_i = \sqrt{4\pi c^2 / V} \sum_{k<k_d} A_i^{(j)}(k) \genfrac{}{}{0pt}{}{\sin \mathbf{kq}}{\cos \mathbf{kq}}.$$

The equation for $A_i^{(j)}$ for $k < k_d$ is the same as Eq. (27). The tensor L_{il} in Eq. (28) is again defined by Eq. (4) with this difference, that the domain of integration is now restricted by the condition $k > k_d$.

We consider first the case where the plasma is in a state of statistical equilibrium. We shall show that we can in that case approximately separate the equations describing the behavior of particles with a screened interaction and the plasma oscillations. Such a kind of problem was considered by Bohm and Pines in their well-known papers[6,7] for a nonrelativistic plasma by a different method.

In an equilibrium state $\overline{N}_{x_i} = \overline{N}_{p_i}$ so that we can write $N_{x_i} = \overline{N}_{p_i} + \delta N_{x_i}$. Because we are dealing with a stationary and uniform case, the corresponding mean-square deviations depend only on coordinate and time differences, i.e., on $q_i - q'_i$.

We substitute the expression $N_{x_i} = \overline{N}_{p_i} + \delta N_{x_i}$ into Eq. (28). Taking into account the fact that in an equilibrium state $\overline{A}_i = 0$, $A_i = \delta A_i$, $F_{ik} = \delta F_{ik}$ we get for small deviations the following approximate equation for δN_{x_i}

$$u_i \partial \delta N_{x_i} / \partial q_i + \frac{e}{c} F_{il} u_l \partial \overline{N}_{p_i} / \partial p_i + \iint\limits_{-\infty}^{t} L_{il} \delta N_{x'_i} d\Omega' u_l \partial \overline{N}_{p_i} / \partial p_l = 0. \tag{29}$$

Using Eq. (29) we eliminate δN_{x_i} from the right-hand side of Eq. (27) for $k < k_d$. The last term in Eq. (29) does not play any role here, as it contains only terms with $k > k_d$. The equation for the $A_i^{(j)}$ becomes

$$\ddot{A}_i^{(j)} + \Omega_k^2 A_i^{(j)} = 0. \tag{30}$$

The frequency Ω_k is different for different components of the vector $A_i^{(j)}$ and is determined from the corresponding dispersion relation for plasma oscillations.

The equation for the change δN_{x_i} due to the screened interaction between the particles has the following form

$$u_i \partial \delta N_{x_i} / \partial q_i + \iint\limits_{-\infty}^{t} L_{il} \delta N_{x'_i} d\Omega' u_l \partial \overline{N}_{p_i} / \partial p_l = 0. \tag{31}$$

We can thus under the given assumptions separate the motion of the particles with screened interactions and the electromagnetic oscillations in the plasma.

We now consider non-equilibrium states in the system. The functions N_{x_i} will consist of two parts corresponding to equilibrium and non-equilibrium parts of the plasma $N_{x_i} = N_{x_i}^{(\text{non-eq})} + N_{x_i}^{(\text{eq})}$. We shall assume that the deviation from equilibrium is small ($N_{x_i}^{(\text{non-eq})} \ll N_{x_i}^{(\text{eq})}$) so that we can neglect any correlation between the non-equilibrium particles in the plasma.

The transition to equilibrium will in this case be determined by two factors, first the screened interaction between the non-equilibrium electrons and the equilibrium electrons in the plasma, and second the interaction with the plasma oscillations. The equation for $N_{x_i}^{(\text{eq})}$ which describes these processes has the following form

$$u_i \partial N_{x_i}^{(\text{non-eq})} / \partial q_i + \frac{e}{c} F_{il} u_l \partial N_{x_i}^{(\text{non-eq})} / \partial p_i + \iint\limits_{-\infty}^{t} L_{il} u_l \{N_{x'_i}^{(\text{non-eq})} \partial N_{x_i}^{(\text{eq})} / \partial p_i + N_{x'_i}^{(\text{eq})} \partial N_{x_i}^{(\text{non-eq})} / \partial p_i\} d\Omega' = 0. \tag{32}$$

The electromagnetic field tensor F_{il} is determined in this equation by the value of the four-dimensional potential of the plasma waves excited by the non-equilibrium electrons

$$\ddot{A}_i^{(j)} + \Omega_k^2 A_i^{(j)} = \sqrt{\frac{4\pi}{V}} e \int u_i N_{x_i}^{(\text{non-eq})} \genfrac{}{}{0pt}{}{\sin \mathbf{kq}}{\cos \mathbf{kq}} d^3k d^4p. \tag{33}$$

Equations (32) and (33) constitute also a set from which we can obtain transport equations for the first distribution functions for the charged particles and the field oscillators. The method of obtaining these equations is similar to the one given in reference 8.

As in the foregoing, we restrict our considerations to the electrons in the plasma. The relativistic Fokker-Planck equation for the function F_1 differs then from Eq. (25) only through additional terms in the coefficients for the diffusion and for the systematic friction caused by the emission of plasma waves. We denote the corresponding extra terms by $D_{\alpha\beta}^{(em)}$ and $A_{\alpha}^{(em)}$. Each of them can be split into two parts determined respectively by the emission of transverse and of longitudinal waves.

The coefficients caused by the emission of transverse waves in an electron plasma differ from zero only if the plasma is in a decelerating medium. We do not consider this case here. The extra coefficients are thus completely determined by the emission of longitudinal plasma waves and are of the following form

$$D_{\alpha\beta}^{(\mathrm{em})} = \frac{e^2 \varkappa T}{2\pi} \int \frac{k_\alpha k_\beta}{k^2} \delta(\Omega_k^{\parallel} - \mathbf{kv})\, d^3k,$$

$$A_{\alpha}^{(\mathrm{em})} = \frac{e^2}{2\pi} \int \frac{k_\alpha \Omega_k^{\parallel}}{k^2} \delta(\Omega_k^{\parallel} - \mathbf{kv})\, d^3k. \tag{34}$$

Equations (34) differ from the corresponding nonrelativistic expressions, obtained in reference 8, only in that now the plasma oscillation frequency is determined from the relativistic dispersion relation for longitudinal waves*

$$1 = \frac{4\pi e^2}{\varkappa T \omega} \int \frac{(u_x/\gamma)^2 F^{(0)}(p)}{\omega - u_x k/\gamma}\, d^3p, \quad k \parallel x, \quad \gamma = 1/\sqrt{1-(v/c)^2}.$$

We consider now the limiting expressions for the coefficients for the diffusion and systematic friction. We find in the nonrelativistic approximation for the case of fast non-equilibrium particles ($v \gg \sqrt{\kappa T/m}$) from Eq. (26) the following expressions

$$A_x = A_y = 0, \quad A_z = \frac{e^2\omega_L^2}{v^2} \ln \frac{r_d}{a}, \quad v \parallel z, \quad a = \frac{e^2}{m_0 v^2};$$

$$D_{\alpha\beta} = 0 \quad \text{for } \alpha \neq \beta, \quad D_{zz} = \frac{e^2\omega_L^2}{v^3} \varkappa T \ln \frac{r_d}{a},$$

$$D_{xx} = D_{yy} = \frac{e^2\omega_L^2}{2v} m \ln \frac{r_d}{a}. \tag{35}$$

The corresponding expressions for $D_{\alpha\beta}^{(em)}$ and $A_{\alpha}^{(em)}$ found from Eqs. (34) are of the form (compare with references 10 and 11)

$$A_x^{(\mathrm{em})} = A_y^{(\mathrm{em})} = 0, \quad A_z^{(\mathrm{em})} = \frac{e^2\omega_L^2}{v^2} \ln \frac{v}{r_d\omega_L} = \frac{e^2\omega_L^2}{v^2} \ln \frac{v}{v_T};$$

$$D_{\alpha\beta}^{(\mathrm{em})} = 0 \quad \text{for } \alpha \neq \beta, \quad D_{zz}^{(\mathrm{em})} = \frac{e^2\omega_L^2}{v^3} \varkappa T \ln \frac{v}{r_d\omega_L},$$

$$D_{xx}^{(\mathrm{em})} = D_{yy}^{(\mathrm{em})} = \frac{e^2\omega_L^2}{4v}. \tag{36}$$

In the ultrarelativistic case, when the velocity of the non-equilibrium particles is close to that of light but the electron temperature is $\kappa T \ll m_0 c^2$, the equations for the coefficients are the same as Eqs. (35) and (36), provided one replaces in them v by c. For the coefficients of the systematic friction we have, for instance,

$$A_z = \frac{e^2\omega_L^2}{c^2} \ln \frac{r_d}{a}, \quad A_z^{(\mathrm{em})} = \frac{e^2\omega_L^2}{c^2} \ln \frac{c}{r_d\omega_L}.$$

It is clear from the expressions given here that the total coefficients of the systematic friction and of diffusion along the direction of motion are independent of the choice of $k_d = 1/r_d$. In the ultrarelativistic approximation we get, for instance, the following expressions

$$A_z + A_z^{(\mathrm{em})} = \frac{e^2\omega_L^2}{c^2} \ln \frac{\delta}{a},$$

$$D_{zz} + D_{zz}^{(\mathrm{em})} = \frac{e^2\omega_L^2}{c^3} \varkappa T \ln \frac{\delta}{a}, \quad \delta = \frac{c}{\omega_L}.$$

One can easily obtain also the expressions for the coefficients for the case $\kappa T \gg m_0 c^2$.

It follows from the formulae obtained here that taking the emission of plasma waves into account leads only to a slight change in the expressions under the logarithm sign. This consideration of the emission of plasma waves, done here, does therefore not lead to any essential change in the relaxation time. We must, finally, bear in mind that the results obtained here refer to that case where the number of non-equilibrium electrons is small and where the main plasma is in an equilibrium state.

We considered in reference 8, in connection with a discussion of Langmuir's paradox, an example where these conditions were not satisfied, i.e., where the initial state of the whole system was essentially non-equilibrium. It then turned out that, for instance, the transfer of energy of the electrons in the beam to the electrons in the plasma takes place over a time interval appreciably shorter than the relaxation time determined by the processes considered in the foregoing. The derivation of a transport equation for this case is a separate problem.

It is also of interest to use the chain of relativistic equations for the distribution functions obtained in the present paper to obtain transport equations when there are external fields present and for a basis for the hydrodynamic approximation.

---

*One must take u/γ instead of γu in the dispersion relations derived in Sec. 4 of reference 1.

Some of the questions mentioned in the above will be considered in the future.

I use this opportunity to express my gratitude to Academician N. N. Bogolyubov for his interest in the present paper and for discussing the results obtained.

---

[1] Yu. L. Klimontovich, JETP **37**, 735 (1959), Soviet Phys. JETP **10**, 524 (1960).

[2] S. T. Belyaev and G. I. Budker, Dokl. Akad. Nauk SSSR **107**, 807 (1956), Soviet Phys. Doklady **1**, 218 (1956).

[3] N. N. Bogolyubov, Проблемы динамической теории в статистической физике (Problems of the Dynamical Theory in Statistical Physics) Gostekhizdat, 1946.

[4] L. D. Landau, Physik Z. Sowjetunion **10**, 154 (1936); JETP **7**, 203 (1937).

[5] S. V. Temko, JETP **31**, 1021 (1956), Soviet Phys. JETP **4**, 898 (1957).

[6] D. Bohm and D. Pines, Phys. Rev. **82**, 625 (1951).

[7] D. Pines and D. Bohm, Phys. Rev. **85**, 338 (1952); D. Bohm and D. Pines, Phys. Rev. **92**, 609 (1953).

[8] Yu. L. Klimontovich, JETP **36**, 1405 (1959), Soviet Phys. JETP **9**, 999 (1959).

[9] P. C. Clemmow and A. J. Willson, Proc. Roy. Soc. (London) **A237**, 117 (1956); Proc. Cambridge Phil. Soc. **53**, 222 (1957).

[10] A. A. Vlasov, Теория вибрационных свойств электронного газа и ее применения, Уч. зап. МГУ Sci. Notes, Moscow State Univ., No. 76 (1944).

[11] B. I. Davydov, Физика плазмы и проблемы управляемых термоядерных реакций (Plasma Physics and Problems of Controlled Thermonuclear Reactions) Vol. 1, U.S.S.R. Acad. Sci. Press, 1958, p. 77.

Translated by D. ter Haar
235

SOVIET PHYSICS JETP VOLUME 11, NUMBER 4 OCTOBER, 1960

ON THE THEORY OF QUADRUPOLE RELAXATION OF NUCLEAR SPINS IN LIQUIDS

K. A. VALIEV

Physico-Technical Institute, Kazan' Branch, Academy of Sciences, U.S.S.R.

Submitted to JETP editor October 23, 1959

J. Exptl. Theoret. Phys. (U.S.S.R.) 38, 1222-1232 (April, 1960)

Quadrupole relaxation of nuclear spins of diamagnetic atoms in liquids is treated theoretically. The calculations are made on the assumption that the thermal motion of the liquid particles is a free translational diffusion. This assumption is valid for metal and salt melts and for weakly solvated ions in electrolyte solutions. It is found that $T_2^{-1} \sim \eta/T$ (η is the viscosity of the liquid) which is in good agreement with the measurements of T_2^{-1} for the nuclear spin of I^{127} in aqueous solutions of NaI and KI salts.

1. INTRODUCTION

ONE of the reasons for the lack of a complete theory of liquids and of liquid solutions is our poor knowledge of the potential of interaction between the particles of a liquid, particularly at small distances. Therefore, it is difficult to obtain unambiguous results on structure and on the motion of particles in a liquid from a comparison of the physical properties of the liquid with a theory which utilizes an approximate interaction potential.

However, if we study liquids by the method of magnetic resonance, the potential of the interaction between the magnetic moments of the particles can be determined quite accurately. Therefore, in a comparison between theory and experiment the only unknowns are the data on the structure of the liquid and the constants which characterize the motion of its particles (the diffusion coefficient or the correlation time). Investigations carried out during the last few years by the method of magnetic resonance have demonstrated the great promise of this method, particularly for the investigation of the structure of a liquid and of the nature of motion of its particles. In the first place a study was made of homogeneous diamagnetic liquids (water). It was shown that the magnetic resonance line in water is narrowed as a result of the influence of thermal motion: the thermal motion averages out the magnetic fields with which the magnetic particles act on one another, and this leads to line narrowing.[1] Considerable progress was made in the study by the nuclear magnetic resonance method of internally hindered rotations of molecules in solid molecular substances. Later studies were extended to solutions of diamagnetic and paramagnetic salts in various solvents. It turned out that the shape and the width of the magnetic-resonance line due to paramagnetic ions dissolved in a dilute solution depend primarily on the structure of the complex formed by the ion and the molecules of the solvent, and on the nature of motion of the particles of this complex.[2,3] The same situation was also observed in solutions of some diamagnetic ions whose nuclei possess large quadrupole moments.[4] It became clear from this work that the dissolved ions can play the role of probes which are very convenient for the study of the nature of thermal motion and of structure in electrolyte solutions. It is obvious that this conclusion also applies fully to liquid melts of metals (alloys) and of salts.

However, the number of experimental investigations of solutions of electrolytes and ionic liquids (metal and salt melts) carried out by the magnetic resonance method is so far comparatively small. The reason for this lies partly in the lack of a theory which would enable one to interpret the experimental results unambiguously. Such a theory must, by starting with a specific model of the liquid, predict the line shape and its behavior as a function of the temperature, the external field etc. First attempts of this kind were the investigations of McConnell[5] and McGarvey.[6] They based their work on a model which assumes the existence in a solution of a paramagnetic salt of a stable solvated complex, and they investigated the contribution to the width of the electron resonance line made by the random rotation of the complex. They considered the complex to be a rigid microcrystal. Comparison with experiment showed that such a mechanism for the broadening of the resonance line turns out to be the principal one only in rare cases. In a joint paper by Al'tshuler and the present author[6] it is shown that in solutions of paramagnetic electrolytes the principal mechanism of line broadening is the interaction of the electron spin of the ion with the internal thermal vibrations of the solvated complex ion.[3] A theory based on a similar line-broadening mechanism turned out to be justified also in the case of nuclear magnetic resonance lines of diamagnetic ions whose nuclei possess an electric quadrupole moment, under the condition that the ions form stable solvated complexes in water.[4]

In this paper we investigate the theory of the width of nuclear magnetic-resonance lines in liquids in which the atoms under investigation have a quadrupole moment and do not form stable complexes with other particles of the liquid. This assumption is applicable, for example, to the quadrupole relaxation of nuclear spins of halogen ions in aqueous solutions of electrolytes, since, as is well known from physical-chemistry studies, the halogen ions do not form stable associations (complexes) with the molecules of the solvent. With certain limitations, a molecule of water may be represented by a point charge; the choice of the value of the effective charge of the molecule will affect the value of the calculated line width, leaving unaltered the physically important dependence of the line width on the temperature and on the nature of the thermal motion of the particles. A similar situation also exists in the case of alloys of metals and ionic salts, and in these cases the charge (ionic) model of the liquid is quite accurate. On the basis of the foregoing we assume that the thermal motion of the particles of the liquid represents free translational diffusion. This assumption will be justified best of all in the case of liquids at temperatures considerably above their melting point. Near the melting point microcrystals can exist in the melt; the quadrupole relaxation of nuclear spins in these microcrystals will evidently be determined by random rotation or by internal vibrations. These mechanisms are similar to those studied by us in reference 4.

We now elucidate the essence of the relaxation mechanism under consideration at present.

We single out of the bulk of the liquid one ion whose nucleus has an electric quadrupole moment. The other particles, regarded as point charges and occupying, generally speaking, random positions with respect to the singled-out ion, will give rise at its nucleus to a resultant inhomogeneous field **E**. Due to diffusion the relative position of the particles will change; this will lead to random variations of the electric field **E** with time. By acting on the quadrupole moment of the nucleus the field **E** can affect its spin. Random shifts of the energy sublevels of the nuclear spin will result from this interaction, and this will give rise to secular broadening of the resonance line and to broadening due to relaxation transitions between the sublevels.

2. THE METHOD OF CALCULATION

The Hamiltonian for a system of spins of nuclei possessing quadrupole moments has the following form in a strong magnetic field

$$\hat{H} = -\gamma\beta_N \mathbf{H}_0 \sum_i \mathbf{I}_i + \hat{H}'. \tag{1}$$

The energy of the internal interactions H' is a small perturbation compared to the Zeeman energy of the spins; in our problem it represents the energy of the nuclear quadrupole moments in the electric fields due to the surrounding particles.

If we neglect the thermal motion of the particles of the system, then the broadening of the resonance line caused by the perturbation H' can be calculated in the following manner. The (secular) part of H' diagonal with respect to the spin of the particle under consideration will result in a displacement of the spin levels of this particle. For a system containing a large number of particles such displacements will form a continuum giving a line of a certain width $\Delta\omega$ which can be evaluated by means of the formulas:[1]

$$\langle \Delta\omega^2 \rangle = T_2^{-2} = \hbar^{-2} \langle | H'_{mm} |^2 \rangle. \tag{2}$$

The averaging indicated by the angular brackets is taken over the space and the spin variables.

We now must take into account the effect on the line width of the thermal motion of the particles. In our problem the thermal motion of the particles represents a translational diffusion. Since diffusion is a random process the matrix element H'_{mm} which depends on the spatial coordinates of the particles of the system will be a random function of the time. The square of the matrix element H'_{mm} can be represented in the form of the Fourier integral

$$\langle | H'_{mm}(t) |^2 \rangle = \int_{-\infty}^{+\infty} J_{mm}(\omega)\, d\omega; \tag{3}$$

where $J_{mm}(\omega)$ is a function describing the frequency spectrum of the perturbation. According to the theory of random processes, the spectral function $J_{mm}(\omega)$ is determined by the correlation function $g_{mm}(\tau)$:

$$J_{mm}(\omega) = \Omega_{mm}^2 \int_{-\infty}^{+\infty} e^{-i\omega\tau} g(\tau)\, d\tau, \qquad \Omega_{mm}^2 = \langle | H'_{mm} |^2 \rangle; \tag{4}$$

$$g_{mm}(\tau) = \Omega_{mm}^{-2} \langle H'_{mm}(t+\tau) H'^{*}_{mm}(t) \rangle. \tag{5}$$

We shall evaluate the quantity T_2^{-1}, which characterizes the secular line broadening, by means of the formula[1]

$$T_2^{-1} = \hbar^{-2} J_{mm}(0), \tag{6}$$

which is sufficiently accurate when rapid motion occurs in the system.

The exponential function $\exp(-\tau/\tau_C)$ is often adopted for the correlation function $g_{mm}(\tau)$. However, in those cases when the distribution density $U(q_0, q)$ of the spatial coordinates q of the system is known, the function $g(\tau)$ can be calculated directly. Our case is just of this kind. H'_{mm} depends on the radius vector $\mathbf{R}_A$ $(R_A, \theta_A, \varphi_A)$ from the center of mass of the nucleus under consideration to the charge e_A. The distance $\mathbf{R}_A$ varies as a result of the process of diffusion, and therefore the distribution $U(\mathbf{R}_A)$ is a solution of the free translational diffusion equation[7]

$$U(R_A, \tau;\ R_A^0,\ 0) = \frac{1}{(2\pi)^3}\int_0^\infty e^{-2k^2 D\tau} \sum g_l(kR_A)\, g_l^*(kR_A^0)$$

$$\times\ Y_l^m(\theta, \varphi)\, Y_l^{m*}(\theta_0, \varphi_0)\, k^2 dk, \tag{7}$$

$$g_l(x) = (2\pi)^{3/2} i^l J_{l+1/2}(x) / \sqrt{x}, \tag{8}$$

$D = kT/6\pi\eta a$ is the diffusion constant, a is the ionic radius.

The function U is equal to the probability density of finding the charge e_A at the instant of time τ within the volume dv, at a distance $\mathbf{R}_A$ from the nucleus under consideration if at zero time it was at a distance $\mathbf{R}_A^0$ from the nucleus within the element of volume dv_0. In (7) the solution of the diffusion equation is written in the form of an expansion in terms of spherical harmonics, which is convenient for the subsequent averaging.

In place of (5) we now have

$$g_{mm}(\tau) = \Omega_{mm}^{-2} \int H'_{mm}(q)\, H'^{*}_{mm}(q_0)\, U(q,\ q_0)\, dq\, dq_0. \tag{9}$$

The matrix elements nondiagonal with respect to spin $H'_{mm'}$; $|m - m'| \neq 0$ give rise to an additional non-secular line broadening due to the decrease in the lifetime of the spin in a given state due to relaxation transitions between different states. The probability of these transitions is determined by the formula[1]

$$w_{mm'} = \hbar^{-2} J_{mm'}(\omega) = \frac{\Omega_{mm}^2}{\hbar^2} \int_{-\infty}^{+\infty} \exp(-i\omega_{mm'}\tau)\, g(\tau)\, d\tau, \tag{10}$$

and the corresponding relaxation time by the formula[8]

$$T_1^{-1} = (2I + 1) \sum_{l>k} w_{lk} (E_l - E_k)^2 \Big/ \sum_{l>k} (E_l - E_k)^2. \tag{11}$$

3. THE ENERGY OF THE QUADRUPOLE MOMENT OF A NUCLEUS IN THE FIELD OF A POINT CHARGE

The energy of the quadrupole moment of a nucleus in an inhomogeneous electric field produced by external charges can be represented in the form of the scalar product of the electric quadrupole moment tensor for the nucleus D_{ik} and the electric field gradient tensor at the nucleus[9]

$$H' = \sum_{i,k} \tfrac{1}{6} D_{ik} (\nabla \mathbf{E})^{ik}, \qquad (\nabla \mathbf{E})^{ik} = \partial^2 \varphi / \partial x_i \partial x_k. \tag{12}$$

In the representation in which I^2 and I_z are diagonal the five independent components of the tensor D_{ik} are quadratic functions of the components of the nuclear spin

$$D_0 = \tfrac{1}{2} C\,(3I_z^2 - I(I+1)), \qquad D_{\pm 1} = \tfrac{3}{2} C\,\{I_z I_\pm\},$$

$$D_{\pm 2} = 3CI_\pm^2, \qquad I_\pm = I_x \mp iI_y,$$

$$\{I_i I_j\} = I_i I_j + I_j I_i, \qquad C = eQ / I(2I - 1). \tag{13}$$

We choose the origin of the laboratory system xyz at the center of mass of the nucleus under consideration, and we direct the z axis along the external magnetic field. We denote by $\mathbf{R}_A$ $(R_A, \theta_A, \varphi_A)$ the radius vector of the charge e_A. In spherical polar coordinates, the components of the tensor $(\nabla \mathbf{E})^{ik}$ can be written in the form

$$(\nabla \mathbf{E})^0 = 3\sqrt{\frac{16\pi}{5}} \sum e_A R_A^{-3} Y_2^0 (\varphi_A, \theta_A),$$

$$(\nabla \mathbf{E})^{\pm 1} = \sqrt{\frac{24\pi}{5}} \sum e_A R_A^{-3} Y_2^{\pm 1} (\theta_A, \varphi_A),$$

$$(\nabla \mathbf{E})^{\pm 2} = \sqrt{\frac{6\pi}{5}} \sum e_A R_A^{-3} Y_2^{\pm 2} (\theta_A, \varphi_A). \tag{14}$$

We can easily evaluate the non-zero matrix elements of the operator for the quadrupole energy of the nucleus (12)

$$H'_{mm} = \sqrt{\frac{\pi}{5}}\, C(1+\gamma)(3m^2 - I(I+1)) \sum e_A R_A^{-3} Y_2^0$$

$$= A_{mm} \sum_A e_A R_A^{-3} Y_2^0, \tag{15}$$

$$H'_{m,\, m\pm 1} = \sqrt{\frac{\pi}{10}}\, C(1+\gamma)\, \{I_z I_\mp\}_m^{m\pm 1} \sum e_A R_A^{-3} Y_2^{\pm 1}$$

$$= A_{m,\, m\pm 1} \sum e_A R_A^{-3} Y_2^{\pm 1}, \tag{16}$$

$$H'_{m,\, m\pm 2} = \sqrt{\frac{\pi}{10}}\, C(1+\gamma)\, (I_\pm^2)_m^{m\pm 2} \sum e_A R_A^{-3} Y_2^{\pm 2}$$

$$= A_{m,\, m\pm 2} \sum e_A R_A^{-3} Y_2^{\pm 2}. \tag{17}$$

The factors $1+\gamma$ have been introduced into (15) and (16) to take into account the effect called antishielding, which consists of an enhancement of the fields produced at the nucleus by charges external to the ion containing the given nucleus as a result of the deformation of the electron shells of the ion. The numerical values of $|\gamma|$ have been calculated theoretically for most ions having a nuclear quadrupole moment.[10]

4. THE CORRELATION FUNCTION

We now evaluate the correlation function for the matrix elements (15) — (17). The coordinate part of the matrix elements (15) — (17) coincides with the coordinate part of the matrix elements of the energy operator for spin-spin interaction. The correlation function for the latter defined by (5) and (9) has been evaluated by Skrotskiĭ and Kokin.[7] They obtained the following result:

$$g_{mm'}(p) = g(p) = \frac{6}{\pi}\int_0^\infty e^{-px^2}\left(\frac{\sin x}{x} - \cos x\right)^2 x^{-2}dx, \qquad (18)$$

where $p = \tau/\tau_C$, $\tau_C = 2a^2/D$; however, they did not carry out the further evaluation of the integral.

The integral (18) can be evaluated by differentiating it with respect to the parameter p:

$$g'_p(p) = -\frac{6}{\pi}\int_0^\infty e^{-px^2}\left(\frac{\sin x}{x} - \cos x\right)^2 dx. \qquad (19)$$

The resulting integral can be easily evaluated by means of breaking it up into parts:

$$g'_p(p) = -\frac{3}{\sqrt{\pi}}\left[p^{1/2}(e^{-1/p} - 1) + \frac{1}{2}p^{-1/2}(e^{-1/p} + 1)\right]. \qquad (20)$$

The correlation function (18) can now be rewritten

$$g(p) = -\frac{3}{2\sqrt{\pi}}\int_0^p [2p^{1/2}(e^{-1/p} - 1) + p^{-1/2}(e^{-1/p} + 1)]\,dp + \text{const}, \qquad (21)$$

the integration constant is determined from the condition $g(\infty) = 0$.

On carrying out the integration required in (21) we obtain the final form of the correlation function for the matrix elements (15) — (17):

$$g(p) = \frac{3}{\sqrt{\pi}}\left[\frac{\sqrt{\pi}}{3}\Phi(p^{-1/2}) + \frac{1}{3}p^{1/2}e^{-1/p} - p^{1/2} + \frac{2}{3}p^{3/2}(1 - e^{-1/p})\right]; \qquad (22)$$

it is normalized to the values $g(0) = 1$ and $g(\infty) = 0$; $\Phi(x)$ is the error function.

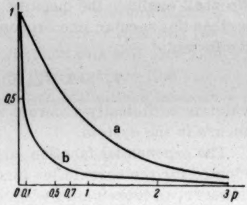

a – graph of the function exp(–p), b – graph of the function (22).

It is appropriate to make a few remarks on the form of the function g(p). As can be seen from (22) and from the figure, the function g(p) differs appreciably from exp(–p). Yet the exponential function is often chosen for the correlation function for quite different random processes perturbed by different motions. Such a choice is dictated both by a desire for simplicity of calculation, and also apparently by the widespread opinion that the exponential form of the correlation function necessarily follows from the Markov character of the process. We see that although the diffusion process is a Markov process, the correlation function obtained by us does not have an exponential form. There is no doubt that the simplification of the correlation function to exponential form introduces a definite error into the results as has been specifically established, in particular, by Skrotskiĭ and Kokin.[7]

5. THE RELAXATION TIMES T_2 AND T_1

We evaluate the normalized spectral densities of the matrix elements in accordance with (2), (10), and (22). The correlation function can now be conveniently written in the form

$$g(p) = \frac{3}{2\sqrt{\pi}}\int_p^\infty [2x^{1/2}(1 - e^{-1/x}) - x^{-1/2}(1 + e^{-1/x})]\,dx; \qquad (23)$$

and with this definition the constant of integration will be equal to zero. We denote the normalized spectral density by

$$j(\omega) = \int_{-\infty}^{+\infty} e^{-i\omega\tau} g(\tau)\,d\tau = \frac{3\tau_c}{\pi^{1/2}}\int_0^\infty \cos\alpha p\,dp\int_p^\infty [2x^{1/2}(1 - e^{-1/x}) - x^{-1/2}(1 + e^{-1/x})]\,dx, \qquad (24)$$

where

$$\alpha = \omega\tau_c, \qquad \omega = \lambda\omega_0, \qquad \lambda = |m - m'|,$$

ω_0 is the nuclear spin precession frequency. The integral (24) can be evaluated by changing the order of integration:

$$j(\omega) = \frac{3\tau_c}{\pi^{1/2}}\int_0^\infty [2x^{1/2}(1 - e^{-1/x}) - x^{-1/2}(1 + e^{-1/x})]\,dx\int_0^x \cos\alpha p\,dp$$
$$= 3\tau_c\,[(z^{-3} - 2z^{-5}) + e^{-z}\cos z\,(z^{-3} + 4z^{-4} + 2z^{-5}) + e^{-z}\sin z\,(z^{-3} - 2z^{-5})], \qquad (25)$$

where

$$z = (2\alpha)^{1/2} = (2\lambda\omega_0\tau_c)^{1/2}.$$

Expansions of the function (25) in the limiting cases $z \ll 1$ (rapid motion) and $z \gg 1$ (slow motion) are given in reference 7.

$$j(\lambda\omega_0) = \frac{2\tau_c}{5}\left(1 - 5\sqrt{2\lambda\omega_0\tau_c}\,/\,12\right) \qquad \text{for } z < 1,$$

$$j(\lambda\omega_0) = \frac{2\tau_c}{5}\left[\delta_{\lambda 0} + \frac{15}{2}(1 - \delta_{\lambda 0})(2\lambda\omega_0\tau_c)^{-3/2}\right] \qquad \text{for } z > 1. \tag{26}$$

We can easily obtain the averaged squares of the matrix elements

$$\Omega^2_{mm'} = \langle |H'_{mm'}(0)|^2\rangle = |A_{mm'}|^2 (N/V)(e_A^2/24a^3), \tag{27}$$

since

$$\sum_A \langle R_A^{-6} |Y_2^\lambda|^2\rangle \doteq N/(24a^3V).$$

In a liquid the condition $z \ll 1$ is practically always fulfilled. In this case we obtain for the relaxation time T_2

$$T_2^{-1} = \frac{2\pi}{75\hbar^2}[ee_AQ(1+\gamma)]^2\left[\overline{\frac{3m^2 - I(I+1)}{I(2I-1)}}\right]^2 \frac{N}{V}\frac{\tau_c}{(2a)^3}. \tag{28}$$

The factor contining the spins is equal to 1 and 0.56 for spins $^3/_2$ and $^5/_2$ respectively.

Under the condition $z \ll 1$ the probabilities of relaxation transitions are equal to:

$$I = {}^3/_2 \qquad w({}^3/_2, {}^1/_2) = w(-{}^1/_2, -{}^3/_2) = 12U,$$

$$w({}^3/_2, -{}^1/_2) = w({}^1/_2, -{}^3/_2) = 12U, \tag{29}$$

$$I = {}^5/_2 \qquad w({}^5/_2, {}^3/_2) = w(-{}^3/_2, -{}^5/_2) = 80U,$$

$$w({}^3/_2, {}^1/_2) = w(-{}^1/_2, -{}^3/_2) = 32U,$$

$$w({}^5/_2, {}^1/_2) = w(-{}^1/_2, -{}^5/_2) = 40U,$$

$$w({}^3/_2, -{}^1/_2) = w({}^1/_2, -{}^3/_2) = 72U, \tag{30}$$

$$U = 2\pi(1/150\hbar^2)(ee_AQ(1+\gamma)/I(2I-1))^2 N\tau_c/V(2a)^3. \tag{31}$$

By utilizing formula (11) and the probabilities (29) and (30), we find that the relaxation time T_1 for spins $^3/_2$ and $^5/_2$ is, respectively,

$$T_1^{-1} = \frac{8\pi}{225}\hbar^{-2}(ee_AQ(1+\gamma))^2(N/V)\tau_c/8a^3,$$

$$T_1^{-1} = \frac{16\pi}{1875}\hbar^{-2}(ee_AQ(1+\gamma))^2(N/V)\tau_c/8a^3. \tag{32}$$

6. AQUEOUS SOLUTIONS OF ELECTROLYTES

We have investigated the quadrupole relaxation of nuclear spins in diamagnetic solutions of electrolytes in reference 4, where we used as our basis the assumption that around ions in solution stable hydrated (solvated) complexes are formed consisting of molecules of the solvent, or of molecules of the solvent together with ions of the electrolyte dissociated in the solution. For aqueous complexes of Al^{3+} and Ga^{3+} ions, which form stable hydrated complexes in solution, we obtain good agreement between the calculated and the measured values of the width of resonance lines. For I^-, Br^-, Na^+ ions the measured line widths do not agree with those calculated on the assumption of the existence of a stable complex. This is apparently associated with the fact that the lifetimes of the hydrated complexes of the I^-, Br^-, Na^+ ions are shorter than the relaxation times T_1 (or T_2) calculated by us for these ions, while the complexes of the Al^{3+} and Ga^{3+} ions live longer than the lattice relaxation times of their nuclear spins (10^{-4} sec). It is natural to assume that the I^-, Br^-, Na^+ ions do not form stable complexes at all in aqueous solution (this also follows from investigations in physical chemistry), and that the relative motion of the molecules of the solvent and of the ions of the dissociated electrolyte represents free translational diffusion. Then in order to determine the line widths and the spin-lattice relaxation times for the I^-, Br^-, Na^+ ions (and for other non-solvated ions) we can utilize formulas (28) and (32).

Let us calculate T_2^{-1} for I^- ions in aqueous solution. The antishielding coefficient $1+\gamma$ for the I^- ion is equal to[10] 179.85, the nuclear constants for the I^{127} isotope are: spin equal to $^5/_2$, and quadrupole moment $Q = 0.7$ b. Instead of $2a$ one should now naturally take the sum of the radii of the I^- ion and of the water molecule $2a = r_{I^-} + r_{H_2O} = 2.16 + 1.45 = 3.61$ A. Moreover, the diffusion coefficient for water at 23° C is equal to[11] 2×10^{-5}, so that $\tau_c = 2a^2/D = 3 \times 10^{-11}$ sec. The number of particles per unit volume is equal to $N/V = 3 \times 10^{22}$. We shall determine the effective charge of the water molecules later by means of comparison with experiment. On substituting the above values of the constants into (28) we obtain

$$T_2^{-1} = 6.9 \cdot 10^5 (e_A/e)^2. \tag{33}$$

Itoh and Yamagata[12] have investigated the variation of T_2^{-1} for the nuclear spins of the I^- ions in aqueous solution. They found that the dependence of T_2^{-1} on the temperature has a close resemblance to the temperature dependence of the ratio η/T for any given solution. Formula (28) predicts just such a dependence

$$\tau_c = (12a^3\pi/k)\,\eta/T, \qquad T_2^{-1} \sim \tau_c \sim \eta/T. \tag{34}$$

Further, the isothermals of the quantity T_2^{-1} must be proportional to the viscosity of the solution:

$$T_2^{-1} \sim \eta. \tag{35}$$

Itoh and Yamagata[12] have studied the dependence of T_2^{-1} on the concentration of the solution, and this dependence has turned out to be considerable in a solution of NaI and not very great in solutions of

KI. At first glance formula (28) does not show any dependence on the concentration of the solution. However, the viscosity of the liquid depends on the concentration of the solution: the experimentally observed dependence of T_2^{-1} on the concentration agrees closely with the dependence of the viscosity on the concentration in accordance with (35).

We now turn to formula (33) and determine the effective charge of the water molecule. On substituting the value of $T_2^{-1} = 7 \times 10^3$ sec^{-1} obtained[12] for 23° C and extrapolated to infinite dilution we get

$$e_A = 0{,}1\,e. \qquad (36)$$

As may be seen, the effective charge of the water molecule obtained from the study of quadrupole relaxation in non-associated solutions is even somewhat smaller than the usually adopted values ~ 0.5 e.

An exact calculation of T_2^{-1} taking into account the dipole nature of the water molecules and their rotational motion will be given by us elsewhere.

In concluding this section we note the following. In the presence of a stable solvated (hydrated) ionic shell the relaxation of nuclear spin proceeds by means of the interaction of the quadrupole moment of the nucleus with the normal vibrations of the complex; in this case the temperature dependence of the width of the resonance line is determined by the equation[3,4]

$$T_2^{-1} \sim T^{-1/2} \coth\,(\hbar\omega_0 / 2kT), \qquad (37)$$

where ω_0 is the frequency of the characteristic vibrations of the complex which amounts to (4 to 16) $\times 10^{13}$ sec^{-1}. Relation (37) was verified by the study of the widths of electron resonance lines for a whole series of paramagnetic ions which form stable complexes in solution;[3] so far there have been no experiments on the study of the temperature dependence of the widths of nuclear magnetic resonance lines of diamagnetic ions solvated in solution. On the other hand, if an ion does not form a stable solvated complex, and the motion of the neighboring particles consists of free diffusion, then relation (34) must be satisfied. A comparison of (34) and (37) shows that a study of the temperature dependence of T_2^{-1} can yield a completely unambiguous determination of the occurrence of complex formation in solution.

7. MELTS OF METALS

In metallic crystals having a cubic structure the energy of the nuclear quadrupole moment is equal to zero, and the principal role in the spin relaxation of the nuclei is played by their interaction with the conduction electrons and among themselves: the spin-lattice relaxation (the relaxation time T_1) is determined by the interaction with the conduction electrons, while the line width (the relaxation time T_2) is determined by the magnetic interaction of the nuclei among themselves.[13,14] A result of this is the inequality $T_1 \neq T_2$. As a crystal is heated various lattice defects are produced: the cubic structure of the lattice is destroyed, and this results in the appearance of quadrupole broadening of magnetic resonance lines which has been experimentally established for Al^{27} nuclei in metallic aluminum.[14] If the structure of the crystal has symmetry lower than cubic (for example, in gallium), then quadrupole effects occur even in a perfect lattice without any defects.[15]

Thus, from experiments on magnetic resonance in metals it follows that the quadrupole energy of nuclei is due primarily to the electric fields produced by ionic cores in the metal lattice; the electric fields at the nuclei due to the conduction electrons have symmetry close to spherical, which is characteristic of S-state electrons, and as a result of their high symmetry cannot produce quadrupole splitting of the nuclear spin energy levels. Apparently, basically the same situation also exists in a metallic melt. But since in a melt the instantaneous configurations of the ion positions which vary with time do not have any symmetry, the fields produced at the nuclei are, generally speaking, different from zero, and give rise to relaxation effects, whose magnitude may be computed from formulas (28) and (32).

A calculation which we have made for Li and Na yielded values of T_1 and T_2 greater than the experimentally observed ones.[13] The Li^6, Li^7, and Na^{23} nuclei have small quadrupole moments and, therefore, the quadrupole effects are small. Al^{27} has a somewhat larger quadrupole moment. The relaxation time calculated with the aid of (28) is $T_2\,(Al^{27}) = 3 \times 10^{-2}$ sec, which also exceeds the experimentally found value[14] $T_2 = T_1 = 2.1 \times 10^{-3}$ sec by a factor of ~ 15. (For the evaluation of $T_2\,(Al^{27})$ the following values of the constants were adopted: $e_A = e$, i.e., it was assumed that the Al ions in the melt are singly charged; the metallic radius of the Al atom $a = 1.4$ A, $I = 5/2$, $Q = 0.156$ b, $N/V = 10^{23}$, $D = 2 \times 10^{-5}$ and $\tau_c = 2a^2/D = 10^{-11}$ sec, $1 + \gamma = 3.59$. The value of $1 + \gamma$ which we have utilized was calculated[10] for the Al^{3+} ion: for a singly charged ion the value of $1 + \gamma$ will probably be greater, since the antishielding effect is associated with the deformability of the electron shell of the atom.)

Our results show that in lithium, sodium, and aluminum melts the quadrupole relaxation of nuclear spins plays a subordinate role; other mechanisms predominate. However, in an aluminum melt, so far as we can judge from our calculations, the rate of quadrupole relaxation of nuclei differs from the rate of relaxation due to the dominant mechanism by a factor of ~ 10. We can expect that in the case of metals having a quadrupole moment of ~ 1 b, quadrupole relaxation will give a contribution comparable to the contribution of the mechanisms predominant in Li, Na, Al, and will possibly become dominant. It should be noted that the antishielding effects, on which the rate of quadrupole relaxation depends in a large measure, are quite insignificant for the Li^+, Na^+, and Al^+ ions. For ions which are isoelectronic with the inert gases the antishielding coefficient $|\gamma|$ increases as the number of the electrons in the ion increases: for the series of ions Na^+, K^+, Rb^+, Cs^+ the values of γ are equal to 4.53, 12.84, 49.3, and 110 respectively.[10] This shows that quadrupole effects will be large for heavy atoms. For example, metallic indium is convenient for carrying out experiments: it has a relatively low melting point and a large quadrupole moment (for the isotope In^{115} $I = 9/2$ and $Q = 1.16$ b). We can assume that the antishielding effects will also be large for the In ion; according to Rhoderick's estimates[16] made on the basis of an experiment in a mixed single crystal of InSb, $\gamma\,(\mathrm{In}) \approx 1000$.

8. MELTS OF IONIC SALTS

Formulas (28) and (32) which we have obtained may be found applicable to interpreting widths of resonance lines and the spin-lattice relaxation time of nuclear spins in melts of salts, for example, of the NaCl type. The new feature which has to be taken into account in discussing melts of salts as compared to melts of metals and solutions of electrolytes consists of the difference in the sign of the charges of the ions composing the melt. This means that ions of different sign can appear near the ion under consideration as a result of the process of diffusion; this circumstance will in some way affect the relaxation times T_1 and T_2, and this, generally speaking, can be taken into account by introducing a certain factor into the right hand side of (28) and (32). The functional dependence of T_1 and T_2 on the temperature and on the viscosity expressed by (34) and (35) will remain valid.

We now estimate the order of magnitude of the factors in (28) and (32). X-ray investigations show the existence in liquids of a sharply pronounced short-range order with atomic configurations corresponding to close packing.[17] On the basis of this we can assume that atoms which are the nearest neighbors of the ion under consideration have a configuration corresponding to one of the close packed configurations, for example, octahedral. If we assume that all the atoms of this octahedron have charges of the same magnitude and of the same sign, then the field gradient ∇E at the center of the octahedron will be due only to the displacements of the atoms from their equilibrium positions in the octahedron, the magnitude of the components will be given by $\nabla E \sim e_A a^{-4} Q_i$, where a is the equilibrium distance between the atoms, Q_i are linear combinations of the displacements of the atoms from their equilibrium positions in the octahedron, $a \approx 3$ A; the magnitude of Q_i can be estimated[17] from the width of the first maximum of the radial distribution function of the particles in the liquid: $Q_i \approx 0.5$ A.

On the other hand, let us assume that in the process of diffusion either ions with charges of different sign or vacancies have appeared in the neighborhood of the ion under consideration. Then, as a simple calculation shows, the components of the tensor ∇E differ from zero even in the case of the correct atomic configuration; the magnitude of the components is given by $\nabla E \sim e_A a^{-3}$. It is clear that the ratio of the gradients in the second and in the first case is equal to $a/Q_i \sim 6$, while the ratio of the magnitudes of T_2^{-1} amounts to ~ 36. Consequently, in a salt melt, if we admit the possibility of formation of coordination spheres for the ions consisting of particles of charges of different sign, the magnitude of T_2^{-1} increases by a factor of 10 to 100 and attains a value of $\sim 10^5$ sec^{-1} (~ 100 oe). Such an estimate of the width agrees with the result of Flynk and Seymour:[18] in a melt of bismuth iodide these authors were unable to observe the nuclear resonance of Bi^{209} ($I = 9/2$, $Q = 0.4$ b), even though their spectroscope permitted them to observe lines of width up to 40 oe.

---

[1] Bloembergen, Purcell, and Pound, Phys. Rev. **73**, 679 (1948).

[2] B. M. Kozyrev, Trans. Faraday Soc. **19**, 135 (1955).

[3] S. A. Al'tshuler and K. A. Valiev, JETP **35**, 947 (1958), Soviet Phys. JETP **8**, 661, (1959).

[4] K. A. Valiev, JETP **37**, 109 (1959), Soviet Phys. JETP **10**, 77 (1960).

[5] H. J. McConnell, J. Chem. Phys. **25**, 709 (1956).

[6] B. R. McGarvey, J. Phys. Chem. **61**, 1232 (1957).

[7] G. V. Skrotskiĭ and A. A. Kokin, JETP 36, 481 (1959), Soviet Phys. JETP 9, 335 (1959).

[8] C. J. Gorter, Paramagnetic Relaxation (Russ. Transl.), IIL, 1949, p. 105.

[9] L. D. Landau and E. M. Lifshitz, Теория поля (Field Theory), Moscow, Gostekhizdat, 1948, p. 116. (Engl. Tr., Addison-Wesley, 1951).

[10] R. M. Sternheimer and H. M. Foley, Phys. Rev. 102, 731 (1956). T. P. Das and R. Bersohn Phys. Rev. 102, 733 (1956). E. G. Wikner and T. P. Das, Phys. Rev. 109, 360 (1958).

[11] J. H. Simpson and H. Y. Carr, Phys. Rev. 111, 1201 (1958).

[12] J. Itoh and Y. Yamagata, J. Phys. Soc. Japan 13, 1182 (1958).

[13] D. F. Holcomb and R. E. Norberg, Phys. Rev. 98, 1074 (1955).

[14] J. J. Spocas and C. P. Slichter, Phys. Rev. 113, 1462 (1959).

[15] Knight, Hewitt, and Pomerantz, Phys. Rev. 104, 271 (1956).

[16] E. H. Rhoderick, Phil. Mag. 3, 545 (1958).

[17] V. I. Danilov, Proceedings of the Conference on the Physics of the Liquid State, Kiev, 1954, p. 11.

[18] C. P. Flynk and E. F. W. Seymour, Proc. Phys. Soc. A73, 945 (1959).

Translated by G. Volkoff
236

ON THE ANALOGY BETWEEN THE WEAK AND THE ELECTROMAGNETIC INTERACTIONS

É. M. LIPMANOV

Stalingrad State Pedagogical Institute

Submitted to JETP editor October 31, 1959

J. Exptl. Theoret. Phys. (U.S.S.R.) 38, 1233-1236 (April, 1960)

The analogy between the weak and the electromagnetic interactions is presented in such a way that the electric current and the charged currents in the weak interaction are obtained from a single symmetrical expression which involves the operators $\frac{1}{2} + \tau$ and $1 + \gamma_5$ after the requirements of conservation of the electric, leptonic, and baryonic charges and of vanishing of the photon mass are imposed. A definite "chirality" is ascribed to particles of half-integral spin, which is conserved in weak interactions. Doublets of "bare" Fermi particles in the weak and electromagnetic interactions are classified in terms of the values of the electric charge, the leptonic or baryonic charge, and the chirality.

THE hypothesis of Gershteĭn and Zel'dovich[1] and of Feynman and Gell-Mann,[2] that there is conservation of the vector current in weak interactions, indicates the existence of a deep analogy between the weak and the electromagnetic interactions. A concrete formulation of this analogy is proposed in the present paper. Together with the requirements of conservation of electric, leptonic, and baryonic charges and of chirality, this makes it possible to set up a complete expression for the weak current of the "bare" particles, which is in qualitative agreement with all available experimental data on the decays of ordinary and strange particles.

In what follows we use the hypothesis that there are two isotopic leptonic doublets ($\nu_1 e^-$) and ($\nu_2 \mu^-$);[3] the isospins of all baryons are assumed to be equal to $\frac{1}{2}$, in accordance with Gell-Mann's hypothesis of global symmetry.[4] When the hyperons are included in the treatment the table of the properties of fermions that was presented earlier[3] takes a new form* (see Table I). Here letters with the tilde denote antiparticles; l, n, e are the leptonic, baryonic, and electric charges,

$$Y^0 = 2^{-1/2}(\Lambda^0 - \Sigma^0), \qquad Z^0 = 2^{-1/2}(\Lambda^0 + \Sigma^0), \tag{1}$$

γ_5 is the chirality in weak interactions;[3,7] the new strangeness S′ of a particle is calculated by the formula

$$e = I_z + {}^1/_2(l + n + S').$$

TABLE I

	I_z	l	n	e	γ_5	S'
e	$-^1/_2$	-1	0	-1	$+1$	0
ν_1	$^1/_2$	-1	0	0	$+1$	0
μ	$-^1/_2$	$+1$	0	-1	$+1$	-2
ν_2	$^1/_2$	$+1$	0	0	$+1$	-2
p	$^1/_2$	0	$+1$	$+1$	$+1$	0
n	$-^1/_2$	0	$+1$	0	$+1$	0
$\widetilde{Y}^0$	$^1/_2$	0	-1	0	$+1$	0
$\widetilde{\Sigma}^+$	$-^1/_2$	0	-1	-1	$+1$	0
Z^0	$^1/_2$	0	$+1$	0	-1	-2
Σ^-	$-^1/_2$	0	$+1$	-1	-1	-2
$\widetilde{\Xi}^-$	$^1/_2$	0	-1	$+1$	$+1$	$+2$
$\widetilde{\Xi}^0$	$-^1/_2$	0	-1	0	$+1$	$+2$

Table I shows that definite chiralities are assigned to all fermions except the neutral hyperons Λ^0 and Σ^0; their chiralities can be ±1, depending on whether they occur in the Z or the Y doublet:*

$$N = \begin{pmatrix} p \\ n \end{pmatrix}, \qquad Y = \begin{pmatrix} \Sigma^+ \\ Y^0 \end{pmatrix}, \qquad Z = \begin{pmatrix} Z^0 \\ \Sigma^- \end{pmatrix}, \qquad \Xi = \begin{pmatrix} \Xi^0 \\ \Xi^- \end{pmatrix}. \tag{2}$$

We shall take as the primary weak processes the interactions of the weak currents with charged vector mesons $X_\mu^\pm$.[2]

Then the Hamiltonians of the electromagnetic and weak interactions can be written in the form

$$H^{(0)} = e j_\mu^{(0)} A_\mu, \tag{3}$$

$$H = H^{(+)} + H^{(-)} \qquad H^{(+)} = g_1 j_\mu^{(+)} X_\mu^+,$$

$$H^{(-)} = g_1 j_\mu^{(-)} X_\mu^-, \tag{4}$$

---

*For antiparticles the signs of all numerical entries in the table are changed.

*The chirality of a particle indicates whether the wave function of the particle appears in the weak current with the factor $1 + \gamma_5$ or $1 - \gamma_5$, and accordingly corresponds to the eigenvalues $\gamma_5 = \pm 1$.

where e is the charge of the electron; $g_1 \sim g^{1/2}$, and g is the constant of the Fermi interaction. We now assume that all three currents $j^{(0)}$, $j^{(+)}$, and $j^{(-)}$ have the same isotopic structure.* Since for all fermions the electric current $j^{(0)}$ has a structure of the form $B/2 + \tau_z$, the corresponding structure of the weak currents must have the form

$$j_\mu^{(+)} \sim (B/2 + \tau_+) \text{ and } j_\mu^{(-)} \sim (B/2 + \tau_-).$$

Here the operator B is defined by $B = l + n + S'$.

The correct expression for the electric current of the fermions is obtained from the following more general expression:

$$\begin{aligned} & i\,(\bar{l}_1 + \bar{l}_2 + \overline{N} + \bar{\tilde{Y}} + \bar{Z} + \bar{\tilde{\Xi}}) \\ & \quad \times (B/2 + \tau_z)\, O_\mu\, (l_1 + l_2 + N + \tilde{Y} + Z + \tilde{\Xi}), \\ & \qquad l_1 = \begin{pmatrix} \nu_1 \\ e^- \end{pmatrix}, \qquad l_2 = \begin{pmatrix} \nu_2 \\ \mu^- \end{pmatrix}, \qquad O_\mu = \gamma_\mu (1 + \gamma_5) \end{aligned} \tag{5}$$

by imposing the requirements of conservation of the electric, leptonic, and baryonic charges, of conservation of chirality in weak interactions,[7] and of gauge invariance of the interaction.[9] It has the usual form

$$\begin{aligned} j_\mu^{(0)} &= i\,[(\bar{l}_1 \gamma_\mu (B/2 + \tau_z)\, l_1) + \ldots + (\bar{\tilde{\Xi}} \gamma_\mu (B/2 + \tau_z)\, \tilde{\Xi})] \\ &= -i\,[(\bar{e} \gamma_\mu e) + (\bar{\mu} \gamma_\mu \mu) - (\bar{p} \gamma_\mu p) \\ &\quad + (\bar{\tilde{\Sigma}}^+ \gamma_\mu \tilde{\Sigma}^+) + (\bar{\Sigma}^- \gamma_\mu \Sigma^-) - (\bar{\tilde{\Xi}}^- \gamma_\mu \tilde{\Xi}^-)]. \end{aligned} \tag{6}$$

In a similar way we get the expressions for the weak currents from general expressions of the type of Eq. (5) by using the conservation laws that have been mentioned (without gauge invariance)†

$$\begin{aligned} & i\,(\bar{l}_1 + \bar{l}_2 + \overline{N} + \bar{\tilde{Y}} + \bar{Z} + \bar{\tilde{\Xi}})\,(B/2 + \tau_-)\, O_\mu\, (l_1 + l_2 + N + \tilde{Y} \\ & \quad + Z + \tilde{\Xi}) \rightarrow\ j_\mu^{(-)} = i\,[(\bar{l}_1 O_\mu \tau_- l_1) + \ldots + (\bar{\tilde{\Xi}} O_\mu \tau_- \tilde{\Xi})] \\ & \quad + \frac{1}{2}\, i\,[(\bar{Z} O_\mu N) + (\bar{\tilde{Y}} O_\mu \tilde{\Xi})] = i\,[(\bar{e} O_\mu \nu_1) + (\bar{\mu} O_\mu \nu_2) + (\bar{n} O_\mu p) \\ & \quad + (\bar{\tilde{\Sigma}}^+ O_\mu \tilde{Y}^0) + (\bar{\Sigma}^- O_\mu Z^0) + (\bar{\tilde{\Xi}}^0 O_\mu \tilde{\Xi}^-)] \\ & \quad + \frac{1}{2}\, i\,[(\bar{Z}^0 O_\mu p) + (\bar{\Sigma}^- O_\mu n) + (\bar{\tilde{Y}}^0 O_\mu \tilde{\Xi}^-) + (\bar{\tilde{\Sigma}}^+ O_\mu \tilde{\Xi}^0)], \end{aligned} \tag{7}$$

$$j_\mu^{(+)} = j_\mu^{(-)*}. \tag{8}$$

Thus the violation of isotopic invariance in the weak and electromagnetic interactions is of precisely the same character for all. We note that conservation of chirality in the expressions (5) and (7) is attained automatically, and the other requirements are imposed from outside. The requirement of gauge invariance, for example, leads to the exclusion of terms that do not conserve parity.[11,12] Furthermore the electric charge is regarded as a conserved integer quantity on an equal footing with the leptonic and baryonic charges and only "accidentally" (the isotopic structure $\frac{1}{2} + \tau_Z$ of the current) coincides with the coupling constant with the electromagnetic field.*

The expressions that have been obtained for the weak currents evidently allow us to explain all existing experimental data on the decays of ordinary and strange particles: they contain no terms with change of the strangeness S by two units; the empirical rule $\Delta S/\Delta e = +1$ is satisfied for processes with change of strangeness;[2] and there are no terms that lead to the production of pairs in the decay of hyperons.†

It is easy to see that these results are a direct consequence of our choice of the values of the chiralities of hyperons and the requirement of conservation of chirality in weak interactions.‡ This choice is not an accidental one, but is occasioned by the following considerations. It is obvious that one can carry out a classification of leptonic doublets in the weak interactions according to all possible combinations of leptonic charge, chirality, and sign of electric charge. The possible leptonic doublets are shown in Table II. In the leptonic case the primed doublets are not observed.

TABLE II

	l	γ_5	e
l_1	−1	+1	−1
l_2	+1	+1	−1
$\tilde{l}_1$	+1	−1	+1
$\tilde{l}_2$	−1	−1	+1
l'_1	−1	+1	+1
l'_2	+1	+1	+1
$\tilde{l}'_1$	+1	−1	−1
$\tilde{l}'_2$	−1	−1	−1

This is evidently connected with the fact that the mass of the neutrino is identically zero [if the primed and unprimed leptonic doublets existed simultaneously in the "world," then each of the two neutrinos and antineutrinos would occur in two different doublets ($\nu_1' \equiv \nu_1$, etc.)]. If in Table II we replace the leptonic charge by the baryonic charge, we get a table of possible baryonic doublets. Evidently they all actually exist (cf. Table III).

---

*The analogy between the weak and electric currents based on the idea of an intermediate vector meson has been studied by Schwinger and by Salam and Ward.[5,6]

†According to the hypothesis of the conserved vector current, in all three of these currents one must add the corresponding mesonic currents.

*This conception of the electric charge is clearly expressed in a paper by Zel'dovich[8] (cf. also reference 9).

†For discussion see a paper by Dalitz.[10]

‡It must be noted that "chirality" is not a charge, since it is conserved only in the weak currents.

TABLE III

	n	χ_5	e
$\tilde{Y}$	−1	+1	−1
Z	+1	+1	−1
Y	+1	−1	+1
$\tilde{Z}$	−1	−1	+1
$\tilde{\Xi}$	−1	+1	+1
N	+1	+1	+1
Ξ	+1	−1	−1
$\tilde{N}$	−1	−1	−1

We note that the scheme we have given for the weak and electromagnetic interactions of "bare" particles, in which definite chiralities are ascribed to the particles, corresponds to the general feature of these interactions, that they are incapable of giving rise to a finite proper mass of particles when this mass is initially zero (this result is a direct consequence of the fact that these interactions do not change the chirality of the particles), and therefore in the absence of strong interactions all the particles involved in them can be regarded as devoid of rest mass. The strong interactions remove the degeneracy, but do not change the number of independent particles.

I take occasion to express my sincere gratitude to Ya. B. Zel'dovich and B. Pontecorvo for their constant attention to and interest in this work and for valuable comments, and also my sincere thankfulness to A. Z. Dolginov for a discussion.

---

[1] S. S. Gershteĭn and Ya. B. Zel'dovich, JETP **29**, 698 (1955), Soviet Phys. JETP **2**, 576 (1956).

[2] R. Feynman and M. Gell-Mann, Phys. Rev. **109**, 193 (1958).

[3] É. M. Lipmanov, JETP **37**, 1054 (1959), Soviet Phys. JETP **10**, 750 (1960).

[4] M. Gell-Mann, Phys. Rev. **106**, 1296 (1957).

[5] J. Schwinger, Ann. Phys. **2**, 407 (1957).

[6] A. Salam and J. Ward, Nuovo cimento **11**, 568 (1959).

[7] E. Sudarshan and R. Marshak, Proc. Intern. Conf. on Mesons, Padova-Venezia, 1957.

[8] Ya. B. Zel'dovich, Dokl. Akad. Nauk SSSR **91**, 1317 (1953).

[9] N. N. Bogolyubov and D. V. Shirkov, Введение в квантовую теорию волновых полей (Introduction to the Quantum Theory of Wave Fields), Gostekhizdat, 1957.

[10] R. H. Dalitz, Rev. Modern Phys. **31**, 823 (1959).

[11] V. G. Solov'ev, JETP **33**, 537 (1957), Soviet Phys. JETP **6**, 419 (1958).

[12] S. Gupta, Canad. J. Phys. **35**, 1309 (1957).

Translated by W. H. Furry
237

SOVIET PHYSICS JETP VOLUME 11, NUMBER 4 OCTOBER, 1960

ON THE STRUCTURE OF THE S MATRIX IN THE THEORY OF ELASTIC AND INELASTIC SCATTERING OF NONRELATIVISTIC PARTICLES

Yu. V. TSEKHMISTRENKO

Institute of Physics, Academy of Sciences, Ukrainian S.S.R.

Submitted to JETP editor November 31, 1959

J. Exptl. Theoret. Phys. (U.S.S.R.) **38**, 1237-1244 (April, 1960)

Integral relations for the components of the S matrix describing a nuclear reaction with two channels (one channel is the elastic scattering of a nonrelativistic particle and the other is inelastic scattering with excitation of the nucleus) are derived from general principles of causality, unitarity, and symmetry, and the analytic properties of some components of the S matrix are established. For simplicity the treatment is confined to the case of spherically symmetrical scattering. In agreement with the results of Wigner[1] and of Baz',[2] the excitation function of the elastic scattering has a break at the threshold of the inelastic process. The form of the excitation function of the inelastic process near threshold is found in the general case.

1. INTRODUCTION

A number of papers[3-6] have been devoted to the determination of the mathematical structure of the S matrix (S function) for the scattering of nonrelativistic particles by a nucleus of finite size or by a potential field. As van Kampen has shown,[4] the S function for the scattering of a nonrelativistic particle by a nucleus of finite size has the form

$$S(\lambda) = e^{-2i\alpha\lambda} \prod_n \frac{1-\lambda/\Lambda_n}{1-\lambda/\Lambda_n^*} \frac{1+\lambda/\Lambda_n^*}{1+\lambda/\Lambda_n} \prod_m \frac{1-\lambda/iP_m}{1+\lambda/iP_m}. \qquad (1)$$

The singularities of $S(\lambda)$ in the upper half-plane are simple poles located on the imaginary axis. It is evidently impossible to establish the character of the distribution of poles in the lower half-plane from general considerations. It is also necessary to note that the general requirements of causality, unitarity, and symmetry do not provide the possibility of determining even the order of the poles in the lower half-plane. Generally speaking, despite a widespread impression (cf., e.g., reference 6), there is no basis for believing that they are only simple poles.

It must be remarked that the theory of the elastic scattering of a particle by a nucleus of finite size that has no internal degrees of freedom does not have any concrete applications in atomic and nuclear physics. In actual fact, when the energy of the incident particle is large enough there must necessarily occur a change of state of the bombarded system. Therefore the formula (1) for the S function of the elastic scattering of a particle by a nucleus must be regarded as only an approximate formula that holds for $\epsilon/E \gg 1$, where $E = k^2/2M$ is the energy of the particle and ϵ is the excitation energy of the nucleus. The Breit-Wigner formula, which can be obtained from Eq. (1) (cf. reference 6), is also approximate. Attempted modifications of the Breit-Wigner formula to take into account the channels of reactions other than elastic scattering are much inferior in rigor to the S function of the theory of "pure" scattering. This theory allows us to establish the structure (1) of the S function on the basis of three fundamental principles — causality, unitarity, and symmetry. The formulation of the principles of unitarity and symmetry is quite unambiguous. The causality principle is another matter. After the discussion of this question in the literature we can now regard as established two noncontradictory formulations of the principle of causality: a) the direct formulation proposed by van Kampen[4] (the probability of finding the particle outside the nucleus at the time $t = t_1$ is smaller than this same probability at $t = -\infty$); b) the "indirect" formulation proposed by Heisenberg[7] (the completeness relation must be fulfilled for the wave functions of particles outside the nucleus).

It is a matter of definite interest to establish with mathematical rigor, on the basis of the principles just mentioned, the integral relations between the components of the S matrix (when inelastic-scattering channels are present), and to determine the structure of the components that correspond to the elastic scattering, thus generalizing Eq. (1). In carrying out this program we shall rely on the second formulation of the causality principle. This choice is made on the following considerations: simplicity of the formulation; automatic establishment of the connection of the poles and residues of the S matrix with the eigenvalues of the energy of the system and the normalization coefficients of the bound states; the possibility of a much easier approach to long-range potentials than in the van Kampen formalism. If, unlike Ning Hu,[3] we use exact expressions for the wave functions outside the nucleus in deriving the structure of the S function in the case of a long-range potential, the form of the S function is basically unchanged, except that now not all of its poles will be connected with energy levels of the system (on this point see references 4, 8, and 9).

2. NOTATION. FORMULATION OF SYMMETRY AND UNITARITY PROPERTIES

Let us consider reactions of the type $n + C = n' + C'$, where C is the bombarded system and n and n′ are the incident and scattered particles. For simplicity we shall regard the nucleus C as infinitely heavy. We assume that the energy spectrum of C is purely discrete with nondegenerate levels. We write for the corresponding eigenfunctions $\psi_j(\xi)$, where j numbers off the levels in order of increasing energy and ξ is the internal coordinates of the system C. We take the entire interaction of C with the particle to be spherically symmetrical and localized inside a sphere of radius a. For $r > a$ we can expand the wave function $\Psi_l(E, r, \xi)$ of the system in a series of the functions $\psi_j(\xi)$:

$$\Psi_l(E, r, \xi) = \sum_j \Phi_{lj}(E, r)\,\psi_j(\xi). \tag{2}$$

As is the usual practice,[10] we call j the channel number and l the number of the open channel. Thus $\Phi_{jj}(E, r)$ contains both the incident and scattered waves, and $\Phi_{l \neq j}(E, r)$ only the diverging wave. Obviously $\Psi_l(E, r, \xi)$ are essentially the same as the functions $\Psi^{(+)}$ introduced by Schwinger and Lippmann.[11] In order hereafter not to obscure the general picture by cumbersome calculations, we shall confine ourselves to the case of just two levels, and let the distance between them be $\epsilon = k_0^2/2M$.

Setting $K = (k^2 - k_0^2)^{1/2}$, we can write more detailed expressions for $\Phi_{lj}(E, r)$:

$$\Phi_{11} = A\,(e^{-ikr} - S_{11}e^{ikr}), \qquad \Phi_{12} = AS_{12}e^{iKr},$$

$$\Phi_{21} = AS_{21}e^{ikr}, \qquad \Phi_{22} = A\,(e^{-iKr} - S_{22}e^{iKr}). \tag{3}$$

Obviously we must require that

$$\Phi_{2l} = 0, \quad \text{if } E < \varepsilon. \tag{4}$$

Let us now examine all the conclusions that can be drawn about the properties of the functions S_{lj} without resorting to the completeness relation. We shall regard S_{lj} as a function of k (or K) for positive and negative k (or K). We use the condition of the conservation of the number of particles in the form that expresses the equality of the flux of the converging wave to that of the diverging wave. This leads to the set of relations:

$$|S_{11}|^2 = 1, \qquad (E < \varepsilon), \qquad kK^{-1}|S_{21}|^2 + |S_{22}|^2 = 1,$$

$$|S_{11}|^2 + Kk^{-1}|S_{12}|^2 = 1\ (E > \varepsilon). \tag{5}$$

The next group of relations comes from the obvious fact that under the replacement $k \rightarrow -k$ (or $K \rightarrow -K$) the function $\Psi_l(E, r, \xi)$ must go over into itself (apart from a constant factor). Here $\psi_j(\xi)$ can of course be regarded as real. These relations are[*]

$$S_{11}^{-1}(k) = S_{11}(-k), \qquad S_{11}(-k) = -S_{12}(-k)/S_{12}(k),$$

$$S_{22}^{-1}(K) = S_{22}(-K), \qquad S_{22}(-K) = -S_{21}(-K)/S_{21}(K). \tag{6}$$

3. NORMALIZATION AND COMPLETENESS CONDITIONS. INTEGRAL RELATIONS FOR THE COMPONENTS OF THE S MATRIX

The writing of the normalization and completeness relations for $\Psi_l(E, r, \xi)$ is a step beyond the framework of the Schrödinger-equation formalism. Even if we assume that the Schrödinger equation is valid for all r, the completeness relation does not follow from the Hermitian property of the Hamiltonian, as is the case, for example, in the treatment of "pure" elastic scattering.[3] The functions $\Psi_l(E, r, \xi)$ are eigenfunctions of a non-Hermitian operator (cf. e.g., reference 11). This can indeed be seen from the fact that the requirement that there be no converging waves in part of the channels is equivalent to the imposition of a non-Hermitian boundary condition at infinity. On the other hand, as is well known, the "Hermitian" solution of the Schrödinger equation, which automatically satisfies the completeness condition, cannot describe the scattering problem.

---

[*] If our two states of the target nucleus are due to spin splitting, the relations (6) are changed. In fact it is not difficult to show that with a suitable choice of the quantization axis for the spin the replacement $k \rightarrow -k$ (or $K \rightarrow -K$) must be accompanied by multiplication of the spin functions ψ_1 and ψ_2 by the matrix σ_2 (in this case ψ_1 and ψ_2 are eigenfunctions of σ_3). As can easily be perceived, this leads to a change of the signs of the fractions in Eq. (6). In the final analysis this difference is unimportant, since these relations are not used in the derivation of the analytical structure of the functions S_{11} and S_{22} that determine all observable quantities.

The normalization condition (7) and completeness condition (8) are written down by analogy with the corresponding conditions for "Hermitian" solutions:

$$\int dr \sum_l \Phi_{lj}(E, r)\Phi^*_{l'j}(E', r) = \delta(k-k')\delta_{ll'}, \tag{7}$$

$$\int dk \sum_l \Phi_{lj}(E, r)\Phi^*_{lj'}(E, r') = \delta(r-r')\delta_{jj'}. \tag{8}$$

From Eq. (7) we can find the coefficient A

$$A = 1/\sqrt{2\pi} \tag{9}$$

and the relation

$$S_{21}S^*_{11} + kK^{-1}S_{22}S^*_{12} = 0. \tag{10}$$

For $j = j' = 1$ the condition (8), after some simple manipulations, multiplication by $e^{-ik(r+r')}$, and integration with respect to the variable $\rho = r + r'$ from 2A to infinity (A > a), with the use of Eqs. (5) and (6), gives the result (for $E > \epsilon$):

$$|S_{11}|^2 + |S_{21}|^2 = 1, \tag{11}$$

$$\pi\theta(k)S_{11A}(k) + \pi\theta(-k)S^*_{11A}(-k) + i\int_{-\infty}^{\infty} \frac{S_{11A}(k')}{k'-k}dk' + i\int_{k_0}^{\infty} dk' \frac{S_{11A}(-k') - S^*_{11A}(k')}{k'+k} = 4\pi i \sum_s \frac{|c_{1s}|^2 \exp(2ik_sA)}{k_s - k}, \tag{12}$$

$$S_{11A}(k) = e^{2ikA}S_{11}(k);\quad \theta(x) = 1 \text{ for } x > 0;\quad \theta(x) = 0 \text{ for } x < 0. \tag{13}$$

By analytical calculations one can obtain the integral relation that follows from Eq. (8) for $j = j' = 2$ ($E > \epsilon$):

$$|S_{22}|^2 + |S_{12}|^2 = 2kK^{-1} - 1, \tag{14}$$

$$\pi\frac{K}{k}S_{22A}(k) - i\int_{k_0}^{\infty}\frac{S^*_{22A}(k')\,dk'}{K+K'} - i\int_{k_0}^{\infty}\frac{S_{22A}(k')\,dk'}{K-K'} + i\int_0^k dk' \frac{e^{2iK'A}}{K-K'}|S_{12}(k')|^2 = -4\pi i \sum_s \frac{|c_{2s}|^2 \exp(2iK_sA)}{K-K_s}, \tag{15}$$

$$S_{22A}(k) = e^{2iKA}S_{22}(k). \tag{16}$$

For $j = 1$, $j' = 2$ the condition (8) gives an extremely complicated integral relation between the components of the S matrix that correspond to different input channels. We shall not concern ourselves with the study of this relation.

Let us turn to the simplification of the relations (12) and (15). From the fact that the relation $|S_{11}|^2 = 1$ becomes invalid for $E = \epsilon$ we can draw the conclusion that S_{11} depends on K. Because the root is multiple valued, S_{11} must be considered on a Riemann surface, which we get by cutting the two k planes from $k = k_0$ to $+\infty$ and from $k = -k_0$ to $-\infty$ and connecting them crosswise along the cuts. Let K take positive values along the upper edges of the cuts in the plane of integration. According to the meaning of the integral $\int_{-\infty}^{\infty}$ in the left member of Eq. (12) the integration is taken along the upper edge of the cut in the right half-plane, and along the lower edge in the left half-plane (the path C, see Fig. 1). Since we intend eventually to apply Cauchy's theorem, we transform our integral in such a way that the integration may also go along the upper edge of the cut in the left half-plane. If we denote the path of integration so obtained by C′, then we have $\int_C = \int_{C'} + \int_{\text{l.c.}}$, where $\int_{\text{l.c.}}$ is the integral around the left-hand cut in the positive direction. We now use the fact that Eq. (12) must be valid for all $A > a$. This means that $\int_{k_0}^{\infty}$ must cancel with $\int_{\text{l.c.}}$. This will happen automatically if

$$S^{(l)}_{11A}(-k) = S^{(u)*}_{11A}(k), \tag{17}$$

where $S^{(l)}_{11A}(k)$ and $S^{(u)}_{11A}(k)$ are the values that $S_{11A}(k)$ takes on the lower and upper edges of the cuts. Finally the relation (12) takes the form

$$\pi S_{11A}(k) + i\int_{C'}\frac{S_{11}(k')}{k'-k}dk' = 4\pi i\sum_s \frac{|c_{1s}|^2\exp(2ik_sA)}{k_s-k}, \tag{12'}$$

where S_{11A} now means only the values of the function on the upper edges of the cuts.

To simplify the relation (15), in the integral $\int_{k_0}^{\infty}$ we must go over to the new variable K. If we write

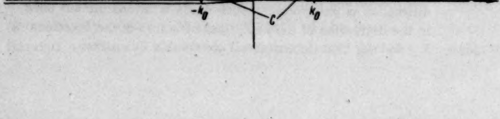

FIG. 1

$$Kk^{-1}S_{22A}(k) = \mathcal{S}_{22A}(K), \tag{18}$$

then Eq. (15) becomes

$$\pi\mathcal{S}_{22A}(K) - i\int_0^\infty \frac{\mathcal{S}^*_{22A}(K')}{K+K'}\,dK' - i\int_0^\infty \frac{\mathcal{S}_{22A}(K')}{K-K'}\,dK'$$
$$+ i\int_0^{k_0} \frac{\exp(2iKA)}{K-K'}\,|S_{12}(k)|^2\,dk = -4\pi i\sum_s \frac{|c_{2s}|^2\exp(2iK_sA)}{K+K_s}. \tag{15'}$$

Let us transform the integral

$$\int_0^\infty dK'\left[\frac{\mathcal{S}^*_{22A}(K')}{K+K'} + \frac{\mathcal{S}_{22A}(K')}{K-K'}\right].$$

We note that $\mathcal{S}_{22A}$ depends also on the function $(K^2 + k_0^2)^{1/2}$. We construct the suitable Riemann surface by cutting the two K planes from ik_0 to $-ik_0$ and joining them crosswise. The plane of integration is characterized by the fact that in it $(K^2 + k_0^2)^{1/2}$ takes positive values on the right-hand edge of the cut. In the integral

$$\int_0^\infty dK'\,\frac{\mathcal{S}^*_{22A}(K')}{K+K'}$$

we make the change of variable of integration $K' \rightarrow -K'$. If we write $\mathcal{S}_{22A}(K)$ to denote the function $\mathcal{S}_{22A}$ with $(K^2 + k_0^2)^{1/2}$ replaced by $-(K^2 + k_0^2)^{1/2}$, the requirement that A be arbitrary leads to the relation

$$\mathcal{S}^*_{22A}(-K) = \mathcal{S}'_{22A}(K) \tag{19}$$

(otherwise there appears in Eq. (15′) an additional integral from 0 to infinity, which is a function of A and K and must vanish identically, which is impossible).

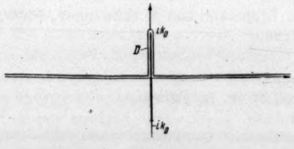

FIG. 2

In the left member of Eq. (15′) let us separate the integral over the path D (see Fig. 2) and some remaining integral over K′ from 0 to ik_0 and over k from 0 to k_0. After a number of transformations it turns out that Eq. (15′) is equivalent to two independent relations:

$$\pi\mathcal{S}_{22A}(K) - i\int_D \frac{\mathcal{S}_{22A}(K')\,dK'}{K-K'} = -4\pi i\sum_s \frac{|c_{2s}|^2\exp(2iK_sA)}{K-K_s}, \tag{20}$$

$$S_{22}(k) + S_{22}(-k) + |S_{12}|^2 = 0, \quad E < \varepsilon. \tag{21}$$

In Eq. (21) S_{22} and S_{12} are to be understood as the analytic continuations of the corresponding functions into the "nonphysical" region $k < k_0$.

4. CONCLUSIONS ABOUT THE MATHEMATICAL STRUCTURE OF THE S-MATRIX COMPONENTS AND THE BREIT-WIGNER FORMULA

We can now show without difficulty that the functions S_{11A} and $\mathcal{S}_{22A}$ are meromorphic: the former, with respect to k in the part of the k plane above the contour C′ (Fig. 1), and the latter, with respect to K in the part of the K plane above the contour D (Fig. 2). The proof is based on application of Cauchy's theorem and use of the fact that A is arbitrary. Let us consider the integral

$$i\int_{C'} \frac{S_{11A}(k')\,dk'}{k'-k}$$

in Eq. (12′). Adding and subtracting the integral along an infinitely small semicircle passing above the point $k' = k$ and the integral along an arc of infinite radius (to close the path of integration), and using Eq. (12′), we get

$$i\int_{C'} \frac{S_{11A}(k')\,dk'}{k'-k} = -2\pi\sum_s \frac{\operatorname{Res} S_{11A}(k_s)}{k_s-k} - \pi S_{11A}(k)$$
$$-\int_\Gamma \frac{S_{11A}(k')\,dk'}{k'-k}. \tag{22}$$

Thus S_{11A} is a meromorphic function of k in the upper half of the k plane, with simple poles on the imaginary axis, and

$$\int_\Gamma \frac{S_{11A}(k')\,dk'}{k'-k} = 0$$

(Γ is the arc of infinite radius). The analytic continuation of $S_{11A}(k)$ into the lower half-plane can be constructed on the basis of the values of the function on the lower edges of the cuts as defined by Eq. (17). Taking into account Eqs. (5), (6), (13), and (17), we can write the explicit form of $S_{11}(k)$:

$$S_{11}(k) = e^{-2i\alpha_1 k}\frac{f_1(k)K + f_2(k)}{f_1(-k)K + f_2(-k)}\,\Pi(k) \qquad (0 < \alpha_1 < a), \tag{23}$$

where $\Pi(k)$ is a product of the type of that in Eq. (1), and $f_1(\lambda)$ and $f_2(\lambda)$ are integral functions with no common zeroes, which for real λ have the properties (for all $k > k_0$):

$$\frac{f_1(-k)}{f_2(-k)} = -\frac{f^*_1(k)}{f^*_2(k)}, \qquad \left|\frac{f_1(k)K + f_2(k)}{f_1(-k)K + f_2(-k)}\right|^2 < 1, \tag{24}$$

$$\int_\Gamma e^{i\beta\lambda}\frac{f_1(\lambda)\Lambda + f_2(\lambda)}{f_1(-\lambda)\Lambda + f_2(-\lambda)}\,d\lambda = \begin{cases} 0, & \text{if } \beta > 0 \\ \infty, & \text{if } \beta < 0 \end{cases}, \tag{25}$$

with β arbitrarily small in absolute value. Obviously only the quantities k_s can be zeroes of $f_1(-\lambda)\Lambda + f_2(-\lambda)$ in the upper half-plane.

In a quite analogous way we can determine the structure of the component $S_{22}(k)$:

$$S_{22}(k) = e^{-2i\alpha_2 K}\frac{g_1(K)k + g_2(K)}{g_1(-K)k + g_2(-K)}\Pi(K) \qquad (0 < \alpha_2 < a). \tag{26}$$

The properties of g are quite analogous to those of f (in the various statements we must make the replacements $f \to g$, $k \rightleftarrows K$, $\lambda \rightleftarrows \Lambda$).

Let us consider the reaction of the scattering of the particle by the unexcited nucleus ($l = 1$, cf. reference 2). This case is interesting through the presence of the threshold process of the inelastic scattering (with energy loss) of the particle. Using the well known formulas for the integrated effective cross sections for elastic and inelastic scattering (σ_e and σ_r), expressed in terms of S_{11} [see Eq. (23)], we find, in agreement with reference 2, that the excitation function σ_e has a vertical tangent at $k = k_0$ (which corresponds to a break or a point of inflection), and near the threshold σ_r is proportional to $(k^2 - k_0^2)^{1/2}$.

Strictly speaking, of course, these conclusions are valid for not very large energies, when we can neglect the contribution of partial waves with nonzero orbital angular momenta.

SUMMARY

We have succeeded in establishing with mathematical rigor the structure of the S functions of spherically symmetrical elastic scattering of a nonrelativistic particle by a nucleus of finite size when this nucleus has one excited state. In so doing we have used only the physical requirements of conservation of the total number of particles, of symmetry, and of completeness of the system of wave functions outside the nucleus. It has been found that because their arguments are multiple-valued these S functions are not analytic in the whole plane, but S_{11A} is analytic in k above the contour C′ (Fig. 1), and S_{22A} is analytic in K above the contour D (Fig. 2); furthermore in the upper half-plane these functions have simple poles, whose positions are given by the eigenvalues of the energy of the system. From the general form of S_{11} there follow with complete rigor the well known conclusions about the behavior of the excitation functions of elastic and inelastic scattering at the threshold of the inelastic process. The formulas (23) and (26) approximately describe the scattering of slow neutrons by nuclei for which the energy spectrum is characterized by the smallness of the distance between the first two levels in comparison with the distance to the next level. As is well known, such a structure is a property both of many even nuclei and also of many odd nuclei.

In conclusion I express my deep gratitude to Professor A. S. Davydov for a helpful discussion of this work.

---

[1] E. P. Wigner, Phys. Rev. **73**, 1002 (1948).

[2] A. Baz', JETP **33**, 923 (1957), Soviet Phys. JETP **6**, 709 (1958).

[3] Ning Hu, Phys. Rev. **74**, 131 (1948); Russian Translation: Prob. sovr. fiz. **2**, 13 (1957).

[4] N. van Kampen, Phys. Rev. **91**, 1267 (1953); Russian Translation: Prob. sovr. fiz. **2**, 244 (1957).

[5] N. Khuri, Phys. Rev. **107**, 1148 (1957). D. Y. Wong, Phys. Rev. **107**, 302 (1957). A. Klein and C. Zemach, Bull. Am. Phys. Soc. **3**, 68 (1958).

[6] B. W. Lee, Phys. Rev. **112**, 2122 (1958).

[7] W. Heisenberg, Z. Physik **120**, 513, 673 (1943); Z. Naturforsch. **1**, 608 (1946).

[8] S. T. Ma, Phys. Rev. **71**, 195 (1947).

[9] R. Jost, Helv. Phys. Acta **20**, 256 (1947).

[10] A. S. Davydov, Теория атомного ядра (Theory of the Atomic Nucleus), Fizmatgiz, 1958.

[11] B. A. Lippmann and J. Schwinger, Phys. Rev. **79**, 469 (1950).

Translated by W. H. Furry
238

SOVIET PHYSICS JETP VOLUME 11, NUMBER 4 OCTOBER, 1960

DISINTEGRATION OF COSMIC-RAY NUCLEI BY SOLAR PHOTONS

N. M. GERASIMOVA and G. T. ZATSEPIN

P. N. Lebedev Physics Institute, Academy of Sciences, U.S.S.R.

Submitted to JETP editor August 16, 1959; resubmitted October 30, 1959

J. Exptl. Theoret. Phys. (U.S.S.R.) **38**, 1245-1252 (April, 1960)

A calculation is made of the effect of disintegration of cosmic-ray nuclei in the field of solar photons, leading to the production of correlated showers in the atmosphere. The energy of the disintegrated nuclei is found to be of the order of 10^{16} ev per nucleon, and their flux of the order of 10^{-4} to 10^{-3} km^{-2} hour^{-1} sr^{-1}. As a result of the divergence of the photonuclear disintegration products before they enter the atmosphere, the distances between the shower cores turn out to be approximately of the order of 1 km.

INTRODUCTION

BECAUSE of the Doppler effect, the energy of solar-radiation photons is sufficient to cause the disintegration of cosmic-ray nuclei if the energy of the nuclei is high.[1]

If, in the coordinate system of the sun, the photon possesses an energy ϵ_0, and a cosmic-ray nucleus with mass M possesses an energy $E = \gamma Mc^2$, then, in the coordinate system in which the nucleus is at rest, the photon energy is given by

$$\varepsilon = \varepsilon_0 (\gamma + \sqrt{\gamma^2 - 1} \cos \alpha) \approx 2\gamma \varepsilon_0 \cos^2 \frac{\alpha}{2}, \qquad (1)$$

where α is the angle between the direction of motion of the photon and that of the nucleus in the coordinate system of the sun (Fig. 1).

Since the mean energy of a solar photon amounts to about 1 Mev, and the photodisintegration of nuclei occurs at a photon energy of about 10^7 ev, nuclei with energy corresponding to $\gamma \approx 10^7$, i.e., $E \approx 10^{16}$ ev per nucleon, can undergo photodisintegration.

A nucleus undergoing photodisintegration decays into two or more fragments, depending on the reaction type: (γ, n), (γ, p) or $(\gamma, 2n)$, (γ, np), $(\gamma, 3\alpha)$ The moving fragments all reach the earth's atmosphere practically simultaneously (the relative delay is of the order of 10^{-12} sec), and each of them produces an extensive air shower. Thus, the photodisintegration effect of the nuclei should lead to the existence of correlated air showers.

The divergence of nuclear fragments before reaching the atmosphere is determined by the distance from the earth at which the photodisintegration occurs, and by the angles of emission of the fragments in the coordinate system of the sun. An estimate shows that the distances between the shower cores should be of the order of 1 km. The divergence due to the deflection of the charged particles by the magnetic fields is negligible. (For a field of 10^{-5} gauss, the deviation would be of the order of 10^{-2} cm.)

The study of correlated showers can yield information about the composition of cosmic-ray nuclei in the range of ultra-high energies. In fact, when one photonucleon is emitted from a nucleus of atomic weight A, two particles are produced, one with nucleon mass and the other with a mass greater by a factor of $(A-1)$. Their energies will also differ by a factor of $(A-1)$. Therefore, one of the correlated showers will have about $(A-1)$ more particles than the other. This provides the possibility of determining the atomic weight of the original nucleus.

Unfortunately, as will be shown in the following discussion, an estimate of the number of expected photodisintegrations of nuclei before they reach the earth's atmosphere yields a very small value. However, arrays having an effective area of the order of several square kilometers are at present being planned for the detection of EAS. There is hope that such arrays will yield sufficient material not only to assess the effect of correlated showers, but also to investigate some features of this phenomenon. It is therefore of interest to consider this process in somewhat greater detail. (In reference 1, an arithmetical error was committed, as a result of which the effect has been overestimated by a factor of 100.)

NUMBER OF PHOTODISINTEGRATIONS

In the calculation, we shall use the diagram shown in Fig. 1. The following notation has been

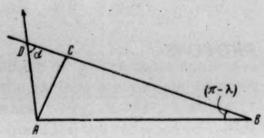

FIG. 1. Diagram of the motion of a nucleus in the field of solar photons. A – position of the sun; B – position of the earth; AD – direction of motion of the photon; DC – direction of motion of the nucleus.

chosen: distance from the sun A to the earth B, AB = R_0. Distance from the sun A to the nucleus D moving towards the earth, AD = R. Distance from the nucleus D to the earth B, DB = L. The angle between the direction of the photon stream and the motion of the nucleus at an arbitrary point of the trajectory of the nucleus, angle ADC = α. The same angle at the moment of the arrival of the nucleus at the earth, $\alpha = \lambda$. It is evident that

$$R = R_0 \sin\lambda / \sin\alpha, \quad L = R_0(\sin\lambda / \tan\alpha - \cos\lambda),$$
$$-dL = R_0\, d\alpha / \sin^2\alpha. \tag{2}$$

We shall assume that the energy spectrum of the solar photons corresponds to black-body radiation. For the calculation, we set T = 5800° K, which corresponds to kT = 0.5 ev.

The number of photons per cm^3 at a distance R from the sun in the energy interval ϵ_0, $\epsilon_0 + d\epsilon_0$ is

$$\rho(\varepsilon_0)\,d\varepsilon_0 = \frac{\rho_0}{(kT)^3}\,\frac{R_0}{R^2}\,\frac{\varepsilon_0^2\, d\varepsilon_0}{e^{\varepsilon_0/kT}-1}, \tag{3}$$

where the constant ρ_0 is chosen so that the energy flux per cm^2/sec at a distance R_0 from the sun corresponds to the solar constant $\overline{K} = 0.15$ watts/cm^2. We have

$$\overline{K} = \frac{c\rho_0}{(kT)^3}\int_0^\infty \frac{\varepsilon_0^3\, d\varepsilon_0}{e^{\varepsilon_0/kT}-1} = c\rho_0 kT\cdot 3!\ \zeta(4), \tag{4}$$

where $\zeta(4)$ is the Riemann ζ function [$\zeta(4) = 1.082$], and c is the velocity of light. Hence, $\rho_0 = \overline{K}/ckT \cdot 3!\,\zeta(4) = 0.96 \times 10^7$ photons/cm^3.

Let us denote the effective cross section for the photodisintegration of a nucleus of type g by $\sigma_g(\epsilon)$, where ϵ is the photon energy in the coordinate system of the sun. The probability of photodisintegration of the nucleus before it reaches the earth can be written in the form

$$W_g(\gamma) = \int_\infty^0 dL \int_0^\infty \rho(\varepsilon_0)\,\sigma_g\left(2\gamma\varepsilon_0\cos^2\frac{\alpha}{2}\right) 2\cos^2\frac{\alpha}{2}\, d\varepsilon_0, \tag{6}$$

where the factor $2\cos^2(\alpha/2)$ appears because of the head-on motion of the nucleus and of the photons. We assume the velocity of the nucleus to be equal to the velocity of light:

$$1 + \frac{v}{c}\cos\alpha \approx 2\cos^2\frac{\alpha}{2}.$$

In order to find the number of disintegrating nuclei, it is necessary to know the energy spectrum of the nuclei.

There are no data on the energy spectrum of nuclei of each type in the high-energy range. There is only information about the energy spectrum of all particles taken together, and the spectrum in the region of interest $E \approx 10^{16}$ ev can be approximated by a power law[2]

$$F(>E) = B(E/10^{16})^{-\varkappa}, \tag{7}$$

where $\kappa = 1.8$, and $B = 10^{-11}$ particles cm^{-2} sec^{-1} sr^{-1} (reference 2).

We shall assume that the energy spectrum of various nuclei is of the same form. The fraction of nuclei of type g among all particles with an energy higher than a given value remains then constant in the energy range of interest. If we denote this fraction by δ_g, then, for the number of nuclei of type g having an energy higher than E, we obtain a formula analogous to Eq. (7) in which, instead of B, we have to write δ_g. In order to pass from the variable E to γ, we make a substitution in Eq. (7) according to the formula

$$E_g = A_g mc^2\gamma,$$

where A_g is the atomic weight of the nucleus g. The integral spectrum of nuclei of the type g is then obtained in the form

$$F_g(>\gamma) = \frac{\delta_g B}{A_g^{\varkappa}}\left(\frac{mc^2\gamma}{10^{16}\ \text{ev}}\right)^{-\varkappa}, \tag{8}$$

and the differential spectrum is

$$F_g(\gamma)\,d\gamma = B_g\gamma^{-(\varkappa+1)}\,d\gamma; \tag{9}$$

where $\kappa = 1.8$, and $B_g = 2 \times 10^{-11}\,\delta_g(10^7/A_g)^{1.8}$ particles cm^{-2} sec^{-1} sr^{-1}. Multiplying Eq. (6) by Eq. (7) and integrating over $d\gamma$, we obtain the total number of disintegrations of nuclei of type g occurring per unit time [using Eq. (2)]:

$$N_g = \frac{2B_g R_0\rho_0}{\sin\lambda\,(kT)^3}\int_0^\lambda d\alpha \int_0^\infty d\varepsilon_0 \int_{\varepsilon'}^\infty \frac{\varepsilon_0^2}{\exp(\varepsilon_0/kT)-1}\,\sigma\left(2\gamma\varepsilon_0\cos^2\frac{\alpha}{2}\right)$$
$$\times\,\gamma^{-(\varkappa+1)}\cos^2\frac{\alpha}{2}\,d\gamma, \tag{10}$$

where ϵ_g is the threshold energy for the photonuclear reaction on nuclei of type g, and $\epsilon' = \epsilon_g/2\epsilon_0\cos^2(\alpha/2)$.

The integration yields

$$N_g = 2B_g\rho_0 R_0(2kT/\varepsilon_g)^{\varkappa}(2+\varkappa)!\,\zeta(3+\varkappa)\,f(\lambda,\varkappa)\,I_g \tag{11}$$

[for the chosen value of $\kappa = 1.8$, $\zeta(3+\kappa) = 1.04$], where

$$I_g = \int_1^\infty \sigma_g(y\varepsilon_g)\, y^{-(\kappa+1)}\, dy, \tag{12}$$

where $y = \epsilon/\epsilon_g$ and the function $\sigma_g(y\epsilon_g)$ can be well approximated by the expression

$$\sigma_g(y\varepsilon_g) = c_g(y-1)\, e^{-a_g(y-1)}. \tag{13}$$

The constants a_g and c_g are found from the experimental data on the energy dependence of the effective cross section for the photonuclear reaction[3-11]

$$a_g = 1/(y_m - 1), \tag{14}$$

$$c_g = e a_g \sigma_{max}, \tag{15}$$

$\sigma_{\max}$ is the value of the maximum effective cross section attained for $y = y_m$.

As a result of integration (12), we obtain the differences of complete and incomplete gamma functions, which is very inconvenient for calculation, as it is necessary to take the values of these functions with a large number of signs. One can, however, derive an approximate expression for I_g which is more convenient for making calculations if we substitute an exponential function $\exp[-\sqrt{\kappa(\kappa-1)}\,(y-1)]$ for the power function $y^{-(\kappa+1)}$ under the integral. For such a substitution, the solution coincides with the exact one for $a \gg 1$ and $a_g \ll 1$, while, for $a_g \approx 1$, the value of I_g will be negligibly higher.

As a result, we obtain

$$I_g \approx c_g / [a_g + \sqrt{\kappa(\kappa-1)}]^2. \tag{16}$$

The function $f(\lambda, \kappa)$ [see Eq. (11)] depends little on κ and, therefore, in computing the values of this function, we set $2(1+\kappa) = 5$ for simplicity, and obtain

$$f(\lambda) = (1/\sin\lambda)\left\{\tfrac{5}{4}\sin\tfrac{1}{2}\lambda + \tfrac{5}{24}\sin\tfrac{3}{2}\lambda + \tfrac{1}{40}\sin\tfrac{5}{2}\lambda\right\}, \tag{17}$$

$f(\lambda) \to 1$ for $\lambda \to 0$; $0.9 < f(\lambda) < 1$ in the range $0 < \lambda < \pi/2$; $f(\lambda) \to 16/15(\pi-\lambda)$ for $\lambda \to \pi$. Substituting Eq. (16) and also the numerical values of the corresponding constants (see Table I) into Eq. (11), we find that the number of particles produced in photodisintegrations of nuclei of type g per hour over an area of 1 km^2 and within an angle of 1 sr is

$$N_g = 3.9\,\delta_g\left(\frac{10^7\,\mathrm{ev}}{\varepsilon_g}\right)^{1.8} \frac{10^{24} C_g}{(a_g + 1{,}2)^2}\, f(\lambda). \tag{18}$$

The numbers obtained show that the expected effect amounts to a quantity of the order of $10^{-4}\,\mathrm{hr}^{-1}\,\mathrm{km}^{-2}\,\mathrm{sr}^{-1}$, and does not depend greatly on the atomic weight of the nuclei.

The real value differs from the calculated one apparently by not more than one order of magnitude. The contribution of other photonuclear reactions will increase the effect by not more than a factor of 3 to 5. The increase in the number of detected showers when the sun is near the zenith is found to be negligible. In fact, the angular dependence $f(\lambda)$ of the disintegration probability increases with decreasing angle $\pi - \lambda$ only slowly during the passage of particles near the sun:

$$f(\lambda) \approx 1/(\pi - \lambda). \tag{19}$$

This leads to the fact that the disintegration probability, averaged over the angle of 1 sr along the direction pointing towards the sun, is greater than for angles $\lambda \approx 0$ by only a factor of 3.5. Averaging over one day will give a coefficient differing little from one.

The approximation made in the calculation because of the exchange of the true sun spectrum for the black-body spectrum with temperature T = 5800° K does not lead to an appreciable error, since the relative contribution of different regions of the solar spectrum to the photodisintegration process is very close to the relative contribution of these regions to the energy flux of solar emission. The contribution of the different spectral regions is shown in Fig. 2: the dotted line 1 shows the contribution to the energy flux, and the curve 2 shows the contribution to the number of photodisintegrations. The maxima of both curves lie in the visible part of the spectrum. The greatest uncertainty in the calculation of the number of disintegrations is due to the constant B which appears

TABLE I

	ε_g, Mev	ε_m, Mev	σ, mb	a_g	C_g, mb	N_g, $\mathrm{km}^{-2}\mathrm{hr}^{-1}\mathrm{sr}^{-1}$
He^4	20.5	24	1.3	5.9	20.8	$0.4 \cdot 10^{-4}$
C^{12}	19.5	21.3	13	11.1	397	$0.6 \cdot 10^{-4}$
N^{14}	17.5	22.5	16	3.6	113	$0.7 \cdot 10^{-4}$
O^{16}	19.0	22.5	8	5.25	127	$0.3 \cdot 10^{-4}$
Fe^{56}	13.0	17.7	75	2.8	570	$0.6 \cdot 10^{-4}$

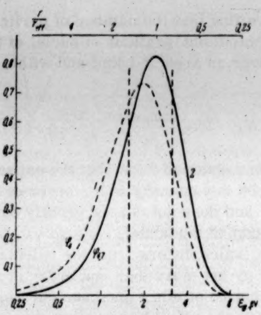

FIG. 2. Curve 1 – energy-flux distribution of the solar spectrum; curve 2 – contribution of photons of different energies to the photonuclear process, and also the energy distribution of nuclei undergoing photodisintegrations. The x axis at the bottom of the figure represents the energy of photons in ev (vertical dotted lines enclose the optical region of the spectrum). The top scale of the x axis refers to curve 2, and represents the energy of the nuclei expressed in units of $\gamma/\gamma_{\text{eff}}$ ($\gamma = E/Mc^2$). The y axis represents the corresponding values of the functions in arbitrary units.

in the expression of the energy spectrum of cosmic rays. If an error by a factor of 2 is made in the estimate of the total energy of EAS, on the basis of which the primary-particle spectrum is normalized, then this leads to an error in the constant B by approximately a factor of 4.

In the detection of correlated showers, the effective solid angle for the observation may amount to 2 or 3 sr.

Taking all these factors into account, one can expect, for an array with an effective area of 1 km², a number of detected photodisintegrations equal to 10^{-4} to 10^{-3} per hour, provided that a considerable percentage of ultra-high-energy cosmic-ray particles consists not of protons but of more complex atomic nuclei.

ENERGY DISTRIBUTION OF DISINTEGRATING NUCLEI

For the majority of nuclei, the energy dependence of the effective photodisintegration cross section has the shape of a narrow resonance curve. Because of this, and also because of the sharply decreasing form of the energy spectrum of cosmic rays, a considerable contribution to the number of photodisintegrations, determined by the integral $I_\sigma(12)$, is made only by a very narrow range of values of y close to y = 1. If, for an estimate of the distribution with respect to γ, we set $y = y_m$ = const, we obtain the condition

$$2\gamma\varepsilon_0\cos^2(\alpha/2)/\varepsilon_T = y_m \approx 1. \tag{20}$$

Hence, it follows for $\cos^2(\alpha/2)$ = const that $d\ln\gamma = -d\ln\epsilon_0$. Therefore, the distribution of the nuclei undergoing photodisintegration with respect to γ should be represented by the same curve as the distribution of the contribution of various regions of the solar spectrum, if the x axis represents $\ln\epsilon_0$ or $-\ln\gamma$. Thus, curve 2 in Fig. 2 shows also the approximate energy spectrum of nuclei undergoing photodisintegration. The values of γ_{eff} corresponding to the maximum of curve 2 are given in Table II for the case $\cos^2(\alpha/2) = 1$. Evidently, for other values of α, we have

$$\gamma_{\text{eff}}(\alpha) = \gamma_{\text{eff}}(\alpha = 0)/\cos^2(\alpha/2). \tag{21}$$

TABLE II

	γ_{eff}	E_{eff}, ev
He^4	$5.1\cdot10^6$	$2\cdot10^{16}$
C^{12}	$4.5\cdot10^6$	$5.4\cdot10^{16}$
N^{14}	$4.7\cdot10^6$	$6.6\cdot10^{16}$
O^{16}	$4.6\cdot10^6$	$7.3\cdot10^{16}$
Fe^{56}	$3.5\cdot10^6$	$2\cdot10^{17}$

For $\lambda \neq 0$, the trajectory of the nucleus moving towards the earth is characterized by various values of α and, therefore, for an estimate of the distribution with respect to γ, it is reasonable to introduce the quantity $[\cos^2(\alpha/2)]_{1/2}$ corresponding to an angle $\alpha_{1/2}$ such that[12]

$$\int_0^{\alpha_{1/2}}\left(\cos\frac{\alpha}{2}\right)^{2(1+\varkappa)}d\alpha = \frac{1}{2}\int_0^{\lambda}\left(\cos\frac{\alpha}{2}\right)^{2(1+\varkappa)}d\alpha. \tag{22}$$

We give here the values of $[\cos^2(\alpha/2)]_{1/2}$ for various values of λ:

λ: 0 $\pi/4$ $\pi/2$ $3\pi/4$
$[\cos^2(\alpha/2)]_{1/2}$: 1 0.97 0.9 0.84

ESTIMATE OF THE DETECTION PROBABILITY OF CORRELATED SHOWERS AS A FUNCTION OF THE DISTANCE BETWEEN THE CORES

The distance between a photonucleon and a nucleus is, at the earth, equal to

$$r = \theta L, \tag{23}$$

where θ is the angle between the directions of the nucleon and of the nucleus in the coordinate system of the earth.

We shall assume that the distribution of the fragments in the coordinate system of the nucleus is isotropic, so that the probability of emission of a particle within an angle θ_c, $\theta_c + d\theta_c$ is given by the formula

$$W(\theta_c)\,d\theta_c = \tfrac{1}{2}\sin\theta\,d\theta_c, \tag{24}$$

where θ_c is the angle, in the coordinate system of the nucleus, between the direction of emission of a particle and the direction of motion of the nucleus towards the earth before the decay. For a velocity of emission of the nucleon and nucleus equal to βc, the angular distribution in the coordinate system of the earth can be written in the form

$$W(\theta)\,d\theta = \gamma^2\theta\,d\theta/\beta^2\sqrt{1-(\gamma\theta/\beta)^2} \quad \text{for } \theta \leqslant \beta/\gamma,$$
$$W(\theta) = 0 \quad \text{for } \theta > \beta/\gamma, \tag{25}$$

since

$$\theta \approx (\beta/\gamma)\sin\theta_c \quad \text{for } \beta \ll 1.$$

For simplicity, let us assume henceforth that in photodisintegration the nuclei are always emitted from the nucleus at the same velocity. The lateral distribution function $\rho(r)$ in its differential form is given by the equation

$$d\rho(r) = \frac{W(\theta)\,d\theta}{2\pi L^2\theta\,d\theta} = \frac{1}{2\pi(L\beta/\gamma)}\,\frac{1}{\sqrt{1-(\gamma r/\beta L)^2}}\,dN, \tag{26}$$

where dN is the number of nuclei undergoing disintegration at a distance L, L + dL from the earth, corresponding to the integrand (10). It is very difficult to carry out an accurate integration of this expression. The problem is, however, simplified if we take into account that, for the nuclei undergoing disintegration, the range of important values of γ is small (see Fig. 2). Therefore, in integrating the expression (26) over γ (or over y), it is permissible, in the factor standing before dN, to set $y = y_{\text{eff}}$, the value of which can be obtained from Eq. (21) on the basis of Table II and the values of $[\cos^2(\alpha/2)]_{1/2}$ for various values of λ. To obtain the lateral distribution it is now only necessary to perform an integration over dL, i.e., over $d\alpha$; this presents no difficulties.

The probability of observation of shower cores at different distances from each other is shown in Fig. 3. Curve 1 was calculaed for $\lambda = 0$, and curve 2 for $\lambda = 3\pi/4$.

To determine the value of r_0 it is necessary to estimate the velocity of photonucleons β. For light nuclei, the majority of photonucleons will be due to a direct photoeffect, so that the energy of a photonucleon is given by the formula

$$E_n = \varepsilon_T(y_{\text{eff}} - 1), \qquad \beta_{\text{eff}} = \sqrt{2E_n/mc^2}. \tag{27}$$

The values of β_{eff} calculated from this formula for all nuclei are close to $\beta = 0.07$. Hence, the value r_0 ($\lambda = 0$), according to Eq. (26) and the values of γ_{eff} given in the table, is of the order of r_0 ($\lambda = 0$) = 2 km. It is evident that our calculation leads to an overestimate in the value of r_0, since not all photonucleons are due to the direct photoeffect.

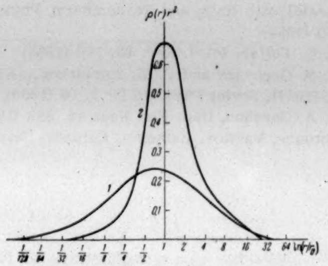

FIG. 3. Graph of the detection probability of shower cores at various distances from each other; x axis represents $\ln(r/r_0)$ and the y axis $\rho(r)r^2$ in arbitrary units.

Special experiments for the detection of correlated showers have not been carried out. However, during the observation of EAS in 1950 at an altitude of 3860 m,[13] a case was detected which is of considerable interest. High-density showers were recorded at two extreme points 1 km apart while at the central point the detected shower-particle flux density was found to be extremely small. The probability of a chance passage of two independent showers of corresponding densities within the resolving time of the array (6 μsec) can be estimated as being 10^{-4} during the whole period of observation of 1000 hours. An analogous event was observed in 1951 by Éĭdus et al.[14] at sea level. Further experiments with suitable arrays can yield important information on this subject.

---

[1] G. T. Zatsepin, Dokl. Akad. Nauk SSSR **80**, 577 (1951).

[2] K. Greisen, Progress in Cosmic Ray Physics (North-Holland Publishing Co., Amsterdam, 1956) Vol. III (Russ. Transl. IIL, 1958).

[3] T. H. Stix, Phys. Rev. **95**, 782 (1954).

[4] B. H. Flowers and F. Mandle, Proc. Roy. Soc. **A206**, 131 (1951).

[5] Ferguson, Halpern, Nathans, and Jergin, Phys. Rev. **95**, 777 (1954).

[6] V. O. Nicolai and E. L. Goldwasser, Bull. Am. Phys. Soc. **29**, 18 (1954).

[7] R. Nathans and J. Halpern, Phys. Rev. **92**, 940 (1953).

[8] V. Weisskopf, Phys. Rev. **52**, 295 (1946).

[9] Montalbetti, Ratz, and Gordemberg, Phys. Rev. 91, 659 (1953).

[10] E. G. Fuller, Phys. Rev. 96, 106 (1954).

[11] A. N. Gorbunov and V. M. Spiridonov, JETP 33, 21 (1957), Soviet Phys. JETP 6, 16 (1958).

[12] A. A. Gershun, Usp. Fiz. Nauk 46, 388 (1952).

[13] Antonov, Vavilov, Zatsepin, Kutuzov, Skvortsov, and Khristiansen, JETP 32, 227 (1957), Soviet Phys. JETP 5, 172 (1957).

[14] Éĭdus, Adamovich, Ivanovskaya, Nikolaev, and Dulyankina, JETP 23, 440 (1952).

Translated by H. Kasha
239

SOVIET PHYSICS JETP VOLUME 11, NUMBER 4 OCTOBER, 1960

ON THE THEORY OF RELAXATION PROCESSES IN FERRODIELECTRICS WITH WEAK MAGNETIC ANISOTROPY AT LOW TEMPERATURES

V. G. BAR'YAKHTAR and G. I. URUSHADZE

Institute for Technical Physics, Academy of Sciences, Ukrainian S.S.R.

Submitted to JETP editor November 4, 1959

J. Exptl. Theoret. Phys. (U.S.S.R.) 38, 1253-1262 (April, 1960)

We consider the relaxation of the magnetic moment and the equalization of spin and lattice temperatures of ferrodielectrics with a weak magnetic anisotropy in weak magnetic fields. We show that the magnetic dipole interaction establishes the equilibrium of the magnetic moment, both as to its magnitude and as to its direction. The relaxation time of the absolute magnitude of the magnetic moment is in this case of the same order of magnitude as the characteristic time of rotation of the magnetic moment to its equilibrium direction. The relaxation time for the equalization of spin and lattice temperatures is also evaluated.

1. Akhiezer, Bar'yakhtar, and Peletminskiĭ[1] presented a general theory for the relaxation of the magnetic moment in ferrodielectrics; this theory was based upon the fact that there are two types of interaction between spin waves: the strong exchange interaction and the weak relativistic interactions (magnetic dipole interaction and interactions caused by the magnetic anisotropy).

The exchange interaction leads to the establishment of a Bose distribution of the spin waves with a non-equilibrium value of the magnetic moment, but the weak interactions lead to the establishment of an equilibrium value of the magnetic moment both in absolute magnitude and in direction. In the cited paper this scheme was applied to an evaluation of the relaxation time of the magnetic moment in those circumstances where the magnetic anisotropy constant β and the external magnetic field H_0 were sufficiently large. Under those circumstances one can easily check that spin waves with wave vector $\mathbf{k} = 0$ cannot split up into two spin waves with wave vectors $\mathbf{k}$ and $-\mathbf{k}$. The strongest of the "weak" interactions, which describe the processes of the combination of two spin waves into one and the splitting of one spin wave into two, can therefore not cause a change in the number of spin waves with $\mathbf{k} = 0$, which determines the component of the magnetic moment of the body perpendicular to the axis of easiest magnetization.

Because of this, one invokes the relativistic interactions, which describe processes involving a large number of spin waves one of which has a momentum $\mathbf{k} = 0$, to explain the relaxation of the transverse component of the magnetic moment.

The situation is different in crystals with a small magnetic anisotropy constant β in weak magnetic fields $(\beta + H_0/M_0 < 4\pi/3)$, since under those conditions the splitting of a spin wave with $\mathbf{k} = 0$ into two spin waves now turns out to be possible. Because of this it is not necessary, when describing the relaxation of the magnetic moment in such crystals, to take the interactions describing spin wave-spin wave scattering into account, and it is sufficient to restrict ourselves to the magnetic dipole interaction which describes the splitting of one spin wave into two and the amalgamation of two spin waves into one.

We note, finally, the following fact: it is well known (see Néel[2]) that many ferrites, which at low temperatures can be considered to be dielectrics, have a complicated magnetic structure, i.e., they are described not by one but by several magnetic sublattices. This leads to the occurrence of high-frequency branches of the magnetic energy spectrum with a large activation energy, as well as a low-frequency branch (without an activation energy). The contribution of these high-frequency branches to the thermodynamic and transport properties of ferrodielectrics at low temperatures is, of course, exponentially small. One might think that the strong exchange interaction $\gamma(\mathbf{M}_1 \cdot \mathbf{M}_2)$ between uniformly magnetized sublattices could essentially change the interactions between low-frequency spin waves. This would thereby lead to an influencing of the magnetic structure of the transport and relaxation properties of a ferrodielectric at low temperatures.

A detailed analysis (see Appendix) shows that, indeed, the interaction between low-frequency spin waves, which is caused by the energy of exchange between sublattices, turns out to be of the same order of magnitude as the relativistic interaction describing spin wave-spin wave scattering. This enables us to neglect the magnetic structure of a ferrodielectric with weak anisotropy when we study its relaxation processes.

2. The Hamiltonian of a ferrodielectric with cubic symmetry can be written in the form

$$\mathcal{H} = \mathcal{H}^{(s)} + \mathcal{H}^{(p)},$$

$$\mathcal{H}^{(s)} = \int\Big[\frac{1}{2}\alpha\frac{\partial M_l}{\partial x_i}\frac{\partial M_l}{\partial x_i} + \frac{\beta}{2M_0^2}(M_x^2M_y^2 + M_x^2M_z^2 + M_y^2M_z^2) + \frac{\mathbf{H}^2}{8\pi}\Big]dv,$$

$$\mathcal{H}^{(p)} = \frac{1}{2}\frac{\Theta_c a^2}{\mu M_0}\int\Big[\delta_1\frac{\partial M_l}{\partial x_i}\frac{\partial M_l}{\partial x_k}u_{ik} + \delta_2\frac{\partial M_l}{\partial x_i}\frac{\partial M_l}{\partial x_i}u_{kk}\Big]dv, \tag{1}$$

where $\mathbf{M}$ is the magnetic moment density, $\mathbf{H}$ the magnetic field acting in the crystal, u_{ik} the deformation tensor, α a constant connected with the exchange integral $[\alpha \equiv (\Theta_C/\mu M_0)a^2$, where Θ_C is a quantity of the same order of magnitude as the Curie temperature, a the lattice constant, $\mathbf{M}_0$ the saturated magnetic moment, and μ the Bohr magneton], and δ_1 and δ_2 are the magnetostriction constants. The first term in Eq. (1) is the magnetic energy of the ferrodielectric and the second term the exchange part of the magnetostriction energy which is connected with the inhomogeneity of the magnetic moment. Kaganov and Tsukernik[3] have shown that one can neglect the energy of relativistic origin, which describes the magnetostriction effect when there is a uniform magnetization, when one considers relaxation and transport processes in the temperature range $T \gg 2\pi\mu M_0 \sim 1°K$.

If we now make the well-known transition (see Holstein and Primakoff[4] and also Kaganov and Tsukernik[5]) to the creation and annihilation operators of the spin waves, $c_{\mathbf{k}}^+$ and $c_{\mathbf{k}}$, we get

$$\mathcal{H}^{(s)} = \mathcal{H}^{(0)} + \mathcal{H}^{(3)} + \mathcal{H}^{(4)}, \tag{2}$$

$$\mathcal{H}^{0} = \sum_{\mathbf{k}}\varepsilon_{\mathbf{k}}c_{\mathbf{k}}^{+}c_{\mathbf{k}}, \qquad \varepsilon_{\mathbf{k}} = \sqrt{A_{\mathbf{k}}^2 - |B_{\mathbf{k}}|^2}, \tag{3}$$

$$\mathcal{H}^{(3)} = \sum_{1,2,3}\Phi_{12,3}c_1^+c_2^+c_3\Delta(\mathbf{k}_1 + \mathbf{k}_2 - \mathbf{k}_3) + \text{c.c.}, \tag{4}$$

$$\mathcal{H}^{(4)} = \sum_{1,2,3,4}\Phi_{12,34}\,c_1^+c_2^+c_3c_4\Delta(\mathbf{k}_1 + \mathbf{k}_2 - \mathbf{k}_3 - \mathbf{k}_4), \tag{5}$$

where we have used the following notation

$$A_k = \mu M_0(\alpha k^2 + \beta + H_0/M_0 + 2\pi\sin^2\theta_{\mathbf{k}}), \tag{6}$$

$$B_k = 2\pi\mu M_0\sin^2\theta_{\mathbf{k}}e^{-2i\varphi_{\mathbf{k}}},$$

$$\Phi_{12,3} = -\pi\mu(2\mu M_0)^{1/2}V^{-1/2}[\sin 2\theta_1(e^{-i\varphi_1}u_1^* + e^{i\varphi_1}v_1^*)(u_2^*u_3 + v_2^*v_3) + \sin 2\theta_2(e^{-i\varphi_2}u_2^* + e^{i\varphi_2}v_2^*)(u_1^*u_3 + v_1^*v_3) + \sin 2\theta_3(e^{i\varphi_3}u_3 + e^{-i\varphi_3}v_3)(v_1^*u_2^* + v_2^*u_1^*)], \tag{7}$$

$$\Phi_{12,34} = -(\mu^2\alpha/2V)(\mathbf{k}_1\mathbf{k}_2 + \mathbf{k}_3\mathbf{k}_4), \tag{8}$$

$$u_{\mathbf{k}} = \sqrt{(A_{\mathbf{k}} + \varepsilon_{\mathbf{k}})/2\varepsilon_{\mathbf{k}}}, \qquad v_{\mathbf{k}} = -e^{2i\varphi_{\mathbf{k}}}\sqrt{(A_{\mathbf{k}} - \varepsilon_{\mathbf{k}})/2\varepsilon_{\mathbf{k}}}, \tag{9}$$

$c_j \equiv c_{\mathbf{k}_j}$, θ_j and φ_j are the polar angles of the vector $\mathbf{k}_j$. Since $\Phi_{12,34}$ is very small for small k ($\sim \alpha k^2$) the main role in the collisions caused by the operator $\mathcal{H}^{(4)}$ will at not too low temperatures ($T \gg 2\pi\mu M_0$) be played by spin waves with large wave vectors: $\epsilon_{\mathbf{k}} \sim T$, $\alpha k^2 \sim T/\mu M_0 \gg 1$. One sees easily from (6) and (9) that for such values of the wave vector $|v_{\mathbf{k}}| \ll |u_{\mathbf{k}}| \approx 1$.

The considerations given above refer also to the Hamiltonian describing the interaction between spin waves and phonons, $\mathcal{H}^{(p)}$. The Hamiltonian $\mathcal{H}^{(p)}$ expressed in terms of creation and annihilation operators for the spin waves and the phonons is of the form

$$\mathcal{H}^{(p)} = \sum_{1,2,3}\Psi_{12,3}c_1^+c_2b_3\Delta(\mathbf{k}_1 - \mathbf{k}_2 - \mathbf{f}_3) + \text{c.c.} \tag{10}$$

where

$$\Psi_{12,3} = i\frac{a^2\Theta_c}{4\sqrt{\omega_3}}\Big(\frac{\hbar}{2\rho V}\Big)^{1/2}[\delta_1(\mathbf{k}_1\mathbf{e}_3)(\mathbf{k}_2\mathbf{f}_3) + \delta_1(\mathbf{k}_2\mathbf{e}_3)(\mathbf{k}_1\mathbf{f}_3) + 2\delta_2(\mathbf{k}_1\mathbf{k}_2)(\mathbf{e}_3\mathbf{f}_3)], \tag{11}$$

the index 3 indicates the wave vector $\mathbf{f}_3$ and the polarization s of the phonon, $\mathbf{e}_3$ and ω_3 are the polarization unit vector and the frequency of the phonon, b_3^+ and b_3 are the creation and annihilation operators for the phonons and ρ is the density of the medium.

Using Eqs. (4), (5), and (10) for the Hamiltonians $\mathcal{H}^{(3)}$, $\mathcal{H}^{(4)}$, and $\mathcal{H}^{(p)}$, we can now write down the transport equation for the number of spin waves n_1 with wave vector $\mathbf{k}_1$

$$\dot{n}_1 = \dot{n}_1^{\text{coll}} \equiv L_{\mathbf{k}_1}^{(e)}\{n\} + L_{\mathbf{k}_1}^{(r)}\{n\} + L_{\mathbf{k}_1}^{(p)}\{n, N\}, \tag{12}$$

where

$$L_{\mathbf{k}_1}^{(e)}\{n\} = \frac{96\pi}{\hbar}\sum_{2,3,4}|\Phi_{12.34}|^2[(n_1 + 1)(n_2 + 1)n_3n_4 - n_1n_2(n_3 + 1)(n_4 + 1)]\delta(\varepsilon_1 + \varepsilon_2 - \varepsilon_3 - \varepsilon_4)\Delta((\mathbf{k}_1 + \mathbf{k}_2 - \mathbf{k}_3 - \mathbf{k}_4), \tag{13}$$

$$L_{\mathbf{k}_1}^{(r)}\{n\} = \frac{8\pi}{\hbar}\sum_{2.3}\{2|\Phi_{12.3}|^2[(n_1 + 1)(n_2 + 1)n_3 - n_1n_2(n_3 + 1)]\delta(\varepsilon_1 + \varepsilon_2 - \varepsilon_3)\Delta(\mathbf{k}_1 + \mathbf{k}_2 - \mathbf{k}_3) + |\Phi_{23.1}|^2[(n_1 + 1)n_2n_3 - - n_1(n_2 + 1)(n_3 + 1)]\delta(\varepsilon_2 + \varepsilon_3 - \varepsilon_1)\Delta(\mathbf{k}_2 + \mathbf{k}_3 - \mathbf{k}_1)\}, \tag{14}$$

$$L_{\mathbf{k}_1}^{(p)}\{n, N\} = \frac{2\pi}{\hbar}\sum_{2.3}\Big\{|\Psi_{123}|^2[(n_1 + 1)n_2N_3 - n_1(n_2 + 1)(N_3 + 1)]\delta(\varepsilon_1 - \varepsilon_2 - \hbar\omega_3)\Delta(\mathbf{k}_1 - \mathbf{k}_2 - \mathbf{f}_3) + |\Psi_{123}|^2[(n_1 + 1)n_2(N_3 + 1) - n_1(n_2 + 1)N_3]\delta(\varepsilon_1 + \hbar\omega_3 - \varepsilon_2)\Delta(\mathbf{k}_1 + \mathbf{f}_3 - \mathbf{k}_2)\Big\}, \tag{15}$$

N_3 is the number of phonons with momentum $\mathbf{f}_3$ and polarization s. The operator $L_{\mathbf{k}}^{(e)}$ describes the spin wave-spin wave scattering processes caused by the exchange interaction in the transport equation; the operator $L_{\mathbf{k}}^{(r)}$ describes the recombination of two spin waves into one and the splitting up of one spin wave into two, which are caused by the magnetic dipole interaction; the operator $L_{\mathbf{k}}^{(p)}$ describes the emission and absorption of a phonon by a spin wave. Starting from Eqs. (13) to (15) for the operators $L_{\mathbf{k}}^{(e)}$, $L_{\mathbf{k}}^{(r)}$, and $L_{\mathbf{k}}^{(p)}$ one can show by a treatment similar to the one in reference 1 that in the temperature range $\Theta_C \gg T \gg \Theta_C \times (\mu M_0/\Theta_C)^{4/7} \approx 10°\mathrm{K}$ the main role in the transport equation is played by the operator $L_{\mathbf{k}}^{(e)}$ ($L_{\mathbf{k}}^{(e)} \gg L_{\mathbf{k}}^{(r)}, L_{\mathbf{k}}^{(p)}$). To a first approximation one can thus use the equation

$$L_{\mathbf{k}}^{(e)}\{n\} = 0$$

to determine the spin wave distribution function.

The solution of this equation is of the form

$$n_{\mathbf{k}} = \begin{cases} n_0, & \mathbf{k} = 0, \\ [\exp\{(\varepsilon_{\mathbf{k}} - \gamma)/T_s\} - 1]^{-1}, & \end{cases} \tag{16}$$

where γ and n_0 are arbitrary constants which can be connected with the mean values of the absolute magnitude of the magnetic moment $\langle \mathfrak{M}^2 \rangle$ and of the dispersion of the component of the magnetic moment $\langle \mathfrak{M}_\perp^2 \rangle$ perpendicular to the axis of easiest magnetization (the z axis)

$$\langle \mathfrak{M}^2 \rangle = \left\langle \left[\int \mathbf{M}(\mathbf{r}, t)\, dv\right]^2 \right\rangle$$
$$= M_0 V \left[M_0 V - 2\mu \sum_{\mathbf{k}} |v_{\mathbf{k}}|^2 - 2\sum_{\mathbf{k}} \mu_{\mathbf{k}} n_{\mathbf{k}}\right],$$
$$\langle \mathfrak{M}_\perp^2 \rangle = \langle \mathfrak{M}_x^2 \rangle + \langle \mathfrak{M}^2 \rangle = 2\mu n_0 M_0 V,$$
$$\mu_{\mathbf{k}} = \mu A_{\mathbf{k}} / \varepsilon_{\mathbf{k}} = -\partial \varepsilon_{\mathbf{k}} / \partial H. \tag{17}$$

The presence of weak interactions ($L_{\mathbf{k}}^{(p)}, L_{\mathbf{k}}^{(r)}$) causes the quantities γ, T_s, T_p, and n_0 to change in time, but slowly compared to the establishment of the distribution (16).

Proceeding as in reference 1, we can obtain the following equations to determine the quantities γ, n_0, and $\Delta T = T_s - T_p$

$$\Delta\dot{T} + G_1\dot{\gamma} - \varepsilon_0 \dot{n}_0 / c = B_{\gamma\gamma}\gamma + B_{\gamma 0} n_0,$$
$$\Delta\dot{T} + G_2\dot{\gamma} + \varepsilon_0 \dot{n}_0 / c_s = B_{TT}\Delta T, \qquad \dot{n}_0 = -n_0/\tau_\perp, \tag{18}$$

where

$$c_s = \frac{15}{32}\frac{\zeta(5/2)}{\pi^{3/2}}\frac{V}{a^3}\left(\frac{T}{\Theta_c}\right)^{3/2}, \qquad c_p = \frac{2\pi^2}{5}\frac{V}{a^3}\left(\frac{T}{\Theta_D}\right)^3$$

are the spin and phonon specific heats, ϵ_0 the energy of a spin wave with $\mathbf{k} = 0$, and

$$G_1 = -\frac{T}{c_p}\frac{\partial}{\partial T}\sum_{\mathbf{k}} n_{\mathbf{k}}^0 + \frac{c_s + c_p}{c_p}\left(\frac{\partial}{\partial H}\sum_{\mathbf{k}} n_{\mathbf{k}}^0 \Big/ \frac{\partial}{\partial T}\sum_{\mathbf{k}} \mu_{\mathbf{k}} n_{\mathbf{k}}^0\right),$$
$$G_2 = -\frac{T}{c_s}\frac{\partial}{\partial T}\sum_{\mathbf{k}} n_{\mathbf{k}}^0, \tag{19}$$

$$B_{\gamma\gamma} = A\sum_{\mathbf{k}}\left(\frac{\partial L_{\mathbf{k}}}{\partial \gamma}\right)_0 \mu_{\mathbf{k}} = -\frac{8\pi A}{\hbar T}\sum_{123} |\Phi_{12,3}|^2 (\mu_1 + \mu_2 - \mu_3)$$
$$\times n_1^0 n_2^0 (n_3^0 + 1)\, \delta(\varepsilon_1 + \varepsilon_2 - \varepsilon_3)\, \Delta(\mathbf{k}_1 + \mathbf{k}_2 - \mathbf{k}_3),$$

$$B_{\gamma_0} = A\sum_{\mathbf{k}} \mu_{\mathbf{k}}\left(\frac{\partial L_{\mathbf{k}}}{\partial n_0}\right)_0$$
$$= \frac{16\pi A}{\hbar}\sum_{\mathbf{k}} |\Phi_{\mathbf{k},-\mathbf{k};0}|^2 (1 + 2n_{\mathbf{k}}^0)\, \mu_{\mathbf{k}}\, \delta(\varepsilon_0 - 2\varepsilon_{\mathbf{k}}), \tag{20}$$

$$B_{TT} = \left(\frac{1}{c_s} + \frac{1}{c_p}\right)\sum_{\mathbf{k}} \varepsilon_{\mathbf{k}}\left(\frac{\partial L_{\mathbf{k}}}{\partial \Delta T}\right)_0$$
$$= -\frac{2\pi\hbar}{T^2}\frac{c_p + c_s}{c_p c_s}\sum_{123} |\Psi_{123}|^2 \omega_3^2 (n_1^0 + 1)$$
$$\times n_2^0 N_3^0\, \delta(\varepsilon_1 - \varepsilon_2 - \hbar\omega_3)\, \Delta(\mathbf{k}_1 - \mathbf{k}_2 - \mathbf{f}_3), \tag{21}$$

$$\frac{1}{\tau_1} = -\left(\frac{\partial L_0}{\partial n_0}\right)_0 = \frac{8\pi}{\hbar}\sum_{\mathbf{k}} |\Phi_{\mathbf{k},-\mathbf{k};0}|^2 (1 + 2n_{\mathbf{k}}^0)\, \delta(\varepsilon_0 - 2\varepsilon_{\mathbf{k}}),$$
$$A = (1/c_s + 1/c_p)T/G_2\mu. \tag{22}$$

Assuming the quantities ΔT, γ, and n_0 to change with time as $e^{-\lambda t}$ we find the following expressions for the relaxation constants

$$\lambda_{1,2} = \frac{G_1 B_{TT} + B_{\gamma\gamma} \pm \sqrt{(G_1 B_{TT} - B_{\gamma\gamma})^2 + 4B_{TT}B_{\gamma\gamma}G_2}}{2(G_2 - G_1)},$$
$$\lambda_3 = \frac{1}{\tau_\perp}. \tag{23}$$

If $T \gg \Theta_C (\mu M_0/\Theta_C)^{4/7} \gg 2\pi\mu M_0$ we get

$$\lambda_1 \approx \begin{cases} \dfrac{\mu M_0}{\hbar}\left(\dfrac{\mu M_0}{\Theta_c}\right)^{1/2}\dfrac{T}{\Theta_c}\ln^{-1}\dfrac{T}{\mu M_0}, & \dfrac{\mu M_0}{T} \ll \beta + \dfrac{H_0}{M_0} \ll 1 \\ \dfrac{\mu M_0}{\hbar}\left(\dfrac{\mu M_0}{\Theta_c}\right)^{1/2}\dfrac{T}{\Theta_c}, & \beta + \dfrac{H_0}{M_0} \sim 1, \end{cases} \tag{24}$$

$$\lambda_2 = \begin{cases} \left(\dfrac{\hbar}{\rho a^6}\right)[\delta_1^2 + 2(\delta_1 + \delta_2)^2]\left(\dfrac{T}{\Theta_c}\right)^{5/2}, & T \gg \dfrac{\Theta_D^2}{\Theta_c} \\ \left(\dfrac{\hbar}{\rho a^5}\right)\delta_1^2\left(\dfrac{T}{\Theta_c}\right)^2 \exp\left(-\dfrac{\Theta_t^2}{4T\Theta_c}\right), & T \ll \dfrac{\Theta_D^2}{\Theta_c}, \end{cases} \tag{25}$$

where Θ_D is the Debye temperature, $\Theta_t = s_t\hbar/a$, and s_t the velocity of a transverse sound wave.

It is clear from Eqs. (22) and (23) that the relaxation time of the quantity n_0 is determined by the process where a spin wave with wave vector $\mathbf{k} = 0$ splits into two spin waves with wave vectors $\mathbf{k}$ and $-\mathbf{k}$. This process can occur when the energy conservation law

$$\varepsilon_0 = 2\varepsilon_{\mathbf{k}},$$

where ϵ_0 is the energy connected with the uniform precession of the magnetic moment, is satisfied. Kittel[7] has shown that the uniform precession frequency ω_0 and thus $\epsilon_0 = \hbar\omega_0$ is strongly shape dependent. If we consider a ferrodielectric occupying one half of space bounded by one of the crystal planes with the field H_0 in this plane, then

$$\varepsilon_0 = \mu\sqrt{(H_0 + \beta M_0)(H_0 + \beta M_0 + 4\pi M_0)}\,. \tag{26}$$

We can obtain the expression for ϵ_0 from Eqs. (3) and (6) by putting $\mathbf{k} = 0$ and $\theta_{\mathbf{k}} = \pi/2$ which corresponds to a quantum mechanical consideration of uniform oscillations of the magnetic moment.

In evaluating the energy spin wave $\epsilon_{\mathbf{k}}$ we neglect the influence of boundary effects* which is permissible provided the spin-wave mean free path l is much shorter than the dimensions of the specimen L

$$l = \bar{v} / W^{(e)} \approx (\Theta_c / T)^{1/2} a \ll L. \tag{27}$$

When condition (27) is satisfied, the average spin wavelength $\bar{\lambda} \sim (\Theta_C/T)^{1/2} a$ is at the same time much shorter than the dimensions L of the body.

Using (26) one sees easily that the energy conservation law $\epsilon_0 = 2\epsilon_{\mathbf{k}}$ is satisfied, provided

$$\beta + H_0 / M_0 < 4\pi / 3. \tag{28}$$

We do not give here the detailed calculations, but quote the final results for λ_3

$$\lambda_3 = \frac{1}{\tau_\perp} \approx \begin{cases} \dfrac{\mu M_0}{\hbar}\left(\dfrac{\mu M_0}{\Theta_c}\right)^{1/2} \dfrac{T}{\Theta_c}, & \beta + \dfrac{H_0}{M_0} \ll 1, \\ 10^2\, \dfrac{\mu M_0}{\hbar}\left(\dfrac{\mu M_0}{\Theta_c}\right)^{1/2} \dfrac{T}{\Theta_c}\left(\dfrac{4\pi}{3} - \beta - \dfrac{H_0}{M_0}\right)^{1/2}, & \dfrac{4\pi}{3} - \beta - \dfrac{H_0}{M_0} \ll 1. \end{cases} \tag{29}$$

The quantity $\tau_\perp$ tends in this approximation to infinity for $\beta + H_0/M_0 = 4\pi/3$, as should have been expected. This means that it is now necessary to take the relativistic interactions which describe the spin wave-spin wave scattering into account to evaluate $\tau_\perp$, as was done before.[1] Using Eq. (18), and also Eq. (19), we get the following formulae which describe the change in time of the quantities $\langle \mathfrak{M}^2 \rangle$, $\langle \mathfrak{M}_\perp^2 \rangle$, and ΔT

$$\frac{\Delta T}{T} = \frac{\Delta T_0}{T} e^{-\lambda_2 t} + \frac{(2\pi)^2}{3\Gamma(^3/_2)\,\zeta(^3/_2)} \frac{G_2}{G_1} \left(\frac{\Theta_c}{T}\right)^{3/2} \frac{\langle \mathfrak{M}_0^2 \rangle - \overline{\mathfrak{M}}^2}{(M_0 V)^2}$$
$$\times (e^{-\lambda_2 t} - e^{-\lambda_1 t}) + \frac{G_2}{2G_1} \frac{\mu M_0}{\hbar(\lambda_3 - \lambda_1)(2\pi + \beta + H_0 / M_0)} \left(\frac{\mu M_0}{T}\right)^{1/2}$$
$$\times \frac{\langle \mathfrak{M}_{\perp 0}^2 \rangle}{(M_0 V)^2} \left[e^{-\lambda_2 t} - e^{-\lambda_1 t} + \frac{\lambda_3}{\lambda_1} (e^{-\lambda_2 t} - e^{-\lambda_3 t})\right], \tag{30}$$

$$\frac{\langle \mathfrak{M}^2 \rangle - \overline{\mathfrak{M}}^2}{(M_0 V)^2} = \frac{\langle \mathfrak{M}_0^2 \rangle - \overline{\mathfrak{M}}^2}{(M_0 V)^2} e^{-\lambda_1 t} + \frac{3\Gamma(^3/_2)\,\zeta(^3/_2)}{2\pi^2} \left(\frac{\lambda_1}{\lambda_2}\right)^2 \left(\frac{T}{\Theta_c}\right)^{3/2}$$
$$\times \frac{\Delta T_0}{T} (e^{-\lambda_2 t} - e^{-\lambda_1 t}) + \frac{3\Gamma(^3/_2)\,\zeta(^3/_2)}{8\pi^2} \frac{\mu M_0}{\hbar(\lambda_3 - \lambda_1)(2\pi + \beta + H_0/M_0)}$$
$$\times \left(\frac{\mu M_0}{\Theta_c}\right)^{1/2} \left(\frac{T}{\Theta_c}\right) \frac{\langle \mathfrak{M}_{\perp 0}^2 \rangle}{(M_0 V)^2} (e^{-\lambda_1 t} - e^{-\lambda_3 t}), \tag{31}$$

$$\langle \mathfrak{M}_\perp^2 \rangle = \langle \mathfrak{M}_{\perp 0}^2 \rangle e^{-\lambda_3 t}, \tag{32}$$

where ΔT_0, $\langle \mathfrak{M}_{\perp 0}^2 \rangle$, and $\langle \mathfrak{M}_0^2 \rangle$ are the initial values of the temperature difference, the transverse components, and the magnitude of the magnetic moment of the body, while $\overline{\mathfrak{M}^2}$ is the average value of the absolute magnitude of the magnetic moment at the given temperature.

It is clear from the formulae given here that $2/\lambda_3$ is the relaxation time of the transverse component of the magnetic moment of the body.

To elucidate the physical meaning of the relaxation constant λ_1 we assume that $\Delta T_0 = \langle \mathfrak{M}_{\perp 0}^2 \rangle = 0$. We have then

$$\langle \mathfrak{M}^2 \rangle - \overline{\mathfrak{M}}^2 = [\langle \mathfrak{M}_0^2 \rangle - \overline{\mathfrak{M}}^2]\, e^{-\lambda_1 t}. \tag{33}$$

Under those initial conditions $1/\lambda_1$ has thus the meaning of the relaxation time of the mean square of the magnetic moment of the body.

If the initial data are such that $\langle \mathfrak{M}_{\perp 0}^2 \rangle = 0$ and $\langle \mathfrak{M}_0^2 \rangle = \overline{\mathfrak{M}^2}$ then

$$\Delta T = \Delta T_0 e^{-\lambda_2 t}, \tag{34}$$

and we must treat the quantity $1/\lambda_2$ as the time for equalizing the spin and lattice temperatures.

Let us estimate the magnitudes of λ_1, λ_2, and λ_3. Putting

$$\Theta_c \sim 10^3\,^\circ\mathrm{K}, \quad \Theta_l \sim 10^2\,^\circ\mathrm{K}, \quad \beta + H_0 / M_0 \sim 1,$$
$$M_0 \sim 10^3 \text{ emu}, \quad \mu = 10^{-20} \text{ emu},$$
$$\rho = 10\,\mathrm{g/cm^3}, \quad a \approx 2\cdot 10^{-8}\,\mathrm{cm},$$

we get

$$\lambda_1 \sim \lambda_3 \sim 10^8 (T / \Theta_c)\,\mathrm{sec}^{-1}, \qquad \lambda_2 \sim 10^{11} (T / \Theta_c)^{5/2}\,\mathrm{sec}^{-1}.$$

Provided $\beta + H_0/M_0$ is not too close to $4\pi/3$, the relaxation times of the absolute magnitude and of the transverse component of the magnetic moment are thus of the same order of magnitude. One should describe such a relaxation of the magnetic moment phenomenologically by the Bloch equation. In this equation is contained the difference between the relaxation for the case of a small anisotropy and weak fields and the relaxation in the case of large anisotropy or strong fields, when the establishment of the equilibrium value of the magnetic moment is appreciably faster than the rotation of the moment towards its equilibrium direction.

In the temperature range $T \ll \Theta_C (\mu M_0/\Theta_C)^{4/7}$ the main role in the transport equation is played by the operator $L_{\mathbf{k}}^{(r)}\{n\}$. In ferrodielectrics with a small magnetic anisotropy the equilibrium value of the magnetic moment is thus at these temperatures established at the same time as the Bose distribution of the spin waves.

The authors express their deep gratitude to A. I. Akhiezer under whose guidance the paper was prepared and to M. I. Kaganov and V. M. Tsukernik for valuable discussions.

---

*We are indebted to M. I. Kaganov for this remark.

APPENDIX

We consider a ferrodielectric with two magnetic sublattices, the Hamiltonian of which can be written in the form

$$\mathscr{H} = \int\left\{\frac{1}{2}\alpha_1 \frac{\partial \mathbf{M}_1}{\partial x_i}\frac{\partial \mathbf{M}_1}{\partial x_i} + \frac{1}{2}\alpha_2 \frac{\partial \mathbf{M}_2}{\partial x_i}\frac{\partial \mathbf{M}_2}{\partial x_i} + \alpha_{12}\frac{\partial \mathbf{M}_1}{\partial x_i}\frac{\partial \mathbf{M}_2}{\partial x_i} + \gamma \mathbf{M}_1\mathbf{M}_2 + \frac{\mathbf{H}^2}{8\pi}\right\} dv, \tag{A.1}$$

where $\mathbf{M}_j$ is the magnetic moment of the j-th sublattice, $\mathbf{H}$ the magnetic field acting in the ferrodielectric, and α_1, α_2, α_{12}, and γ quantities which are connected with the exchange integrals

$$\alpha_1 \sim \alpha_2 \sim \alpha_{12} \sim \Theta_c a^2 / \mu M_0, \qquad \gamma \sim \Theta_c / \mu M_0.$$

We do not write down here the anisotropy energy which is inessential for the following.

Putting

$$\mathbf{M}_j = \mathbf{M}_{0j} + \mathbf{m}_j, \qquad \mathbf{H} = \mathbf{H}_0 + \mathbf{h}$$

where $\mathbf{M}_{0j}$ is the equilibrium value of the magnetic moment of the j-th sublattice, $\mathbf{H}_0$ the constant magnetic field, in the direction of the z axis, and $\mathbf{m}$ and $\mathbf{h}$ small corrections to $\mathbf{M}_{0j}$ and $\mathbf{H}_0$, we find

$$\mathscr{H} = \int\left\{\frac{1}{2}\alpha_1 \frac{\partial \mathbf{m}_1}{\partial x_i}\frac{\partial \mathbf{m}_1}{\partial x_i} + \frac{1}{2}\alpha_2 \frac{\partial \mathbf{m}_2}{\partial x_i}\frac{\partial \mathbf{m}_2}{\partial x_i} + \alpha_{12}\frac{\partial \mathbf{m}_1}{\partial x_i}\frac{\partial \mathbf{m}_2}{\partial x_i} + \gamma M_{01}^z m_2^z + \gamma M_{02}^z m_1^z + \gamma \mathbf{m}_1\mathbf{m}_2 - \boldsymbol{H}_0(m_1^z + m_2^z) + \frac{\mathbf{h}^2}{8\pi}\right\} dv$$

Going over from $\mathbf{m}$ and $\mathbf{h}$ to their Fourier components

$$\mathbf{m}_j = \frac{1}{V^{1/2}}\sum_{\mathbf{k}} \mathbf{m}_{\mathbf{k}j} e^{i\mathbf{kr}}, \qquad \mathbf{h} = \frac{1}{V^{1/2}}\sum_{\mathbf{k}} \mathbf{h}_{\mathbf{k}} e^{i\mathbf{k}} \tag{A.2}$$

and using the equations of magnetostatics, we get

$$\mathscr{H} = \sum_{\mathbf{k}}\Big[\frac{1}{2}\alpha_1 k^2 \mathbf{m}_{\mathbf{k}1}\mathbf{m}_{-\mathbf{k}1} + \frac{1}{2}\alpha_2 k^2 \mathbf{m}_{\mathbf{k}2}\mathbf{m}_{-\mathbf{k}2} + \alpha_{12}k^2\mathbf{m}_{\mathbf{k}1}\mathbf{m}_{-\mathbf{k}2} + \gamma V^{1/2}(M_{01}^z \mathbf{m}_{\mathbf{k}2}^z + M_{02}^z \mathbf{m}_{\mathbf{k}1}^z)\Delta(\mathbf{k}) + \gamma \mathbf{m}_{\mathbf{k}1}\mathbf{m}_{-\mathbf{k}2} - HV^{1/2}(\mathbf{m}_{\mathbf{k}1}^z + \mathbf{m}_{\mathbf{k}2}^z)\Delta(\mathbf{k}) + (2\pi/k^2)(\mathbf{m}_{\mathbf{k}1} + \mathbf{m}_{\mathbf{k}2}, \mathbf{k}) \times (\mathbf{m}_{-\mathbf{k}1} + \mathbf{m}_{-\mathbf{k}2}, \mathbf{k})\Big]. \tag{A.3}$$

We now define the operators of the magnetic moments $\mathbf{m}_1$ and $\mathbf{m}_2$ by the equations

$$m_1 = (2\mu M_1)^{1/2}(1 - \mu a_1^+ a_1 / 2M_1)^{1/2} a_1 \approx (2\mu M_1)^{1/2}(a_1 - \mu a_1^+ a_1 a_1 / 4M_1),$$

$$m_1^+ = (2\mu M_1)^{1/2} a_1^+ (1 - \mu a_1^+ a_1 / 2M_1)^{1/2} \approx (2\mu M_1)^{1/2}(a_1^+ - \mu a_1^+ a_1^+ a_1 / 4M_1),$$

$$m_1^z = M_1^z - M_1 = -\mu a_1^+ a_1,$$

$$m_2^+ = (2\mu M_2)^{1/2}(1 - \mu a_2^+ a_2 / 2M_2)^{1/2} a_2 \approx (2\mu M_2)^{1/2}(a_2 - \mu a_2^+ a_2 a_2 / 4M_2),$$

$$m_2^- = (2\mu M_2)^{1/2} a_2^+ (1 - \mu a_2^+ a_2 / 2M_2)^{1/2} \approx (2\mu M_2)^{1/2}(a_2^+ - \mu a_2^+ a_2^+ a_2 / 4M_2),$$

$$m_2^z = M_2^z + M_2 = \mu a_2^+ a_2, \qquad m_j^\pm = m_{xj} \pm i m_{yj},$$

$$M_1 = M_{01}^z > 0, \qquad M_2 = -M_{20}^z > 0,$$

$$[a_j(\mathbf{r}, t), a_{j'}(\mathbf{r}', t)] = \delta_{jj'}^+ \delta(\mathbf{r} - \mathbf{r}'). \tag{A.4}$$

Using these formulae one can express the Hamiltonian $\mathcal{H}$ in terms of the variables $a_{\mathbf{k}j}$ and $a_{\mathbf{k}j}^+$

$$a_{\mathbf{k}j} = \frac{1}{V^{1/2}}\sum_{\mathbf{k}} a_j(\mathbf{r}, t)e^{-i\mathbf{kr}}, \qquad a_{\mathbf{k}j}^+ = \frac{1}{V^{1/2}}\sum_{\mathbf{k}} a_j^+(\mathbf{r}, t)e^{i\mathbf{kr}}. \tag{A.5}$$

We then get

$$\mathscr{H} = \mathscr{H}_0 + \mathscr{H}^{(3)} + \mathscr{H}^{(4)}, \tag{A.6}$$

where

$$\mathscr{H}_0 = \sum_{\mathbf{k}}(A_{\mathbf{k}1}a_{\mathbf{k}1}^+ a_{\mathbf{k}1} + A_{\mathbf{k}2}a_{\mathbf{k}2}^+ a_{\mathbf{k}2} + B_{\mathbf{k}}a_{\mathbf{k}1}a_{-\mathbf{k}2} + B_{\mathbf{k}}^* a_{-\mathbf{k}2}^+ a_{\mathbf{k}1}^+),$$

$$A_{\mathbf{k}1} = \mu(\alpha_1 k^2 M_1 + \gamma M_2 + H), \quad A_{\mathbf{k}2} = \mu(\alpha_2 k^2 M_2 + \gamma M_1 - H),$$

$$B_{\mathbf{k}} = \mu(M_1 M_2)^{1/2}(\alpha_{12}k^2 + \gamma). \tag{A.7}$$

We have neglected here the influence of the magnetic dipole interaction on the spectrum; taking it into account does not change the result, but complicates the calculations greatly.

The Hamiltonians $\mathcal{H}^{(3)}$ and $\mathcal{H}^{(4)}$ contain, respectively, three and four operators $a_{\mathbf{k}j}$ and $a_{\mathbf{k}j}^+$.

The Hamiltonian $\mathcal{H}_0$ which is quadratic in the operators $a_{\mathbf{k}j}$ and $a_{\mathbf{k}j}^+$ can be diagonalized by a Bogolyubov canonical transformation[9]

$$a_{\mathbf{k}1} = u_{11}c_{\mathbf{k}1} + v_{12}^* c_{-\mathbf{k}2}^+, \qquad a_{\mathbf{k}2} = u_{22}c_{\mathbf{k}2} + v_{21}^* c_{-\mathbf{k}1}^*, \tag{A.8}$$

where the operators $c_{\mathbf{k}j}$ and $c_{\mathbf{k}j}^+$ satisfy the commutation relations

$$[c_{\mathbf{k}j}, c_{\mathbf{k}'j'}^+] = \delta_{jj'}\Delta(\mathbf{k} - \mathbf{k}')$$

and where u and v satisfy the usual conditions

$$|u_{11}|^2 - |v_{12}|^2 = |u_{22}|^2 - |v_{21}|^2 = 1.$$

If we use the equations of motion

$$\dot{a}_{\mathbf{k}j} = (i/\hbar)[\mathscr{H}, a_{\mathbf{k}j}],$$

we can obtain another four equations to determine u and v, and also the eigenvalues of the Hamiltonian $\mathcal{H}_0$. These equations are of the form

$$u_{11}\varepsilon_{\mathbf{k}1} = A_{\mathbf{k}1}u_{11} + B_{\mathbf{k}}v_{21}, \qquad u_{22}\varepsilon_{\mathbf{k}2} = A_{\mathbf{k}2}u_{22} + B_{\mathbf{k}}v_{12},$$

$$-v_{21}\varepsilon_{\mathbf{k}1} = A_{\mathbf{k}2}v_{21} + B_{\mathbf{k}}u_{11}, \qquad -v_{12}\varepsilon_{\mathbf{k}2} = A_{\mathbf{k}1}v_{12} + B_{\mathbf{k}}u_{22},$$

and hence

$$\varepsilon_{\mathbf{k};\,1,2} = [(A_{\mathbf{k}1} + A_{\mathbf{k}2})^2/4 - B_{\mathbf{k}}^2]^{1/2} \pm (A_{\mathbf{k}1} - A_{\mathbf{k}2})/2,$$

$$v_{12} = v_{21} = (A_{2\mathbf{k}} - \varepsilon_{\mathbf{k}2}) / [B_{\mathbf{k}}^2 - (A_{\mathbf{k}2} - \varepsilon_{\mathbf{k}2})^2]^{1/2},$$

$$u_{11} = u_{22} = -B_{\mathbf{k}} / [B_{\mathbf{k}}^2 - (A_{\mathbf{k}2} - \varepsilon_{\mathbf{k}2})^2]^{1/2}. \tag{A.9}$$

Since $\gamma \gg 1$, we have*

*We note that the expression for ε_1 given in reference 8 is incorrect.

$$\varepsilon_1 \approx (\mu / M)(\alpha_1 k^2 M_1^2 + \alpha_2 k^2 M_2^2 - 2\alpha_{12} k^2 M_1 M_2) + \mu H,$$
$$\varepsilon_2 \approx \mu\gamma M - \mu H + (\mu M_1 M_2 / M)(\alpha_1 + \alpha_2 - 2\alpha_{12}) k^2,$$
$$v_{12} = v_{21} \approx (M_2 / M)^{1/2}, \qquad u_{11} = u_{22} \approx -(M_1 / M)^{1/2},$$
$$M = M_1 - M_2 > 0.$$

We see that one of the branches of the energy spectrum has a large activation energy caused by the exchange interaction between the sublattices. The contribution from the oscillations of the magnetic moments described by the variables $c_{\mathbf{k}2}$ and $c_{\mathbf{k}2}^{+}$ to the thermodynamic and transport properties of the ferrodielectric at low temperatures is thus exponentially small, and when one studies these properties of the ferrodielectric one need only take into account the low-frequency spin waves, described by the operators $c_{\mathbf{k}1}$ and $c_{\mathbf{k}1}^{+}$.

The interactions between the low-frequency spin waves themselves, caused by the exchange energy connected with the inhomogeneities of the magnetic moments and by the magnetic dipole energy, have the same structure as in the case of a ferrodielectric with one magnetic sublattice.

As regards the interactions caused by the exchange energy between sublattices when the magnetization is homogeneous,

$$\mathcal{H}_{int}^{\gamma} = -\frac{\gamma\mu^2}{4}\int\Big[\Big(\frac{M_2}{M_1}\Big)^{1/2}(a_1^+ a_1^+ a_1 a_2^+ + a_1^+ a_1 a_1 a_2)$$
$$+ \Big(\frac{M_1}{M_2}\Big)^{1/2}(a_1^+ a_2^+ a_2^+ a_2 + a_1 a_2^+ a_2 a_2) + 4a_1^+ a_1 a_2^+ a_2\Big] dv,$$

one can use (A.5), (A.8), and (A.9) to show that that part of it which describes the interactions of the low frequency spin waves with one another does not contain the large parameter γ and is of the form

$$\mathcal{H}_{int}^{\gamma} = \sum_{\mathbf{k}_1\mathbf{k}_2\mathbf{k}_3\mathbf{k}_4} \Phi_{\mathbf{k}_1\mathbf{k}_2\mathbf{k}_3\mathbf{k}_4} c_{\mathbf{k}_1 1}^{+} c_{\mathbf{k}_2 1}^{+} c_{\mathbf{k}_3 1} c_{\mathbf{k}_4 1} \Delta(\mathbf{k}_1 + \mathbf{k}_2 - \mathbf{k}_3 - \mathbf{k}_4).$$

where

$$\Phi_{\mathbf{k}_1\mathbf{k}_2\mathbf{k}_3\mathbf{k}_4} \sim \mu^2 / V,$$

i.e., $\mathcal{H}_{\text{int}}^{(\gamma)}$ is a small correction compared with $\mathcal{H}^{(3)}$. This makes it possible to neglect the magnetic structure when studying the low-temperature properties of ferrodielectrics.

---

[1] Akhiezer, Bar'yakhtar, and Peletminskiĭ, JETP **36**, 216 (1959), Soviet Phys. JETP **9**, 146 (1959).

[2] L. Néel, Ann. phys. **3**, 137 (1948).

[3] M. I. Kaganov and V. M. Tsukernik, JETP **36**, 224 (1959), Soviet Phys. JETP **9**, 151 (1959).

[4] T. Holstein and H. Primakoff, Phys. Rev. **58**, 1098 (1940).

[5] M. I. Kaganov and V. M. Tsukernik, JETP **34**, 1610 (1958), Soviet Phys. JETP **7**, 1107 (1958).

[6] A. Akhiezer, J. Phys. (U.S.S.R.) **10**, 217 (1946).

[7] C. Kittel, Phys. Rev. **71**, 270 (1947).

[8] M. I. Kaganov and V. M. Tsukernik, JETP **34**, 106 (1958), Soviet Phys. JETP **7**, 73 (1958).

[9] N. N. Bogolyubov, Лекции по квантовой статистике (Lectures on Quantum Statistics) Kiev, 1947; Bogolyubov, Tolmachev, and Shirkov, Новый метод в теории сверхпроводимости (A New Method in Superconductivity Theory) Acad. Sci. Press, 1958, Fortschr. Phys. **6**, 605 (1958).

Translated by D. ter Haar
240

SOVIET PHYSICS JETP VOLUME 11, NUMBER 4 OCTOBER, 1960

RENORMALIZATION IN PARITY-NONCONSERVATION THEORY

B. L. IOFFE

Submitted to JETP editor November 6, 1959

J. Exptl. Theoret. Phys. (U.S.S.R.) 38, 1263-1275 (April, 1960)

A method is proposed for the renormalization of mass, charge, and wave functions in the parity-nonconservation theory. The method is checked in the case in which the "three-Γ approximation" equation is used for the vertex part.

THE renormalization program (for a theory which is invariant with respect to time reversal) should be somewhat different in parity-nonconservation theory than in ordinary theory, for the reason that the radiative corrections based on an interaction which does not conserve parity contains terms of a type different (pseudoscalar) than those contained in the free Lagrangian. Renormalization in parity-nonconservation theory was considered by d'Espagnat and Prentki[1] and Sekine.[2] The former did not study the problem sufficiently fully, and the latter reached a conclusion that a systematic renormalization program was impossible, which is erroneous from our point of view. It is therefore appropriate to consider this question again.

In the presence of parity nonconservation, the free equations can, generally speaking, have a form that differs from the ordinary. Therefore, we shall first (in Sec. 1) consider the properties of free equations in the presence of parity nonconservation. In Sec. 2 the renormalization program will be given, and in Sec. 3 it will be shown how this program is realized in a concrete example — the calculation of the asymptotic behavior of the Green's function and the vertex parts for large p^2.

1. THE EQUATIONS OF MOTION OF FREE PARTICLES IN PARITY NONCONSERVATION

In parity nonconservation, the equations of motion of free particles generally differ from the form usually taken. At first glance, it can be shown that in such forms of parity violation in which time (combined) parity is not conserved, the observed effects appear in the propagation of a free particle in a vacuum, for example, the rotation of the plane of polarization of light. Actually however, because of nonconservation of parity, no observed effects can arise in the propagation of the free particle in a vacuum. Physically, this is almost obvious, inasmuch as the motion of the free particle is determined by its momentum and the projection of its spin on a certain axis, which do not change by virtue of the laws of conservation, regardless of whether parity is conserved or not.

In the case of bosons with spin zero or one, the hypothesis of parity nonconservation does not change the equations of motion, as can be seen directly from the free Lagrangian. In fact, for bosons with spin zero one can construct only the scalars $(\partial\varphi/\partial x_\nu)^2$ and φ^2 from the field φ and its first derivatives; it is not possible to construct pseudoscalars, so that the ordinary expression for the Lagrangian density

$$L = -\tfrac{1}{2}[(\partial\varphi/\partial x_\nu)^2 + \mu^2\varphi^2] \tag{1.1}$$

does not change upon the consideration of parity nonconservation. For bosons with spin one, for example, for the electromagnetic field A_μ, in addition to the scalar $F_{\mu\nu}^2$ ($F_{\mu\nu} = \partial A_\nu/\partial x_\mu - \partial A_\mu/\partial x_\nu$) which is quadratic over the field, there is also the pseudoscalar $\epsilon_{\mu\nu\lambda\sigma}F_{\mu\nu}F_{\lambda\sigma}$. However, the addition of this pseudoscalar to the Lagrangian

$$L = -\tfrac{1}{4}F_{\mu\nu}^2 - \tfrac{1}{4}\lambda\varepsilon_{\mu\nu\lambda\sigma}F_{\mu\nu}F_{\lambda\sigma} \tag{1.2}$$

does not change the equations of motion, inasmuch as the second term in (1.2) reduces to a total derivative after differentiation by parts.

For particles with spin one-half, the most general expression for the Lagrangian density of free particles in the presence of parity nonconservation differs from the ordinary, which corresponds to the Dirac equation, and has the form*

$$L = \bar{\psi}[\hat{p}(1+\lambda\gamma_5) - m - i\mu\gamma_5]\psi,$$
$$\hat{p} = i\gamma_\mu\partial/\partial x_\mu \equiv i(\beta\partial/\partial t + \beta\alpha\nabla). \tag{1.3}$$

Here, because of the Hermite character of the Lagrangian, the constants λ and μ should be real. The equation for the ψ function

$$[\hat{p}(1+\lambda\gamma_5) - m - i\mu\gamma_5]\psi = 0, \tag{1.4}$$

---

*The following notation is employed:
$\gamma_\mu = (\beta, \beta\alpha)$, $\gamma_5 = -i\gamma_1\gamma_2\gamma_3\gamma_4$, $\gamma_5^2 = 1$, $\hat{a} = a_\mu\gamma_\mu = a_0\beta - \beta\alpha\mathbf{a}$.

follows from (1.3); upon squaring this equation, we easily find the connection between energy and momentum:

$$p^2 = (m^2 + \mu^2)/(1 - \lambda^2) \text{ or } E^2 = \mathbf{p}^2 + (m^2 + \mu^2)/(1 - \lambda^2). \tag{1.5}$$

Thus, account of parity nonconservation leads only to appearance of the effective mass $m_{\text{eff}} = \sqrt{(m^2 + \mu^2)/(1 - \lambda^2)}$.

It is important to note that (1.5) has meaning only for $|\lambda| < 1$. We shall see below that if the terms which do not conserve parity in the free equation appear only because of the interaction, and the ordinary Dirac equation holds for "bare" particles, then $|\lambda|$ actually does not exceed unity.

Invariance relative to time reversal or charge conjugation imposes definite limitations on the general form of the Lagrangian (1.3). It is easy to prove that in the case of T-invariant theory, $\mu = 0$, while in the case of C-invariant theory, on the other hand, $\lambda = 0$. Inasmuch as T-invariant theory possesses the greater interest, we shall consider this case in more detail.*

The free Lagrangian in the T-invariant theory has the form

$$L = \overline{\psi}\,[\hat{p}(1 + \lambda\gamma_5) - m]\,\psi, \tag{1.6}$$

$$p^2 = m^2/(1 - \lambda^2), \qquad |\lambda| < 1. \tag{1.7}$$

In order to carry out the second quantization, we determine the canonically conjugate momentum

$$\pi = \partial L/\partial(\partial\psi/\partial t) = -i\overline{\psi}\beta(1 + \lambda\gamma_5) \tag{1.8}$$

and construct the Hamiltonian

$$H = \pi\partial\psi/\partial t - L = -i\overline{\psi}\gamma\nabla(1 + \lambda\gamma_5)\psi + m\overline{\psi}\psi, \qquad H = H^+. \tag{1.9}$$

The anticommutation relations for canonically conjugate variables taken at the same instant of time can be determined in the following fashion:

$$\{\psi_\alpha(\mathbf{r}, t), \pi_\beta(\mathbf{r}', t)\} = i\delta_{\alpha\beta}\,\delta(\mathbf{r} - \mathbf{r}'). \tag{1.10}$$

Substituting (1.8) in (1.10), we find the value of the anticommutator of the functions ψ and $\overline{\psi}$ at the same instant of time:

$$\{\psi_\alpha(\mathbf{r}, t), \overline{\psi}_\beta(\mathbf{r}', t)\} = (1 - \lambda^2)^{-1}[\gamma_4(1 + \lambda\gamma_5)]_{\alpha\beta}\,\delta(\mathbf{r} - \mathbf{r}'). \tag{1.11}$$

The remaining anticommutators vanish as usual:

$$\{\psi_\alpha, \psi_\beta\} = \{\overline{\psi}_\alpha, \overline{\psi}_\beta\} = 0. \tag{1.12}$$

In accord with the ordinary rules of quantum mechanics, the time dependence of the ψ operator can be obtained from the equation

$$-i\partial\psi/\partial t = \int d^3x'\,[H(x'), \psi(x)]. \tag{1.13}$$

Computing the commutator in (1.13) by means of (1.11), we obtain the equation

$$[\hat{p}(1 + \lambda\gamma_5) - m]\psi \equiv i\gamma_\mu(1 + \lambda\gamma_5)\partial\psi/\partial x_\mu - m\psi = 0, \tag{1.14}$$

as was to be expected. It is interesting to note that if we rewrite (1.14) in the form of the Schrödinger equation

$$i\partial\psi/\partial t = \mathcal{H}\psi, \tag{1.15}$$

then the corresponding Hamiltonian

$$\mathcal{H} = \alpha\mathbf{p} + \beta m(1 + \lambda\gamma_5)/(1 - \lambda^2) \tag{1.16}$$

becomes non-Hermitian. Of course, this is not any defect of the theory, inasmuch as the Hamiltonian (1.9) in second-quantization theory was Hermitian, and the eigenvalues of the energy were real [which also follows directly from (1.7)].

In the method of quantization of (1.10) and (1.11), used by us, the anticommutator $\{\psi_\alpha(\mathbf{r}, t), \overline{\psi}_\beta(\mathbf{r}', t)\}$ is an integral of the motion. It is easy to demonstrate this by calculating the derivative of the anticommutator with respect to time by means of (1.15), (1.16), and (1.11). In the case of any other method of quantization, for example, when just γ_4 appears on the right-hand side of (1.11), the anticommutator will no longer be an integral of the motion.

Equation (1.14) and the anticommutation relations (1.11) do not have the usual form in T-invariant theory with parity nonconservation. One can show, however, that all the physical consequences for the motion of a free particle (or for the motion of a particle in an electromagnetic field) are the same as in the theory with parity conservation. For this purpose, we carry out a transformation of the ψ functions:

$$\psi = S\psi', \qquad \overline{\psi} = \overline{\psi}'\widetilde{S}, \qquad \widetilde{S} = \beta S^+\beta \tag{1.17}$$

and put the matrix S in the form

$$S = A + B\gamma_5, \tag{1.18}$$

where A and B are real numbers. We substitute (1.17) in (1.6), and require that there be no terms $\hat{p}\gamma_5$ in the new expression for the Lagrangian, and that the coefficient of $\hat{p}$ be equal to unity. This leads to the following set of equations for the coefficients A and B:

---

*In C-invariant theory, the term with the time derivative $\partial\psi/\partial t$ does not change as a result of parity violation. Therefore, the commutation relations remain the same as in ordinary theory, and additional problems do not appear in carrying out the renormalization program.

$$(A^2+B^2)\lambda+2AB=0, \qquad A^2+B^2+2AB\lambda=1, \quad (1.19)$$

the solution of which has the form

$$A=\tfrac{1}{2}\left[(1+\lambda)^{-1/2}+(1-\lambda)^{-1/2}\right],$$
$$B=\tfrac{1}{2}\left[(1+\lambda)^{-1/2}-(1-\lambda)^{-1/2}\right]. \quad (1.20)$$

For such values of A and B, the Lagrangian (1.6) is expressed in terms of $\bar{\psi}'$ and ψ', and takes the form

$$L=\bar{\psi}'(\hat{p}-m/\sqrt{1-\lambda^2})\psi', \quad (1.21)$$

where the anticommutation relations (1.11) reduce to the usual:

$$\{\psi'_\alpha(\mathbf{r},t),\ \bar{\psi}'_\beta(\mathbf{r}',t)\}=(\gamma_4)_{\alpha\beta}\,\delta(\mathbf{r}-\mathbf{r}'). \quad (1.22)$$

In the presence of an electromagnetic field the operator $\hat{p}$ should be replaced by $\hat{p}-e\hat{A}$ in the Lagrangian (1.6) because of gauge invariance. It is clear that the transformation (1.17) will hold in this case also and lead to (1.21) with the substitution of $\hat{p}-e\hat{A}$ for $\hat{p}$. We thus see that for the case of the motion of a free particle, or of a particle in an electromagnetic field, the entire effect of the introduction of the parity-nonconserving term $\hat{p}\gamma_5$ into the Lagrangian leads, after transformation of the ψ functions, to the appearance of an effective mass $m_{\text{eff}}=m/\sqrt{1-\lambda^2}$. Inasmuch as the mass of the particles is determined from experiment, it is physically impossible to distinguish between the Lagrangians (1.6) and (1.21).

Some interest attaches to the problem of how the equations change upon introduction of the pseudoscalar term $\lambda\hat{p}\gamma_5$ in the presence of interaction with other fields. In order to make this clear, it suffices to consider how the five covariant expressions formed from ψ functions, scalar, pseudoscalar, tensor, vector, and axial vector, change under the transformation (1.17). Making use of (1.16) and (1.20), it is easy to prove that the scalar, pseudoscalar, and tensor change in the transformation (1.17) according to the law

$$\bar{\psi}O_j\psi=\bar{\psi}'O_j\psi'/\sqrt{1-\lambda^2}, \qquad O_j=S,T,P, \quad (1.23)$$

while the vector and axial vector change as

$$\bar{\psi}O_j\psi=\bar{\psi}'O_j(1-\lambda\gamma_5)\psi'/(1-\lambda^2), \qquad O_j=V,A. \quad (1.24)$$

Equations (1.23) and (1.24) do not have much meaning, because if one considers that the term $\lambda\hat{p}\gamma_5$ arises because of an interaction which does not conserve parity, then the same interaction produces corrections to the vertex part of the interaction under consideration. For the interactions S, T, and P it follows from the T invariance that the general form of the interaction operator cannot contain the matrix γ_5. For vector interactions the correction should have the same form as in electrodynamics, i.e., $1+\lambda\gamma_5$ and, consequently, should compensate the factor $(1-\lambda\gamma_5)/(1-\lambda^2)$ in (1.24). It can be shown that for axial interaction the ratio of the parity-nonconservation term (in the correction to the vertex part) to the parity-conservation term is the same as in the vector interaction, i.e., the correction will also have the form $1+\lambda\gamma_5$ and will be compensated. The latter statements (relative to V and A interactions) hold only for vertex parts with free ends, while for vertex parts with $p^2 \neq m^2_{\text{phys}}$, terms not conserving parity of course remain.

One must also make the following observation. The transformation (1.17) is not unitary. Therefore, in the physical interpretation, it is necessary to assume that the physical particles are described by the functions ψ' (and not by ψ) so that, for example, for a particle at rest, ψ' (and not ψ) has the form $\psi'=\begin{pmatrix}v\\0\end{pmatrix}$, where v is a two-component spinor.

2. RENORMALIZATION IN PARITY-NONCONSERVATION THEORY

As a parity-nonconservation interaction, we consider the interaction of a charged boson* possessing spin zero with a fermion field having the two states X and N. (The interaction in the decay $\Lambda^0 \rightarrow N+\pi$ serves as an example of such interaction.) We shall write down the total Lagrangian in the form

$$L=\bar{\psi}_X(\hat{p}-m_{0X})\psi_X+\bar{\psi}_N(\hat{p}-m_{0N})\psi_N+\varphi^+(p^2-\mu_0^2)\varphi$$
$$+\,g_0\bar{\psi}_X(\alpha+\beta\gamma_5)\psi_N\varphi+\text{Herm. Conj.} \quad (2.1)$$

where m_{0X}, m_{0N}, μ_0 are the bare masses of the corresponding particles, g_0 is the bare charge, $\alpha^2+\beta^2=1$, α and β are real.

As usual (see, for example, reference 3), it is convenient to carry out the renormalization of the mass and of the ψ functions of X and N by considering the equation for the corresponding Green's function which, for example, has the following form for N:

$$\{\hat{p}-m_{0N}-M(\hat{p})\}\,G_N(\hat{p})=1; \quad (2.2)$$

---

*These considerations can be carried through in a quite similar fashion for the case of interaction with a neutral boson field. Of course, it is necessary to bear in mind that in this case N and X cannot be one and the same particle, inasmuch as this would lead to the vanishing of terms which do not conserve parity because of the T invariance and the Hermitian character of the Hamiltonian.

$M(\hat{p})$ is the mass operator:

$$M(\hat{p}) = \frac{g_0^2}{4\pi^3 i} \int d^4k\, (\alpha - \beta\gamma_5)$$

$$\times G_X(\hat{p} + \hat{k})\, \Gamma^+(\hat{p},\ \hat{p} + \hat{k};\ \hat{k})\, D(k^2); \qquad (2.3)$$

$\Gamma^+(\hat{p}, \hat{p}+\hat{k}; \hat{k})$ is the exact vertex part corresponding to the interaction $\bar{\psi}_X(\alpha + \beta\gamma_5)\psi_N\varphi$ (Γ^- corresponds to the Hermitian-adjoint interaction $\bar{\psi}_N(\alpha - \beta\gamma_5)\psi_X\varphi^+$); $D(k^2)$ is the Green's function of the meson.

In T-invariance theory, the general expression for the mass operator should have the form

$$M(\hat{p}) = \hat{p}M_1(p^2) + \hat{p}\gamma_5 M_2(p^2) + M_3(p^2), \qquad (2.4)$$

where M_1, M_2, M_3 are scalar functions of p^2, and the equation for the Green's function (2.2) is written as

$$\{\hat{p} - m_{0N} - \hat{p}M_1(p^2) - \hat{p}\gamma_5 M_2(p^2) - M_3(p^2)\}\, G_N = 1. \qquad (2.5)$$

We transform (2.5) in the following manner:

$$\{\hat{p}\,[1 - M_1(m^2_{\text{phys}})] - \hat{p}\gamma_5 M_2(m^2_{\text{phys}}) - m_{0N} - M_3(m^2_{\text{phys}})$$
$$- \hat{p}\,[M_1(p^2) - M_1(m^2_{\text{phys}})] - \hat{p}\gamma_5\,[M_2(p^2) - M_2(m^2_{\text{phys}})]$$
$$- [M_3(p^2) - M_3(m^2_{\text{phys}})]\}\, G_N = 1, \qquad (2.6)$$

where m_{phys} is the physical mass. It is seen from (2.6) that for $p^2 \to m^2_{\text{phys}}$, the equation for the Green's function G_N has the form

$$Z_2^{-1}\{\hat{p}(1 + \lambda\gamma_5) - m\}\, G_N = 1; \qquad (2.7)$$

$$Z_2^{-1} = 1 - M_1(m^2_{\text{phys}}),$$

$$m = [m_{0N} + M_3(m^2_{\text{phys}})]\, Z_2,\ \lambda = -Z_2 M_2(m^2_{\text{phys}}), \qquad (2.7')$$

that is (with accuracy up to the factor Z_2^{-1}), the form of the equation for the Green's function corresponding to the free equation (1.14).

By studying the free equation (1.14), we came to the conclusion that in the transition to physical particles described by the ordinary Dirac equation (with the observed mass $m_{\text{phys}} = m/\sqrt{1-\lambda^2}$) it is necessary to make the transformation (1.17). Since the Green's function is defined in terms of the T-product as

$$G_{\alpha\beta}(x,\ x') = \langle 0 | T(\psi_\alpha(x),\ \bar{\psi}_\beta(x')) | 0 \rangle, \qquad (2.8)$$

then the transformation of the ψ functions (1.17) produces the following transformation of the Green's function:

$$G = SG'\bar{S}. \qquad (2.9)$$

We now make another numerical renormalization of the ψ functions: $\psi' = Z^{1/2}\psi_R$ and the Green's function: $G' = Z_2 G_R$. Then (2.6) takes the form

$$\Big\{\hat{p} - m_{\text{phys}} - \hat{p}\,\frac{1 - \lambda\gamma_5}{1 - \lambda^2}\, Z_2[M_1(p^2) - M_1(m^2_{\text{phys}})]$$
$$- \hat{p}Z_2\,\frac{\gamma_5 - \lambda}{1 - \lambda^2}\,[M_2(p^2) - M_2(m^2_{\text{phys}})]$$
$$- (Z_2/\sqrt{1-\lambda^2})\,[M_3(p^2) - M_3(m^2_{\text{phys}})]\Big\}\, G_R = 1. \qquad (2.10)$$

For $p^2 \to m^2_{\text{phys}}$, the renormalized Green's function is $G_R \to (\hat{p} - m_{\text{phys}})^{-1}$, i.e., it has the form of the Green's function of a free particle with mass m_{phys}.

Renormalization of the mass and of the ψ functions for the second fermion takes place in precisely the same fashion. Renormalization of the mass and of the wave equations of the boson is carried out just as in ordinary theory, inasmuch as parity nonconservation does not lead to the appearance of terms of a new type in the expression for the polarization operator.

There still remains the charge renormalization. For this purpose, we consider the exact expression for the interaction energy [$a(p^2, (p-k)^2, k^2)$ and $b(p^2, (p-k)^2, k^2)$ are certain functions of p^2, $(p-k)^2$, k^2]:

$$g_0\bar{\psi}_X(\hat{p})\,[a(p^2, (p-k)^2, k^2)$$
$$+ \gamma_5 b(p^2, (p-k)^2, k^2)]\,\psi_N(\hat{p} - \hat{k})\,\varphi(k^2), \qquad (2.11)$$

for $p^2 \to m_X^2$, $(p-k)^2 \to m_N^2$ and $k^2 \to \mu^2$ (m_X, m_N, μ are the physical masses). Then, in accordance with the definition of physical charge, we should have

$$g_0\bar{\psi}_X(m_X)\,[a(m_X^2, m_N^2, \mu^2) + b(m_X^2, m_N^2, \mu^2)\gamma_5]\,\psi_N(m_N)\,\varphi(\mu^2)$$
$$= g\bar{\psi}_{XR}(m_X)\,(\alpha_R + \beta_R\gamma_5)\,\psi_{NR}(m_N)\,\varphi_R(\mu),$$
$$\alpha_R^2 + \beta_R^2 = 1. \qquad (2.12)$$

The renormalized ψ functions are connected with the usual relations

$$\psi_X = Z_{2X}^{1/2}(A_X - B_X\gamma_5)\,\psi_{XR},$$
$$\psi_N = Z_{2N}^{1/2}(A_N + B_N\gamma_5)\,\psi_{NR},\ \varphi = Z_3^{1/2}\varphi_R. \qquad (2.13)$$

We note that for equal masses of N and X, there will be $Z_{2X} = Z_{2N}$, $A_N = A_X$, $B_N = B_X$ and $\lambda_N = -\lambda_X$. This circumstance follows directly from a comparison of the equations of the mass operators (2.3) for N and X. Substituting (2.13) and (2.12), we find the relation between the renormalized and non-renormalized charges (and also the expression for the values of α_R and β_R) at $m_X = m_N$:

$$g^2 = g_0^2 Z_2^2 \widetilde{Z}_1^{-2} Z_3, \quad \alpha_R = \widetilde{Z}_1(a - b\lambda)/(1 - \lambda^2),$$

$$\beta_R = \widetilde{Z}_1(b - a\lambda)/(1 - \lambda^2);$$

$$\widetilde{Z}_1 = (1 - \lambda^2)/\sqrt{(a^2 + b^2)(1 + \lambda^2) - 4ab\lambda}. \qquad (2.14)$$

The expression for the renormalization of the charge (2.14) is materially simplified in the case of the two-component theory. Then, as can be proved (see the following section), $a = b \equiv Z_1^{-1}/\sqrt{2}$, $\lambda = 1 - Z_2$ and, in place of (2.14), we have

$$g^2 = g_0^2 Z_2^2 Z_1^{-2} Z_3 (1+\lambda)^{-2} = g_0^2 Z_2^2 Z_1^{-2} Z_3 (2 - Z_2)^{-2}. \quad (2.14')$$

The exact vertex part (for $p^2 = m^2$) has the form

$$\Gamma^+ = Z_1^{-1}(1+\gamma_5)/\sqrt{2},$$

so that Z_1^{-1} has the meaning of an ordinary renormalized constant in the renormalization of the vertex part.

The remaining part of the proof of the renormalizability of the theory (in particular, the elimination of the so-called "b divergences"), inasmuch as it is not connected with the specific parity nonconservation, can be carried out in the same fashion as in the usual theory.[4-6]

The renormalization that we have carried out will be valid only in the case in which the quantity λ, determined in accord with (2.7), is less than unity in absolute value, $|\lambda| \leq 1$. We now shall show that this is actually the case. For this purpose, we generalize the spectral decomposition of Lehmann-Kallen to the case of noconservation of spatial parity under the preservation of time (combination) parity (see also reference 2): just as in reference 7, we consider the function

$$G_{\alpha\beta}^{(+)}(x, x') = \langle 0 | \psi_{\alpha R}(x) \overline{\psi}_{\beta R}(x') | 0 \rangle,\ G_{\alpha\beta}^{(-)}(x, x') = \langle 0 | \overline{\psi}_{\beta R}(x') \psi_{\alpha R}(x) | 0 \rangle \quad (2.15)$$

and the anticommutator

$$G_{\alpha\beta}^{(a)}(x, x') = \langle 0 | \{\psi_{\alpha R}(x), \overline{\psi}_{\beta R}(x')\} | 0 \rangle. \quad (2.16)$$

in addition to the Feynman Green's function (2.8). (As is well known, the Lehmann-Kallen relations are written down for renormalized functions.) Making use of CP invariance, it is easy to prove that the function $G^{(-)}$ can be expressed in terms of $G^{(+)}$ by means of the equality (C is the charge-conjugation matrix)

$$G^{(-)T}(-\mathbf{r}', t'; -\mathbf{r}, t) = -C\gamma_4 G^{(+)}(-\mathbf{r}, t; -\mathbf{r}', t')\gamma_4 C^{-1} \quad (2.17)$$

and, consequently, all the vacuum averages, including the Feynman Green's function and the anticommutator, are expressed in terms of $G^{(+)}$.

According to Lehmann,[7] the function $G^{(+)}$ can be written as

$$\langle 0 | \psi_{\alpha R}(x) \overline{\psi}_{\beta R}(x') | 0 \rangle = \sum_p \langle 0 | \psi_{\alpha R}(x) | \Phi_p \rangle \langle \Phi_p | \overline{\psi}_{\beta R}(x') | 0 \rangle = \sum_p C_p^\alpha \overline{C}_p^\beta \exp\{-ip(x-x')\}, \quad (2.18)$$

where Φ_p is the state with the 4-momentum p. From a consideration of the relativistic invariance and the CP invariance, the general expression for $\sum C_p^\alpha \overline{C}_p^\beta$ (the summation is taken over all states with 4-momentum p) should have the form

$$(2\pi)^3 \sum_p C_p^\alpha \overline{C}_p^\beta = (\hat{p}_{\alpha\beta} + \delta_{\alpha\beta}\sqrt{p^2})\rho_1(p^2) - (\hat{p}\gamma_5)_{\alpha\beta}\rho_3(p^2) - \delta_{\alpha\beta}\rho_2(p^2) = \{(\hat{p}[1 - f(p^2)\gamma_5])_{\alpha\beta} + \delta_{\alpha\beta}\sqrt{p^2}\}\rho_1(p^2) - \delta_{\alpha\beta}\rho_2(p^2);$$

$$f(p^2) = \rho_3(p^2)/\rho_1(p^2), \quad (2.19)$$

where ρ_1, ρ_2, ρ_3 are real functions. Substituting (2.19) in (2.18), we obtain the general expression for the function $G^{(+)}$, and consequently, for the arbitrary Green's function:

$$G^{(\;)}(x) = \int_0^\infty \{[\hat{p}(1 - f(\varkappa^2)\gamma_5) + \varkappa]\rho_1(\varkappa^2) - \rho_2(\varkappa^2)\}\Delta^{(\;)}(x, \varkappa^2)\,d\varkappa^2; \quad (2.20)$$

Here $\Delta^{(\;)}(x, \kappa^2)$ are the vacuum functions for the boson field with mass κ.

In the momentum representation, Eq. (2.20) is written, for example, for the Feynman function, as

$$G_F(\hat{p}) = \int_0^\infty \frac{[\hat{p}(1 - f(\varkappa^2)\gamma_5) + \varkappa]\rho_1(\varkappa^2) - \rho_2(\varkappa^2)}{p^2 - \varkappa^2 + i\varepsilon}\,d\varkappa^2. \quad (2.21)$$

For the rest of the functions, the rule for bypassing the poles $p = \pm\kappa$ should be chosen in similar fashion.

The functions $f(\kappa^2)$, $\rho_1(\kappa^2)$, $\rho_2(\kappa^2)$ entering into (2.19) – (2.21) satisfy the inequalities

$$\rho_1(\varkappa^2) \geqslant 0,\ 0 \leqslant \rho_2(\varkappa^2) \leqslant 2\varkappa\rho_1(\varkappa^2),\ f^2(\varkappa^2) \leqslant 1. \quad (2.22)$$

The first of the inequalities (2.22) is obtained immediately after multiplying (2.19) by $(\gamma_4)_{\beta\alpha}$ and summing over α. In order to obtain the other inequalities, it suffices to compute the sum

$$\sum_\alpha h_\alpha h_\alpha^* = p_0\{\rho_1(p^2)(\alpha - p)^2 + p^2 x[x - 2f(p^2)] + 2\alpha\rho_2(p^2)\} \geqslant 0; \quad (2.23)$$

$$h_\alpha = \{\gamma_4[\hat{p}(1 + x\gamma_5) - \alpha]\}_{\alpha\gamma} C_p^\gamma, \quad (2.24)$$

x and α are arbitrary real numbers. The second inequality of (2.22) follows from (2.23) for $x = 0$ and $\alpha = \alpha_{\min} = (-\rho_2 + p\rho_1)/\rho_1$, while for

$\alpha = 0$, and $x = x_{\min} = f$, we obtain the third.[*]

A stable particle with physical mass m corresponds to the appearance of a δ function in $\rho_1(\kappa^2)$ $:\rho_1(\kappa^2) = \delta(\kappa^2 - m^2)$. Here, it must be true that $\rho_2(m^2) = 0$ and $f(m^2) = 0$. The latter condition follows from the fact that the operators entering into the determination of the vacuum functions are unrenormalized physical quantities which satisfy the Dirac equation (with physical mass m).

By means of the inequalities (2.22), we can now prove the inequality $|\lambda| \leq 1$ which is of interest to us. For this purpose, let us write down the expression for the Lagrangian (2.1) in unrenormalized functions

$$\begin{aligned} L = {} & Z_{2X}(1-\lambda_X^2)^{-1}\bar{\psi}_{XR}\,[\hat{p}(1-\lambda_X\gamma_5) - \sqrt{1-\lambda_X^2}\,m_{0X}]\,\psi_{XR} \\ & + Z_{2N}(1-\lambda_N^2)^{-1}\bar{\psi}_{NR}\,[\hat{p}(1-\lambda_N\gamma_5) - \sqrt{1-\lambda_N^2}\,m_{0N}]\,\psi_{NR} \\ & + Z_3\varphi_R^+(p^2-\mu_0^2)\varphi_R + Z_1 g\bar{\psi}_{XR}(A_X + B_X\gamma_5) \\ & \times(\alpha+\beta\gamma_5)(A_N+B_N\gamma_5)\,\psi_{NR}. \end{aligned} \tag{2.25}$$

The anticommutator of the ψ functions, taken at the same instant of time, will, in accord with (1.11), be equal to

$$\{\psi_{\alpha R}(\mathbf{r},\ t),\ \bar{\psi}_{\beta R}(\mathbf{r}',\ t)\} = Z_2^{-1}[\gamma_4(1-\lambda\gamma_5)]_{\alpha\beta}\,\delta(\mathbf{r}-\mathbf{r}') \tag{2.26}$$

(the index X or N is omitted). On the other hand, the expression

$$\{\psi_{\alpha R}(\mathbf{r},\ t),\ \bar{\psi}_{\beta R}(\mathbf{r}',\ t)\}$$

$$= \int_0^\infty [\gamma_4(1-f(\varkappa^2)\gamma_5)]_{\alpha\beta}\,\rho_1(\varkappa^2)\,d\varkappa^2\,\delta(\mathbf{r}-\mathbf{r}'). \tag{2.27}$$

follows from (2.20) for the same anticommutator.

Comparing (2.26) and (2.27), we have

$$Z_2^{-1} = \int_0^\infty \rho_1(\varkappa^2)\,d\varkappa^2;$$

$$Z_2^{-1}\lambda = \int_0^\infty f(\varkappa^2)\,\rho_1(\varkappa^2)\,d\varkappa^2, \tag{2.28}$$

$$\lambda = \int_0^\infty f(\varkappa^2)\,\rho_1(\varkappa^2)\,d\varkappa^2 \Big/ \int_0^\infty \rho_1(\varkappa^2)\,d\varkappa^2. \tag{2.29}$$

Since $\rho_1 \geq 0$ and has the component $\delta(\kappa^2 - m^2)$, then, as follows from (2.28), $Z_2^{-1} \geq 1$ and

$$0 \leqslant Z_2 \leqslant 1,$$

i.e., we obtain the usual inequality for Z_2. From (2.29) and the inequalities $\rho_1 \geq 0$ and $f^2 \leq 1$, it follows directly that

$$|\lambda| \leqslant 1.$$

The inequality $|\lambda| \leq 1$ is proved in general form and the renormalization of the δ functions (2.13) carried out above is justified in the same fashion.

Let us now sum up. Renormalization of the mass and charge in the case of a T-invariant parity-nonconserving interaction can be carried out in the same fashion as renormalization in the case of parity conservation. Here, the equation for the renormalized ψ functions in the case of free motion is the usual Dirac equation with physical mass. However the free Lagrangian (2.25) expressed in these ψ functions and the Poisson brackets (2.26) differ from the usual in the presence of terms which do not conserve parity.

3. THE ASYMPTOTIC FORM OF THE GREEN'S FUNCTION AND THE EFFECTIVE CHARGE IN A SERIES WITH WEAK PARITY-NONCONSERVING INTERACTION

For the investigation of the asymptotic behavior (at large p^2) of the Green's function in weak coupling theory, Landau[8] proposed to use the so-called "three-Γ approximation" in which all the terms of order $[g^2 \ln(p^2/m^2)]^n$ are kept in the equations for the Green's functions and the vertex part, while terms of the order $g^{2m}[\ln(p^2/m^2)]^n$ $(m > n)$ are discarded. Solution of such equations for the case of electrodynamics[8] and pseudoscalar theory[9,10] has led, however, to unfavorable results, inasmuch as the Green's functions that are obtained have nonphysical poles at a certain value $p^2 = p_{cr}^2$ and the three-Γ approximation proves inapplicable beyond the pole $(p^2 > p_{cr}^2)$ where the weak coupling becomes effectively strong. This result led Landau and Pomeranchuk[11-13] to conclude that the renormalized charged vanished, so that the theory was unsuitable.

It is to ascertain whether the difficulty that has been pointed out persists in the case of interactions that do not preserve parity, i.e., whether the solutions of the equations in the three-Γ approximation will contain nonphysical poles. By solving this equation, one will be able to test on a concrete example the method of renormalization set up above.

We choose a formal model, namely a scalar symmetric theory, in which both the fermions X and N have isotopic spin one-half, while the meson has isotopic spin one. We shall assume that the fermions enter into the interaction with two components of their wave functions, so that the Hamiltonian of the interaction is written as

---

[*] Interesting consequences may arise if $f(\kappa^2) \to \pm 1$ for $\kappa^2 \to \infty$. In this case, the general proof of Lehmann that the exact Green's functions should disappear as $p^2 \to \infty$ no more rapidly than the free ones will evidently not have adequate rigor in the analysis of the divergences, inasmuch as in the calculation of the polarization operator for parity conservation, the interaction of terms containing a higher divergence can vanish as a result of the renormalization of the operators $1 + f\gamma_5$ or $1 - f\gamma_5$ [see Eq. (3.20)].

$$H_I = g_0\bar{\psi}_X(1+\gamma_5)\tau_i\psi_N\varphi_i + g_0\bar{\psi}_N(1-\gamma_5)\tau_i\psi_X\varphi_i. \qquad (3.1)$$

Inasmuch as it is necessary for us to test our scheme of renormalization, we shall solve the corresponding set of equations directly, not using the renormalization group.[14,15] The set of equations for the Green's function and the vertex parts will have the form (see reference 10)

$$\{\hat{p} - m_0 + 3\frac{g_0^2}{4\pi^3 i}\int d^4k\,(1-\gamma_5)\,G_X(\hat{p}-\hat{k})$$
$$\times\Gamma^+(\hat{p}-\hat{k},\ \hat{p};\ \hat{k})\,D(k^2)\}\,G_N(\hat{p}) = 1, \qquad (3.2)$$

$$\{\hat{p} - m_0 + 3\frac{g_0^2}{4\pi^3 i}\int d^4k\,(1+\gamma_5)\,G_N(\hat{p}-\hat{k})$$
$$\times\Gamma^-(\hat{p}-\hat{k},\ \hat{p};\ \hat{k})\,D(k^2)\}\,G_X(\hat{p}) = 1, \qquad (3.2')$$

$$\{k^2 - \mu_0^2 - 2\frac{g_0^2}{4\pi^3 i}\int d^4p\,Sp\,[(1+\gamma_5)\,G_N(\hat{p})$$
$$\times\Gamma^-(\hat{p},\ \hat{p}+\hat{k};\ \hat{k})\,G_X(\hat{p}+\hat{k})]\}\,D(k^2) = 1, \qquad (3.3)$$

$$\Gamma^+(\hat{p},\ \hat{p}-\hat{k};\ -\hat{k}) = 1 + \gamma_5 + \frac{g_0^2}{4\pi^3 i}\int d^4q\,\Gamma^+(\hat{p},\ \hat{p}-\hat{q};-\hat{q})$$
$$\times G_N(\hat{p}-\hat{q})\,\Gamma^-(\hat{p}-\hat{q},\ \hat{p}-\hat{q}-\hat{k};\ -\hat{k})$$
$$\times G_X(\hat{p}-\hat{k}-\hat{q})\,\Gamma^+(\hat{p}-\hat{q}-\hat{k},\ \hat{p}-\hat{k};\ \hat{q})\,D(q^2), \qquad (3.4)$$

$$\Gamma^-(\hat{p},\ \hat{p}-\hat{k};\ -\hat{k}) = 1 - \gamma_5 + \frac{g_0^2}{4\pi^3 i}\int d^4q\,\Gamma^-(\hat{p},\ \hat{p}-\hat{q};\ -\hat{q})$$
$$\times G_X(\hat{p}-\hat{q})\,\Gamma^+(\hat{p}-\hat{q},\ \hat{p}-\hat{q}-\hat{k};\ -\hat{k})$$
$$\times G_N(\hat{p}-\hat{q}-\hat{k})\,\Gamma^-(\hat{p}-\hat{q}-\hat{k},\ \hat{p}-\hat{k};\ \hat{q})\,D(q^2). \qquad (3.4')$$

Here Γ^+ and Γ^- are vertex parts corresponding to the interaction $\bar{\psi}_X(1+\gamma_5)\tau_i\psi_N\varphi_i$, $\bar{\psi}_N(1-\gamma_5)\times\tau_i\psi_X\varphi_i$, m_0 and μ_0 are the bare masses (we consider the masses of N and X to be equal).

In the two-component theory, the exact vertex part Γ^+ should be proportional to $1+\gamma_5$, while Γ^- is proportional to $1-\gamma_5$:

$$\Gamma^+(\hat{p},\ \hat{p}-\hat{k};\ -\hat{k}) = (1+\gamma_5)\,s^+(\hat{p},\ \hat{p}-\hat{k};\ -\hat{k}),$$
$$\Gamma^-(\hat{p},\ \hat{p}-\hat{k};\ -\hat{k}) = (1-\gamma_5)\,s^-(\hat{p},\ \hat{p}-\hat{k};\ -\hat{k}), \qquad (3.5)$$

where s^+ and s^- are operators which do not contain the matrix γ_5 (but only $\hat{p}$ and $\hat{k}$). This proof follows directly from perturbation theory. In fact, any diagram for the vertex part Γ^+ contains the factor $1+\gamma_5$ in its left angle. Therefore, if the rest of the expression is written in the form

$$(1+\gamma_5)\,M + (1-\gamma_5)\,N,$$

where M, N are operators which do not contain γ_5, then the terms with N makes no contribution to Γ^+.

Being interested in the asymptotic behavior of the Green's functions, we can throw away terms with the mass and seek solutions of Eqs. (3.2) – (3.4′) in the form[8-10]

$$G_N(\hat{p}) = (\hat{p}/p^2)\,[1 + f_N(p^2)\,\gamma_5]\,F_N(p^2),$$
$$G_X(\hat{p}) = (\hat{p}/p^2)\,[1 + f_X(p^2)\,\gamma_5]\,F_X(p^2), \qquad D(k^2) = \varphi(k^2)/k^2,$$
$$s^{\pm}(\hat{p}-\hat{k},\ \hat{p};\ -\hat{k}) = s_0^{\pm}\,[(p-k)^2,\ p^2,\ k^2]$$
$$-\ \hat{k}\hat{p}/(k^2+p^2)\,s_1^{\pm}[(p-k)^2,\ p^2,\ k^2]; \qquad (3.6)$$

we consider the functions $F_N(p^2)$, $F_X(p^2)$, $\varphi(k^2)$, s_0, s_1 to be slowly changing functions of their arguments.

If we set $f_N = -f_X \equiv f$, $s^+ = s^- \equiv s$, $F_N = F_X \equiv F$, then Eqs. (3.2′) and (3.4′) coincide with Eqs. (3.2) and (3.4), respectively. Thus, it is necessary to solve the following set of equations:

$$\Big\{\hat{p} + 6\,\frac{g_0^2}{4\pi^3 i}\,(1-\gamma_5)\int\frac{d^4k}{k^2}\,[1 - f((p-k)^2)]\,\frac{\hat{p}-\hat{k}}{(p-k)^2}$$
$$\times F\,[(p-k)^2]\,s(\hat{p}-\hat{k},\ \hat{p};\ \hat{k})\,\varphi(k^2)\}$$
$$\times(\hat{p}/p^2)\,[1 + \gamma_5 f(p^2)]\,F(p^2) = 1, \qquad (3.7)$$

$$\Big\{k^2 - 4\,\frac{g_0^2}{4\pi^3 i}\int\frac{d^4p}{p^2}\,[1 - f(p^2)]\,F(p^2)$$
$$\times[1 - f((p+k)^2)]\,F((p+k)^2)$$
$$\times\,\mathrm{Sp}\,[\hat{p}s(\hat{p},\ \hat{p}+\hat{k};\ \hat{k})\,(\hat{p}+\hat{k})/(p+k)^2]\}\,\varphi(k^2)/k^2 = 1, \qquad (3.8)$$

$$s(\hat{p},\ \hat{p}-\hat{k};\ \hat{k}) = 1 + 4\,\frac{g_0^2}{4\pi^3 i}\int\frac{d^4q}{q^2}\,\frac{\hat{p}-\hat{q}}{(p-q)^2}\,\frac{\hat{p}-\hat{q}-\hat{k}}{(p-q-k)^2}$$
$$\times[1 - f((p-q)^2)]\,[1 - f((p-q-k)^2)$$
$$\times F((p-q)^2)\,F((p-q-k)^2)\,s(\hat{p},\ \hat{p}-\hat{q};\ -\hat{q})$$
$$\times\,s(\hat{p}-\hat{q},\ \hat{p}-\hat{q}-\hat{k};\ -\hat{k})$$
$$\times\,s(\hat{p}-\hat{q}-\hat{k},\ \hat{p}-\hat{k};\ \hat{q})\,\varphi(q^2). \qquad (3.9)$$

Multiplying (3.7) by $1-\gamma_5$ and $1+\gamma_5$, successively, we can convert this equation to a set of two equations

$$\Big\{\hat{p} + 12\,\frac{g_0^2}{4\pi^3 i}\int\frac{d^4k}{k^2}\,\frac{\hat{p}-\hat{k}}{(p-k)^2}\,[1 - f((p-k)^2)]\,F((p-k)^2)$$
$$\times\,s(\hat{p}-\hat{k},\ \hat{p};\ \hat{k})\,\varphi(k^2)\Big\}\,(\hat{p}/p^2)\,[1 - f(p^2)]\,F(p^2) = 1, \qquad (3.10)$$

$$[1 + f(p^2)]\,F(p^2) = 1. \qquad (3.11)$$

Comparing Eqs. (3.8) – (3.10) with the corresponding equations in scalar theory with parity conservation,* it is easy to ascertain that, except for the difference in the coefficients for g_0^2, the only change arising as a result of parity nonconservation reduces to the appearance of the function $[1-f(p^2)]F(p^2)$ in place of the function $F(p^2)$. Therefore, all the discussions carried out previously[9,10] remain valid, and we can immediately write down the set of differential equations for the functions $\Phi(p^2) = [1-f(p^2)]F(p^2)$, $\varphi(p^2)$ and $s_0(p^2)$ (which are analogous to Eqs. (50) – (52) of reference 10):

---

*The equations in scalar theory (for large p^2) have the same form and the same values of the coefficients as in the equations of pseudoscalar theory. Therefore, we can, for example, compare (3.8) – (3.10) with the corresponding formulas of the work of Galanin and others.[10]

$$\begin{aligned} d\Phi(\xi)/d\xi &= 6\varkappa s_0^2(\xi)\Phi^3(\xi)\varphi(\xi), \\ d\varphi(\xi)/d\xi &= 8\varkappa s_0^2(\xi)\Phi^2(\xi)\varphi^2(\xi), \\ ds_0(\xi)/d\xi &= -4\varkappa s_0^3(\xi)\Phi^2(\xi)\varphi(\xi). \end{aligned} \tag{3.12}$$

Here $\kappa = g_0^2/4\pi$; $\xi = \ln(p^2/\Lambda^2)$, Λ is the cutoff momentum; we shall consider Φ, φ and s_0 to be unrenormalized. The values of the coefficients on the right-hand side of (3.12) are changed in comparison with the coefficients in Eqs. (50) – (52) of reference 10 in correspondence with the change of coefficients in the formulas for G, Γ, and D (there is an additional factor of four in the formulas for G and Γ, and of two in the formula for D). Solutions of Eqs. (3.12) corresponding to the initial conditions for $\xi = 0$, $\Phi = \varphi = s_0 = 1$ have the form

$$\Phi(\xi) = Q^{-1/2}, \quad \varphi(\xi) = Q^{-2/3}, \quad s_0(\xi) = Q^{1/3}, \qquad Q = 1 - 12\varkappa\xi. \tag{3.13}$$

The functions $F(\xi)$ and $f(\xi)$ can be found from (3.13) and (3.11), and are seen to be equal to

$$F = (1 + Q^{1/2})/2Q^{1/2}, \qquad f = (Q^{1/2} - 1)/(Q^{1/2} + 1). \tag{3.14}$$

In order to carry out charge renormalization on the basis of Eq. (2.14′), it is necessary to express the values of Z_1, Z_2, Z_3 and λ in terms of the values of the functions F, φ, s_0, s. From the renormalization conditions for the functions $\varphi(\xi)$ and $s_0(\xi)$ we have $\varphi = Z_3\varphi_R$, $s_0 = Z_1^{-1}s_{0R}$ and the relations

$$Z_3 = \varphi(\mu^2/\Lambda^2) \approx Q_\Lambda^{2/3}, \qquad Z_1^{-1} = s_0(m^2/\Lambda^2) = Q_\Lambda^{-1/3}, \qquad Q_\Lambda^{-1} = 1 + 12(g_0^2/4\pi)\ln(\Lambda^2/m^2). \tag{3.15}$$

In order to express Z_2 and λ in terms of F and f, we write the equation for the Green's function of the N particle in the form (2.7) in the vicinity of $p^2 = m^2$:

$$Z_2^{-1}\hat{p}(1 + \lambda\gamma_5)(\hat{p}/p^2)[1 + f(m^2/\Lambda^2)\gamma_5]F(m^2/\Lambda^2) = 1. \tag{3.16}$$

We then find

$$\lambda = f(m^2/\Lambda^2),$$

$$\begin{aligned} Z_2 &= F(m^2/\Lambda^2)(1 - \lambda^2) \\ &= F(m^2/\Lambda^2)[1 - f^2(m^2/\Lambda^2)] = 1 - f(m^2/\Lambda^2), \end{aligned} \tag{3.17}$$

and Eq. (2.14′) for the coupling between the bare and the renormalized charges takes the form

$$\begin{aligned} g^2 &= g_0^2 Z_1^{-2} Z_2^2 Z_3 (1 + \lambda)^2 \\ &= g_0^2 s_0^2\left(\frac{m^2}{\Lambda^2}\right) F^2\left(\frac{m^2}{\Lambda^2}\right)\varphi\left(\frac{m^2}{\Lambda^2}\right)\left[1 - f^2\left(\frac{m^2}{\Lambda^2}\right)\right] \\ &= g_0^2 s_0^2\left(\frac{m^2}{\Lambda^2}\right)\Phi^2\left(\frac{m^2}{\Lambda^2}\right)\varphi\left(\frac{m^2}{\Lambda^2}\right). \end{aligned} \tag{3.18}$$

Substituting (3.13) in (3.16), we have

$$g^2 = g_0^2\,[1 + 3(g_0^2/\pi)\ln(\Lambda^2/m^2)]^{-1}. \tag{3.19}$$

The renormalized functions are expressed in terms of the experimental charge in the following fashion:

$$\begin{aligned} &\Phi_R = Q_\Lambda^{-1/2}\Phi = Q_R^{-1/2}, \qquad \varphi_R = Q_R^{-2/3}, \qquad s_{0R} = Q_R^{1/3}, \\ &G_{NR} = \frac{\hat{p}}{p^2}\,\frac{F(p^2)}{F(m^2)}\,[1 - f(p^2)\lambda + (f - \lambda)\gamma_5]\,\frac{1}{1-\lambda^2} \\ &\qquad = \frac{\hat{p}}{p^2}\,\frac{1}{2}\,Q_R^{-1/2}[1 + Q_R^{1/2} - \gamma_5(1 - Q_R^{1/2})], \\ &\frac{F(p^2)}{F(m^2)} = \frac{Q_\Lambda^{1/2} + Q_R^{1/2}}{(Q_\Lambda^{1/2} + 1)\,Q_R^{1/2}}, \qquad f(p^2) = -\frac{Q_\Lambda^{1/2} - Q_R^{1/2}}{Q_\Lambda^{1/2} + Q_R^{1/2}}, \\ &\lambda = -\frac{Q_\Lambda^{1/2} - 1}{Q_\Lambda^{1/2} + 1}, \\ &Q = Q_R/Q_\Lambda, \qquad Q_R = 1 - 12(g^2/4\pi)\ln(p^2/m^2), \\ &Q_\Lambda = 1 - 12(g^2/4\pi)\ln(\Lambda^2/m^2). \end{aligned} \tag{3.20}$$

It is not difficult to see that f and λ actually satisfy the conditions $f^2 \leq 1$, $\lambda^2 \leq 1$. The value of the cutoff limit comes from the expression for the renormalized G, Γ, D. In the same way, we have shown that one can systematically and without contradiction carry out the renormalization in the three-Γ approximation in the theory with parity nonconservation.

We shall now analyze the results obtained. First of all, it is evident that the difficulty from the vanishing of the renormalized charge remains in the theory under consideration with parity nonconservation: the renormalized Green's functions have a nonphysical singularity. However, if it can be so expressed, the situation becomes more favorable. The fact is that if we denote the coefficients on the right side of Eqs. (3.12) by a, b and c, respectively, then the presence or absence of a nonphysical pole will be determined by the sign of the quantity $2(a+c)+b$ (there is no pole for $2(a+c)+b<0$). According to the theorem of Lehmann, a and b must be positive. Therefore, the only possibility of removal of the pole is connected with the presence of a large negative coefficient c. In pseudoscalar symmetrical theory with parity conservation, $a = 3/2$, $b = 4$, $c = -1$. Introduction of parity nonconservation changes the coefficients and they become equal to $a = 6$, $b = 8$, $c = -4$, i.e., the coefficients a and c increase by a factor of four while b increases by only a factor of two. Thus consideration of parity nonconservation increases the relative role of the coefficient c.

We note that the introduction of additional fields can improve the situation materially. Thus, for example, if we assume the presence of a scalar meson χ with isotopic spin 0 in addition to the pseudoscalar meson π with isotopic spin 1, then in parity nonconservation the corresponding coefficients are shown to be $a = 2$, $b_\pi = b_\chi = 4$, $c_\pi = c_\chi = -2$ and the value of $2(a + c_\pi) + b_\pi$, or of what is equal to it, $2(a + b_\chi) + c_\chi$ approaches 0 even more closely.

The author is grateful to I. Ya. Pomeranchuk, A. D. Galanin, and G. M. Gandel'man for useful discussions.

---

[1] B. d'Espagnat and J. Prentki, Nuovo cimento **6**, 1129 (1957).

[2] K. Sekine, Nuovo cimento **11**, 87 (1959).

[3] Galanin, Ioffe, and Pomeranchuk, Dokl. Akad. Nauk SSSR **98**, 361 (1954).

[4] F. J. Dyson, Phys. Rev. **75**, 1736 (1949).

[5] A. Salam, Phys. Rev. **82**, 217 (1951).

[6] J. C. Ward, Proc. Phys. Soc. (London) **64**, 54 (1951).

[7] H. Lehmann, Nuovo cimento **11**, 342 (1954).

[8] Landau, Abrikosov, and Khalatnikov, Dokl. Akad. Nauk SSSR **95**, 497, 773, 1177; **96**, 261 (1954).

[9] Abrikosov, Galanin, and Khalatnikov, Dokl. Akad. Nauk SSSR **97**, 793 (1954).

[10] Galanin, Ioffe, and Pomeranchuk, JETP **29**, 51 (1955), Soviet Phys. JETP **2**, 37 (1956).

[11] L. D. Landau and I. Ya. Pomeranchuk, Dokl. Akad. Nauk SSSR **102**, 489 (1955).

[12] I. Ya. Pomeranchuk, Dokl. Akad. Nauk SSSR **103**, 1001 (1955); **104**, 51 (1955); **105**, 461 (1955); JETP **29**, 869 (1955), Soviet Phys. JETP **2**, 739 (1956).

[13] Pomeranchuk, Sudakov, and Ter-Martirosyan, Phys. Rev. **103**, 784 (1956).

[14] N. N. Bogolyubov and D. V. Shirkov, JETP **30**, 77 (1956), Soviet Phys. JETP **3**, 57 (1956).

[15] V. V. Sudakov, JETP **31**, 729 (1956), Soviet Phys. JETP **4**, 616 (1957).

Translated by R. T. Beyer
241

SOVIET PHYSICS JETP VOLUME 11, NUMBER 4 OCTOBER, 1960

DISTRIBUTION OF THE TRANSVERSE MOMENTUM OF SHOWER PARTICLES IN JETS

É. G. BOOS and Zh. S. TAKIBAEV

Institute of Nuclear Physics, Academy of Sciences, Kazakh S.S.R.

Submitted to JETP editor November 6, 1959

J. Exptl. Theoret. Phys. (U.S.S.R.) 38, 1276-1284 (April, 1960)

Experimental data are presented on the distribution of the transverse momenta of secondary shower particles in jets produced by cosmic rays. Transverse momentum distributions that follow from various theories and also from various phenomenological descriptions of multiple production of mesons are analyzed and systematized. Comparison with the experiments narrows the possible choice of a scheme for description of the elementary process of multiple meson production.

THE theoretical formulas for the transverse-momentum distribution of mesons p⊥, calculated in an arbitary system of coordinates, can be readily compared with the experimental data obtained in the laboratory system (l.s.). However, good agreement between the p⊥ distribution with the experimental distribution is a necessary but insufficient condition for the correctness of a theoretical description, since it reflects simultaneously the angle and energy distributions of the generated particles. It is found, as follows from the analysis below, that the distribution of the transverse momenta becomes in many cases insensitive to the choice of different versions of the theory.

1. TRANSVERSE MOMENTUM DISTRIBUTION RESULTING FROM DIFFERENT VERSIONS OF THE THEORETICAL AND PHENOMENOLOGICAL DESCRIPTION OF MULTIPLE MESON PRODUCTION

a) One of the first theories of multiple production of mesons is the Heisenberg field theory,[1] based on the use of the nonlinear Lagrangian interaction. The energy spectrum ($\sim d\epsilon'/\epsilon'^2$) of the generated mesons in the center-of-mass system (c.m.s.), resulting from this theory, was experimentally confirmed by shower analysis.[2-9] The anisotropy in the angular distribution of the mesons generated at large energies (10^{11} ev) was explained by Heisenberg qualitatively by using the uncertainty principle. In a direction perpendicular to the motion of the colliding nucleons, the dimension of the generation region is $\hbar/\mu_\pi$, and consequently, $p_\perp \sim 1$.* In this case the mesons with momentum $p \gg \mu_\pi$ are scattered within an angle

$$\theta' \sim p_\perp / p \sim 1/p.$$

As the energy increases, the degree of angular anisotropy of the generated particles increases. Later on, Symanzik* chose a function that reflects this law, and used this function to calculate the angular distribution in the laboratory system for the so-called "maximum-anisotropy" case.[10]

In the present paper we calculate the meson transverse-momentum distribution both in the "maximum anisotropy" assumption and in the assumption of angular isotropy in the c.m.s. The corresponding curves are shown in Fig. 1; the pertinent equations are

$$\frac{dN}{N dp_\perp} = \frac{3p_\perp}{(p_\perp^2+1)^{5/2}}, \quad \frac{dN}{N dp_\perp} = \frac{p_\perp}{(p_\perp^2+1)^{3/2}}; \tag{1}$$

$N^{-1} dN/dp_\perp$ is the relative differential intensity of the generated mesons.

b) In the Landau hydrodynamic theory[11] the c.m.s. energy of the generated mesons is uniquely related with the angle θ' between the directions of motion of the center of mass and of the primary particle. Assuming that all the secondary particles are pions, we can obtain the transverse-momentum distribution in the following parametric form:

$$\frac{dN}{N dp_\perp} = \frac{C_2}{4C_1} \frac{\mu_\pi}{M} \frac{\exp[-L/3 + 2\sqrt{L^2-\lambda^2}/3]\,(1+e^{-2\lambda})^2}{2e^{-2\lambda} - \lambda[1+\exp(-2\lambda)]/3\sqrt{L^2-\lambda^2}},$$

$$p_\perp = 2\frac{C_1 M}{\mu_\pi} \frac{\exp[-L/6 + \sqrt{L^2-\lambda^2}/3]}{1+\exp(-2\lambda)}, \qquad \lambda < \left|\frac{\sqrt{3}}{2} L\right|, \tag{2}$$

$L = \ln \gamma_C$; γ_C is the c.m.s. Lorentz factor (nucleon-nucleon collision is assumed); C_1 and C_2 are constants of order unity, determined from the Landau

---

*The transverse momentum $p_\perp$ of the particles is measured in units of pion rest mass.

*We are very grateful to Mr. Symanzik for sending us the unpublished manuscript containing this calculation.

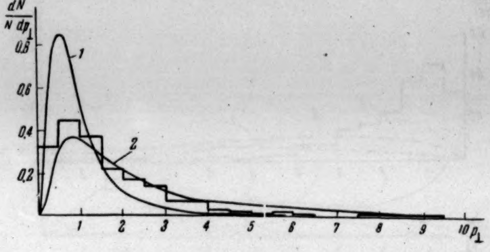

FIG. 1. Transverse-momentum distributions of the mesons according to Heisenberg's theory,[1,10] and the experimental distribution. Curves 1 and 2 are obtained under the assumption of maximum anistropy,[10] and isotropy of the angular distribution in the c.m.s., respectively.

integral conditions;[11] M is the nucleon mass.

The corresponding distributions for $\gamma_c = 20$ and 100 are given in Fig. 2 (curves 1 and 2). It follows from the form of the distribution that the majority of the particles have $p_\perp \gtrsim M/\mu_\pi$. Such a result does not agree with experiment.

Milekhin and Rozental'[12] have interpreted the occurence of so large transverse momenta as the consequence of the second stage of the expansion of an ideal liquid — conical scattering. They calculated the distribution of the transverse momentum of the generated mesons, starting with the assumption that such a distribution is determined exclusively by thermal motion in a one-dimensional relativistic current of a nucleonic liquid (see reference 13). The use of a Bose distribution for the pions and its integration over the longitudinal components[12] of the momentum $p_\parallel$ makes the distribution of the mesons over $p_\perp$ depend on the critical temperature T_c at which the system begins to disintegrate. The corresponding distribution* for different values of the parameter $T_c/\mu_\pi = 1/3$, $1/2$, 1, and 1.5 is shown in Fig. 2 (curves 3 — 6).

In a three-dimensional version of hydrodynamic theory,[14] Milekhin has shown that the transverse hydrodynamic velocity is much smaller than the thermal velocity. Therefore the transverse-momentum distribution of the generated mesons coincides with that obtained earlier.[12] (The disintegration temperature of the system is assumed to be $1\mu_\pi$.)

c) It is interesting to examine also the statistical theory, first employed by Fermi[15] to explain the Schein stars. At large energies, the thermodynamic approximation is applicable. Using Eq. (45) of reference 15 for the number of mesons dN generated in a phase-space element $d\tau$ we obtain a transverse-momentum distribution

$$N^{-1}dN/dp_\perp = \frac{\gamma^3 p_\perp^2}{af(\rho)} \int_{-1}^{+1} (1-y^2)\,dy \int_{-1}^{+1} (1-\eta^2)^{-3/2} \times \left\{ \exp\left[\frac{\gamma p_\perp}{(1-\eta^2)^{1/2}} (1-\rho\eta y) \right] - 1 \right\}^{-1} d\eta,$$

$$f(\rho) = \left[\frac{1+\rho^2}{\rho^3} \ln \frac{1+\rho}{1-\rho} - \frac{2}{\rho^2} \right], \tag{3}$$

where $a = 2.413$ and ρ is the nucleon collision parameter.* Calculations based on (3) were made[15] at an average value $\bar{\rho} = 0.959$.[15] The quantity $\gamma = \mu_\pi/T$ is expressed in terms of the energy of the colliding nucleons. Since $\gamma_c \lesssim 100$ for most of the compared showers, we have assumed, following Fermi, that equilibrium takes place only for the

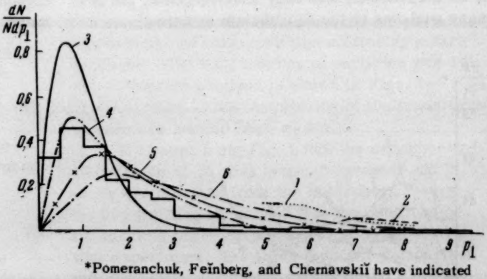

FIG. 2. Transverse-momentum distributions according to Landau's hydrodynamic theory.[11] Curves 1 and 2 are obtained for values of the Lorentz factor $\gamma_c = 20$ and 100. Curves 3 to 6 are obtained in the one-dimensional version[12,14] for various disintegration temperatures: $T_c/\mu_\pi = 1/3$, $1/2$, and 1.5.

---

*We choose a system of units in which the Boltzmann constant and the velocity of light are equal to unity.

*Pomeranchuk, Feĭnberg, and Chernavskiĭ have indicated the difficulties connected in this theory with the choice of the meson-production volume and the introduction of the impact parameter.[16]

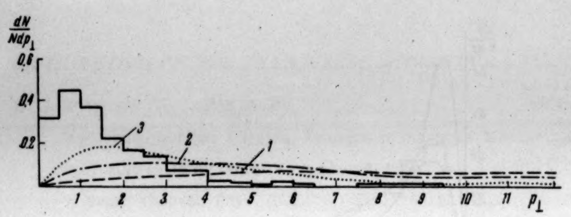

FIG. 3. Transverse-momentum distributions obtained from Fermi's theory,[15] taking account of the angular momentum in the c.m.s. Curves 1, 2, and 3 correspond to values $\alpha\gamma_c(\gamma_c - 1) = 100$, 10 and 0.5.

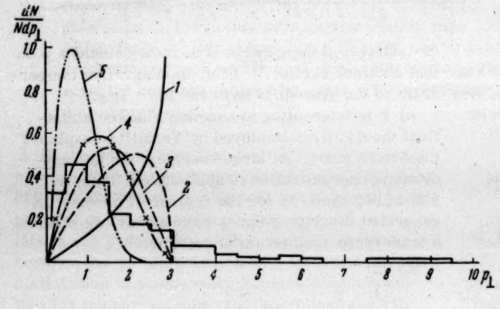

FIG. 4. Transverse-momentum distributions obtained under the assumption that the generated mesons are monoenergetic ($p_0 = 3$) in the c.m.s. Curves 1 to 5 correspond to various degrees of anisotropy: n = 0, 1, 2, 3, and 10.

pion gas; in other words, we have neglected the possible production of heavy particles.

Using the expression[15] for the energy density ξ, we can write for the energy balance

$$\frac{4}{3}\pi\frac{\hbar^3}{\mu_\pi^3}\frac{1}{\gamma_c}\xi = 2M\alpha(\gamma_c - 1), \tag{4}$$

hence

$$\gamma = [\pi\alpha\gamma_c(\gamma_c - 1)]^{-1/4}. \tag{5}$$

The quantity α can be treated in Eq. (4) either as the factor by which the production volume is increased[16]

$$\Omega = \Omega_1/\alpha \qquad (\Omega_1 \approx \hbar^3/\mu_\pi^3\gamma_c),$$

or as the fraction of energy transferred by the primary nucleons to the equilibrium system.[17]

The distributions shown in Fig. 3 have been obtained by numerically integrating (3) for $\alpha(\gamma_c - 1)\gamma_c = 100$, 10, and 0.5.

It is appropriate to note here that the choice of the form of the phase volume is important in the calculation of the distribution over the transverse momenta, and incidentally also in the calculation of the angular distribution and the total number of particles. Various qualitative models frequently encountered in the literature make use of the assumption that the mesons are monoenergetic. Let us see how this assumption influences the distribution over the transverse momenta at different degrees of angular anisotropy in the system of meson emission [this may be both the center of mass, as well as the system connected with each

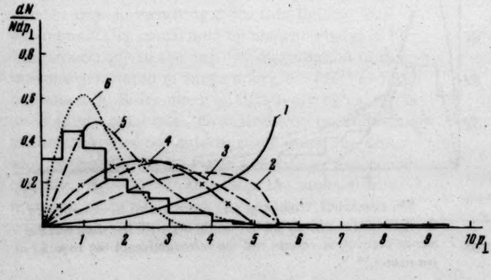

FIG. 5. Transverse-momentum distributions obtained under the assumption that the mesons are monoenergetic ($p_0 = 5.7$). Curves 1 to 6 correspond to n = 0, 1, 2, 3, 10, and 16.

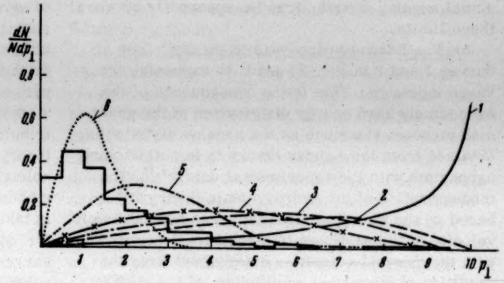

FIG. 6. Transverse-momentum distributions obtained under the assumption that the mesons are monoenergetic ($p_0 = 10$). Curves 1 to 6 correspond to n = 0, 1, 2, 3, 10, and 50.

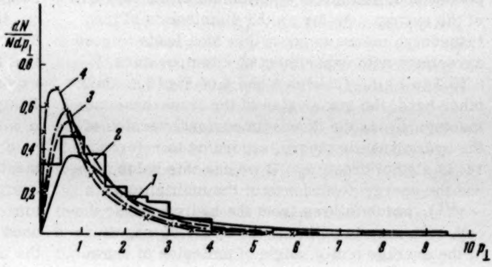

FIG. 7. Transverse-momentum distribution of the mesons obtained under the assumption of angular anisotropy ($\sim\cos^{2n}\theta'$) and of an energy spectrum from Heisenberg's theory.[1] Curves 1 to 4 correspond to n = 0, 1, 2, and 3. The histogram is the same as in the preceding figures.

of the meson emission centers (fire ball).[18-20] If the angular distribution is approximated by the function $\cos^{2n}\theta'$, the distribution by transverse momenta will have the form

$$\frac{dN}{Ndp_\perp} = (2n+1)\left(1-\frac{p_\perp^2}{p_0^2}\right)^{n-1/2}\frac{p_\perp}{p_0^2}, \qquad 0 \leqslant p_\perp \leqslant p_0, \qquad (6)$$

where p_0 is the proposed value of the meson momentum. The calculation was made for different values of n and p_0, and more will be said below regarding the specific choice of p_0. Results of the calculations are illustrated in Figs. 4 – 6.

d) In conclusion, let us consider the frequently encountered version of the theory,[21-22] in which the Heisenberg energy spectrum is combined with an isotropic angular distribution. In the center-of-mass system, such a distribution has the form

$$dN = C\frac{p^2dp}{(1+p^2)^2}\cos^{2n}\theta' d\Omega, \qquad d\Omega = -d\cos\theta'. \qquad (7)$$

Making the substitution $p = p_\perp/\sin\theta'$ and integrating over the angles, we arrive at a transverse-momentum distribution dependent on n:

$$\frac{dN}{Ndp_\perp} = 3\frac{p_\perp\left(\sqrt{1+p_\perp^2}-p_\perp\right)}{\sqrt{1+p_\perp^2}\,\left((1+p_\perp^2)^{1/2}+p_\perp\right)}, \qquad n=1, \qquad (8)$$

$$\frac{dN}{Ndp_\perp} = 5\frac{p_\perp\left(\sqrt{1+p_\perp^2}-p_\perp\right)}{\left(\sqrt{1+p_\perp^2}+p_\perp\right)}, \qquad n=2, \qquad (9)$$

$$\frac{dN}{Ndp_\perp} = \frac{7}{4}\frac{p_\perp\left(p_\perp+4\sqrt{p_\perp^2+1}\right)}{\left(p_\perp+\sqrt{1+p_\perp^2}\right)^4}, \qquad n=3. \qquad (10)$$

The corresponding distributions for different values of n are shown in Fig. 7.

2. COMPARISON WITH EXPERIMENTAL DATA

The experimental distribution of the transverse momenta of the generated particles was obtained from showers registered in emulsions.[2-6,23,24] We selected stars with energies $E > 10^{11}$ ev, which can be considered with high degree of probability, as being produced in nucleon-nucleon collisions. The momentum of the secondary shower particles was determined from multiple-scattering measurements. The total number of particles was 161. The histogram obtained is shown in Figs. 1–7. The maximum in the distribution of the transverse momenta is located near $p_\perp = 1$.

a) It is seen from Fig. 1 that the experimental distribution of $p_\perp$ lies between curves 1 and 2, which are obtained from the Heisenberg theory for two limiting cases, and that the positions of the maxima of the curves are in good agreement with experiment. It follows from the comparison that the assumed limiting values of the c.m.s. angular distribution of the mesons are correct. The actual angular distributions lie apparently between these limits.

b) The Landau hydrodynamic theory[11] (see curves 1 and 2 in Fig. 2) leads to excessive transverse momenta. This is the consequence of the exceedingly hard energy distribution of the generated mesons, inasmuch as the angular distribution obtained from the Landau theory is in satisfactory agreement with the experimental data.[3,4,18] The modernization of the hydrodynamic theory[12,13] is based on the idea that the transverse hydrodynamic velocity of the particles is insignificant compared with the thermal velocities determined from the condition of statistical equilibrium of the elements of the system. As far as the distribution of the transverse momenta goes, this idea leads to good agreement with experiment at a temperature $T_c = (0.5 \text{ to } 1)\,\mu_\pi$ (curves 5 and 6 of Fig. 2). On the other hand, the mean value of the transverse momentum $\overline{p}_\perp$ in the three-dimensional version of the hydrodynamic theory, according to reference 14, is also of order μ_π. If we use this value of $\overline{p}_\perp$ and the energy dependence of the multiplicity ($n \sim \gamma_c^{1/2}$), which follows from the hydrodynamic theory, it is easy to estimate the order of magnitude of the average c.m.s. angle of emission of shower particles, $\overline{\theta}'$:

$$n \sim \gamma_c^{1/2}, \qquad \overline{p} \sim M\gamma_c^{1/2}, \qquad \overline{\theta}' \sim \overline{p}_\perp/\overline{p} \sim (\mu_\pi/M)\,\gamma_c^{-1/2}.$$

The value of $\overline{\theta}'$ estimated in this manner is much less than the average value of the angle ($\sim 2\sqrt{2/\pi L}$), estimated from the angular distribution given in the paper by Milekhin.[14] This lack of agreement may indicate that in the three-dimensional version of the hydrodynamic theory[14] it is either necessary to forego the dependence $n \sim \gamma_c^{1/2}$, or the order of magnitude claimed for the transverse momentum is incorrect.

c) From a comparison of the experimental distribution with the curves calculated from the Fermi theory (see Fig. 3), it follows that for no reasonable values of the quantity $\alpha\gamma_c(\gamma_c - 1)$ is agreement with experiment reached. If the quantity α is taken to mean an inelasticity coefficient, then for $\gamma_c = 10$ the values of α corresponding to curves 1, 2, and 3 of Fig. 3 are 1, 0.1, and 0.05, respectively. It is easy to see that with increasing γ_c the discrepancy with experiment increases. The quantity α can be estimated by stipulating that the energy spectrum of the theory agree with experiment. This calculation, carried out by Baktybaev for the showers considered, yields $\alpha \simeq 0.01$.

d) The distribution over the transverse momenta corresponding to the assumption of monoenergetic generated mesons contains the momentum p_0 as a parameter. In the calculations we used a quantity p_0, equal to the average value of the meson momentum. This value depends on the system of coordinates in which the analysis is made. For the center-of-mass system and the excited-volume systems, respectively,[19,20] the values obtained for p_0 were 5.7 and 3 (Figs. 4 and 5).

Inasmuch as values of $p_\perp$ up to 10 are seen on the histogram, we decided to plot these curves for $p_0 = 10$ (Fig. 6).

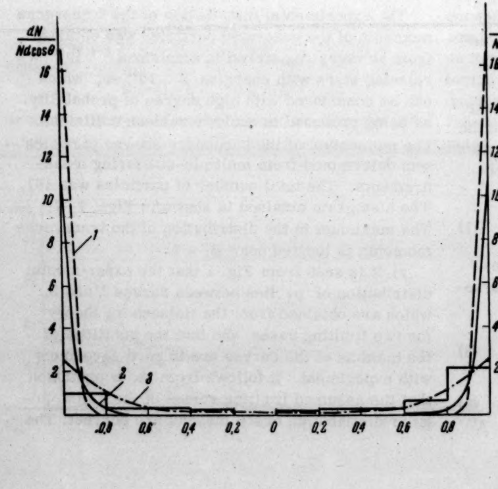

FIG. 8. Histogram of the angular distribution of the particles in the c.m.s., and differential angular distributions obtained under the assumption of an angular anisotropy $\sim\cos^{2n}\theta'$. Curves 1, 2, and 3 correspond to n = 16, 10, and 2.

A monoenergetic and isotropic meson distribution $(n = 0)$ leads to a transverse-momentum distribution (curves 1 of Figs. 4, 5, and 6) which does not agree at all with the experimental data. It follows from Fig. 4 that for no value of n do the curves agree with the histogram of the distribution of transverse momenta. A considerable fraction $(\sim 15\%)$ of the particles has a value $p_\perp > 3$. For large values of p_0, agreement with experiment is reached only for $n > 10$ (when $p_0 = 5.7$ and 10, and accordingly when $n = 16$ and 50).

Figure 8 shows the histogram of the overall c.m.s. angular distribution of the shower particles.[2-4,6,9,23] The ordinates are the relative differential meson densities, $N^{-1}\,dN/d\cos\theta'$, as functions of $\cos\theta'$. Curves 1 to 3 correspond to $n = 16$, 10, and 2.

From a comparison of Figs. 5, 6, and 8 it follows that the values $n > 10$ lead to a sharp angular anisotropy, which does not agree with the observed c.m.s. angular distribution. Thus, the assumption that the generated mesons are monoenergetic does not lead, for an anisotropic angular distribution $(\sim \cos^{2n}\theta')$, to an agreement between the distribution over $p_\perp$ and the experimental distribution.

e) The distribution of the transverse meson momenta obtained by assuming an anisotropic angular distribution $(\sim \cos^{2n}\theta')$ and an energy spectrum from the Heisenberg theory, is compared with the histogram on Fig. 7. Unlike the preceding case, the curves agree with the experimental distribution for considerably lower values of n, which is in agreement with the c.m.s. angular distribution of the mesons, shown in Fig. 8.

CONCLUSION

A comparison between different versions of the theory and experiment leads to the following conclusions:

1) It is impossible to explain the observed distribution of the transverse momenta by assuming the generated mesons to be monoenergetic, since a condition of sharp anistropy is imposed on the angular distribution. It is natural to assume that the anisotropy in the angular distribution of the mesons is greater than in the c.m.s. than in the system of excited volumes. A direct comparison with the experimental c.m.s. angular distribution shows that the experimental angular distribution is much less anisotropic even in this system. This contradiction disappears if it is assumed that the energy spectrum of the generated mesons is similar to the spectrum that follows from the Heisenberg theory.[1]

2) The Landau hydrodynamic theory[11] shifts the distribution of $p_\perp$ towards the larger transverse momenta, owing to the exceedingly hard energy spectrum predicted by this theory for the generated mesons. In the revised version of the theory,[14] as in the one-dimensional version,[12] the distribution of the transverse momenta is in good agreement with experiment, but it does not follow from the hydrodynamics, and is introduced by superposing the thermal motion of the particles on the hydrodynamic motion, which is assumed to be less developed in the transverse direction.

3) The Fermi theory[15] in the thermodynamic approximation leads to a distribution of transverse momenta which does not agree with experiment.

4) In the Heisenberg theory[1,10] the distribution over the transverse momenta is in satisfactory agreement with experiment. The generated-particle energy spectrum derived from this theory has found experimental verification.[2-9] The angular distribution does not follow directly from the theory, but is qualitatively explained by Heisenberg, starting with a correct representation of the order of magnitude of the mean transverse momenta. The c.m.s. angular distribution function, introduced by Symanzik on the basis of these representations, is confirmed both by the distribution over $p_\perp$ and by direct comparison[3,4,25] with experiment.

5) Analysis shows that distribution of the transverse momenta of the generated particles is described satisfactorily both by the hydrodynamic theory, in which only thermal motion of the particles is important in the transverse direction, and by the Heisenberg field theory. The experimentally observed distribution over the transverse momenta thus does not allow us to give preference to either of the foregoing versions of the theory of multiple production of mesons.

---

[1] W. Heisenberg, Z. Physik **133**, 65 (1952); Kosmische Strahlung, Berlin–Heidelberg–Gottingen, 1953.

[2] Schein, Glasser, and Haskin, Nuovo cimento 647 (1955); M. Schein, Proc. Seventh Rochester Conf., N.Y., 1957. M. Schein, Trans. Int. Conf. on Cosmic Rays, Moscow, 1959 (in press).

[3] Boos, Vinitskiĭ, Takibaev, and Chasnikov, JETP **34**, 622 (1958), Soviet Phys. JETP **7**, 430 (1958).

[4] Zh. S. Takibaev, Trans. Phys. Inst. Acad. Sci. Kazakh S.S.R. **1**, 36 (1958).

[5] Edwards, Losty, Perkins, Pinkay, and Reynolds, Phil. Mag. **3**, 237 (1958).

[6] Debenedetti, Garelli, Tallone, and Vigone, Nuovo cimento **4**, 1142 (1956).

[7] Fenyves, Combosi, and Suranyi, Nuovo cimento **11**, 21 (1959).

[8] É. G. Boos and Zh. S. Takibaev, Trans. Int. Conf. on Cosmic Rays, Moscow 1959 (in press); Vinitskiĭ, Takibaev, Golyak, and Chasnikov, ibid.

[9] L. V. Lindern, Z. Naturforsch. **11a**, 340 (1956).

[10] K. Symanzik, Kosmische Strahlung, Springer Verlag, Berlin-Heidelberg-Gottingen 1953, p. 563.

[11] L. D. Landau, Izv. Akad. Nauk SSSR, Ser. Fiz. **17**, 51 (1953); S. Z. Belen'kiĭ and L. D. Landau, Usp. Fiz. Nauk 56, 1 (1955).

[12] G. A. Milekhin and I. L. Rozental', JETP **33**, 197 (1957), Soviet Phys. JETP **6**, 154 (1958).

[13] I. L. Rozental', JETP **31**, 278 (1956), Soviet Phys. JETP **4**, 217 (1958).

[14] G. A. Milekhin, JETP **35**, 1185 (1958), Soviet Phys. JETP **8**, 829 (1959).

[15] E. Fermi, Usp. Fiz. Nauk **46**, 71 (1952).

[16] I. L. Pomeranchuk, Dokl. Akad. Nauk SSSR **78**, 889 (1951). E. L. Feĭnberg and D. S. Chernavskiĭ, ibid. **81**, 795 (1951).

[17] M. Krezchmar, Z. Physik **150**, 247 (1958).

[18] Ciok, Coghen, Cierula, Holynski, Jurak, Miesowicz, Samievska, and Pernegr, Nuovo cimento **10**, 741 (1958).

[19] C. Cocconi, Phys. Rev. **111**, 1699 (1958).

[20] K. Niu, Nuovo cimento **10**, 925 (1958).

[21] Bradt, Kaplon, and Peters, Helv. Phys. Acta **23**, 24 (1950).

[22] Castagnolli, Cortini, Franzinetti, Manfredini, and Moreno, Nuovo cimento **10**, 1539 (1953).

[23] Hopper, Biswas, and Darby, Phys. Rev. **84**, 457 (1951).

[24] M. Demeyretal, Nuovo cimento **9**, 92 (1952).

[25] E. Lohrmann, Nuovo cimento **5**, 1074 (1957).

Translated by J. G. Adashko
242

SOVIET PHYSICS JETP VOLUME 11, NUMBER 4 OCTOBER, 1960

LEPTONIC DECAYS OF HYPERONS WITH EMISSIONS OF PIONS

I. S. TSUKERMAN

Scientific Information Institute, Academy of Sciences, U.S.S.R.

Submitted to JETP editor November 9, 1959

J. Exptl. Theoret. Phys. (U.S.S.R.) 38, 1285-1287 (April, 1960)

The total probabilities for leptonic decays of hyperons with emission of a pion, $Y \to N(Y') + l + \nu + \pi$, ($l$ denotes an electron or μ meson) are estimated in the case of the simplest matrix element of the universal V-A interaction for one of the possible perturbation theory diagrams.

IN view of the successes of the universal theory of weak interactions[1] it is of interest to study theoretically leptonic decays of hyperons. The probability of such decays was first obtained by Behrends and Fronsdal[2] and Feynman and Gell-Mann,[1] and the energy spectra and angular distributions by Shekhter;[3,4] experimentally a few events of leptonic hyperon decays were observed.[5]

In this work we consider hyperon decay processes of the type

$$Y \to N(Y') + l + \nu + \pi, \qquad (1)$$

where in addition to leptons a pion is emitted:

$$\Lambda^0 \to n + l^- + \tilde{\nu} + \pi^+, \quad \Lambda^0 \to p + l^- + \tilde{\nu} + \pi^0;$$
$$\Sigma^- \to n + l^- + \tilde{\nu} + \pi^0, \quad \Sigma^- \to p + l^- + \tilde{\nu} + \pi^-,$$
$$\Sigma^+ \to p + l^- + \tilde{\nu} + \pi^+; \quad \Xi^- \to \Lambda^0 + l^- + \tilde{\nu} + \pi^0,$$
$$\Xi^0 \to \Lambda^0 + l^- + \tilde{\nu} + \pi^+$$

[the letters and subscripts Y, N, π, l (μ, e), ν refer here and in the following to hyperons, nucleons, pions, charged leptons (μ meson, electron), and neutrinos]. All these decays are described (see Okun'[6]) by the universal weak interaction Hamiltonian

$$H_{\rm inc} = (G/\sqrt{2})\,(\bar{\psi}_N \gamma_\alpha (1 + \gamma_5)\,\psi_Y)\,(\bar{\psi}_l \gamma_\alpha (1 + \gamma_5)\,\psi_\nu) \qquad (2)$$

(we consider the case $C_V = -C_A = G/\sqrt{2}$). In the absence of a consistent theory of strong interactions we use for the description of process (1) a phenomenological matrix element. The invariant matrix element for the strongly interacting particles in this process contains eight unknown scalar functions of the invariants constructed out of the four-momenta of the various interacting particles and can be written as

$$M'_\alpha = f_1 \gamma_\alpha + f_2 (\gamma_\alpha \hat{k} - \hat{k} \gamma_\alpha) + f_3 k_\alpha + f_4 p_{\pi\alpha}$$
$$+ g_1 \gamma_\alpha \gamma_5 + g_2 (\gamma_\alpha \hat{k} - \hat{k} \gamma_\alpha)\,\gamma_5 + g_3 k_\alpha \gamma_5 + g_4 p_{\pi\alpha} \gamma_5, \qquad (3)$$

where $k = p_l + p_\nu$, p being the four-momentum of the particle in question. We make use of one of the possible perturbation theory diagrams (see figure) to estimate the probability of the decay (1); the weak interaction acts at the point O and the loop represents the virtual strong interactions.

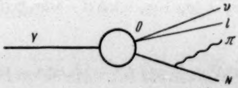

Since it is not possible at this time to determine the unknown functions f and g we consider the simplest case obtained by taking $f_1 = g_1 = 1$ and f_i, $g_i = 0$ ($i = 2, 3, 4$), the matrix element for the decay (1) becomes

$$M = \frac{G}{(2\pi)^8 \sqrt{2}} \left(\bar{\psi}_N \gamma_5 \frac{g}{\sqrt{4\pi E_\pi}} \frac{1}{\hat{p}_N + \hat{p}_\pi - m_N} (1 + \gamma_5)\,\gamma_\alpha \psi_Y \right)$$
$$\times\, (\bar{\psi}_l (1 + \gamma_5)\,\gamma_\alpha \psi_\nu), \qquad (4)$$

where g is the strong interaction coupling constant ($g^2/4\pi = 14$). E and m are the total energy and mass of the particle and we use the system of units in which $\hbar = c = 1$.

The decay probability is calculated from the usual formula

$$W = (2\pi)^{-8} \int \langle |M|^2 \rangle \, d^3p_N d^3p_\pi d^3p_l d^3p_\nu \, \delta\,(p_Y - p_N - p_\pi - p_l - p_\nu);$$

where we make use of the method of Dalitz[7] (see also Okun' and Shebalin[8]) to reduce the integration over d^3p_N, d^3p_π, d^3p_l, d^3p_ν to the invariant integration over d^4Q^*, d^4R^* ($Q^* = p_l + p_\nu$, $R^* = p_l - p_\nu$) followed by the integration over d^4Q, d^4R ($Q = p_N + p_\pi$, $R = p_N - p_\pi$).

Neglecting the electron mass in comparison with the masses of all other particles and assuming that the condition $\Delta/m_Y \ll 1$ is satisfied, where $\Delta = m_Y - (m_N + m_\pi)$, we find for the decays (1) with the emission of an electron or μ meson respectively the following expressions for the total

Decay	τ_e, sec	τ_μ, sec	$10^8\ \tau_e^{\mathrm{Sh}}$, sec	$10^8\ \tau_\mu^{\mathrm{Sh}}$, sec	$10^{10}\ \tau$, sec
$\Lambda^0 \to p + l^- + \tilde{\nu} + \pi^0$	29	—	1.7	10.6	2.4
$\Lambda^0 \to n + l^- + \tilde{\nu} + \pi^+$	76	—			2.4
$\Sigma^- \to n + l^- + \tilde{\nu} + \pi^0$	0.48	3.15	0.3	0.7	1.7
$\Sigma^- \to p + l^- + \tilde{\nu} + \pi^-$	0.57	0.79			1.7
$\Sigma^+ \to p + l^- + \tilde{\nu} + \pi^+$	0.77	0.93			0.8
$\Xi^- \to \Lambda^0 + l^- + \tilde{\nu} + \pi^0$	0.0033	—	0.8	3.1	~10
$\Xi^0 \to \Lambda^0 + l^- + \tilde{\nu} + \pi^+$	0.0051	—			~10

probabilities:*

$$W \approx \frac{2^7 G^2 (g^2/4\pi)}{1\cdot 3\cdot 5\cdot 7\cdot 9\cdot 11\cdot 13\pi^5}\left(\frac{m_N}{2m_Y}\right)^{3/2} \frac{\sqrt{m_\pi}\,\Delta^{13/2}}{(m_Y+m_N-\Delta/2)(1-\Delta/2m_Y)^{3/2}(1+\Delta/2m_\pi)^2}, \tag{5}$$

$$W \approx \frac{G^2 (g^2/4\pi)}{2^7\cdot 3\pi^4}\left(\frac{m_N}{2m_Y}\right)^{3/2} \frac{\sqrt{m_\pi}\sqrt{\Delta/2 + 3m_\pi/2}\,K^6}{(m_Y + m_N - \delta/2)(1-\delta/2m_Y)^{3/2}(1+\delta/2m_\pi)^2}, \tag{6}$$

where

$$K^6 = \Big[\left(\Delta^4 - \tfrac{1}{6} m_\pi^2\Delta^2 + \tfrac{41}{24} m_\pi^4\right)\Delta^{*2} + \left(\tfrac{1}{3} m_\pi^2\Delta - 4\Delta^3\right)\tfrac{1}{2}\Delta^{*3}$$
$$+ \left(6\Delta^2 - \tfrac{1}{6} m_\pi^2\right)\tfrac{5}{16}\Delta^{*4} - \tfrac{7}{8}\Delta\Delta^{*5} + \tfrac{21}{128}\Delta^{*6}$$
$$- \tfrac{61}{3} m_\pi^6 \left(1 - \frac{\Delta^*}{2\sqrt{\Delta m_\pi}}\right)\Big],$$

$$\Delta^* = m_Y - (m_N + m_\pi + m_\mu) = \Delta - m_\mu,$$

$$\delta = m_Y - m_N - m_\pi + m_\mu = \Delta + m_\mu.$$

It follows from a comparison of theory and experiment for hyperon leptonic decays (see Shekhter[4]) that the effective weak interactions coupling constant is approximately an order of magnitude smaller than its usual value $G = 10^{-5}/m_p^2$ (m_p – mass of the proton). This fact may be due to a renormalization of the C_V and C_A coupling constants due to the strong interactions. Following Shekhter[4] we take $G = 10^{-6}/m_p^2$. The table shows the hyperon lifetimes τ_e and τ_μ, corresponding to electron and μ-meson decays with the emission of a pion, as calculated from Eqs. (5) and (6) using the above value for the coupling constant. For purposes of comparison we also list in the table the hyperon lifetimes τ_e^{Sh} and τ_μ^{Sh} referring to the normal leptonic decays and taken from Shekhter.[4] The lifetimes τ_e, τ_μ for the cascade hyperon were calculated from Eqs. (5) and (6) with the nucleon mass replaced by the mass of the lambda particle; the crossed out entries refer to reactions energetically forbidden.

The author is sincerely grateful to L. B. Okun' for supervising this research and to I. G. Ivanter and K. A. Ter-Martirosyan for useful discussions.

---

*It should be noted that the transition to the limit $m_\pi = 0$ is not allowed in Eqs. (5) and (6), since they were derived on the assumption $2m_\pi \gg \Delta$ or Δ^*.

[1] R. P. Feynman and M. Gell-Mann, Phys. Rev. **109**, 193 (1958). E. C. Sudarshan and R. E. Marshak, Phys. Rev. **109**, 1860 (1958).

[2] R. E. Behrends and C. Fronsdal, Phys. Rev. **106**, 345 (1957).

[3] V. M. Shekhter, JETP **35**, 458 (1958), Soviet Phys. JETP **8**, 316 (1959).

[4] V. M. Shekhter, JETP **36**, 1299 (1959), Soviet Phys. JETP **9**, 920 (1959).

[5] J. Hornbostel and E. O. Salant, Phys. Rev. **102**, 502 (1956). Crawford, Cresti, Good, Kalbfleisch, Stevenson, and Ticho, Phys. Rev. Lett. **1**, 377 (1958). Nordin, Orear, Reed, Rosenfeld, Solmitz, Taft, and Tripp, Phys. Rev. Lett. **1**, 380 (1958).

[6] L. B. Okun', Usp. Fiz. Nauk **68**, 449 (1959), Ann. Rev. Nuc. Sci. **9** (1959).

[7] R. H. Dalitz, Phys. Rev. **99**, 915 (1955).

[8] L. B. Okun' and E. P. Shebalin, JETP **37**, 1775 (1959), Soviet Phys. JETP **10**, 1252 (1960).

Translated by A. M. Bincer

SOVIET PHYSICS JETP VOLUME 11, NUMBER 4 OCTOBER, 1960

ON CERTAIN GENERAL PROPERTIES OF THE PHOTON PROPAGATION FUNCTION IN QUANTUM ELECTRODYNAMICS

A. A. ANSEL'M

Leningrad Physico-Technical Institute, Academy of Sciences, U.S.S.R.

Submitted to JETP editor November 14, 1959

J. Exptl. Theoret. Phys. (U.S.S.R.) **38**, 1288-1296 (April, 1960)

By considering jointly the spectral representation of the photon Green's function and the renormalizability property, the behavior of the D function is investigated for very large energies and $e^2 = {}^1\!/_{137}$, and for very large charges but not too high energies. With an accuracy to within a numerical parameter it was possible to establish the dependence of the D function on charge in the first case, and on energy in the second case.

AT present it is still an open question whether the difficulties that occur when quantum field theory is applied to phenomena taking place at small distances indicate an internal inconsistency of the theory or whether they are due to the inadequacy of the existing calculation methods. Although objections have been raised repeatedly against the double-limit proof of the zero-charge, the arguments of Landau and Pomeranchuk (which, however, refer only to electrodynamics) are still quite convincing, even if they have only qualitative character (see, for example, the article by Landau[1]).

In this connection it appears to be of interest to try to investigate the photon Green's function for very large energies, using only the most general features of the theory: positive definiteness of probabilities, renormalizability, gauge invariance, etc. This can be accomplished partially. As will be seen below, the qualitative concepts used in the investigation can be made self-consistent, which leads us to conclude, for example, that it is not possible to prove rigorously the existence of a zero-charge using only renormalizability and the Lehmann expansion. At the same time, although these two conditions do not, of course, determine the propagation function completely, they do allow us to say more than one should have expected about its qualitative properties.

In the first section of this paper we investigate the behavior of the photon Green's function in the region of energies much larger than the critical energy (corresponding to the unphysical pole appearing in the Green's function in the usual calculations). Up to a numerical constant it is possible to establish the dependence of the D function on the charge, and it turns out that the D function either does not depend on the charge at all or is exponentially small. The last case corresponds to the non-logarithmic character of the divergence of the renormalized constant in the exact solution of the equations of quantum electrodynamics and seems to be entirely possible.

In the second section we shall consider a model of quantum electrodynamics for very large values of the renormalized coupling constant. It is possible to find the explicit dependence of the Green's function on the energy in a wide region. It should be noted that these results can be obtained only by making the very critical assumption that the role of the mass term in the Lagrangian does not become too important as the coupling constant increases.

In conclusion we shall discuss the problem of the zero charge in connection with the preceding considerations. It will be noted that our results do not in any way refute the arguments of Landau and Pomeranchuk, who considered the Hamiltonian directly, although our discussion starts from the very beginning with the assumption that there is no zero charge (i.e., that it is possible to use the basic general principles of the theory consistently with a nonvanishing value of the renormalized charge).

1. THE PHOTON GREEN'S FUNCTION FOR VERY LARGE ENERGIES

The renormalized photon propagation function $D_c = d_c/k^2$ is a function of two variables: the dimensionless ratio k^2/m^2 (k is the energy-momentum vector of the particle, and m is the mass of the electron) and the square of the renormalized charge e^2. Gell-Mann and Low showed from the renormalizability requirement of the theory that the function d_c $(k^2/m^2,\ e^2)$ can be expressed in terms of a function of a single variable in the asymptotic region $k^2/m^2 \gg 1$:[2]

$$e^2 d_c (k^2/m^2, e^2) = F\,(k^2\varphi(q(e^2))/m^2, \tag{1}$$

where F and φ are inverse functions, and $q(e^2)$ nearly coincides with e^2 for small values of the charge:

$$q(e^2) = e^2[1 - (5/9\pi)e^2 + \ldots]. \tag{2}$$

Introducing the functions

$$h(x) = F(e^x), \qquad g(x) = \ln \varphi(x),$$

$$\psi(x) = h(-x^{-1}), \qquad \chi(x) = -1/g(x), \tag{3}$$

we rewrite (1) in the form

$$e^2 d_c = h[\xi + g(q(e^2))] = \psi[\chi(q(e^2))(1 - \chi(q(e^2))\,\xi)^{-1}],$$
$$\xi = \ln(k^2/m^2), \tag{4}$$

where h and g, and ψ and χ are inverse functions.

As is known, perturbation theory gives the following expressions for the functions $\chi(x)$ and $\psi(x)$ for small positive x:

$$\chi(x) = x/3\pi, \qquad \psi(x) = 3\pi x, \qquad 0 < x \ll 1, \tag{5}$$

which leads to the known expression for $e^2 d_c$:[3]

$$e^2 d_c = e^2[1 - (e^2/3\pi)\,\xi]^{-1}, \qquad e^2 \ll 1, \qquad e^2 d_c \ll 1. \tag{6}$$

This means that the functions g and h are determined by perturbation theory for the following values of the argument:

$$g(x) = -3\pi/x \ \text{ for } 0 < x \ll 1,$$

$$h(x) = -3\pi/x \ \text{ for } x < 0,\ |x| \gg 1. \tag{7}$$

The Green's function d_c can be written in the form of an expansion in terms of the masses:[2,4]

$$d_c(k^2/m^2, e^2) = 1 + k^2 \int_0^\infty d\varkappa^2 \sigma(\varkappa^2, e^2)/(k^2 + \varkappa^2) \tag{8}$$

and is therefore an increasing function of k^2 (or $\xi = \ln(k^2/m^2)$, if we consider space-like $k^2 > 0$):

$$\frac{\partial}{\partial k^2} d_c(k^2/m^2, e^2) = \int_0^\infty d\varkappa^2 \varkappa^2 \sigma(\varkappa^2, e^2)/(k^2 + \varkappa^2)^2 > 0. \tag{9}$$

Since, for values of ξ which go up to $+\infty$ and for small values of e^2 which start from zero, the argument of the function $h(x)$, which is equal to $\xi + g(e^2) \approx \xi - 3\pi/e^2$, varies from $-\infty$ to $+\infty$, the function $h(x)$ is an increasing function of its argument everywhere (see Fig. 1). Two cases are possible:

1) $h[\xi + g(q(e^2))] \to \infty$ for $\xi \to \infty$ (curve *1*),

2) $h[\xi + g(q(e^2))] \to \beta$ for $\xi \to \infty$ (curve *2*),

where β is a numerical constant which is independent of the value of the renormalized charge.

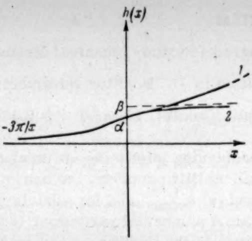

FIG. 1

The behavior of $g(x)$ [the inverse function of $h(x)$] is shown in Fig. 2. In case 2 the argument of $g(x)$ changes only from zero to β, so that $q(e^2)$ is limited from above by the value $q(e^2) = \beta$. There exists, therefore, a maximal value of the renormalized charge for which quantum electrodynamics is valid: $e^2 \le e_1^2$, $q(e_1^2) = \beta$. We note that then $e_1^2 \le \beta$, since e_1^2 is the value of the function $e_1^2 d_c(k^2/m^2, e_1^2)$ for $k^2 = 0$ and β is the value of the function $e_1^2 d_c(k^2/m^2, e_1^2)$ for $k^2 \to \infty$, and d_c must increase as k^2 increases. This result was obtained by Gell-Mann and Low.[2]

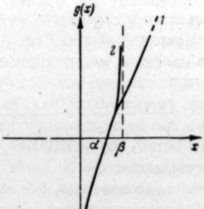

FIG. 2

The behavior of the functions $\psi(x)$ and $\chi(x)$ is shown in Figs. 3 and 4. For $\xi = 1/\chi(e^2)$ (which corresponds to $(e^2/3\pi)\,\xi = 1$ for small values of the charge) the argument of the function $\psi(x)$ jumps from $+\infty$ to $-\infty$. If the first approximation $\psi(x) = 3\pi x$ is used, this discontinuity represents an unphysical pole in the Green's function ("zero charge"). If we consider the function $\psi(x)$ as shown in Fig. 3, we see that $\psi(x)$ remains continuous for $x = \pm\infty$ [it is equal to α, the root of

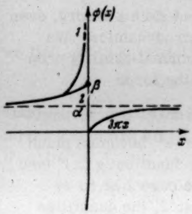

FIG. 3

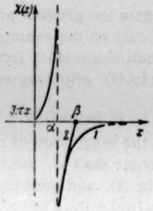

FIG. 4

the function $g(x)$]. These curves, of course, do not prove in any sense the absence of the zero charge. To decide this question, we must first find out how adequately the figures represent these functions, if the latter are derived directly from a study of the Hamiltonian itself. This problem will be discussed below.

Let us now attempt to obtain some information on the behavior of the Green's function for very large energies $\xi \gg \xi_0$, $\xi_0 = -g(e^2) \approx 3\pi/e^2$. If $h(x)$ were a function in the argument of which small terms could be neglected in comparison with large terms, even if the small terms are not small as compared with unity, we could conclude immediately that for $\xi \gg 3\pi/e^2$, e^2d_c does not depend on the charge: $e^2d_c = h(\xi)$. However, $h(x)$ may have exponential character, and then, of course, the dependence on the charge remains in force for arbitrarily large values of ξ.

Let us now try to calculate the value of the ratio $h(x+y)/h(x)$, when $x \gg y$ ($x \to \infty$) and $y \gtrsim 1$. For this purpose we consider $R(y)$:

$$\begin{aligned} R(y) &= h[\eta + g(e'^2)]/h[\xi + g(e'^2)] \\ &= \Big[1 + p^2\int_0^\infty d\varkappa^2\sigma(\varkappa^2, e'^2)/(p^2+\varkappa^2)\Big] \\ &\times\Big[1 + k^2\int_0^\infty d\varkappa^2\sigma(\varkappa^2, e'^2)/(k^2+\varkappa^2)\Big]^{-1}, \end{aligned} \tag{10}$$

when $\eta - \xi = y$ remains a finite quantity and η and $\xi \to \infty$; e'^2 is arbitrary. ($R(y)$ is independent of e'^2.) Under these conditions $p^2/k^2 = e^y \equiv \lambda$ is a finite quantity, while $p^2 \to \infty$ and $k^2 \to \infty$. Each of the integrals in the numerator and the denominator of (10) goes to ∞ if $d_c \to \infty$, i.e., we have case 1 (cf. the figures). In case 2 we have $R \to \beta/\beta = 1$. This value of $R(y)$ is included as a special case in the subsequent discussion, and we shall, therefore, assume that the integrals in (10) do not diverge. The R is written in the form

$$R = \lambda F(\lambda)/F(1), \qquad F(\lambda) = \int_0^\infty d\varkappa^2\sigma(\varkappa^2, e'^2)/(\lambda k^2 + \varkappa^2). \tag{11}$$

$F(\lambda)$ and $F(1)$ go to zero for $k^2 \to \infty$. Therefore

$$\frac{F(\lambda)}{F(1)} = \frac{\partial}{\partial k^2}F(\lambda)\Big/\frac{\partial}{\partial k^2}F(1) = \lambda\frac{\partial F}{\partial\lambda}\Big/\Big(\frac{\partial F}{\partial\lambda}\Big)_{\lambda=1}, \tag{12}$$

or

$$(\partial F/\partial\lambda)_{\lambda=1}/F(1) - \lambda(\partial F/\partial\lambda)/F(\lambda) = 0. \tag{13}$$

Integrating the last equation, we find*

$$R/\lambda = F(\lambda)/F(1) = \lambda^k, \qquad k = (\partial F/\partial\lambda)_{\lambda=1}/F(1),$$

or

$$R(y) = e^{\nu y}, \quad \nu = 1 - \lim_{k^2\to\infty}\Big[k^2\int_0^\infty \frac{\sigma(\varkappa^2, e'^2)\,d\varkappa^2}{(k^2+\varkappa^2)^2}\Big/\int_0^\infty \frac{\sigma(\varkappa^2, e'^2)\,d\varkappa^2}{k^2+\varkappa^2}\Big]. \tag{14}$$

We have therefore proved the following property of the function h:

$$h(x+y)/h(x) \to e^{\nu y}, \qquad x \to \infty, \tag{15}$$

where the numerical parameter ν is given by (14). $R(y)$, and hence ν, do not depend on e'^2, which was included in (10) in an arbitrary way. Nevertheless, ν cannot be calculated by perturbation theory because its applicability requires not only $e'^2 \ll 1$ but also $e'^2\ln(k^2/m^2) \ll 1$. The function $\nu(k^2)$, which becomes ν in the limit $k^2 \to \infty$, is zero for $e'^2 \ll 1$, $e'^2\ln(k^2/m^2) \ll 1$ (perturbation theory), depends on k^2 in a complicated manner for $e'^2\ln(k^2/m^2) \sim 1$, and becomes equal to the above-mentioned number ν for $k^2 \to \infty$.

From (14) we find the following limitations on ν:

$$0 \leqslant \nu \leqslant 1. \tag{16}$$

If we set

$$h(x) = e^{\nu x}P(x), \tag{17}$$

we see that the function $P(x)$ has the following property:

$$P(x+y)/P(x) \to 1, \qquad x \to \infty. \tag{18}$$

Going back to formula (4), we have now

$$e^2d_c(k^2/m^2, e^2) = \exp\{\nu g(q(e^2))\}(k^2/m^2)^\nu P(\ln(k^2/m^2)),$$
$$\ln(k^2/m^2) \gg g(q(e^2)). \tag{19}$$

The function $g[q(e^2)]$ has for small e^2 the form[5]

$$\begin{aligned} g(q(e^2)) = &-3\pi/q(e^2) - \tfrac{9}{4}\ln q(e^2) + C_1 q(e^2) \\ &+ C_2[q(e^2)]^2 + \dots. \end{aligned} \tag{20}$$

---

*It can be easily shown that the value of $F(\lambda)/F'(1)$, at which, in fact, the cancellation in the derivation of (13) was carried out, is finite.

We see from (19) that we must take the first two terms of this expansion. Then we have, finally,

$$e^2 d_c(k^2/m^2, e^2) = \exp\{-3\pi\nu/e^2\}(e^2)^{-9\nu/4}(k^2/m^2)^\nu P(\ln(k^2/m^2)),$$
$$e^2 \ll 1, \qquad (e^2/3\pi)\ln(k^2/m^2) \gg 1.$$

If we considered the next approximation for the function $q(e^2)$, we would find, according to (2), that this only introduces an unessential constant factor on the right hand side of (20). The energy dependence given by formula (20) is almost trivial and could have been predicted without calculations. The result given above is useful only in that it leads to a connection between the value of the parameter ν with the characteristic integrals (14). Indeed, if $\int \kappa^{-2}\sigma(\kappa^2)\,d\kappa^2$ converges and $\int \sigma(\kappa^2)\,d\kappa^2$ diverges (case 1), the dependence of σ on powers of κ^2 can only have the form $(\kappa^2)^{\nu-1}$ for $0 \le \nu \le 1$, which gives at once an energy dependence of the type (20). The case $\nu = 0$ corresponds to a logarithmic divergence of the renormalized coupling constant,

$$Z_3^{-1} = 1 + \int \sigma(\kappa^2)\,d\kappa^2$$

and does indeed occur in the perturbation theory, as was mentioned above. For a finite renormalization (case 2), as in the case of a logarithmic divergence, $e^2 d_c$ does not depend on the charge in the region of large energies. As is seen from (20), the quantity $e^2 d_c$, as a function of the charge, is exponentially small for $\nu > 0$, and can therefore not be expanded in a perturbation series. Here the circumstance that the derivation of (20) was based on the property (1), which was obtained in reference 2 precisely with the help of perturbation theory, is probably not essential for the validity of (20), since the renormalizability property reflects only the most general aspects of the theory. If $\nu \neq 0$, Z_3^{-1} diverges like $\Lambda^{2\nu}$ (Λ is the cut-off momentum).

It should be emphasized that, although the case $\nu = 0$ is intuitively regarded as the most probable, there do not seem to exist any special reasons for excluding values of $\nu \neq 0$.

In the following section we shall discuss quantum electrodynamics for large values of the renormalized coupling constant, where the cases $\nu = 0$ and $\nu \neq 0$ both seem to be perfectly acceptable, even if they lead to D functions of completely different qualitative behavior.

2. THE PHOTON GREEN'S FUNCTION FOR LARGE VALUES OF THE RENORMALIZED COUPLING CONSTANT

Since we are not able to construct a quantitative theory of strong coupling, it is of interest to investigate the general properties of such a theory, even if only on the example of electrodynamics. We shall again start from the renormalizability property (4), which we rewrite in the form

$$q(e^2) = h[g(e^2 d_c) - \xi]. \tag{21}$$

If the magnitude of the charge e^2 becomes much larger than α, the root of the function $g(x)$ (see Fig. 2), and goes to infinity in case 1 or to e_1^2 [$q(e_1^2) = \beta$, $g(\beta) = \infty$] in case 2, the quantities $g(e^2 d_c)$ and $g[q(e^2)]$ in formulas (21) and (4) increase beyond limit. If at the same time the energy does not become too large, so that the inequalities $g(e^2 d_c) \gg \xi$ or $g[q(e^2)] \gg \xi$ are fulfilled, we can use the property (15) of the function $h(x)$ and write

$$d_c(k^2/m^2, e^2) = e^{-2} q(e^2)(k^2/m^2)^\nu = d_c(1, e^2)(k^2/m^2)^\nu. \tag{22}$$

The quantity $q(e^2)/e^2$ equals $d_c(1, e^2)$, i.e., the value of the asymptotic Green's function for $k^2 = m^2$. It follows from the derivation that we have neglected those terms in (22) which are small in comparison with $d_c(1, e^2)$, although they may be greater than, or of the order of, unity, if only $d_c(1, e^2)$ is large.

In the discussion above we have made one very critical assumption. The criterion for the applicability of (22) is given by the inequalities $\xi \ll g(e^2 d_c)$ or $\xi \ll g[q(e^2)]$, which limit the quantity k^2/m^2 from above. On the other hand, formulas (4) and (20) have asymptotic character, i.e., terms which vanish as k^2/m^2 increases are omitted in these expressions. It is clear that, if these terms grow very fast with increasing e^2 (roughly speaking, faster than $\sim \exp[g(e^2)]$), it is impossible to find a region of values of k^2/m^2 which are large enough that these terms can be neglected, but still sufficiently small to satisfy the above-mentioned inequalities. We shall assume that this difficulty does not occur, basing our supposition on the rather natural hypothesis that the mass term in the Lagrangian cannot have too much importance for very large values of the renormalized charge.

Formula (22) determines the dependence of d_c on energy in a rather wide region. The exact expression (not the asymptotic one) for d_c should have branch points at the threshold values of k^2 which are multiples of the square of the mass. In the asymptotic theory $m^2 \to 0$, and all branch points converge to the point $k^2 = 0$. In this case the character of the branching is $(k^2)^\nu$. This throws, perhaps, some light on the meaning of the parameter ν.

It is easy to find the spectral function $\sigma(\kappa^2, e^2)$ corresponding to expression (22). Since

$$\varkappa^2\sigma(\varkappa^2, e^2) = \pi^{-1}\operatorname{Im} d_c(-\varkappa^2/m^2, e^2), \tag{23}$$

we find, after substitution of (22),

$$\varkappa^2\sigma(\varkappa^2, e^2) = \pi^{-1} d_c(1, e^2)(\varkappa^2/m^2)^\nu \sin\pi\nu. \tag{24}$$

Equation (24) is valid with an accuracy up to terms which are small in comparison with $d_C(1, e^2)$ if $\kappa^2/m^2 \gg 1$, but

$$\ln(\varkappa^2/m^2) \ll g(e^2 d_c),\ g(q(e^2)).$$

In the case $\nu = 0, 1$, $d_C(k^2/m^2, e^2) = d_C(1, e^2)$ with the same accuracy, and $\sigma/d_C(1, e^2) \to 0$ with increasing e^2. If, in this case, the renormalization is finite, $d_C(1, e^2) \to \beta/e_1^2$ and $\sigma(\kappa^2, e^2)$ itself goes to zero.

Let us consider the case $\nu = 0$ in more detail. Since the basic term in σ which is proportional to $d_C(1, e^2)$ vanishes, it is desirable to determine the next term of the expansion. It follows from formula (23) and the renormalizability condition (4) that the dependence of σ on κ^2 and e^2 in the asymptotic region has the form

$$\varkappa^2\sigma(\varkappa^2, e^2) = e^{-2} f[\ln(\varkappa^2/m^2) + g(q(e^2))], \tag{25}$$

where $f[x]$ is some function which, in the case $\nu = 0$, satisfies condition (18). The asymptotic expression for $d_C(k^2/m^2, e^2)$ for $\nu = 0$ consists of a term independent of k^2/m^2, $d_C(1, e^2)$, and a term which is an increasing function of it. The latter is small in the region under consideration, since for $\nu = 0$

$$d_c(k^2/m^2, e^2)/d_c(1, e^2) \to 1. \tag{26}$$

We can easily obtain the increasing part of d_C, starting from (25). We have

$$d_c\left(\frac{k^2}{m^2}, e^2\right) \approx k^2 \int\limits_{\sim m^2}^{\infty} d\varkappa^2 e^{-2} f[\ln(\varkappa^2/m^2)$$
$$+ g(q(e^2))]/\varkappa^2(\varkappa^2 + k^2).$$

Since the integral converges, the important values of κ^2 are $\kappa^2 \lesssim k^2$, i.e.,

$$\ln(\varkappa^2/m^2) \leqslant \ln(k^2/m^2) \ll g(q).$$

Inasmuch as f satisfies property (18), we obtain at once

$$d_c(k^2/m^2, e^2) \approx e^{-2} f[g(q(e^2))] \ln(k^2/m^2) \tag{27}$$

or, adding the constant term to d_C,

$$d_c(k^2/m^2, e^2) = d_c(1, e^2) + e^{-2} f[g(q(e^2))] \ln(k^2/m^2). \tag{28}$$

Using condition (26), we rewrite (28) in the form

$$d_c(k^2/m^2, e^2) = d_c(1, e^2)[1 + \Delta(e^2)\ln(k^2/m^2)], \tag{29}$$

$$\Delta(e^2) = f[g(q(e^2))]/e^2 d_c(1, e^2) \to 0. \tag{30}$$

Now the $\sigma(\kappa^2, e^2)$ corresponding to (29) is

$$\varkappa^2\sigma(\varkappa^2, e^2) = d_c(1, e^2)\Delta(e^2). \tag{31}$$

Equation (30) is, of course, equivalent to the above-mentioned condition $\sigma/d_C(1, e^2) \to 0$ for increasing e^2. If the renormalization is finite, $q(e^2) \to \beta$ and $d_C(1, e^2) \to \beta/e_1^2$ for $e^2 \to e_1^2$. Here $\sigma(\kappa^2, e^2)$ goes to zero like $\Delta(e^2)$, which in its own right must vanish faster than $[g(q)]^{-1}$, as can be seen from the definition (30) and the convergence of the integral

$$\int^{\infty} \sigma(\varkappa^2)\, d\varkappa^2 = e^{-2}\int^{\infty} f(x)\, dx.$$

If the renormalization is infinite, it is easily shown from (30) that $\Delta(e^2) \sim [g(q)]^{-1}$. In order to see this, we write (30) in the form

$$\Delta(e^2) = f[g(q(e^2))]/q(e^2) = f(g(x))/x = f(y)/h(y),$$
$$x = q(e^2), \qquad y = g(x),$$

and compute $f(y)/h(y)$ for large values of y:

$$\frac{f(y)}{h(y)} = f\left(\ln\frac{p^2}{m^2} + g'\right) \Bigg/ p^2 \int\limits_{\sim m^2}^{\infty} d\varkappa^2 f\left(\ln\frac{\varkappa^2}{m^2} + g'\right) \Bigg/ \varkappa^2(p^2 + \varkappa^2),$$
$$y = \ln(p^2/m^2). \tag{32}$$

Since we are concerned with the case of infinite renormalization, the values $\kappa^2 \sim p^2$ are important in the integral of formula (30), so that we may pull out of the integral the slowly varying function f at the point $\ln(p^2/m^2) + g'$. Then

$$\Delta(e^2) = f(y)/h(y) \approx \frac{1}{\ln(p^2/m^2)} = 1/y = 1/g(q(e^2)). \tag{33}$$

The function $\sigma(\kappa^2, e^2)$ may in this case go to zero for increasing e^2, if $d_C(1, e^2)\Delta(e^2) \to 0$, or it may stay finite and even increase. To resolve this question, we must understand the behavior of $d_C(1, e^2)$ for large values of the charge, which cannot be done in the framework of our techniques. It may turn out that, if $d_C(1, e^2)\Delta(e^2) \to 0$, that part of $\sigma(\kappa^2, e^2)$ becomes important which corresponds to the terms neglected in (4), as these vanish for $m^2/k^2 \to 0$. Nothing is known about the dependence of these terms on the charge. It should be noted, however, that by virtue of formula (9) the imaginary part of these terms for $k^2 < 0$, which is also the imaginary part of the total σ, is a negative quantity and can, therefore, never be greater (in terms of absolute values) than the calculated part of σ. In general, the case for which $\sigma(\kappa^2, e^2) \to 0$ is physically very improbable. Indeed, the function $\sigma(\kappa^2, e^2)$ is a sum of the squares of the moduli of the electromagnetic-field-operator matrix elements which connect such states as, for example, the vacuum and an electron-positron pair. The condition $\sigma(\kappa^2, e^2) \to 0$ will imply, in particular, that as the charge increases, the cross section for the scattering of an electron by another electron with arbitrary momentum transfer much larger than m^2 decreases. If, on the other hand, the momentum transfer goes to zero, the quantum effects should disappear and the cross section should be of the Rutherford type, i.e., it should increase rapidly as a function of the charge. But this means that the cross section must change very rapidly in a relatively small interval of momentum transfers near $k^2 \sim m^2$.

All this seems, of course, very strange; however, one could argue that it is not unnatural to assume that electrodynamics has limited applicability for large charges. In any case, the idea that the theory becomes gradually worse as the charge increases seems rather phantastic.

There are thus two possibilities left, and the choice between these two is apparently very difficult. In the case $\nu > 0$ we have for d_C the functions (22) and for $\sigma(\kappa^2, e^2)$ formula (24), and in the case $\nu = 0$ formulas (29) and (31), respectively. These formulas have the character of expansions in terms of quantities which are small for strong coupling.

3. CONCLUSION

Our whole analysis of the behavior of the D function hinges on the possibility of making the renormalizability of the theory consistent with Lehmann's spectral representation (i.e., with the analyticity properties of the theory). By themselves these two suppositions are indeed not contradictory; however, this does not mean that the theory is internally consistent if it is examined fully, i.e., if we consider the Hamiltonian. For a better understanding of this circumstance we briefly outline the arguments of Landau and Pomeranchuk[1] concerning the "zero charge" in the light of our previous discussion.

As is known,[2] the connection between the renormalized and the bare charges e^2 and e_0^2, respectively, is (in our notation)

$$e_0^2 = h[g(q(e^2)) + L], \tag{34}$$

where $L = \ln(\Lambda^2/m^2)$ and Λ is the cut-off momentum. In going over to a local theory $\Lambda \to \infty$, and e_0^2 increases from small values until it reaches the value $\alpha = h(0)$ [the root of the function $g(x)$, see Figs. 1 and 2] for $L = -g[q(e^2)]$. In the neighborhood of this point the unrenormalized Green's function is equal to

$$e_0^2 d_0(\Lambda^2/k^2, e_0^2) = h[-(L-\xi) + g(e_0^2)] \approx h[-(L-\xi)] \tag{35}$$

and is, therefore, independent of e_0^2.

It is important that even if h has exponential character ($\nu \neq 0$), this assertion remains true, since $g(e_0^2)$ is small in comparison with unity for $e_0^2 \sim \alpha$. On the other hand, $e_0^2 d_0$ is the vacuum expectation value of the T product of two operators $U = e_0 A$ (A is the electromagnetic potential), and the fact that $e_0^2 d_0$ is independent of e_0^2 seems to be due to the neglect of the free term in the Lagrangian. (The latter is proportional to $e_0^{-2} U^+ U$, whereas the interaction is of the order of $U^+ U$.) Furthermore, in order to avoid a "zero charge", the function $g(e_0^2)$ should have the behavior shown in Fig. 2, which implies that $e_0^2 d_0$ will again start to depend on e_0^2. This seems surprising, not so far as the Lehmann expansion or the renormalizability property is concerned, but looking at it within the framework of the Lagrangian formalism; for the neglect of a term $\sim e_0^{-2} U^+ U$ in comparison with a term $\sim U^+ U$ can hardly become less justifiable as e_0^2 increases. There is thus good reason to assume that the functions g and h do not have the behavior shown in Figs. 1 and 2, if they are determined with the help of the Hamiltonian. Nevertheless, regardless of whether the zero charge does or does not exist in reality, it seems useful to study the general features of the theory. We summarize the results obtained:

1) In the real electrodynamics with $e^2 = 1/137$ at energies much larger than the critical value $[(e^2/3)\ln(k^2/m^2) \gg 1]$ the function d_C is either independent of the charge or exponentially small [formula (20)]. The last case corresponds to a non-logarithmic divergence of the exact expressions.

2) In an electrodynamics with a very large coupling constant it is possible (with an accuracy within a numerical constant) to determine the dependence of the function d_C on the energy in a fairly wide region. It has either the form (22) [the corresponding function σ is given by (24)] or the form (29) [the function σ is given by (31)].

In conclusion I should like to thank V. N. Gribov, K. A. Ter-Martirosyan, I. T. Dyatlov, and V. M. Shekhter for numerous useful comments.

---

[1] W. Pauli, Niels Bohr and the Development of Physics, London, Pergamon Press (1958).

[2] M. Gell-Mann and F. Low, Phys. Rev. **95**, 1300 (1954).

[3] Landau, Abrikosov, and Khalatnikov, Dokl. Akad. Nauk SSSR **95**, 497, 773, and 1177 (1954).

[4] H. Lehmann, Nuovo cimento **11**, 342 (1954).

[5] N. N. Bogolyubov and D. V. Shirkov Введение в квантовую теорию полей (Introduction to the Theory of Quantized Fields), Gostekhizdat (1957); Engl. Transl., Interscience, N.Y. (1959).

Translated by R. Lipperheide
244

SOVIET PHYSICS JETP VOLUME 11, NUMBER 4 OCTOBER, 1960

MOMENTS OF INERTIA OF ODD ATOMIC NUCLEI

Yu. T. GRIN', S. I. DROZDOV, and D. F. ZARETSKIĬ

Submitted to JETP editor November 17, 1959

J. Exptl. Theoret. Phys. (U.S.S.R.) **38**, 1297-1303 (April, 1960)

An expression is derived for the moment of inertia of odd nuclei, with the effect of pair correlation taken into account. The theory is compared with the experiments.

It is well known that in the mass number regions $150 < A < 190$ and $A > 225$ the atomic nuclei are deformed and have rotational levels in addition to single-particle levels. Experiments show that the moments of inertia of odd nuclei are larger than those of neighboring even nuclei on the average by 10 – 20% in units of the moment of inertia for a solid, and in some cases by as much as 30 and even 60% (the ground state of Dy^{161}).

In a number of papers[1] the formula for the moments of inertia of even and odd nuclei was derived and the difference between them was calculated on the basis of the single-particle model,[2] but without taking consistently into account effects due to pair correlations. The inclusion of pair correlations substantially reduces the moment of inertia of the nucleus in comparison to the moment of a solid.[3,4]

In this work use is made of the Green's function technique for a finite system with an odd number of particles.[5] For the calculation of the moment of inertia we make use of the method developed by Migdal[3] for even-even nuclei.

The moment of inertia J is determined by the expression

$$J = \langle M^x \rangle / \Omega, \qquad (1)$$

where

$$\langle M^x \rangle = \sum_{\lambda\lambda'} M^x_{\lambda\lambda'} \rho_{\lambda'\lambda}$$

is the average value of the projection of the angular momentum of the system on the x axis, which is perpendicular to the symmetry axis z of the nucleus; $\rho_{\lambda\lambda'}$ is the density matrix, and Ω is the angular velocity whose direction coincides with the x axis. In a previous paper by the authors[5] the density matrix $\rho_{\lambda\lambda'}$ (Eq. 25) for an odd system was calculated for a statistical perturbation. In the case of a rotation of the system the perturbation of the Hamiltonian, as was shown by Migdal,[3] is of the form

$$\hat{V} = -\hat{V}^{+} = \hat{M}^x \Omega M / M_{\rm eff},$$

where M is the nucleon mass, $M_{\rm eff}$ is the effective mass of the quasiparticle and for Δ' it is convenient to introduce the notation $\Delta' = i f(\mathbf{r}) \Omega M / M_{\rm eff}$.

If we use the density matrix $\rho_{\lambda\lambda'}$ obtained in reference 5 to evaluate the expression (1) we obtain

$$J = \sum_{\lambda\lambda'} \frac{(E_\lambda E_{\lambda'} - \varepsilon_\lambda \varepsilon_{\lambda'} - \Delta^2) \, |M^x_{\lambda\lambda'}|^2 - \Delta \dot{M}^x_{\lambda\lambda'} f_{\lambda'\lambda}}{2E_\lambda E_{\lambda'} (E_\lambda + E_{\lambda'})} \frac{M}{M_{\rm eff}} + {\sum_\lambda}' \frac{2 (E^2_{\lambda_0} + \varepsilon_\lambda \varepsilon_{\lambda_0} + \Delta^2) \, |M^x_{\lambda\lambda_0}|^2 + \Delta (\dot{M}_{\lambda\lambda_0} f_{\lambda_0\lambda} + \dot{M}_{\lambda_0\lambda} f_{\lambda\lambda_0})}{E_{\lambda_0} (\varepsilon^2_\lambda - \varepsilon^2_{\lambda_0})}, \qquad (2)$$

where $E_\lambda = \sqrt{\epsilon^2_\lambda + \Delta^2}$, ϵ_λ is the single-particle energy measured from the chemical potential ϵ_0, and λ_0 is the state occupied by the odd particle. The prime in the single summation over λ indicates that the state with energy $\epsilon_\lambda = \epsilon_{\lambda_0}$ should be omitted. For a nucleus with N nucleons, Δ is determined from the expression

$$\Delta(N) = \tfrac{1}{2} \, | 2E_0(N) - E_0(N+1) - E_0(N-1) | , \qquad (3)$$

where $E_0(N)$ denotes the energy of the ground state of the system. The integral equation for f takes the form

$$\sum_{\lambda\lambda'} \varphi_\lambda \varphi^*_{\lambda'} \frac{(\varepsilon_\lambda - \varepsilon_{\lambda'})^2 f_{\lambda\lambda'} + 2\Delta \dot{M}^x_{\lambda\lambda'}}{2E_\lambda E_{\lambda'} (E_\lambda + E_{\lambda'})} + \sum_{\lambda(\varepsilon_\lambda = \varepsilon_{\lambda_0})} \varepsilon_{\lambda_0} E^{-2}_{\lambda_0} (\varphi_\lambda \varphi^*_{\lambda_0} f_{\lambda\lambda_0} - \varphi_{\lambda_0} \varphi^*_\lambda f_{\lambda_0\lambda}) + {\sum_\lambda}' \frac{\varphi_\lambda \varphi^*_{\lambda_0} (2E_{\lambda_0} - \varepsilon_\lambda + \varepsilon_{\lambda_0}) \, [(\varepsilon_\lambda - \varepsilon_{\lambda_0})^2 f_{\lambda\lambda_0} + 2\Delta \dot{M}^x_{\lambda\lambda_0}]}{E_{\lambda_0} (\varepsilon^2_{\lambda_0} - \varepsilon^2_\lambda)(\varepsilon_{\lambda_0} - \varepsilon_\lambda)} - {\sum_\lambda}' \frac{\varphi_{\lambda_0} \varphi^*_\lambda (2E_{\lambda_0} - \varepsilon_{\lambda_0} + \varepsilon_\lambda) \, [(\varepsilon_{\lambda_0} - \varepsilon_\lambda)^2 f_{\lambda_0\lambda} + 2\Delta \dot{M}^x_{\lambda_0\lambda}]}{E_{\lambda_0} (\varepsilon^2_{\lambda_0} - \varepsilon^2_\lambda)(\varepsilon_{\lambda_0} - \varepsilon_\lambda)} = 0. \qquad (4)$$

The first term in this expression corresponds to the equation for f for an even-even nucleus, and the first term in (2) corresponds to the moment of inertia of such a nucleus.[3]

We write f as $f = f^0 + f'$, where f^0 denotes the solution of the integral equation for an even-even nucleus. Insofar as Eq. (4) differs from the integral equation for f for an even-even nucleus by the addition of a single summation over λ the modification of its solution will be quasiclassically small in comparison with f^0 (see Appendix). Therefore in the single summation over λ we may replace f by f^0. Then expression (2) becomes

$$J = J_e(\varkappa) - \sum_{\lambda\lambda'} \frac{\Delta \dot{M}^x_{\lambda\lambda'} f'_{\lambda'\lambda}}{2E_\lambda E_{\lambda'}(E_\lambda + E_{\lambda'})} \frac{M}{M_{\text{eff}}}$$

$$+ \sum_\lambda{}' \frac{2(E^2_{\lambda_0} + \varepsilon_\lambda \varepsilon_{\lambda_0} + \Delta^2)\,|M^x_{\lambda\lambda_0}|^2 + \Delta(\dot{M}^x_{\lambda\lambda_0} f^0_{\lambda_0\lambda} + \dot{M}^x_{\lambda_0\lambda} f^0_{\lambda\lambda_0})}{E_{\lambda_0}(\varepsilon^2_\lambda - \varepsilon^2_{\lambda_0})}$$

$$\times \frac{M}{M_{\text{eff}}}, \tag{5}$$

$$J_e(\varkappa) = \sum_{\lambda\lambda'} \frac{(E_\lambda E_{\lambda'} - \varepsilon_\lambda \varepsilon_{\lambda'} - \Delta^2)\,|M^x_{\lambda\lambda'}|^2 - \Delta \dot{M}^x_{\lambda\lambda'} f^0_{\lambda'\lambda}}{2E_\lambda E_{\lambda'}(E_\lambda + E_{\lambda'})}. \tag{6}$$

Here $\kappa = \beta\omega_0/2\Delta$, the parameter on which the moment of inertia of an even-even nucleus depends,[3] is evaluated for values of Δ and β corresponding to the odd nucleus. From the integral equation (4) we obtain the following equation for f′:

$$\sum_{\lambda\lambda'} \varphi_\lambda(\mathbf{r})\,\varphi^*_{\lambda'}(\mathbf{r}) \frac{(\varepsilon_\lambda - \varepsilon_{\lambda'})^2 f'_{\lambda\lambda'}}{2E_\lambda E_{\lambda'}(E_\lambda + E_{\lambda'})}$$

$$+ \frac{\varepsilon_{\lambda_0}}{E^2_{\lambda_0}} \sum_{\substack{\lambda \\ (\varepsilon_\lambda = \varepsilon_{\lambda_0})}} (\varphi_\lambda \varphi^*_{\lambda_0} f^0_{\lambda\lambda_0} - \varphi_{\lambda_0} \varphi^*_\lambda f^0_{\lambda_0\lambda})$$

$$+ \sum_\lambda{}' \frac{\varphi_\lambda \varphi^*_{\lambda_0}(2E_{\lambda_0} - \varepsilon_\lambda + \varepsilon_{\lambda_0})\,[(\varepsilon_\lambda - \varepsilon_{\lambda_0})^2 f^0_{\lambda\lambda_0} + 2\Delta \dot{M}^x_{\lambda\lambda_0}]}{E_{\lambda_0}(\varepsilon^2_{\lambda_0} - \varepsilon^2_\lambda)(\varepsilon_{\lambda_0} - \varepsilon_\lambda)}$$

$$- \sum_\lambda{}' \frac{\varphi_{\lambda_0} \varphi^*_\lambda(2E_{\lambda_0} - \varepsilon_{\lambda_0} + \varepsilon_\lambda)\,[(\varepsilon_{\lambda_0} - \varepsilon_\lambda)^2 f^0_{\lambda_0\lambda} + 2\Delta \dot{M}^x_{\lambda_0\lambda}]}{E_{\lambda_0}(\varepsilon^2_{\lambda_0} - \varepsilon^2_\lambda)(\varepsilon_{\lambda_0} - \varepsilon_\lambda)} = 0 \tag{7}$$

and the following equation for f^0:

$$\sum_{\lambda\lambda'} \varphi_\lambda(\mathbf{r})\,\varphi^*_{\lambda'}(\mathbf{r})\,[2\Delta \dot{M}^x_{\lambda\lambda'}$$

$$+ (\varepsilon_\lambda - \varepsilon_{\lambda'})^2 f^0_{\lambda\lambda'}]/2E_\lambda E_{\lambda'}(E_\lambda + E_{\lambda'}) = 0. \tag{8}$$

Multiplying Eq. (7) by f^0 and Eq. (8) by f′ and integrating over **r** we obtain respectively

$$\sum_{\lambda\lambda'} \frac{(\varepsilon_\lambda - \varepsilon_{\lambda'})^2 f'_{\lambda\lambda'} f^0_{\lambda'\lambda}}{2E_\lambda E_{\lambda'}(E_\lambda + E_{\lambda'})} + 2\Delta \sum_\lambda \frac{(\dot{M}^x_{\lambda\lambda_0} f^0_{\lambda_0\lambda} - \dot{M}^x_{\lambda_0\lambda} f^0_{\lambda\lambda_0})}{(\varepsilon^2_{\lambda_0} - \varepsilon^2_\lambda)(\varepsilon_{\lambda_0} - \varepsilon_\lambda)}$$

$$+ \sum_\lambda{}' \frac{2\Delta(\dot{M}^x_{\lambda\lambda_0} f^0_{\lambda\lambda_0} + f^0_{\lambda_0\lambda} \dot{M}^x_{\lambda_0\lambda})}{E_{\lambda_0}(\varepsilon^2_{\lambda_0} - \varepsilon^2_\lambda)}$$

$$+ \frac{2}{E_{\lambda_0}} \sum_\lambda{}' \frac{|f^0_{\lambda\lambda_0}|^2(\varepsilon_{\lambda_0} - \varepsilon_\lambda)}{\varepsilon_{\lambda_0} + \varepsilon_\lambda} = 0, \tag{9}$$

$$\sum_{\lambda\lambda'} [2\Delta \dot{M}^x_{\lambda\lambda'} f'_{\lambda'\lambda}$$

$$+ (\varepsilon_\lambda - \varepsilon_{\lambda'})^2 f^0_{\lambda\lambda'} f'_{\lambda'\lambda}]/2E_\lambda E_{\lambda'}(E_\lambda + E_{\lambda'}) = 0. \tag{10}$$

It follows from Eq. (8) that the matrix $f^0_{\lambda\lambda'}$ has the same symmetry properties as the matrix $\dot{M}^x_{\lambda\lambda'}$. Therefore $\dot{M}^x_{\lambda\lambda_0} f^0_{\lambda_0\lambda} - \dot{M}^x_{\lambda_0\lambda} f^0_{\lambda\lambda_0} = 0$. Eliminating f′ from the expression for the moment of inertia by making use of Eqs. (9) and (10) we find:

$$J = J_e(\varkappa) + \frac{M}{M_{\text{eff}}} \sum_\lambda{}' \frac{2(E^2_{\lambda_0} + \varepsilon_\lambda \varepsilon_{\lambda_0} + \Delta^2)\,|M^x_{\lambda\lambda_0}|^2 + 2\Delta(f^0_{\lambda\lambda_0} \dot{M}^x_{\lambda_0\lambda} + f^0_{\lambda_0\lambda} \dot{M}^x_{\lambda\lambda_0}) + (\varepsilon_\lambda - \varepsilon_{\lambda_0})^2 |f^0_{\lambda\lambda_0}|^2}{E_{\lambda_0}(\varepsilon^2_\lambda - \varepsilon^2_{\lambda_0})} \tag{11}$$

In this manner it is seen that J is independent of f′ and there is no need for solving Eq. (7).

A solution of the integral equation (8) for f^0 can be expressed in an analytic form only for an oscillator potential. In what follows we evaluate terms containing f^0 for such a potential. According to Migdal,[3] f^0 has the form

$$f^0(\mathbf{r}) = -(g_1 + g_2)\,\dot{M}^x(\mathbf{r})/2\Delta\,(g_1\nu_1^2 + g_2\nu_2^2),$$

$$g(\nu) = \frac{\sinh^{-1}\nu}{\nu\sqrt{1+\nu^2}}, \quad g_1 = g(\nu_1), \quad g_2 = g(\nu_2),$$

$$\nu_1 = \frac{(\omega_z - \omega_y)}{2\Delta}, \quad \nu_2 = \frac{(\omega_z + \omega_y)}{2\Delta}, \tag{12}$$

where ω_z, $\omega_x = \omega_y$ are the corresponding frequencies. By substituting (12) into (11) and setting $\epsilon_{\lambda_0} = 0$ we reduce (11) to the form

$$J = J_e(\varkappa) + \sum_\lambda{}' \frac{|\dot{M}^x_{\lambda\lambda_0}|^2}{4\Delta^3} \left[\frac{1}{\nu^2_\lambda} - \frac{g_1 + g_2}{g_1\nu_1^2 + g_2\nu_2^2}\right]^2 \frac{M}{M_{\text{eff}}}, \tag{13}$$

where $\nu_\lambda = \epsilon_\lambda/2\Delta$.

In the quasiclassical approximation the nonvanishing matrix elements of $\dot{M}^x$ are equal in the representation (n_x, n_y, n_z). In the representation $(N, n_z, \Lambda, \Omega)$, where N is the principal quantum number, and Λ and Ω are the projections of the orbital and total angular momenta on the z axis, the quasiclassical equality of matrix elements will also hold provided that the degeneracy of energy levels in this representation is taken into account and the effective expressions $|\dot{M}^x_{\lambda\lambda_0}|^2_{\text{eff}}$ are used, corresponding to the two possible transitions to the degenerate level. Then Eq. (13) becomes

$$J_0 = J_e(\varkappa_0) + \frac{(N - n_z)\,n_z}{\Delta} \nu_1^2 \left[\frac{1}{\nu_1^4} + \frac{1}{\nu_2^4} - \frac{2(g_1 + g_2)}{(g_1\nu_1^2 + g_2\nu_2^2)}\right.$$

$$\left. \times \left(\frac{1}{\nu_1^2} + \frac{1}{\nu_2^2}\right) + \frac{2(g_1 + g_2)^2}{(g_1\nu_1^2 + g_2\nu_2^2)^2}\right] \frac{M}{M_{\text{eff}}}, \tag{14}$$

Insofar as M differs little from M_{eff} we set in what follows $M/M_{\text{eff}} \approx 1$.

For deformed nuclei $\nu_1 \sim 1$, $g_1 \sim 0.6$, $\nu_2 \sim 10$, and $g_2 \sim 0.03$. It follows from Eq. (14) that terms connected with f^0 can be as large as 25% of the first term. However the dependence of these terms on ν_1 is much weaker than that of the first term. In addition, it follows from Eq. (14) that the summation over λ is important only within the one shell which contains the state λ_0, because the principal contribution to J_o comes from terms corresponding to the minimal energy ϵ_λ.

Let us consider the difference between the moments of inertia of an odd nucleus and the neighboring even-even nucleus:

$$\delta J = J_o - J_e = J_e(\varkappa_o) - J_e(\varkappa_e)$$

$$+ \sum_\lambda \frac{|M_{\lambda\lambda_0}|^2}{4\Delta^3}\left[\frac{1}{\nu_\lambda^2} - \frac{g_1 + g_2}{g_1\nu_1^2 + g_2\nu_2^2}\right]^2 \tag{15}$$

The last term in Eq. (15) is always positive. For an oscillator potential $\kappa = \hbar\omega_0\beta/2\Delta$. Since $\Delta_e > \Delta_o$, and β does not vary much between neighboring nuclei, we have in a majority of cases $\kappa_o > \kappa_e$ and $\delta J > 0$, in agreement with experiment. Let us estimate the dependence of the main term in δJ on the number of particles in the system, A. Since

$$\sum_\lambda{}' |M^x_{\lambda\lambda_0}|^2 \sim A^{2/3}, \ \varepsilon_\lambda \sim \Delta \sim \varepsilon_0 A^{-2/3},$$

it follows that $\delta J \sim A^{4/3}/\epsilon_0$. The moment of inertia of a solid goes as $J_s \sim A^{5/3}/\epsilon_0$ and therefore

$$\delta J / J_s \sim A^{-1/3}. \tag{16}$$

The experimentally observed sharp jumps in δJ correspond to those cases when the odd particle occupies states which in the limit of small deformations go over into states with a large orbital angular momentum l. The dependence on l is particularly clear in the example of a rectangular potential well, when

$$\varepsilon_\lambda + \varepsilon_0 = \varepsilon_\lambda^0 + \beta(m^2/l^2 - 1/3)\varepsilon_\lambda^0,$$

where ϵ_λ^0 is measured from the bottom of the well. In that case the main term in Eq. (15) has the form

$$\delta J \approx [\Delta l^4 / 2(\beta\varepsilon_{\lambda_0}^0)^2][l^2/m^2 - 1].$$

This formula illustrates the strong dependence of the moment of inertia on the state occupied by the odd particle.

We discuss next the limiting value of J. In the limit as $\Delta \to 0$ $(\nu \to \infty)$, according to Migdal,[3] $J_e(\kappa) \to J_s$, and the second term in Eq. (14) tends to zero. This is understandable since in the case of a solid $\delta J/J_s \sim 1/A$ and terms of this order in A are not included in our formula.

Let us discuss the limitations on the permissible values of the parameters β and Δ imposed by the criterion of applicability of perturbation theory $\rho'_{\lambda\lambda'} \ll 1$. We assume that $\Delta \ll \epsilon_0 A^{-1/3} \sim \omega_0$, which is always valid for a nucleus. Since the perturbation V goes as $A^{2/3}/J$ (where $J \sim A^{5/3}/\epsilon_0$), it follows from the condition $\rho'_{\lambda_0\lambda} \ll 1$ that

$$\beta \gg A^{-2/3}, \quad \Delta \ll \varepsilon_0 A^{1/3}\beta^2. \tag{17}$$

For deformed nuclei these conditions are always satisfied ($\beta \sim A^{-1/3}$, $\Delta \sim \epsilon_0 A^{-2/3}$) and, therefore, perturbation theory is applicable.

The calculation of the difference of the moments of inertia of even and odd nuclei was carried out using the formula

$$\delta J = \sum_\lambda \frac{4\Delta |M^x_{\lambda_0\lambda}|^2}{\epsilon_\lambda^2} - \frac{2(g_1 + g_2)\nu_2^2 g_2}{\Delta(\nu_1^2 g_1 + \nu_2^2 g_2)^2}\left[n_z(N - n_z) + \frac{N + n_z}{2}\right]$$

$$+ J_e(\varkappa_o) - J_e(\varkappa_e). \tag{18}$$

The main term in expression (18) is the first term. It gives the principal dependence of δJ on the state of the odd nucleon λ_0. In deriving it no specific form was used for the nuclear potential. It was therefore calculated using the wave functions for the Nilsson potential,[6] which gives a good description of the state of the odd particle in a deformed nucleus. The second term in Eq. (18) was obtained by utilizing the oscillator potential. It contributes to δJ less than the first term (~ 25%) and, furthermore, depends rather smoothly on the state λ_0. Therefore the evaluation of the second term utilizing asymptotic wave functions of a deformed oscillator in the representation $(N, n_z, \Lambda, \Omega)$ introduces no significant errors.

Migdal[3] obtained an expression for $J_e(\kappa)$, where $\kappa = \hbar\omega_0\beta/2\Delta$ and $\hbar\omega_0 = 41\ A^{-1/3}$ Mev.[6] In order to calculate the difference $J_e(\kappa_o) - J_e(\kappa_e)$ it is necessary to know Δ_o, Δ_e, β_o, and β_e for neighboring nuclei. The quantity Δ may be obtained from data on nuclear masses and binding energies with an accuracy not better than 10 or 15%.[7] In many cases, particularly for odd proton nuclei, the necessary data for Δ do not exist. Therefore in those cases Δ was found by interpolation. In those cases when one of the neighboring Δ_e and Δ_o could not be determined directly we made use of the relation

$$\Delta_e = \Delta_o + 1/\rho_0,$$

where ρ_0 is the density of single-particle levels near the Fermi surface for particles of the given type. The values of β were taken from references 2, 8, and 9. Values of β corresponding to the neighboring nuclei were used in those cases when β was not known. The results of a comparison of theory and experiment are shown in Tables I and II. It is seen that the theory gives a satisfactory description of the dependence of the moments of inertia of odd nuclei on the state occupied by the odd particle. In several cases such a comparison may be useful for a classification of the state occupied by the odd nucleon in the Nilsson scheme. The tables also make it possible to estimate the quantity Δ in those cases when it is not known from other data.

The authors express their gratitude to S. T. Belyaev and A. B. Migdal for useful discussions.

APPENDIX

Let us find the solution of Eq. (7) for $\mathbf{f}'(\mathbf{r})$, under the assumption that the nonvanishing matrix elements $\mathrm{f}'_{\lambda\lambda'}$, similarly to $\mathrm{f}^0_{\lambda\lambda'}$, are quasi-classically equal for a given λ. Then utilizing the quasi-classical independence of $\varphi_\lambda\varphi^*_{\lambda'}$, $\dot{\mathrm{M}}_{\lambda\lambda'}$, $\mathrm{f}^0_{\lambda\lambda'}$, and $\mathrm{f}'_{\lambda\lambda'}$ on λ' for a fixed λ and employing the well known method[3] for evaluating the sums we reduce Eq. (7) to the form

$$\frac{1}{2}(\nu_1^2 g_1 + \nu_2^2 g_2) f'(\mathbf{r})\rho(\varepsilon_0, \mathbf{r})$$

$$= \frac{1}{4\Delta^2}\left(\frac{1}{\nu_1^2} + \frac{1}{\nu_2^2}\right)\dot{M}^x(\mathbf{r})|\varphi_{\lambda_0}|^2 + \frac{f^0(\mathbf{r})|\varphi_{\lambda_0}|^2}{\Delta}, \tag{A.1}$$

where $\rho(\epsilon_0, \mathbf{r})$ is the density of particles with energy ϵ_0. Introducing into Eq. (A.1) the expression

TABLE I. Relative change of the moments of inertia for nuclei with an odd number of neutrons

Nucleus	Classification of the state occupied by the odd particle $(N, n_z, \Lambda, \Omega)$	β_o	β_e	$\Delta_o^{(n)}$ Mev	$\Delta_e^{(n)}$ Mev	$\delta J/J_s$, %	
						Experiment	Theory
$_{64}\mathrm{Gd}^{155}$	$521\,{}^3/_2$	0.31	0.3	1	1.15	26	22
$_{64}\mathrm{Gd}^{157}$	$521\,{}^3/_2$	0.31	0.41	0.8	1	17	16
$_{66}\mathrm{Dy}^{161}$	$642\,{}^5/_2$	0.3	0.35	0.9	1.1	62	47
$_{66}\mathrm{Dy}^{161}$	$521\,{}^3/_2$	0.3	0.35	0.9	1.1	15	14
$_{66}\mathrm{Dy}^{161}$	$523\,{}^5/_2$	0.3	0.35	0.9	1.1	13	17
$_{66}\mathrm{Dy}^{163}$	$523\,{}^5/_2$	0.3	0.36	0.7	0.9	14	14
$_{68}\mathrm{Er}^{167}$	$633\,{}^7/_2$	0.29	0.33	0.7	0.9	27	23
$_{70}\mathrm{Yb}^{173}$	$512\,{}^5/_2$	0.28	0.31	0.6	0.8	7	9
$_{72}\mathrm{Hf}^{177}$	$514\,{}^7/_2$	0.27	0.29	0.6	0.75	7	9
$_{72}\mathrm{Hf}^{179}$	$624\,{}^9/_2$	0.26	0.31	0.6	0.75	16	12
$_{90}\mathrm{Th}^{229}$	$633\,{}^5/_2$	0.22	0.22	0.65	0.85	23	21
$_{90}\mathrm{Th}^{231}$	$633\,{}^5/_2$	0.23	0.23	0.67	0.87	21	20
$_{92}\mathrm{U}^{233}$	$633\,{}^5/_2$	0.24	0.24	0.43	0.67	17	16
$_{92}\mathrm{U}^{233}$	$631\,{}^3/_2$	0.24	0.24	0.43	0.67	17	15
$_{92}\mathrm{U}^{235}$	$743\,{}^7/_2$	0.24	0.24	0.62	0.81	22	22
$_{94}\mathrm{Pu}^{239}$	$743\,{}^7/_2$	0.26	0.26	0.44	0.71	28	20
$_{94}\mathrm{Pu}^{241}$	$622\,{}^5/_2$	0.27	0.27	0.35	0.44	7	5
$_{96}\mathrm{Cm}^{245}$	$624\,{}^7/_2$	0.26	0.26	0.5	0.7	8	5
		0.20	0.20	0.5	0.7	8	10
$_{96}\mathrm{Cm}^{245}$	$734\,{}^9/_2$	0.26	0.26	0.5	0.7	19	10
		0.20	0.20	0.5	0.7	19	20

TABLE II. Relative change of the moments of inertia for nuclei with an odd number of protons

Nucleus	N, n_z, Λ, Ω	β_o	β_e	$\Delta_o^{(p)}$ Mev	$\Delta_e^{(p)}$ Mev	$\delta J/J_s$, %	
						Experiment	Theory
$_{67}\mathrm{Ho}^{165}$	$523\,{}^7/_2$	0.32	0.39	0.8	0.9	8	15
$_{69}\mathrm{Tm}^{169}$	$523\,{}^7/_2$	0.35	0.34	0.78	0.9	13	21
$_{75}\mathrm{Re}^{183}$	$514\,{}^9/_2$	0.21	0.23	0.75	0.85	3	4
$_{75}\mathrm{Re}^{187}$	$402\,{}^5/_2$	0.19	0.24	0.75	0.85	2	3
$_{91}\mathrm{Pa}^{233}$	$642\,{}^5/_2$	0.24	0.24	0.5	0.6	112	35
$_{93}\mathrm{Np}^{237}$	$642\,{}^5/_2$	0.25	0.25	0.5	0.6	29	27
$_{93}\mathrm{Np}^{239}$	$642\,{}^5/_2$	0.26	0.26	0.5	0.65	33	29
$_{93}\mathrm{Np}^{237}$	$523\,{}^5/_2$	0.25	0.25	0.5	0.6	11	11
$_{93}\mathrm{Np}^{239}$	$523\,{}^5/_2$	0.26	0.26	0.5	0.65	10	12
$_{95}\mathrm{Am}^{241}$	$523\,{}^5/_2$	0.27	0.27	0.45	0.55	10	9
$_{95}\mathrm{Am}^{243}$	$523\,{}^5/_2$	0.27	0.27	0.45	0.55	11	9

for $f^0(\mathbf{r})$ from Eq. (12) we obtain

$$f' = \frac{\dot{M}^x(\mathbf{r})\,|\varphi_{\lambda_0}|^2}{2\Delta^2\rho(\epsilon_0,\mathbf{r})}\,\frac{(\nu_2^2-\nu_1^2)(g_1\nu_2^2-g_2\nu_1^2)}{\nu_1^2\nu_2^2(g_1\nu_1^2+g_2\nu_2^2)}.$$

Since $\rho(\epsilon_0, \mathbf{r})$ depends on $\mathbf{r}$ only weakly we have $\rho(\epsilon_0, \mathbf{r})V = \rho_0$, where ρ_0 is the level density at the Fermi surface, and V is the volume of the system. Since $|\varphi_{\lambda_0}|^2$ is a rapidly oscillating function it may be replaced by 1/2V. Thus the matrix $f'_{\lambda\lambda'}$ has the properties assumed in the derivation of $f'(\mathbf{r})$. Estimating f' for $\nu_1 \sim 1$, $\nu_2 \sim 10$ we find that

$$f'/f^0 \approx 1/2\rho_0\Delta \sim A^{-1/3}.$$

Consequently the function f' is quasiclassically small in comparison with f^0.

---

[1] D. Inglis, Phys. Rev. **97**, 701 (1955). A. Bohr and B. Mottelson, Dan. Mat. Fys. Medd. 30, 1 (1955). B. Mottelson and S. Nilsson, Dan. Mat. Fys. Skr. **1**, 8 (1959).

[2] O. Prior, Ark. Fysik **14**, 451 (1959).

[3] A. B. Migdal, JETP **37**, 249 (1959), Soviet Phys. JETP **10**, 176 (1960).

[4] S. Belyaev, Dan. Mat. Fys. Medd. **31**, 11 (1959).

[5] Grin', Drozdov, and Zaretskiĭ, JETP **38**, 222 (1959), Soviet Phys. JETP **11**, 162 (1960).

[6] S. Nilsson, Dan. Mat. Fys. Medd. **29**, 16 (1955).

[7] V. A. Kravtsov, Usp. Fiz. Nauk **65**, 3 (1958). A. H. Wapstra, Physica **21**, 367, 385 (1955). J. R. Huizenga, Physica **21**, 410 (1955).

[8] Alder, Bohr, Huus, Mottelson, and Winther, Revs. Modern Phys. **28**, 432 (1956).

[9] V. G. Nosov, JETP **37**, 886 (1959), Soviet Phys. JETP **10**, 631 (1960).

Translated by A. M. Bincer
245

SOVIET PHYSICS JETP VOLUME 11, NUMBER 4 OCTOBER, 1960

CONTRIBUTION TO THE THEORY OF ELECTRON GAS CONDUCTIVITY IN A STRONG MAGNETIC FIELD

V. G. SKOBOV

Leningrad Physico-Technical Institute, Academy of Sciences, U.S.S.R.

Submitted to JETP editor November 18, 1959

J. Exptl. Theoret. Phys. (U.S.S.R.) 38, 1304-1310 (April, 1960)

The conductivity of an electron gas in perpendicular electric and magnetic fields is investigated for $\omega\tau \gg 1$ (τ is the electron relaxation time, ω is the cyclotron frequency). Elastic scattering of electrons on fixed short-range force centers is considered. Interaction between the electrons and the scatterers is treated without the aid of perturbation theory. In the final result the conductivity is expressed as a function of the magnetic field and the exact amplitude for scattering of a zero energy electron on a single center in the absence of a magnetic field.

In the recent work of Adams and Holstein,[1] galvanomagnetic phenomena were studied in a strong magnetic field. Here, the interaction of the electrons with different scatterers was considered by the authors as a perturbation, which required the assumption of a finite width of the electron levels for the elimination of divergences that appear in the Born approximation.

In the present work, the conductivity of an electron gas is computed for a strong magnetic field in the case $\omega\tau \gg 1$, where τ is the relaxation time of the electrons, $\omega = eH/m$ (the system of units is used for which $\hbar = c = 1$). Only elastic scattering of the electrons on randomly-arranged immovable centers is considered; the radius of action of these centers is assumed to be small in comparison with the wavelength of the electrons and with the mean distance between scatterers. The interaction of the electrons with the scatterers is considered without the aid of perturbation theory, inasmuch as the Born approximation, strictly speaking, is not suitable at low energies. Limiting ourselves to the case in which the directions of the electric and magnetic fields are perpendicular, we begin our calculations with the general expression for the conductivity tensor obtained by Kubo:[2]

$$\sigma_{\mu\nu} = \frac{e^2}{\Omega}\int_0^\infty e^{-\epsilon t}dt\int_0^\beta d\lambda\,\mathrm{Sp}\,\{\rho v_\nu(-i\lambda)\,v_\mu(t)\},$$

$$\rho = \exp(-\beta\mathcal{H})/\mathrm{Sp}\exp(-\beta\mathcal{H}), \tag{1}$$

$\mathcal{H}$ is the total Hamiltonian of the system in the absence of an electric field; $v_\mu(t)$ is the Heisenberg operator of the μ component of the velocity of the electron; $\epsilon > 0$; $\beta = 1/kT$; Ω is the normalized volume; $\mu, \nu = x, y, z$. The diagonal elements of the tensor $\sigma_{\mu\nu}$ can be written in the much simpler form

$$\sigma_{\mu\mu} = \frac{\beta e^2}{\Omega}\,\mathrm{Re}\,\{\mathrm{Sp}\,\rho v_\mu(0)\,X_\mu\}, \tag{2}$$

$$X_\mu = \int_0^\infty e^{-\epsilon t}dt\,e^{i\mathcal{H}t}v_\mu(0)\,e^{-i\mathcal{H}t}. \tag{3}$$

For calculation of $\sigma_{\mu\nu}$, it is convenient to put the operator X_μ in the form

$$X_\mu = \frac{1}{2\pi}\int_{-\infty}^{+\infty} dE\,\frac{1}{E-\mathcal{H}-i\epsilon}\,v_\mu(0)\,\frac{1}{E-\mathcal{H}+i\epsilon}. \tag{4}$$

The identity of Eqs. (3) and (4) can easily be seen by taking their matrix elements in the representation of the Hamiltonian $\mathcal{H}$ and carrying out integration over t in (3) and integration over E in (4).

We shall now consider separately the cases of Boltzmann statistics and Fermi statistics.

1. NONDEGENERATE ELECTRON GAS

In this case, it can be assumed that $\mathcal{H}$ is the Hamiltonian of a single electron in the field of the scattering centers, i.e., $\mathcal{H} = \mathcal{H}_0 + V$, where

$$\mathcal{H}_0 = (\mathbf{p} - e\mathbf{A})^2/2m, \qquad V = \sum_i V_i.$$

Here **A** is the vector potential of the magnetic field **H**, V_i is the Hamiltonian of interaction of the electron with the i-th scattering center, located at the point $\mathbf{r}_i$.

We write the vector **A** in the form $A_x = A_z = 0$; $A_y = Hx$. The eigenfunctions and the eigenvalues of the operator $\mathcal{H}_0$ have the form

$$\Psi_{nk_yk_z}(\mathbf{r}) = \exp[i(k\ y + k_z z)]\varphi_n(x/l - lk_y),$$
$$E_{nk_z} = \omega(n+\tfrac{1}{2}) + k_z^2/2m,$$

where φ_n is the Hermite function of n-th order and $l = (eH)^{-1/2}$. The matrix elements of the operators $v_x(0)$ and $v_y(0)$ are determined by the formula

$$(n'k_y'k_z' \mid v_x(0) + iv_y(0) \mid nk_yk_z')$$
$$= -i(2\omega/m)^{1/2} n^{1/2} \delta_{n',n-1}\delta_{k_y'k_y}\delta_{k_z'k_z},$$
$$(n'k_y'k_z' \mid v_x(0) - iv\ (0) \mid nk_yk_z)$$
$$= i(2\omega/m)^{1/2}(n+1)^{1/2}\delta_{n',n+1}\delta_{k_y'k_y}\delta_{k_z'k_z}. \tag{5}$$

In what follows, we shall denote the sets of quantum numbers nk_yk_z by the Greek letters α, β, etc.

Following Luttinger and Kohn,[3] we introduce the "scattering operator" $T^{(\pm)}(E)$, which is determined by the relation

$$(E - \mathcal{H} \pm i\varepsilon)^{-1} = G_E^{(\pm)} + G_E^{(\pm)} T^{(\pm)}(E) G_E^{(\pm)},$$
$$G_E^{(\pm)} = (E - \mathcal{H}_0 \pm i\varepsilon)^{-1}. \tag{6}$$

The operator $T^{(\pm)}(E)$ can be written in the form of a series

$$T^{(\pm)}(E) = \sum_j T_j^{(\pm)}(E) + \sum_{j \neq k} T_j^{(\pm)}(E) G_E^{(\pm)} T_k^{(\pm)}(E) + \ldots, \tag{7}$$

where the "operator of scattering on the j-th center" $T_j^{(\pm)}(E)$ satisfies the integral equation

$$T_j^{(\pm)}(E) = V_j + V_j G_E^{(\pm)} T_j^{(\pm)}(E).$$

The matrix element $(\beta \mid T_j^{(+)}(E) \mid \alpha)$ for $E = E_\alpha$ is the amplitude of the transition from the state α to the state β in the scattering of the electron on the j-th center. In reference 4, the author calculated the amplitude of scattering of an electron of low energy on the short-range potential V in a strong magnetic field [it was assumed that the radius of action of the scattering potential $r_0 \ll (2mE)^{-1/2}$]. According to the results of reference 4,

$$(\beta \mid T_j^{(+)}(E_\alpha) \mid \alpha) = \Psi_\beta^*(\mathbf{r}_j)\Psi_\alpha(\mathbf{r}_j)\frac{2\pi f/m}{1 + ifK(E_\alpha)}, \tag{8}$$

where

$$K(E) = l^{-2}\sum_{n=0}^{N}[2m(E - n\omega - \omega/2)]^{-1/2},$$

f is the exact scattering amplitude of a zero energy free electron on the potential V; N in the expression for K is so defined that the last term in the sum over n would be purely imaginary.

By a method completely analogous to that used in reference 4 for the derivation of (8), it can be shown that the matrix elements $T_j^{(+)}(E)$ are determined by an expression similar to (8), i.e., that (8) maintains its force if we replace E by E_α in the argument of $T_j^{(+)}$ and in K. The matrix elements of the operator $T_j^{(-)}(E)$ are connected in simple fashion with the matrix elements of $T_j^{(+)}(E)$:

$$(\alpha \mid T_j^{(-)}(E) \mid \beta) = (\beta \mid T_j^{(+)}(E) \mid \alpha)^*.$$

Expressing X_μ and ρ in terms of the operator $T(E)$, determined by Eq. (7), one can compute the elements of the tensor $\sigma_{\mu\nu}$ for $\mu, \nu = x, y$. It is shown that in the approximation $\omega\tau \gg 1$ and $\beta^{-1}\tau \gg 1$, it is sufficient to consider a single scattering center and multiply the expression obtained in this case for the number of collisions of the electron per unit time by the number of such centers. Therefore, in what follows, in order to make the calculations clearer, we shall understand by $T(E)$ the scattering operator on a single center.

Substituting (4) in (3), we have

$$X_\mu = X_\mu^{(0)} + X_\mu^{(1)} + X_\mu^{(2)}.$$

Here $X_\mu^{(0)}$ does not depend on the operator $T(E)$; $X_\mu^{(1)}$ is proportional to the first power of $T(E)$, and $X_\mu^{(2)}$ is proportional to the second.

$$(\beta \mid X_\mu^{(0)} \mid \alpha) = i(\beta \mid v_\mu(0) \mid \alpha)/\omega_{\beta\alpha}. \tag{9}$$

$$(\beta \mid X_\mu^{(1)} \mid \alpha) = i\sum_\gamma \{(\beta \mid v_\mu(0) \mid \gamma)\frac{1}{\omega_{\beta\gamma}}(\gamma \mid T^{(+)}(E_\beta) \mid \alpha)\frac{1}{\omega_{\beta\alpha} + i\varepsilon}$$
$$- \frac{1}{\omega_{\alpha\beta} - i\varepsilon}(\beta \mid T^{(-)}(E_\alpha) \mid \gamma)\frac{1}{\omega_{\alpha\gamma}}(\gamma \mid v_\mu(0) \mid \alpha)\}, \tag{10}$$

where $\omega_{\alpha\beta} = E_\alpha - E_\beta$. In obtaining (10), we took it into account that $T^{(+)}(E)$ has a pole only in the lower half of the complex plane E, while $T^{(-)}(E)$ has a pole only in the upper half-plane. The operator X_μ has a simple physical meaning. $X_\mu^{(0)}$ is the operator of the μ-th coordinate of the electron relative to its center of rotation in the absence of collisions, while $X_\mu - X_\mu^{(0)}$ describes the mean change of X_μ under the action of the scattering of the electron on the potential V. We note that $X_\mu^{(0)}$ makes no contribution to $\sigma_{\mu\mu}$, inasmuch as the term corresponding to it is purely imaginary. One can generally omit $X_\mu^{(2)}$ in the calculation of $\sigma_{\mu\nu}$ in the approximation under consideration, since

$$\sum_{\alpha\alpha'} T^{(-)}(E) \mid \alpha)\frac{1}{E - E_\alpha - i\varepsilon}(\alpha \mid v_\mu(0) \mid \alpha')$$
$$\times \frac{1}{E - E_{\alpha'} + i\varepsilon}(\alpha' \mid T^{(+)}(E)$$

disappears on summation over the x coordinate of the center of rotation of the electron (l^2k_y), because of the orthogonality of Hermite functions of different order. We recall that only $\Psi_\alpha(\mathbf{R})$ and $\Psi^*_{\alpha'}(\mathbf{R})$, which enter into the matrix elements of the operators $T^{(+)}(E)$ and $T^{(-)}(E)$, depend on k_y; here **R** is the radius vector of the scattering center.

Let us consider the operator $\rho(\mathcal{H})$. We can represent the quantity $\exp(-\beta\mathcal{H})$ in it in the form

$$\exp(-\beta\mathcal{H}) = S(i\beta)\exp(-\beta\mathcal{H}_0),$$

where $S(i\beta)$ is determined by the equation

$$-\frac{\partial}{\partial\beta}S(i\beta) = S(i\beta)V(i\beta) \tag{11}$$

and the boundary condition $S(0) = 1$. By direct substitution it can easily be shown that the solution of (11) (with accuracy up to terms of higher order in the operator T') is given by the formula

$$(\alpha\,|\,S(i\beta)\,|\,\gamma) = \delta_{\alpha\gamma} - \frac{1-\exp(\beta\omega_{\gamma\alpha})}{\omega_{\gamma\alpha}}(\alpha\,|\,T'(E_\alpha)\,|\,\gamma), \tag{12}$$

where T' is determined by the integral equation

$$(\alpha\,|\,T'(E_\alpha)\,|\,\gamma) = (\alpha\,|\,V\,|\,\gamma) + \sum_\delta(\alpha\,|\,T'(E_\alpha)\,|\,\delta)\left(\frac{1}{\omega_{\alpha\delta}}\right)_P(\delta\,|\,V\,|\,\gamma);$$

(here the index P means that the integral over E is taken in the sense of the principal value). The solution of this equation differs from the matrix elements $(\alpha|T^{(\pm)}(E_\alpha)|\gamma)$ only in the fact that it does not contain $\operatorname{Re} K(E_\alpha)$.

Substituting the expressions (9), (10), and (12) obtained for X_μ and $\exp(-\beta\mathcal{H})$ in (1) and (2), we obtain, after tedious but elementary transformations,

$$\sigma_{xx} = \beta n_e e^2\sum_{\alpha\gamma}\rho_0(E_\alpha)\,|\,(\alpha\,|\,X^{(0)}\,|\,\gamma)\,|^2\,2\pi \times\sum_\lambda|\,(\gamma\,|\,T^{(+)}(E_\lambda)\,|\,\lambda)\,|^2\delta(E_\lambda - E_\alpha), \tag{13}$$

$$\sigma_{yx} = -n_e e^2/m\omega, \tag{14}$$

where

$$\rho_0(E) = Z^{-1}\exp(-\beta E), \qquad Z = \operatorname{Sp}\exp(-\beta\mathcal{H}_0),$$

n_e is the electron concentration. In the derivation of (13), we made use of the "optical theorem" for the operator $T(E)$:

$$-2\operatorname{Im}(\alpha\,|\,T^{(+)}(E)\,|\,\alpha) = 2\pi\sum|\,(\alpha\,|\,T^{(+)}(E_\beta)\,|\,\beta)\,|^2\,\delta(E_\beta - E)$$

and also of the fact that

$$\operatorname{Re}(\beta\,|\,T^{(+)}(E_\alpha)\,|\,\alpha)(\alpha\,|\,T'(E_\alpha)\,|\,\beta) = |\,(\beta\,|\,T^{(+)}(E_\alpha)\,|\,\alpha)\,|^2.$$

The validity of these expressions follows from the explicit form of the matrix elements of $T^{(+)}$ and T'.

Thus σ_{xx} and σ_{yy} are proportional to the mean square of the Larmor radius of the electron and to the frequency of collisions with the scatterers. Equation (14) shows that $Y^{(1)}$ makes no contribution to σ_{yx} in the given approximation, i.e., the average change of the y coordinate of the electron under action of the collisions is equal to zero if the electric field is directed along the x axis.

We shall compute σ_{xx} in two different limiting cases. Substituting (8) and (9) in (13), we have

$$\sigma_{xx} = \beta\frac{n_e e^2}{m\omega}\sum_\alpha\rho_0(E_\alpha)(n_\alpha + 1/2)\,\nu(E_\alpha), \tag{15}$$

$$\nu(E) = n_p\frac{4\pi f^2}{(1+fK'')^2 + (fK')^2}\,\frac{K'(E)}{m}. \tag{16}$$

We use here $K = K' - iK''$; n_p is the number of scatterers per unit volume. The quantity $\nu(E)$ is the total number of collisions of the electron with energy E per unit time. In the limiting case $\beta\omega \ll 1$, we have substantially $n_\alpha \approx (\beta\omega)^{-1}$ in (14), and the well-known classical formula

$$\sigma_{xx} \approx n_e e^2/m\omega^2\tau \tag{17}$$

is obtained for σ_{xx}, where

$$1/\tau = \sum_\alpha\rho_0(E\ )\,\nu(E_\alpha).$$

In the other limiting case $\beta\omega \gg 1$, if all the electrons are in states with $n_\alpha = 0$, σ_{xx} has the form

$$\sigma_{xx} \approx \beta\frac{n_e e^2}{m}\,n_p f^2\left(\frac{2\pi\beta}{m}\right)^{1/2}\operatorname{Ei}\left(\frac{\beta f^2}{4ml^4}\right). \tag{18}$$

Here,

$$\operatorname{Ei}(u) = \int_0^\infty\frac{dz}{z+u}\exp(-z),$$

that is, in the limiting quantum case, σ_{xx} is almost independent of the value of the magnetic field.

2. DEGENERATE ELECTRON GAS

In the case of Fermi statistics, it is appropriate to calculate in the second-quantization representation. We introduce the operators a^+_α of creation of an electron in the state α and the operators a_β of annihilation of an electron in the state β. The properties of these operators are defined by well-known commutation relations

$$a_\alpha a_\beta + a_\beta a_\alpha = \overset{+}{a}_\alpha\overset{+}{a}_\beta + \overset{+}{a}_\beta\overset{+}{a}_\alpha = 0, \qquad \overset{+}{a}_\alpha a_\beta + a_\beta\overset{+}{a}_\alpha = \delta_{\alpha\beta}.$$

The operators $\mathcal{H}$ and X_μ are single particle operators and have the form

$$\mathscr{H} = \mathscr{H}_0 + V, \qquad \mathscr{H}_0 = \sum_\alpha (E_\alpha - \zeta)\hat{n}_\alpha,$$

$$V = \sum_{\alpha \neq \beta} a_\alpha^+ a_\beta (\alpha | V | \beta), \qquad X_\mu = \sum_{\alpha\beta} a_\alpha^+ a_\beta (\alpha | X_\mu | \beta). \quad (19)$$

Here ζ is the chemical potential and $\hat{n}_\alpha = a_\alpha^+ a_\alpha$ is the operator of the number of electrons in the state α.

The operator $\exp(-\beta\mathscr{H})$ can, as in the nondegenerate case, be written in the form

$$\exp(-\beta\mathscr{H}) = S(i\beta)\exp(-\beta\mathscr{H}_0).$$

where, under the given approximation $(\omega\tau \gg 1)$,

$$S(i\beta) = 1 + \sum_{\alpha\gamma} a_\alpha^+ a_\gamma \frac{1 - \exp(\beta\omega_{\gamma\alpha})}{\omega_{\gamma\alpha}} (\alpha | T'(E_\alpha) | \gamma). \quad (20)$$

We now substitute (19) and (20) in (1) and (2), and make use of the relations

$$Z^{-1}\,\mathrm{Sp}\,[e^{-\beta\mathscr{H}_0}\hat{n}_\alpha] = f(E_\alpha),$$

$$Z^{-1}\,\mathrm{Sp}\,[e^{-\beta\mathscr{H}_0}\hat{n}_\alpha\hat{n}_\gamma] = f(E_\alpha)f(E_\gamma) \qquad (\alpha \neq \gamma)$$

etc. where $f(E)$ is the Fermi function.

Carrying out transformations similar to those used in the derivation of (13), and making use of the identity

$$f(E_\alpha) - f(E_\gamma) = [1 - \exp(\beta\omega_{\alpha\gamma})]f(E_\alpha)[1 - f(E_\gamma)],$$

$$\beta f(E)[1 - f(E)] = df(E)/d\zeta,$$

we get

$$\sigma_{xx} = \sigma_{yy} = \frac{e^2}{\Omega}\sum_\alpha \frac{df(E_\alpha)}{d\zeta} l^2 (n_\alpha + 1/2)\nu(E_\alpha), \quad \sigma_{yx} = -n_e e^2/m\omega, \quad (21)$$

where $\nu(E)$ is given by Eq. (16).

In the limiting quantum case $1 \ll \beta(\zeta - \omega/2) < \beta\omega$, all the electrons are found in states with $n = 0$, and we get

$$\sigma_{xx} = \frac{1}{4\pi}\frac{n_p e^2 f^2 \omega}{\zeta - \omega/2} \quad (22)$$

from Eq. (21) with the aid of (16).

In order to obtain the final expression for the conductivity, it is still necessary to take into account the dependence of the chemical potential ζ on the magnitude of the magnetic field. This dependence can easily be found from the condition

$$n_e(\zeta) = n_e^{(0)}(\zeta_0).$$

Here $n_e^{(0)}$ and ζ_0 are the electron concentration and the chemical potential in the absence of the magnetic field, respectively. In the case under study,

$$\zeta - \omega/2 = 4\zeta_0^3/9\omega^2$$

and the final expression for σ_{xx} has the form

$$\sigma_{xx} = 9n_p e^2 f^2 \omega^3 / 16\pi\zeta_0^3. \quad (23)$$

In the case $\omega \ll \zeta$, (21) can be reduced to the form

$$\sigma_{xx} = \frac{e^2}{(2\pi)^2}\left(\frac{2m}{\omega}\right)^{1/2} \int_{\omega/2}^{\infty} dE \frac{df(E)}{d\zeta} I(E)\nu(E), \quad (24)$$

where

$$I(E) = \sum_n \frac{n + 1/2}{(E/\omega - n - 1/2)^{1/2}}.$$

The summation is carried out over all n for which the radicand is non-negative.

For computation of K' and I, we introduce the notation $E = \omega(N + \epsilon + \frac{1}{2})$, where N is an integer, $0 \leq \epsilon < 1$, and make use of the summation formula of Poisson, which is written in the form

$$\sum_{k=-\infty}^{+\infty} \exp(i2\pi kx) = \sum_{n=-\infty}^{+\infty} \delta(x - n). \quad (25)$$

Multiplying (25) by the function $\varphi(x)$, and integrating over x from 0 to $N + \epsilon$, we get

$$\sum_{n=0}^{N} \varphi(n) = \frac{1}{2}\varphi(0) + \sum_{k=-\infty}^{+\infty} \int_0^{N+\varepsilon} dx\,\varphi(x)\exp(i2\pi kx).$$

By means of this formula, it is not difficult to obtain an expression for I and K' in the case $N \gg 1$:

$$I(E) \approx \frac{4}{3}\left(N + \varepsilon + \frac{1}{2}\right)^{3/2}\left[1 + \frac{3}{2}\left(N + \varepsilon + \frac{1}{2}\right)^{-1/2} \times \sum_{k=1}^{\infty} \frac{\cos(2\pi k\varepsilon - \pi/4)}{(2k)^{1/2}}\right],$$

$$K'(E) \approx (2m\omega)^{1/2}\left(N + \varepsilon + \frac{1}{2}\right)^{1/2}\left[1 + \left(N + \varepsilon + \frac{1}{2}\right)^{-1/2} \times \sum_{k=1}^{\infty} \frac{\cos(2\pi k\varepsilon - \pi/4)}{(2k)^{1/2}}\right]. \quad (26)$$

As ϵ tends to zero, the behavior of the series appearing in Eq. (26) is accurately described by the function $\frac{1}{2}\epsilon^{-1/2}$. This function serves as an integrating factor; therefore in integration over E in (24), we can neglect the departure of the denominator of (16) from unity, for all terms except the term corresponding to the product of the series entering into (26). As a result, the product $I(E)\nu(E)$ can be written in the form

$$\left(\frac{E}{\omega}\right)^2\left[1 + \frac{5}{2}\left(\frac{\omega}{E}\right)^{1/2} \sum_{k=1}^{\infty} \frac{\cos(2\pi k\varepsilon - \pi/4)}{(2k)^{1/2}} + \frac{3\omega}{4E}\frac{1}{2\varepsilon + f^2/l^2}\right]$$

with accuracy to within a common factor.

Expanding the last component in the brackets in a Fourier series and integrating over E in (24) for the case $1 < \beta\omega \ll \beta\zeta$, we obtain

$$\sigma_{xx} \approx \frac{8}{3\pi} e^2 n_p f^2 \left(\frac{\zeta}{\omega}\right)^2 \left\{ 1 + \frac{3}{8}\frac{\omega}{\zeta} \ln \frac{2l^2}{f^2} + \sum_{k=1}^{\infty} (-1)^k \left[A_k \cos\left(\frac{2\pi k\zeta}{\omega} - \frac{\pi}{4}\right) + B_k \cos\left(\frac{2\pi k\zeta}{\omega}\right)\right]\right\}, \quad (27)$$

where

$$A_k = \frac{2\pi^2 k}{\beta\omega \sinh(2\pi^2 k/\beta\omega)} \frac{5}{2}\left(\frac{\omega}{\zeta}\right)^{1/2} (2k)^{-1/2},$$

$$B_k = -\frac{2\pi^2 k}{\beta\omega \sinh(2\pi^2 k/\beta\omega)} \frac{3\omega}{4\zeta} \operatorname{Ci}\left(\frac{\pi k f^2}{l^2}\right).$$

The asymptotic expression of the cosine integral has the form

$$\operatorname{Ci} z \approx \ln \gamma z \qquad (z \ll 1), \qquad \gamma = 1.7\ldots,$$

for small values of the argument; therefore the term in the conductivity proportional to B_k can play an important role, especially if ω/ζ is not too small.

In conclusion, I express my thanks to L. É. Gurevich for suggesting the topic and for constant interest in the work, and to S. V. Maleev for useful discussions.

---

[1] E. N. Adams and T. D. Holstein, J. Phys. Chem. Solids **10**, 254 (1959).

[2] R. Kubo, J. Phys. Soc. Japan **12**, 570 (1957).

[3] J. M. Luttinger and D. W. Kohn, Phys. Rev. **109**, 1892 (1958).

[4] V. G. Skobov, JETP **37**, 1467 (1959), Soviet Phys. JETP **10**, 1039 (1960).

Translated by R. T. Beyer
246

SOVIET PHYSICS JETP VOLUME 11, NUMBER 4 OCTOBER, 1960

ROTATIONAL ENERGY AND MOMENTS OF INERTIA OF NON-AXIAL NUCLEI

A. S. DAVYDOV, N. S. RABOTNOV, and A. A. CHABAN

Moscow State University

Submitted to JETP editor November 19, 1959

J. Exptl. Theoret. Phys. (U.S.S.R.) **38**, 1311-1315 (April, 1960)

It is shown that if the moments of inertia of a non-axially symmetric nucleus depart from their hydrodynamic values, then there is but little change in the dependence of the ratios of the energies of rotational levels on the ratio of the energies of two rotational states with spin 2.

1. Davydov and Filippov[1] and Davydov and Rostovskiĭ[2] have developed a theory of the rotational states of nuclei which do not have axial symmetry. It was shown that the ratios of the energies of the rotational states to the energy of the first excited state with spin 2 were uniquely determined, provided that the same ratio was known for the second level with spin 2. It was also demonstrated that the relative probabilities of electric quadrupole transitions between the rotational levels are also uniquely determined by the same energy ratio.

These results follow from two simplifying assumptions: a) the internal state of the nucleus does not change when it rotates (the adiabatic approximation) and b) the principal moments of inertia of the nucleus can be expressed in terms of only two parameters, A and γ, through the equations

$$I_i = A \sin^2(\gamma - 2\pi i / 3) \qquad (i = 1, 2, 3). \tag{1}$$

Such a relation between the moments of inertia and γ holds in the hydrodynamic model of the nucleus, and we shall refer to this approximation as the hydrodynamic approximation.

It is natural to wonder how much the results obtained in references 1 and 2 depend on the simplifying assumptions. MacDonald[3]* has used the relation

$$I_i = I_i^H [(I_i^H / I_i^R)^{1/2} + p]^{-2}, \tag{2}$$

where I_i^R are the moments of inertia of the solid body, I_i^H are the moments of inertia that coincide with (1) when $A = 4B\beta^2$, and where p is a new parameter, taken to be 0.1 or 0.2. The relation (2) has the property that $I_i = I_i^R$ as $p \to 0$; for $p \neq 0$ and $\gamma \to 0$, the moment $I_3 \to 0$; for $p \neq 0$ and $\beta \to 0$, all $I_i \to 0$.

Formula (2) can be considered an empirical one, taking into account the departure of the moments of inertia from their hydrodynamic values. MacDonald considered only levels with spin 2. It will be shown below that in this case it is impossible to say which is the more important, the nonadiabaticity or the deviations of the moments of inertia from their hydrodynamic values.

In this paper we consider, in the adiabatic approximation, the rotational states of non-axial nuclei having arbitrary moments of inertia. We shall show that in the general case the ratios of the rotational energy levels can be expressed through two parameters: ξ – the ratio of the energies of two spin-2 levels, and η – a parameter that depends on the nature of the collective motions which define the rotation of the nucleus. A comparison of our results with experiment shows that the hydrodynamic approximation is good enough for computing the ratios of rotational energy levels. Discrepancies between theory and experiment are due to an interaction between the rotation and the internal state of the nucleus.

2. In the adiabatic approximation, the rotational energy operator for a non-axial even-even nucleus is

$$H = \tfrac{1}{2} \sum_{i=1}^{3} a_i J_i^2 ,$$

where $a_i = \hbar^2/I_i$; the J_i are the projections of the angular momentum on the principal direction in the nucleus, while the I_i are its principal moments of inertia.

As was pointed out in reference 1, the rotation states of an even-even nucleus are related to the totally-symmetric representation of the D_2 group; only such states will be considered here. It is easy to show that the energy of a rotational state of spin 2 is determined by the equation

$$E^2 - 2(a_1 + a_2 + a_3)E + 3(a_1a_2 + a_1a_3 + a_2a_3) = 0.$$

---

*The authors would like to thank N. MacDonald for sending a preprint of his paper prior to publication.

If $E_1(2)$ and $E_2(2)$ are the roots of this equation, then it follows that

$$\Sigma a_i / E_1(2) = \tfrac{1}{2}(1+\xi), \quad (a_1a_2 + a_1a_3 + a_2a_3) / E_1^2(2) = \tfrac{1}{3}\xi, \tag{3}$$

where

$$\xi = E_2(2) / E_1(2) > 1.$$

The energies of all rotational states will be written in terms of the dimensionless quantity $\epsilon = E/E_1(2)$. Then the energies of rotational states with spin 3 and 5 can be expressed in terms of the experimentally-measureable ratio ξ through the formulas

$$\varepsilon(3) = 1 + \xi, \qquad \varepsilon_1(5) = 4 + \xi, \qquad \varepsilon_2(5) = 1 + 4\xi.$$

The energies of rotational states with other values of the spin depend not only on the parameter ξ but also on another parameter η,

$$\eta = a_1a_2a_3 / E_1^3(2). \tag{4}$$

For example, the energies of levels with spin 4 and 6 are given by

$$\varepsilon^3 - 5(1+\xi)\varepsilon^2 + 4[\xi^2 + \tfrac{19}{3}\xi + 1]\varepsilon - 40[\tfrac{1}{3}\xi(1+\xi) + 7\eta] = 0,$$

$$\varepsilon^4 - 14(1+\xi)\varepsilon^3 + 49[1 + 4\xi + \xi^2]\varepsilon^2 - [36(\xi^3+1) + 578\xi(1+\xi) + 3888\eta]\varepsilon + [252\xi(1+\xi^2) + 889\xi^2 + 13608(1+\xi)\eta] = 0.$$

If the moments of inertia are determined by formula (1), then

$$\eta = \eta_{\text{hydr}} = \xi^2 / 18(1+\xi),$$

and the energies of all rotational states depend only on ξ, which in this case is greater than or equal to 2. In general, however, there is a second parameter η, whose values lie in a certain interval determined by ξ.

To find the limits of the variation of η with ξ, we note that according to (3) and (4) the quantities $a_i/E_1(2)$ $(i = 1, 2, 3)$ are the roots of the cubic equation

$$x^3 - \tfrac{1}{2}(1+\xi)x^2 + \tfrac{1}{3}\xi x - \eta = 0.$$

The condition that the roots of this equation be real and positive implies that η must lie in the following intervals, whose end points depend on ξ:

$$\xi^2(3-\xi) \leqslant 54\eta \leqslant 3\xi - 1 \qquad (1 < \xi \leqslant 3),$$

$$0 \leqslant 54\eta \leqslant 3\xi - 1 \qquad (\xi \geqslant 3). \tag{5}$$

Figure 1 shows the ratios $\epsilon_1(4)$ and $\epsilon_2(4)$ as functions of ξ for various values of η satisfying the inequalities (5). The cross hatched area is bounded by two curves, $\eta_{\text{hydr.}}$ (corresponding to the hydrodynamic approximation) and η_{MD} (corresponding to moments of inertia determined by (2) with $\beta = p = 0.2$). Figure 2 shows $\epsilon_1(6)$ as a function of ξ and η, for the range defined by (5).

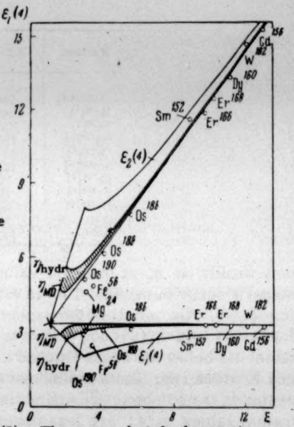

FIG. 1. Possible values of the ratios $\varepsilon_1(4)$ and $\varepsilon_2(4)$ for various values of the parameters ξ and η.

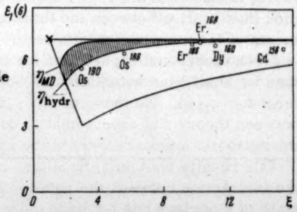

FIG. 2. Possible values for the ratio $\varepsilon_1(6)$ for various values of the parameters ξ and η.

It should be noted, naturally, that the values of η in (5) correspond to all possible ratios of the principal moments of inertia, including some that are utterly unrealistic. For example, in Figs. 1 and 2, the point marked with a cross corresponds to the rotation of the nucleus as a rigid sphere ($I_1 = I_2 = I_3$; $\xi = 1$); in such cases η is zero or close to it.

At present it is considered that the moments of inertia in the nucleus are intermediate between their hydrodynamic values and those obtaining for a rigid body. Hence the actual ratios of the moments of inertia correspond apparently to values of η for which the energy ratios $\epsilon_i(J)$ are displaced from their hydrodynamic values toward the cross hatched area. Taking this into account, we conclude that the energy ratios $\epsilon_i(J)$ depend

Experimental results for the ratios ϵ

Nucleus	$E_1(2)$ (kev)	ξ	$\varepsilon(3)$	$\varepsilon_1(4)$	$\varepsilon_2(4)$	$\varepsilon_1(6)$
Os^{190}[4,6]	186.7	2.99	4.04	2.94	5.12	5.61
Mg^{24}[4]	1368	3.09	3.82	3.01	4.61	—
Fe^{56}[7]	845	3.49	4.54	2.47	4.85	—
Os^{188}[5]	155	4.09	5.10	3.08	6.17	—
Os^{186}[5]	137,2	5,60	6,63	3.16	7,73	6.33
Sm^{152}[5]	122.3	8.92	10.14	3.01	11.68	—
Er^{166}[8]	80,7	9,76	10,67	3.29	11.87	6.76
Er^{168}[8]	79,9	10,29	11,22	3,31	12.47	6.86
Dy^{160}[9]	87,0	11.16	12.11	3,27	13,35	6.70
Gd^{156}[4,5]	89,0	13,01	14,0	3.24	15.34	6.56
W^{182}[5]	100.9	12.11	13.20	3,26	14.68	—

only weakly on η, at least for values of η which actually occur in nuclei. This is especially true for $\xi \geq 4$. Almost all of the experimental values for $\epsilon_1(4)$ and $\epsilon_1(6)$ now known to us (see the table) lie below the cross hatched area in Figs. 1 and 2, which represents the theoretically allowed region in the adiabatic approximation. The experimental values $\epsilon_2(4)$ are less than the theoretically predicted ones for all values of η satisfying the inequalities (5). This shows that the agreement between theory and experiment cannot be improved by modifying the moments of inertia so that they lie somewhere between the hydrodynamic ones and those corresponding to a rigid body. Furthermore, it follows from Fig. 1 that if we formally pick those ratios between the three principal moments of inertia which minimize the disagreement between theory and experiment for the ratios $\epsilon_1(4)$, then we shall have automatically worsened the agreement for $\epsilon_2(4)$. We thus conclude that the difference between theory and experiment is due to the use of the adiabatic approximation in the calculations.

Our results lead us to hope that corrections for the interaction between the rotation and the internal state of a nucleus can be made using the hydrodynamic-model dependence of the moments of inertia on the parameter γ, which describes the departure of the nucleus from axial symmetry. The values of the relative energies $\epsilon_1(4)$, $\epsilon_2(4)$ and $\epsilon_1(6)$ are much less sensitive to departures of the parameter η from its hydrodynamic value than they are to deviations from the adiabatic condition.

---

[1] A. S. Davydov and G. F. Filippov, JETP **35**, 440 (1958), Soviet Phys. JETP **8**, 303 (1959); Nucl. Phys. **8**, 237 (1958).

[2] A. S. Davydov and V. S. Rostovskiĭ, JETP **36**, 1788 (1959), Soviet Phys. JETP **9**, 1275 (1959); Nucl. Phys. **12**, 58 (1959).

[3] N. MacDonald, Nucl. Phys. **14**, 70 (1959).

[4] B. S. Dzhelepov and L. K. Peker, Схемы распада радиоактивных ядер (Decay Schemes for Radioactive Nuclei), U.S.S.R. Acad. Sci., 1958.

[5] B. S. Dzhelepov and L. K. Peker, Возбужденные состояния радиоактивных ядер (Excited States of Radioactive Nuclei), preprint RP-218, Joint Inst. Nuc. Res.

[6] Nielsen, Poulsen, Sheline, and Jensen, Nucl. Phys. **10**, 475 (1959).

[7] S. Cook, Nucl. Phys. **7**, 480 (1958).

[8] Jacob, Mihelich, Harmatz, and Handley, Bull. Am. Phys. Soc. **3**, 358 (1958).

[9] E. P. Grigor'ev and M. P. Avotina, Izv. Akad. Nauk SSSR, Ser. Fiz. **24**, 324 (1960), Columbia Tech. Transl., in press.

Translated by R. Krotkov
247

SOVIET PHYSICS JETP VOLUME 11, NUMBER 4 OCTOBER, 1960

ON THE EQUILBRIUM SHAPE OF ATOMIC NUCLEI

G. F. FILIPPOV

Moscow State University

Submitted to JETP editor November 19, 1959

J. Exptl. Theoret. Phys. (U.S.S.R.) **38**, 1316-1319 (April, 1960)

The equilibrium shape of atomic nuclei has been found for the case when the deformations are small and the external nucleons do not interact among themselves.

IN the initial phases of the development of the collective model of A. Bohr and Mottelson[1] it was assumed that the equilibrium shape of deformed atomic nuclei has an axis of symmetry. With this assumption it was possible to explain the properties of the experimentally observed rotational excitations.[2] A number of calculations[3,4] also confirmed this hypothesis. However, as new experimental data accumulated, there appeared in the rotational spectra of some nuclei certain anomalies, which could not be accounted for by introducing simple corrections to the rotational states corresponding to an axially symmetric equilibrium shape. These anomalies become understandable if their appearance is related to deviations of the equilibrium shape from axial symmetry.[5,6] In this connection it becomes necessary to reconsider the theoretical evidence for the existence of a symmetry axis in deformed nuclei which has up to now appeared in the literature.

The problem of the equilibrium shape of a nucleus with a single external nucleon has been investigated by A. Bohr.[3] The operator for the energy of the interaction of the external nucleon with the deformations of the core was chosen in the form

$$H_{int} = (k\beta / j(j+1))[\cos\gamma(3j_\zeta^2 - j^2) + \sqrt{3}\sin\gamma(j_\xi^2 - j_\eta^2)], \tag{1}$$

where k is some constant of the order of magnitude of the kinetic energy of the outer nucleon; j is the total angular momentum of the outer nucleon; j_ξ, j_η, and j_ζ are its projections on the axes fixed in the core; β and γ are collective coordinates which characterize the deviation of the shape of the nuclear core from spherical symmetry. Expression (1) is valid for the case in which the spin-orbit interaction of the external nucleon is large in comparison with H_{int}, so that the angular momentum j is an approximate integral of the motion.

Averaging the operator H_{int} over the coordinates of the external nucleon, we can find the interaction energy ϵ as a function of the coordinates of the core β and γ and then determine the values of β and γ for which $\epsilon(\beta, \gamma)$ summed with the potential energy of the free oscillations of the core, $V(\beta) = \frac{1}{2}C\beta^2$, has a minimum. These values of β and γ determine the equilibrium shape of the core completely.

To simplify the problem further, A. Bohr assumed that the equilibrium shape of the core is axially symmetric. Then not only j, but also j_ζ (the symmetry axis coincides with the ζ axis) becomes an approximate integral of the motion, and H_{int} is to be averaged over the state of the external nucleon with a definite angular momentum j and definite projection j_ζ on the ζ axis of the core.

Let $j_\zeta = \Omega$ and $\Phi(j, \Omega)$ be the wave function of the outer nucleon; then

$$\varepsilon_{\Omega 0}(\beta, \gamma) = (\Phi(j, \Omega) | H_{int} | \Phi(j, \Omega)) \equiv (j, \Omega | H_{int} | j, \Omega)$$
$$= (k\beta / j(j+1)) \cos\gamma (3\Omega^2 - j(j+1)). \tag{2}$$

It is easily seen that the interaction energy $\epsilon_{\Omega 0}(\beta, \gamma)$ has a minimum for $\gamma = 0$, if $3\Omega^2 - j(j+1) < 0$, and for $\gamma = \pi$, if $3\Omega^2 - j(j+1) > 0$.

This result, therefore, would seem to justify the initial assumption about the axial symmetry of the equilibrium shape. This, however, is not actually the case: the energy of the interaction of the external nucleon with the deformations of the core has been computed only in first order of perturbation theory, and we must know the contribution from higher-order terms.

In second-order perturbation theory the correction to the interaction energy due to the nondiagonal (with respect to j) terms of the operator H_{int} is different from zero. This correction $[\epsilon_{\Omega 1}(\beta, \gamma)]$ is always negative, since we are interested in the equilibrium shape of the ground state of the nucleus: moreover, it is proportional to $\beta \sin^2\gamma$, so that we can write it in the form

$$\varepsilon_{\Omega 1}(\beta,\gamma) = -b\beta\sin^2\gamma,$$

where $b > 0$.

Similarly we write

$$\varepsilon_{\Omega 0}(\beta,\gamma) = a\beta\cos\gamma,$$

where we set $a > 0$ for definiteness. Then

$$\varepsilon(\beta,\gamma) \approx \varepsilon_{\Omega 0}(\beta,\gamma) + \varepsilon_{\Omega 1}(\beta,\gamma) = a\beta\cos\gamma - b\beta\sin\gamma. \quad (3)$$

At the point $\gamma = \pi$ the interaction energy will have a minimum even if $\epsilon_{\Omega 1}(\beta,\gamma)$ is included, so long as $\frac{1}{2}a - b > 0$. If the opposite inequality holds, we obtain a maximum instead of a minimum. The quantity $\frac{1}{2}a - b$ depends on j and Ω. Therefore, a special investigation is required for each nucleon state in order to find the value of $\frac{1}{2}a - b$.

Bohr's proof of the existence of an axis of symmetry for a nucleus with a single external nucleon can therefore not be considered completely correct. There is still less justification for taking this proof over for the case of nuclei with a large number of nucleons.

Birbrair, Peker, and Sliv[4] showed under very general assumptions that $\partial\epsilon/\partial\gamma = 0$ for $\gamma = 0, \pi$.

However, from this it is also impossible to draw any conclusions about the axial symmetry of the equilibrium shape of the nucleus, since we must still find the sign of the second derivative.

For a more exact solution of the problem of the equilibrium shape of a nucleus with a single external nucleon, we do not make Bohr's assumption about the axial symmetry of the equilibrium shape, but keep all other restrictions. We seek the wave function of the external nucleon in the form of a superposition of states with different values of j and require that it be an eigenfunction of the operator H_{int}. As a result, we obtain the secular equation

$$|\varepsilon\delta_{\Omega\Omega'} - (j,\Omega\,|\,H_{int}\,|\,j,\Omega')| = 0, \quad (4)$$

the roots of which are the average values of the interaction energy in the $\frac{1}{2}(2j+1)$ different states of motion of the outer nucleon.

The diagonal matrix elements of the operator H_{int} were introduced above [Eq. (2)]. Among the nondiagonal elements, the following are different from zero:

$$(j,\Omega\,|\,H_{int}\,|\,j,\Omega+2) = (j,\Omega+2\,|\,H_{int}\,|\,j,\Omega)$$
$$= (k\beta/2j(j+1))\sin\gamma\,[3(j-\Omega)(j-\Omega-1)$$
$$\times(j+\Omega+1)(j+\Omega+2)]^{1/2}. \quad (5)$$

The secular equations for different values of j are easily found:

$$x = 0 \quad (j = 1/2), \quad (6a)$$

$$x^2 - 9 = 0 \quad (j = 3/2), \quad (6b)$$

$$x^3 - 84x - 160\cos 3\gamma = 0 \quad (j = 5/2), \quad (6c)$$

$$x^4 - 378x^2 - 1728\,x\cos 3\gamma + 8505 = 0 \quad (j = 7/2), \quad (6d)$$

$$x^5 - 1188x^3 - 9504\cos 3\gamma x^2 + 171072x$$
$$+ 1119744\cos 3\gamma = 0 \quad (j = 9/2), \quad (6e)$$

$$x^6 - 3003x^4 - 36608\,x^3\cos 3\gamma$$
$$+ 1550835x^2 + 22214400\,x\cos 3\gamma$$
$$- 63149625 + 39424000\cos^2 3\gamma = 0 \quad (j = 11/2). \quad (6f)$$

The ϵ and x belonging to a given j are connected by the relation $\epsilon = k\beta x/j(j+1)$.

The solutions of equations (6c) to (6e) are shown in Figs. 1 to 3 as functions of γ. It is easily seen that a single external nucleon in the states under consideration leads to an axially-symmetric deformation. The exact solution, therefore, gives the same result as the approximate treatment of A. Bohr.

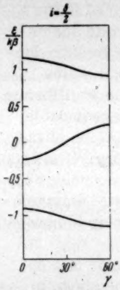

FIG. 1

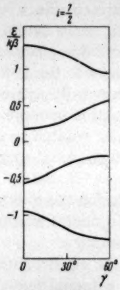

FIG. 2

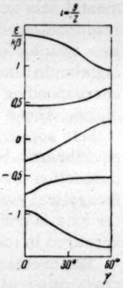

FIG. 3

Let us now turn our attention to many-particle configurations. If only one of the shells is filled, the equilibrium shape of the nucleus will remain axially symmetric as before. The only exception to this is the configuration with three nucleons in the $j = 5/2$ shell, which has an energy minimum at $\gamma = \pi/6$. It is noteworthy, however, that if the shell is less than half-filled the interaction energy has a minimum at $\gamma = \pi/3$ (oblate ellipsoid of revolution) and a maximum at $\gamma = 0$ (prolate ellipsoid of revolution). Once the shell is more than half-filled, the maximum and minimum change places. Special consideration must therefore be given to those nuclei in which the external nucleons fill up less than half of one shell and more than half of another.

By direct calculation, using the curves of Figs.

1 to 3, we convince ourselves that the configurations

$$(^5/_2)^1\,(^7/_2)^{-1},\quad (^5/_2)^1\,(^7/_2)^{-3},\quad (^5/_2)^2\,(^7/_2)^{-1},$$

$$(^5/_2)^2\,(^7/_2)^{-2},\quad (^5/_2)^2\,(^7/_2)^{-3},\quad (^5/_2)^1\,(^9/_2)^{-1}$$

etc. correspond to an equilibrium shape without axial symmetry. As an example we show in Fig. 4 the interaction energy ϵ_1 corresponding to four nucleons in the $j = ^5/_2$ shell, the energy ϵ_2 corresponding to two nucleons in the $j = ^7/_2$ shell, and the total energy $\epsilon = \epsilon_1 + \epsilon_2$, which has a minimum at the point $\gamma \approx ^2/_3\pi$.

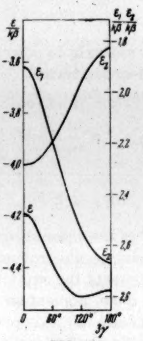

FIG. 4

We have shown, therefore, that the many-particle configurations lead in many cases to a non-axially symmetric equilibrium shape. To realize these configurations it is necessary that the neutrons and protons fill different shells, as is indeed the case in heavy and intermediate nuclei.

In the case of strongly deformed nuclei H_{int} cannot be regarded as a small quantity, so that our calculations cannot be directly applied. However, the qualitative result illustrated by Figs. 1 to 3 should be preserved in the case of strong deformations: the energy of one part of the states of the external nucleon is a minimum for an axially symmetric oblate shape of the core and a maximum for a prolate shape, while the energy of another part of the states of the external nucleon has the opposite behavior — it has a maximum for an axially symmetric oblate shape and a minimum for a prolate shape. Even for strongly deformed nuclei there exist, therefore, configurations in which the competition between the external nucleons leads to a non-axially symmetric shape. This is confirmed by the calculations of Gursky,[7] Geĭlikman,[8] and Zaikin,[9] who considered the equilibrium deformation of the core using explicit forms of the single particle potential but neglecting the spin-orbit interaction.

In many-particle configurations the motions of the external nucleons may turn out to be strongly correlated, which leads to an additional interaction of the nucleons with the deformations of the core. The equilibrium shape for one of the possible types of correlations was investigated earlier.[10]

In conclusion the author thanks A. S. Davydov for valuable comments.

---

[1] A. Bohr and B. Mottelson, Kgl. Danske Videnskab. Selskab, Mat.-Fys. Medd. **27**, Nr. 16 (1953).

[2] Alder, Bohr, Huus, Mottelson, and Winther, Revs. Modern Phys. **28**, 432 (1956).

[3] A. Bohr, Kgl. Danske Videnskab. Selskab, Mat.-Fys. Medd. **26**, Nr. 14 (1953).

[4] Birbrair, Peker, and Sliv, JETP **36**, 803 (1959), Soviet Phys. JETP **9**, 566 (1959).

[5] A. S. Davydov and G. F. Filippov, JETP **35**, 440 and 703 (1958), Soviet Phys. JETP **8**, 303 (1959).

[6] D. van Patter, Nucl. Phys. **14**, 42 (1959/60).

[7] M. Gursky, Phys. Rev. **98**, 1205 (1955).

[8] B. T. Geĭlikman, JETP **35**, 989 (1958), Soviet Phys. JETP **8**, 690 (1959).

[9] D. A. Zaikin, JETP **35**, 529 (1958), Soviet Phys. JETP 8, 365 (1959).

[10] A. S. Davydov and G. F. Filippov, JETP **36**, 1497 (1959), Soviet Phys. JETP **9**, 1061 (1959).

Translated by R. Lipperheide
248

SOVIET PHYSICS JETP VOLUME 11, NUMBER 4 OCTOBER, 1960

NONRESONANCE ABSORPTION OF OSCILLATING MAGNETIC FIELD ENERGY BY A FERROMAGNETIC DIELECTRIC, II

M. I. KAGANOV and V. M. TSUKERNIK

Physico-Technical Institute, Academy of Sciences, Ukrainian S.S.R.

Submitted to JETP editor November 23, 1959

J. Exptl. Theoret. Phys. (U.S.S.R.) 38, 1320-1325 (April, 1960)

Spin-wave theory is used to calculate the imaginary part of the transverse magnetic susceptibility of a ferromagnetic dielectric.

WE have previously studied the nonresonance absorption of alternating magnetic field energy by a ferromagnetic dielectric, with the field in the direction of easy magnetization.[1] The present paper discusses the analogous problem for a field perpendicular to the direction of easy magnetization. Unlike the case of the "longitudinal" field (in the direction of easy magnetization), the energy of the "transverse" field can be absorbed even when dissipative processes are absent if the field frequency coincides with that of ferromagnetic resonance. We shall not consider ferromagnetic resonance and the associated questions such as the shape of the absorption line. Our results therefore pertain basically to frequencies far from resonance.

The dissipative processes associated with energy absorption result from the interaction between the magnetic field and spin waves. As previously,[1] we shall assume saturation magnetization of the ferromagnetic dielectric at a given temperature ($T \ll \Theta_C$). The sample is thus a single domain and is also assumed to be of sufficient purity for the disregard of impurities.

1. The Hamiltonian of the ferromagnet in an alternating magnetic field $\mathbf{h}$ is

$$\mathcal{H} = \mathcal{H}_0 + \mathcal{H}_{int}, \qquad \mathcal{H}_{int} = -\int \hat{\mathbf{M}}\mathbf{h}\,dv, \tag{1}$$

where $\hat{\mathcal{H}}_0$ is the part of the Hamiltonian which does not contain the alternating magnetic field.

Let the field $\mathbf{h}$ be monochromatic and polarized circularly in a plane perpendicular to the easy magnetization axis, which is the direction of the static field $H_0(0, 0, H_0)$:

$$h_x = h_0 \cos(\omega t - \mathbf{kr}),$$
$$h_y = h_0 \sin(\omega t - \mathbf{kr}), \qquad k = \omega / c. \tag{2}$$

Introducing the operators a and a^* through the formulas[2,3]

$$\hat{M}^+ \equiv \hat{M}_x + i\hat{M}_y = (2\mu M_0)^{1/2} a^* (1 - \mu a^* a / 2M_0)^{1/2},$$
$$\hat{M}^- \equiv \hat{M}_x - i\hat{M}_y = (2\mu M_0)^{1/2} (1 - \mu a^* a / 2M_0)^{1/2} a \tag{3}$$

and expanding the radicals in powers of a^*a, we obtain, up to third-order terms,

$$\hat{\mathcal{H}}_{int} = -\tfrac{1}{2}(2\mu M_0)^{1/2}\int (a^* h^- + a h^+)\,dv$$
$$+ \frac{\mu}{8M_0}(2\mu M_0)^{1/2}\int (a^* a^* a h^- + a^* a a h^+)\,dv, \tag{4}$$

where

$$h^\pm = h_x \pm i h_y.$$

The first integral in the interaction Hamiltonian (4) describes resonance absorption of the magnetic field since it represents the excitation of a spin wave with crystal quasimomentum $\hbar\mathbf{k}$ and energy $\hbar\omega$. As already mentioned, this process will not be considered here. We confine our attention to the second integral in (4).

When the temperature T is higher than the characteristic temperature of magnetic interaction $2\pi\mu M_0 \sim 1°\mathrm{K}$ we can neglect the magnetic interaction energy in the unperturbed part $\hat{\mathcal{H}}_0$ of the Hamiltonian compared with the exchange energy.[2,3] We know that in this case

$$a = \frac{1}{V^{1/2}}\sum_\lambda a_\lambda e^{i\mathbf{k}_\lambda \mathbf{r}}, \qquad a^* = \frac{1}{V^{1/2}}\sum_\lambda a^*_\lambda e^{-i\mathbf{k}_\lambda \mathbf{r}}, \tag{5}$$

where a^*_λ and a_λ are the creation and annihilation operators of the spin wave with quasimomentum $\hbar\mathbf{k}_\lambda$.

Substituting (5) in (4), we obtain

$$\hat{\mathcal{H}}_{int} = \frac{\mu h_0}{8M_0}\left(\frac{2\mu M_0}{V}\right)^{1/2} e^{i\omega t}\sum_{\lambda\mu\nu} a_\lambda a_\mu a^*_\nu + \mathrm{c.c.}\ (\mathbf{k}_\lambda + \mathbf{k}_\mu = \mathbf{k}_\nu + \mathbf{k}). \tag{6}$$

It thus appears that the nonresonance absorption of magnetic field energy is associated with the production of two spin waves through the "collision" of a photon with a spin wave. Photon absorption is also possible in the following perturbation approximations through processes in which a larger number of spin waves participate. The most important of these processes is of the fifth order in the operators a_λ and a^*_λ, and occurs in the second perturbation approximation because of exchange-interaction terms in $\hat{\mathcal{H}}_0$ which are of the fourth order in a_λ and a_λ^* and because of the resonance term in (4). Although the photon absorption probability due to this process contains as a factor the large constant of the exchange interaction, its importance is reduced by the high power of the temperature (the number of spin waves being proportional to $T^{3/2}$). Therefore the process under consideration plays the principal part at some not too low temperature. In accordance with (6) the probability for this process is

$$W^{n_\lambda n_\mu n_\nu 1_\omega}_{n_\lambda+1\, n_\mu+1\, n_\nu-1\, 0_\omega} = \frac{2\pi}{\hbar} \left| (\mathcal{H}_{int})^i_f \right|^2 \delta(E_i - E_f)$$
$$= \frac{\pi}{4} \frac{\mu^3 h_0^2}{V\hbar M_0} (n_\lambda + 1)(n_\mu + 1) n_\nu \delta(\varepsilon_\lambda + \varepsilon_\mu - \varepsilon_\nu - \hbar\omega)$$
$$\times \Delta(\mathbf{k}_\lambda + \mathbf{k}_\mu - \mathbf{k}_\nu - \mathbf{k}), \qquad (7)$$

where n_λ is a spin-wave occupation number and

$$\Delta(\mathbf{k}) = \begin{cases} 1 \text{ for } & \mathbf{k} = 0, \\ 0 \text{ for } & \mathbf{k} \neq 0; \end{cases}$$

ϵ_λ is the energy of the spin wave with the wave vector k_λ. For $\Theta_c \gg T \gg 2\pi\mu M_0$ we have

$$\varepsilon_\lambda = \Theta_c (a\mathbf{k}_\lambda)^2 + \mu H_e, \qquad H_e = H_0 + \beta M_0. \qquad (8)$$

β being the anisotropy constant. (8) is also valid for $H_e \gg 2\pi M_0$ at all low temperatures.

The magnetic energy absorption coefficient is

$$\Gamma = Q \Big/ \frac{h_0^2}{8\pi} V,$$

where Q is the amount of energy absorbed per second in the entire volume:

$$Q = \sum_{\lambda\mu\nu} \hbar\omega \left\{ W^{n_\lambda n_\mu n_\nu 1_\omega}_{n_\lambda+1\, n_\mu+1\, n_\nu-1\, 0_\omega} - W^{n_\lambda\ \ n_\mu\ \ n_\nu\ \ 0_\omega}_{n_\lambda-1\, n_\mu-1\, n_\nu+1\, 1_\omega} \right\}. \qquad (9)$$

From (7) and (9) we obtain

$$\Gamma = \frac{\pi^2}{4} \frac{\mu^3 \omega}{M_0} \sum_{\lambda\mu\nu} (n_\lambda n_\mu - n_\lambda n_\nu - n_\mu n_\nu - n_\nu)\, \delta(\varepsilon_\lambda + \varepsilon_\mu - \varepsilon_\nu - \hbar\omega)$$
$$\times \Delta(\mathbf{k}_\lambda + \mathbf{k}_\mu - \mathbf{k}_\nu - \mathbf{k}). \qquad (10)$$

When the frequency of the field **h** is large compared with the reciprocal of the spin-wave relaxation time the n_λ in (10) may reasonably be regarded as equilibrium Bose functions:

$$n_\lambda = (e^{\varepsilon_\lambda/T} - 1)^{-1}. \qquad (11)$$

The frequency limitation does not apply to the case under consideration since the field **h**, which is perpendicular to the equilibrium magnetic moment of the ferromagnet, appears quadratically in the expression for the spin-wave energy.* Therefore the distribution function of n_λ $(\dot{n}_\lambda \sim \dot{\epsilon}_\lambda)$ is not affected in the approximation which is linear in **h**.

(10) and (11) thus determine the absorption coefficient Γ at all frequencies.

Our study is subject to a high-frequency condition ($\hbar\omega \ll \Theta_c$), since we are using the dispersion law (8), which is valid only at low energies ($\epsilon_\lambda \ll \Theta_c$), and it follows from energy conservation that $\hbar\omega = \epsilon_\lambda + \epsilon_\mu - \epsilon_\nu$.

The wave vector **k** of the magnetic field is practically always small compared with the wave vector of the spin wave, and can be neglected. When the summation in (10) is changed to integration over all angles we obtain

$$\Gamma = \frac{1}{32\pi^2} \frac{w^2 T^2}{\mu M_0 \Theta_c^3} \omega (1 - e^{-\hbar\omega/T}) I(\eta, \nu), \qquad (12)$$

where

$$w = \mu^2/a^3, \qquad \eta = \mu H_e/T, \qquad \nu = \hbar\omega/T,$$

and $I(\eta, \nu)$ is defined by

$$I(\eta, \nu) = \iint \frac{e^{x+y}\, dx\, dy}{(e^x - 1)(e^y - 1)(e^{x+y-\nu} - 1)}, \qquad (13)$$

with the region of integration given by the inequalities

$$(\nu - \eta)^2 \leqslant 4(x - \eta)(y - \eta), \qquad x > \eta, \qquad y > \eta. \qquad (14)$$

Performing a single integration in (13) in accordance with (14), we can represent $I(\eta, \nu)$ by

$$I(\eta, \nu) = \int_\eta^\infty \frac{e^y}{(e^y - 1)(1 - e^{y-\nu})} \ln \frac{\exp\{\eta + (\eta - \nu)^2/4(y - \eta)\} - 1}{\exp\{\eta + (\eta - \nu)^2/4(y - \eta)\} - e^{\nu - y}} dy. \qquad (13')$$

2. We now compute (13) (or (13′)) in the different limiting cases.

Low frequencies ($\nu \ll 1, \eta$). In (13′) ν can now be set equal to zero. Introducing the new variable $z = y/\eta$, we obtain

$$I(\eta, 0) = \eta \int_1^\infty \frac{e^{\eta z}}{(e^{\eta z} - 1)^2} \ln \frac{\exp\{\eta[1 + 1/4(z - 1)]\} - e^{-\eta z}}{\exp\{\eta[1 + 1/4(z - 1)]\} - 1} dz. \qquad (15)$$

(15) will now be integrated for large and small values of H_e ($\eta \ll 1$, $\eta \gg 1$).

a) $\eta \ll 1$. Expanding all exponentials in powers of η, we obtain after integration

$$I(\eta, 0) \approx \frac{4}{\eta\sqrt{3}} \left\{ \ln(2 + \sqrt{3}) - \frac{2}{\sqrt{3}} \ln 2 \right\} \approx \frac{2.1}{\eta\sqrt{3}}. \qquad (16)$$

b) $\eta \gg 1$. The argument of the logarithm is now expanded about unity, from which it differs very little, yielding the following approximate expression for (15):

$$I(\eta, 0) \approx \eta e^{-\eta} \int_0^\infty \exp\left\{ -\eta \left[y + \frac{1}{4(y - 1)} \right] \right\} dy.$$

The method of steepest descents easily leads to the result

---

*For $\omega\tau \ll 1$, where τ is the relaxation time, we can consider quasi-static energy levels of the spin waves.[1]

$$I(\eta, 0) \approx \sqrt{\pi\eta/2}\, e^{-3\eta}. \tag{17}$$

Resonance frequency ($\nu = \eta$). At $\hbar\omega = \mu H_e$ the absorption is mainly of resonance character. Calculations are shown here only for the purpose of estimating the contribution of nonresonance absorption near resonance.

At $\nu = \eta$ we easily obtain from (13′):

$$I(\eta, \eta) = \int\limits_{\eta}^{\infty} \frac{e^y}{(e^y - 1)(1 - e^{y-\eta})} \ln \frac{1 - e^{-\eta}}{1 - e^{-y}}\, dy.$$

a) $\eta = 1$. When, as previously, we make the substitution $y = \eta z$ and expand the exponentials in powers of η, we obtain

$$I(\eta, \eta) \approx \frac{1}{\eta} \int\limits_0^{\infty} \frac{z\,dz}{e^z - 1} = \frac{\pi^2}{6\eta}. \tag{18}$$

b) $\eta \gg 1$. After expansion of the logarithm about unity we obtain

$$I(\eta, \eta) \approx e^{-\eta}. \tag{19}$$

High frequencies. High frequencies are understood to be those which are high compared with at least one of the frequencies $T/\hbar$ or $\mu H_e/\hbar$, but small compared with $\Theta_c/\hbar$.

a) $1 \gg \nu \gg \eta$. We may substitute $\eta = 0$ in (13′). Substituting the new variable $z = y/\nu$ and expanding the exponentials in powers of ν, we obtain

$$I(0, \nu) \approx \frac{2}{\nu} \int\limits_0^{\infty} \frac{\ln|2z - 1|\, dz}{z(z-1)} = \frac{3\pi^2}{20\nu}. \tag{20}$$

b) $\nu \gg 1 \gg \eta$. It is now more convenient to use (13) for $I(\eta, \nu)$. Substituting $\eta = 0$, we find that for $\nu \gg 1$ most of the integral comes from the region of integration about the point with the coordinates $x = y = \nu/2$. We can therefore neglect unity compared with e^x and e^y. We thus have

$$I(0, \nu) \approx \iint \frac{dx\,dy}{e^{x+y-\nu} - 1} \qquad (4xy \geqslant \nu^2;\ x > 0,\ y > 0).$$

After integrating once we have

$$I(0, \nu) \approx -\int\limits_0^{\infty} \ln\left[1 - \exp\left\{-\frac{(\nu - 2x)^2}{4x}\right\}\right] dx.$$

Taking $\nu \gg 1$ into account, we obtain

$$I(0, \nu) \approx \sqrt{2\nu} \int\limits_0^{\infty} \frac{z^{1/2}\,dz}{e^z - 1} = \zeta(3/2) \sqrt{\frac{\pi\nu}{2}}. \tag{21}$$

c) $\eta \gg \nu \gg 1$. The asymptotic value (13′) now does not differ from its value for $\eta \gg 1$ at low frequencies [see Eq. (17)].

d) $\nu \gg \eta \gg 1$. We again use (13) for $I(\eta, \nu)$. Since $\eta \gg 1$ while $x, y > \eta$, we have

$$I(\eta, \nu) \approx \iint \frac{dx\,dy}{e^{x+y-\nu} - 1}, \qquad (\nu - \eta)^2 < 4(x - \eta)(y - \eta),\quad x > \eta,\quad y > \eta.$$

After a single integration and expansion of the logarithm about unity, the method of steepest descents yields

$$I(\eta, \nu) \approx \sqrt{\pi\nu/2}. \tag{22}$$

3. Using the asymptotic values of $I(\eta, \nu)$, we derive the following values of the absorption coefficient. For $\mu H_e \ll T$:

$$\Gamma \approx \frac{0.53\omega}{8\sqrt{3}\,\pi^2} \frac{w^2 T^2}{\mu M_0 \Theta_c^2} \frac{\hbar\omega}{\mu H_e} \qquad (\hbar\omega \ll \mu H_e \ll T),$$

$$\Gamma \approx \frac{\omega}{192} \frac{w^2 T^2}{\mu M_0 \Theta_c^3} \qquad (\hbar\omega = \mu H_e \ll T),$$

$$\Gamma \approx \frac{3\omega}{640} \frac{w^2 T^2}{\mu M_0 \Theta_c^3} \qquad (T \gg \hbar\omega \gg \mu H_e),$$

$$\Gamma \approx \frac{\zeta(3/2)\,\omega}{32\sqrt{2}\,\pi^{3/2}} \frac{w^2 T^2}{\mu M_0 \Theta_c^3} \sqrt{\frac{\hbar\omega}{T}} \qquad (\hbar\omega \gg T \gg \mu H_e).$$

For $\mu H_e \gg T$:

$$\Gamma \approx \frac{\omega}{32\sqrt{2}\,\pi^{3/2}} \frac{w^2 \hbar\omega}{\mu M_0 \Theta_c^2} \sqrt{\frac{\mu H_e T}{\Theta_c^2}} \exp\left\{-\frac{3\mu H_e}{T}\right\} \quad (\hbar\omega \ll T \ll \mu H_e),$$

$$\Gamma \approx \frac{\omega}{32\pi^2} \frac{w^2 T^2}{\mu M_0 \Theta_c^3} \exp\left\{-\frac{\hbar\omega}{T}\right\} \qquad (\hbar\omega = \mu H_e \gg T),$$

$$\Gamma \approx \frac{\omega}{32\sqrt{2}\,\pi^{3/2}} \frac{w^2 T^2}{\mu M_0 \Theta_c^3} \sqrt{\frac{\mu H_e}{T}} \exp\left\{-\frac{3\mu H_e}{T}\right\} \quad (\mu H_e \gg \hbar\omega \gg T),$$

$$\Gamma \approx \frac{\omega}{32\sqrt{2}\,\pi^{3/2}} \frac{w^2 T^2}{\mu M_0 \Theta_c^3} \sqrt{\frac{\hbar\omega}{T}} \qquad (\hbar\omega \gg \mu H_e \gg T).$$

With the absorption coefficient Γ known, the dispersion equation for a circularly polarized electromagnetic wave can be used to determine the imaginary part of the transverse magnetic susceptibility

$$\mu''_\perp = \mu'_\perp \Gamma/\omega,$$

where $\mu'_\perp$ is the real part of the magnetic susceptibility. At low frequencies ($\omega \ll g B_e$) we have $\mu'_\perp = B_e/H_e$, where $B_e = H_e + 4\pi M_0$; at high frequencies ($\omega \gg g B_e$) the result is $\mu'_\perp = 1$.

An estimate of $\mu''_\perp$ near resonance shows that nonresonance absorption is entirely negligible in this region, while it evidently plays an important part far from resonance.

The authors wish to express their sincere appreciation to A. I. Akhiezer and V. G. Bar'yakhtar for valuable discussions.

---

[1] M. I. Kaganov and V. M. Tsukernik, JETP **37**, 823 (1959), Soviet Phys. JETP **10**, 587 (1960).

[2] T. Holstein and H. Primakoff, Phys. Rev. **58**, 1098 (1940).

[3] M. I. Kaganov and V. M. Tsukernik, JETP **34**, 1610 (1958), Soviet Phys. JETP **7**, 1107 (1958).

Translated by I. Emin
249

SOVIET PHYSICS JETP VOLUME 11, NUMBER 4 OCTOBER, 1960

MAGNETIC RESONANCE IN RHOMBOHEDRAL WEAK FERROMAGNETICS

E. A. TUROV and N. G. GUSEĬNOV

Institute of Metal Physics, Academy of Sciences, U.S.S.R.

Submitted to JETP editor November 23, 1959

J. Exptl. Theoret. Phys. (U.S.S.R.) 38, 1326-1331 (April, 1960)

On the basis of Dzyaloshinskii's ideas on the nature of weak ferromagnetism, resonance frequencies are calculated for rhombohedral weak ferromagnetic crystals of the α-Fe_2O_3 and $MnCO_3$ type. Account is taken of the effect on the resonance of anisotropy in the basal plane, and the dependence of the resonance frequencies on the magnitude and direction of the magnetizing field is obtained. The theoretical formulas are compared with experimental data on α-Fe_2O_3.

1. Magnetic resonance is the most direct method of studying the energy spectrum of magnetic crystals. The peculiarities of the energy spectrum of weak ferromagnetics, which result from the peculiar nature of weak ferromagnetism as a property of antiferromagnetic crystals conditional on a definite symmetry, are most evident in the conditions of magnetic resonance, and especially in the form of the dependence of the resonance frequencies on the magnitude and direction of the magnetizing field. Therefore it is of interest to study the conditions of magnetic resonance in weak ferromagnetics by means of the Hamiltonian proposed by Dzyaloshinskiĭ[1] on the basis of symmetry considerations, and to compare the results obtained with the existing experimental data.

Since the only weak ferromagnetic for which there are experimental data on magnetic resonance, α-Fe_2O_3, belongs to the rhombohedral syngony, all our calculations will relate to crystals of this symmetry. Moreover the other best studied weak ferromagnetic, $MnCO_3$,[1,2] has a crystal lattice isomorphic with the α-Fe_2O_3 lattice.

The most complete experimental study of magnetic resonance in hematite was made by Kumagai et al.[3] In their work the dependence of resonance frequency on the magnitude and direction of the external field H was studied. In particular, it was shown that the usual Kittel resonance formula for a uniaxial ferromagnetic, with no account taken of anisotropy in the basal plane, agrees poorly with experimental data on the dependence of resonance frequency on the magnitude of a field H lying in the basal plane. Furthermore the experiment gave a very simple dependence of the magnitude of the resonance field H_θ at a given frequency on the angle θ between the direction of this field and the trigonal axis [111] of the crystal:

$$H_\theta = H_\perp / \sin\theta, \tag{1}$$

where $H_\perp$ is the resonance field for $\theta = \pi/2$.

There has been only one attempt at a theoretical explanation of the experimental laws for resonance in hematite. This attempt, by Shimizu,[4] is based on old ideas about weak ferromagnetism, such as the explanation based on the presence in an α-Fe_2O_3 crystal of fine ferromagnetic impurities. For this impurity ferromagnetism, Shimizu included in the anisotropy energy terms through the sixth order; in consequence, by choice of the numerical values of the three anisotropy constants that appeared in the theory, he succeeded in giving a satisfactory explanation of the experimental data of Kumagai et al.[3] in the range of fields in which there is saturation. However, description of the resonance phenomenon in hematite on the basis indicated came into contradiction with static measurements of the magnetic properties of α-Fe_2O_3. In particular, it was found that the magnetic susceptibility in the direction of the trigonal axis should be appreciably larger than the susceptibility in the basal plane,* which was contrary to experiment.[5]

In the present work it will be shown that on the basis of the ideas developed by Dzyaloshinskiĭ on the nature of weak ferromagnetism, it is possible to give a more natural explanation of the observed resonance properties of hematite; furthermore, this explanation is in good agreement with the static measurements of magnetization and susceptibility of these crystals.

---

*The susceptibility in the direction of the [111] axis should, according to Shimizu, be the resultant of the transverse antiferromagnetic susceptibility and of a susceptibility connected with rotation of the spontaneous magnetic moment of the ferromagnetic impurities.

2. We shall start with the following Hamiltonian, proposed by Dzyaloshinskii[1] on the basis of symmetry considerations for rhombohedral crystals of the α-Fe_2O_3 or $MnCO_3$ type:

$$\mathcal{H} = \tfrac{1}{2} Bm^2 + \tfrac{1}{2} bm_z^2 + \tfrac{1}{2} al_z^2 + q(l_x m_y - l_y m_x) + d(3l_x^2 l_y - l_y^3)\, l_z + e(l_x^6 - l_y^6 - 15 l_x^4 l_y^2 + 15 l_x^2 l_y^4) - \mathrm{mh}. \tag{2}$$

Here the z axis is the trigonal axis, and the x axis is directed along one of the twofold axes in the (111) plane; $\mathbf{m} = (\mathbf{M}_1 + \mathbf{M}_2)/2M_0$, $\boldsymbol{l} = (\mathbf{M}_1 - \mathbf{M}_2)/2M_0$, where $\mathbf{M}_1$ and $\mathbf{M}_2$ are the sublattice magnetizations, for which, in accordance with the basic assumptions of spin-wave theory, the relations $\mathbf{M}_1^2 = \mathbf{M}_2^2 = M_0^2$ hold; or

$$l^2 + m^2 = 1, \qquad \mathbf{lm} = 0. \tag{3}$$

The parameters that appear in (2) have the following meanings: the exchange interaction parameter $B > 0$ leads to an antiferromagnetic arrangement of the sublattice magnetizations; the parameter $q > 0$ causes a disturbance of the strict antiparallelism of the vectors $\mathbf{M}_1$ and $\mathbf{M}_2$, so that a weak spontaneous moment $\mathbf{m} \perp \boldsymbol{l}$ appears; a and b are fourth- and sixth-order anisotropy constants, which for hematite satisfy the conditions*[1]

$$a > 0, \quad e + d^2/4a > 0.$$

The last term in (2) represents the energy of the magnet in the external field $\mathbf{H} = \mathbf{h}/2M_0$. In the Hamiltonian (2) two fourth-order terms, not important for present purposes, have been omitted.

3. The spectrum of characteristic oscillations of the vectors $\mathbf{m}$ and $\boldsymbol{l}$ for rhombohedral weak ferromagnetics, with neglect of anisotropy in the basal plane (i.e., for $d = e = 0$), was calculated by Borovik-Romanov[2] and one of the authors[6,7] for the case in which the field **H** lies in the basal plane. We shall first generalize the results of these works to the case of arbitrary direction of **H**.

Let **H** make an angle θ with the [111] axis. Then, upon neglect of the c and d terms in (2) and upon supposing (without loss of generality) that **H** lies in the xz plane, it is easy to find, from the condition of minimum $\mathcal{H}$ with attention to (3), the following equilibrium values of $\mathbf{m}$ and $\boldsymbol{l}$ (for $h \ll B$):

$$m_{x0} = (q + h\sin\theta)/B, \qquad m_{y0} = 0, \quad m_{z0} = h\cos\theta/(B+b),$$
$$l_{x0} = l_{z0} = 0, \qquad l_{y0} = l_0 = \sqrt{1 - m_0^2} \approx 1. \tag{4}$$

By considering, furthermore, small uniform oscillations of $\mathbf{m}$ and $\boldsymbol{l}$ about the values $\mathbf{m}_0$ and $\boldsymbol{l}_0$, we find in the usual way[8,9] the characteristic frequencies of these oscillations:

$$\omega_1 = (\gamma/2M_0)\sqrt{h\sin\theta\,(q + h\sin\theta)}, \tag{5}$$

$$\omega_2 = (\gamma/2M_0)\sqrt{Ba + q(q + h\sin\theta) + h^2\cos^2\theta}, \tag{6}$$

where $\gamma = ge/2mc$ is the magnetomechanical ratio (ω = angular frequency).

Oscillations of frequency ω_1 can be excited by radio waves of the centimeter range, and in fact they were observed in resonance experiments of Kumagai et al.[3] The second branch of the oscillations is related to much higher frequencies, of order 10^{12} to 10^{13} cps. Observation of it requires larger fields, $H \sim 10^4$ to 10^5 oe, and electromagnetic radiation of wavelength $\lambda \sim 10^{-1}$ to 10^{-2} cm.

Solution of the resonance formula (5) for the external field H gives the experimentally established relation (1), with

$$H_\perp = \sqrt{(H_\mathrm{D}/2)^2 + (\omega_1/\gamma)^2} - H_\mathrm{D}/2,$$
$$H_\mathrm{D} = q/2M_0. \tag{7}$$

Thus even without allowance for anisotropy in the basal plane, the theory explains well the observed dependence of the magnitude of the resonance field **H** on its direction in a plane passing through the trigonal axis. However, the theoretical relation (7) between the resonance field $H_\perp$ in the basal plane and the frequency ω_1 is poorly satisfied experimentally. Therefore, as has already been pointed out by Vonsovskiĭ and Turov,[7] here it is necessary to take account of anisotropy in the basal plane, described by the d and e terms in the Hamiltonian (2). This will be done below.

4. Let the field **H** lie in the (111) plane and make an angle φ with the x axis. Then from the minimum condition for the complete Hamiltonian (2) in the range of fields $h^* < h \ll B$, we find

$$\mathbf{m}_0 \parallel \mathbf{H}, \qquad m_0 = (q+h)/B, \qquad l_0 = \sqrt{1 - m_0^2} \approx 1, \tag{8}$$

$\boldsymbol{l}_0$ lies in the plane perpendicular to **H** and makes with the (111) plane an angle

$$\delta = (d/a)\cos 3\varphi. \tag{9}$$

The field h^* represents an effective anisotropy field in the basal plane; for $h > h^*$ saturation occurs, in the sense that $\mathbf{m}_0 \parallel \mathbf{H}$. Approximately,

$$h^*_1 = 36B(e + d^2/4a)/q. \tag{10}$$

---

*Under these conditions, in the equilibrium state (at $H = 0$) **m** is directed along one of the twofold axes in the basal plane, and **l** is in the vertical plane perpendicular to it and makes a small angle with the basal plane.

For hematite in particular, as will be clear from the estimates made below, $H^* = h^*/2M_0 \sim 10^2$ oe.

Knowing the equilibrium vectors $\mathbf{m}_0$ and $\boldsymbol{l}_0$, we can calculate anew the spectrum of oscillations of the system about this equilibrium state. A very laborious calculation on the basis of the complete Hamiltonian (2), with attention to the relations (8) and (9), leads to the following two characteristic frequencies of oscillation for this case:

$$\omega_1 = (\gamma / 2M_0) \sqrt{h(h+q) + 36B(e + d^2/4a)\cos 6\varphi}\,. \qquad (11)$$

$$\omega_2 = (\gamma / 2M_0) \sqrt{Ba + q(q+h) + 9Bd + 6Be\cos 6\varphi}\,, \qquad (12)$$

As is clear from (12), the fourth- and sixth-order anisotropy is practically without effect on the second resonance frequency, since the d and e terms that occur in it are always small in comparison with the term Ba. On the contrary, for the first resonance frequency ω_1 the role of anisotropy in the basal plane can be appreciable if the field H is not very large. The range of fields in which there is an effect of anisotropy of higher than second order is, as a rule, appreciably larger for the weakly ferromagnetic crystals under consideration than for ordinary ferromagnetics of the same symmetry, since in the present case the role of "anisotropy constants" is played not by the parameters d and e themselves, but by quantities proportional to the geometric mean of $e + d^2/4a$ and of the exchange parameter B. Consequently, in this respect weak ferromagnetics are similar to ordinary antiferromagnetics.

5. We now show under what conditions the oscillations of frequencies ω_1 and ω_2 are excited. For this purpose we find the susceptibility of a weak ferromagnetic with respect to a high-frequency magnetic field $\mathbf{h}_\omega$; we start with the equation of motion for the magnetic moments $\mathbf{M}_1$ and $\mathbf{M}_2$ of the sublattices:

$$d\mathbf{M}_j / dt = \gamma[\mathbf{M}_j \times \mathbf{H}_j], \qquad j = 1, 2. \qquad (13)$$

Here the effective fields $\mathbf{H}_j$ acting on the sublattices are found from the Hamiltonian (2) and the relation $\mathbf{H}_j = -\partial\mathcal{H}/\partial\mathbf{M}_j$. We shall consider that the external field consists of a constant field $H = H_x$, directed along the x axis in the basal plane, and of a high-frequency alternating field $\mathbf{h}_\omega$, whose amplitude is small in comparison with H_x. A standard calculation gives the following expression for the high-frequency tensor susceptibility:

$$\chi_{\alpha\beta} = \begin{vmatrix} \chi_{xx} & 0 & 0 \\ 0 & \chi_{yy} & \chi_{yz} \\ 0 & \chi_{zy} & \chi_{zz} \end{vmatrix}, \qquad \chi_{xx} = \chi_0\omega_2^2/(\omega_2^2 - \omega^2),$$

$$\chi_{yy} = (M_x/H_x)\omega_1^2/(\omega_1^2 - \omega^2), \qquad \chi_{zz} = \chi_0\omega_1^2/(\omega_1^2 - \omega^2),$$

$$\chi_{yz} = -\chi_{zy} = i\chi_0(\omega/\gamma H)\,\omega_1^2/(\omega_1^2 - \omega^2),$$

$$M_x = \chi_0(H_D + H), \quad \chi_0 = 4M_0^2/B.$$

From the formulas presented it is evident that the oscillations of frequency ω_1 are excited when the high-frequency field is perpendicular to the constant field, and the oscillations of frequency ω_2 when it is parallel to it. The presence of nondiagonal elements of the tensor $\chi_{\alpha\beta}$ shows that there is gyrotropy in the medium.

It is possible to allow for a damping term in equation (13), for example in the form proposed by Landau and Lifshitz;[10] this was done for ordinary antiferromagnetics by Kaganov and Tsukernik[11] and also by Seĭdov.[12] If the width $\Delta\omega$ of the resonance line is then determined from the expressions obtained for $\chi_{\alpha\beta} = \chi'_{\alpha\beta} - i\chi''_{\alpha\beta}$, it turns out that in weak ferromagnetics, just as in antiferromagnetics,[11] $\Delta\omega$ is connected with the dimensionless damping parameter α of the Landau-Lifshitz equation of motion by the following relation: $\Delta\omega \approx \alpha\omega_E$ ($\omega_E = \gamma B/2M_0$ is the so-called exchange frequency).

We remark that the analogous relation for ordinary ferromagnetics has the form $\Delta\omega \approx \gamma\omega_0$, where ω_0 is the resonance frequency.[13] Consequently, if the parameter α in antiferromagnetics (and in weak ferromagnetics) had the same nature and the same order of magnitude as in ferromagnetics, then $\Delta\omega$ would be about three orders of magnitude larger in the former than in the latter. However, no great differences are observed between the line widths for antiferromagnetics and for ferromagnetics. Apparently the question of the formal description of relaxation terms in the equations of motion for antiferromagnetics and weak ferromagnetics, and also of the nature of the line widths in them, needs to be subjected to a special and more detailed study.*

6. We apply the theoretical results obtained to the discussion of the resonance properties of hematite.[3] It has already been indicated that the theory explains well the experimentally established formula (1) for the dependence of the magnitude of the resonance field on its direction in a plane passing through the [111] axis. Kumagai et al.[3] also investigated the relation between the frequency ω_1 and a resonance field H lying in the basal plane. We rewrite formula (11), which should describe this relation, in the following form:

$$\omega_1/\gamma = \sqrt{H(H + H_D) + H_\Delta^2\cos 6\varphi},$$

$$H_\Delta^2 = 36B(e + d^2/4a)/4M_0^2. \qquad (14)$$

Thus in the resonance formula (14) there occur two unknown parameters† H_Δ and H_D. The first

---

*Cf. also the work of Dayhoff.[14]

†If we do not include the g factor; this we set equal to 2.

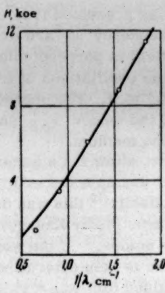

of these can be estimated from the angular dependence of the resonance field (i.e., the dependence of H on φ for given frequency ω_1), observed by Anderson et al.[15] and less precisely by Kumagai et al.[3] This estimate gives approximately $H_\Delta = 1450$ oe. A value of the parameter H_D was selected by the criterion of best fit between theory and experiment for the dependence of ω_1 on H. The figure shows the theoretical curve for the relation between $1/\lambda = \omega_1/2\pi c$ and a resonance field H directed along the "easy axis" x [this corresponds to $\cos 6\varphi = 1$ in formula (14)], for $H_D = 22{,}800$ oe. The experimental data[3] are plotted as points. As is evident from the figure, there is completely satisfactory agreement between theory and experiment except in the low-field range. This was likewise the case in the work of Shimizu.[4] Presumably, because of various crystal defects, the saturation of the magnetization assumed by us is not present at fields $\lesssim 2000$ oe. In fact, from magnetization curves of hematite taken by other authors[16] it is clear that saturation in the basal plane is not attained at field strengths below 1000 to 2000 oe, whereas according to (10) saturation should occur for an ideal crystal at fields

$$H \sim H^* = H_\Delta^2 / H_D \sim 100 \text{ oe}.$$

The important superiority of our theory is that, in contrast to the theory of Shimizu, it leads to good agreement of the resonance experiments with the results of static measurements of the spontaneous magnetization M_s and of the transverse antiferromagnetic susceptibility χ of hematite. The fact is that from the statistics of the measurements it is possible to determine in an independent way the field H_D responsible for the weak ferromagnetism,[1,6] since $H_D = M_s/\gamma$. According to data of Néel and Pauthenet,[5] at room temperature $M_s \approx 0.4$ cgs emu and $\chi = 2 \times 10^5$; consequently $H_D \approx 2 \times 10^4$ oe, which is very close to the value $H_D = 22{,}800$ oe found above from resonance measurements.*

For more detailed comparison of theory with experiment and for resolution of the still remaining difficulties in the low-field range, it is necessary to carry out experimental studies of both the magnetic and the resonance properties of hematite (or $MnCO_3$) on the same monocrystalline specimens.

The authors express their deep gratitude to S. V. Vonsovskiĭ for discussions of the results and for valuable advice.

---

[1] I. E. Dzyaloshinskiĭ, JETP **32**, 1547 (1957), Soviet Phys. JETP **5**, 1259 (1957).

[2] A. S. Borovik-Romanov, JETP **36**, 766 (1959), Soviet Phys. JETP **9**, 539 (1959).

[3] Kumagai, Abe, Ono, Hayashi, Shimada, and Iwanaga, Phys. Rev. **99**, 1116 (1955).

[4] M. Shimizu, J. Phys. Soc. Japan **11**, 1078 (1956).

[5] L. Néel and R. Pauthenet, Compt. rend **234**, 2172 (1952); L. Néel, Revs. Modern Phys. **25**, 58 (1953).

[6] E. A. Turov, JETP **36**, 1254 (1959), Soviet Phys. JETP **9**, 890 (1959).

[7] S. V. Vonsovskiĭ and E. A. Turov, J. Appl. Phys. **30** (Suppl.), 9S (1959).

[8] M. I. Kaganov and V. I. Tsukernik, JETP **34**, 106 (1958), Soviet Phys. JETP **7**, 73 (1958).

[9] E. A. Turov and Yu. P. Irkhin, Izv. Akad. Nauk SSSR, Ser. Fiz. **22**, 1168 (1958), Columbia Tech. Transl. p. 1158.

[10] L. D. Landau and E. M. Lifshitz, Physik. Z. Sowjetunion **8**, 153 (1935).

[11] M. I. Kaganov and V. M. Tsukernik, JETP **34**, 524 (1958), Soviet Phys. JETP **7**, 361 (1958).

[12] Yu. M. Seĭidov, Физика металлов и металловедение (Phys. of Metals and Metallurgy) **7**, 443 (1959).

[13] Yager, Galt, Merritt, and Wood, Phys. Rev. **80**, 744 (1950).

[14] E. S. Dayhoff, J. Appl. Phys. **29**, 344 (1958).

[15] Anderson, Merritt, Remeika, and Yager, Phys. Rev. **93**, 717 (1954).

[16] Bizette, Chevallier, and Tsai, Compt. rend. **236**, 2043 (1953).

Translated by W. F. Brown, Jr.
250

*This agreement can be improved further by taking for the g factor a value slightly greater than 2.

SOVIET PHYSICS JETP VOLUME 11, NUMBER 4 OCTOBER, 1960

Letters to the Editor

INVESTIGATION OF NUCLEAR MAGNETIC RESONANCE IN ADSORBED GAS

A. A. GALKIN and I. V. MATYASH

Institute of Radiophysics and Electronics, Academy of Sciences, Ukr. S.S.R.

Submitted to JETP editor December 19, 1959

J. Exptl. Theoret. Phys. (U.S.S.R.) **38**, 1332-1334 (April, 1960)

COMPARATIVELY little work has been devoted to the study of physical properties of adsorbed gas. Indeed, only isothermal adsorption and heat capacity of thin films of gas have been studied in any degree of detail.[1-4] Therefore, it is of definite interest to carry out investigations of nuclear magnetic resonance (n.m.r.) in thin films of a substance, since from the form of the resonance curves it is possible to evaluate the interaction between the molecules of the adsorbed gas and to study the effect of the substratum.

In order to study the problems indicated above, n.m.r. investigations were undertaken in thin films of hydrogen, water, and methane adsorbed by activated charcoal. The investigations were carried out by means of the spin-echo method,[5] which enables us to measure in a comparatively simple way the longitudinal and the transverse relaxation times (T_1 and T_2), and also to evaluate the self-diffusion coefficients.

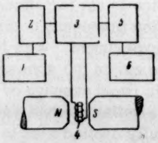

FIG. 1

The block diagram of the apparatus is shown in Fig. 1. The rectangular pulse generator 1 enabled us to obtain: a) two or three pulses with independent control of their length, repetition frequency and the time interval between them; b) a single pulse, followed by a series of equidistant pulses with independent control of the pulse length and the time interval between them. The pulse generator modulates the radiofrequency oscillator 2 stabilized by a quartz crystal and operating at a frequency of 14 Mcs. In order to avoid overloading the radiofrequency amplifier the latter is separated from the oscillator by the r-f bridge 3 one of whose arms contains the coil with the sample 4; the r-f amplifier 5 has a gain of $\sim 10^5$. The signal from the detector was applied to the input 6 of an IO-4 oscillograph.

A magnetic field of 3300 oe was produced by a permanent magnet with pole pieces 110 mm in diameter and with a 40 mm gap. The magnet was provided with coils which made it possible for the magnetic field to be varied by ± 50 oe.

This apparatus enabled us to measure the longitudinal and transverse relaxation times (T_1 and T_2) in the range $10^{-4} - 10$ sec.

For the determination of T_1 three pulses were applied to the sample and the relaxation time was determined by analyzing the intensity of the stimulated echo signal as a function of the time between the first and the third pulses.[5] A study of the intensity of the spin echo signal as a function of the time between two pulses enabled us to calculate the relaxation time T_2 and the self-diffusion coefficient. Moreover, the dependence of the intensity of the spin echo on the time elapsed from the application of a single orienting pulse and a series of equidistant pulses enabled us to determine T_2 directly.[5]

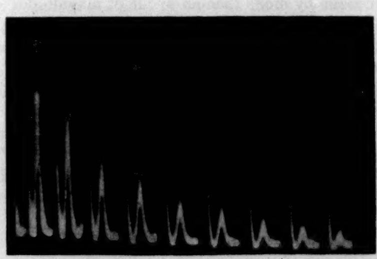

FIG. 2

As an illustration Fig. 2 shows a spin echo oscillogram from which the relaxation time T_2 was determined for hydrogen adsorbed on charcoal at a temperature of 77° K.

The table summarizes data on the measurement of the relaxation times T_1 and T_2 for hydrogen, methane, and water adsorbed on charcoal, and also an evaluation of the self-diffusion coefficient (D), and of the activation energy (Q) obtained by the n.m.r. method at different temperatures.

From the table it may be seen that at a temperature of 77° K the width of the n.m.r. line in hydrogen adsorbed on charcoal is 0.2 oe, while according

Substance	T, °K	10^3T_1, sec	10^3T_2, sec	ΔH, oe	$10^2\cdot D$, cm²/sec	Q, joule/mole	Notes
H_2	90	2	1.4	0.2	2.7	590	Monomolecular layer
	77	5	1.3	0.2	2.4		
	20.4	10	0.1	2			
	20.4	20	8	0.03	$2\cdot10^{-2}$		Liquid film
H_2	14_{liq}	200	200	10^{-3}		1200	In free state according to data of reference 6.
	14_{sol}		2.3	0.1	0.1		
	11		0.23	1.0			
CH_4	290	20	1.9		4	760	Monomolecular layer
	90	8	2.1		2.5		
	77	7	2.6		2.1		
H_2O	290	1	0.7				10 Steam pressure
		2	0.7				20 over charcoal
		10	5				70 in mm Hg
		15	6				170
		3000	2000				In free state

to Bloom's data[6] hydrogen has an absorption line of 0.1 oe width only near its freezing point (liquid hydrogen gives a line width of 10^{-3} oe). It should be pointed out that at a temperature in the neighborhood of 25°K the n.m.r. line width in hydrogen adsorbed on charcoal increases to 2 oe. It is of definite interest to make an estimate of the coefficient of internal friction for water. According to n.m.r. data the viscosity of water in the adsorbed state increases by more than an order of magnitude.

Thus, an analysis of the results of this investigation shows that physical properties of adsorbed gases can be successfully studied by the n.m.r. method which significantly extends the range of possibilities in the study of molecular physics.

[1] A. van Itterbeek and W. van Dingenen, Physica **4**, 389, 1169 (1937).

[2] K. Tanaka and K. Yamagata, Bull. Chem. Soc. Japan **28**, 90 (1955).

[3] W. A. Steeble, Proc. First Conference on Low Temperature Physics, Madison, 1958, p. 603.

[4] A. Odajima, J. Phys. Soc. Japan **14**, 308 (1959).

[5] H. Y. Carr and E. M. Purcell, Phys. Rev. **94**, 630 (1954).

[6] M. Bloom, Physica **23**, 378 (1957).

Translated by G. Volkoff
251

OBSERVATION OF SPONTANEOUS COHERENT RADIATION OF A FERRITE IN A RESONATOR

A. P. ALEKSANDROV, Ya. I. KHANIN, and
É. G. YASHCHIN

Radiophysics Institute, Gor'kiĭ State University

Submitted to JETP editor December 31, 1959

J. Exptl. Theoret. Phys. (U.S.S.R.) **38**, 1334-1337 (April, 1960)

IN recent years there have been published a number of researches related to spontaneous coherent radiation of electron spin systems in the microwave range. In the majority of cases,[1-3] generation is accomplished by use of paramagnetics that possess, at liquid-helium temperatures, very long spin-lattice relaxation times (from milliseconds to minutes). Such a choice is not fortuitous, for the duration of the relaxation processes determines the time scale of the experiment. With long relaxation times, it is easy to excite the spin system by the method of adiabatic rapid passage or with the aid of 180° pulses. A similar method (a 45° pulse) has been successfully applied also to the excitation of organic free radicals[4] possessing relaxation times from 0.03 to 0.1 μsec.

For the overwhelming majority of ferrites, the relaxation times τ, estimated from the width of the ferromagnetic resonance line, are much smaller than the figures mentioned. This circumstance substantially complicates the technical application of the indicated method for excitation of ferrites. Furthermore there is a difficulty in principle, in that τ is of the order of magnitude of, or less than, the time constant of the apparatus. Therefore we used a somewhat different principle, consisting of this: that the resonance excitation of the ferrite is carried out at a frequency ν_1 different from the frequency ν_2 of spontaneous radiation.* The acts of excitation and radiation are separated by a time interval $t_2 - t_1$, during which the external magnetic field is changed from the value $H_1 = 2\pi\nu_1/\gamma$ to $H_2 = 2\pi\nu_2/\gamma$, where γ is the gyromagnetic ratio for the electron. In order that the precession of the magnetic moment of the ferrite may not become practically extinguished during the time $t_2 - t_1$, this interval must not greatly exceed τ.

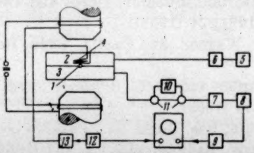

FIG. 1. Block diagram of the experimental arrangement: 1, ferrite; 2 and 3, resonators; 4, pulse coil; 5, generator; 6 and 7, attenuators; 8, detector; 9, broadband amplifier; 10, resonator-filter; 11, waveguide switches; 12, synchronizer; 13, thyratron current-pulse generator.

A block diagram of the experimental arrangement is shown in Fig. 1. The ferrite 1 is fastened in an opening in the common wall of the rectangular resonators 2 and 3. The dimensions of the resonators correspond to the TE_{012} mode; the fastening point of the ferrite coincides with an antinode of the magnetic field of each. The resonator block is placed between the poles of an electromagnet. Resonator 2, designed to excite precession in the ferrite, is connected by means of a waveguide with generator 5 and tuned to its frequency ν_1. The resonator Q is approximately 300; the excitation power is of the order of a few watts. By means of the two-winding coil 4, located inside resonator 2, there is produced a pulsed magnetic field parallel to the constant field H_0 of the electromagnet. The change of the total field with time is shown in Fig. 2. For $|H - H_1| \lesssim \Delta H$, where ΔH is the half width of the resonance line of the ferrite, the ferrite interacts with the high-frequency field in 2, and there is excited a precession of the magnetic moment, with precession angle θ. In the succeeding interval of time, the precession frequency does not coincide with the characteristic frequencies of the resonators $(\nu_1 < \nu < \nu_2)$, and the angle θ decreases under the influence of relaxation processes alone:

$$\theta = \theta_0 \exp\{-(t - t_1)/\tau\}. \qquad (1)$$

When, finally, H passes through the values $|H - H_2| \lesssim 2\pi\Delta\nu_2/2\gamma$ ($\Delta\nu_2$ = tuning band of the resonator 3 to frequency ν_2), the ferrite radiates a short pulse. This pulse is further detected, amplified by the broadband amplifier 9, and observed with the aid of a fast oscillograph.

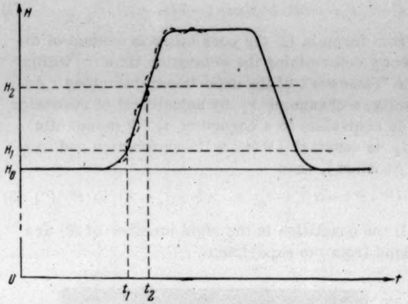

FIG. 2. Change of magnetic field with time.

In the experiment, the excitation frequency used was ν_1 = 8900 Mcs. The electromagnet field H was kept equal to 3050 oe, with the value of the pulsed field 700 oe. The frequency could be varied over the range 9000 to 9800 Mcs by adjustment of the resonator 3. In order that the antinode of the field might not move with respect to the ferrite in this process, the adjustment was made by simultaneous and symmetrical movement of two pistons. The slope of the pulse front, $dH/dt = 3 \times 10^{10}$ oe/sec, insured over the range of adjustment mentioned a value $t_2 - t_1 = (3 \text{ to } 15) \times 10^{-9}$ sec.

The process of coherent radiation of a spin system placed in a resonator has been described by Faĭn.[5] He considered, in particular, the case of a resonator tuned to the characteristic frequency of the system, when the radiation field is absent at the initial instant. In our case the precession frequency changes continuously, and radiation occurs when $|\nu - \nu_2| \lesssim \nu_2/2$. However, it is possible to estimate the radiated energy and power by using Faĭn's results, if one replaces the actual process of frequency change by a step change and assumes the frequency to be constant during the radiation process. The duration of the act of radiation, Δt_2, is easily determined from knowledge of dH/dt and $\Delta\nu_2$. The time of complete transfer of the energy of the ferrite into radiation, estimated by formula (56) of Faĭn's paper for the specimens used, was of order 10^{-8} sec, whereas $\Delta t_2 \sim 10^{-9}$sec. Consequently, in our experiment the ferrite is able to radiate only a part of its energy. For this case, the formula mentioned can be simplified, and we get for the power in the pulse the simple expression

$$P = \mathrm{const} \cdot \Delta t_2 \theta_0^2 \exp \{-2(t_2 - t_1)/\tau\}. \qquad (2)$$

From formula (2) the possibility is evident of directly determining the relaxation time τ within the framework of the experiment described. Actually, a change of ν_2 by adjustment of resonator 3 is equivalent to a change of t_2. If meanwhile Δt_2 is constant [H (t) a linear function and $\Delta\nu_2$ a constant], then

$$\ln(P'/P'') = 2(t_2'' - t_2')/\tau, \quad \tau = 2(t_2'' - t_2')/\ln(P'/P''). \qquad (3)$$

All the quantities in the right member of (3) are found from the experiment.

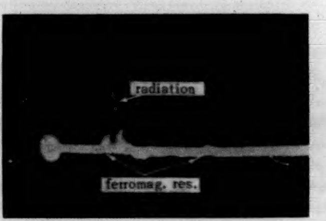

FIG. 3. Signals due to radiation and to ferromagnetic resonance on the oscillograph screen.

Figure 3 shows a photograph of the picture on the oscillograph screen. The large pulse is caused by the radiation at $H = H_2$, and the two small ones by ferromagnetic resonance at $H = H_1$. The correctness of this interpertation was confirmed by special checks. In the first place, it was established that the carrier frequency of the large pulse coincided with ν_2 and of the smaller with ν_1. For this purpose, there was connected in the line, in front of the detector, the adjustable resonator-filter 10. In the second place, it was shown that the radiation pulse was absent in all cases in which the magnetic field did not reach the value H_2. In the third place, the dependence of the size of the radiated pulse on Δt_2 was verified qualitatively. The fact is that the slope of the pulse front of the magnetic field was slightly oscillatory, as is shown by the dashed curve in Fig. 2. Consequently the interval Δt_2 should also oscillate with change of t_2, and the dependence P(t) expressed by formula (2) ceases to be purely exponential. On the experimentally obtained graphs of P(t), the corresponding fluctuations are clearly indicated; this, unfortunately, greatly complicates the determination of the relaxation time.

The specimens used in this research were of yttrium iron garnet, of diameter from 0.5 to 1.0 mm, with polished surface of spherical form.

In closing, we wish to express our deep gratitude to A. G. Gurevich, G. A. Smolenskiĭ, and K. P. Belov, who kindly provided the ferrite specimens; to A. M. Leonov, who took an active part in the construction of the apparatus; and to V. M. Faĭn for valuable advice.

---

*A similar idea was used in the work of Hoskins,[6] where an experiment with ruby is described.

---

[1] Combrisson, Honig, and Townes, Compt. rend. **242**, 2451 (1956).

[2] Feher, Gordon, Buehler, Gere, and Thurmond, Phys. Rev. **109**, 221 (1958).

[3] Chester, Wagner, and Castle, Phys. Rev. **110**, 281 (1958).

[4] D. E. Kaplan and M. E. Browne, Phys. Rev. Letters **2**, 454 (1959).

[5] V. M. Faĭn, Изв. Высш. шк., Радиофизика (News of the Colleges, Radiophysics) **2**, 167 (1959).

[6] R. H. Hoskins, Phys. Rev. Letters **3**, 174 (1959).

Translated by W. F. Brown, Jr.
252

FORMATION OF PIONS IN πN COLLISIONS

A. I. LEBEDEV and V. A. PETRUN'KIN

P. N. Lebedev Physics Institute, Academy of Science, U.S.S.R.

Submitted to JETP editor January 3, 1960

J. Exptl. Theoret. Phys. (U.S.S.R.) **38**, 1337-1338 (April, 1960)

THE model of Lindenbaum and Sternheimer[3] offers only a qualitative explanation for the observed momentum distribution of π mesons from the reaction $\pi + N \rightarrow 2\pi + N$ at kinetic energies 1.0 and 1.4 Bev (in the laboratory frame of reference). According to this model, the meson arises from the formation of an isobaric state ($T = 3/2$, $J = 3/2$, $l = 1$) with finite width. On the other hand, Fermi's statistical theory does not explain these distributions, while within the framework of this theory a calculation of the isobars, as particles of mass M = 1.32 nucleon masses, also leads to only qualitative agreement with experiment. Rus'kin[5] has attempted to improve the agreement by taking into account a resonance $\pi\pi$ interaction, a new particle Π being introduced, with mass $M = 0.47$ nucleon masses, which decays into two π mesons. We have made analogous calculations, which do in-

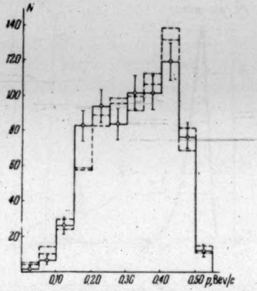

FIG. 1. Momentum distribution of all π mesons (π^+, π^-, π^0) from the reactions $\pi^- + p \rightarrow \pi^- + \pi^+ + n$, $\pi^- + \pi^0 + p$ at an energy of 1 Bev (number of mesons N as a function of momentum p in the center-of-mass system). The solid histogram is drawn through the experimental points of reference 1, while the dot-dash one was calculated from the statistical theory, taking into account the isobar with M = 1.32 and a Π particle (M = 0.47). The dashed histogram was calculated taking into account the finite width of the isobaric state (3/2, 3/2, 1).

deed improve agreement with experiment but not to the extent quoted in reference 5. We wish to point out that it is possible to describe the experimental data just as well without taking into account the meson-meson interaction, but including instead in the statistical theory the effect of the finite width of the isobar which decays to give π mesons.

To do this we take into account the interaction in the final state;[6] in our case the final state is $\pi + \pi + N$ and we consider only the interaction between the meson and the nucleon. We then have for the part of the cross section which corresponds to the formation of a π meson through the isobaric state

$$d\sigma_1 = (p^{-2}\sin\delta_{33})^2\, d\mathbf{p}_1\, d\mathbf{p}_2\, d\mathbf{p}_3\, \delta\left(\sum_{i=1}^{3} E_i - E_0\right)\delta\left(\sum_{i=1}^{3} \mathbf{p}_i\right),$$

where the phase δ_{33} describes the resonance scattering of mesons by nucleons and p is the modulus of the relative meson-nucleon momentum. Integration of this formula leads to the result of Lindenbaum and Sternheimer. The total cross section for the reaction $\pi + N \rightarrow 2\pi + N$ has the form

$$d\sigma = C_1\, d\sigma_1 + C_2\, d\sigma_2,$$

where $d\sigma_2$ is the cross section for the formation of three particles without interaction, while C_1 and C_2 are determined by the statistical weights for the formation of a π meson plus the isobar (M = 1.32) and two π mesons plus a nucleon. $d\sigma_1$ and $d\sigma_2$ are normalized to the same number of mesons.

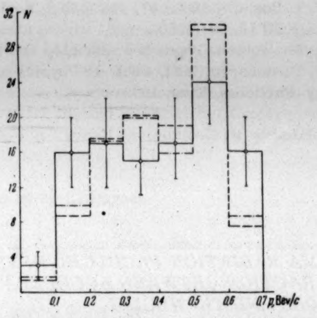

FIG. 2. Same as Fig. 1, but at 1.4 Bev. The experimental points were taken from reference 2.

Figures 1 and 2 show the results of integrating this formula over all variables (except the momentum of one particle), namely the momentum distribution of the mesons in the center-of-mass system for incident-meson energies 1.0 and 1.4 Bev. It is clear that the calculated histograms agree with the experimental data just as well as the results of statistical-theory calculations with account of $\pi\pi$ interaction. Thus the experimental data can be described without invoking the particle Π (M = 0.47), particularly since the existence of such a particle implies a peak in the momentum distribution of the recoil nucleons, a peak which is not observed in the new, more comprehensive data at 1 Bev.[1]

If we take into account the second resonance state (T = ½, J = 3/2, l = 2) in the πN system[7] as a second isobar with mass M = 1.52, then agreement between theory and experiment becomes worse. (Such a second resonance state would correspond to a π meson with kinetic energy ~ 600 Mev in the laboratory frame of reference.) This is because both the π meson from the decay of this isobar and the recoil meson contribute to the momentum spectrum just where the observed spectrum has a plateau or even a dip.

In conclusion, the authors would like to express their gratitude to I. A. Egorova for doing the laborious numerical computations.

---

[1] I. Derado and N. Schmitz, Preprint, 1959.

[2] Eisberg, Fowler, Lea, Shephard, Shutt, Thorndike, and Whittemore, Phys. Rev. **97**, 797 (1955).

[3] R. M. Sternheimer and S. J. Lindenbaum, Phys. Rev. **109**, 1723 (1958).

[4] A. I. Nikishov, JETP **30**, 601 (1956), Soviet Phys. JETP **3**, 634 (1956).

[5] V. I. Rus'kin, JETP **37**, 105 (1959), Soviet Phys. JETP **10**, 74 (1960).

[6] K. M. Watson, Phys. Rev. **88**, 1163 (1952).

[7] B. Pontecorvo, Int'l. Conf. on Physics of High-energy Particles, Kiev, 1959

Translated by R. Krotkov
253

GAMMA RADIATION PRODUCED IN THE INTERACTION BETWEEN ACCELERATED C^{12} IONS AND TIN NUCLEI

V. A. KARNAUKHOV and Yu. Ts. OGANESYAN

Submitted to JETP editor January 14, 1960

J. Exptl. Theoret. Phys. (U.S.S.R.) **38**, 1339-1340 (April, 1960)

COMPOUND nuclei with large excitation energy and angular momentum are produced in nuclear reactions caused by accelerated heavy ions. Strutinskiĭ[1] assumes that during the decay of such a compound nucleus the main part of the angular momentum is carried off by gamma radiation, i.e., the emission of nucleons is accompanied by a gamma-ray cascade.

The present paper is devoted to the study of the gamma-ray energy spectrum appearing during the irradiation of Sn with C^{12} ions, accelerated to about 78 Mev. According to estimates, the maximum excitation energy of the compound nucleus in this case amounts to ~ 66 Mev, and the maximum angular momentum amounts to $\sim 45\,\hbar$. The experiments were carried out with the extracted beam of the 150-cm cyclotron of the Atomic Energy Institute of the U.S.S.R. Academy of Sciences. The intensity of the beam was $\sim 5 \times 10^6$ particles/sec. The 24 mg/cm^2 tin target was set at 45° to the incident beam. The gamma rays in the 0.4- to 4-Mev energy range were registered with a scintillation gamma spectrometer, consisting of a CsI crystal (3 cm diameter, 3 cm height), an S-993 photomultiplier and an ÉLA-2 multichannel analyzer.[2] The channel width was 0.075 Mev. The energy resolution of the Cs^{137} photopeak (0.661 Mev) was $\sim 11\%$. A miniature proportional counter, mounted on the entrance diaphragm, was used to monitor the beam. To absorb the soft x rays appearing when the carbon ions pass through the target, a lead foil $\sim 150\,\mu$ thick was placed in front of the crystal. The distance between the target and the spectrometer crystal could be varied from 0.2 to 5 cm. In the experiments for determining the background, the ion energy was decreased below the Coulomb barrier of tin nuclei for C^{12} ions by inserting a $60\,\mu$ aluminum foil at a distance of 15 cm from the crystal. In processing the spectra, the spectral sensitivity of the instrument and the line shape, obtained during the registration of monochromatic gamma rays,[3] were taken into account.

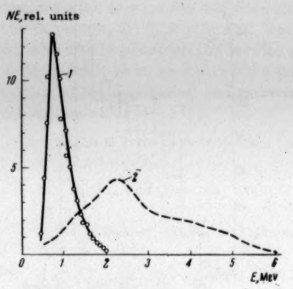

FIG. 1

Figure 1 (curve 1) shows the corrected gamma spectrum in the form NE = f(E) [N is the number of gamma quanta in the channel with an energy E]. The distance R between the crystal and the target was 5 cm. The spectrum has the form of a continuous distribution with a maximum at E = 0.8 Mev. Figure 1 (curve 2) also shows the gamma-ray spectrum from the reaction $Sm^{150}(n, \gamma)$ with thermal neutrons (unresolved portion[4]), which is typical of the case of a compound nucleus with an angular momentum practically the same as in the ground state. This spectrum has a peak energy of about 2 Mev.

Comparison of these two spectra indicates that in our case the transition of the nucleus to the ground state takes place overwhelmingly with emission of softer gamma quanta than emitted in radiative neutron capture.

An attempt was also made to estimate experimentally the mean number of gamma quanta emitted during the disintegration of the compound nucleus. For this purpose the distance between the crystal and the target was decreased to its minimum; this increased the probability of simultaneous registration of successively emitted gamma quanta.

Figure 2 shows corrected gamma-ray spectra obtained for R = 5 cm (a) and R = 0.2 cm (b) normalized to make the areas under the respective curves, plotted in NE and E coordinates, equal.

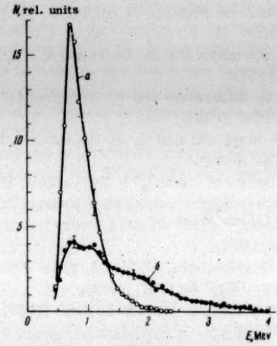

FIG. 2

This normalization takes account of the change in the registration efficiency of the radiation with a change in the distance between the target and the crystal. From a comparison of the spectra it can be seen that with the decreasing target-to-crystal distance the relative number of pulses corresponding to 1.5- to 4-Mev gamma quanta increases. It must be assumed that this is caused by the presence of cascades consisting of relatively soft gamma rays which, being simultaneously registered, simulate gamma quanta of higher energy. The mean number of simultaneously registered gamma quanta for $R = 0.2$ cm, found from the ratio of the areas under curves (a) and (b) (Fig. 2), is ~ 1.8.

To determine the mean number of gamma quanta in a cascade, it is essential to know not only the counting efficiency of the spectrometer, but also the angular distribution of the gamma quanta. At present, there are no data on the angular distribution of gamma quanta emitted by a compound nucleus with a large angular momentum, and therefore a sufficiently precise determination of this quantity is difficult. According to our rough estimates this number is apparently not less than 10.

The authors are grateful to Professor G. N. Flerov for valuable advice, and to A. B. Malinin for help in carrying out the experiment.

---

[1] V. M. Strutinskiĭ, Тр. Всесоюзной конференции 1957 г. по ядерным реакциям при малых и средних энергиях, (Trans. of the All-Union Conference on Nuclear Reactions at Low and Medium Energies) 1957, Acad. Sci. Press, p. 522.

[2] Mel'nikov, Artemenkov, and Golubov, Приборы и техника эксперимента (Instr. and Meas. Engg.) No. 6, 57 (1957).

[3] N. V. Konstantinov, Некоторые вопросы инженерной физики (Some Problems of Engineering Physics) Moscow Physics and Engineering Institute Press, No. 3, 32 (1957).

[4] Groshev, Demidov, Lutsenko, and Pelekhov, Trans. of the Second International Conference on the Peaceful Uses of Atomic Energy, Geneva 1958, Acad. of Sci. Press, vol. I, p. 281.

Translated by Z. Barnea
254

BETA DECAY OF P^{32}

B. V. GESHKENBEĬN

Submitted to JETP editor January 14, 1960

J. Exptl. Theoret. Phys. (U.S.S.R.) 38, 1341-1342 (April, 1960)

THE β transition in P^{32} appears to be an allowed $1^+ \rightarrow 0^+$ transition. Therefore the β spectrum of P^{32} must have a Fermi shape and a polarization equal to v/c. However experimental results[1-3] have indicated a small deviation from the Fermi shape for the spectrum and from the designated polarization value. The aim of the present paper is to offer a possible explanation of these experimental results.

Since $\log ft = 7.9$ for P^{32}, while for Gamow-Teller transitions $\log ft \sim 4$, this means that the matrix element $\int\sigma$ in this case must be about 30 – 40 times smaller than its normal value. Therefore we must examine second-forbidden terms. The transition in question may have contributions from terms of the form $\int\sigma r^2$, $\int(\sigma r)r$, $\int[\alpha r]$ and $\int\gamma_5 r$. The first two matrix elements are small in comparison to the last two. The matrix element $\int[\alpha r]$ introduces into the spectrum a term which is proportional to the β-electron energy, but since there is no such term experimentally observed in the P^{32} spectrum, we set this matrix element equal to zero. Therefore we shall consider further only the matrix element $\int\gamma_5 r$.

Let us introduce the relation $x = \int\gamma_5 r/\int\sigma$. In β transitions having a normal value of $\log ft$ we have $x \sim (v/c)_{\text{nucl}}\rho_{\text{nucl}}/\lambda\!\!\!^{-}_{\text{Compton}} \sim 0.002$. (We use a system of units in which $\hbar = c = m_e = 1$.) Because of the smallness of $\int\sigma$, the value of x for P^{32} must be about 30 – 40 times larger, i.e., $x \sim 0.06 - 0.08$. For these values of x it is necessary to take into account not only the terms proportional to x, but also terms of the order of x^2.

Assuming the correctness of the theory of weak interactions,[4,5] we obtain the following equations for the correction constant C and for the polarization $<\sigma>$:

$$C = \left(1 - \tfrac{2}{3} qy + \tfrac{1}{3} q^2y^2\right)L_0 + 2\left(y - \tfrac{1}{3} qy^2\right)N_0 + y^2(M_0 + 2L_1),$$
$$\langle\sigma\rangle = -D/C, \qquad (1)$$

whereupon D is obtained from C by substituting

$$L_0 \to L_0' = (L_0^2 - P_0^2)\sin(\delta_{-1} - \delta_1),$$
$$M_0 \to M_0' = (M_0^2 - Q_0^2)\sin(\delta_{-1} - \delta_1),$$
$$N_0 \to N_0' = \tfrac{1}{2}[(L_0 + P_0)^{1/2}(M_0 + Q_0)^{1/2}$$
$$+ (L_0 - P_0)^{1/2}(M_0 - Q_0)^{1/2}]\sin(\delta_{-1} - \delta_1),$$
$$L_1 \to L_1' = (L_1^2 - P_1^2)^{1/2}\sin(\delta_{-2} - \delta_2).$$

For determination of the functions L_0, M_0, N_0, etc. see references 6 and 7; δ_1, δ_{-1}, δ_2, δ_{-2} are Coulomb phases; q is the neutron momentum. If we use the relation $Ze^2 \ll 1$, and the explicit expressions for the functions L_0, M_0, . . . ,[6,8] we obtain the following simple equations for the β spectrum and for the longitudinal polarization of the β electrons in P^{32}:

$$C = 1 + a/\varepsilon, \qquad \langle\sigma\rangle = -v(1 - a/\varepsilon), \qquad (2)$$

where $a = \tfrac{2}{3}x[1 - (Ze^2/2\rho + \tfrac{2}{3}\epsilon_0)x]^{-1}$, ϵ_0 is the spectral end-point energy. In deriving Eq. (2) we neglected terms in x^2 if they were multipled by small quantities, i.e., a necessary condition for the validity of these equations is

$$x^2 \ll 1 - \left(Ze^2/2\rho + \tfrac{2}{3}\varepsilon_0\right)x.$$

Equations (1) and (2) convert into Morita's equation[9] if we drop the quadratic terms in x^2. For a value of $x = 0.08$ we obtain $a = 0.18$ which agrees with experimental data.[1-3] The deviation of the spectrum from a Fermi shape and of the polarization from v/c also occurs for In^{114} ($1^+ \to 0^+$ transition).[2,3] The formally required value $a \sim 0.3$ is obtained for a value of $x = 0.057$. Although such a large value of x seems improbable because the quantity log ft equals 4.4 for In^{114}, it cannot be strictly ruled out.

In conclusion I wish to express my thanks to Academician A. I. Alikhanov, Professor V. A. Berestetsko, B. L. Ioffe, and V. A. Lyubimov for their interest in and discussion of the work.

---

[1] Porter, Wagner, and Freedman, Phys. Rev. **107**, 135 (1957).

[2] Johnson, Johnson, and Langer, Phys. Rev. **112**, 2004 (1958).

[3] L. A. Mikaélyan and P. E. Spivak, Материалы конференции по физике частиц высоких энергий (Trans. Conf. on Physics of High-Energy Particles) Kiev, 1959.

[4] R. P. Feynman and M. Gell-Mann, Phys. Rev. **109**, 193 (1958).

[5] E. C. G. Sudarshan and R. E. Marshak, Phys. Rev. **109**, 1860 (1958).

[6] E. I. Konopinski and G. E. Uhlenbeck, Phys. Rev. **60**, 308 (1958).

[7] B. S. Dzhelepov and L. I. Zyryanova, Влияние электрического поля атома на бета-распад (Effect of Atomic Electric Field on Beta Decay) Acad. of . Sci. Press, 1956.

[8] B. V. Geshkenbeĭn, JETP **33**, 1535 (1957), Soviet Phys. JETP **6**, 1187 (1958).

[9] M. Morita, Phys. Rev. **113**, 1584 (1959); **114**, 1080 (1959).

Translated by D. A. Kellogg
255

ON THE DECAY OF Σ HYPERONS

CHOU KUANG-CHAO

Joint Institute of Nuclear Studies

Submitted to JETP editor January 27, 1960

J. Exptl. Theoret. Phys. (U.S.S.R.) **38**, 1342-1343 (April, 1960)

THE experimental data on the probabilities and asymmetry coefficients of the decays of Σ hyperons by various channels evidently satisfy the rule $|\Delta I| = \tfrac{1}{2}$. If the $|\Delta I| = \tfrac{1}{2}$ rule receives final experimental confirmation, it will be necessary to renounce the theory of the universal weak interaction between charged currents.[3] At present it is desirable to have more data to test this rule.

Let us denote the amplitudes for the processes $\Sigma^+ \to p + \pi^0$, $\Sigma^+ \to n + \pi^+$, and $\Sigma^- = n + \pi^-$ by A_+, A_0, and A_-, respectively, where $A = a + ib(\boldsymbol{\sigma}\mathbf{k})$; **k** is the unit vector in the direction of motion of the nucleon. The absence of asymmetry in the decays $\Sigma^\pm \to n + \pi^\pm$ means that for these processes

$$\mathrm{Re}(ab^*) = 0. \qquad (1)$$

There are three ways to satisfy the condition (1): 1) a = 0, 2) b = 0, 3) the phases of a and b differ by 90°. Since the interaction of pion and nucleon in the final state is small, the third possibility violates the conservation of time parity.

Many authors[2,3] have shown that the rule $|\Delta I| = \frac{1}{2}$ holds only for $a_0 = b_- = 0$ or $a_- = b_0 = 0$. To choose from among the three cases the one that exists in nature, one could use measurements of the polarization of the nucleons from the decay of polarized $\Sigma^\pm$ particles produced in reactions $\pi^\pm + p \rightarrow \Sigma^\pm + K^+$.

Denoting the polarization vectors of nucleons and Σ hyperons by **P** and $\mathbf{P}_\Sigma$, we get

$$\mathbf{P} = \frac{2\operatorname{Re}(ab^*)}{|a|^2+|b|^2}\mathbf{k} + \frac{|a|^2-|b|^2}{|a|^2+|b|^2}\mathbf{P}_\Sigma + \frac{2|b|^2}{|a|^2+|b|^2}(\mathbf{P}_\Sigma\mathbf{k})\mathbf{k} + \frac{2\operatorname{Im}(ab^*)}{|a|^2+|b|^2}[\mathbf{k}\times\mathbf{P}_\Sigma]. \qquad (2)$$

In particular $\mathbf{P} = 2(\mathbf{P}_\Sigma\mathbf{k})\mathbf{k} - \mathbf{P}_\Sigma$ for $a = 0$; $\mathbf{P}_\Sigma = \mathbf{P}$ for $b = 0$; and for the third case **P** has a component along the direction of $\mathbf{k}\times\mathbf{P}_\Sigma$.

It is obvious that a measurement of the direction of the polarization vector of the nucleons will not only give information to test the rule $|\Delta I| = \frac{1}{2}$, but can also help to choose one solution from the two that are possible ($a_0 = b_- = 0$ or $a_- = b_0 = 0$) if this rule holds.

If there is no transverse polarization of the neutrons from Σ^- decay, this means that the initial Σ^- particle is unpolarized. In this case the absence of asymmetry in the Σ^- decay does not lead to Eq. (1). The quantity $\operatorname{Re}(ab^*)$ can be determined from a measurement of the longitudinal polarization of the neutrons.

---

[1] E. C. G. Sudarshan and R. E. Marshak, Phys. Rev. **109**, 1860 (1958). R. P. Feynman and M. Gell-Mann, Phys. Rev. **109**, 193 (1958).

[2] F. S. Crawford, Jr. et al., Phys. Rev. **108**, 1102 (1957). F. Eisler et al., Phys. Rev. **108**, 1353 (1957).

[3] R. E. Sawyer, Phys. Rev. **112**, 2135 (1958). G. Takeda and M. Kato, Progr. Theoret. Phys. **21**, 441 (1959). B. d'Espagnat and J. Prentki, Phys. Rev. **114**, 1366 (1959). B. T. Feld, Preprint. R. H. Dalitz, Revs. Modern Phys. **31**, 823 (1959). M. Gell-Mann, Revs. Modern Phys. **31**, 834 (1959).

Translated by W. H. Furry
256

ON THE PROCESS $e^- + p \rightarrow \Lambda + \nu$

V. M. SHEKHTER

Leningrad Physico-Technical Institute, Academy of Sciences, U.S.S.R.

Submitted to JETP editor January 27, 1960

J. Exptl. Theoret. Phys. (U.S.S.R.) **38**, 1343-1345 (April, 1960)

So far only two decays $\Lambda \rightarrow p + e^- + \bar{\nu}$ have been found,[1] although according to the universal V-A interaction theory (without, however, taking into account the renormalization of the decay coupling constants) approximately 20 times as many events should have been seen. The rarity of hyperon leptonic decays makes the study of them very difficult. For this reason it becomes of interest to study the inverse process

$$e^- + p \rightarrow \Lambda + \nu, \qquad (1)$$

which is due to the same interaction as the β decay of the Λ hyperon, but whose statistics may, in principle, be made rather large.

The threshold for reaction (1) in the laboratory system is $(m_\Lambda^2 - m_p^2)/2m_p = 194$ Mev, and, up to the threshold for Λ photoproduction ($e^- + p \rightarrow e^- + \Lambda + K^+$), which is equal to $[(m_\Lambda + m_K)^2 - m_p^2]/2m_p = 912$ Mev, reaction (1) is the only source of Λ hyperons (together with $e^- + p \rightarrow \Sigma^0 + \nu$, $\Sigma^0 \rightarrow \Lambda + \gamma$).

The matrix element for process (1) (in the notation introduced in reference 3) has the form (where we ignore the electron mass)

$$M = (\bar{u}_\Lambda\{\gamma_\alpha(C_V - C_A\gamma_5) - \sigma_{\alpha\beta}(p_\Lambda - p_p)_\beta(B_V + B_A\gamma_5)\}u_p) \times (\bar{u}_\nu\gamma_\alpha(1+\gamma_5)u_e), \qquad (2)$$

with the form factors C_V, C_A, B_V, B_A functions of the square of the momentum transfer

$$-Q^2 = (p_p - p_\Lambda)^2 = 2m_pW + (m_\Lambda - m_p)^2, \qquad (3)$$

where W is the kinetic energy of the Λ hyperon in the laboratory system. If E is the energy of the incident electron and $\epsilon \equiv 2m_pE + m_p^2$ is the total energy in the center-of-mass system then

$$0 \leqslant -Q^2 \leqslant 2m_pE\left(1 - \frac{m_\Lambda^2}{\varepsilon^2}\right) = \varepsilon^2\left(1 - \frac{m_p^2}{\varepsilon^2}\right)\left(1 - \frac{m_\Lambda^2}{\varepsilon^2}\right). \qquad (4)$$

The cross section for process (1) for a given E and Q^2 is given by*

$$d\sigma = \frac{d(-Q^2)}{16\pi E^2 m_p^2}\{(C_V^2 + C_A^2)[8m_p^2E^2 - (4m_pE + Q^2)(m_\Lambda^2 - m_p^2 - Q^2)] - (C_A^2 - C_V^2)2m_\Lambda m_pQ^2 - (B_A^2 - B_V^2)2m_\Lambda m_pQ^4$$
$$+ (B_V^2 + B_A^2)[-8m_p^2E^2 + (4m_pE - m_\Lambda^2 + m_p^2)(m_\Lambda^2 - m_p^2 - Q^2)] - 2C_VB_VQ^2(m_\Lambda + m_p)[(m_\Lambda - m_p)^2 - Q^2]$$
$$+ 2C_AB_AQ^2(m_\Lambda - m_p)[(m_\Lambda + m_p)^2 - Q^2] - 2[C_VC_A + C_AB_V(m_\Lambda + m_p) - C_VB_A(m_\Lambda - m_p)$$
$$- B_VB_A(m_\Lambda^2 - m_p^2)]Q^2[-4m_pE + m_\Lambda^2 - m_p^2 - Q^2]\}. \qquad (5)$$

For a "pure" V-A interaction ($C_V = -C_A \equiv F/\sqrt{2}$, $B_V = B_A = 0$) formula (5) simplifies into

$$d\sigma \doteq \frac{d(-Q^2)\,F^2}{4\pi E m_p}(\varepsilon^2 - m_\Lambda^2); \quad \sigma = \frac{F^2}{2\pi}\varepsilon^2\left(1 - \frac{m_\Lambda^2}{\varepsilon^2}\right)^2. \quad (6)$$

The second of these formulas is valid to the extent that the Q^2 dependence of F may be ignored. This dependence will become important, presumably, at $-Q^2 \sim m_K^2$.[6] In any case the magnitude of the form factors should fall off rapidly for $-Q^2 \gg m_K^2$. Therefore, at high energies the effective range of variation of $-Q^2$ is smaller than is given by Eq. (4). One may suppose that in effect $0 \leq -Q^2 \leq Q_0^2$, $Q_0^2 \sim m_K^2$. If at the same time $E \gg m_\Lambda$, and consequently $m_p E \gg -Q^2$, then only the first term in Eq. (5) is important so that

$$d\sigma = \frac{d(-Q^2)}{2\pi}(C_V^2 + C_A^2). \quad (7)$$

For $C_V^2 + C_A^2 \equiv F^2 \approx \text{const}$ $(0 \leq -Q^2 \leq Q_0^2)$

$$\sigma \sim \frac{F^2}{2\pi}Q_0^2 \sim \frac{F^2}{2\pi}m_K^2 \sim \frac{F^2}{G^2}\cdot 2\cdot 10^{-39}\ \text{cm}^2 \quad (8)$$

where $G = 1.41 \times 10^{-49}$ erg cm^3 is the Feynman–Gell-Mann constant.[2] If $F^2/G^2 \sim 1/20$ then $\sigma \sim 10^{-40}$ cm^2. In a similar fashion we find

$$\sigma \approx (F/G)^2\cdot 7\cdot 10^{-40}\ \text{cm}^2 \approx 0.35\cdot 10^{-40}\ \text{cm}^2, \quad (9)$$

for $E = 400$ Mev, when the upper limit on the range of variation of $-Q^2$ in Eq. (4) is of order m_K^2 and we may use for estimate purposes the second of the formulas (6).

With a cross section of the order of 10^{-40} cm^2 the probability for the process (1) is equal to 10^{-17} for a 10 cm path length of an electron in liquid hydrogen of density $\sim 10^{22}$ atoms/cm^3. Consequently, approximately $10^{18} - 10^{19}$ electrons are needed to observe the reaction. With accelerator intensities of 10^{13} electrons per second this figure is not so fantastic. If instead of hydrogen heavier elements are used then for the same number of atoms in 1 cm^3 the necessary number of electrons is decreased by a factor Z. Theoretically, however, the analysis of the experimental results becomes in this case much more complicated since the proton is initially bound. We only remark that in the case of a nucleus some of the reactions $e^- + p \rightarrow \Lambda + \nu$ will result in the formation of Λ hyperfragments.

The experimental study of the process (1) presents, naturally, a number of difficulties, connected in part with the necessity of observing a Λ hyperon in the presence of considerable background. Nevertheless such a study is of interest particularly since by varying the energy E it is possible in this way to directly investigate the Q^2 dependence of the form factors.

Along with the reaction (1) it is possible to study the reactions $e^- + p \rightarrow \Sigma^0 + \nu$ and $e^- + n \rightarrow \Sigma^- + \nu$. In view of the absence of intense μ^--meson beams the corresponding processes involving μ^- mesons in place of e^- are hardly possible experimentally.

The author is grateful to I. M. Shmushkevich for pointing out the feasibility of studying process (1) and for discussions.

---

*If one neglects the mass difference between the Λ hyperon and the proton (in which case, according to Eq. (3), $-Q^2 = 2m_p W$) as well as the "magnetic" form factors of the type B_V and B_A, then the expression for the cross section with all covariants of the 4-fermion interaction taken into account is the same as the expression describing the cross section for electron-neutrino scattering.[4] (In formula (1) of reference 4 g_S^2 should stand next to $W^2 + 2WE$ and not $W^2 + WE$, and $(2g_V g_A + g_S g_T + g_P g_T)$ next to $W^2 - 2WE$, not $W^2 - WE$).

For $B_A = 0$, $m_\Lambda \approx m_p$, expression (5) coincides with the result obtained by Berestetskiĭ and Pomeranchuk[5] for the cross section for the process $e^- + p \rightarrow n + \nu$.

---

[1] Crawford, Cresti, Good, Kalbfleisch, Stevenson, and Ticho, Phys. Rev. Lett. **1**, 377 (1958). Nordin, Orear, Reed, Rosenfeld, Solmitz, Taft, and Tripp, Phys. Rev. Lett. **1**, 380 (1958).

[2] R. P. Feynman and M. Gell-Mann, Phys. Rev. **109**, 198 (1958).

[3] Belov, Mingalev, and Shekhter, JETP **38**, 541 (1960), Soviet Phys. JETP **11**, 392 (1960).

[4] V. M. Shekhter, JETP **34**, 257 (1958), Soviet Phys. JETP **7**, 179 (1958).

[5] V. B. Berestetskiĭ and I. Ya. Pomeranchuk, JETP **36**, 1321 (1959), Soviet Phys. JETP **9**, 936 (1959).

[6] N. Cabibbo and R. Gatto, Nuovo cimento **13**, 1086 (1959).

Translated by A. M. Bincer
257

INELASTIC INTERACTIONS OF 9 Bev PROTONS WITH FREE AND BOUND NUCLEONS IN EMULSION

N. P. BOGACHEV, S. A. BUNYATOV, Yu. P. MEREKOV, V. M. SIDOROV, and V. A. YARBA

Joint Institute for Nuclear Research

Submitted to JETP editor January 27, 1960

J. Exptl. Theoret. Phys. (U.S.S.R.) **38**, 1346-1348 (April, 1960)

IN an emulsion stack exposed to the proton synchrotron of the High-Energy Laboratory of the Joint Institute for Nuclear Research, 243 cases of inelastic interactions (140 pp and 103 pn) of

9-Bev protons with free and bound nucleons of the emulsion were recorded by scanning along the tracks. The selection of the events was made according to the criteria enumerated in reference 1 and described earlier in greater detail.[2]

To obtain the energy and angular characteristics of the secondary particles, measurements of multiple Coulomb scattering and ionization were carried out on all tracks inclined at an angle no greater than 5° to the plane of the emulsion. There were 144 such tracks of pp events and 108 of pn events. The method of measurement and analysis of the results was described in reference 3. The mean value of spurious scattering in pellicles in which momentum measurements were made was 0.3μ for a 1000μ cell and 0.7μ for a 2000μ cell, which corresponds to the Coulomb scattering of a singly charged particle with $p\beta = 5$ Bev/c. All secondary tracks with $p\beta \leq 1.6$ Bev/c were identified; in the region of higher $p\beta$ values the ionization vs $p\beta$ curves for π mesons and protons overlap. After allowance for the geometric correction[3] it was found that particles with $p\beta \leq 1.6$ Bev/c constituted 78% of the total number of particles.

All secondary particles whose angle of emission with reference to the direction of the primary proton in the laboratory system was greater than 20° were identified. This means that all π^- mesons emitted in the center-of-mass system (c.m.s.) of the colliding nucleons in the backward hemisphere were identified. The proportion of unidentified protons emitted in the backward hemisphere in the c.m.s. can be estimated by making use of the symmetry of the angular distribution of secondary particles from pp interactions with respect to the 90° direction in the c.m.s. The corresponding value did not exceed 6% of the number of identified protons in the backward hemisphere in the c.m.s. Hence, practically only identified particles fall in the backward hemisphere in the c.m.s.

For the pp interactions, the angular distributions of the charged π mesons and protons emitted in the c.m.s. in the backward hemisphere are shown in Fig. 1 (N is the number of particles in relative units). The median angle of emission in the c.m.s. was $(16 \pm 6)^\circ$ for protons and $(38 \pm 10)^\circ$ for π mesons. Thus the angular distributions of the protons and π mesons are anisotropic, as has also been observed[4] at 6.2 Bev. This is in contradiction to the statistical theory assumption of isotropy of the secondary particle distribution in the c.m.s., at least in its variant in which the influence of the conservation of angular momentum is not taken into account.

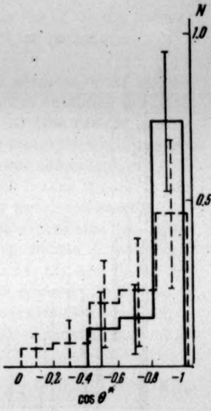

FIG. 1. C.m.s. angular distribution of protons and charged π mesons from pp interactions. Solid line – protons (43 tracks); broken line – π mesons (20 tracks).

The mean numbers n_p and n_π of protons and charged π mesons for one act of inelastic pp interaction found from the number of protons and π mesons in the backward hemisphere in the c.m.s. are $n_p = 1.3 \pm 0.3$ and $n_\pi = 1.9 \pm 0.3$. The corresponding values calculated from statistical theory[5] are $n_p = 1.2$ and $n_\pi = 2.3$. The number of negative π mesons in each pp event, if the production of antiprotons and strange particles is neglected, is determined from the law of charge conservation. Thus, knowing the total number of charged π mesons, one can estimate the number of π^+ and π^- mesons for one act of interaction. The values found are $n_{\pi^+} = 1.3 \pm 0.3$ and $n_{\pi^-} = 0.61 \pm 0.06$.

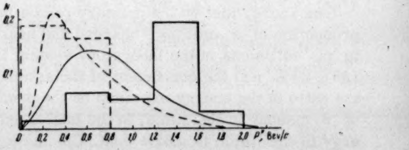

FIG. 2. C.m.s. momentum spectra of protons and charged π mesons from pp interactions. Histograms – experimental data; smooth curves – according to statistical theory.[5] The areas under all four curves are the same. Solid lines – protons (43 tracks); broken lines – π mesons (20 tracks).

The momentum spectra for protons and charged π mesons emitted in the c.m.s. in the backward hemisphere is shown for pp interactions in Fig. 2. It is seen from the figure that the π-meson and proton spectra are displaced, with respect to the theoretical spectrum, towards the lower and higher momenta, respectively. The same is also observed[4]

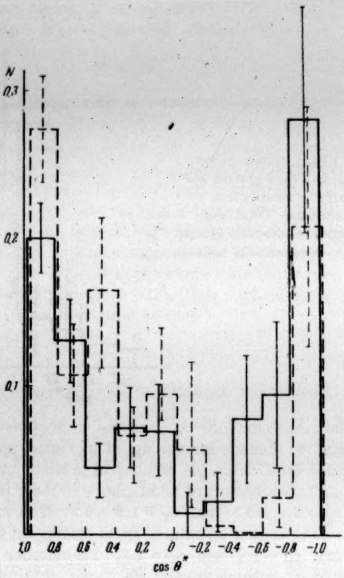

FIG. 3. C.m.s. angular distributions of secondary particles from pp interactions (solid line) and pn interactions (broken line).

at 6.2 Bev. The mean momenta in the c.m.s. for protons and charged π mesons are $P_p^* = (1.2 \pm 0.1)$ Bev/c and $P_\pi^* = (0.4 \pm 0.1)$ Bev/c, and according to statistical theory,[6] $P_p^* = 0.79$ Bev/c and $P_\pi^* = 0.51$ Bev/c.

The energy lost by the primary proton in the production of π mesons (charged and neutral) in pp collisions in the laboratory system is $(36 \pm 2)\%$, and the coefficient of inelasticity, i.e., the ratio of the energy expended on the production of π mesons in the c.m.s. to the total kinetic energy in the c.m.s. is 0.52 ± 0.03. Calculations based on statistical theory[6] give for the energy loss in the laboratory system a much greater value (58%). Even if the contribution from peripheral collisions is taken to be 20%, the theoretical energy loss in the laboratory system will not drop below 50%.

For pp and pn interactions the angular distributions in the c.m.s. were constructed for secondary charged particles on whose tracks scattering and ionization measurements were made (Fig. 3). A geometric correction here was introduced in accordance with reference 3. It was assumed that the velocity of the unidentified particles in the c.m.s. was equal to the velocity of the center of mass. The angular distributions of the secondary particles in the c.m.s. for pp interactions are symmetric. In contrast to the pp interactions, the angular distributions of the secondary particles from pn interactions are asymmetric. The respective coefficients of asymmetry are $\Delta_{pp} = 0.08 \pm 0.36$ and $\Delta_{pn} = 1.05 \pm 0.32$, which confirms the results obtained earlier.[2] Here $\Delta = (N_F - N_B)/C$, where N_F and N_B are the numbers of particles emitted forward and backward in the c.m.s. and C is the number of interactions. The existence of an asymmetry in the c.m.s. angular distributions of secondary charged particles from pn interactions cannot, in general, be explained from the point of view of statistical theory.

Hence the experimental results obtained in the present work and earlier[2,3] indicate that the nucleon-nucleon interaction at energies of 6 — 9 Bev are not described by the statistical theory of multiple production. The data of the present article on the momentum and angular distributions of secondary protons and mesons do not contradict the conclusion as regards the important role of collisions with a small momentum transfer (peripheral collisions).[7]

The authors thank V. I. Veksler and Academician V. P. Dzhelepov for their interest in this work

---

[1] Bogachev, Bunyatov, Merekov, and Sidorov, Dokl. Akad. Nauk SSSR **121**, 617 (1958), Soviet Phys.-Doklady **3**, 785 (1959).

[2] Bogachev, Bunyatov, Gramenitskiĭ, Lyubimov, Merekov, Podgoretskiĭ, Sidorov, and Tuvdendorzh, JETP **37**, 1225 (1959), Soviet Phys. JETP **10**, 872 (1960).

[3] Bogachev, Bunyatov, Vishki, Meretov, Sidorov, and Yarba, Preprint, Joint Inst. Nucl. Res. O-391; JETP **38**, 432 (1960), Soviet Phys. JETP **11**, 317 (1960).

[4] Kalbach, Lord, and Tsao, Phys. Rev. **113**, 330 (1959).

[5] Barashenkov, Belyakov, Bubelev, Wang, Mal'tsev, Ten Gyn, and Tolstov, Nuclear Phys. **9**, 74 (1958).

[6] V. S. Barashenkov and V. M. Mal'tsev, Preprint, Joint Inst. Nucl. Res. R-433 (1959).

[7] V. I. Veksler, Report at the 8th International Conference on High Energy Physics, Kiev, 1959.

Translated by E. Marquit
258

ON ELASTIC SCATTERING OF PHOTONS BY THE NUCLEAR COULOMB FIELD

C. EFTIMIU and C. VREJOIU

Parhon University, Bucharest

Submitted to JETP editor February 1, 1960

J. Exptl. Theoret. Phys. (U.S.S.R.) 38, 1348-1350 (April, 1960)

As is known, the only evaluations of the cross section for elastic scattering of photons by the nuclear Coulomb field have been made either at zero angle of incidence[1] or at very small angles (of the order of a degree) and at high energies (of the order of tens and hundreds of Mev).[2] On the other hand, experiments carried out to detect this effect (see reference 3), are concerned with angles greater than $15 - 20°$ and with energies of the order of a Mev. Thus, in order to compare theory and experiment, it is necessary to find an approximation which is valid within the experimental region. In what follows we shall describe two approximations whose region of validity is significantly better suited to this situation than are those of previously used methods.

As is known (see reference 2), the main difficulty in calculating the given effect consists of calculating expressions of the type

$$T = \frac{1}{\pi^2 i}\int d^4p \operatorname{Sp}\{\hat{e}(i\hat{p}+1)^{-1}\hat{e}'(i\hat{p}-i\hat{k}'+1)^{-1}\gamma_0(i\hat{p}-i\hat{k}' - i\hat{q}+1)^{-1}\gamma_0(i\hat{p}-i\hat{k}+1)^{-1}\}, \tag{1}$$

where $k \equiv (\mathbf{k}, \mathbf{w})$ and $k' \equiv (\mathbf{k}', \mathbf{w})$ indicate the initial and final photon 4-momenta e and e' are its initial and final polarization; $q \equiv (\mathbf{q}, 0)$ is the "recoil" momentum with respect to which the integration is carried out ($\hbar = c = m_e = 1$). The expression (1) leads in the usual manner to the equation

$$T = \frac{6}{\pi^2 i}\int_0^1 dx \int_0^x dy \int_0^y dz \int d^4p\, \frac{S(p;\, k,\, k',\, q;\, x,\, y,\, z)}{(p^2+L)^4}, \tag{2}$$

where S represents in principle the result of the calculation following (1), and

$$L = 1 - i\varepsilon + q^2x(1-x) + \Omega^2(k,\, k',\, q;\, x,\, y,\, z) \equiv \mu^2 + \Omega^2. \tag{3}$$

In order to reduce the number of different integrations and thus permit carrying the calculations to a conclusion, it is expedient to introduce into equation (1) the expansion

$$(i\hat{p}-i\hat{k}+1)^{-1} = (i\hat{p}-i\hat{k}'+1)^{-1} + (i\hat{p}-i\hat{k}'+1)^{-1}\, i\hat{\Delta}\,(i\hat{p}-i\hat{k}'+1)^{-1} + \ldots, \tag{4}$$

which leads to an expression for T in the form of an expansion in the terms of the parameter $\Delta = |\mathbf{k} - \mathbf{k}'|$.

We calculated the matrix element of the investigated process in this manner, retaining the first two terms of the expansion (4) (the results are given in reference 4). The integration with respect to $\mathbf{q}$ must then be carried out numerically.

Another possibility, which makes it easy to find an analytical expression for the cross section, comes out of the form of the expression (2). After integrating with respect to p in this expression, L appears in terms of $1/L$, $1/L^2$, and $\ln L$. If we expand these functions in powers Ω^2/μ^2, we can easily complete the integration with respect to x, y, z, and q. Such an expansion is permissible, provided

$$\omega^2 + 2\Delta^2 < 4. \tag{5}$$

After normalizing and summing over the polarizations, we obtain the final expression

$$\frac{d\sigma}{d\Omega} = (\alpha Z)^4 \frac{r_0^2}{32}\frac{\omega^4}{m^4}\Big\{\Big[c_1 - c_2\frac{\omega}{m}\sin\frac{\theta}{2} + c_3\sin^2\frac{\theta}{2}\Big]^2(1+\cos\theta) + \Big[c_4\frac{\omega}{m} - c_5\sin\frac{\theta}{2}\Big]^2\sin^2\frac{\theta}{2}\cos^4\frac{\theta}{2}\Big\}, \tag{6}$$

where $c_1, \ldots, c_5$ are numerical coefficients.[5] Coefficients for terms of the order of ω^2/m^2, $\omega\Delta/m^2$ and Δ^2/m^2 are calculated in reference 5. It is found that the coefficients of terms independent of ω and of those linear in ω become zero as a result of gauge invariance. Equation (6) shows that the cross section decreases with increasing scattering angle θ, and that this decrease is more rapid at higher energies. This fact agrees with experimental data. It is evident that $d\sigma/d\Omega\ (\omega, 180°) = 0$, as was to have been expected.

The authors wish to thank Prof. V. Novak for his constant interest in the work and his valuable suggestions.

---

[1] F. Rohrlich and R. L. Gluckstern, Phys. Rev. **86**, 1 (1952).

[2] H. Bethe and F. Rohrlich, Phys. Rev. **86**, 10 (1952).

[3] A. M. Bernstein and A. K. Mann, Phys. Rev. **110**, 805 (1958).

[4] C. Eftimiu and C. Vrejoiu, Bull. Acad. R.P.R. (in press).

[5] C. Eftimiu and C. Vrejoiu, Bull. Acad. R.P.R. (in press).

Translated by D. A. Kellogg

DETERMINATION OF THE FIRST IONIZATION POTENTIALS OF NEODYMIUM AND PRASEODYMIUM BY THE SURFACE IONIZATION METHOD

N. I. IONOV and M. A. MITTSEV

Leningrad Physico-Technical Institute, Academy of Sciences, U.S.S.R.

Submitted to JETP editor February 2, 1960

J. Exptl. Theoret. Phys. (U.S.S.R.) **38**, 1350-1351 (April, 1960)

THE ionization potentials V of the majority of rare earth elements have not yet been determined spectroscopically. This is primarily due to the extreme complexity of the optical spectra of these elements. An attempt made to determine these values from the electrical conductivity of flames[1] did not produce the anticipated results. A surface-ionization method described earlier[2] has been used in the present work to determine the ionization potentials of neodymium and praseodymium atoms.

As is shown in the theory of surface ionization of atoms on composite surfaces,[2,3] if V significantly exceeds the maximum value of the localized work function of the surface, then the logarithm of the ion current from the surface must be a linear function of the surface inverse temperature 1/T. Furthermore if atoms of two different elements are simultaneously ionized on the surface (occurring in numbers n_1 and n_2 per second), the relation of their ion currents J_1/J_2 with the surface is determined by the equation:

$$\log(J_1/J_2) = \log(n_1A_1/n_2A_2) + 5040\,(V_1 - V_2)/T\,.$$

($A = Q_+/Q_0$ is the ratio of the statistical sum of the states of the positive ion Q_+ and of the atom Q_0).

Therefore the slopes of the plots of the $\log J_1/J_2 = f(1/T)$ can be used to find the ionization potential difference $(V_1 - V_2)$ for atoms of the two elements being compared.

For our comparison element we selected indium, whose value V = 5.79 ev has been determined reliably by spectroscopic means. In order to obtain and measure the currents J_1 and J_2, atomic fluxes produced by vaporizing metallic In, Nd and Pr in a special evaporator were directed onto a heated tungsten filament 0.005 cm in diameter. The filament temperature was measured with an optical pyrometer. The steadiness of the atomic flux density arriving at the filament (i.e., the values n_1 and n_2) was monitored by observing the stability of the ion current during the course of the measurements with the filament at $T_0 = 2700°K$.

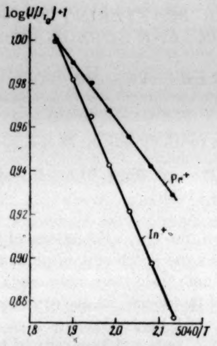

FIG. 1

Figure 1 shows plots of $\log(J/J_{T_0})$ versus 1/T for surface ionization of atoms of In and Pr, from which it can be seen that within the temperature interval 2300 to 2700°K this relation can be satisfactorily approximated by straight lines. Analogous results were obtained for the ionization of Neodymium atoms.

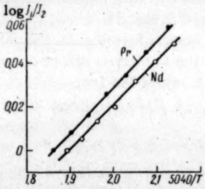

FIG. 2

Figure 2 shows plots of $\log(J_1/J_2)$ versus 1/T for the ratio of Nd and Pr ion currents to the indium ion current in the tungsten filament temperature interval 2300 to 2700°K. The average values of $V_1 - V_2$, found from eight independent determinations of the slope for the pair Pr-In and from ten determinations for the pair Nd-In, turned out to be respectively (0.22 ± 0.01) and (0.19 ± 0.02) ev. It is necessary to introduce a correction into the differences $V_1 - V_2$ determined by slope of the plots in Fig. 2, because of the temperature dependence of the ratio of the statistical sums A of the ionized elements. This correction amounts to 0.09 ev for indium in the filament temperature interval from 2300 to 2700°K. Unfortunately it is not presently possible to evaluate the magnitude of the correction for the case of Nd and Pr, since the energy level diagrams of the atoms and positive ions of these elements are not known.

The corrections may amount to several hundredths ev. In the case of lanthanum, for example, where the atomic and ionic energy level diagrams are known, the correction for the above temperature interval amounts to 0.04 ev. Thus our values of the ionization potentials for atoms of neodymium and praseodymium, not taking into account the possibility of excited atomic and ionic states near the ground state, turned out to be:

$$V_{\mathrm{Pr}} = 5.79 - 0.09 - 0.22 = (5.48 \pm 0.01)\ \text{ev},$$

$$V_{\mathrm{Nd}} = 5.79 - 0.09 - 0.19 = (5.51 \pm 0.02)\ \text{ev}.$$

We would like to remark in conclusion that our results might be viewed as experimental confirmation of the validity of the theoretical equations[3] for the surface ionization of indium, neodymium and praseodymium atoms on incandescent tungsten.

---

[1] L. Rolla and G. Piccardi, Phil. Mag. **7**, 286 (1929).

[2] I. N. Bakulina and N. I. Ionov, JETP **36**, 1001 (1959), Soviet Phys. JETP **9**, 709 (1959).

[3] É. Ya. Zandberg and N. I. Ionov, Usp. Fiz. Nauk **67**, 581 (1959), Soviet Phys.-Uspekhi **2**, 255 (1959).

Translated by D. A. Kellogg
260

THE LINE SHAPE OF THE NUCLEAR ACOUSTIC RESONANCE

N. G. KOLOSKOVA and U. Kh. KOPVILLEM

Kazan' State University

Submitted to JETP editor February 8, 1960

J. Exptl. Theoret. Phys. (U.S.S.R.) 38, 1351-1353 (April, 1960)

RECENTLY there appeared in the literature a number of articles on nuclear acoustic resonance in which the line shape $A(\omega)$ of the nuclear acoustic resonance absorption and the relaxation process in acoustically-excited spin systems is interpreted on the basis of the existing theory of nuclear magnetic resonance (cf. references 1 and 2).

Our investigation of the character of the interaction of the ultrasonic field with the nuclear spin system in cubic crystals, based on the quantum theory of irreversible processes,[3] shows that the above-mentioned method of interpretation of acoustic magnetic resonance data is unfounded and leads to erroneous conclusions. While the line shape of ordinary paramagnetic resonance is determined by the Fourier transform of the auto-correlation function $G_M(t)$ of the magnetic moment M of the spin system,[3] the line shape of the acoustic nuclear resonance is analogously determined by means of the auto-correlation function $G_K(t)$ of the nuclear quadrupole moment K_0 of the spin system. Since M and K_0 are described by a linear and bilinear function of the spin variables, respectively, the character of the time variation of M and K_0 differs for dipole-dipole ($\mathcal{H}_d$), exchange ($\mathcal{H}_{ex}$), and other inner interactions, and the functions $G_M(t)$ and $G_K(t)$ do not coincide.

In particular, in the case when the longitudinal sound wave propagates along the [110] axis and a strong static magnetic field H parallel to the z axis forms an angle θ with the [110] axis, we obtained

$$A(\omega) = \sum_a \omega^2 \frac{\langle |K(\omega_a)|^2 \rangle}{VkT} \Bigl(1 - \sum_{\omega_\gamma \neq 0} \frac{\Delta^2_{a\gamma}}{\omega^2_\gamma}\Bigr) (2\pi\Delta^2_{a0})^{-1/2}$$

$$\times \exp\Bigl\{-\frac{1}{2\Delta^2_{a0}}\Bigl(\omega - \omega_a + \sum_\gamma \frac{\Delta^2_{a\gamma}}{\omega_\gamma}\Bigr)^2\Bigr\}, \qquad (1)$$

where the coefficients for the transition $a = \xi$, in the course of which the magnetic quantum number m of nuclei with spin I changes by ±2, are calculated according to the formula

$$K(\omega_\xi) = \frac{K_0}{4I(2I-1)}\Bigl[\frac{3}{4} + \frac{S_{44}}{S_{11}} + \Bigl(\frac{S_{44}}{S_{11}} - \frac{3}{4}\Bigr)\sin^2\theta\Bigr] S_{11}\varepsilon_1 \sum_j [I_x^{j2} - I_y^{j2}],$$

$$\Delta^2_{\xi 0} = \frac{1}{6} I(I+1) \sum_{k(\neq j)} \{(P^{jk}_{xx} + P^{jk}_{yy})^2 + 8P^{jk2}_{zz}\},$$

$$\mathcal{H}_{\mathbf{d}} + \mathcal{H}_{\mathbf{ex}} = \sum_{j>k} \sum_{\alpha,\beta} P^{jk}_{\alpha\beta} I^j_\alpha I^k_\beta,$$

$$\Delta^2_{\xi 1} = \frac{5}{3} I(I+1) \sum_{k(\neq j)} (P^{jk2}_{xz} + P^{jk2}_{yz}),$$

$$\Delta^2_{\xi 2} = \frac{1}{6} I(I+1) \sum_{k(\neq j)} \{(P^{jk}_{xx} - P^{jk}_{yy})^2 + 4P^{jk2}_{xy}\}.$$

Here ϵ_1 is the mean value of the time-dependent component of the deformation tensor ϵ; $S_{\eta\eta}$ are the components of the fourth-rank tensor relating ϵ with the tensor of the electric field gradient on the nucleus [see (1), (2), and (14) in reference 4]; $\Delta^2_{\xi 0}$ is the adiabatic second moment of the resonance line, $\Delta^2_{\xi 1}$ and $\Delta^2_{\xi 2}$ are the nonadiabatic second moments for transitions with m changing by ±1 and ±2, respectively (cf. reference 5), and ω_1 and ω_2 are the corresponding transition frequencies; V is the volume of the crystal, k the Boltzmann constant, and T the temperature. The form of the components of the tensor $P^{jk}_{\alpha\beta}$ is indicated in reference 6.

According to (1), the absorption curve $A(\omega)$ consists of a series of $(a = \xi, \ldots .)$ Gaussian lines, shifted by a distance $\Sigma_\gamma \Delta^2_{\alpha\gamma}/\omega_\gamma$ from the resonance frequencies ω_a. The width of these lines (at half the intensity) is calculated from the expression $\Delta\nu_{1/2} = 2.35\,\Delta_{a0}$. The coefficient $\Delta^2_{\epsilon 0}$ differs from the corresponding result $<(\Delta\nu)^2>$ of Van Vleck[5] in that $\Delta^2_{\epsilon 0d}$ for the $\mathcal{H}_d$ interaction is twice $<(\Delta\nu)^2>_d$, and $\Delta^2_{\epsilon 0}$ depends on the value of the isotropic exchange interactions. Therefore, the acoustic magnetic resonance is a much-promising method of investigation of exchange interactions in crystals.

Furthermore, it follows from our calculations that if $\Delta\nu_{1/2}$ in a crystal is determined by dislocation-type defects, then for $I = 3/2$ and $I = 5/2$ the ratio δ of the ultrasonic resonance width and the magnetic resonance width are respectively $\delta(3/2) = \sqrt{5/3}$, and $\delta(5/2) = \sqrt{12/5}$. The experimental values are $\delta(3/2) = 1.7$ (reference 1) and $\delta(5/2) > \delta(3/2)$ (reference 2).

We note that in the event of the excitation of free nuclear precession about the direction of H by an ultrasonic moment, the form of the decrease in the nuclear induction signal G with time will be described by the function $G_K(t)$ obtained from $A(\omega)$ by a Fourier transform [cf. reference 3, (3.17)]. Since $G_K(t) \neq G_M(t)$, it follows that ultrasonic moment methods can yield new results compared with the usual spin-echo method.

The authors express their deep gratitude to S. A. Al'tshuler for a discussion of the results.

---

[1] W. G. Proctor and W. A. Robinson, Phys. Rev. **104**, 1344 (1956).

[2] D. I. Bolef and M. Menes, Phys. Rev. **114**, 1441 (1959).

[3] R. Kubo and K. Tomita, J. Phys. Soc. Japan **9**, 888 (1954).

[4] E. F. Taylor and N. Bloembergen, Phys. Rev. **113**, 431 (1959).

[5] J. H. Van Vleck, Phys. Rev. **74**, 1168 (1948).

[6] U. Kh. Kopvillem, JETP **34**, 1040 (1958), Soviet Phys. JETP **7**, 719 (1958).

Translated by Z. Barnea
261

BETA AND GAMMA SPECTRA OF THE Sb^{113} *AND* Sb^{115} *ISOTOPES*

V. L. CHUKHLADZE, D. E. KHULELIDZE, and I. P. SELINOV

Submitted to JETP editor February 1, 1960

J. Exptl. Theoret. Phys. (U.S.S.R.) **38**, 1353 (April, 1960)

RECENTLY Selinov and his co-workers[1] discovered the new antimony isotopes Sb^{113} and Sb^{115}. The isotopes were obtained by the method of absorption of the approximate values of their end-point beta spectra.

The beta and gamma spectra of these isotopes were investigated with a double-lens beta spectrometer. The positron spectrum of Sb^{113} was found to consist of two components with end-point energies of 1.85 ± 0.02 and 2.42 ± 0.02 Mev. The values of log ft are 4.4 and 4.7. The end-point energy of the positron spectrum of Sb^{115} is 1.51 ± 0.02 Mev, and log ft = 4.25. The shape of the spectra is resolved. In the conversion-electron spectrum of Sb^{115} a gamma line with an energy of 0.499 ± 0.002 Mev was found. The conversion coefficient α_K is 0.00625. The ratio of the conversion coefficients of the K and L shells is about 6. According to preliminary data, eight gamma lines were observed in the Sb^{113} gamma spectrum, which was investigated with a scintillation spectrometer. The data on the Sb^{113} gamma spectrum are being published in the transactions of the 10th Conference on Nuclear Spectroscopy.

---

[1] Selinov, Grits, Khulelidze, Bliodze, Demin, and Kushakevich, Атомная энергия (Atomic Energy) **5**, 660 (1958).

Translated by Z. Barnea
262

A ROTATORY MAGNETO-MECHANICAL EFFECT IN A LOW PRESSURE PLASMA

V. L. GRANOVSKIĬ and É. I. URAZAKOV

Moscow State University

Submitted to JETP editor March 1, 1960

J. Exptl. Theoret. Phys. (U.S.S.R.) **38**, 1354-1355 (April, 1960)

IT has been pointed out in the literature[1] that in a low pressure positive column the gas should rotate around the axis of the column if a longitudinal uniform constant magnetic field is applied. One can attempt to detect this effect using a thin solid plate put into the gas which should be dragged by the rotation of the gas. We have performed such experiments.

The positive column was produced in a vertical cylindrical tube which contained activated electrodes at both ends and which was completely symmetrical about both the vertical axis and the horizontal plane. The presence of activated electrodes at both ends enabled us to change the direction of the current in the tube. The upper electrode was pierced, and through it was passed a thin quartz fiber (length 30 cm, diameter $20\,\mu$) hanging along the axis of the tube. The fiber supported a vertically suspended rectangular mica plate with a mirror stuck on it in the middle. This enabled us to observe the position of the plate by the usual means of a light beam and scale.

Two coils with a narrow gap between them to let the light beam through were put on the tube. The current passing through the coils produced a constant magnetic field in the tube which was parallel to the tube axis and to the current in it. The degree of uniformity of the field over the tube was not less than 97%. The coils and the tube were put in coaxial positions by regulating screws which could raise the base of the coils.

We performed the experiments in inert gases, mainly in argon, and partly in neon. The gas pressure was varied between 100 and $500\,\mu$ Hg. The following observations were made:

1. When a constant magnetic field was applied to the plasma the plate suspended in it deviated from its initial position; once the vibrations around the new equilibrium position were damped out the plate remained deflected at a constant angle. Such a deflection was observed in both gases and for all pressures and magnetic fields (from 100 to 800 oe) used. The deflection was appreciable (more than several degrees) and could easily be observed, even without a scale.

The stationary character of the effect in a system with a constantly acting restoring force (the elasticity of the fiber) shows that the effect is produced by the constant magnetic field and not by the turbulent inductive electrical field which is produced when the magnetic field appears.

2. When we reversed the direction of the magnetic field the deflection of the mobile system was also reversed.

3. However, when the direction of the current in the tube was reversed, the direction of the deflection of the suspended system remained the same. This shows that the effect is not caused by the plasma current and the applied magnetic field not being completely parallel, for otherwise the effect would reverse its sign when the direction of the current in the tube was reversed.

A possible cause of this magneto-mechanical effect is that the magnetic field produces a rotation of the positive column around its longitudinal axis. This could be caused by the diffusion of the ions and electrons in the plasma in the magnetic field in a direction perpendicular to this field and to the direction of the concentration gradient ("Hall diffusion current," see reference 2). The concentration gradient is in the radial direction in a cylindrical plasma and the "Hall diffusion currents" of the free electrons and of the ions must be in opposite azimuthal directions. The momenta of the two currents are unequal and the gas as a whole will thus begin to rotate.[1]

Further quantitative studies of this effect will enable us to verify the correctness of this interpretation.

---

[1] W. H. Bostick and M. A. Levine, Phys. Rev. **97**, 13, (1955).

[2] L. Spitzer Jr., Physics of Fully Ionized Gases, Interscience, New York, 1956.

Translated by D. ter Haar
263

ON THE HOLE COMPONENT OF THE FERMI SURFACE IN BISMUTH

N. B. BRANDT

Moscow State University

Submitted to JETP editor March 3, 1960

J. Exptl. Theoret. Phys. (U.S.S.R.) **38**, 1355-1356 (April, 1960)

As reported previously,[1,2] new high-frequency oscillations associated with a group of holes were observed during a study of the anisotropy of magnetic susceptibility in Bi at very low temperatures. Further investigation showed that the shape of the Fermi surface for this group consists, to a first approximation, of an ellipsoid of rotation, elongated along the trigonal axis, which has the following parameters. Area of the principal sections: perpendicular $S_1 = 6.75 \times 10^{-42}$ gm^2 cm^2/sec^2 and parallel to the trigonal axis $S_2 = 25.75 \times 10^{-42}$ gm^2 cm^2/sec^2; hole concentration $n^H = 0.34 \times 10^{18}$ cm^{-3}; bounding

Fermi energy $E_0^H \simeq 2.5 \times 10^{-14}$ erg ($E_0^H/k \simeq 180°K$); effective mass in the plane perpendicular to the trigonal axis $m_1^H = m_2^H = 0.05\,m_0$ (m_0 is the free electron mass) and in the direction of the trigonal axis $m_3^H = 0.7\,m_0$.

The magnitude of the anisotropy of the hole surface and the value of the effective masses are in good agreement with recently published work on cyclotron resonance[3] in Bi ($m_1^H = m_2^H = 0.068\,m_0$ and $m_3^H = 0.92\,m_0$) and on the anomalous skin effect[4] ($m_3^H/m_1^H = 12.8$). In these works, and also in Reneker's, this group of holes has been described by the anomalously small value of bounding energy ($E_0^H = 0.18 \times 10^{-14}$ erg, $E_0^H/k = 13°K$) which was suggested by Heine[6] and by Strelkov and Kalinkina[7] to explain the appreciable electronic specific heat of Bi.

We should point out that n^H in one ellipsoid of revolution is 0.34×10^{18} cm^{-3}, and is practically equal to the concentration of electrons in Shoenberg's three-ellipsoid model, $n^e = 0.39 \times 10^{-18}$ cm^{-3}. These two groups of 'light' electrons and holes must evidently be responsible for the galvanomagnetic properties of Bi. The difference between the mean effective masses of the electrons in Shoenberg's three-ellipsoid model,

$$\overline{m}^e = [m_1(m_2m_3 - m_4^2)]^{1/3} = 0.053m_0$$

and of the holes in the one-ellipsoid model,

$$\overline{m}^H = (m_1^2 m_3)^{1/3} = 0.13m_0$$

agrees well with the difference of mean mobilities $\overline{\tau}/\overline{m}$ of the electrons and holes ($\overline{\tau}^e/\overline{m}^e \simeq 2\overline{\tau}^H/\overline{m}^H$) assuming approximately the same relaxation times.

Since the heat capacity of the 'light' holes is negligibly small compared with the observed[7] linear term in the heat capacity of Bi, we must assume that there exist at least three groups of carriers.[8,1]

---

[1] Brandt, Dubrovskaya, and Kytin, JETP **37**, 572 (1959), Soviet Phys. JETP **10**, 670 (1960).

[2] N. B. Brandt, Приборы и техника эксперимента (Instrum. and Meas. Engg.) No. **2** (1960).

[3] Galt, Yager, Merritt, and Cetlin, Phys. Rev. **114**, 1496 (1959).

[4] G. E. Smith, Phys. Rev. **115**, 1561 (1959).

[5] D. H. Reneker, Phys. Rev. **115**, 303 (1959).

[6] V. Heine, Proc. Phys. Soc. **A69**, 513 (1956).

[7] I. N. Kalinkina and P. G. Strelkov, JETP **34**, 616 (1958); Soviet Phys. JETP **7**, 426 (1958).

[8] N. B. Brandt and V. A. Venttsel, JETP **35**, 1083 (1958), Soviet Phys. JETP **8**, 757 (1959).

Translated by R. Berman

PRODUCTION OF A Σ HYPERON BY 8.3 Bev/c NEGATIVE π MESONS

WANG KANG-CHANG, WANG CHU-CHIEN, V. I. VEKSLER, N. M. VIRYASOV, I. VRANA, TING TA-CHAO, KIM HU IN, E. N. KLADNITSKAYA, A. A. KUZNETSOV, A. MIKHUL, NGUYEN DIN TU, A. V. NIKITIN, and M. I. SOLOV'EV

Joint Institute for Nuclear Research

Submitted to JETP editor March 24, 1960

J. Exptl. Theoret. Phys. (U.S.S.R.) **38**, 1356-1359 (April, 1960)

ONE event of production and decay of a $\overline{\Sigma}^-$ hyperon was found out of 40,000 pictures obtained by a beam of negative 8.3 ± 0.6 Bev/c pions in a propane bubble chamber[1] with a constant magnetic field of 13,700 oe. A photograph and diagram of this event are shown. A π^- meson (track 1) gives a star at point O, from which emerge four charged particles of high energy (tracks 2, 6, 7, 16), two K^0 mesons (tracks 4, 5, 14, 15), and one particle of low energy (short track 17). The track of the positively charged particle 2 is deflected at point A. At a distance of 7.7 mm from the point of deflection is a six-prong star. The center of the star lies in the plane of tracks 2 and 3 within the limits of the error of measurement (47′). The decay of particle 2 at point A into particle 3 and a neutral particle N in the direction AB is in very good agreement with the kinematics of a Σ decay (see Table I). Track 3 is that of a π^+ meson.

The momentum of particle N was determined by equating the perpendicular components of the momenta of particles 3 and N at point A.

Assuming a decay according to the scheme $\Sigma^+ \rightarrow \pi^+ + n$, we obtain M_2 = 1182 ± 14 Mev.

The energy and momentum balance at point B is given in Table II. Star B has five positive particles (tracks 8, 9, 11, 12, 13) and one negative (track 10). The negative particle is a π meson. Tracks 9, 11, 12, 13 stop in the chamber and we take them to be protons. Particle 8 has a high momentum and escapes from the chamber. From the measurements of ionization* and momentum it follows that track 8 belongs to a π^+ meson. The measurement of the energy balance at point B shows that the energy of the charged particles of the star is already much larger than the kinetic energy of a neutron with a momentum of 1628 ± 100 Mev/c. Consequently, star B can be caused only by the annihilation of an antineutron on a carbon nucleus. The most probable reaction is

$$\overline{n} + C \rightarrow He_2^4 + 4p + 3n + \pi^+ + \pi^- + n\pi^\circ.$$

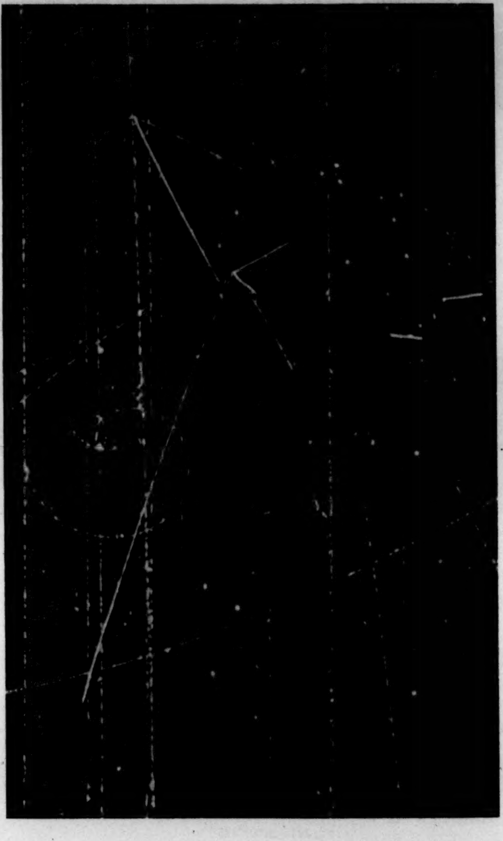

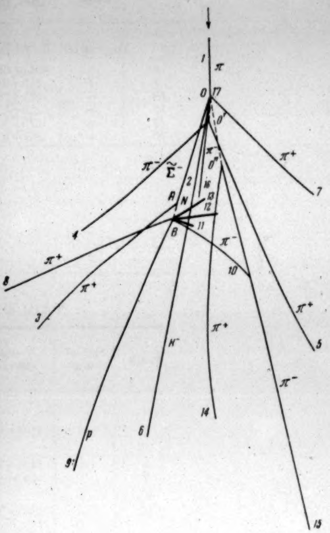

TABLE I. Kinematics at Point A

Track	Sign of charge	P_{meas}, (Mev/c)	P_{cal}, (Mev/c)	Particle	Angle
2	+	1104±600	1798±100	$\bar{\Sigma}^-$	
3	+	244±10		π^+	$\varphi(3.2)=39°38'\pm20'$
AB	0		1628±100	$\bar{n}$	$\varphi(AB.2)=5°29'\pm20'$

The energy carried away by neutrons should be added to the energy of the charged particles. Assuming that on the average they carry away the same energy as the protons, $E_n = 144 \pm 5$ Mev; also, the binding energy of the nucleons in the nucleus is $E_b = 64$ Mev. Assuming that, apart from charged π mesons, there are still neutral π mesons which carry away, on the average, half the energy of the charged π mesons, $E_{\pi^0} \approx \frac{1}{2}E_{\pi^\pm} = 645$ Mev, then the total energy in the star is $E_{\text{tot}} = 2336$ Mev.

The energy obtained in this way is close to the

TABLE II. Kinematics at Point B

Track	Sign of charge	P_{meas}, (Mev/c)	P_{cal}, (Mev/c)	Particle	E_{kin}, (Mev/c)	E_{mass}, (Mev)	Total E (Mev)
AB	0		1628 ± 100	$\bar{n}$	940 ± 100	$2 \cdot 939$	2818 ± 100
8	+	1044 ± 55		π^+	920 ± 56	140	
9	+	445 ± 9		p	101 ± 3		
10	—	183 ± 25		π^-	90 ± 20	140	
11	+	228 ± 4		p	27 ± 2		
12	+	270 ± 5		p	38 ± 2		
13	+	257 ± 5		p	27 ± 2		
ΔP			703	$\sum E = 1203 \pm 60 + 280$			$=1483 \pm 60$
				$E_n = 3(48 \pm 3)$			$=144 \pm 5$
				$E_b = 8 \cdot 8$			$=64$
							1691 ± 61
				E_{π°			645
				Total energy at point B			2336

TABLE III. Kinematics at Point O

Track	Sign of charge	P_{meas}, (Mev/c)	P_{cal}, (Mev/c)	Particle	Visible E_{kin}, (Mev)	E_{mass}, (Mev)	Total E (Mev)
1	—	—	8300 ± 600	π^-	8200 ± 600	$140 =$	8340 ± 600
2	+	1104 ± 600	1798 ± 100	$\bar{\Sigma}^-$	964 ± 80	1196	
V_1^0	0		654 ± 29	K^0 or $\bar{K}^0$	323 ± 27	494	
6	—	1456 ± 70		K^-	1043 ± 60	494	
7	+	790 ± 45		π^+	663 ± 45	140	
V_2^0	0		1475 ± 71	$\bar{K}^0$ or K^0	1060 ± 60	494	
16	—	300 ± 50		π^-	190 ± 50	140	
	0			N		939	
					$(4243 \pm 138) + 3897 = 8140 \pm 138$		

TABLE IV. Kinematics at Points O′ and O″

Track	Sign of charge	P_{meas}, (Mev/c)	P_{cal}, (Mev/c)	Particle	Angle	Angle of noncoplanarity
V_1^0	0		654 ± 29	K^0 or $\bar{K}^0$		$\eta = 33'$
4	—	324 ± 25		π^-	$\varphi(V_1^0, 4) = 41^\circ 18' \pm 15'$	
5	+	453 ± 22		π^+	$\varphi(V_1^0, 5) = 24^\circ 43' \pm 15'$	
V_2^0	0		1475 ± 71	$\bar{K}^0$ or K^0		$\eta = 8'$
14	+	207 ± 8		π^+	$\varphi(V_2^0, 14) = 26^\circ 50' \pm 15'$	
15	—	1299 ± 70		π^-	$\varphi(V_2^0, 15) = 5^\circ 3' \pm 15'$	

total annihilation energy of the antineutron. Consequently, at point A there occurred the decay $\bar{\Sigma}^- \rightarrow \pi^+ + \bar{n}$.

The probability of a chance coincidence in one picture of various events which may have imitated the phenomenon under consideration is, according to our estimate, $\sim 10^{-9}$.

We consider the most probable reaction in the primary star to be

$$\pi^- + \mathrm{C} \rightarrow \bar{\Sigma}^- + K^0 + \bar{K}^0 + K^- + p + \pi^+ + \pi^- + \text{recoil nucleus}$$

For the lifetime of the $\bar{\Sigma}^-$ we obtained the value $(1.18 \pm 0.07) \times 10^{-10}$ sec.

Hence, the data presented is evidence of the fact that we have observed a new type of particle, the charged antihyperon $\bar{\Sigma}^-$.

---

*S. Otwinowski and I. Vrana studied the possibility of measuring the ionization in our chamber. Out of 60 different pictures 40 m of track, the momentum and nature of which were known, were measured. It was found that for a track length 20 cm one may reliably (96%) separate π mesons and protons up to a momentum of 1200 Mev/c. The measured value of the ionization of track 8 (of length 20 cm) was 1.02 ± 0.19, and should be, by the β^{-2} law (Blinov et al.[3]), 1.86 for a proton and 1.04 for a π meson.

---

[1] Wang Kang-Chang, Solov'ev, and Shkobin, Приборы и техника эксперимента (Instrum. and Meas. Engg.) No. 1, 41 (1959).

[2] S. Otwinowski, Report, High-Energy Laboratory, Joint Institute for Nuclear Research, 1960.

[3] Blinov, Krestnikov, and Lomanov, JETP 31, 762 (1956), Soviet Phys. 4, 661 (1957).

[4] Willis, Fowler, and Rahm, Phys. Rev. 108, 1046 (1957).

Translated by E. Marquit
265

SOVIET PHYSICS JOURNALS

Published in English by the American Institute of Physics

Soviet Physics—JETP

A translation, beginning with 1955 issues of "Zhurnal Eksperimental'noi i Teoreticheskoi Fiziki" of the USSR Academy of Sciences. Leading physics journal of Soviet Union. Similar to "The Physical Review" in quality and range of topics. Outstanding new work is most likely to appear in this journal.

Twelve issues, approximately 4000 pages. $75 domestic, $79 foreign. Libraries $35 domestic, $39 foreign. Single copies, $8.*

Soviet Physics—SOLID STATE

A translation, beginning with 1959 issues of "Fizika Tverdogo Tela" of the USSR Academy of Sciences. Offering results of theoretical and experimental investigations in the physics of semiconductors, dielectrics, and on applied physics associated with these problems. Also publishes papers on electronic processes taking place in the interior and on the surface of solids.

Twelve issues, approximately 2000 pages. $55 domestic, $59 foreign. Libraries $25 domestic, $29 foreign. Single copies, $8.*

Soviet Physics—TECHNICAL PHYSICS

A translation, beginning with 1956 issues of "Zhurnal Tekhnicheskoi Fiziki" of the USSR Academy of Sciences. Contains work on plasma physics and magnetohydrodynamics, aerodynamics, ion and electron optics, and radio physics. Also publishes articles in mathematical physics, the physics of accelerators, and molecular physics.

Twelve issues, approximately 2000 pages, $55 domestic, $59 foreign. Libraries $25 domestic, $29 foreign. Single copies, $8.*

Soviet Physics—ACOUSTICS

A translation, beginning with 1955 issues of "Akusticheskii Zhurnal" of the USSR Academy of Sciences. Devoted principally to physical acoustics but includes electro-, bio-, and psychoacoustics. Mathematical and experimental work with emphasis on pure research.

Four issues, approximately 500 pages. $12 domestic, $14 foreign. (No library discounts.) Single copies, $4.

Soviet Physics—DOKLADY

A translation, beginning with 1956 issues of the physics sections of "Doklady Akademii Nauk SSSR," the proceedings of the USSR Academy of Sciences. All-science journal offering four-page reports of recent research in physics and borderline subjects.

Six issues, approximately 1500 pages. $35 domestic, $38 foreign. Libraries $15 domestic, $18 foreign. Single copies Vols. 1 and 2, $5; Vol. 3 and later issues, $7.*

Soviet Physics—CRYSTALLOGRAPHY

A translation, beginning with 1957 issues of the journal "Kristallografiya" of the USSR Academy of Sciences. Experimental and theoretical papers on crystal structure, lattice theory, diffraction studies, and other topics of interest to crystallographers, mineralogists, and metallurgists.

Six issues, approximately 1000 pages. $25 domestic, $27 foreign. Libraries $10 domestic, $12 foreign. Single copies, $5.*

SOVIET ASTRONOMY—AJ

A translation, beginning with 1957 issues of "Astronomicheskii Zhurnal" of the USSR Academy of Sciences. Covers various problems of interest to astronomers and astrophysicists including solar activity, stellar studies, spectroscopic investigations of radio astronomy.

Six issues, approximately 1100 pages. $25 domestic, $27 foreign. Libraries $10 domestic, $12 foreign. Single copies, $5.*

Soviet Physics—USPEKHI

A translation, beginning with September, 1958, issue of "Uspekhi Fizicheskikh Nauk" of the USSR Academy of Sciences. Offers reviews of recent developments comparable in scope and treatment to those carried in "Reviews of Modern Physics." Also contains reports on scientific meetings within the Soviet Union, book reviews, and personalia.

Six issues, approximately 1700 pages. (Contents limited to material from Soviet sources.) $45 domestic, $48 foreign. Libraries $20 domestic, $23 foreign. Single copies $9.*

*For libraries of nonprofit academic institutions.
Subscription prices subject to annual variation, depending on size of Russian originals.

Please send orders and inquiries to

American Institute of Physics
335 East 45 Street, New York 17, N.Y.

CONTENTS—continued

		Page	Russian Reference	
On the Theory of Quadrupole Relaxation of Nuclear Spins in Liquids	K. A. Valiev	883	38,	1222
On the Analogy between the Weak and Electromagnetic Interactions	É. M. Lipmanov	891	38,	1233
On the Structure of the S Matrix in the Theory of Elastic and Inelastic Scattering of Nonrelativistic Particles	Yu. V. Tsekhmistrenko	894	38,	1237
Disintegration of Cosmic-Ray Nuclei by Solar Photons	N. M. Gerasimova and G. T. Zatsepin	899	38,	1245
On the Theory of Relaxation Processes in Ferrodielectrics with Weak Magnetic Anisotropy at Low Temperatures	V. G. Bar'yakhtar and G. I. Urushadze	905	38,	1253
Renormalization in Parity-Nonconservation Theory	B. L. Ioffe	911	38,	1263
Distribution of the Transverse Momentum of Shower Particles in Jets	É. G. Boos and Zh. S. Takibaev	920	38,	1276
Leptonic Decays of Hyperons with Emission of Pions	I. S. Tsukerman	927	38,	1285
On Certain General Properties of the Photon Propagation Function in Quantum Electrodynamics	A. A. Ansel'm	929	38,	1288
Moments of Inertia of Odd Atomic Nuclei	Yu. T. Grin', S. I. Drozdov, and D. F. Zaretskiĭ	936	38	1297
Contribution to the Theory of Electron-Gas Conductivity in a Strong Magnetic Field	V. G. Skobov	941	38,	1304
Rotational Energy and Moments of Inertia of Non-Axial Nuclei	A. S. Davydov, N. S. Rabotnov, and A. A. Chaban	946	38,	1311
On the Equilibrium Shape of Atomic Nuclei	G. F. Filippov	949	38,	1316
Nonresonance Absorption of Oscillating Magnetic Field Energy by a Ferromagnetic Dielectric. II	M. I. Kaganov, and V. M. Tsukernik	952	38,	1320
Magnetic Resonance in Rhombohedral Weak Ferromagnetics	E. A. Turov and N. G. Guseĭnov	955	38,	1326

LETTERS TO THE EDITOR

		Page	Russian Reference	
Investigation of Nuclear Magnetic Resonance in Adsorbed Gas	A. A. Galkin and I. V. Matyash	959	38,	1332
Observation of Spontaneous Coherent Radiation of a Ferrite in a Resonator	A. P. Aleksandrov, Ya. I. Khanin, and É. G. Yashchin	960	38,	1334
Formation of Pions in πN Collisions	A. I. Lebedev and V. A. Petrun'kin	962	38,	1337
Gamma Radiation Produced in the Interaction between Accelerated C^{12} Ions and Tin Nuclei	V. A. Karnaukhov and Yu. Ts. Oganesyan	964	38,	1339
Beta Decay of P^{32}	B. V. Geshkenbeĭn	965	38,	1341
On the Decay of Σ Hyperons	Chou Kuang-Chao	966	38,	1342
On the Process $e^- + p \to \Lambda + \nu$	V. M. Shekhter	967	38,	1343
Inelastic Interactions of 9-Bev Protons with Free and Bound Nucleons in Emulsion	N. P. Bogachev, S. A. Bunyatov, Yu. P. Merekov, V. M. Sidorov, and V. A. Yarba	968	38,	1346
On Elastic Scattering of Photons by the Nuclear Coulomb Field	C. Eftimiu and C. Vrejoiu	971	38,	1348
Determination of the First Ionization Potentials of Neodymium and Praseodymium by the Surface Ionization Method	N. I. Ionov and M. A. Mittsev	972	38,	1350
The Line Shape of the Nuclear Acoustic Resonance	N. G. Koloskova and U. Kh. Kopvillem	973	38,	1351
Beta and Gamma Spectra of the Sb^{113} and Sb^{115} Isotopes	V. L. Chukhladze, D. E. Khulelidze, and I. P. Selinov	974	38,	1353
A Rotatory Magneto-Mechanical Effect in a Low-Pressure Plasma	V. L. Granovskiĭ and E. I. Urazakov	974	38,	1334
On the Hole Component of the Fermi Surface in Bismuth	N. B. Brandt	975	38,	1355
Production of a Σ Hyperon by 8.3-Bev/c Negative π Mesons	Wang Kang-Chang, Wang Chu-chien, V. I. Veksler, N. M. Viryasov, I. Vrana, Ting Ta-Chao, Kim Hu In, E. N. Kladnitskaya, A. A. Kuznetsov, A. Mikhul, Nguyen Din Tu, A. V. Nikitin, and M. I. Solov'ev	976	38,	1356

SOVIET PHYSICS JETP VOLUME 11, NUMBER 4 OCTOBER, 1960

CONTENTS

Page Russian Reference
Long-lived Lutetium Isotopes . . . . V. A. Romanov, M. G. Iodko, and V. V. Tuchkevich 733 **38**, 1019
Investigation of the Relative Intensities of Some Conversion Lines of the Spectrum of Neutron-Deficient Lutetium Isotopes . . . . M. G. Iodko, V. V. Tuchkevich, V. A. Romanov, and O. M. Kresin 739 **38**, 1027
Large Cosmic-Ray Intensity Fluctuations in the Stratosphere . . . . A. N. Charakhch'yan, V. F. Tulinov, and T. N. Charakhch'yan 742 **38**, 1031
Anomalies in the Modulus of Elasticity and in Internal Friction in the Alloy Fe_3Pt . . . . G. I. Kataev and Z. D. Sirota 747 **38**, 1037
Investigation of the Line Width and Shape in the Paramagnetic Resonance Spectrum of the Cr^{+++} Ion in Corundum Single Crystals . . . . A. A. Manenkov and V. B. Fedorov 751 **38**, 1042
Internal Conversion Pairs in the Decay of Neutral π Mesons . . . . Yu. A. Budagov, S. Viktor, V. P. Dzelepov, P. F. Ermolov, and V. I. Moskalev 755 **38**, 1047
Ionization of Gases by Negative Ions . . . . Ya. M. Fogel', A. G. Koval', and Yu. Z. Levchenko 760 **38**, 1053
The Isentropic Compressibility of Aluminum, Copper, Lead, and Iron at High Pressures . . L. V. Al'tshuler, S. B. Kormer, M. I. Brazhnik, L. A. Vladimirov, M. P. Speranskaya, ... and A. I. Funtikov 766 **38**, 1061
Energy Spectrum of Mesons from Nuclear Disintegrations Produced by 9-Bev Protons . . . . Yu. T. Lukin, Zh. S. Takibaev, and E. V. Shalagina 776 **38**, 1074
Photoproduction of Charged Pions near Threshold . . . . M. I. Adamovich, E. G. Gorzhevskaya, V. G. Larionova, V. M. Popova, S. P. Kharlamov, ... and F. R. Yagudina 779 **38**, 1078
The $Al^{27} \rightarrow Na^{24}$, $Co^{59} \rightarrow Mn^{56}$, and $P^{31} \rightarrow Na^{24}$ Reactions in the 260-Mev Gamma-Ray Energy Range . . . . A. N. Gorbunov, F. P. Denisov, and V. A. Kolotukhin 783 **38**, 1084
Piezomagnetism in the Antiferromagnetic Fluorides of Cobalt and Manganese . . . . A. S. Borovik-Romanov 786 **38**, 1088
Elastic Scattering of 240-330 Mev π^- Mesons by Hydrogen . . . . V. G. Zinov and S. M. Korenchenko 794 **38**, 1099
Investigation of the Decay Scheme of As^{76} by the γ-γ Coincidence Method . . . . N. N. Delyagin and A. A. Sorokin 799 **38**, 1106
Resonance Scattering of Gamma Rays by Se^{76} . . . . N. N. Delyagin 803 **38**, 1111
Fragment Production by 100-Mev Protons . . . . U. R. Arifkhanov, M. M. Makarov, N. A. Perfilov, and V. P. Shamov 806 **38**, 1115
The Existence of New Isotopes of Light Nuclei and the Equation of State of Neutrons . . . . Ya. B. Zel'dovich 812 **38**, 1123
Multiple Production of Jet Particles in Peripheral Collisions . . . . Yu. A. Romanov and D. S. Chernavskiĭ 819 **38**, 1132
The Thermodynamic Average of Functions of the Displacement of Atoms in a Non-Ideal Crystalline Lattice . . . . V. I. Peresada 825 **38**, 1140
Polarization Effects in the Scattering of Electrons by Deuterons . . . . G. V. Frolov 831 **38**, 1148
Resonance Absorption of High-Frequency Sound Energy by Semiconductor Current Carriers in a Magnetic Field . . . . E. P. Pokatilov 835 **38**, 1153
Scattering of Electrons by Nuclei according to the α-Particle Model . . . . E. V. Inopin and B. I. Tishchenko 840 **38**, 1160
Allowance for the Medium in Radiation Corrections to Coulomb Scattering . . . . M. L. Ter-Mikaelyan 845 **38**, 1167
Polarization of Deuterons Elastically Scattered on Zero-Spin Nuclei . . . . G. M. Budyanskiĭ 847 **38**, 1170
On the Quantum-Mechanical Calculations of the Pressure in Solids . . . . G. M. Gandel'man and E. S. Pavlovskiĭ 851 **38**, 1176
Coherent Electron Radiation in a Synchrotron. III . . . . M. S. Rabinovich and L. V. Iogansen 856 **38**, 1183
Quantum Oscillations of the Photoelectric Yield of Metals in a Magnetic Field . . . . G. E. Zil'berman and I. O. Kulik 859 **38**, 1188
The Effect of an External Electric Field on the Shape of the Intrinsic Absorption Edge in Non-Conducting Crystals . . . . D. S. Bulyanitsa 868 **38**, 1201
On the Build-up of Electromagnetic Waves in a Plasma Moving in a Non-Dispersive Dielectric in the Presence of a Constant Magnetic Field . . . . G. G. Getmantsev and V. O. Rapoport 871 **38**, 1205
A Relativistic Transport Equation for a Plasma. II . . . . Yu. L. Klimontovich 876 **38**, 1212

(Contents continued on inside back cover)